ISTANBUL TECHNICAL UNIVERSITY ★ GRADUATE SCHOOL OF SCIENCE ENGINEERING AND TECHNOLOGY

POLYTECHNIC UNIVERSITY OF TURIN ★ DOCTORAL SCHOOL

A METHODOLOGY FOR ENERGY OPTIMIZATION OF BUILDINGS CONSIDERING SIMULTANEOUSLY BUILDING ENVELOPE HVAC AND RENEWABLE SYSTEM PARAMETERS

Ph.D. THESIS

Meltem BAYRAKTAR

Department of Architecture - Construction Sciences Programme

Department of Energy - Energetics Programme

NOVEMBER 2015

ISTANBUL TECHNICAL UNIVERSITY ★ GRADUATE SCHOOL OF SCIENCE ENGINEERING AND TECHNOLOGY

POLYTECHNIC UNIVERSITY OF TURIN ★ DOCTORAL SCHOOL

A METHODOLOGY FOR ENERGY OPTIMIZATION OF BUILDINGS CONSIDERING SIMULTANEOUSLY BUILDING ENVELOPE HVAC AND RENEWABLE SYSTEM PARAMETERS

Ph.D. THESIS

Meltem BAYRAKTAR
(502072608 - 161788)

Department of Architecture - Construction Sciences Programme

Department of Energy - Energetics Programme

Thesis Advisor: Prof. Dr. A. Zerrin YILMAZ
Thesis Advisor: Prof. Dr. Marco PERINO

NOVEMBER 2015

İSTANBUL TEKNİK ÜNİVERSİTESİ ★ FEN BİLİMLERİ ENSTİTÜSÜ

TORİNO POLİTEKNİK ÜNİVERSİTESİ ★ FEN BİLİMLERİ ENSTİTÜSÜ

BİNALARDA YAPI KABUĞU, MEKANİK SİSTEMLER VE YENİLENEBİLİR ENERJİ SİSTEMLERİ PARAMETRELERİNİN EŞ ZAMANLI ENERJİ OPTİMİZASYONU İÇİN BİR YÖNTEM

DOKTORA TEZİ

Meltem BAYRAKTAR
(502072608 - 161788)

Mimarlık Anabilim Dalı - Yapı Bilimleri Programı

Enerji Anabilim Dalı - Enerji Bilimi Programı

Tez Danışmanı: Prof. Dr. A. Zerrin YILMAZ
Tez Danışmanı: Prof. Dr. Marco PERINO

KASIM 2015

Meltem Bayraktar, a **joint Ph.D.** student of **ITU Graduate School of Science Engineering and Technology**, student ID **502072608**, and **Politecnico di Torino**, **Department of Energy**, student ID **161788**, successfully defended the thesis entitled **"A METHODOLOGY FOR ENERGY OPTIMIZATION OF BUILDINGS CONSIDERING SIMULTANEOUSLY BUILDING ENVELOPE HVAC AND RENEWABLE SYSTEM PARAMETERS"**, which she prepared after fulfilling the requirements specified in the associated legislations, before the jury whose signatures are below.

Thesis Advisor:	**Prof. Dr. Ayşe Zerrin YILMAZ** İstanbul Technical University	.....
Thesis Advisor:	**Prof. Dr. Marco PERINO** Politecnico di Torino	.....
Jury Members:	**Prof. Dr. Figen KADIRGAN** İstanbul Technical University	.....
	Prof. Dr. İsmail Cem PARMAKSIZOĞLU İstanbul Technical University	.....
	Ass. Prof. Dr. Stefano CORGNATI Politecnico di Torino	.....
	Ass. Prof. Dr. Valentina SERRA Politecnico di Torino	.....
	Prof. Dr. Hasan HEPERKAN Yıldız Technical University	.....

Date of Submission : 13 July 2015
Date of Defense : 13 November 2015

FOREWORD

It is my pleasure to acknowledge the roles of several individuals who were instrumental for completion of this PhD research.

First of all, I would like to express my deepest gratitude to my joint PhD supervisors, Professor Ayşe Zerrin Yılmaz, Istanbul Technical University and Professor Marco Perino, Politecnico di Torino, for their patient guidance, enthusiastic encouragement and valuable critiques of this research work. It would not have been possible to complete this study without their support.

I would also like to thank Dr. Yi Zhang of IESD, De Montfort University for taking his time to guide me into the field of optimization and for his advice.

I would like to extend my appreciation to my committee members: Professor Figen Kadırgan, Professor Cem Parmaksızoğlu and Professor Hasan Heperkan, for providing invaluable advice and guidance throughout my research.

During my PhD work, I was fortunate to be involved in an international research project, CityNet, funded by European Union under FP6 Marie Currie Action - Research Training Network. The project gave me a great chance to work with excellent researchers in my field and to gain a valuable experience. I wish to express my gratitude to European Commission for the financial support and to Professor Ursula Eicker for providing us with such a great opportunity.

I would also like to thank my former colleagues from CityNet research group, from Department of Energy at Politecnico di Torino and from Department of Environmental Control at Istanbul Technical University. An incomplete list includes Ivan Korolija, Jerko Labus (whom I will always remember with a smile), Julie Ann Futcher, Tobias Schulze, Rafal Strzalka, Graeme Stuart, Fabio Zanghirella, Francesco Causone, Alice Gorrino, Feride Şener Yılmaz, Mine Aşçıgil Dinçer and Neşe Ganiç. They have been a great source of moral support.

I greatly appreciate the support and well wishes from my friends, Elif Aydın Çınar, Yeliz Erkoç, Evren Akgöz, Başak Kundakçı, Ece Kalaycıoğlu, Burcu Çiğdem Çelik, Sinem Bahadır and Güneş Uyar. I am grateful to them for being always there for me and for their care and great concern.

Finally, I wish to thank my parents Adnan and Fevziye Bayraktar for always standing by my side, for their endless love and encouragement my whole life.

November 2015 Meltem Bayraktar

TABLE OF CONTENTS

Page

ABBREVIATIONS

ASHRAE : American Society of Heating, Refrigerating and Air-Conditioning Engineers
BIPV/T : Building-integrated photovoltaic/thermal
BPIE : Building Performance Institute Europe
BPS : Building Performance Simulation
CAPFT : Capacity as a Function of Temperature curve
CIBSE : Chartered Institution of Building Services Engineers
CMAES : Covariance matrix adaptation evolution strategy
CO2 : Carbon dioxide
CO2-eq : Carbon dioxide equivalent
COP : Coefficient of performance
EER : Energy Efficiency Ratio
EF : Energy factor
EIR : Energy input ratio
EIRFPLR : Energy Input Ratio as a Function of Part-load Ratio
EIRFT : Energy Input Ratio as a Function of Temperature
EPBD : European Energy Performance of Buildings Directive
FHR : First-hour rating
GA : Genetic algorithm
GC : Global cost
GHG : Greenhouse gas
HDE : Hybrid differential evolution
HJ : Hooke Jeeves
HVAC : Heating, Ventilating and Air-Conditioning
ID : Identification
IEA : International Energy Agency
IEQ : Indoor Environmental Quality
IESNA : Illuminating Engineering Society of North America
IGDAS : Istanbul Gas Distribution Industry and Trade Incorporated Company
IPCC : Intergovernmental Panel on Climate Change
ISKI : Istanbul Water and Sewerage Administration
ISO : Organization for Standardization
LCC : Life cycle cost
MOGA : Multiple objective genetic algorithm
Mtoe : Million Tonnes of Oil Equivalent
NBEC : Normalized boiler efficiency curve
NIBS : National Institute of Building Sciences
NN : Neural network
NPGA : Niched Pareto genetic algorithm
NPV : Net-present value
NSGA : Non-dominated sorting genetic algorithm
nZEB : nearly zero energy buildings

PCM **:** Phase Change Material
PEN **:** Penalty value
PEUI **:** The primary energy use intensity
PMV **:** Predicted mean vote
PPD **:** Percentage people dissatisfied
PPM **:** Parts per million
PSO **:** Particle swarm optimization
PV **:** Photovoltaic
REA **:** Robust evolutionary algorithm
SC **:** Solar collector
SHGC **:** Solar heat gain coefficient
SI **:** Sensitivity index
SBP **:** Simple payback
SPEA **:** Strength Pareto evolutionary algorithm
SRI **:** Solar Reflectance Index
S/V **:** Surface area to volume ratio
SWH **:** Solar water heating
TEDAS **:** Turkish Electricity Distribution Company
Tvis **:** Visible transmittance
W-t-w **:** Window-to-wall
VAT **:** Value added tax

NOMENCLATURE

BL	: Boiler type
$\mathbf{c_1}$	: Cognitive acceleration coefficient
$\mathbf{c_2}$	: Social acceleration coefficient.
$\mathbf{CI_i}$	: The carbon dioxide equivalent intensity index in g.EqCO^2/kWh for each available energy source
CL	: Chiller type
$\mathbf{CO2_{target}}$	: User set overall CO_2 emission amount
$\mathbf{CO2_{actual}}$	: Actual building overall CO2 emission amount
$\mathbf{CO2_{emission}}$	: The overall building CO2 emission amount
$\mathbf{d}$	: Real discount rate
$\mathbf{D}$	: Nominal discount rate
$\mathbf{D_{max}}$	: Maximum of output values
$\mathbf{D_{min}}$	: Minimum of output values
DL	: Artificial lighting control type
$\mathbf{E}$	: Nominal escalation rate
$\mathbf{E_0}$	: Annually recurring energy cost at base-date price
$\mathbf{e_e}$	: Real constant price escalation rate for energy
$\mathbf{e_w}$	: Constant price escalation rate for water.
$\mathbf{En_i}$	: Energy consumptions in different fuel forms
$\mathbf{EC_{actual}}$	: Allowable capacity of the actual equipment
$\mathbf{EC_{autosize}}$	: Required equipment capacity determined via autosizing calculation
$\mathbf{gbest}$	: gbest of the group
$\mathbf{GC}$	: Global cost
GT	: Glazing type
$\mathbf{H}$	: Internal heat production rate of an occupant per unit area
$\mathbf{I}$	: Present-value investment cost
$\mathbf{I_0}$	: Investment cost at base date
iEW	: External wall insulation thickness
$\mathbf{Inf}$	: Inflation rate
iR	: Roof insulation thickness
$\mathbf{L}$	: All the modes of energy loss from body
$\mathbf{M}$	: Present-value maintenance cost
$\mathbf{M_0}$	: Annually recurring uniform maintenance cost in base year
$\mathbf{Met}$	: Metabolic rate
$\mathbf{n}$	: Study period
Ort	: Orientation
$\mathbf{pbest_i}$	: pbest of particle i
$\mathbf{PEN_{Capacity}}$	: Calculated penalty for being above or below user-set capacity limits
$\mathbf{PEN_k}$	: Main penalty value
$\mathbf{PEN_{Comfort}}$	: Penalty value due to violation of comfort criteria
$\mathbf{PEN_{payback}}$	: Penalty value due to violation of payback time criteria

$\mathbf{PPD_{actual}}$: Calculated PPD index for actual building
$\mathbf{PPD_{target}}$: Target PPD index set by designer
$\boldsymbol{PVtyp}$: Photovoltaic module type
$\boldsymbol{PVnum}$: Number of available photovoltaic modules
$\mathbf{q}$: Nonnegative constant as penalty power factor
$\mathbf{r_1}$: Uniformly distributed random number between 0 and 1
$\mathbf{r_2}$: Uniformly distributed random number between 0 and 1
$\mathbf{R_0}$: Replacement cost at base-date price
$\mathbf{Rep}$: Present-value capital replacement cost
$\boldsymbol{RT}$: Roof type
$\mathbf{S}$: Present-value scrap cost
$\mathbf{S_0}$: Scrap cost at base-date price
$\boldsymbol{SCnum}$: Number of available solar thermal modules
$\boldsymbol{SCtyp}$: Solar thermal module type
$\mathbf{SF_{Lower}}$: User-defined sizing factor to determine undersizing limit
$\mathbf{SF_{Upper}}$: User-defined sizing factor to determine oversizing limit
$\mathbf{SI}$ **:** Sensitivity index
$\mathbf{SPB_{target}}$: Target simple payback index set by designer
$\mathbf{SPB_{calculated}}$: Calculated simple payback index for actual building
$\mathbf{t}$: Future cash occurs at the end of year t (service life)
$\mathbf{TC_{actual}}$: Calculated thermal comfort metric for actual building
$\mathbf{TC_{target}}$: Target thermal comfort metric set by designer
$\boldsymbol{\mu_{ec}}$: Equipment capacity penalty parameter
$\boldsymbol{\mu_{em}}$: CO2 emission penalty parameter
$\boldsymbol{\mu_{cf}}$: Occupants thermal comfort penalty parameter
$\boldsymbol{\mu_{k}}$: Penalty parameter
$\boldsymbol{\mu_{pb}}$: Payback period penalty parameter
$\boldsymbol{\mu_{maxcap}}$: User-assigned maximum equipment capacity penalty parameter
$\boldsymbol{\mu_{mincap}}$: User-assigned minimum equipment capacity penalty parameter
$\mathbf{V_i^k}$: Velocity of particle i at iteration k
$\mathbf{x_i^k}$: Position of particle i at iteration k
$\mathbf{W_0}$: Annually recurring water cost at base-date price
$\boldsymbol{WTW}$: Window-to-wall ratio
$\boldsymbol{\omega}$: Inertia weight factor
$\boldsymbol{\chi}$: Constriction coefficient
$\boldsymbol{\varphi}$: Sum of acceleration coefficients

LIST OF TABLES

Page

LIST OF FIGURES

Page

A METHODOLOGY FOR ENERGY OPTIMIZATION OF BUILDINGS CONSIDERING SIMULTANEOUSLY BUILDING ENVELOPE HVAC AND RENEWABLE SYSTEM PARAMETERS

SUMMARY

Energy is the vital source of life and it plays a key role in development of human society. Any living creature relies on a source of energy to exist. Similarly, machines require power to operate. Starting with Industrial Revolution, the modern life clearly depends on energy. We need energy for almost everything we do in our daily life, including transportation, agriculture, telecommunication, powering industry, heating, cooling and lighting our buildings, powering electric equipment etc. Global energy requirement is set to increase due to many factors such as rapid industrialization, urbanization, population growth, and growing demand for higher living standards. There is a variety of energy resources available on our planet and non-renewable fossil fuels have been the main source of energy ever since the Industrial Revolution.

Unfortunately, unsustainable consumption of energy resources and reliance on fossil fuels has led to severe problems such as energy resource scarcity, global climate change and environmental pollution. The building sector compromising homes, public buildings and businesses represent a major share of global energy and resource consumption. Therefore, while buildings provide numerous benefits to society, they also have major environmental impacts. To build and operate buildings, we consume about 40 % of global energy, 25 % of global water, and 40 % of other global resources. Moreover, buildings are involved in producing approximately one third of greenhouse gas emissions. Today, the stress put on the environment by building sector has reached dangerous levels therefore urgent measures are required to approach buildings and to minimize their negative impacts.

We can design energy-efficient buildings only when we know where and why energy is needed and how it is used. Most of the energy consumed in buildings is used for heating, cooling, ventilating and lighting the indoor spaces, for sanitary water heating purposes and powering plug-in appliances required for daily life activities. Moreover, on-site renewable energy generation supports building energy efficiency by providing sustainable energy sources for the building energy needs. The production and consumption of energy carriers in buildings occur through the network of interconnected building sub-systems. A change in one energy process affects other energy processes. Thus, the overall building energy efficiency depends on the combined impact of the building with its systems interacting dynamically all among themselves, with building occupants and with outdoor conditions. Therefore, designing buildings for energy efficiency requires paying attention to complex interactions between the exterior environment and the internal conditions separated by building envelope complemented by building systems.

In addition to building energy and CO_2 emission performance, there are also other criteria for designers to consider for a comprehensive building design. For instance,

building energy cost is one of the major cost types during building life span. Therefore, improving building efficiency not only addresses the challenges of global climate change but also high operational costs and consequent economic resource dependency. However, investments in energy efficiency measures can be costly, too. As a result, the economic viability of design options should be analysed carefully during decision-making process and cost-effective design choices needs to be identified. Furthermore, while applying measures to improve building performance, comfort conditions of occupants should not be neglected, as well.

Advances in science and technologies introduced many approaches and technological products that can be benefitted in building design. However, it could be rather difficult to select what design strategies to follow and which technologies to implement among many for cost-effective energy efficiency while satisfying equally valued and beneficial objectives including comfort and environmental issues. Even using the state-of-the-art energy technologies can only have limited impact on the overall building performance if the building and system integration is not well explored. Conventional design methods, which are linear and sequential, are inadequate to address the inter-depended nature of buildings. There is a strong need today for new methods that can evaluate the overall building performance from different aspects while treating the building, its systems and surrounding as a whole and provide quantitative insight information for the designers. Therefore, in the current study, we purpose a simulation-based optimization methodology where improving building performance is taken integrally as one-problem and the interactions between building structure, HVAC equipment and building-integrated renewable energy production are simultaneously and dynamically solved through mathematical optimization techniques while looking for a balanced combination of several design options and design objectives for real-life design challenges.

The objective of the methodology is to explore cost-effective energy saving options among a considered list of energy efficiency measures, which can provide comfort while limiting harmful environmental impacts in the long term therefore financial, environmental and comfort benefits are considered and assessed together. During the optimization-based search, building architectural features, building envelope features, size and type of HVAC equipment that belong to a pre-designed HVAC system and size and type of considered renewable system alternatives are explored simultaneously together for an optimal combination under given constraints.

The developed optimization framework consists of three main modules: the optimizer, the simulator, and a user-created energy efficiency measures database. The responsibility of the optimizer is to control the entire process by implementing the optimization algorithm, to trigger simulation for performance calculation, to assign new values to variables, to calculate objective function, to impose constraints, and to check stopping criteria. The optimizer module is based on GenOpt optimization environment. However, a sub-module was designed, developed and added to optimization structure to enable Genopt to communicate with the user-created database module. Therefore, every time the value of a variable is updated, the technical and financial information of a matching product or system equipment is read from the database, written into simulation model, and fed to the objective formula. The simulator evaluates energy-related performance metrics and functional constraints through dynamic simulation techniques provided by EnergyPlus simulation tool. The database defines and organizes design variables and stores user-collected cost related, technical and non-technical data about the building energy

efficiency measures to be tested during the optimization. An updated version of Particle Swarm Optimization with constriction coefficient is used as the optimization algorithm.

The study covers multi-dimensional building design aims through a single-objective optimization approach where multi objectives are represented in a ε-Constraint penalty approach. The primary objective is taken as minimization of building global costs due to changes in design variables therefore it includes minimization of costs occur due to operational energy and water consumption together with ownership costs of building materials and building systems. Moreover, a set of penalty functions including equipment capacity, user comfort, CO_2 emissions and renewable system payback period are added to the main objective function in the form of constraints to restrict the solution region to user-set design target. Consequently, multi-objective design aims are translated into a single-objective where the penalty functions acts as secondary objectives.

The performance of the proposed optimization methodology was evaluated through a case study implementation where different design scenarios were created, optimized and analysed. A hypothetical base-case office building was defined. Three cities located in Turkey namely Istanbul, Ankara and Antalya were selected as building locations. Therefore, the performance of the methodology in different climatic conditions was investigated. An equipment database consists of actual building materials and system equipment commonly used in Turkish construction sector was prepared. In addition, technical and financial data necessary for objective function calculation were collected from the market. The results of the case studies showed that application of the proposed methodology achieved giving climate-appropriate design recommendations, which resulted in major cost reductions and energy savings.

One of the most important contributing factors of this thesis is introducing an integrative method where building architectural elements, HVAC system equipment and renewable systems are simultaneously investigated and optimized while interactions between building and systems are being dynamically captured. Moreover, this research is distinctive from previous studies because it makes possible investigating actual market products as energy efficiency design options through its proposed database application and a sub-program that connect optimization engine with the data library. Therefore, application of the methodology can provide support on real-world building design projects and can prevent a mismatch between the optimization recommendations and the available market solutions.

Furthermore, another contributing merit of this research is that it achieves formulating competing building design aims in a single objective function, which can still capture multi-dimensions of building design challenge. Global costs are minimized while energy savings are achieved, CO_2-equivalent emission is reduced, right-sized equipment are selected, thermal comfort is provided to users and target payback periods of investments are assured.

To conclude, the proposed methodology links building energy performance requirements to financial and environmental targets and it provides a promising structure for addressing real life building design challenges through fast and efficient optimization techniques.

BİNALARDA YAPI KABUĞU, MEKANİK SİSTEMLER VE YENİLENEBİLİR ENERJİ SİSTEMLERİ PARAMETRELERİNİN EŞ ZAMANLI ENERJİ OPTİMİZASYONU İÇİN BİR YÖNTEM

ÖZET

Temel yaşam kaynağımız olan enerji insanlığın gelişiminde can alıcı bir rol oynamaktadır. Ekosistemi oluşturan tüm canlılar varlıklarını sürdürebilmek için enerjiye ihtiyaç duyarlar. Benzer şekilde makinelerin işleyebilmesi için de dış bir enerji kaynağına ihtiyaçları vardır. Sanayi devrimi ile birlikte modern hayatta enerjiye olan bağımlılığımız her geçen gün artmaktadır. Günlük hayatta ulaşım, iletişim, tarım, sanayi faaliyetleri, binalarımızı ısıtmak, soğutmak ve havalandırmak, cihazlarımızı çalıştırmak gibi neredeyse tüm temel işlemleri yerine getirebilmek için enerjiye gereksinim duymaktayız.

Günümüzde, küresel enerji ihtiyacı sanayileşme, kentleşme, nüfus artışı ve bireylerin daha iyi yaşam kalitesi beklentisi gibi çeşitli sebeplerden ötürü hızlı bir artış göstermektedir. Uluslararası Enerji Ajansı'nın verilerine göre enerji ihtiyacı önümüzdeki yıllarda daha da ivmelenerek artacaktır.

Dünyamızda çok çeşitli enerji kaynakları mevcuttur fakat konvansiyonel fosil yakıtlar artan talebi karşılamada birinci sırada yer almaktadırlar. Günümüzde, enerji kaynaklarının bilinçsiz tüketimi ve enerji ihtiyacının fosil yakıtlara dayalı olarak karşılanıyor olması, küresel iklim değişikliği, fosil yakıtların tükenmesi ihtimali ve çevresel tahribat gibi tüm insanlığı tehdit eden ciddi sorunlara yol açmaktadır. Enerji bilinci ile geliştirilen yeni politikalar, enerjinin verimli kullanılmasına dair yürütülen kampanyalar, ulusal ve uluslararası boyutta çıkarılan bağlayıcı direktifler ile standartlar, temiz enerji teknolojilerine yapılan yatırımlar gibi pek çok önlem ise küresel sorunlarla başa çıkabilmede önemli potansiyele sahiptir. Ancak, sorunlarla mücadele için geliştirilecek stratejilerin tanımı ve içeriği uygulanacağı alana göre değişiklik göstermektedir. Uluslararası Enerji Ajansı'nın çalışmaları konutlar, iş yerleri ve kamu binalarını kapsayan yapı sektörünün küresel enerji ve kaynak tüketiminde oldukça önemli bir paya sahip olduğunu göstermektedir. Binaların toplumsal ihtiyaçları karşılamada önemli bir işlevleri olmasına karşılık çevresel olarak yol açtığı sorunlar artık göz ardı edilemez. Binaların yapım ve işletme dönemlerinde küresel enerjinin % 40'ı, küresel su tüketiminin % 25'i ve diğerküresel kaynakların % 40'ı tüketilmektedir. Dahası küresel CO_2 emisyonlarının üçte biri binalardan kaynaklanmaktadır. Dolayısıyla bu günlerde yapı sektörünün tabiat üzerinde oluşturduğu baskı tehlikeli seviyelere ulaşmıştır ve binaların neden olduğu olumsuz etkilerin azaltılmasını sağlayacak önlemler acilen alınmalıdır.

Binalarda tüketilen enerjinin büyük bölümü bina kullanıcılarına gerekli ısıl ve görsel konfor şartlarını sağlayabilmek niyetiyle iç mekanları ısıtmak, soğutmak, havalandırmak ve aydınlatmak için kullanılmaktadır. Ayrıca kullanıcılar için sıcak su hazırlamak ve ev veya ofislerimizdeki elektrikli cihazları çalıştırmak için de önemli miktarlarda enerji tüketilmektedir. Enerji ihtiyacı düşük ve enerjiyi verimli kullanan

binaların tasarlanması binanın enerjiye nerede, ne zaman ve ne için ihtiyaç duyacağının önceden belirlenmesi ve enerjinin nasıl kullanılacağının öngörülmesi ile mümkün olabilir. Enerji kullanımına ek olarak yenilenebilir sistemler ile yerinde enerji üretimi bina enerji ihtiyacının karşılanmasında sürdürülebilir çözümler sunar ve binanın toplam enerji verimliliği üzerinde önemli bir etkisi vardır. Dolayısıyla, binalarda enerjinin üretim ve tüketimi, birbiriyle ve binayla bağlantılı alt sistemlerden oluşan bir ağ üzerinde gerçekleşir. Bir enerji sürecinde oluşan bir değişim diğer tüm süreçleri etkiler. Bu nedenle, binanın toplam verimi, binanın kendisinin, alt sistemler, bina kullanıcıları ve dış ortam koşulları ile olan bütünsel ve dinamik etkileşimine bağlıdır ve enerji etkin bina tasarımı çevresel etmenlerin, iç koşulların, iç ve dış ortamı birbirinden ayıran yapı kabuğunun ve tamamlayıcı bina sistemlerinin bütünleşik olarak ele alındığı bir tasarım sürecini gerektirir.

Yüksek performanslı bina tasarlarken binanın enerji ve CO_2 emisyonu kriterleri açısından gösterdiği performansa ek olarak, başka göz önünde bulundurulması gereken kriterler de mevcuttur. Örneğin, binaların enerji maliyeti binanın işletme dönemindeki en büyük maliyet giderlerinden birini oluşturur. Bu nedenle enerji verimliliğini artırmak yalnızca iklim değişikliği ile mücadele etmeye destek olmakla kalmaz aynı zamanda enerji maliyetlerinin düşürülmesi, enerjide dışa bağımlılığın azaltılması ve dolayısıyla ekonomik olarak da güçlenmeyi beraberinde getirir. Ne var ki, enerji verimliliği alanında yapılan yatırımların da maddi olarak bir bedeli vardır. Bu nedenle bina tasarımı sürecinde binanın enerji performansına etki eden tasarım kararlarının ve seçilen sistemlerin ekonomik anlamda elverişliliğinin de incelenmesi ve maliyet-etkin enerji çözümlerinin belirlenmesi önemlidir.

Maliyetlere ilaveten enerji verimliliğini artırıcı önlemler planlanırken binanın kullanıcılarına sağlayacağı konfor düzeyinin de göz önüne alınması gereklidir. Konfor koşulları kullanıcı sağlığı ve esenliği ile doğrudan ilişkilidir. Ayrıca, örneğin ofis binaları gibi kullanıcıların maaş giderlerinin diğer kalamlere göre yüksek olduğu bina tiplerinde konfor koşullarının kurumsal maliyetlere de ciddi anlamda etkisi olacaktır.

Günümüzde bilim ve teknoloji alanındaki ilerlemeler enerji etkin bina tasarımında faydalanılabilecek yeni yaklaşımlar ve ürünleri ortaya çıkardı. Fakat ele alınan bir bina için çok çeşitli seçeneklerin arasından hangi tasarım stratejilerinin izlenmesi gerektiği ve hangi teknolojik ürünlerin kullanılmasının maliyet-etkin enerji verimliliğini sağlarken, binanın CO_2 emisyonlarını azaltacağı ve aynı zamanda da bina kullanıcılarına gerekli konforu sağlayacağını saptamak oldukça güç olabilir. Eğer bina ve sistem entegrasyonu erken tasarım aşamasında araştırılarak planlanmamışsa, sadece son teknoloji ürünlerin kullanılması istenilen performansta binaların yapılması için yeterli olmayacaktır.

Genel manasıyla karar verme, çeşitli seçenekler arasından birbiriyle çatışan hedefleri ve kısıtları en uygun şekilde sağlayan seçeneği bulmayı gerektirir. Bina tasarım sürecinde ise binanın enerji davranışının kompleks olması, bina performansına etki eden çok sayıda parametrenin bulunması ve enerji, maliyet, çevresel performans, kullanıcı konforu gibi tasarım hedeflerinin birbirleriyle çelişiyor olması gibi nedenlerden dolayı tüm beklentileri karşılayan tasarım seçeneğini bulmak tasarımcı açısından oldukça zorlu bir karar verme sürecidir. Mimarlar, makine mühendisleri, aydınlatma tasarımcıları ve yenilenebilir enerji mühendisleri gibi tasarım sürecinde görev alan çeşitli uzmanların sırasıya kendi uzmanlıkları açısından katkılarını ortaya koydukları doğrusal ve ardışık olan mevcut tasarım yaklaşımları zaten kompleks bir

doğaya sahip binalarda enerji verimliliğini sağlamada yetersiz kalmaktadırlar. Günümüzde, bina ve sistem tasarımını bütüncül olarak ele alırken bina performansını farklı açılardan değerlendirebilecek ve nicel verilerle tasarımı destekleyecek yenilikçi yöntemlere ihtiyaç vardır. Bu nedenle mevcut çalışmada, binanın kendisi, bina mekanik sistemleri ve binaya entegre yenilenebilir enerji sistemleri arasındaki bağlantıyı bütüncül bir bakış açısıyla ele alabilen, enerji verimliliğini birbirleriyle çelişen farklı tasarım hedeflerini dengeleyerek sağlayabilen ve en ideal tasarım seçenekleri birleşimini matematiksel arama teknikleri ile simultane ve dinamik olarak hesaplayabilen bir simülasyona dayalı optimizasyon yöntemi önerilmektedir.

Geliştirilen yöntemin temel amacı, binanın enerji performansına etki eden binaya ve bina sistemlerine dair farklı alanlardan çeşitli tasarım seçeneklerini içeren bir listeden binanın işletme döneminde enerji verimliliğini maliyet-etkin, konforlu ve çevreye etkisi azaltılmış şekilde sağlacak en ideal kombinasyonu matematiksel optimizasyon teknikleri ile belirlemektir. Yöntemin optimizasyon temelli arama sürecinde, binaya dair en uygun mimari etmenler, yapı kabuğu seçenekleri, ön seçimi yapılmış önerilen bir mekanik sistemin cihazlarının tipi ve cihaz kapasiteleri ve binaya entegre edilecek yenilenebilir enerji sistemlerine ait cihazların tipi ve kurulu güçleri verilen sınır koşullar altında eş zamanlı olarak araştırılır.

Ayrıca, maliyet-etkin enerji verimliliğine ek olarak binadaki mekanik sistemlerin su tüketme performansının iyileştirilmesi de bir tasarım amacı olarak göz önüne alınır ve binanın su tüketimi alanındaki verimliliğine de katkı sağlanır.

Geliştirilen optimizasyon yöntemi optimizör, simulatör ve kullanıcı tarafından hazırlanan ve enerji verimliliği önlemlerine dair seçenekler içeren veritabanı uygulaması olmak üzere üç ana modülden oluşmaktadır.

Optimizör modülü tüm süreci yönetir, optimizasyon algoritmasını çalıştırır, performans hesabı için simulasyon uygulamasını başlatır, karar değişkenlerine yeni değerler atar, amaç fonksiyonunu hesaplar, sistem kısıtlarını uygular ve durdurma kriterinin sağlanıp sağlanmadığını denetler. Optimizör, GenOpt yazılımı temel alınarak geliştirilen bir optimizasyon altyapısına sahiptir. GenOpt'un mevcut yapısına yazar tarafından geliştirilen bir alt modül eklenerek optimizasyon algoritmasının tasarlanan veritabanı modülü ile dinamik etkileşimde olması sağlanmıştır. Böylelikle optimizasyon esnasında karar değişkenine yeni bir değer atandığında, bu değerin temsil ettiği bir enerji verimliliği çözümü ve çözüme dair teknik ve ekonomik veriler veritabanından okunarak simülasyon modeline aktarılır ve amaç fonksiyonuna iletilir.

Simulatör modülü, bina performansına dair ölçütleri ve fonksiyonel kısıtları EnergyPlus enerji modelleme motorunu kullanarak dinamik olarak hesaplar.

Veritabanı modülü ise optimizasyon esnasında test edilecek karar değişkenlerine yani dolayısıyla enerji verimliliği çözümlerine dair mali, teknik ve teknik olmayan verileri tanımlar, düzenler ve saklar.

Optimizasyon süreci, tasarımcı tarafından tanımlanan ve başlangıç koşullarını temsil eden referans bir binaya performans iyileştirici önlemlerin geliştirilmesi motivasyonu ile başlar. Optimizör modülü tanımlanan optimizasyon yapısının arama prensiplerine göre karar değişkenlerine yeni değerler atayarak enerji verimliliği çözümleri kombinasyonları yaratır ve alternatif tasarım senaryoları üretir. Her optimizasyon iterasyonunda, binaya dair mimari etmenler, kabuk seçenekleri ve mekanik sistem cihazlarına (birincil enerji dönüşümü yapan cihazlar örn. kazan, soğutma grubu) ait

seçenekler arasından arama prensipleri uyarınca yeni bir kombinasyon oluşturulur. Oluşturulan kombinasyon için öncelikle yaz ve kış tasarım günleri için bina ısıl yükleri ve gerekli cihaz kapasitesitelerini tahmin etmek üzere boyutlandırma hesabı koşturulur. Yük ve kapasite belirlendikten sonra binaya önerilmiş olan cihazlar ile binanın ihtiyacının uyumlu olup olmadığı tesbit edilir. Düşük veya yüksek kapasiteli cihaz önerileri kısıt fonksiyonları kullanılarak çözüm uzayından elenir. Elenmeyen kombinasyonlar için pik yükün karşılanabilir olmasının yanında, yıl boyunca tam ve kısmi yükte de en ideal dinamik performansı gösteren cihazın seçilmesi hedeflenir. Ayrıca, birincil enerji dönüşümü yapan cihazların yanında, soğutma kulesi, fan coil üniteleri gibi sistemi tamamlayıcı bağımlı cihazların da boyutlandırma hesabı yapılır. Bina mekanik sistemine ek olarak, aynı adımda binaya entegre edilmesi hedeflenen yenilenebilir enerji sistemi alternatifleri için de kurulu güç/ boyut hesabı yapılır ve sistemlerin temel bileşenleri olan panel/modül gibi elementler yine veritabanındaki cihaz kütüphanesinden tüm yıllık performansı göz önüne alınarak seçilir. Optimizasyon önceden tanımlanmış durdurma kriterine ulaşana kadar iterasyona devam eder.

Bu çalışmada, çok yönlü olan bina tasarım hedefleri, seçilen ana amaç dışında kalan hedeflerin, ε-Kısıtı yaklaşımıyla ceza fonskiyonları olarak tanımlandığı tek amaçlı optimizasyon problemi olarak formülize edildi. Önerilen yöntemin ana amaç fonksiyonu binanın işletme döneminde enerji tüketimi maliyeti, su tüketimi maliyeti ve binada enerji verimliliği önerileri kapsamında kullanılan yapı kabuğu malzemeleri ve binayı ısıtma soğutma amaçlı kullanılan mekanik sisteme ait cihazların toplam sahip olma maliyetlerini içerir. Optimizasyonun hedefi ise toplam maliyetin minimize edilmesidir. Bunun dışında, mekanik sistem cihazlarının sağlaması gereken kapasite aralığı, binanın kullanıcıya sağladığı ısıl konfor düzeyi, binanın enerji tüketimi sebebiyle yaydığı CO_2 emisyonu miktarı ve binaya entegre edilen yenilenebilir enerji sistemi alternatifinin geri ödeme süresi ceza fonksiyonları biçiminde ikincil amaçlar olarak ana amaç fonksiyonuna eklenir ve çözüm uzayını kullanıcı tarafından belirlenen mümkün bölgeye doğru taşır. Çalışma, maliyeti yüksek fakat verimliliği artırıcı yapı kabuğu ürünleri, mekanik sistem cihazları gibi önerilere hangi dereceye kadar yatırım yapmanın akıllıca olacağı, binanın mimari özellikleri ile mekanik sistem çözümlerinin nasıl entegre edilmesi gerektiği, enerji üreten yenilenebilir enerji sistemi uygulamaları ile enerji tüketen bina sistemlerinin ideal bileşiminin nasıl olması gerektiği gibi sorulara erken tasarım sürecinde cevap vermeyi hedeflemektedir.

Önerilen yöntem arama tekniği olarak kısıtlama katsayıları kullanan Parçacık Sürü Optimizasyonu algoritmasını kullanmaktadır.

Tez çalışması kapsamında, geliştirilen yöntemin başarısı ve uygulanabilirliği farklı tasarım seçeneklerinin optimize edildiği örnek vaka çalışmaları üzerinden değerlendirildi. Öncelikle enerji verimliliği kritlerleri göz önüne alınmadan tasarlanmış varsayılan bir ofis binası tanımlandı. İstanbul, Ankara ve Antalya şehirleri binanın alternatif konumları olarak seçildi böylelikle yöntemin performansı farklı iklim koşullarında değerlendirildi. Türkiye yapı sektöründe bina ve sistem tasarımında sıklıkla kullanılan yapı malzemeleri, mekanik sistem ve yenilenebilir sistem cihazlarının mali ve teknik bilgilerini içeren detaylı bir veri tabanı hazırlandı. Ek olarak, amaç fonksiyonu hesabında gerekli olan piyasalara ait ekonomik veriler ve enerji ve su kullanımına dair tarife bilgileri de edinildi.

Vaka çalışması kapsamında yapılan hesaplama sonuçları, geliştirilen yöntemin enerji ve toplam maliyetleri önemli ölçüde düşüren ve aynı zamanda iklim koşullarına uygun çözüm önerileri üretebildiğini gösterdi. Dahası önerilen tasarım seçenekleri aynı zamanda CO_2 emisyon oranlarını da düşürerek hedeflenenden daha iyi CO_2 performansı elde edildi. Benzeri şekilde yeni öneriler kullanıcı ısıl konfor koşullarını iyileştirerek optimize edilmiş binada hedeflenen konfor aralığını yakalayabildi.

Bu tez çalışmasının en önemli katkılarından birisi bina yapı kabuğu, mekanik sistemleri ve binaya entegre yenilenebilir enerji sistemleri cihazlarının bütünleşik ve eş zamanlı ele alınarak değerlendirilmesi ve birbirine bağlı bu elementler arası ilişkinin dinamik olarak gözlenerek optimizasyonun yürütülmesidir.

Ayrıca, bu araştırmayı diğer araştırmalardan ayıran taraf veritabanı modülü ve de veri tabanını optimizasyon ortamı ile ilişkilendiren alt modülü sayesinde, piyasada mevcut gerçek malzeme ve cihazlara ait verileri kullanarak hesaplama yapabilmesi böylelikle gerçek hayatta karşılaşılan enerji verimliliğini artırıcı önlemler arasından söz konusu bir bina için en uygun seçeneği ve kombinasyonları bulmaya olanak tanımasıdır. Böylelikle optimizasyon sonucu geliştirilen öneriler ile gerçek hayatta mevcut seçenekler arasında eşleştirme yapılır ve farklar oluşmaz. Fakat, malzeme ve cihazlara dair veriler edinilirken doğru ve tutarlı verilerin toplanmasına özen gösterilmelidir.

Buna ilaveten, bu çalışmanın bir diğer katkısı ise birbiriyle çelişen ve yarışan çok boyutlu bina tasarımı hedeflerini tek amaçlı fonksiyon olarak formüle edebilmesidir. Toplam global maliyetler en aza indirgenirken enerji verimi artırılır, eşdeğer CO_2 hedeflenen değerin altına düşürülür ve kullanıcı ısıl konforu istenen aralığa çekilir, doğru boyutlandırılmış cihazlar seçilir ve yenilenebilir enerji sistemi yatırımlarından hedeflenen geri ödeme süresini yakalayabilen seçenekler belirlenir.

Çoklu tasarım hedeflerini kapsamanın yanında, esneklik sağlayan veri tabanı yapısı sayesinde çok sayıda karar değişkeni aynı anda hesaba katılabilir.

Bu çalışma Parçacık Sürü Optimizasyonu yöntemine dayalı olduğu için geniş bir çözüm uzayını otomatik olarak çok daha az sayıda arama teşebbüsü ile zamandan tasarruf ederek araştırabilir.

Yöntemin uygulanması, binanın mimari öğeleri ile mühendislik sistemlerinin bir arada verimli bir şekilde çalışmasını sağlar. Yöntem her ikisi de oldukça güç karar verme süreçlerini içeren fakat enerji verimliliği için de önemli potansiyellere sahip yeni binaların tasarımı veya mevcut binaların yenileme çalışmaları kapsamında kullanılabilir.

Sonuç olarak, geliştirilen yöntem bina enerji performansı ihtiyaçlarını mali ve çevresel hedefler ile ilişkilendirerek gerçek hayatta karşılaşılan tasarım güçlüklerini çözebilecek hızlı ve etkin bir optimizasyon yöntemi ortaya koyar.

1. INTRODUCTION

1.1 Background

Energy is the vital source of life and it plays a key role in development of human society. Any living creature relies on a source of energy to exist. Similarly, machines require power to operate. Starting with Industrial Revolution, the modern life clearly depends on energy. We need energy for almost everything we do in our daily life, including transportation, agriculture, telecommunication, powering industry, heating, cooling and lighting our buildings, powering electric equipment etc.

Global energy requirement is set to increase due to many factors such as rapid industrialization, urbanization, population growth, and growing demand for higher living standards. The data given in Figure 1.1, taken from BP Statistical Review of World Energy June 2012, displays an ever-increasing trend for global primary energy consumption from 1965 until 2011 (BP, 2012, p. 42).

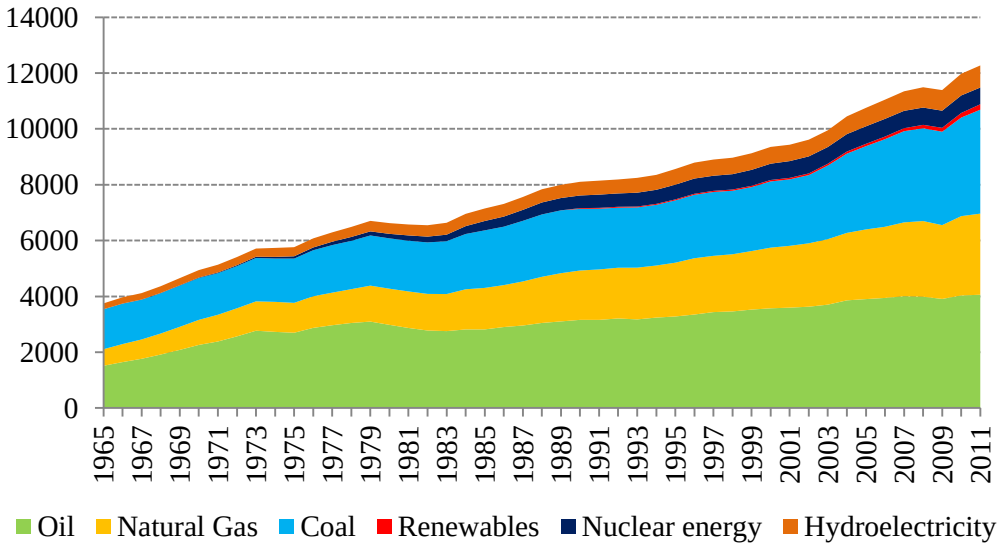

Figure 1.1 : World total primary energy consumption from 1965 to 2011 (Mtoe).

Similarly, global energy use is expected to increase 53 % by 2035 according to the projections in the International Energy Agency's (IEA) 2011 International Energy Outlook (IEA, 2011a).

There is a variety of energy resources available on our planet and non-renewable fossil fuels have been the main source of energy ever since the Industrial Revolution. Global fuel shares given in 2011 Key World Energy Statistics book by International Energy Agency shows that in 2009 more than 80 percentage of the total primary energy supply share belonged to conventional fossil fuels (oil: 32.8 %, coal: 27.2 % , natural gas: 20.9 %, biofuels and waste: 10.2 %, nuclear: 5.8 %, other (includes geothermal, solar, wind, heat, etc.): 0.8 % (IEA, 2011b)). Moreover, many projections show that fossil fuels will most likely continue to dominate the global energy mix in the near future.

Unfortunately, unsustainable consumption of energy resources and reliance on fossil fuels in the last century has led to severe problems such as energy resource scarcity, global climate change and environmental pollution.

Fossil fuels are available on earth in limited quantity and excessive use of fossil fuels has introduced the risk of conventional resource depletion. Moreover, fossil fuels must be burnt to release their stored energy and the burning process leads to many environmental impacts and consequently health impacts from smog, acid rain, and toxic air pollution. Scientists believe that key factor in global climate change is increasing greenhouse gas (GHG) levels in the atmosphere due to fuel burning (IPCC, 2007a). The concentration of carbon dioxide (CO_2) in the atmosphere is increasing at an accelerating rate from decade to decade. The average atmospheric CO_2 level was at 315.97 parts per million (ppm) in 1959 and has risen to 395.93 ppm in October 2014 according to measurements of Mauna Loa Observatory (CO2Now, 2014).

Dealing with global climate change and energy resource scarcity is not an easy task. Fortunately, governments, corporations and individuals globally acknowledge that pressure on the environment caused by human activities requires urgent action. For instance, in 2007, European Union (EU) leaders agreed on an integrated approach to climate and energy policy and they committed to transforming Europe into a highly energy-efficient, low carbon economy. A unilateral commitment was made to cut Europe’s emissions by at least 20% of 1990 levels, increasing the share of renewables in the EU's energy mix to 20%, and achieving the 20% energy efficiency target by 2020 (EU, 2012). Since EU is on track to meet its 2020 target, even new goals are set such as 40% cut in greenhouse gas emissions compared with 1990 level

by 2030 and 80-95% cut by 2050 as announced in the "Roadmap for Moving to a Competitive Low Carbon Economy in 2050" guide (EU, 2011).

Similarly, Turkey's National Action Plan for Climate Change defines several goals that should be targeted for adapting to the effects of the climate change (IDEP, 2012).

A sustainable way of living supported by energy efficiency policies, binding standards, carbon quotas, information campaigns, investments on clean energy technologies, etc. offers a great potential to face global challenges. However, definition and the content of the strategies vary by sector they are applied to. Therefore, it is critical to understand where and how energy and other resources are consumed. According to numbers published by IEA, residential, commercial and public services together with agriculture represented 37% of the total global final energy consumption in 2009 followed by industry (27%), transport (27%) and non-energy use (9%) (IEA, 2011b).

The building sector compromising homes, public buildings and businesses represent a major share of global energy and resource consumption. The findings of the 4th Assessment Report of the Intergovernmental Panel on Climate Change (IPCC) shows that at present, buildings contribute as much as one third of total global greenhouse gas emissions. Therefore, the efficiency in the building sector has become a priority for countries across the globe (IPCC, 2007a).

Unfortunately, building related GHG emissions are projected to grow if new strategies are not urgently adopted (IPCC, 2007a). However, energy efficiency in the buildings sector also offers a significant potential for reductions for greenhouse gas emission as well. IPCC estimated that there is global potential to avoid about 30 per cent of the projected GHG emissions in the building sector by 2020 if various technological options were introduced. They emphasize that since buildings consume great amounts of energy, even small improvements can make significant impacts (IPCC, 2007a).

There is a growing interest in high energy performance building design, as it is now accepted as an encouraging solution to deal with the increasing pressure placed on environment by building sector. The recast of European Energy Performance of Buildings Directive (EPBD) in 2010 targets for all new buildings in the EU to be

‘Nearly Zero-Energy Buildings’ from 2020 and for new buildings occupied and owned by public authorities by 2018 (EPBD, 2010).

In addition to building energy performance and CO_2 emission targets, there are also other criteria to consider when approaching buildings. For instance, building energy cost is one of the major cost types during building life span. Therefore, improving building efficiency not only addresses the challenges of global climate change but also high operational costs and consequent economic resource dependency. However, investments in energy efficiency measures can be costly, too. As a result, the economic viability of a design decisions should be analysed carefully during decision-making process. The recast of EPBD now obliges Member States to assure that minimum energy performance requirements for buildings or building units are set with a view to achieving cost-optimal level that is the energy performance level, which leads to the lowest cost during the estimated economic lifecycle (EPBD, 2010).

Furthermore, while applying measures to improve building performance, comfort conditions of occupants should not be neglected, as well. Comfort is linked with occupants’ health, well-being and productivity. Especially in commercial buildings, employee comfort reduce absenteeism and health-care costs, therefore it has an influence on operational business costs. However, providing comfort is also linked with energy consumption levels (Wyon, 1996).

Advances in science and technology introduced many approaches and technological products that can be benefitted in building design. However, it could be rather difficult to select what design strategies to follow and which technologies to implement among many for cost-effective energy efficiency while satisfying equally valued and beneficial design objectives. Even using the state-of-the-art energy technologies can only have limited impact on the overall building performance if the building and system integration is not well explored.

Whole Building Design concept, which refers to a design and construction technique that incorporates an integrated design approach and an integrated team process, is introduced in the last decade to support creation of high energy performance buildings (WBDG, 2014). Whole Building Design views the building as a system, rather than a collection of components and it requires a multi-disciplinary strategy

that effectively integrates all aspects of site development, building design, construction, and operations and maintenance.

Creating a high energy efficiency building requires an in-depth understanding of the interrelationships between various building elements and the benefits or drawbacks of each design decision is required to be quantified in the context of the whole building design concept. Therefore, there is a strong need today for new methods that can evaluate the overall building performance from different aspects while treating the building, its systems and surrounding as a whole and provide quantitative insight information for the decision-making process.

1.2 Research Objective

We can design energy-efficient, comfortable, healthy and economic high performance buildings only when we know where and why energy is needed and how it is used. Buildings are very complex dynamic energy systems that energy is converted, transferred, used or even sometimes produced in a dynamic manner. Most of the energy consumed in buildings is used for heating, cooling, ventilating and lighting the indoor spaces to create a thermally and visually comfortable built-environment for its occupants. Energy is also needed for sanitary water heating purposes and powering plug-in appliances required for daily life activities. Moreover, on-site energy generation supports building energy efficiency by providing sustainable energy sources for the building energy needs. Therefore, the production and consumption of energy carriers in buildings occur through the network of interconnected building sub-systems. As mentioned by Zięb ik and Hoinka (2013) a change in one energy process affects other energy processes. Thus, the overall building energy efficiency depends on the combined impact of the building with its systems interacting dynamically all among themselves, with the building occupants and with outdoor conditions. Therefore, assessing building energy performance requires paying attention to complex interactions between the exterior environment and the internal conditions separated by building envelope complemented by building systems.

Making a design decision in general involves selection of the best or the most suitable design option among all the feasible alternatives while satisfying multiple conflicting design objectives and constraints. Therefore, in building design problem,

due to the complex nature of building energy behaviour and numerous influential elements and conflicts in design aims such as energy, economy, environmental performance and user comfort, it is a serious challenge to find the best design option and system configuration that satisfies all the expectations. Conventional design methods, which are linear and sequential, are inadequate to address the inter-depended nature of buildings (IPCC, 2007b). Thus, as highlighted by Ziębik and Hoinka (2013) energy carriers and their relations with outdoor and indoor conditions should be investigated as a whole and the building and system integration should be investigated starting from early stages of the design process.

The physical phenomena of energy and mass flow occurring within a building can be described in detail through mathematical equations. The building energy model is then used to predict the behaviour of actual building under different boundary conditions. Building performance simulation is a computer-based solution of building energy model and it is becoming now an integral part of the design process to predict quantitative information about building performance (Crawley et al, 2005).

When building performance is expressed as a function of input parameters, many design alternatives can be investigated for building lifetime from energy, economy and environment perspectives. However, designers still need to carry out hundreds of calculations to explore a very large design space and handle huge amount of data while looking for the optimal combination of several energy efficiency measures. This time-consuming and labour intensive trial-and-error process can lead to improved results but in many cases, it is extremely unlikely to achieve the best solution (Attia et al., 2013).

In order to address the difficulties inherited in decision making via simulation, simulation-based optimization methods, which integrates optimization techniques into simulation analysis has been introduced. Coupling mathematical programming techniques with a simulation engine automate the search for the optimal or near optimal solutions in the design space, speed up the calculations and have a potential to improve iteratively the solutions to multi-objective, multi-criterion design problems in a variety of fields (Fu et al. 2005). Due to its potential to automate the input and output, assess many options, and perform many simulations by mathematical means, optimization techniques also caught the attention of the

building research community as a promising approach to multi-dimensional building design problem.

There is a strong need today for fast and efficient optimization methods to address real-life building design challenges. Therefore, the focus of this research is to offer a simulation-based building design optimization methodology that can take into account the perspective of whole-building design concept and integration issues.

The objective of the methodology is to explore cost-effective energy saving options among a considered list of energy efficiency measures, which can also provide comfort while limiting harmful environmental impacts in the long term therefore financial, environmental and comfort benefits are considered and assessed together. During the optimization-based search, building architectural features, building envelope features, size and type of HVAC equipment that belong to a pre-designed HVAC system and size and type of considered renewable system alternatives are explored simultaneously together for an optimal combination under given constraints.

The study covers multi-dimensional building design aims through a single-objective optimization approach where multi objectives are represented in a ε-Constraint penalty approach. The primary objective is taken as minimization of building global costs due to changes in design variables therefore it includes minimization of costs occur due to operational energy and water consumption together with ownership costs of building materials and building systems. Moreover, a set of penalty functions including equipment capacity, user comfort, CO_2 emissions and renewable payback period are added to the main objective function in the form of constraints to restrict the solution region to user-set design target. Consequently, multi-objective design aims are translated into a single-objective where the penalty functions acted as secondary objectives.

The method is based on a proposed database structure that includes technical and financial product information therefore; it allows for consideration of actual product constraints and can provide decision support in building design projects based on available technology options. Moreover, the methodology is designed to be capable of evaluating large number of parameters fast and effectively in a time-efficient manner.

The methodology aims to answer design questions such as to what extent it is wise to invest in expensive but higher efficiency products for building envelope and HVAC system equipment, how to integrate building architectural features with building systems, what are the optimal combinations of renewable energy options and energy conversion systems, as early as possible in the design process.

The application of the methodology ensures that architectural elements and the engineering systems work efficiently together for true efficiency and it can be used as a decision-support tool for both new building design and renovation projects since both processes provide significant opportunities to improve building performance but also goes through a complicated decision making process.

The developed optimization procedure implements a Particle Swarm Optimization technique and it is based on the combination of EnergyPlus simulation tool and an enhanced GenOpt based environment that is specifically designed to be in simultaneous interaction with a proposed database application that stores information on energy efficiency measures.

Within the scope of the work, the motivation of the work is explained, the background that supports the methodology is introduced, the research gap is discussed, the details of the methodology is presented and the performance of the methodology is assessed through a case study application.

1.3 Thesis Chapter Overview

This thesis is organized as follows.

Chapter 1 provides a background summary and explains the motivation of this thesis work.

Chapter 2 includes a literature review on whole-building design approach. Basics of high performance building design are introduced with a focus on energy efficiency. The chapter also summarizes the most influential factors to consider for a successful building and system design including outdoor conditions, building architectural design characteristics, indoor conditions, building system characteristics and building integrated renewable system characteristics. Moreover, building simulation concept and its importance in energy efficient building design practices are discussed.

Chapter 3 investigates the optimization phenomenon and presents a review of the history of simulation-based building performance optimization and the most commonly used techniques by highlighting their relevant assets and limitations. Moreover, the current research status of simulation-based building performance optimization is introduced. The chapter also identifies the research gaps, and explains where the current research fits within what has already been accomplished.

Chapter 4 includes the description of the proposed building performance optimization methodology and explains the essential steps of the developed structure.

Chapter 5 includes the implementation of the proposed optimization model on a group of case studies. Comprehensive analyses were conducted through a hypothetical office building to quantify the success of the method in terms of thermal comfort, energy consumption, CO_2 emission and economy. A detailed description of the case study building is given, the database that includes technical and financial information about the considered energy efficiency measures is explained and the results are documented.

Chapter 6 summarizes current concept, major accomplishments achieved in this thesis and conclusions drawn from the work. It also discusses the limitations of work and outlines the future directions of research in order to improve the proposed methodology.

2. HIGH ENERGY PERFORMANCE BUILDINGS

2.1 Introduction

Buildings served as a protective shelter to people for many centuries but they also respond to several needs of society nowadays. People of modern life spend most of their time indoors for several activities including living, working, shopping, entertainment etc. and buildings are expected to provide comfortable and healthy indoor conditions to the people who are using it.

While buildings provide numerous benefits to society, they also have major environmental impacts. To build and operate buildings, we consume about 40% of global energy, 25% of global water, and 40% of global resources. Moreover, buildings are involved in producing approximately one third of greenhouse gas emissions (UNEP, 2011). Today, the stress put on the environment by building sector has reached dangerous levels therefore urgent measures are required to approach buildings and to minimize their negative impacts.

Fortunately, there is a growing public awareness of environmental issues and human health concerns due to buildings. The professionals in the building sector are beginning to realize that conventionally designed, constructed and operated buildings are not sufficient to address global environmental challenges. As a result, new design concepts are being developed and high energy performance buildings, which exceed current requirements of basic building standards, are evolving.

In this chapter, main definitions and requirements of building performance will be explained with a special focus on energy-efficiency in the built environment. The main factors that influence building energy performance will be introduced and methods and tools for assessing building performance will be summarized.

2.2 Basics of High Performance Building Design

There is not a single globally acknowledged definition of building performance because it is an ever-evolving process. A report on terms and definitions for high-

performance buildings by Erhorn and Kluttig (2011) shows that there are 23 different terms are used in 14 different European Union Member States for high-performance buildings. The terms relate mostly to one of the three following options: low energy consumption, low emissions and sustainable or green aspects. According to the report, “low energy house”, “passive house” and “energy saving house” are the terms used in the highest number to refer to building energy performance attribute. There are also other popular terms such as “eco-building”, “green building” and “sustainable building” used frequently to underline building ecological performance.

United States Energy Independence and Security Act expands the scope of the high performance attributes and defines a high-performance building as a building that integrates and optimizes on a life-cycle basis all major high-performance attributes, including energy conservation, environment, safety, security, durability, accessibility, cost-benefit, productivity, sustainability, functionality and operational considerations (Public Law 110 – 140, 2007).

Regardless of different terminology used in different countries, the main expectations from high performance buildings are very similar: to use as minimum energy and resources possible, to improve the health, comfort and productivity of their occupants and to limit the harmful environmental effects during building entire lifespan.

Whole Building Design Guide by the United States National Institute of Building Sciences (NIBS) mentions six fundamental principles for sustainable design to achieve high performance buildings: Optimize Site Potential, Optimize Energy Use, Protect and Conserve Water, Optimize Building Space and Material Use, Enhance Indoor Environmental Quality (IEQ), and Optimize Operational and Maintenance Practices (NIBS, 2014).

Land development for construction can contributes to flooding, deforestation, and loss of biodiversity, therefore creating High Performance buildings should start with sustainable site selection and planning (NIBS, 2014).

Moreover, buildings consume large amounts of energy during construction and operation phases therefore, it is essential to reduce energy use, apply passive solar techniques, increase efficiency, and maximize the use of renewable energy sources (NIBS, 2014).

Similarly, buildings use a large portion of municipally supplied water for cleaning, personal hygiene, heat transfer, and for landscaping however, water efficiency receives little attention in building design and operation. Potable water also has embedded energy due to the effort to bring drinkable water to our buildings. To address water related environmental concerns, high performance building should use water efficiently, and reuse or recycle water for on-site use, when feasible (NIBS, 2014).

In addition, energy and water are used not only during building operation but also during production of building materials or equipment. There is embodied energy to mine or harvest natural resources and raw materials; to manufacture the products; and to transport them to building site and to install. Moreover, during material and equipment life-cycle, other natural resources are consumed, landscapes are destroyed, and pollutants are released into the nature as well where raw materials are extracted from the earth, are transformed into the concrete, steel, glass, rubber, and other construction materials. Therefore, in high performance buildings, sustainably produced and recyclable materials that minimize life-cycle environmental impacts and contribute to occupant safety and health should be used (NIBS, 2014).

A healthy indoor environment promotes comfort, productivity, health and well-being of the building users therefore; the physical, chemical and biological properties of the indoor air must be assured at all times. Hazardous gases such as volatile organic compounds from building materials, products, and furnishings should be avoided by appropriate ventilation and moisture control and selection of non-toxic materials. Moreover, appropriate levels of thermal, visual and acoustic comfort must be provided to ensure the total quality of the indoor environment (NIBS, 2014).

Lastly, operational phase of a building starts after completion of construction however, operating and maintenance issues should be planned at early design stages for better integration and consequently for improved overall performance. The operational phase of building is quite longer than the design and construction phases and the lifecycle cost of the operational life could be highest in whole building life cycle. Therefore, to operate a high performance building, professionals need make sure that the building would perform as it is intended. High performance operation requires good planning, integration and control of occupants, processes, mechanical, electrical, renewable energy systems and, information technology (NIBS, 2014).

As explained above, high performance building design requires simultaneous realization of several objectives including life-cycle economics, energy-efficiency, environmental impact, occupant productivity and health, durability and building functionality.

The economic and environmental performance of the building is strongly influenced by building energy behaviour. Moreover, building energy consumption and occupant's comfort are closely related, too. Therefore, within many of the high-performance building attributes the energy-efficiency lies at the heart. An assessment report on high performance buildings by U.S National Institute of Building Sciences (2008) says, "Energy efficiency should be a cornerstone of a high-performance building. All energy consuming systems and products should be designed to achieve the highest level of energy efficiency consistent with the other design attributes" (p.13).

The focus of this current work is therefore to develop a methodology for addressing building performance challenges with a special emphasis on building operational energy efficiency.

2.3 Building Energy Performance

Operational energy is the dominant part of the energy consumption due to the long building lifetimes. Therefore, the intent of the current study is to directly target the reduction of the dominant operational energy component. Therefore, the embodied energy component is neglected in this research for simplification.

Most of the energy consumed in building operational phase is used for heating, cooling, ventilating and lighting the space to create a thermally and visually comfortable built-environment for its occupants, and water heating and powering plug-in appliances needed for daily life activities.

The thermal and visual performance of a building involves complex interactions between the exterior environment and the internal environment separated by building envelope. Moreover, Heating, Ventilating and Air-Conditioning (HVAC) and lighting systems complement the architectural design and they are adopted to control and adjust the internal environmental factors such as temperature, humidity, illuminance when necessary.

The building energy performance includes the integrated effects of the whole building with its lighting, mechanical systems and control systems interacting dynamically all among themselves and with the building occupants. Moreover, on-site energy generation supports building energy efficiency by providing sustainable methods of heating, cooling, and powering the building.

Identification and determination of the best combinations of building and system parameters, which influence building energy balance, is key to the whole building energy efficiency. However, there are many factors drive energy demand and consequent consumption in buildings. Understanding the effect of individual factor is at vital importance.

Buildings interact with their external environment through complex dynamic processes and respond to the continually changing outdoor and indoor conditions. How buildings interact with the environment creates building's need for energy. The fundamental physics encountered within and around a building includes various thermal forces at play including the heat of the sun entering the building, the heat generated by building occupancy and appliances, and the transfer of energy across the building enclosure due to the difference in temperature between building and the environment (Nasrollahi, 2009).

The process of determining what energy changes are occurring in the environment inside a structure is called building energy balance. In order to reduce the energy demand, it is first important to understand how energy demand is created, how energy is distributed throughout a building, and how each parameter contributes to the building energy balance (Zięb ik and Hoinka, 2013).

The following sections mention only the most influential elements for a successful energy-efficient building and system design, where a detailed analysis is beyond the scope of this work. Influential factors are mentioned under five main categories: outdoor environment, building architectural design characteristics, indoor environment, building system characteristics and renewable energy system characteristics.

2.3.1 Outdoor environment

Macro and micro climate surrounding a building have a major effect on building energy performance and the integration of climatic data is a driving factor in the

building design. Macro-climate represents the climate of a larger area such as a region or a country where micro-climate is the localized climate in building site (ESRU, 2006).

The successful design of buildings relies on an appropriate understanding and controlling of climatic influences at the building site through prevailing climatic conditions when unwanted and benefiting when useful. When designing an individual building the outdoor climate is to be regarded as a given condition.

Cooling and heating loads are partially driven by weather patterns specific to a particular climate region. Lovell (2009) explain that different locations in the world, with their specific climatic conditions, certainly present different priorities and they require different design approaches.

As climatic elements change dynamically, buildings respond to the changes simultaneously. The main climatic elements that affect building heat balance are solar radiation, ambient temperature, air humidity, precipitation, air movement, and sky condition. The influence of climate on building performance was explored in many studies (Erell et al., 2003; Lam et al., 2005; Ochoa and Capeluto, 2008; Manioglu and Yilmaz, 2008) and the design strategies that needs to be incorporated into the process for different climatic zones are discussed. The studies highlights that dynamic nature of the environment must be incorporated into a design response in the form of daily, seasonal, and annual cycles of heat transfer, air pressure changes, and humidity levels.

Furthermore, site conditions have an important role in the building design among numerous factors. Each building site offers its own conditions and imposes limits on the design flexibility.

The building site might limit the size and shape of the building. Moreover, careful site selection and building placement are essential for optimal daylight and solar utilization.

The variations in localized climate around a building create the site-specific microclimate. The environmental conditions at the site area are a combination of macroclimate as well as the microclimate. Therefore, building site also affects the air movement, temperatures, rain penetration, humidity etc. around the building through vegetation and topography.

Taking advantage of the physical features of the building site and microclimate reduces heating and cooling loads, and therefore lowers overall energy consumption as mentioned in the literature studies.

Akbari et al (1997) documented the dramatic differences in cooling-energy requirement between houses on landscaped and unlandscaped sites.

Parker (1981) measured the cooling-energy savings from well-planned landscaping and found that properly located trees and shrubs around a mobile trailer reduced the daily air-conditioning electricity use by as much as 50%.

Robitu et al (2006) introduced a numerical approach based on coupling the CFD model of airflow, in which the influence of trees is considered as source terms, and the radiation exchange, completed with thermal conduction.

Therefore, site conditions should be considered carefully and necessary arrangements need to be realized prior to building design.

2.3.2 Building architectural design characteristics

2.3.2.1 Orientation

Building orientation is one of the main factors in reducing building energy demand and keeping the interior conditions in comfort range. Decisions made in adjusting the building orientation will have impacts on the energy performance of the building over its entire life cycle mainly with regard to solar radiation and wind. Proper building orientation can diminish the unwanted effects of severe weather a great deal. Therefore, it is very important to orient a building to optimize the effects of the nature (Nasrollahi, 2013).

Orientation of building determines the amount of radiation the building receives. A good orientation should allow maximum access to the sun when needed; or, likewise, eliminate it when unwanted. Moreover building orientation should provide maximum natural light in all climatic conditions.

The best orientations for a building can literally vary from location to location and should be evaluated accordingly. The past studies by Yohanis and Norton (2002), Jaber and Ajib (2011); Al-Tamimi et al., (2011) showed approaches for optimal orientation selection in different climate zones.

2.3.2.2 Building form

Building form is one of the basic determinants of the building energy performance and the comfort of residents. Form refers to the shape or configuration of a building and it is mainly determined by the building's height, width, and depth (Harvey, 2012).

The building form also defines the building footprint, building volume, floor-to-floor height and more importantly, the size and the orientation of the exterior envelope exposed to the outdoor environment.

The surface area to volume ratio (S/V) is a significant factor determining the magnitude of the heat transfer in and out of the building. The larger the S/V ratio, the greater the heat gain or loss for a given volume of space is.

There is a trade-off between a compact form that minimizes conductive heat transfer through the envelope and a form that facilitates daylighting, solar gain, and natural ventilation therefore it should be developed considering the trade-offs.

The role of building form in energy consumption has been investigated by several researchers including Depecker et al.(2001); AlAnzi et al. (2009), Danielski et al. (2012); Ling at al., (2007) where their work showed that the building morphology is an important design parameter in the process of energy-efficient building design.

2.3.2.3 Building envelope

Building envelope thermally and physically separates the interior and the exterior building environments. It includes the outer elements of a building such as foundations, walls, roof, windows, doors and floors.

Building envelope is an integral part of a building and functions as a thermal shell. It regulates how well the building can benefit from solar radiation, daylight, wind and natural ventilation and provides the ability to control of solar radiation, heat flow, airflow and moisture. Therefore, appropriate selection and arrangement of building envelope elements can enhance the comfort and energy performance a great deal (Harvey, 2012).

Building envelope consists of the following elements:

Opaque building elements

As summarized by Harvey (2012), opaque elements of the building include walls, roof, floor etc. Thermo-physical properties of the layers comprising the building elements determine the energy-flow behaviour and the energy storage capacity of the building.

Heat transfer through the opaque building elements is a combination of convective, radiative and conductive processes.

Building elements such as walls, roofs consist of multi layers and total heat transfer coefficient (U-value, W/m2.K) is used to estimate how much heat can be transferred through a building element.

In addition to heat transfer, thermal mass enables building materials to absorb, store, and later release thermal energy. Due to thermal mass buildings can absorb and store excess thermal energy when the building's thermal load is high and release the energy when the load is low. This way, thermal mass moderates temperature swings inside a building. Appropriately sized thermal mass can help buildings manage their thermal energy resources

Radiation is a significant component of heat transfer in buildings in both heating and cooling. Solar radiation incident on building envelope can be absorbed, reflected and transmitted depending on the surface characteristics and consequently it influences interior and exterior surface temperatures, heat flow entering the building, light distribution and the occupant's comfort. For opaque components, reflectivity, absorptivity, emissivity and long wave radiation behaviour characterize the surface behaviour.

Abundant literature is available on impact of the thermal resistance of building envelope against heat flow (e.g. Kim and Moon, 2009) and many studies shows how to determine the appropriate values for the overall heat transfer coefficients for building opaque elements. (e.g. Farhanieh and Sattar, 2006; Sanea and Zedan, 2011; Al-Homoud, 2005; and Bojic et al., 2002). These studies reveal that appropriate arrangement of thermal resistance of building envelope significantly reduces building loads.

Similarly, there is significant research carried out about the relationship between the building thermal mass and the thermal performance. Gregory et al (2008), Balaras

(1996), Al Sanea et al (2012), Cheng et al (2005), and Zhou et al (2008) investigated the different aspects and applications of building thermal mass. The results conclude that thermal mass has the ability to significantly reduce the building energy requirements and improve internal temperatures. Optimum amount of thermal mass should be estimated for true energy efficiency.

The significance of total solar reflectance and optical properties of the exterior facade has been well studied by Joudi et al (2011), Filho et al. (2010), Berdahl et al (2008), Synnefa et al (2007), and Stathopoulou at al. (2009).

Shading

Nasrollahi (2009) explains that solar shading is a part of building envelope and it controls the amount of sunlight that strikes and enters into a building. Accordingly, it blocks the solar radiation incident on the exposed surfaces of a building and reduces heat gain, modifies thermal gains and influences daylighting levels. Shading of surfaces can be achieved by the self-shading profiles of buildings such as in H-type or L-type buildings or by integrated building shading elements. The use of well-designed sun controls save energy, reduce heat and glare, improve occupant's comfort.

Solar and visual transmittance, thermal resistance, location and dimensions of shading element together with any control strategy associated with it determines the performance of the shading device in term of energy and visual performance.

The performance of building solar shading in terms of energy and daylighting and optimal shading design for better Indoor thermal environmental conditions was explored deeply by many researcher such as Ho et al (2008), Alzoubi and Al-Zoubi (2010), Palmero-Marrero and Oliveira (2010), Kim et al (2012), Bessoudo et al (2010), and Datta (2001).

Finally, there is extensive research about control strategies for shading devices. Moeseke and de Herde (2007) investigated the impact of control rules on the efficiency of shading devices and free cooling for office buildings. Guillemin and Molteni (2002) explored energy-efficient controller for shading devices self-adapting to the user wishes. Tzempelikos and Athienitis (2007) discussed the impact of shading design and control on building cooling and lighting demand.

Transparent building elements

Transparent elements such as windows and skylights allow the direct admittance of solar gains into the building. Major portion of the solar radiation is transmitted directly to the interiors, while the remaining small fraction is absorbed and/or reflected back. Furthermore, an element may also be openable (e.g. skylight, window, door, etc.), thereby allowing for air exchanges between the building and its surroundings. Thus, the transparent buildings components affect the building energy balance a great deal

Nasrollahi (2009) mentions that according to the diurnal changes in sun's position, the intensity of solar radiation differs considerably among the exterior surfaces of the building. Therefore location and orientation of transparent elements changes the amount of solar radiation enter the building.

Nasrollahi (2009) also explains that the area of the transparent elements also influences the building energy performance. The dimension of transparent elements (with and length) and the ratio between the total glazed area of the building and the total wall area which is called as window-to-wall ratio (w-t-w) are the influential parameters.

Heat is transferred through the transparent components by conduction, convection and radiation.

Solar heat gain coefficient (SHGC) refers to the fraction of incident solar heat admitted through a window glazing both directly transmitted, and absorbed and subsequently released inward.

Visible transmittance (Tvis) refers to the fraction of visible light transmitted through a window glazing. It is an optical property that indicates the amount of visible light transmitted.

U-Value is a rate of non-solar heat transfer through transparent components and it measures the ability of the component to reduce heat gain.

Air leakage defines heat loss and gain occurs by infiltration through cracks in the assembly of transparent components. It is indicated by an air leakage rating expressed as the equivalent m3 of air passing through a square meter of window area.

In addition to the air leakage there is also natural ventilation can be provided to the building through operable transparent building elements such as windows. Ventilation lets in the fresh air and exhausts room air. This way heat is transported by the convective means and: the thermal energy is associated with the air replaced.

The studies about the impact of glazing area on building energy performance appear frequently in the literature. For example, Kontoleon and Bikas (2002) discussed the influence of glazed openings percentage and type of glazing on the thermal zone behaviour. Su and Zhang (2010) highlight the environmental performance optimization of window-to-wall ratio for different window type in hot summer and cold winter zone in China based on life cycle assessment. Hassouneh et al (2010) explore influence of windows on the energy balance of apartment buildings in Amman highlighting the selection of the optimum window size for each direction.

Furthermore, visual and energy performance of windows regarding solar and optical properties were deeply investigated in a wide scope as well. Nilsson and Roos (2009) review the evaluation of optical and thermal properties of coatings for energy efficient windows Karlsson and Roos (2001) inspect the heating and cooling energy impact of low thermal emittance values for architectural glazings. Johnson et al. (2004) systematically explores the influence of glazing systems on component loads and annual energy use in prototypical office buildings.

Nabinger and Persily (2011) describe the retrofits and the results of the pre- and post-retrofit assessment of building airtightness, ventilation, and energy use. Hassan et al, (2007) investigate the effects of window combinations on ventilation characteristics for thermal comfort in buildings.

2.3.3 Indoor environment

Indoor conditions are another factor significantly influences the thermal behaviour and thermal comfort inside a space and as mentioned by Nasrollahi (2009) buildings are expected to provide an environment that does not harm the health of its occupants.

Internal loads which are generated within the building itself impact the building energy balance a great deal. In buildings, the main source of internal heat gain is artificial lighting, occupants, and plug loads such as equipment and appliances.

Occupants generate both sensible and latent heat components according to the activity level. Activity level of people together with dynamic change in density determines the heat gain from the people occupy a space.

The influence of occupancy is shown in many studies. For example, Davis and Nutter (2010) investigate the occupancy profiles to characterize occupancy factors for common university building types. Diaconu (2011) explores the effect of occupancy pattern and ventilation on the energy savings potential of a Phase Change Material (PCM) wall system. Richardson et al. (2008) presents a thorough and detailed method for generating realistic occupancy data for United Kingdom households, based upon surveyed time-use data. Kwok et al. (2011) discuss the critical role of building occupancy rate in building cooling load prediction and how it significantly improves predictive accuracy.

Interior lighting is a basic requirement of buildings and it constitutes a major fraction of the building's internal load. A lighting system is set up in order to create required illuminance levels inside. The installed interior lighting power (W) or lighting power density (W/m2) determines the amount of electricity consumed by the lighting system and the heat given off at the same time. In the literature Yun et al. (2012) investigates the effects of occupancy and lighting use patterns on lighting energy consumption. Lam et al. (2006) discusses the impacts of lighting density on heating and cooling loads in different climates in China. Linhart and Scartezzini (2011) explore the influence of Lighting Power Density on visual comfort and. energy efficiency. They conclude that energy-efficient lighting with Lighting Power Density of less than 5 W/m2 is already achievable in today’s office rooms without jeopardizing visual comfort and performance.

Similarly, plug loads that are a proportion of the building loads contribute a great deal to building energy balance. Equipment Power Density (W/m2) that comes from a careful estimate of the amount, size, and type of the equipment will determine the amount of heat realized by the equipment and the amount of electricity consumed. Yao and Steemers (2005) propose a method of formulating energy load profile for domestic buildings in the United Kingdom. Turiel et al (1987) discusses the estimation of energy intensity by end-use for commercial buildings. Srinivasan et al. (2011) establishes plug-load densities for use in energy simulation of K-12 schools.

In addition to interior loads, the operational patterns of each building (days building is open and schedule for typical start and end of day), the target comfort levels, temperature set points etc. influence the building energy behaviour.

2.3.4 Building system characteristics

As explained in the previous section, a building itself act as a system and depending on its interaction with outside environment energy is required to maintain the internal conditions. The amount of required energy depends on the building architectural characteristics, climate and building site and it can be lowered or sometimes eliminated by designing buildings in harmony with its surroundings. On the other hand, sometimes it may not be possible to achieve the ultimate building load-avoidance on every building by only arranging design parameters, especially where it is obliged to maintain buildings in a narrow temperature range. In this case, the required heating, cooling, ventilation and lighting should be provided through building systems and a good architectural design will help to reduce the number of hours during the year when the systems are needed. Therefore, building systems must work in concert with the building shape, orientation, envelope, electrical equipment, and site characteristics (Harvey, 2012).

The energy performance of building systems depends on the properties of each system.

2.3.4.1 HVAC system

HVAC is an acronym that stands for "heating, ventilating and air conditioning." The main purpose of an HVAC system is to regulate the climate within a residential or commercial environment to keep its occupants comfortable. An HVAC System consists of a chain of components designed to heat, ventilate or cool a specific area while maintaining defined environmental conditions. HVAC systems come in a broad range of sizes and complexity from the simplest fireplace, used for comfort heating, to the extremely reliable total air-conditioning systems that can be found in complex buildings (Grondzik and Furst, 2000).

Today, HVAC systems account for a large portion of national and global energy consumption and represent an opportunity for significant energy savings.

HVAC systems are used for indoor climate control and they can include functions such as heating, cooling, supply of fresh air, air movement, filtration and where required by the climate, humidification and dehumidification.

Heating, Ventilating and Air Conditioning is a huge field and there is a large variety of HVAC systems available today. A detailed discussion of HVAC systems is beyond the scope of this work. Only the most commonly used types of HVAC systems will be briefly mentioned and the parameters that influence the energy efficiency of systems will be highlighted.

For the purposes of this study, HVAC system types are broken down into two broad categories as central systems and local systems.

Central systems

As explained by Grondzik and Furst (2000), central systems serve multiple spaces from one base location. They use a series of equipment to distribute cooling/heating media to exchange heat and supply conditioned air from one point to more than one room. Central systems are built-up systems assembled and installed on the site.

A central HVAC system may serve one or more thermal zones and has its major components located outside of the zone or zones being served, usually in some convenient central location in, on, or near the building. Central HVAC systems will have as many points of control (thermostats) as there are zones.

Central HVAC systems come in a variety of different types and most conventional centralized systems fall within one of the following three categories depending on the nature of the thermal energy transfer medium used by the system: All-Air System, All-Water System, or Air-Water System (Westphalen and Koszalinski, 2001a).

All-air systems are central systems, which provide complete sensible and latent heating and cooling of the air supply and deliver cooled or heated air from a central point via ducting, distributing air through a series of grilles or diffusers to the room or rooms being served.

All-water hydronic system delivers the hot or cold-water from a chiller or heating boiler to individual heat transfer devices (terminal units) located in each room of the building through a network of pipes. When heating is required, the terminal units

draw heat from the water and when cooling is required these reject heat to the water. All-water systems only control indoor temperature.

An air-water system is a hybrid system of all-air and all-water type of systems. Air-and-water systems condition spaces by distributing both conditioned air for primary ventilation and water to local terminal units installed in the spaces for additional conditioning.

The components of a central system fall into two broad categories: "primary components" and "secondary components.

Primary components, often called "central plant" equipment, convert energy from fuel or electricity into heating and cooling energy in the form of hot water, steam, chilled water or refrigerant: Refrigeration equipment options include water chillers and direct-expansion equipment. A refrigeration system must also reject the heat that it removes using a water cooling or air cooling. Water-cooled chillers require condenser water pumps and cooling towers to reject heat.

Boilers produce hot water or steam to distribute to heating coils. Pumps circulate chilled water, hot water, and cooling tower water.

Secondary components, sometimes called "system" equipment, deliver heating and cooling to occupied spaces: Air handling equipment may be centrally located or several air handlers may be distributed throughout a facility. Ducts, plenums and shafts distribute air. Terminal units are devices at the end of a duct or pipe that transfer desired heating or cooling to the conditioned space. Some types commonly used with central HVAC systems include fan-coil units, induction units, and convectors (Grondzik and Furst, 2000).

Controls are used to make components work together efficiently.

Local systems

Local air-conditioning systems are self-contained factory made assemblies consisting of a heat and/or cool source (depending on climate and occupancy demands), a fan, a filter, and control devices. The most common local air-conditioning systems include window units, package air-conditioners, rooftop units and heat pumps (Grondzik and Furst, 2000).

The cooling is delivered directly to the supply air in a refrigerant evaporator coil. These units are sometimes also referred as direct-expansion units.

HVAC energy performance

HVAC systems utilize energy in many forms. Fuel sources for generation of heating and cooling include electricity, coal, natural gas, propane, oil etc. Furthermore, energy is also required to distribute heating and cooling within a building, reject the heat discharged by cooling systems to the environment, and move air for ventilation purposes. (Westphalen and Koszalinski, 2001a)

As Westphalen and Koszalinski discuss (2001a) the energy performance of HVAC systems depends on several factors including system type, system size, efficiency of plant equipment, efficiency of distribution system components, system control etc. Estimation of HVAC energy use is strictly tied to the system type and the systems choice depends mainly on system constraints, architectural constraints and financial constraints.

Haines and Myers (2010) explains that determining the correct size of HVAC equipment is key to achieving energy efficiency moreover it also influences first cost and operating costs. For HVAC systems, the thermal loads come primarily from five sources including building envelope, lighting, occupancy, plugged-in equipment and ventilation and they should be all taken into account during sizing calculations. A proper HVAC system should always be able to effectively satisfy the peak heating and cooling loads that the building experiences throughout the year. Overcapacity equipment has a higher initial cost, costs more to operate, and may be less effective than optimally sized equipment thus safety sizing factors should be chosen carefully.

As highlighted by Westphalen and Koszalinski (2001a), the efficiency of plant equipment is another factor that determines the energy performance of HVAC systems. Equipment efficiency is a measure of how much energy is effectively converted into heating and cooling the built environment. More efficient systems use less energy to achieve the same degree of conditioning. Efficiency ratios such as Energy Efficiency Ratio (EER) or coefficient of performance (COP) is determined at full load and under standard test conditions however, many central plant units spend a significant part of their operating life at below full load. Therefore, part load off-reference equipment efficiency due to changing building load and environmental conditions should be also considered.

Similarly, the full load and part load-efficiency of the distribution system equipment including fans and pumps affects overall HVAC energy performance significantly. Good part-load efficiency for distribution systems often involves variable speed drives along with components to allow drives to operate at lower frequencies as often as possible.

Application of HVAC control helps operating the building systems in strict accordance with demand; thereby it avoids unnecessary use of energy. Supply fan speed controls, cooling capacity controls, demand-controlled ventilation supports increasing the operational efficiency.

HVAC energy performance was deeply investigated in several studies.

Salsbury and Diamond (2000) proposed a method for performance validation and energy analysis of HVAC systems using simulation.

Wang et al. (2011) explained an approach for energy performance comparison of heating and air-conditioning systems for multi-family residential buildings.

Lombard et al. (2011) reviewed energy related aspects of HVAC systems with the aim of establishing a common ground for the analysis of their energy efficiency. The paper focused on the map of energy flow to deliver thermal comfort: the HVAC energy chain.

Shahrestani et al. (2013) attempted to characterize the performance of 36 HVAC&R systems based on the simultaneous dynamic simulation.

Haniff et al. (2013) provided a detailed review on heating, ventilation and air conditioning (HVAC) scheduling techniques for buildings towards energy-efficient and cost-effective operations.

Vakiloroaya et al. (2014) investigated and reviewed the different technologies and approaches, and demonstrates their ability to improve the performance of HVAC systems in order to reduce energy consumption.

The studies concluded that several factors such as climatic conditions, expected thermal comfort, initial and capital cost, the availability of energy sources and the application of the building must be considered to properly design and select an energy-efficient HVAC system.

2.3.4.2 Lighting system

Lighting plays a key role in our daily lives where it makes possible to carry out activities at night, or where natural light is not available. However, providing artificial light consumes, almost one fifth of the globally generated electricity (IEA, 2006). Moreover, artificial lighting also introduces heat into the space and increase building cooling loads. Therefore, lighting system significantly impacts a building's overall energy consumption and operating costs.

Sustainable Design Guide by Los Alamos National Laboratory (LANL, 2013) mentions that the lighting energy use depends on several factors including the area of the lighted space, lighting needs, the efficiency of the lighting system, daylighting availability, lighting control as well as the number of hours of use.

Boreham and Hadley (2009) summarize that luminaries and control units together form a lighting system. A luminaire is a complete lighting unit, comprised of a light source (lamp or lamps), together with the parts that distribute the light, position and protect the lamps, and connect the lamps to the power supply. Lighting efficiency measures the lamps ability to convert input electric power into luminous power. Therefore, using more efficient lamps consumes less energy to produce same illuminance levels as a less efficient lamp. There are various lamp types are available today with varying efficiencies including Incandescent, tungsten halogen, fluorescent, metal halide, low-pressure sodium, high-pressure sodium, light emitting diodes.

Moreover, as Ander (2003) explains, building's ability to benefit from daylight also influences the need for artificial lighting. Daylighting is the controlled admission of natural light (direct sunlight and diffuse skylight) during daylight hours into a building through building openings such as windows and skylights. A building designed to take advantage of daylighting will have electric lighting system controls that turn the electric lights off or dim them when sufficient daylighting is available. The electric lights operate only to maintain set lighting conditions that the daylighting cannot meet. Therefore, an electric lighting system integrated with building architectural design and daylighting controls reduce the lighting demand and consequently the energy consumption.

In the literature, many research studies investigated the influence of a variety of factors on the building lighting consumption.

Krarti et al. (2005) developed a simplified method to estimate energy savings of artificial lighting use from daylighting

Doulos et al. (2008) aimed to quantify energy savings in daylight responsive systems and explored the role of dimming electronic ballasts.

Li et al. (2008) studied the lighting and cooling energy performances for a fully air-conditioned open-plan office when solar control films together with daylight-linked lighting controls are being used.

Mardaljevic et al. (2009) reviewed the historical basis of current compliance methods for achieving daylit buildings, proposes a technical basis for development of better metrics, and provides two case study examples to stimulate dialogue on how metrics can be applied in a practical, real-world context.

Yun et al. (2012) investigated the effects of occupancy and lighting use patterns on lighting energy consumption through field survey.

Shen et al. (2014) carried out energy and visual comfort analysis of lighting and daylight control strategies and they compared the energy and visual comfort performance of seven independent and integrated lighting and daylight control strategies.

2.3.4.3 Water heating system

Water heating accounts for approximately 17 % of a residential building energy use in USA (EIA, 2013), and 14 % in Europe (ODYSSEE-MURE, 2009) and after heating and cooling, it is typically the largest energy user in the home. In commercial buildings, however water heating forms a small fraction of energy consumption and it comes last after space conditioning, lighting and powering office equipment.

American Society of Heating, Refrigerating and Air-Conditioning Engineers (ASHRAE) Handbook HVAC System and Equipment (2008) mentions three main categories of water heating systems including instantaneous (tankless) water heaters storage water heaters, combination of space and water heating systems.

Demand (tankless or instantaneous) water heaters heat water directly circulating water through a large coil and there is no storage tank continuously maintaining hot water. Demand systems produce a limited amount of hot water

Storage water heaters heat and store water in an insulated storage tank ready for use at all times. Many fuel options are available, including electricity, natural gas, oil, and propane.

Combination space and water heating systems use a boiler plant as the heat source by circulating hot water from the boiler through a heat exchanger in a well-insulated water heater tank.

Moreover, as mentioned by Ibrahim et al. (2014a) there are also renewable energy supported water heater systems such as heat pump water heaters where a heat pump transfers energy from the surrounding air or ground to water in a storage tank and solar water heaters where energy of sun is used as the heat source.

The energy consumption due to water heating depends on several factors including hot water demand, water heater temperature, first-hour rating (FHR) and energy factor (fhr).

The FHR measures the amount of hot water the heater can supply per hour (starting with the tank full of hot water.

The EF indicates overall unit efficiency based on the amount of hot water produced per unit of fuel consumed over a typical day

There are several studies in the literature concerning the energy and economic performances of several water-heating options.

Hegazy (2007) investigated the effect of inlet design on the performance of storage-type domestic electrical water heaters for energy conservation.

Carboni and Montanari (2008) proposed a quantitative approach able to forecast the profitability of the introduction of domestic solar thermal systems operating in parallel with the most common systems for heating domestic sanitary water.

Nikoofard et al. (2014) evaluated the impact on energy consumption and GHG emissions as well as the techno-economic feasibility of retrofitting solar domestic hot water (DHW) heating systems to all houses in the Canadian housing stock.

Ibrahim et al. (2014b) presented the dynamic modelling of a domestic hybrid water heating system. The system is composed of a solar collector, a heat pump water heater, a wind turbine, a battery and a hot water storage tank

Hepbasli and Kalinci (2009) reviewed heat pump water heaters systems in terms of energetic and exergetic aspects.

2.3.5 Building integrated renewable system

As explained in previous sections, improving buildings energy efficiency requires climate responsive building design for demand reductions, application of more efficient building systems. Moreover, a good integration between building and its systems is also essential.

While working on strategies for demand-side efficiency it is also equally important to develop supply-side solutions. One approach to making buildings more energy-efficient is to require the use of renewable energy systems capable of generating power or energy that can be used by the building occupants. As the term suggests, renewable technologies rely on the resource being constantly renewed

Building-related renewable energy provides an opportunity to reduce building environmental impact and bring energy directly and efficiently to end users. As explained by Bronin (2012), building-related renewable energy is primarily solar heating, photovoltaic, wind, biomass and geothermal technologies, which are incorporated into inhabited structures and used by those structures' occupants. The amount of energy that can be acquired from building related renewables are limited to what sources are available on or around the building.

The energy output of the renewable systems depends on energy production capabilities of each technology and the site conditions.

Building integrated renewable technologies were frequently studied from many different perspectives.

Kalogirou (2004) evaluated the performances of a solar water heating and a solar space/water heating system.

Ardente et al. (2005) studied the energy and the environmental performances of the solar thermal collector for sanitary warm water demand. A life cycle assessment

(LCA) was performed following the international standards of series International Organization for Standardization (ISO) 14040.

Dalton et al (2009) presented an analysis of the technical and financial viability of grid-only, Renewable Energy System-only and grid/ Renewable Energy System hybrid power supply configurations for a large-scale grid-connected hotel.

Cucchiella et al. (2012) presented a model to define the profitability of a Photovoltaic (PV) building integrated system.

Marino et al. (2013) presented an energetic, economic and environmental analysis of two different configurations of a self-sufficient system for energy production from renewable sources in buildings.

Fong and Lee (2014) proposed a hybrid renewable cooling system for office building application by utilizing both the solar energy and the ground source.

Oh et al. (2014) suggested a cost-effective method for integration of existing grids with new and renewable energy sources in public buildings in Korea.

The studies highlighted that a good integration of renewable systems with the building for a better efficiency is required starting with the early design phases.

2.4 Building Performance Simulation

As discussed in previous sections, overall building performance depends on several factors, which are related with characteristics of climate, building site, building architectural characteristics, indoor conditions, building HVAC systems, and on-site energy generation. Moreover, all the design factors are in constant interaction. Therefore, designing buildings for energy efficiency is a challenge. Clear and reliable information on the buildings performance is required for understanding the building behaviour and addressing the needs of building design.

Built environment is becoming more complex, as the expectations from buildings increasing due to economic, environmental and social pressures. High energy performance buildings cannot be designed using only conventional knowledge, rules of thumb, or traditional methods, which are mono-disciplinary, restricted in scope and static in time domain. Therefore, computerized building simulation has been

introduced over the last fifty years to provide support for evaluating buildings performance (Hensen and Lambert, 2011).

According to Fishwick (1995), computer simulation is the discipline of designing a model of an actual theoretical system, executing it on a digital computer and analysing the execution output. A simulation model is actually a mathematical model acting as the imitation of the operation of a real-world process or system over time. It allows describing and analysing the behaviour of a system, calculating the impact of certain inputs and decisions on outcomes, therefore, asking "what if" questions about the real system, and aiding the design process by providing insight data.

Until the mid-1960s only simple hand-calculation methods were available for calculating energy consumption in buildings. However, as the power of computers grew, more resourceful building simulations tools started to appear. Since the first introduction of the building simulation discipline, it has been constantly evolving and as a result, a large variety of Building Performance Simulation (BPS) tools which are scientifically and internationally validated are available today (Hensen and Lambert, 2011).

Building performance simulation can model the thermal, visual, ventilation and other energy consuming processes taking place within a proposed design in response to changing climate conditions and provide information about how the building is expected to perform. Moreover, BPS can support decision making by providing information on building environmental impact, thermal and visual comfort, daylighting benefits and related costs as well. By doing so, designers can preview and improve the performance of interdependent building features such as orientation, shape, building envelope, various mechanical systems and building related renewables and can effectively integrate the building envelope and systems for cost-effective design solutions. Therefore, computer simulation tools are an essential component of the whole-building design process.

Building performance simulation can be used not only in the design stages of new energy efficient buildings, but also in the planning stages of energy retrofits for existing buildings, and the development of building energy codes and standards.

There are quite a big number of tools in use nowadays and their capabilities vary in a wide range (DOE, 2014). Some tools focuses on only certain issues inherited in

building energy problems while others provide a more general view. The core tools in the building energy field are the whole building energy simulation programs that can provide users with building performance indicators such as energy use and demand, temperature, humidity, and costs (Crawley et al., 2008). These tools can carry out not only energy efficiency calculations but also daylighting and comfort calculations.

Crawley et al., (2008) compared the features and capabilities of twenty major building energy simulation programs namely BLAST, BSim, DeST, DOE-2.1E, ECOTECT, Ener-Win, Energy Express,Energy-10, EnergyPlus, eQUEST, ESP-r, IDA ICE, IES/VES, HAP, HEED, PowerDomus, SUNREL, Tas, TRACE and TRNSYS in the following 14 categories: General Modeling Features, Zone Loads, Building Envelope and Daylighting, Infiltration, Ventilation and Multizone Airflow, Renewable Energy Systems, Electrical Systems and Equipment, HVAC Systems, HVAC Equipment, Environmental Emissions, Economic Evaluation, Climate Data Availability, Results Reporting, Validation, and User Interface, Links to Other Programs, and Availability. Their study concluded that even among the 'mature' tools, there is not a common language to describe what the tools could do. Identification of simulation needs is essential in determining the simulation tool. They encourage users to consider adopting a suite of tools, which would support the range of simulation needs. Lastly, validation of simulation results is key to correct tool selection. Therefore, BESTEST-like procedures can support users with detailed information on the accuracy of the considered tools.

Whole-building simulation has been used in a wide variety of research attempts in the last decade and only a few of them are mentioned below:

Griffith et al. (2003) employed EnergyPlus to study the influence of some advanced building technologies over the building performance of a building in Teterboro airport and DOE-2.1E to analyse the effect of such common measures as optimized envelope system and schedules.

Ibanez et al. (2005) evaluated the influence of the phase change materials on different parts of the envelope of a room through TRNSYS Program.

Ellis and Torcellini (2005) carried out research on the reliability of EnergyPlus in simulating tall buildings and the outcomes from their research proved accuracy and reliability of EnergyPlus in simulating on a tall building.

Griffith and Crawley (2006) used EnergyPlus to propose a methodology for evaluating the energy performance for the United States commercial building sector to estimate the technical potential of zero-energy buildings.

Kalogirou (2011) used TRNSYS Program to see how the energy demand behaves with a hybrid photovoltaic-thermal solar system in a building in Nicosia, Cyprus and determined overall the energy consumption.

Zhai et al. (2011) studied the effects of the ventilation in summer with the EnergyPlus simulation software. They compared experimental and simulated measures of indoor temperature in three distinct building offices.

Bojić et al. (2011) compared energy consumption, energy costs and environment impact of three systems used for space heating, and space cooling of an office building in Kragujevac, Serbia. Three investigated systems are a system with a natural gas boiler and convective baseboard heaters for water space heating and window air conditioners for air space cooling, a system with a natural gas boiler and individual air reheaters for air space heating and a chiller plant for air space cooling, and an air-to-air heat pump for air space heating, and cooling. The systems are modeled and simulated by using EnergyPlus software.

Zhou and Park (2012) demonstrated how much energy use will be reduced if the simulation -assisted building energy management and control system is applied to a representative large office building.

Boyano et al. (2013) explored the energy saving potentials in office buildings across Europe by simulating several currently available scenarios.

Ochs et al. (2013) used the simulation tools MATLAB Simulink and TRNSYS 17 to model a renovated multi-family house.

Xiaoqi et al. (2014) proposed an innovative Energy Saving Alignment Strategy (ESAS) to reduce building energy demands. They explored the application of ESAS in the context of public housing through EnergyPlus simulation.

Mohamad et al. (2014) calculated the annual energy load of the windows offset thermal bridges for a typical French house by combining a developed MATLAB code and EnergyPlus energy simulation program.

Gustafsson et al. (2014) used dynamic simulation to compare the energy performance of three innovative HVAC systems: (A) mechanical ventilation with heat recovery (MVHR) and micro heat pump, (B) exhaust ventilation with exhaust air-to-water heat pump and ventilation radiators, and (C) exhaust ventilation with air-to-water heat pump and ventilation radiators, to a reference system: (D) exhaust ventilation with air-to-water heat pump and panel radiators. System A was modelled in MATLAB Simulink and systems B and C in TRNSYS 17.

Building simulation supports the understanding of how a given building operates according to certain criteria and enables comparisons of different design alternatives. The application of whole-building simulation and analysis has demonstrated a significant energy efficiency potential in many research studies. However, high energy performance building design involves handling the complex relationship between building and systems while considering numerous design parameters.

Many simulation runs, which are based on a trial-and-error approach, are required to be carried out by designer until finding a satisfactory solution. The success of this human-driven approach is based on skills and experience of the designer and it requires a significant amount of time to scan the entire design space.

To achieve an optimal design solution with less time and labour, the building simulation models can be solved iteratively by automated computer programming methods. This procedure is known as simulation-based optimization and it offers a great potential for overcoming the drawbacks of impracticality of simulation only methods (Nguyen et al. (2014).

2.5 Summary

Buildings are expected to create necessary conditions for its occupants. In order to create healthy environments, some internal environmental factors need to be controlled and adjusted.

Heat needs to be added to or removed from a space by passive or active means to maintain thermal comfort. Light needs to be provided to ensure visual comfort.

Indoor spaces need to be supplied with fresh air for good indoor air quality. All these vital requirements determine the building demand for energy.

Many studies suggest that energy performance of buildings is multi-dimensional and depends on several factors that are related to building architectural characteristics, indoor conditions, building systems, building-related renewable systems and site and climate conditions. Moreover, combined impact of these elements determines the building overall performance. A wide range of literature exists regarding the parameters influence building energy behaviour and how these parameters should be adjusted for better energy efficiency. However as a result of the inter-dependent interactions between building elements and the large number of parameters that impacts the building energy efficiency, it can be rather difficult to find the optimum design solution for a particular building that will satisfy many competing design objectives including energy efficiency, user comfort, cost, environmental impacts.

Building performance simulation tools are introduced in order to overcome the complexity of design problem of complex buildings. Such tools simulate the proposed design's response to climate and season. Therefore, designers can preview and improve the performance of interdependent building features such as orientation, building envelope, and various mechanical systems. Application of simulation in design process let different design scenarios be explored, analysed and compared for better efficiency. However, this task can be quite complicated and difficult due to complex nature of building energy behaviour and conflicts in economical, energy and comfort aspects. Many simulation attempts might be required until finding the best combination of many performance measures. It is believed that on the way to better building energy performance, this obstacle can be tackled with combination of mathematical optimization techniques with building performance simulation to automate the search for an optimal design.

3. SIMULATION-BASED BUILDING OPTIMIZATION

3.1 Introduction

Computer simulation is a powerful tool in analysis of complex real systems where models of systems are expressed in mathematical equations and then the behaviour of the models are observed under different conditions. As explained in the previous chapter, the simulation studies allow users to calculate and analyse the performance of a system in consideration. However, in real world complex problems, the performance usually depend on several factors and decision making often involves a challenge of simultaneously satisfying many conflicting objectives. Therefore, although proven effective, still the traditional scenario-based manual simulation methods can be quite labour-intensive and weak at finding the best solution for complex system problems.

In order to address the difficulties inherited in decision making via simulation, simulation-based optimization methods, which integrates optimization techniques into simulation analysis has been introduced (Fu, 2002). Optimization is a field of mathematics that deals with finding the extreme values of a function, subject to various constraints. During a simulation-optimization process, a simulation model and an optimization solver interact dynamically to explore a search space until an optimal solution based on an objective function and established constraints is obtained. The output of simulation corresponds to the function that is aimed to be minimized or maximized. The solver iteratively changes the values of the variables of the simulation model according to a search strategy. Therefore, simulation-based optimization techniques introduce the possibility of finding the best input variable values from among all possibilities without explicitly evaluating each possibility (Carson and Maria, 1997).

The integration of optimization techniques with simulation automate the search for the optimal or near optimal solutions in the design space, speed up the calculations and improve the solutions to multi-variable, multi-objective, and multi-criterion

problems. Therefore, in parallel with the advances in computing power in the last decade, the possibility of optimizing simulation models started to draw a significant attention in research community (Fu et al. 2005). Today, simulation-based optimization methods are successfully applied to a wide range of fields including engineering design in mechanical, civil, and chemical engineering, economics, production operations, transportation engineering, manufacturing, molecular biology, and finally building and systems design. (Papadrakakis and Lagaros, 2002; Qi et al, 2014; Gansterer et al., 2014; Chaudhry and Drake, 2009; Wells et al, 2012; Fesanghary et al., 2012).

Buildings are complex energy systems that consist of several interacting sub-systems, and as summarized in Chapter II, energy performance of buildings depends on numerous factors. Application of simulation-based optimization methods in building design started to draw attention of researchers especially in the last decade in order to support the development of cost-effective, environmentally friendly, highly energy-efficient buildings by bridging the gap between the steps of whole building design process.

This chapter introduces the basics of the optimization phenomenon. The following sections give main definitions; introduce optimization techniques and shares background on building design optimization. The optimization theory is discussed from building performance perspective and optimization tools and performance optimization methods which are used frequently for building design optimization are highlighted. Finally, the most recent studies in building design optimization field are summarized and the research gap is identified.

3.2 Simulation-based Optimization Basics

3.2.1 Main definitions

Carson and Maria (1997) explain that when the mathematical model of a system is studied using simulation, it is called a simulation model. In simulation-based analyses, system behaviour at specific values of input variables is evaluated by running the simulation model and the influence of some specific changes to design parameter values are tested manually by the user through a simulation experiment. However, when large numbers of input variables are involved and the simulation

model is complex, the simulation experiment may become computationally unfeasible.

As discussed by Dellino et al. (2014), simulation–optimization approach, which is based on the merging of optimization and simulation techniques, introduced the possibility of repeated analysis of the problem until finding a set of design parameters providing the best simulated performance.

A dictionary definition of the term optimization is an act, process, or methodology of making something (as a design, system, or decision) as fully perfect, functional, or effective as possible (Merriam-Webster, 2013). In mathematics, optimizations is defined as a mathematical programming technique for finding the maximum or minimum values of a specified function of several variables subject to a set of constraints without having to enumerate all of the possibilities (Liberti, 2008).

Any problem in which certain parameters need to be determined to satisfy constraints can be formulated as an optimization problem.

As mentioned by Rao (2009), existence of optimization methods can be traced back to the days of Newton, Lagrange, and Cauchy. However, development of the simplex method by Dantzig in 1947 for linear programming problems was the first technique to be referred as optimization. Since then, different modeling techniques have been developed to meet the requirement of different type of optimization problems.

The general single-objective, non-linear, constrained optimization problem can be written in the following generic form (Venter, 2010):

$$\begin{aligned} \text{Minimize : } & f(x) && R^n \rightarrow R \\ \text{Subject to } & g_j(x) \leq 0, && j = 1, \ldots, m. \\ & h_k(x) = 0, && k = 1, \ldots, p. \\ & x_{iL} \leq x_i \leq x_{iU} && k = 1, \ldots, n. \end{aligned} \tag{3.1}$$

In the equation 3.1, function f(x) represents the objective function, the functions $g_i(x)$ and $h_j(x)$ are the inequality and equality constraint functions, respectively. The vector $x = (x_1, \ldots, x_n)$ represents n design variables that are varied to reach the optimum. They are also called independent variables. The search space is defined by the upper and lower bounds, x_{iL} and x_{iU}, of the design variables, as side constraints.

The optimization problem in this equation is an abstraction of the problem of making the best possible choice of a vector in R_n from a set of candidate choices. The variable x represents the choice made; the constraints represent firm requirements or specifications that limit the possible choices and the objective value f(x) represents the cost of choosing x.

Objective function represents an equation to be maximized or minimized in the optimization theory under certain constraints. It defines the relationship between the design variables and quantifies the performance of the design. The efficiency and success of any optimization problem is greatly influenced by the properties and the formulation of the objective function.

Yang (2013) explains that for any optimization problem, the integrated components of the optimization process are the optimization algorithm, an efficient numerical simulator and a realistic-representation of the physical processes that designer wish to model and optimize. Carson and Maria (1997) illustrate a generic simulation optimization scheme as given in Figure 3.1. The optimization problem is introduced to the optimizer module as input. The optimizer module implements optimization algorithms and calls simulation model to generate the data. The output of the simulation model is used by the optimization strategy to provide feedback. This in turn guides further input to the simulation model. The simulation output is checked against an optimization criteria and a decision is made to accept the proposed solution or to continue the search process. The loop lasts until a stopping criterion is satisfied. Once the optimization process starts, it runs automatically without user interference. When the optimization is completed optimum or near-optimum solutions are returned.

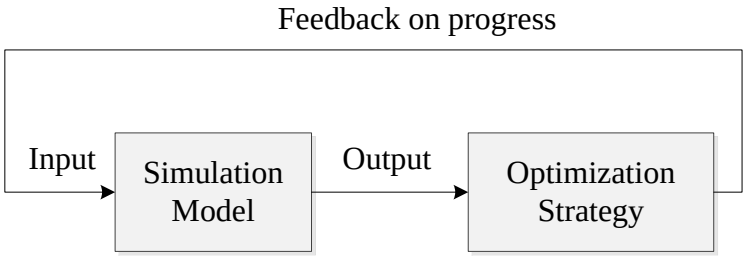

Figure 3.1 : A generic simulation-based optimization scheme.

Yang (2013) mentions three main issues in the simulation-driven optimization approach to consider carefully, and they are the efficiency of an algorithm, the efficiency and accuracy of a numerical simulator, and assigning right algorithms to the right problem.

As Yang (2013) further explains, simulations could be the most laborious part in an optimization process as they often require the evaluation of objective function many times using extensive computational tools. Therefore, an efficient solver is crucial. Moreover, an efficient optimizer is very important to ensure the optimal solutions are reachable.

However, despite its importance, there are no agreed guidelines for choosing the right algorithms for the right problems and no universally efficient algorithms for all types of problems are available. The choice of the algorithm largely depends on the type of the problem, the nature of an algorithm, the desired quality of solutions, the available computing resource, time limit, availability of the algorithm implementation, and the expertise of the decision-makers (Yang, 2013).

3.2.2 Classification of optimization problems

Formulating a real life problem as an optimization case strictly depends on the nature of the particular problem and there are many dimensions to consider before selecting solution techniques. There is not a definite classification of optimization problems in the literature and the classification can be carried out based on several different criteria as illustrated by Yang (2010), Raphael and Smith (2013) and Rao (2009) . However, in the current work the optimization problem is sorted into five broad categories following the common literature: nature of variables, shape of objective function, type of data, number of objectives, and type of constraints.

3.2.2.1 Nature of variables

As Yang (2010) explains, design variables can be continuous variables or discrete variables. A continuous variable can take any numerical value in some interval (with lower and upper bounds). However, a discrete variable can take only distinct, separate values typically from a list of permissible values. Both continuous and discrete variable could exist together in an optimization problem.

3.2.2.2 Shape of objective function

Based on the nature of equations for the objective function and the constraints, optimization problems can be classified as linear and nonlinear programming problems. If the objective function and all the constraints are linear functions of the independent variables, the optimization problem is called a linear programming problem; if not then it is called non-linear programming. Geometric and quadratic programming problems belong to the class of non-linear programming problems (Yang 2010).

3.2.2.3 Type of data

Based on deterministic nature of the variables, optimization problems can be classified as deterministic or stochastic programming problems. In, deterministic programming problems all the design variables are deterministic and the output of the simulation model can be fully determined by the parameter values and the initial conditions. On the other hand, stochastic optimization problems include random variables that can be expressed probabilistically. Therefore, problems having stochastic elements are generally not solved analytically (Ohnari, 1998).

3.2.2.4 Number of objectives

Based on the number of objective functions, optimization problem can be classified as single-objective and multi-objective problems. As previously explained in equation 3.1 that there is only a unique objective function to satisfy in single-objective optimization problem. However, multi-objective optimization deals with the task of simultaneously optimizing two or more conflicting objectives (Yang, 2010).

As summarized by Bandyopadhyayand and Saha, (2013), single objective optimization problems can be solved by application of calculus-based techniques, enumerative techniques and random techniques and it is possible to determine between any given pair of solutions if one is better than other is.

Multi-objective optimization problem can be described in mathematical terms as in equation 3.2 (Rao, 2010):

$$Find\ x = \begin{Bmatrix} x_1 \\ x_2 \\ \dots \\ x_n \end{Bmatrix}$$

Which minimizes $f_1(x),\ f_2(x),\ \dots,\ f_k(x)$

Subject to $g_j(x) \leq 0 \qquad j = 1, 2, \dots, m$ (3.2)

Where k denotes the number of objective functions to be minimized. Any or all of the functions may be nonlinear.

As Rao (2010), Caramia and Dell'Olmo (2008) and many others discuss, no solution vector x exist that minimizes all the k objectives simultaneously. Therefore, Pareto optimum solution concept is introduced in the literature. A feasible solution x is called Pareto optimal if there exist no other feasible solution y such that $f_i(y) \leq f_i(x)$ for $i = 1, 2, \dots, k$ with $f_i(y) < f_i(x)$ for at least one j. Thus, a feasible vector x is called Pareto optimal if there is no other feasible solution y that would reduce some objective function without causing a simultaneous increase in at least one other objective function. In other words, in the Pareto frontier none of the components can be improved without deterioration of at least one of the other components. Therefore, there is no single optimal solution but rather a set of optimal trade-offs exists.

Adding more than one objective to an optimization problem adds complexity. There are quite a number of methods available for solving a multi-objective optimization problem in the literature however only a short summary will be given.

Bandyopadhyayand and Saha (2013) categorize the approaches for solving multi-objective optimization problem as aggregating approaches, population-based non-Pareto approaches and Pareto-based approaches.

Aggregating approaches belongs to traditional methods where a multi-objective problem is often solved by combining its multiple objectives into one single-objective scalar function (Caramia and Dell'Olma, 2008). This group mainly includes weighted-sum approach, ε-Constraint approach, goal programming-based approach, and goal attainment-based approach.

In weighted-sum approach different objectives are combined using some weights w_i , i = 1, . . . , n (where n is the number of objectives). Then using these weights the

objective functions are merged into a new single function to be optimized as shown in equation 3.3.

$$min \sum_{i=1}^{n} w_i . f_i(x)$$
$$\sum_{i=1}^{n} w_i = 1 \qquad w_i > 0, \quad i = 1 \ldots . . n \quad x \in S, \tag{3.3}$$

The weighted-sum approach is simple and easy to implement however, there are two major drawbacks. As explained by Caramia and Dell'Olma (2008), the appropriate selection of the weights, which is up to the decision maker could be a challenge. Moreover, non-convex parts of the Pareto set cannot be reached by minimizing convex combinations of the objective functions.

In ε-Constraint approach designer chooses one objective out of n as the primary objective function to be minimized; the rest of the objectives are then constrained to be less than or equal to given target value, ε_i .

If $f_j(x)$ is taken as the objective function to be minimized, constraint approach takes the following form given in equation 3.4:

$$minf_j(x)$$
$$f_i(x) \leq \varepsilon_i, \quad \forall i \in \{1, \ldots, n\} \backslash \{j\} \qquad x \in S \tag{3.4}$$

ε-Constraint approach is efficient, easy to implement and it is able to achieve efficient points in a non-convex Pareto curve. However, selecting appropriate values for the ε vector is required to be addressed carefully (Bui and Alam, 2008).

In Goal programming-based approach designer assigns targets or goals (T_i) that wishes to achieve for each objective ($f_i(x)$). The optimum solution is then defined as the one that minimizes the deviations from the set goals as shown in equation 3.5 (Rao, 2009).

$$min \sum_{i=1}^{k} |f_i(x) - T_i| \qquad subject\ to\ x \in X, \tag{3.5}$$

In Goal attainment-based approach the designer is required to provide, along with the target vector, a weight vector w_i, relating the relative under- or overattainment of the objectives (Bandyopadhyayand and Saha, 2013).

Population-based non-Pareto approaches and Pareto-based approaches belong to metaheuristics Evolutionary Methods, (Zitzler, 1999). As stated by Surry et al. (1995), population-based search algorithms consider trying to use the population to hold solutions that represent different trade-offs.

Bhuvaneswari (2014) explains that, in Population-based non-Pareto approaches, the population of an evolutionary algorithm is used to diversify the search for the different objectives. Subpopulations are used to optimize each objective independently which are then shuffled together to obtain a new population to work on. Bandyopadhyayand and Saha, (2013) introduces some example to this approach as following: Vector evaluated genetic algorithm (number of subpopulations are generated by applying proportional selection according to each objective function in turn.), Lexicographic ordering (the objectives are ranked in order of importance by the user. The optimization is performed on these objectives according to this order.), Game theory-based approach (a player is associated with each objective.). Bhuvaneswari (2014) sees the main disadvantage of this approach generally as not directly incorporating the concept of Pareto dominance.

In Pareto-based approach, as described by Bhuvaneswari (2014), the aim is to determine an entire Pareto optimal solution set or a representative subset by attempting to promote the generation of multiple non-dominated solutions by making use of the actual definition of Pareto-optimality. Pareto optimal sets can be of varied sizes but the size of the Pareto set usually increases with the increase in the number of objectives. There are a few examples mentioned here representing Pareto-based approaches as given by Bandyopadhyayand and Saha, (2013):

Multiple objective genetic algorithm (MOGA): An individual is assigned a rank corresponding to the number of individuals in the current population by which it is dominated. This method has a very slow convergence rate, and there are some problems related to niche size parameters.

Niched Pareto genetic algorithm (NPGA): Pareto dominance-based tournament selection with a sample of the population is used to determine the winner between

two candidate solutions. This method suffers from the problem of selecting an appropriate value of the niche size parameter.

Non-dominated sorting genetic algorithm (NSGA): All non-dominated individuals are classified into one category, with a dummy fitness value proportional to the population size. This method has a very high convergence rate, but it also suffers from problems related to the niche size parameter.

Strength Pareto evolutionary algorithm (SPEA): This algorithm implements elitism explicitly by maintaining an external population called an archive. Its most limiting aspect is the use of clustering.

Strength Pareto evolutionary algorithm 2 (SPEA2): the fitness assignment is entirely based on the strength of the archive members. This method suffers from computationally expensive fitness and density calculations.

Elitist non-dominated sorting genetic algorithm (NSGA-II): The individuals in a population undergo nondominated sorting as in NSGA, and individuals are given ranks based on this.

Bui and Alam (2008) explain two major issues with application of Multi-objective Evolutionary Methods: how to get close to the Pareto optimal front since this is not an easy task, because converging to the Pareto optimal front is a stochastic process. In addition, how to keep diversity among the solutions in the obtained set is underlined. Evolutionary algorithms cannot guarantee finding optimal solutions in a finite amount of time and population approach may be computationally expensive. Moreover, a good parameter tuning is also required for maintaining a diverse population in order to prevent premature convergence (Zitzler 1999).

3.2.2.5 Type of constraints

Constrained optimization is the minimization of an objective function subject to constraints on the possible values of the design variables. However, some optimization problems do not involve any constraints and such problems are called unconstrained optimization problems (Rao, 2009).

In general, the constraints represent some functional relationships among the design variables and other design parameters. Constraints can be either equality constraints or inequality constraints.

There are several methods are available for solving an unconstrained nonlinear optimization problem and they are classified into two broad categories by Rao (2009) as direct search methods and descent (gradient) methods. Direct methods cover random search method, grid search method, univariate search methods, and pattern search method. Descent methods include Steepest descent (Cauchy) method, Fletcher–Reeves method, Newton's method, Marquardt method, Quasi-Newton methods.

There are also many methods available to deal with constrained nonlinear optimization problem. Rao (2009) classifies all the methods into two broad categories: direct methods and indirect methods. Direct methods include Random search methods, heuristic search methods, objective and constraint approximation methods, methods of feasible directions, generalized reduced gradient method. Indirect methods include transformation of variables technique and sequential unconstrained minimization techniques. In this work, only the penalty function methods that belong to sequential unconstrained minimization techniques will be discussed.

As mentioned by Weise (2009) the penalty methods are one of the most popular approaches for dealing with constraints. The idea of a penalty function method is to solve the general constrained optimization by first converting it to an equivalent unconstrained form. Then, this equivalent unconstrained problem is solved using a suitable unconstrained algorithm (Venter, 2010).

As explained by Rao (2010), the constraints are combined with the objective function f(x) in equation 3.6, resulting in a new function φ (x) which is then actually optimized.

$$Find\ x\ that\ \text{minimizes}\ f(x)$$

$$\text{Subject to} \qquad (3.6)$$

$$g_j(x) \leq 0, \quad j = 1,2,\ldots,m$$

This problem is converted into an unconstrained minimization problem by constructing a function of the form in equation 3.7.

$$\varphi_k = \varphi(X, r_k) = f(x) + r_k \sum_{j=1}^{m} G_j[g_j(x)] \tag{3.7}$$

Where G_j is some function of the constraint, g_j, and r_k is a positive constant known as the penalty parameter. The second term of the on the right side of the equation 3.7 is called penalty term.

Combining objective function with constraints is done in a way to ensure that an infeasible solution candidate has always a worse $\varphi_k$value than a feasible one with the same objective values.

The penalty function formulations for inequality constrained problems can be divided into two categories: interior and exterior methods.

In the interior penalty function methods, which are also called barrier methods, a new function (φ function) is constructed by augmenting a penalty term to the objective function. The penalty term is chosen such that its value will be small at points away from the constraint boundaries and will tend to infinity as the constraint boundaries are approached. The main formula for barrier methods has the following form in equation 3.8:

$$\varphi(\mathrm{X}, r_k) = f\,(X) - \, r_k \sum_{j=1}^{m} \frac{1}{g_j(X)} \tag{3.8}$$

In the exterior penalty function method, the φ function is generally taken as in equation 3.9

$$\varphi(\mathrm{X}, r_k) = f\,(X) + \, r_k \sum_{j=1}^{m} (g_j(X))^{q} \tag{3.9}$$

where r_k is a positive penalty parameter, the exponent q is a nonnegative constant, and the bracket function $(g_j(X))$ is defined as in equation 3.10

$$\begin{aligned} \Big(g_j(X)\Big) &= max\big(g_j(X), 0\big) \\ &= \begin{cases} g_j(X) & if\ g_j(X) > 0 (constraint\ is\ violated) \\ 0 & if\ g_j(X) \leq 0 (constraint\ is\ satisfied) \end{cases} \end{aligned} \tag{3.10}$$

Equation 3.9 shows that the effect of the second term on the right side is to increase $\varphi(X, r_k)$ in proportion to the q^{th} power of the amount by which the constraints are violated. Thus there will be a penalty for violating the constraints, and the amount of penalty will increase at a faster rate than will the amount of violation of a constraint for $q > 1$.

Gunaratne and Wu (2011) highlights the advantage of using a penalty function method that it is easy to implement, and does not require solving a nonlinear system of equations in every time step. However, the biggest drawback of these methods is related to the value of the penalty parameter. Jensen and Bard (2003) explain that this influence of penalty term is counterbalanced by f(x). Therefore, if the magnitude of the penalty term is small relative to the magnitude of f(x), minimization of φ_k may not result in feasible solutions. Moreover setting penalty term extremely large may lead to numerical ill-conditioning (Venter, 2010). However, if the value of the penalty term is made suitably large, the penalty term will exact such a heavy cost for any constraint violation that the minimization of the augmented objective function will yield a feasible solution (Jensen and Bard, 2003).

Weise (2009) discusses that a penalty for infeasibility can be integrated into the objective functions for several ways including static and dynamic approaches. Similarly, Deb and Agrawal (1999) claim that "although many researchers use adaptive variation of penalty parameters and penalty functions, the general conclusion is that these variations are specific to a problem and cannot be generalized". Therefore, contributions of the penalty terms are recommended to be adjusted relative to the magnitude of the objective function through design of experiment studies.

3.2.3 Optimization Algorithms

Deb (2012) describes an optimization algorithm as a procedure, which is executed iteratively by comparing various solutions until an optimum, or a satisfactory solution is found. The optimization algorithms require repetitive application of certain procedures therefore; they are executed through computers. The optimization field has advanced rapidly in the past few decades due to the development of computer power and as explained by Deb (2012), several new optimization methods,

computational techniques, and algorithms have been introduced to solve various problems that vary in nature.

There are many classification systems of optimization algorithms available in the literature however, in this research; the algorithms will be broadly classified into two distinct types, local algorithms and global algorithms, as suggested by Venter (2010).

3.2.3.1 Local optimization algorithms

Gaspero (2003) explains that the local optimization techniques are based on the iterative exploration of a solution space where a single design point is updated from one iteration to the next by applying local changes. According to Venter (2010), many of the local optimization algorithms are gradient-based where algorithms make use of gradient information to find the optimum solution. Therefore, the gradient-based approach requires a mathematical expression of the objective function. Some popular algorithms are mentioned below.

For the one-dimensional search, some of the popular algorithms include the Golden Section search, the Fibonacci search, and many variations of polynomial approximations.

One of the classical gradient-based optimization algorithms is Newton's algorithm. Newton's algorithm is an unconstrained algorithm that is derived from a second-order Taylor series expansion of the objective function about an initial design point.

For unconstrained problems, two very popular methods are the Fletcher-Reeves and the Broyden- Fletcher-Goldfarb-Shanno (BFGS) methods. The Fletcher-Reeves method makes use of conjugate search directions to reach the optimum.

For constrained optimization problems, Sequential Unconstrained Minimization Techniques and direct (or constrained) methods are available. The direct methods directly solve the non-linear constrained optimization problem. Sequential Linear Programming algorithm, the Modified Method of Feasible Directions algorithm, and the Sequential Quadratic Programming algorithm are commonly encountered in engineering.

Even though few in number, Venter (2010) also mentions that there are also non-gradient based local search algorithms are available such as Powell's algorithm,

Nelder-Mead simplex algorithm and Rosenbrock algorithm. They all are capable of solving non-linear, unconstrained optimization problems.

Local optimization algorithms are suitable for optimization problems with large numbers of design variables and they assure finding good results in reasonable calculation times, however they are trapped in local optimum.

3.2.3.2 Global optimization algorithms

The objective of global optimization is to find the globally best solution in the possible or known presence of multiple local optima. Venter (2010) argues that global optimization algorithms provide a much better chance of finding the global or near global optimum than the local algorithms. However, no algorithm can guarantee convergence on a global optimum in the general sense.

Global optimization algorithms are generally classified as either deterministic or stochastic algorithms.

Yagan and Tham (2006) mention that in classical deterministic optimization, it is assumed that perfect information is available about the objective function and this information is used then to determine the search direction in a deterministic manner at every step of the algorithm. However, such information may not be available for many design problems.

Deterministic methods for global optimization include branch methods, Cutting plane methods, and Interval methods. One popular general-purpose deterministic global optimization algorithm is the DIRECT algorithm. The algorithm locates promising sub-regions in the design space and then further explores each sub-region by using a local search technique (Venter, 2010).

Spall (2004) highlights that stochastic methods use randomness to be able to escape local optima, therefore the search for the optimal solution involves uncertainty due random nature of variables. The objective function is written as an expected value based on the random variables with probability distributions. A variety of computational methods then can be used to maximize or minimize the expected value.

Stochastic algorithms are mostly random search algorithms that use a population set. Examples include simulated annealing, tabu search, genetic algorithms, evolutionary

programming, particle swarm optimization, ant colony optimization, cross-entropy, stochastic approximation, multi-start and clustering algorithms (Zabinsky, 2003).

Population-based algorithms do not require any gradient information and they concern a population of solutions at a time. These methods are typically inspired by nature.

Liberty (2008) explains that stochastic algorithms are suitable for problems that are highly nonlinear, high dimensional, or otherwise inappropriate for classical deterministic algorithms. They are robust algorithms but they also require high computational time and power.

To summarize, an optimization problem can be approached by a number of different ways and there is no single optimization algorithm exists to solve all optimization problems.

All search methods have at least some limitations therefore, it is important to investigate and understand the nature of the problem first, and then select a suitable algorithm.

3.3 Simulation-based Building Design Optimization

Today buildings are becoming even more complex both in architectural and system design due to the constraints put on building performance by regulations. For instance, as explained by Attia (2013), the recast of the European Performance of Buildings Directive (EPBD) requires all new buildings to be "nearly zero energy" buildings (nZEB) by 2020, including existing buildings undergoing major renovations. The expectations from the building performance is increasing now and in order to achieve higher levels of building performance, there are more energy use-reducing options and technologies now has to be taken into account.

Making a design decision in general involves selection of the best or the most suitable design option among of all the feasible alternatives while satisfying multiple conflicting design objectives and constraints. In building design problem, due to the complex nature of building energy behaviour, numerous influential elements and conflicts in design aims such as economy, environmental performance and user comfort, it is a serious challenge to find the best design option and system configuration that satisfies all the expectations.

Building regulations, energy efficiency guidelines, and rule-of-thumb design methods has been used for conventional building design for years but they are now found to be inadequate addressing the requirements of highly energy-efficient building design.

Dynamic building simulation has become a powerful tool nowadays to evaluate the overall building performance. With support of simulation tools designers can investigate many design alternatives and a better design is iteratively proposed based on the performance of previous designs. However, this iterative trial-and-error process that is carried out manually cannot efficiently guide the design process to an optimal solution especially for complicated designs.

Simulation-based optimization techniques have been successfully applied to many real-world engineering design problems to support the complicated decision-making process (April et al., 2003; Ding et al., 2006; Fu et al., 2005). Moreover, due to its potential to automate the input and output, assess many options, and perform many simulations by mathematical means, it caught the attention of the building research community as well. In a building optimization study, the optimization process is usually occurs as the coupling between a building simulation program and an optimization 'engine' which may consists of one or several optimization algorithms or strategies as illustrated in Figure 3.2 by Nguyen et al. (2014).

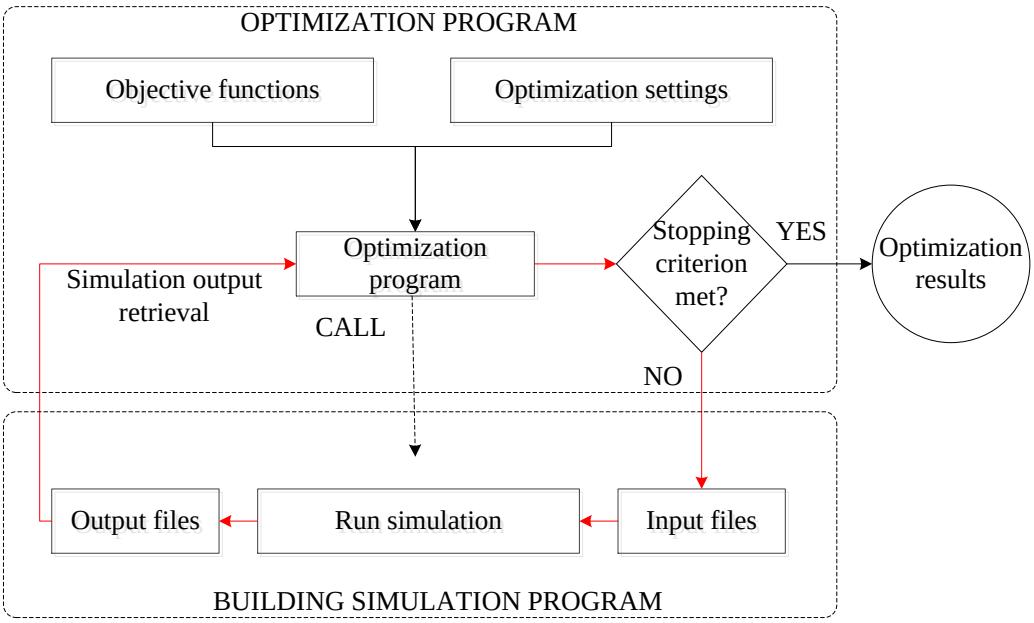

Figure 3.2 : The generic coupling loop applied to simulation-based optimization in building performance studies.

Earliest study in the field is conducted in a PhD research by Wright (1986) about the design optimization of HVAC systems in 1986. He implemented direct search methods to building simulation. Since then many researchers investigated the nature of the building design optimization problem and have studied the potential and applicability of simulation-based building optimization methods and possible obstacles were discussed from different perspectives in several studies including Palonen et al. (2001), Wright and Farmani (2001), Holst (2003), Wang et al (2005), Nassif et al. (2005), Caldas (2006), Fong et al. (2006), Hasan et al. (2008), Castro-Lacouture et al. (2009), Wright and Mourshed (2009), Mossolly et al. (2009), Kämpf and Robinson (2010), Bambrook et al. (2011), Fesanghary et al., (2012), Rapone and Saro (2012), Evins et al. (2012), Eisenhower et al. (2012), Nguyen and Reiter (2013), Wright et al. (2013), Nguyen et al. (2014), Petri et al. (2014), Ramallo-González and A. P, Coley (2014).

Nyungen et al. (2014) explored the trend of international optimization studies in the field of building science within the last two decades and he concluded that the interest on optimization techniques among building research has increased sharply since the year 2005 although the first efforts were found much earlier.

3.3.1 Optimization variables, design objectives and design space

Attia et al. (2013) reviewed 165 publications in building performance optimization field and found out that most frequently used variables are either energy related or economic related. According to their study, most common design variables includes building layout and form, geometry, position and density of fenestration, building envelope and fabric constructions, daylighting performance and automated control of solar shadings, natural ventilation strategies, shape and functional structure of buildings as well as heat source utilization, heating, ventilating, and air-conditioning (HVAC) systems sizing, HVAC system control parameters and/or strategy, thermal comfort, HVAC system configuration synthesis, managing of energy storage and automated model calibration. simultaneous optimization of building envelope and HVAC elements, simultaneous optimization of building construction, HVAC system size, and system supervisory control, simultaneous optimization of building construction, HVAC elements and energy supply system including renewable energy systems.

Evins et al. also contributed that, out of the 74 building performance optimization studies that they reviewed, the most frequently addressed category was building envelope in nearly 40% of works, followed by form, systems and renewables each accounted for around 20% of works, with controls and lighting occurring in very few cases.

Nguyen et al. (2014) explains that in building design optimization, design variables with integer or discrete values could be used. Discrete variables generally make the optimization problem nonconvex and cause the simulation output to be disordered and discontinuous. Therefore, solving optimization problems with discrete variables could be more difficult. Moreover, even with optimization problems where all inputs are continuous parameters, the nature of the building simulation programs itself could generate discontinuities in the simulation output.

In the literature, several optimization objectives were adopted in single or multi-objective form. Machairas et al. (2014) and Evins et al. (2013) mention in their review studies that the most frequently addressed design objectives are building energy consumption, life cycle cost, initial and operating costs, CO2 emission, environmental impact, and user comfort. Moreover, Nguyen et al. claim that about 60% of the building optimization studies used the single objective approach.

Attia et al. (2013) discussed in their building performance optimization review that the size and complexity of the addressed solution spaces vary in a wide range since some studies in the literature used detailed building simulation tools while others used simplified ones. There are three common strategies adopted in order to reduce the simulation time: using custom simplified thermal model instead of existed detailed software, using detailed simulation tools simulating geometrically simplified models: and finally, using detailed simulation tools for simulating a model only for a representative period.

A survey carried out by Nguyen et al. (2014) tells that EnergyPlus and TRNSYS are the mostly-used dynamic building simulation programs in optimization studies.

3.3.2 Search methods for building design optimization

Various optimization algorithms are available to couple with building simulation tools. Each algorithm has its own benefits as well as limitations therefore selection of

optimization algorithm directly depends on the nature of the optimization problem in consideration.

As explained previously, in simulation-based building optimization, the objective function is estimated using building simulation and since simulation tools make approximation of reality, it causes objective function to be non-linear, non-smooth and discontinuous for some parameters. As highlighted by Attia (2013) the deterministic algorithms need the evaluation functions to have particular mathematical properties like the continuity and the derivability consequently, methods might fail to contribute reliable results while handling discontinuous building and HVAC problems with highly constrained characteristics and multi-objective functions. Alternatively, gradient-free methods are based on stochastic approaches are more suitable to building applications since they allow exploration of the whole search space, eventually focusing on regions of interest only, and finally converging towards a near-optimal solution. With methods of this type, no hypothesis about the regularity of objective functions is necessary. This makes them easier to couple to building assessment tools. Therefore, as mentioned by Nguyen et al. (2014), stochastic population-based algorithms are the most frequently used methods in building performance optimization.

The performance of several optimization algorithms were tested and analysed in some studies. Wetter and Wright (2004) compared the performance of nine optimization algorithms using numerical experiments. Their study dealt with four main optimization classes: direct search algorithms (the coordinate search, the Hooke–Jeeves, and two versions of the Nelder–Mead simplex algorithm), stochastic population-based algorithms (a simple genetic algorithm (GA) and two particle swarm optimization (PSO) algorithms), a hybrid particle swarm Hooke–Jeeves algorithm and a gradient-based algorithm (the discrete Armijo gradient algorithm). The analyses are carried out through a simple and a complex simulation model.

Direct search methods do not require any information on the derivatives of the objective function. A General Pattern Search (GPS) algorithm defines some point around the current point and aims at the point with an objective function more desirable than the current point’s and searches along each coordinate direction for a decrease in objective function.

The Hooke–Jeeves algorithm has the same convergence properties on smooth cost functions as the coordinate search algorithm. However, it makes progressively bigger steps in the direction that has reduced the cost in previous iterations.

Stochastic population-based algorithms studied in the work belong to the family of evolutionary algorithms.

Genetic algorithm (GA) is a population-based algorithm that mimics the process of natural evolution. It generates solutions to optimization problems using techniques inspired by natural evolution, such as inheritance, mutation, selection, and crossover. PSO algorithm was proposed first by Eberhart and Kennedy (1995). Individuals are here called particles, and they move round in the search-space according to simple mathematical formula over the particle's position and velocity. The change of each particle from one iteration to the next is modeled based on the social behaviour of flocks of birds or schools of fish.

The hybrid global optimization algorithm does a PSO on a mesh for the first iterations. Afterwards, it starts the Hooke–Jeeves algorithm.

The Nelder Mead simplex algorithm attempts to minimize a scalar-valued nonlinear function of n real variables using only function values, without any derivative information.

Armijo is a line search method, which can be used to minimize smooth functions. It approximates gradients by finite differences, with the difference increment reduced as the optimization progresses.

The analysis by Wetter and Wright (2004) showed that the gradient-based Armijo method failed far from the optimal solution even for the simpler problem. Similarly, the Nelder–Mead algorithm did not perform well on the test problems as well. It required a high number of simulations, and in one test case, it failed far from the minimum. Neither of the algorithms is recommended for building performance optimization problems.

Moreover, according to results the coordinate search algorithm tends to fail far from the minimum if the detailed simulation model is used. On the same problems, the Hooke–Jeeves algorithm also jammed less frequently compared to the coordinate search algorithm, which may be due to the larger steps that are taken in the global exploration.

Both GA and PSO algorithms performed well, where the simple GA got close to a solution with a low number of simulations. However, the biggest cost reduction was obtained with the hybrid PSO-Hooke Jeeves algorithm but it required a greater number of simulations.

Similarly, Kämpf et al. (2010) analysed the performance of two hybrid algorithms that are Particle swarm optimization coupled with Hooke Jeeves (PSO-HJ) and covariance matrix adaptation evolution strategy coupled with hybrid differential evolution algorithms (CMAES/HDE) in optimizing 5 standard benchmark functions through EnergyPlus simulation tool. The results showed that CMAES/HDE performed better than the PSO-HJ in solving the benchmark functions with 10 dimensions or less. However, if the number of dimensions is larger than 10, the PSO-HJ performed better.

Moreover Brownlee et al. (2011) investigated the performance of five multi-objective algorithms, namely IBEA, MOCell, NSGA-II, SPEA2 and PAES on a multi-objective problem concerning window placement. The results showed that NSGA-II showed the best performance among all.

3.3.2.1 Building performance optimization tools

There are several computer tools are available to solve an optimization problem once it has been properly formulated. Numerous decent algorithms are implemented in these programs to deal with different kind of optimization issues.

Some tools include optimization algorithm libraries that can search for best design option for general optimization problems.

Nyungen et al. (2014), Machairas et al. (2014) and Attia et al. (2013) explored the stand-alone optimization tools used in building optimization studies and the most frequently mentioned tools are found to be GenOpt, Matlab Optimization Toolbox, and modeFrontier. Some less frequent tools are named as GENE_ARCH, Dakota, jEPlus, Topgui and Toplight. Moreover Nguyen et al. (2014) mentioned a new free tool, MOBO, as showing promising capabilities to become the major optimization engine in coming years.

In this study, only the tools that caught the most of the attention of research community will be introduced shortly.

GenOpt®

GenOpt is a generic optimization program developed at Lawrence Berkeley National Laboratory that has implemented a number of optimization algorithms (GenOpt, 2012). It is a stand-alone program that is designed to be coupled with any simulation program that reads from and writes to text files. GenOpt is designed to work with programs where the derivative of the cost function is not available or may not even exist. GenOpt can handle single-objective optimization with continuous and discrete variables and some constraints.

The algorithms that are available in GenOpt's library are: Coordinate Search Algorithm, Hooke-Jeeves Algorithm, Multi-Start GPS Algorithms, Discrete Armijo Gradient, Particle Swarm Optimization, Hybrid Generalized Pattern Search Algorithm with Particle Swarm Optimization Algorithm, Simplex Algorithm of Nelder and Mead with the Extension of O'Neill, Interval Division Algorithms, and Algorithms for Parametric Runs.

Since one of GenOpt's main application fields is building energy use or operation cost optimization, GenOpt has been designed such that it addresses the special properties of optimization problems in this area.

GenOpt has been used in several building optimization studies including Wetter and Wright (2004), Djuric et al. (2007), Coffey (2008), Hasan et al. (2008), Magnier et al. (2009), Kämpf et al. (2010), Coffey et al. (2010), Seo et al. (2011), Boonbumroong et al. (2011), Stephan et al. (2011), Asadi et al. (2012), Rapone and Saro (2012), Bigot et al. (2013), Ali et al. (2013), Cvetković and Bojić (2014), Ferrara (2014), Joe et al. (2014).

MATLAB® Optimization Toolbox

Optimization Toolbox™ extends the MATLAB® technical computing environment with tools and widely used algorithms for standard and large-scale optimization. These algorithms solve constrained and unconstrained continuous and discrete problems. The toolbox includes functions for linear programming, quadratic programming, nonlinear optimization, nonlinear least squares, solving systems of nonlinear equations, multi-objective optimization, and binary integer programming Moreover, MATLAB Global Optimization Toolbox includes global search, multistart, pattern search, genetic algorithm, and simulated annealing solvers (Matlab, 2012a).

MATLAB optimization environment has been used in a variety of studies including Shea et al. (2006), Jacob et al. (2010), Hamdy et al. (2011), Asadi et al. (2012), Trubiano et al. (2013), Asadi et al. (2014), Murray et al. (2014).

modeFRONTIER®

modeFRONTIER is an integration platform for multi-objective and multi-disciplinary optimization. It provides a seamless coupling with third party engineering tools, enables the automation of the design simulation process, and facilitates analytic decision making. modeFRONTIER has a rich optimization algorithm library covering deterministic, stochastic and heuristic methods for both single and multi-objective problems including Levenberg-Marquart, Broyden–Fletcher–Goldfarb–Shanno, Sequential quadratic programming, Multi-objective Genetic Algorithm (MOGA-II),Adaptive range Multi-objective Genetic Algorithm (ARMOGA), Fast Multi-objective Genetic Algorithm (FMOGA-II), Non-dominated Sorting Genetic Algorithm (NSGA-II), Multi-objective Particle Swarm Optimization and Multi-objective Simulated Annealing (Esteco, 2014).

MATLAB optimization environment has been used in a variety of studies including Suga et al. (2010), Hoes et al. (2011), Shi (2011), Loonen et al. (2011), Padovan and Manzan (2014), Manzan (2014), Baglivo et al. (2014).

3.3.3 Research gap

The literature review carried out within the scope of this work reveals that building performance optimization studies centres around two main aims: to develop mathematical search techniques and optimization algorithms that can effectively address building design optimization problem, and to develop approaches that can more efficiently formulate the building optimization problem.

Some of the studies regarding the development of advanced search techniques are briefly mentioned below.

Wright and Zhang (2005) introduced a new evolutionary algorithm operator (an ageing operator) that prevents topology dominance by penalizing solutions that have a dominant topology through a synthesis of HVAC system configurations.

Hamdy et al. (2009), aimed to evaluate how combinations of optimization algorithms can achieve faster and/or better solutions for multi-objective optimization problems.

Kamps and Robinson (2009) developed a hybrid of the covariance matrix adaptation evolution strategy (CMAES) and hybrid differential evolution (HDE) algorithms coupled with an efficient backwards ray tracing technique. They concentrated on the formulation of the new hybrid algorithm and its testing using standard benchmarks as well as a solar optimization problem.

Evins et al. (2010) investigated the configuration of a Genetic Algorithm for optimization of solar gain, in terms of various seeding, selection and fitness options as well as different parameter values.

Caldas and Norford (2012) used the concepts of generative and goal-oriented design to propose a computer tool that can help the designer to generate and evaluate certain aspects of a solution towards an optimized behaviour of the final configuration by adopting a micro-GA procedure.

Eisenhower et al. (2012) developed an approach to perform optimization of building energy models using a meta-model generated from sample design and operation scenarios of the building around its baseline.

Tresidder et al. (2012) used Kriging surrogate modelling optimization techniques on a building design problem with discrete design choices through comprehensive analysis using a multi-processor computer.

In addition to efforts aimed at improving search techniques, there are also several studies concerning definition and mathematical formulation of building design optimization problem. As introduced in the previous sections, building performance optimization is a multi-parametric and multi-dimensional problem with constraints and discontinuities. Wide range of parameters are available as independent variables from different perspectives such as building architectural design elements (e.g. building envelope constructions, building form, orientation, aspect ratio), HVAC system elements (e.g. system type, equipment type, efficiency, and operation characteristics), and energy generation (e.g. system type, equipment type, efficiency, and operation characteristics). Moreover, as far as objective functions are concerned, most of the time they are energy consumption, energy cost, capital cost, lifecycle cost environmental impact and the occupant's comfort in single or multi-objective form. Therefore, the studies in building performance optimization field vary in a

wide range from single-objective problems with involvement of fewer variables to multi-objective holistic approaches as briefly summarized below.

Application of optimization techniques for building architectural design has received a notable attention in the research community.

Al-Homoud (2005) presented an optimization model that utilizes a direct search optimization technique incorporated with an hourly building energy simulation program for the optimum thermal design of building envelopes for minimum annual source energy use. Design variables of the study included siting, building shape, glazing, wall and roof construction, massing, infiltration, and operational parameters (lighting, equipment and occupancy load).

Wang et al. (2005) presented a multi-objective optimization model that could assist designers in green building design based on genetic algorithm. Life cycle analysis methodology is employed to evaluate design alternatives for both economic and environmental criteria. Life cycle environmental impacts are evaluated in terms of expanded cumulative exergy consumption. Variables in the model included building orientation, aspect ratio, window type, window-to-wall ratio, wall layer, roof type, and roof layer.

Znouda et al. (2007) presented an optimization method that coupled genetic algorithms, with a simplified tool for building thermal evaluation (CHEOPS) for minimizing the energy consumption of Mediterranean buildings. The aim of the optimization was to identify the best envelope configurations from both energetic and economic points of view. Dimensions of the building envelope and its shape, types of roofing and walls and solar protection represented by solar factors were investigated as design variables.

Yi and Malkawi (2009) developed a new method for performance-based form-making. The research proposed a new representation for building geometry, controlled by introducing hierarchical relationships between points (nodes) to allow the user to explore the building geometry without being restricted to a box or simple form. The Genetic Algorithm was used as the technique for optimization. The objective function for the evaluation included targets surface heat flow, heat gain, heat loss, and volume.

Tuhus-Dubrow and Krarti (2010) developed a simulation–optimization tool based on genetic algorithm to optimize building shape (including rectangle, L, T, cross, U, H, and trapezoid) and building envelope features (including wall and roof constructions, foundation types, insulation levels, and window types and areas) in order to minimize energy use for residential buildings.

Gagne and Anderson (2010) developed a genetic algorithm based methodology for determining the set of facade parameters (window-to-wall ratio, glazing transmissivity, overhang depth, among others) that, for a given massing model, maximizes the space's illuminance within a specified range, while minimizing the space's glare potential. Their approach used the Lightsolve Viewer coupled with an approximation of the Daylighting Glare Probability.

Fesanghary et al. (2012) developed a multi-objective optimization model based on harmony search algorithm to minimize the life cycle cost (LCC) and carbon dioxide equivalent (CO_2-eq) emissions of the buildings by varying building constructions including wall, roof, ceiling and floor construction materials as well as glazing type.

Jin and Jeong (2014) proposed a free-form building shape optimization process based on the genetic algorithm. Geometric modeling of a model free-form building was performed using a parametric design method with Rhinoceros. Their study showed that the proposed process could rapidly predict and optimize the variation of the heat gain and loss characteristics that was caused by changing the building shape.

Furthermore, application of optimization techniques to design and control of HVAC systems has been addressed in several studies.

Wright et al. (2002) investigated the application of a multi-objective genetic algorithm (MOGA) search method in the identification of the optimum pay-off characteristic between the energy cost of a building and the occupant thermal discomfort through the design of a single zone “all outside air” HVAC system. The problem variables were formed from the control system set points and the size of the HVAC components, which was represented by the width, height, number of rows, and number of water circuits of each coil and the supply fan diameter. The maximum water flow rate to each coil was also a problem variable.

Lu et al. (2004) proposed a model-based optimization strategy for the condenser water loop of centralized heating, ventilation and air conditioning (HVAC) systems.

The objective of the work was to minimize the total energy consumption of the condenser water loop. Based on the mathematical models of related components, the operating characteristics of cooling towers, the effects of different ambient environment and the interactions between chillers and cooling towers, the energy efficiency of the condenser water loop was maximized by both variable water flow rate and air flow rate. A modified genetic algorithm was used to search for optimal values of the independent variables.

Nassif et al. (2005) also used multi-criteria GAs to explore optimal control strategies for HVAC systems for the objective functions of energy cost and thermal comfort.

Fong et al. (2006) proposed a simulation-optimization approach for the effective energy management of HVAC system where it is necessary to suggest optimum settings for different operations in response to the dynamic cooling loads and changing weather conditions throughout a year. A metaheuristic simulation–EP (evolutionary programming) coupling approach was developed using evolutionary programming for minimizing energy consumption. The problem parameters to be optimized included chilled water supply temperature of chiller and supply air temperature of Air Handling Unit.

Fong et al. (2009) introduced a robust evolutionary algorithm (REA) to tackle this nature of the HVAC simulation models. REA is based on one of the paradigms of evolutionary algorithm, evolution strategy, which is a stochastic population-based searching technique emphasized on mutation. The REA, which incorporates the Cauchy deterministic mutation, tournament selection and arithmetic recombination, would provide a synergetic effect for optimal search. By using REA for optimization, a monthly reset scheme of both chilled water supply temperature and supply air temperature of a centralized HVAC system was recommended. T The objective was to minimize the monthly energy consumption with both the optimal or an installed centralized heating, ventilating and air conditioning (HVAC) system, appropriate energy management measures would achieve energy conservation targets through the optimal control and operation.

Kusiak et. al. (2011a) presented a data-driven approach for the optimization of a heating, ventilation, and air conditioning (HVAC) system in an office building. A neural network (NN) algorithm was used to build a predictive model. The NN-

derived predictive model is then optimized with a strength multi-objective particle-swarm optimization (S-MOPSO) algorithm. The relationship between energy consumption and thermal comfort measured with temperature and humidity was discussed. The control settings derived from optimization of the model minimize energy consumption while maintaining thermal comfort at an acceptable level. Parameters including air handling unit supply air temperature set point and supply air duct static pressure set point were taken as design variables. The solutions derived by the S-MOPSO algorithm pointed to a large number of control alternatives for an HVAC system, representing a range of trade-offs between thermal comfort and energy consumption.

Kusiak et al. (2011b) presented a data-mining approach for the optimization of a HVAC (heating, ventilation, and air conditioning) system. A predictive model of the HVAC system is derived by data-mining algorithms, using a dataset collected from an experiment conducted at a research facility. To minimize the energy while maintaining the corresponding indoor air quality within a user-defined range, a multi-objective optimization model is developed. The solutions of this model are set points of the control system derived with an evolutionary computation algorithm.

Kusiak and Xu (2012) proposed an optimization model derived by a dynamic neural network based on the concept of a non-linear autoregressive with external input. The energy consumption of a heating, ventilating and air conditioning (HVAC) system is optimized by using a data-driven approach while maintaining indoor room temperature at an acceptable level. The model is solved with three variants of the multi-objective particle swarm optimization algorithm.

Vakiloroaya et al. (2014) developed an optimization methodology to explore the influence of the thermo-economical design optimization of the finned-tube condenser coil on system cost and energy consumption in an existing direct expansion rooftop package air conditioning system. Using this method, the frontal area of the condenser coil is maintained as constant, while other geometrical parameters of the thermal and economic performance of the system are varied and investigated. A mixed heuristic–deterministic optimization algorithm was implemented to determine the synthesis and design variables that influence the cost and energy efficiency of each configuration.

In addition to the optimization studies regarding building and HVAC system elements, renewable energy generation and building integration was studied in several research work as well.

Optimization of sizes, components and control strategies of stand-alone renewable energy systems such as PV and/or Wind and/or Diesel systems has been investigated in the works of Borowy and Salameh (1995), Ashari and Nayar (1996), Chedid and Saliba (1996), Kaiser et al. (1997), Morgan et al (1997), Dufo-Lopez and Bernal-Agustin (2005), and Koutroulis et al (2006). Typically, the optimum design is carried out minimizing the Net Present Cost or by minimizing total cost of the entire hybrid system divided by the energy supplied by the hybrid system.

Smilarly, Boonbumroong et al. (2011) presented a technique on how to optimize the configuration of a typical AC-coupling stand-alone hybrid power system with particle swarm optimization. The minimization of the objective function was evaluated using TRNSYS 16 in assistance with GenOpt optimization program.

While most of current research concentrates on stand-alone renewable system, there appears to be a few studies on grid-connected renewables including feasibility analysis of integrating PV systems into the grid or the optimization of PV panel design for its long-term operation (Ashraf et al, 2004; Celik, 2006; Liu et al, 2012).

Efficiency of building integrated renewable systems is directly related to the dynamic performance of the buildings they serve to. In addition to optimization studies about stand-alone or grid connected renewable systems there has been some attempts to evaluate renewable system performance together with buildings they are integrated.

Charron and Athienitis (2006) conducted a theoretical investigation in order to optimize performance of double façades with integrated photovoltaics and motorized blinds. Key parameters affecting the overall performance of building-integrated photovoltaic thermal (BIPV/T) double façades have been investigated.

Zogou and Stapountzis (2011a) investigated the transient thermal behaviour of the basic structural module of a double-skin photovoltaic façade in real insolation conditions. The results are employed in the validation and further improvement of integration of a BIPV concept to the HVAC system of a building.

Moreover, they examined an improved concept of incorporating PV modules to the south façades of an office building, exploiting both the electricity produced and the

heat rejected by the module, to increase building energy efficiency (Zogou and Stapountzis, 2011b).

Talebizadeh et al. (2011) proposed a Genetic Algorithm based approach to calculate the optimum slope and surface azimuth angles for solar collectors to receive maximum solar radiation. The optimum angles and the collector input solar energies for these angles are calculated in hourly, daily, monthly, seasonally and yearly bases respectively.

Bornatico et al. (2012) presented a methodology for finding the optimal size of the main components for a solar thermal system where particular attention is given to the optimization framework. The use of the PSO algorithm is proposed. They used a weighted-sum approach to combine the objectives of solar fraction (maximized), with energy use and construction cost (minimized). The variables of the study included collector area, tank volume and auxiliary power unit size.

Griego et al. (2012) aimed to evaluate various combinations of energy efficiency and thermal comfort measures to arrive at an optimum set of recommendations for existing residential and new construction residential buildings. The two renewable energy technologies including solar domestic hot water systems and photovoltaic systems evaluated in the study. The optimum point is the minimum annualized energy related costs and the corresponding annual source energy savings.

A simultaneous optimization of building architectural elements, HVAC system design and control and building integrated energy generation would be the most desirable target. However, the problem arises in dealing simultaneously with these potentially conflicting objectives and numerous design variables. There are some studies aimed at developing holistic approaches to combine some of these aspects.

Wright and Farmani (2001) studied the simultaneous optimization of building's fabric construction, the size of heating, ventilating and air conditioning system, and the HVAC system supervisory control strategy with respect to the operating energy cost of the HVAC system. The optimization problem has been solved using a Genetic Algorithm search method through design day calculations. The design variables included ONN/OFF status of the HVAC system, coil width and height, number of rows and water circuits, water flow rate, fan size, building weight, glazing type, glazing area.

Wright et. al. (2002) investigated the application of a multi-criterion genetic algorithm in the search for a non-dominated (Pareto) set of solutions to pay-off between energy cost and occupant discomfort. Optimization variables included HVAC system size (coil and supply fan sizes) and control strategy (supply air temperature and flow rate setpoints for each hour of the day).

Bichiou and Krarti (2011) developed an energy simulation environment to optimally select HVAC system type and its operation settings but together with building envelope features to minimize the life cycle cost of operating a residential building. A wide range of HVAC system types was considered in the study to meet heating and cooling requirements for single-family residential buildings. The considered design variables were: building orientation, building aspect ratio and shape (rectangle, L, T, cross, trapezoid), foundation insulation, wall insulation, roof insulation, infiltration, window type, window-to-wall ratio, thermal mass, overhang dimensions, heating and cooling set points, heating efficiency and HVAC system type. Three optimization algorithms were considered in the simulation environment including Genetic Algorithm, the Particle Swarm Algorithm and the Sequential Search algorithm. Different HVAC system types are investigated separately and prior to comparisons.

Chantrelle et al. (2011) aimed to develop a multicriteria tool, MultiOpt, for the optimization of renovation operations, with an emphasis on building envelopes, heating and cooling loads and control strategies. MultiOpt is based on existing assessment software and methods: it uses a genetic algorithm (NSGA-II) coupled to TRNSYS, and economic and environmental databases. The design variables included external wall type, roof type, ground floor type, intermediate floor type, partition wall type and window type, shade control, namely the threshold value for the illumination of the facade and the dead band associated with the on–off controller. He objective of the optimization was to minimize the values of four criteria: environmental impact, cost, energy consumption and thermal discomfort.

Hamdy et. al. (2011) evaluated the impact of the Finnish national adaptive thermal-comfort criteria on energy performance in an office building. Two fully mechanically air-conditioned single offices are taken as representative zones. A simulation based optimization scheme (a combination of IDA-ICE 4.0 and a multi-objective genetic-algorithm from MATLAB-2008a) was employed to determine the minimum primary

energy use and the minimum room cooling-equipment size required for different thermal comfort levels. The applicability of implementing energy-saving measures such as night ventilation, night set-back temperature, day lighting as well as optimal building envelope and optimal HVAC settings were addressed by investigating design variables including supply air temperature profile, night ventilation control strategy, maximum power of the cooling beam, radiator set-point and night set-back temperature, window U-value, internal shading darkness.

Evins et al. (2012) optimized the cost and energy use of a modular building for different climate types. The variables included constructions (U-values, shading), HVAC and renewables (PV, solar thermal). The objectives were carbon emissions and construction cost, and the optimization was performed using a multi-objective genetic algorithm. Shading was optimized using a local search, which was embedded in the Genetic Algorithm used for all other variables. The heating and cooling systems were modelled in the thermal simulation as ideal loads systems. The different system choices were then applied using the efficiencies and carbon factors. Energy available from solar hot water and PV systems was modelled based on the available incident solar radiation on an angled surface present in the model.

Ihm and Krarti (2012) applied a sequential search technique to optimize the design of residential buildings in Tunisia in order to minimize their life cycle energy costs while maximizing energy efficiency and thermal comfort. In the analysis, design features including orientation, window location and size, glazing type, wall and roof insulation levels, infiltration levels, lighting fixtures, appliances, and efficiencies of heating and cooling systems are investigated as pre-defined energy efficiency measures.

Asadi et al. (2012) proposed a simulation-based multi-objective optimization scheme, a combination of TRNSYS, GenOpt and a Tchebycheff optimization technique, developed in MATLAB to optimize the retrofit cost, energy savings and thermal comfort of a residential building. A wide decision space is considered, including alternative materials for the external walls insulation, roof insulation, different window types, and solar collector types.

Fesanghary et al. (2012) aimed to develop a multi-objective optimization model based on harmony search algorithm to find an optimal building envelope design that

minimizes the life cycle costs and carbon dioxide equivalent (CO2-eq) emissions of the buildings. Several building envelope parameters including wall, roof, ceiling and floor construction materials as well as glazing type are taken as the design variables. All phases of the life of a building including pre-use, use and end-of-life was considered in the study. A series of Pareto optimal solutions was identified, which can help designers to get a better understanding of the trade-off relation between the economic and environmental performances.

Rapone and Saro (2012) studied a typical curtain wall facade of an office in order to find the configuration of parameters including type of glass installed, percentage of glazed surface, depth of the louvers and spacing of the louvers that minimizes the total carbon emissions arising from building operation. A real HVAC system is not modeled instead, an overall annual efficiency of the heating system and a coefficient of performance of the cooling system were assumed to convert the building loads to consumption values. A PSO algorithm coupled to EnergyPlus dynamic energy simulation engine.

To conclude, the literature review showed that building performance optimization has received a great deal of attention in building research community and there is certain amount of work has been done on a variety of issues. Some of the research efforts mainly focused on developing efficient search techniques and algorithms suitable for the building design optimization problem while majority of the studies concentrated on problem formulation.

Most of the problem formulation approaches focused mainly on optimal design of building architectural design characteristics (construction/envelope parameters). Moreover, HVAC system design and efficient operation of individual devices through optimization has been investigated, too. There are also some studies proposed to address renewable system and component design with application of optimization. However, holistic approaches that aim to combine building architectural features, HVAC system features and renewable generation features simultaneously while taking into account various dimensions of building performance are in limited number.

In previous studies when a high number of design variables regarding building architectural design elements are addressed, usually predefined and simplified

HVAC and/or renewable energy generation models were used for investigating the system side. Therefore, the optimal capacities of the HVAC system equipment were explored at only on-reference conditions neglecting the equipment dynamic performance. Similarly, when dynamic system models were integrated, only supervisory control of an entire system, optimal set-point configurations, and the optimal start time were mainly explored. Moreover, balancing HVAC and renewable system options were not deeply investigated and integrated into the optimization models.

Moreover, in many of the studies, design variables are defined in a continuously varying range because of the difficulty for numerical optimization methods to deal with discrete variables. However, this may result in a mismatch between the optimization recommendations and actual products and optimization results may lead to unfeasible solutions by market standards. Even some studies addressed building envelope options as limited discrete parameters still no work provided an approach that can deal with fully dynamic HVAC and renewable operation conditions.

Furthermore, the environmental issues, such as CO2 emissions and the interaction of building with electricity grid have not been taken into account in most studies.

In addition to design variable definition, majority of the studies focused on two objectives either in weight-sum single objective or in multi-objective forms. For instance, carbon dioxide equivalent emissions and investment cost, carbon dioxide equivalent emissions and life cycle cost, energy demand and thermal comfort are sought together. In few cases, some studies proposed three objectives such as energy demand, carbon dioxide equivalent emissions, investment cost, or energy demand, thermal comfort and investment cost are examined together.

In order to address the above mentioned limitations and to contribute to the building design optimization field, a simulation based optimization method that can quantitatively and simultaneously assess combinations of building architectural design elements together with actual technology choices from building envelope, HVAC system equipment and renewable energy generation systems is aimed to be developed.

3.4 Summary

Efficient building design requires is a multi-disciplinary integrated design approach starting from the early design phases. Optimization of building performance through coupling computerized building simulations tools with optimization algorithms provides a promising approach to the practice of high performance building design.

The literature review revealed that there is an ever-increasing interest on building design optimization studies. The application of optimization techniques for the design of the building characteristics, design of building HVAC systems, design of building integrated renewable systems, and design of control strategy setting were investigated in several research studies.

As mentioned earlier, today many optimization methods are available. However, when coupled with building simulation tools; a fast, effective and consistent algorithm would be preferred. Gradient-based algorithms are limited to differentiable functions, can converge to local optimum and consequently, display several weaknesses when coupled with simulation tools. On the other hand, gradient-free algorithms such as GA and PSO have proven to be efficient in terms of building optimization, and are more suitable.

Many design objectives such as life cycle costs, energy consumption, greenhouse gas emissions, indoor air quality, and occupant comfort were aimed to be improved via aggregated single-objective or multi-objective approaches. Studies showed that adding objectives also adds complexity to the design optimization problem.

In the literature, a certain amount of work has been done on optimizing building architectural design characteristics. Moreover, HVAC system design and operation through optimization has been deeply investigated, too. Best combinations of building envelope and HVAC system features were explored in a few studies. There are studies available that aim to address renewable system and component design with application of optimization.

Although the body of literature on building simulation-optimization is extensive, very limited studies have been attempted to include the various dimensions of building performance in one single approach. There is still a strong need for an integrated optimization of building design, HVAC systems, building integrated renewable systems design simultaneously and dynamically.

4. THE METHODOLOGY

4.1 Introduction

There is a growing interest in high energy performance building design, as it is now accepted as an encouraging solution to deal with the increasing pressure placed on environment by building sector. Advances in building science and technology have introduced many approaches and options today that can help improving building performance; however, designing buildings for energy efficiency is still not straightforward. Although buildings have commonalities, they are also unique in the sense that they are built to satisfy different needs in different locations for different purposes. As discussed previously in Chapter II, many studies suggest that energy performance of buildings is a multi-dimensional issue and depends on several factors that are related to building architectural characteristics, indoor conditions, building systems, building integrated renewable systems and site and climate conditions. Moreover, combined impact of these elements determines the building overall performance. A good balance of several design objectives is required to be established through adjusting all the influential building design elements.

In addition to energy efficiency, decision-makers also need to carefully assess economic viability of the energy efficiency measures, and the resulting environmental and comfort performances as well. For instance, the recast of the European Energy Performance of Buildings Directive (2010/31/EU) proposes to define the energy performance of buildings "with a view to achieving cost-optimal levels". Similarly, the directive also targets for all new buildings in the EU to be 'Nearly Zero-Energy Buildings' from year 2020. The cost-optimality and nearly zero-energy perspectives links building performance requirements to energy, environmental and financial targets therefore, it could be rather difficult for designers to select what design strategies to adopt and which technologies to implement among many, while satisfying several equally valued and beneficial objectives driven by individual building needs.

Today, conventional building design practices where team members with different specialties consecutively realize different project goals independent of each other are not capable of addressing the requirements of high energy performance buildings. In conventional approaches, for instance, architect initially works on building architectural design characteristics mainly focusing on building form, massing, orientation, general exterior appearance and envelope. Once the main decisions are made and the concept is complete, the mechanical engineers, lighting designers and renewable energy specialist are invited to design appropriate systems for the building in consideration and to select suitable equipment. Building architectural and envelope design have significant impacts on building energy, lighting, and comfort performance since building loads are directly affected by the overall thermal performance of the building structure. Therefore, even using the state-of-the-art energy technologies at this stage can only have limited impact on the overall efficiency because the passive solar potential of the building is not well explored and integrated with the rest of the building systems. Compensating for an inefficient design later with mechanical systems can be quite costly. Similarly, contributions from renewable systems can be diminished due to late integration and poor planning. The overall energy efficiency depends on the appropriate combination of different design options therefore if the building and system integration is not well considered, the opportunity to design a true high energy performance building can be missed.

Aitken (1998) defines the whole-building concept as "a method of siting, design, equipment and material selection, financing, construction, and long term operation that takes into account the complex nature of buildings and user requirements, and treats the overall building as an integrated system of interacting components" (p.3). Moreover, he emphasize that "a whole building approach requires participation by all stakeholders in the design and building process, including material and equipment manufacturers; designers, builders and developers; building trades and code officials; and end users"(p.3). The definition of whole-building concept reveals that interactions between building and sub-systems are required to be well captured in an integrative manner starting with the early stages for high energy performance building design. Today, new building design methods, which can simultaneously take into account building and system integration, address several influential design

parameters and provide quantitative inside information about the building performance, are highly required to achieve high performance building targets.

As presented in Chapter III, the application of simulation-based optimization methods in building design field started to draw attention of researchers especially in the last decade in order to support the development of cost-effective, environmentally friendly, highly energy-efficient buildings by bridging the gap between the steps of whole building design process. During a simulation-optimization process, a simulation model of a building design scenario and an optimization solver interact dynamically to explore a search space until an optimal solution based on an objective function and established constraints is obtained.

There is certain amount of work has been done through optimization applications on a variety of building design issues. Some of the research efforts in the literature mainly focused on developing efficient search techniques and algorithms suitable for the building design optimization problem while majority of the studies concentrated on problem formulation. The literature review revealed that although effective methodologies presented so far to address building and system design issues, there is still a research need for holistic approaches that aim to combine building architectural features, HVAC system features and renewable generation features simultaneously while taking into account various dimensions of building performance.

Therefore, in the current study, we purpose a simulation-based optimization methodology where improving building performance is taken integrally as one-problem and the interactions between building structure, HVAC equipment and building-integrated renewable energy production are simultaneously and dynamically solved while looking for a balanced combination of several design options and design objectives for real-life design challenges.

The proposed methodology is capable of simultaneously taking into account several influential factors on energy performance including outdoor conditions, building envelope parameters, indoor conditions, HVAC and renewable systems characteristics. During the search for an optimal design scenario, building architectural features, building envelope features, size and type of HVAC equipment

belong to a pre-designed HVAC system and size and type of considered renewable system alternatives are explored together through optimization search techniques.

The objective of the methodology is to explore cost-effective energy efficiency options, which can also provide comfort while limiting harmful environmental impacts in the long term therefore financial, environmental and comfort benefits are considered and assessed together. The methodology specifically aims at supporting cost-effective building and system design for real-world design challenges by minimizing investment and operational costs in long term while ensuring required thermal comfort is provided to user within minimized CO_2 emission rates. Moreover, the cost-effective design choices which provide the energy performance level that leads to the lowest cost during the estimated economic lifecycle are presented to the designer.

Moreover, the methodology not only aims at contributing to cost-effective energy efficiency but also to water conservation by taking into account the influence of HVAC design on mechanical system water use. While the cost of water is generally lower than the cost of energy, conservation of water is no less important since water sources on earth are limited, too.

The methodology aims to answer design questions such as to what extent it is wise to invest in expensive but higher efficiency products for building envelope and HVAC system equipment, how to integrate building architectural features with building systems, what are the optimal combinations of renewable energy options and energy conversion systems, as early as possible in the design process. The methodology can be used as a decision-support tool for both new building design and renovation projects since both processes provide significant opportunities to improve building performance but also goes through a complicated decision making process.

The proposed optimization procedure implements a Particle Swarm Optimization and it is based on the combination of EnergyPlus simulation tool and an enhanced version of GenOpt environment that is developed by the author to be in simultaneous interaction with a database, which provides technical and financial information on existing building materials, HVAC and renewable system equipment. Therefore, the performances of actual materials, equipment and system could be assessed. As a

result, the methodology allows designers to design buildings as an engineered system and supports them in creating true energy-efficient buildings for real-life challenges.

The study cover multi-dimensional building design aims through a single-objective optimization approach where multi objectives are represented in a ε-Constraint penalty approach.

The methodology allows evaluating large number of parameters fast and effectively in a time-efficient manner.

The following sections introduce the details of the methodology and describe the steps that should be taken for a successful implementation. The limitations of the current work are also addressed and the boundary of the methodology is given.

4.2 Optimization Procedure

The success of any optimization study strongly depends on the identification of problem characteristics and development of an approach that can address the needs of the problem. Figure 4.1 illustrates the essential steps taken in this study for setting up the proposed building design optimization model. Each step of the optimization formulation is described in the following sections. The decisions made at each step may influence other steps so the interactions are taken into account carefully.

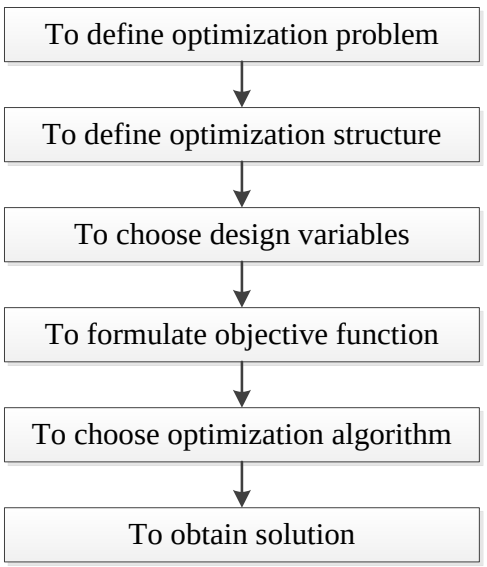

Figure 4.1 : Steps of setting up the proposed building design optimization model.

4.2.1 Problem domain and optimization structure

Before making an attempt to structure an optimization methodology, it is necessary first to define the problem of interest clearly and completely.

Building thermal performance involves complex dynamic interactions between the exterior environment and the internal loads occurring through building envelope and satisfied by building systems. As explained in Los Alamos National Laboratory Sustainable Design Guide (LANL, 2013), "The difficulty is that these various external and internal load conditions and associated utility loads are constantly changing from hour to hour and season to season. Also, the number of potential interacting design alternatives and possible trade-offs is extremely large" (p.53). Therefore, the main problem of the current study is to tackle the difficulty in building design complexity while searching for the optimum combinations of building's architectural characteristics, the size and type of HVAC equipment belong to a pre-designed HVAC system and the size and type of building integrated renewable system component, simultaneously as a whole.

Figure 4.2 depicts the adapted generic building and system energy calculation scheme for the problem formulation. As figure demonstrates, indoor conditions, outdoor conditions and building characteristics all together create building thermal and ventilation requirements. The thermal loads and building ventilation needs are then served by an HVAC system that consists of a primary and a secondary side. The primary side of the system represents components and equipment that convert primary energy to a useful form such as chillers and boilers. Primary side equipment is connected by a network to the secondary side equipment where a conditioned medium is brought to the space of intention (delivered energy) to satisfy the building loads and to provide comfort to occupants. Secondary system equipment could include fans, fan coils, radiators, air handling units, etc.

In addition to building and HVAC system integration, artificial lighting and building daylighting potential are integrated into the calculation procedure as well. Building daylighting potential has impact on the building lighting load and it is directly influenced by properties of building envelope. Moreover, there is a trade-off with heating and cooling load due to artificial lighting use and consequent heat gain. Therefore, the methodology takes into account the interactions between building

envelope, daylighting potential, artificial lighting and HVAC system, too and it certainly contributes to the optimization of natural daylight into the buildings.

Furthermore, the hot water need of the building is served by a water heating system and it is included in the calculation scheme. Sanitary hot water could be produced with the same system used for space heating or it can also be supplied by combined systems or separate systems.

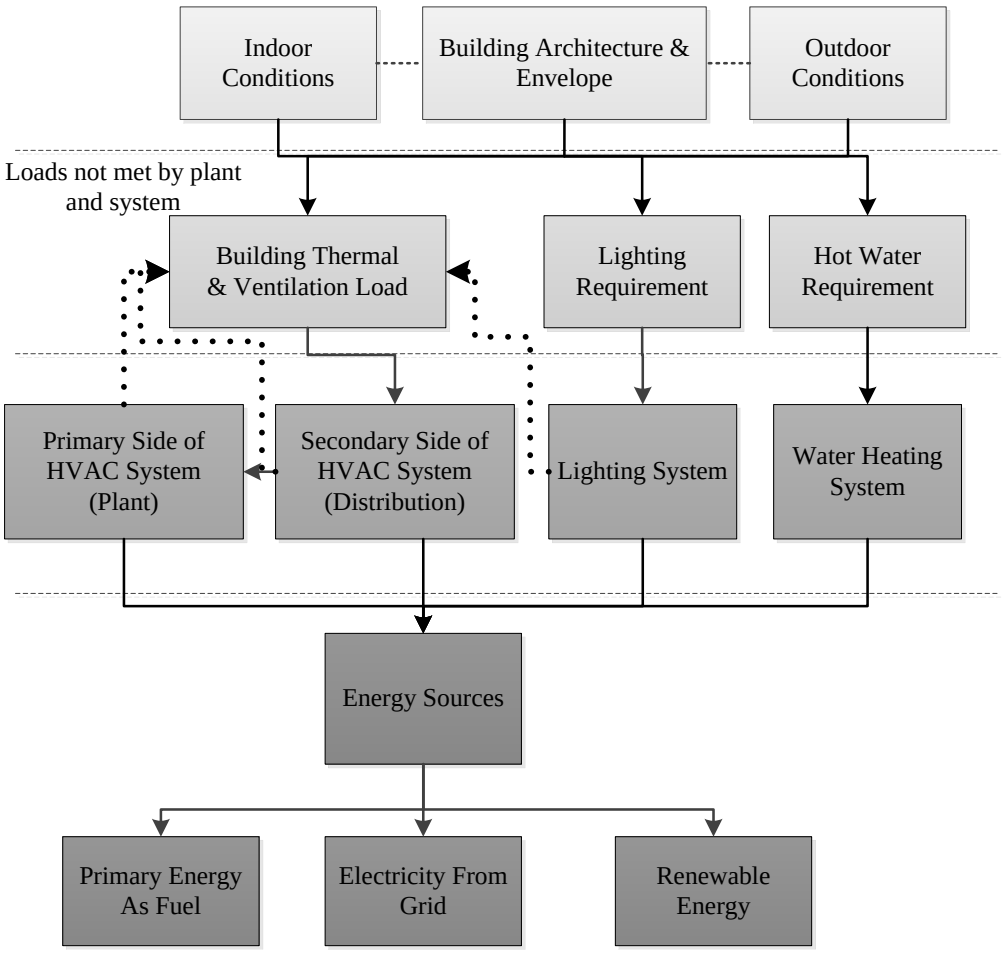

Figure 4.2 : Energy use calculation scheme.

The full coupling of thermal load, secondary system, plant and energy sources where there is a feedback from the supply-side to the demand-side is required for a better understanding of how a building responds to the changing indoor and outdoor environmental factors, as it attempts to meet the dynamic building thermal loads. Therefore, as depicted in the figure, the interactions between the thermal building loads, secondary system models, primary plant models and energy production models are taken into account and closely linked in the methodology.

The building elements and building systems (HVAC, lighting and water heating) interact dynamically and the systems naturally require energy to operate. However, each energy efficiency measure comes with an investment and operating cost. Therefore in the methodology, the energy performance level which leads to the lowest global cost during the building service life is explored. In addition to the building energy performance, the proposed methodology also considers building operational water consumption by especially focusing on HVAC system water use.

Due to the system energy use, the building emits greenhouse gases depending on the energy sources and CO_2 emission level is therefore taken as a design restriction in the methodology.

Similarly, the thermal comfort that is provided indoors is taken as a restriction as a measure of how well the building and the systems is designed and integrated.

The aim of the proposed optimization framework is therefore to configure building architectural and construction options (such as the degree of orientation, amount of insulation material, type of roof coating, type of glazing units, amount of glazed area so on.) and to select elements of a pre-designed HVAC system (such as size, full-load and part-load efficiency of primary side HVAC primary equipment matching an actual equipment available in the market, and size of dependent HVAC equipment including cooling tower, fan coil units etc.) and to select elements of considered renewable energy systems (such as type, efficiency and power of photovoltaic systems and/or solar thermal systems) for cost-effective energy efficiency in the long term while emitting less than a user-set target CO_2 level and providing comfort. The mathematical formulization of the objective function representing the building performance is introduced in detail in the following sections.

Figure 4.3 illustrates the main architecture of the proposed optimization framework. The framework requires interactive collaboration of three main elements: an optimization engine, a dynamic simulation tool and a database where technical and financial information about several alternative energy efficiency measures are kept and fed to the optimization environment.

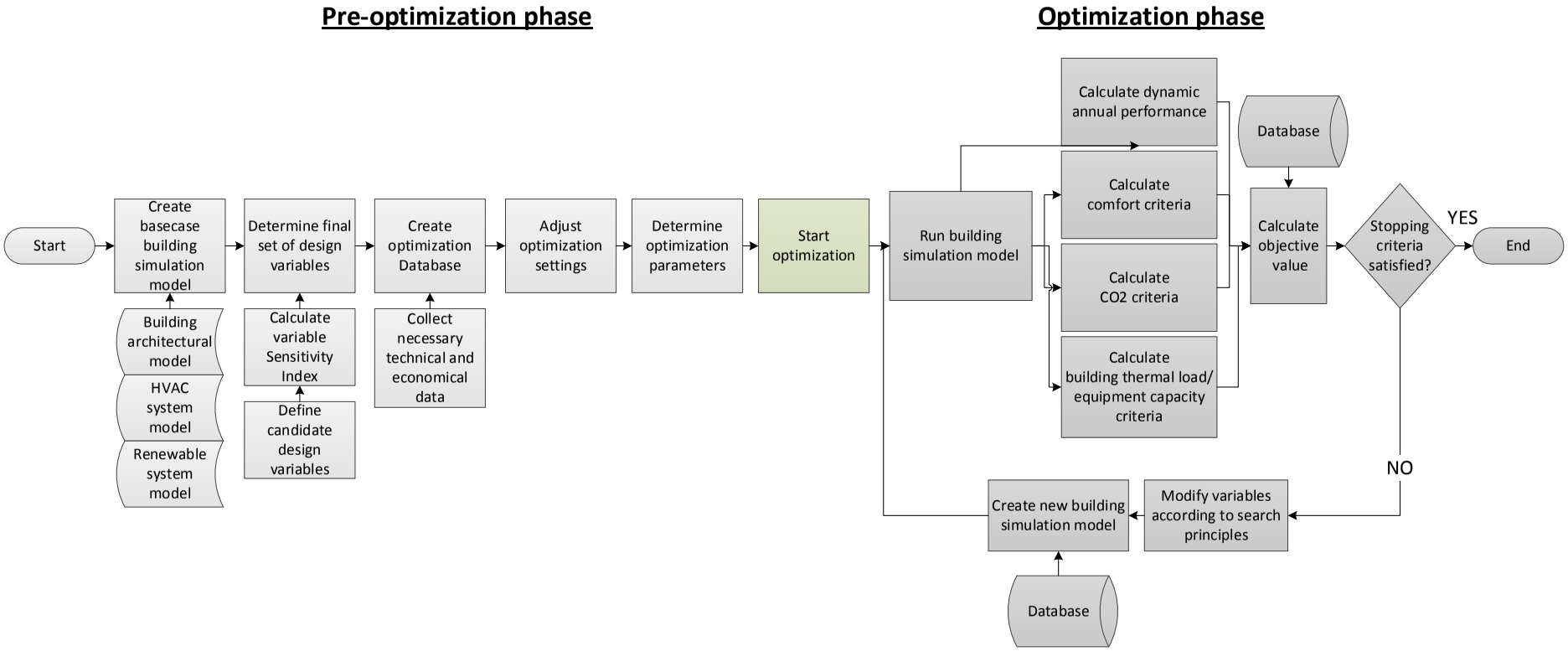

Figure 4.3 : The architecture of the proposed optimization framework.

The optimization process starts with a pre-processing phase where the designer creates a generic simulation model of a base case building scenario that includes information about climate, building location, site information, three dimensional building view, building envelope, plug loads, occupancy type and pattern, pre-designed building systems for comfort heating and cooling, and pre-designed renewable systems to integrate. The base case building constitutes a starting point in the search space and provides an initial reference for comparisons.

Once the base case building is established, the designer selects a variety of energy efficiency measures to investigate therefore prepares a variable list accordingly. Moreover, a database containing technical and financial information about the each energy efficiency measure including a variety of construction products and system component options is also prepared.

The designer then runs test of optimization experiments to determine possible dimensions of the main element of the objective function and imposed constraints. Thus, appropriate optimization parameters related to objective function formula that will lead to a balance between different objectives are determined. Moreover, designer also obtains appropriate optimization algorithm settings suitable for the design problem in consideration through test runs.

The once the required parameters and settings are determined, optimization process starts with the motivation to improve the performance of the base case building, which is calculated through dynamic building simulation, based on the defined objectives and criteria.

At every iteration step of the optimization search, optimization algorithm proposes different values for each optimization variable according to variable definition and optimization search principles. Variables represent actual energy efficiency measures that are stored in the database. Therefore each time a new combination of different measures are proposed by optimization algorithm, the technical information of that technology alternative is read from the database and a corresponding energy model object is created and inserted into the building simulation model. Similarly financial information belongs to that measure is again read from the database and transferred to the objective function formula.

Once the building simulation model of the new design scenario is complete, firstly a design day simulation for summer and winter periods is run to predict the building peak heating and cooling loads due to changes in architectural design variables. Within the same iteration, after the load is established, the optimization algorithm seeks to determine if the proposed HVAC equipment at this step is within the capacity range. If an over or under capacity equipment is proposed by the optimization, then this design combination is eliminated from the search space through application of constraint functions. Therefore it is made sure that suitable plant equipment (boiler, chiller) that can satisfy the calculated thermal load among the user-created equipment database is chosen. In addition, the required capacity of dependent equipment (such as cooling tower, radiator, fan coil units etc.) is also calculated with an aim to complement the design suitably.

If the proposed equipment capacity is within the required capacity range, then the optimization runs an annual simulation considering the full-load and part-load equipment performance. The database contains variety of primary equipment options with varying on-reference and off-reference efficiencies represented by performance curves. Therefore, before final equipment selection, all around the year performance of actual equipment under varying load conditions is observed. At same instance, optimization module also searches the energy generation potential of the considered renewable technologies, evaluates, and compares the performance of different components such as photovoltaic module types or installed power capacity to find the optimal configuration that maximizes the benefit.

The energy and economic performance of the proposed EEM combination is checked against the optimization criteria, and the optimizer module then initiates creating new design scenarios automatically by combining the variable options according to optimization search principles. The iterative search continues until an optimum solution that can balance the design aims while satisfying the optimization constraints is established. Therefore, a right-sized HVAC system that is capable of providing necessary occupant comfort, operating efficiently throughout the year, costing, and emitting less and balanced with renewable technologies is configured among several equipment options.

The simulation module of the developed scheme evaluates energy-related performance metrics and functional constraints. Finally, the database defines and

organizes design variables, contains technical and financial information about design options and stores related non-variable optimization data.

The application of the methodology allows exploring, sizing, comparing and finally selecting equipment options only for one pre-designed HVAC system type during a single optimization run. However, the performances of different HVAC systems can be investigated and compared if they are included in separate optimization runs.

The optimization generates several design alternatives from the assessed packages and marks the energy and water performance level leading to the lowest cost during the estimated economic lifecycle as economic optimum. However, a cost versus primary energy consumption curve is also created from eligible optimization results and cost-effective alternative options for the building in consideration are identified.

4.2.1.1 The optimizer

The responsibility of the optimization module is to regulate the entire process by implementing the optimization algorithm, triggering simulation for performance calculation, interacting with the database, assigning new values to variables to create alternative scenarios, calculating objective function, imposing constraints, and checking stopping criteria.

The literature reviews by Nguyen et al. (2014), Machairas et al. (2014), and Evins (2013) inform that there are several optimization environments available to solve a building optimization problem once it is formulated. Many decent algorithms are implemented in these tools to deal with different kinds of optimization issues.

In this study, a GenOpt based optimization environment is developed and used as the optimizer module of the proposed study.

The structure of GenOpt allows running multiple simulations in parallel. Parallel computation is an important means to improve an algorithm's efficiency since it can drastically reduce computation time. Moreover, GenOpt can easily be coupled with a building simulation program and its rich algorithm library, capability to handle discrete variables and flexible format to add new subroutines makes it a suitable tool for the methodology.

However, GenOpt alone is not capable of interacting with a database to acquire information about design variables and transfer them to building simulation module

for analysis therefore, in the methodology, GenOpt environment is enhanced to communicate with a user-created database through a proposed sub-module.

The general structure of the developed optimization environment is depicted in Figure 4.4.

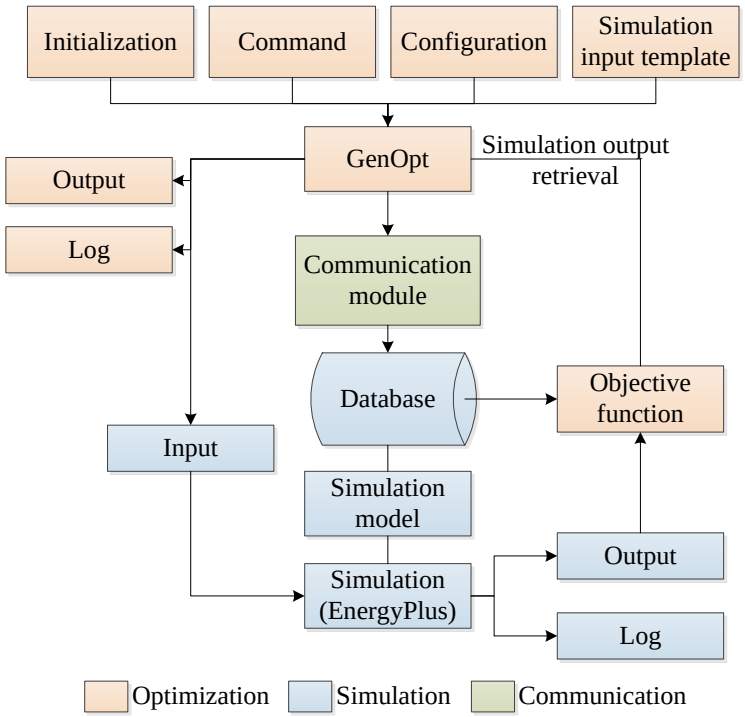

Figure 4.4 : The structure of GenOpt based enhanced optimization environment.

The initialization file specifies the location of input files, output files, log files, etc. It includes the objectives function formula. Moreover, it also shows what number in the simulation output file is a cost function value, and which simulation program is being used.

The command file specifies decision variables' names, initial values, upper/lower bounds, optimization algorithm, etc.

The configuration file contains information related only to the simulation program used.

Simulation input template the location of decision variable in the building simulation input file.

Finally, the database connection module interacts with the database and simulation program to rewrite simulation input file with actual product information.

When the optimization algorithm creates new design combinations based on the variable information written in the command file, the dedicated communication module reads the assigned variable value and matches it with a product in the database. Then all the necessary technical information about that specific product is read from the database and directly written into the simulation input file for the dynamic simulation step. Therefore, technical information regarding actual market products is transferred into the simulation file and they are evaluated with their dynamic performances at every iteration during optimization.

Once the simulation model of the new design combination becomes complete, simulation is run and the simulation output is used for calculating the objective function value along with other necessary data read from the database.

4.2.1.2 The simulator

The main purpose of the simulation module is to calculate performance metrics required for the objective function formula. Due to the integrated nature of the proposed whole-building solution scheme, the simulation module must be capable of calculating building thermal loads, daylighting potential, equipment capacities, energy consumption, CO_2 emission, user comfort index, and on-site energy production simultaneously.

As highlighted in Chapter II there are a great number of simulation tools available with varying capabilities and level of calculation accuracy. However, not many of them have the ability to capture dynamic interactions between building and systems. As expressed by Trcka and Hensen (2010) "The integration of building and HVAC system models is accomplished at different levels. The models can be sequentially coupled (many duct/pipe sizing tools, BLAST, DOE-2, etc.) – without system model feedback to the building model or fully integrated (ESP-r, EnergyPlus, IDA ICE, TRNSYS, etc.) – allowing the system deficiencies to be taken into account when calculating the building thermal conditions" (p.95).

Among the few dynamic building simulation tools, EnergyPlus is employed as the simulation environment in this study due its integrated solution manager, which ensures building, system, and plant interaction. Moreover, EnergyPlus is compliant with the requirements of ANSI/ASHRAE Standard 140-2004 and meets also the general technical requirements of the European Directive on the Energy Performance

of Building therefore it produces reliable results. Furthermore, EnergyPlus offers wide choices for HVAC and renewable system models and its text-based input and output format allows coupling with optimization module.

The comprehensive and powerful qualities of EnergyPlus make it a suitable simulation engine for the proposed methodology.

4.2.1.3 Database

Building design optimization is a multi-variable problem and it requires substantial numerical input. The data needs to be well defined and handled therefore a dedicated database module is developed for organizing input parameters.

The parameters are categorized under two titles: non-variables and variables. Non-variable parameters are required to successfully calculate the objective function; however, they are fixed during a whole optimization run. For instance, energy tariffs, water tariff, discount rates, etc. are handled in this category.

On the other hand, dependent and independent optimization parameters fall under variables category. Independent optimization parameters are design variables that take a numerical input that is allowed to change during the optimization process to find its most favourable value. For example, thickness of insulation material, type of roof coating, type of boiler or chiller equipment is handled as independent variables.

Since the main aim of the methodology is to optimize real-world design challenges, the technical and financial information of the actual market products including building envelope materials, HVAC system equipment and renewable system equipment are stored in the database. Each product or a component is assigned with a unique Identification (ID) number under a product category. During the optimization run, when a product matching the requirements of the design variable is called from the database, all the necessary information related with that ID number is read and technical product information is written into simulation file and the related financial information is fed into the objective function formula.

Dependent variables take new values at each optimization iteration based on the assigned value of the independent variable. For instance, size of cooling tower capacity, or opaque area of wall component is calculated based on the assigned value of chiller capacity or window-to-wall ratio, respectively.

4.2.2 Design variables

Design variables are the input factors within an optimization model that need to be determined and they constitute a design space on which the optimization algorithm will work. Each decision variables has a domain, which is a set of all possible values available for the variable and in the whole-building performance optimization problem, decision variables reflect the whole set of alternative measures that are available for the design of a building and systems.

In the proposed methodology, the optimization problem is addressed as a purely discrete optimization problem where design options are completely described by discrete strings. There are two approaches adopted to define discrete variable sets.

First approach introduces a constraint set of finite, non-zero n discrete integers for each variable as represented by $V = \{V_1, \ldots, V_n\}$. This approach is used to address equipment and component type as a design option. Admissible discrete values of variables are the ID number of equipment from the database that designer wants to investigate through optimization.

In the second approach, the continuous variables are discretized into a discrete set through definition of lower and upper bonds for each variable and the number of intervals. This strategy is used for representing design options that vary in a stepwise manner such as insulation thickness.

Commonly, deciding on the design variables is one of the hardest and crucial steps in formulating any optimization problem. Creative variable definition and selection can dramatically improve the calculation performance in terms of accuracy, computation time and consequently decreases the complexity of the problem. Therefore, eliminating unavailable and insignificant variables is highly required for the success of any optimization procedure. The sensitive parameters can be determined through experience of the designer, common knowledge, and sensitivity analysis.

In a real-life building design optimization problem, there is large number of influential parameters however; some parameters may not be always available for every optimization attempt due to natural causes. Project-specific constraints can limit the design space therefore; the designer should explore the availability of the parameters first, when setting up an optimization model.

Furthermore, among the available decision variables, some can only have a limited impact on the design objectives. Therefore, when the available parameters are determined, the degree to which an input parameter affects the model output can be evaluated through sensitivity analysis.

4.2.2.1 Sensitivity analysis for variable selection

Sensitivity analysis is performed to investigate the relationships between the input and output parameters of a system and to quantitatively compare the changes on the output with respect to the changes in the input. Therefore, designer can determine the most influential parameters or the parameters with insignificant impacts.

Hamby (1994) reviews a large number of sensitivity techniques available for simple to complex models. In this study, the Sensitivity Index method, which is a simple and straightforward technique, is adapted for the variable subset selection. The method calculates the sensitivity index (SI) of the variables that is the output percentage difference when varying one input parameter at a time, from its minimum value to its maximum value as given in equation 4.1.

$$SI = \frac{D_{max} - D_{min}}{D_{max}} \tag{4.1}$$

In the equation, D_{max} and D_{min} represent the maximum and minimum output values resulting from varying the input over its entire range.

In the methodology, the influence of the input parameters on the building heating, cooling and overall operating energy consumption is taken as the sensitivity index criteria.

The main reason to select a local, one-at-a-time technique instead of a global analysis that examines sensitivity with regard to the entire parameter distribution is to reduce the number of trials to a manageable size. The priority is given to obtaining non-sensitive variables within the given boundary conditions and parameter correlation is neglected for simplification.

4.2.3 Objective function and the constraints

Objective function translates a real-word problem to an objective and a constraint equation. The presented model aims at maximizing economic benefits from energy

efficiency investments during a selected time period and to therefore ensure cost-effective energy efficiency is achieved. Moreover, CO_2 emission released during building operation is aimed to be limited to a user-set target while required occupancy thermal comfort is provided. Thus, there are four main performance criteria to consider including economy, energy and water consumption due to HVAC operation, environmental impact due to building energy use, and indoor user thermal comfort.

Adding objectives to an optimization problem adds complexity. For instance, Ishibuchi et al. (1997) mentions that although evolutionary multi-objective optimization algorithms work very well on two-objective problems their search ability is severely deteriorated by the increase in the number of objectives. In the current study; therefore, even though the nature of the problem is multi-objective, the problem is reformulated as a single-objective optimization with some of the objectives acting as constraints. The secondary objectives are introduced in the form of penalty functions based on ε-Constraint method where adding a penalty for infeasibility forces the solution to feasibility and subsequent optimum.

Single-objective formulation takes advantage of being less computationally expensive and providing the best solution directly for a given objective. Moreover, there are a wide range of well-studied heuristic methods that are capable of dealing with this complexity in single-objective optimization.

In the study, the primary objective is taken as minimization of building lifetime global costs including operational cost for energy, water, and ownership cost for building envelope and building system equipment, in comparison to a user-defined base case building. The total global cost is calculated according to the European Standard EN 15459:2007 Energy performance of buildings - Economic evaluation procedure for energy systems in buildings. This method results in a discounted value of all costs for a defined calculation period (EN 15459, 2007).

Global cost is a key economic indicator to show the long term behaviour of a building and it mainly includes initial investment costs, running costs (energy, water, maintenance etc.) replacement costs, disposal costs, residual value at end of life. In addition to the European definition, running water costs due to HVAC system operation and hot water use is also included in the formulation.

Energy and water costs account for the largest share of the building running costs occur during building lifespan therefore they have the high sensitivity and priority in optimization process. Thus, the efficiency of building resource use is incorporated into the formulation.

The secondary objectives in the form of penalty constraints include user discomfort index, CO_2 gas emissions and payback period for renewables.

The general formula to calculate objective function is expressed in equation 4.2 where the constraints are combined with the original objective function (dGC), resulting in a new function of h(x). The function h(x) is then attempted to be optimized by the algorithm that is adopted within this study.

$$h(x) \quad = d\boldsymbol{GC} + \sum_{k=1}^{4} \mu_k PEN_k \tag{4.2}$$

Where,

$h(x)$: Main objective function,

dGC : Global cost difference between any design combination, which is created automatically during optimization and a user-defined base case scenario,

PEN_k : Main penalty value that is the summation of all sub-penalties, where each one evaluates a unique building aspect,

μ_k : Penalty parameter.

Comparing the building performance of each alternative to a base case allows investigating only the influences of design variables; therefore, the cost occurring due to fixed parameters can be avoided.

In the calculation, if a constraint is violated, the cost function dGC is penalized by addition of a large positive value. This way, infeasible solution candidates have always a worse overall objective value than a feasible one and excluded from candidate solutions so that the search direction is pushed back towards to the feasible region.

However, the difficulty of this approach is due to determination of suitable penalty parameter. Each penalty constraint is multiplied by a penalty parameter and summed together. If the magnitude of the each penalty term PEN_k multiplied by its penalty

factor is small relative to the magnitude of main objective dGC, the minimization of overall objective function h(x) will not result in a feasible solution. However, if the value of the penalty parameter is made suitably large, the penalty term will impose a heavy cost for any constraint violation that the minimization of the overall objective function will yield a successful solution.

The severity of the penalty depends on the penalty parameter. If the penalty value is too large, the optimization might create enormously steep valleys at the constraint boundaries and converge to a feasible solution very quickly even if it is far from the optimal. Similarly, if the penalty value is too small penalty can spend so much time in searching an unfeasible region. Therefore, the largeness of the penalty parameter should be decided depending on the particular design problem.

In the methodology, penalty factors are determined experimentally. An optimization test case is conducted during pre-optimization phase to obtain the likely magnitude of objective and the constraints. Then suitable factors, which reflect the priorities of the designer, are chosen to balance main objectives where penalty does not dominate the objective function nor remains ineffective.

Figure 4.5 shows a graphical representation of the objective function formula.

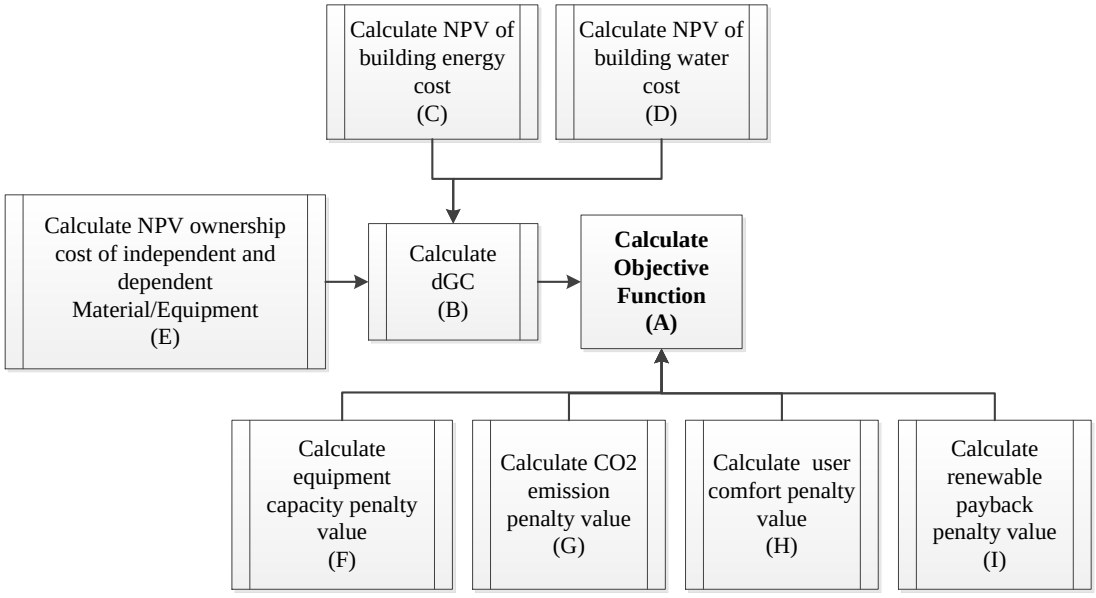

Figure 4.5 : Main objective function calculation algorithm.

Building material and system equipment represent the energy efficiency measures (variables) that will be investigated within the course of the optimization. Dependent material and equipment represent non variables that take values based on the changes

in optimization variables. The each element of the algorithm will be explained in detail in the following sections.

4.2.3.1 Global cost calculation

In the methodology, the main objective, the global cost, is calculated according to net-present value approach, which is a financial analysis technique where all future costs and benefits are discounted to the present to obtain a common reference for comparing competing alternatives in a long-term perspective (Fuller and Petersen, 1995).

There are numerous types of costs occur during service life of a building. In this research however, cost breakdown includes long-term energy costs due to HVAC operation, water heating and lighting energy consumption; water costs due to HVAC system water use and occupancy hot water use; ownership costs due to buying, installing, maintaining and disposing building envelope material and/or HVAC system equipment.

Moreover, if a renewable system alternative is considered, its ownership cost is also added to equipment cost category and energy cost benefits are reflected in energy category. The calculation time period is set by the designer.

All the cost elements of the equation are expressed in net-present value (NPV) and the main formula is given in equation 4.3:

$$GC = \sum_1^n NPV_{Energy} + \sum_1^n NPV_{Water} + \sum_1^n NPV_{Material} + \sum_1^n NPV_{Equipment} \quad (4.3)$$

The financial calculation are carried out from and user perspective therefore all the costs are the prices paid by the customer including VAT and charges.

Net present value of energy cost

Net present value of energy cost is a recurring annual cost that changes from year to year at a constant price escalation rate, and it is calculated for each energy source that is consumed in the building according to the algorithm illustrated in Figure 4.6:

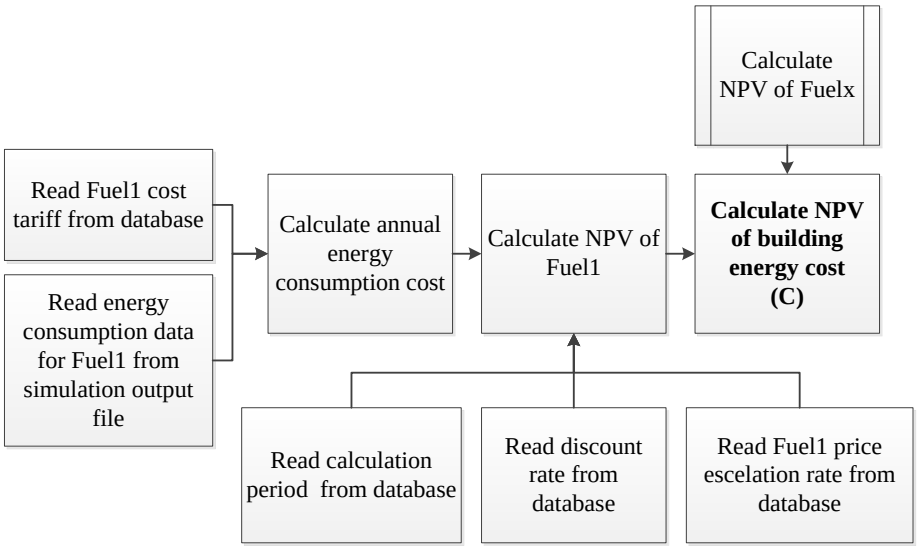

Figure 4.6 : NPV energy cost calculation algorithm.

The NPV cost of each energy source is calculated separately based on the annually recurring cost with an escalation rate formula given in equation 4.4:

$$NPV_{Energy} = E_0 \frac{(1+e_e)}{(d-e_e)}\left[1-(\frac{1+e_e}{1+d})^n\right] \quad (4.4)$$

Where,

NPV_{Energy} : Net present value of energy cost for each energy source,

E_0 : Annually recurring energy cost at base-date price,

n : Study period (number of years which energy consumption recurs),

d : Real discount rate,

e_e : Real constant price escalation rate for energy.

Annual energy cost for each energy source is calculated as a multiplication of annual end-use energy consumption (site energy) obtained through a yearly energy balance calculation performed by EnergyPlus simulation engine and its associated energy tariff stored in the user-created database. Energy cost includes cost due to heating, ventilation air conditioning, artificial lighting, plug loads and water heating purposes.

The real discount rate, d, is used in the formula to discount future costs to the present and is calculated based on the interest rate of an alternative investment corrected with regard to the inflation rate as given in equation 4.5,

$$d = \frac{1 + \mathrm{D}}{1 + Inf} - 1 \tag{4.5}$$

Where,

d : Real discount rate,

D : Nominal discount rate,

Inf : Inflation rate.

Nominal discount rate can be estimated based on market interest rate.

Similarly, the real constant price escalation rate for energy can be calculated according to the following formula:

$$e_e = \frac{1 + \mathrm{E}}{1 + Inf} - 1 \tag{4.6}$$

Where,

E : Nominal escalation rate,

Inf : Inflation rate.

Net present value of water cost

Net present value of water cost is also a recurring cost that changes from year to year at a constant price escalation rate and it is calculated for each water end-use type according to the algorithm illustrated in Figure 4.7.

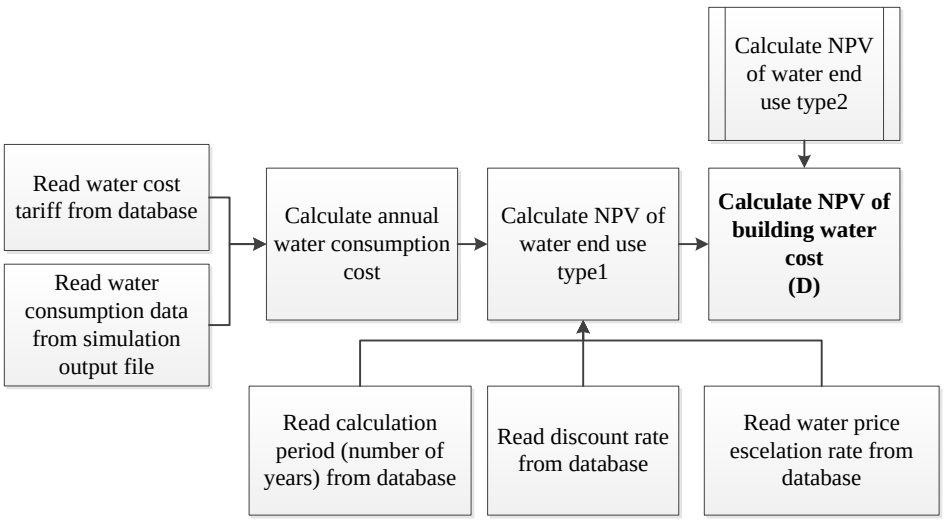

Figure 4.7 : NPV water cost calculation algorithm.

The NPV cost of each end-use type is calculated based on the annually recurring cost with an escalation rate formula given in equation 4.7.

$$NPV_{Water} = W_0 \frac{(1+e_w)}{(d-e_w)}\left[1-(\frac{1+e_w}{1+d})^n\right] \quad (4.7)$$

Where,

NPV_{Water} : Net present value of water cost,

W_0 : Annually recurring water cost at base-date price,

n : Study period (number of years which water consumption recurs),

d : Discount rate,

e_w : Constant price escalation rate for water.

Annual water cost is calculated as a multiplication of annual water consumption obtained through building simulation and its associated water tariff. In the methodology the water cost especially focuses on water use due to HVAC system operation.

Net present value ownership of material, HVAC and renewable system equipment cost

The net-present value ownership cost of different energy efficiency measures (independent and dependent building material, HVAC or renewable system equipment) is calculated according to the algorithm illustrated in Figure 4.8.

The financial information about each material/equipment is stored in a user-created database; therefore at each optimization run, the data is read from the database and transferred to the objective function equations.

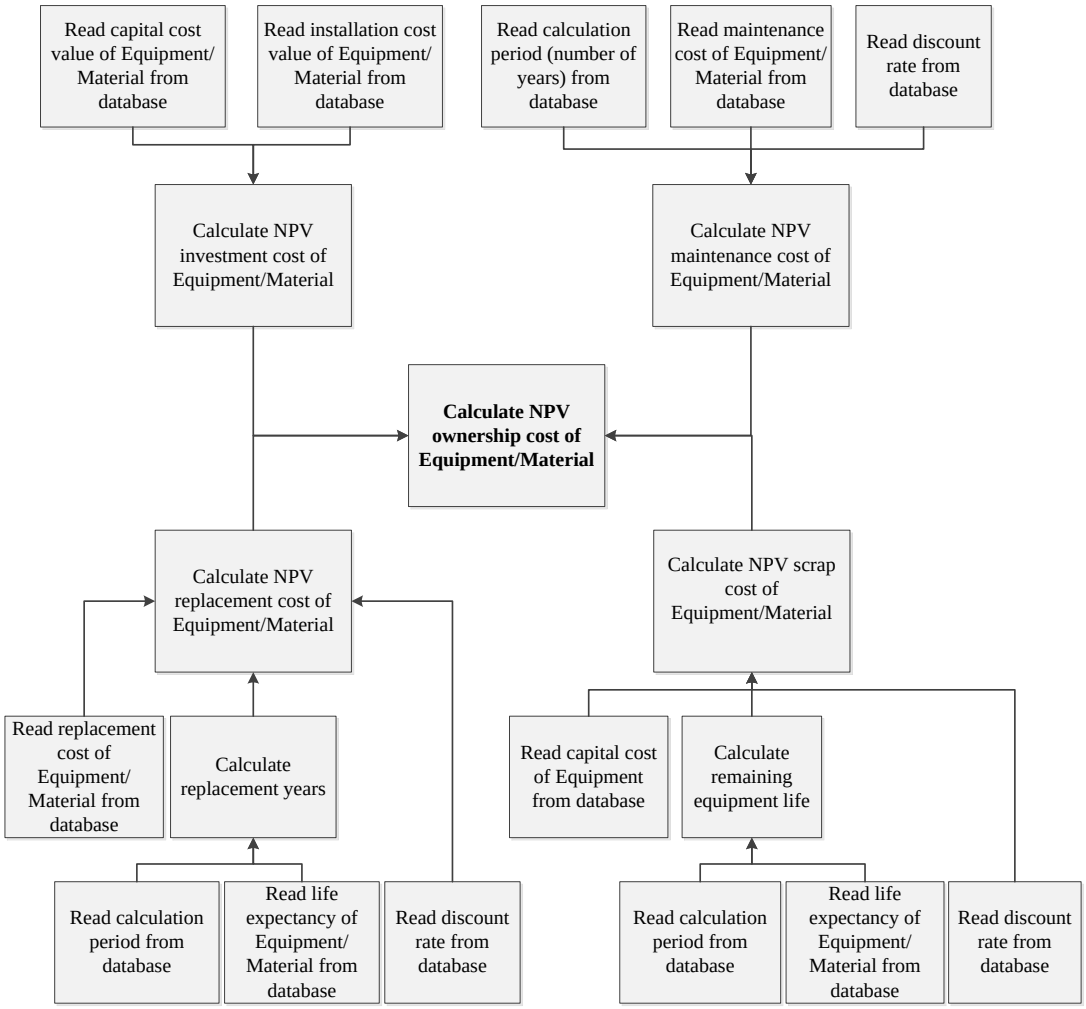

Figure 4.8 : NPV material/equipment ownership cost calculation algorithm.

The algorithm is based on the NPV of initial, maintenance, replacement and scrap cost for the material/equipment life, as given in equation 4.8.

$$NPV_{Material/Equipment} = I + Rep + M - S \tag{4.8}$$

Where,

I : Present-value investment cost,

Rep : Present-value capital replacement cost,

M : Present-value maintenance cost,

S : Present-value scrap cost.

The investment costs include costs for purchasing and installing building envelope material and/or system equipment. The investment takes place in the present

therefore the net present value of the investment cost is equal to the sum of the investment costs, for each material or equipment as given in equation 4.9.

$$I_{Material/Equipment} = \sum_{j=1}^{k} I_k \tag{4.9}$$

Replacement costs occur due to shorter lives of building components than the building and hence they are required to be replaced during the building service life. The replacement cost of a component can be considered as an extra expense equal to the initial investment cost for the component occurring when the service life of the component ends. The present value of replacement cost, which occurs at irregular or non-annual intervals, is calculated according to the formula given in equation 4.10.

$$Rep_{material/equipment} = R_0 \frac{1}{(1+d)^t} \tag{4.10}$$

Where,

$Rep_{material/equipment}$: Present-value of replacement cost occur at year t,

R_0 : Replacement cost at base-date price,

d : Real discount rate,

t : Future cash occurs at the end of year t (service life).

The building components need regular maintenance in order to remain functional during its life span and it is a recurring cost element of the GC. The equation 4.11 below is used to calculate the present-value of annual routine maintenance costs.

$$M_{Material/Equipment} = M_0 \times \frac{(1+d)^n - 1}{d(1+d)^n} \tag{4.11}$$

$M_{Material/Equipment}$: Present-value of replacement cost occur at year t,

M_0 : Annually recurring uniform maintenance cost,

n : Study period (number of years which maintenance recurs),

d : Discount rate.

Scrap cost is a one-time amount cost that occurs once at end of products service life and can include scrap value and removal cost. In this study, however, the removal cost is neglected. The base-date value of scrap cost is estimated as a user-defined percentage of the purchase price. The equation to calculate scrap value is as given below:

$$S_{Material/Equipment} = S_0 \frac{1}{(1+d)^t} \tag{4.12}$$

Where:

$S_{Material/Equipment}$: Present-value of scrap cost occur at year t,

S_0 : Salvage cost at base-date price,

d : Discount rate,

t : Future cash occurs at the end of year t (service life).

In the current study, the NPV ownership cost is calculated through two different approaches:

The change in cost due to change in the value of discrete variable with stepwise definition is calculated based on the multiplication of unit value of the variable with its current value. For example, adding insulation to a wall is calculated as the amount of insulation (m^3) times unit value of the insulation (TL/m^3).

On the other hand, the change in cost due to change in the value of a standard discrete variable is calculated based on the actual price of the component. For instance, while selecting a boiler, all the cost information of the equipment at that instance is directly obtained from the equipment database. By doing so, optimization algorithm can individually evaluate the economic performance of each component in the database.

4.2.3.2 Penalty functions

In the current study, the constraints regarding the HVAC equipment sizing, greenhouse gas emissions, indoor comfort levels and renewable system payback period are imposed in the form of penalty functions.

The equation 4.13 shows the elements of main penalty function:

$$\sum PEN = \mu_{ec}PEN_{Capacity} + \mu_{em}PEN_{Emission} + \mu_{cf}PEN_{Comfort} + \mu_{pb}\mathrm{PEN}_{\mathrm{PayBack}} \quad (4.13)$$

Equipment capacity

In the current study, ideal primary side HVAC equipment is aimed to be selected via optimization with rest of the design variables from a database, simultaneously. As explained previously, the optimization algorithm firstly combines design variables, runs a design day simulation, and determines the required equipment loads. Then, it tries to assess the annual performance at the same instance. In the equipment library, there exists a wide range of equipment with varying capacities and dynamic performances. Therefore, to prevent a capacity mismatch between the recommended equipment's actual capacity and the required capacity occurs due to new combination of design variables, a penalty is added to the main objective every time an equipment violates sizing rules set by the designer. The calculation steps of the equipment capacity penalty function are depicted in Figure 4.9.

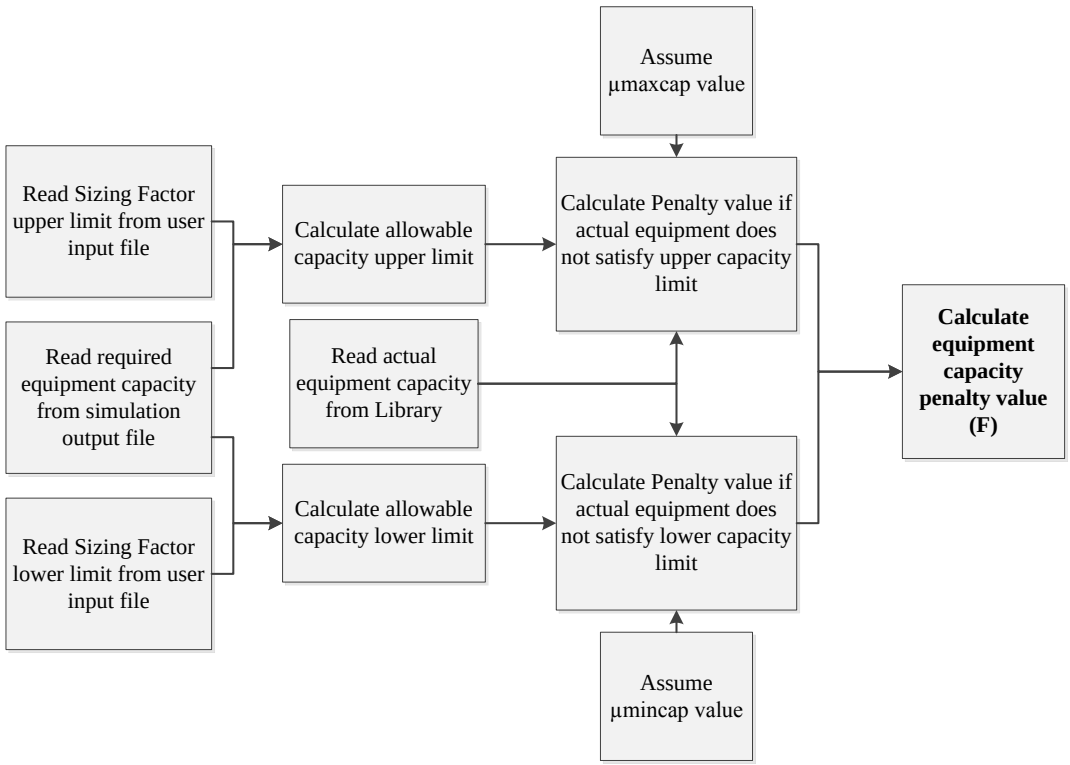

Figure 4.9 : Equipment capacity penalty value calculation algorithm.

The penalty calculation formula is based on equation 4.14.

$$EC_{autosize} * SF_{Lower} \leq EC_{actual} \leq EC_{autosize} * SF_{Upper} \quad (4.14)$$

Where,

EC_{actual} : Capacity of the actual equipment in database,

$EC_{autosize}$: Required equipment capacity determined via autosizing calculation,

SF_{Lower} : User-defined sizing factor to determine undersizing limit,

SF_{Upper} : User-defined sizing factor to determine oversizing limit.

Therefore, the penalty function for equipment capacity becomes as following:

$$PEN_{Capacity} = \mu_{maxcap}\left(max\left(0,\ \left(EC_{actual} - EC_{autosize} * SF_{Upper}\ \right)\right)\right)^{q} + \mu_{mincap}\left(max\left(0,\ \left(EC_{autosize} * SF_{Lower} - EC_{actual}\right)\right)\right)^{q} \quad (4.15)$$

Where,

$PEN_{Capacity}$: Calculated penalty for being above or below user-set capacity limits,

μ_{maxcap} : User-assigned maximum equipment capacity penalty parameter,

μ_{mincap} : User-assigned minimum equipment capacity penalty parameter,

q : Nonnegative constant as penalty power factor.

CO_2 emission

A good environmental performance of a building is aimed to be assured by setting a minimum-achievable performance target in the form of penalty. Therefore, while optimization searches for the optimum combination of design variables in terms of economic viability, it also makes sure the proposed building emits less than a target level during operational phase.

There are several different types of greenhouse gases with varying levels of global warming potential. The major ones are carbon dioxide, water vapour, methane, and nitrous oxide; however, in this study the target emission is restricted only to CO_2 because CO_2 remains in the atmosphere longer than the other major heat-trapping gasses and is the dominant source of global warming.

The metric used in the penalty function equation is described as the overall annual amount of carbon dioxide equivalence emitted by the building in kg due to the operational energy consumption from different energy sources. When the emitted overall CO_2 emission exceeds the target, a penalty which is calculated according to steps illustrated in Figure 4.10 is added to the main objective function.

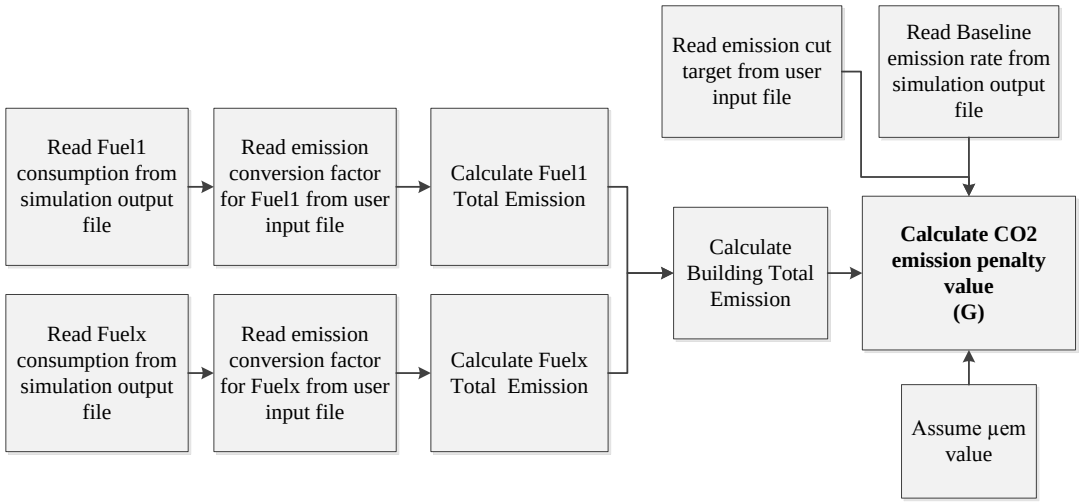

Figure 4.10 : CO_2 emission penalty value calculation algorithm.

The equation 4.16 describes mathematically the penalty formulation.

$$PEN_{Emission} = \mu_{em}\left(max\left(0,\ \left(CO2_{actual} - CO2_{target}\right)\right)\right)^{q} \qquad (4.16)$$

Where,

$PEN_{Emission}$: Penalty value due to violation of CO_2 emission criteria,

$CO2_{actual}$: Proposed building overall CO_2 emission amount,

$CO2_{target}$: User set overall CO_2 emission target,

μ_{em} : User-assigned CO_2 emission penalty parameter,

q : Nonnegative constant as penalty power factor.

The overall building CO_2 emission amount, for either actual case or base case, is a summation of CO_2 emission due to different energy sources used in the building and is calculated according to the equation 4.17:

$$CO2_{emission} = \sum_{1}^{i} CI_i En_i \tag{4.17}$$

Where,

$CO2_{emission}$: Overall building CO_2 emission amount,

CI_i : Carbon dioxide equivalent intensity index in kg.EqCO2/kWh for each available energy source,

En_i : Energy consumptions in different fuel forms.

The carbon dioxide equivalent intensity indexes are determined by public bodies according to the nature of the national energy market.

User thermal comfort

When performing a building design optimization, it is also crucial to maintain thermal comfort in the building. For instance, if the thermal comfort is not included in the calculations, it is very likely that the design that turns up as cost-effective, could lead to overheating or underheating problems. Therefore, in the current study, thermal comfort is added to the objective function as a penalty to make sure that design alternatives, which violate a user-set thermal comfort criterion is eliminated from design alternatives and the solution region is restricted to a comfort zone.

The penalty function for thermal comfort is defined mathematically as following:

$$PEN_{Comfort} = \mu_{cf} \left(max \left(0, \left(TC_{actual} - TC_{target} \right) \right) \right)^{q} \tag{4.18}$$

Where,

$PEN_{Comfort}$: Penalty value due to violation of comfort criteria,

TC_{target} : Target thermal comfort metric set by designer,

TC_{actual} : Calculated thermal comfort metric for proposed building,

μ_{cf} : User-assigned weighting factor for thermal comfort penalty function,

q : Nonnegative constant.

Thermal comfort can be defined as ‘that condition of mind which expresses satisfaction with the thermal environment’ (EN ISO 7330, 2006). The determination

of thermal comfort level is not straight forward since it results from a combination of environmental factors and personal factors including air and radiant temperature, humidity, air velocity, activity level of occupant and clothing insulation. There are many techniques available for estimating likely thermal comfort. In this study, however, Predicted Mean Vote (PMV) and Percentage People Dissatisfied (PPD) is adapted as suggested by EN ISO 7730 (2006), EN ISO 15251 (2007) and ASHRAE 55 (2004) standards. PPD is a quantitative measure of the thermal comfort of a group of people at a particular thermal environment and described as the percentage of occupants that are dissatisfied with the given thermal conditions. PPD is calculated according to equation 4.19 given in EN ISO 7330.

$$PPD = 100 - 95e^{-(0.03353PMV^4 + 0.2179PMV^2)} \tag{4.19}$$

The PPD can be deduced from the Predicted Mean Vote (PMV) as suggested in EN ISO 7730 given in equation 4.20:

$$PMV = (0.303e^{-0.036Met} + 0.28)(H - L) \tag{4.20}$$

Where,

Met : Metabolic rate,

H : Internal heat production rate of an occupant per unit area,

L : All the modes of energy loss from body.

PMV is representative of what a large population would think of a thermal environment using a seven-point thermal sensation scale. It is derived from the physics of heat transfer and empirical correlations.

Accordingly, when the thermal comfort criterion is taken as PDD index, the penalty function takes the following mathematical form:

$$PEN_{Comfort} = \mu_{cf}\left(max\left(0,\ \left(PPD_{actual} - PPD_{target}\right)\right)\right)^q \tag{4.21}$$

Where,

$PEN_{Comfort}$: Penalty value due to violation of comfort criteria,

PPD_{actual} : calculated PPD index for proposed building,

PPD_{target} : Target PPD index set by designer,

q : nonnegative constant.

The PMV-PPD indices are included in the national and international thermal comfort standards. Therefore, the designer can select the target PPD metric according to recommended values and can define the boundaries of the comfort zone.

The PDD index of actual building is however computed through building simulation at each optimization step. For multi-zone buildings, PDD is calculated for each zone during occupied times and then each PPD can be used as an individual comfort penalty otherwise an average PPD of all zones representing the whole building can be adopted.

Figure 4.11 represents calculations steps for comfort penalty through an average PPD index approach.

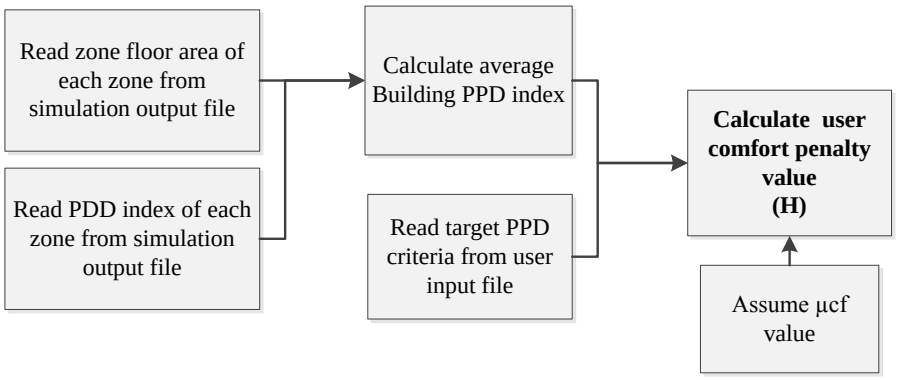

Figure 4.11 : User thermal comfort penalty value calculation algorithm.

Setting up a thermal comfort metric requires taking into account a range of environmental and personal factors however in the current study, it is assumed that all environmental factors other than air temperature and radiant temperature are constant. Commonly, control strategies are implemented in building simulation to maintain air temperatures within standard-defined comfort limits. However, in the optimization study HVAC plant equipment is selected from the equipment library based on a capacity calculation. Therefore, a capacity mismatch can be prevented through comfort criteria check, too. Moreover, radiant temperature is influenced a great deal by the change in building envelope design variables and thermal comfort can be improved based on radiant temperature.

Payback period for renewable systems

The payback period is the time in which the initial cash outflow of an investment is expected to be recovered from the cash inflows generated by the investment. Therefore, payback period measures the time required to recover initial investment costs. The payback period of a given investment is an important measure of whether or not to undertake the investment, since longer payback periods are typically not desirable for investors.

In the current study, a penalty is added to the main objective to set a limit on the payback period of a considered renewable system based on designer's expectancy. The simple payback method is used to calculate payback period as explained in Figure 4.12.

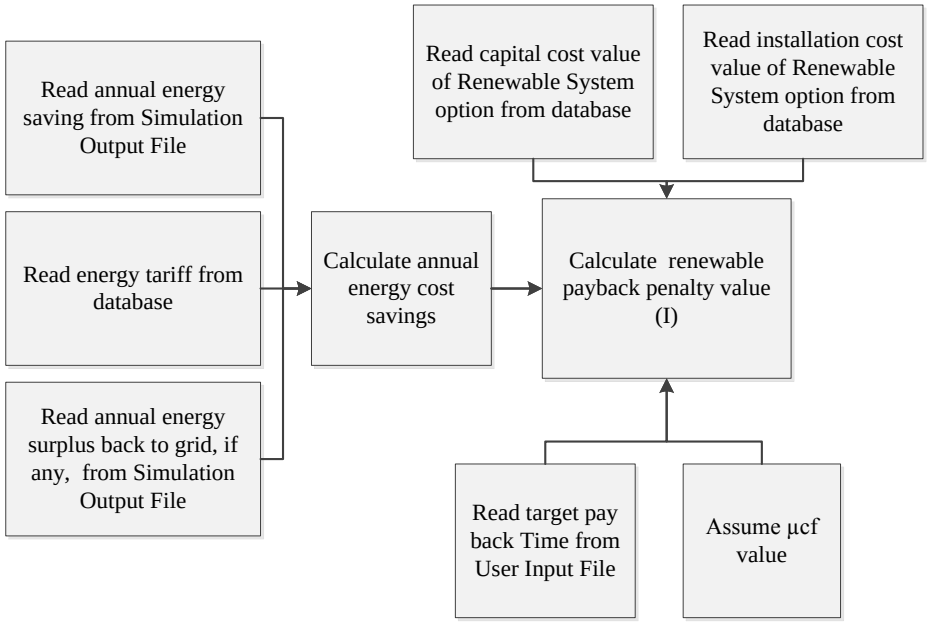

Figure 4.12 : Renewable payback period penalty value calculation algorithm.

The calculation algorithm is based on the equation 4.22.

$$PEN_{payback} = \mu_{pb}\left(max\left(0,\ \left(SPB_{actual} - SPB_{target}\right)\right)\right)^{q} \qquad (4.22)$$

Where,

$PEN_{payback}$: Penalty value due to violation of payback time criteria,

SPB_{actual} : Calculated simple payback index for proposed building,

SPB_{target} : Target simple payback index set by designer,

μ_{pb} : Payback period penalty parameter,

q : Nonnegative constant.

The simple payback (SPB) is formulated as in equation 4.23 for renewable system investments in the study (Fuller and Petersen, 1995):

$$SPB = \frac{dI_0}{[dE_0 + dM_0]} \tag{4.23}$$

Where,

dI_0 : Additional investment cost,

dE_0 : Savings in energy cost in year t,

dM_0 : Difference in maintenance cost in year t.

SBP is a practical method and it does not use discounted cash flows in the payback calculation. For instance, dE and dM are assumed to be the same every year, which means price escalation is not taken into account. Moreover, non-annually recurring additional costs such as replacements costs are ignored in SPB, too.

4.2.4 Optimization Algorithm

It is well known that all optimization methods have at least some limitations therefore, selecting a good algorithm is strictly depends on the nature of the considered problem.

In this study, the considered building design optimization problem has a multi-dimensional nature with multi-constraints expressed in single-objective formulation. There are a large number of variables involved and they are all represented in discrete form. Thus, objective function is likely to be discontinuous. There is no derivative information available and many local optima might occur.

The main expectations from the optimization algorithm in this study are the following: being capable to deal with above mentioned problem nature, being able to manage black box functions provided by building simulation tools, providing reduced computation time, being simple, robust and easy to implement.

As discussed in pervious chapter population based heuristic techniques are found to be effective dealing with constraint discrete optimization problems where they

provide the ability of escaping from local plateau. Particle Swarm Optimization belongs to the population-based evolutionary algorithms class and it is successfully applied to the building design optimization problem in the literature. It has its own pros and cons. However, in this research Particle Swarm Optimization is chosen as computation technique due to following advantages over other similar techniques: PSO is a simple but powerful search technique that can rapidly converge towards an optimum. It is easier to implement PSO and there are fewer parameters to adjust. It is free from the complex computation. Moreover, several studies suggest that PSO has the same effectiveness for finding the true global optimal solution for single-objective optimization as the Genetic Algorithms but with significantly better computational efficiency (Hassan et al., 2005; Panda and Padhy, 2008; Yang et al., 2008; Peyvandi et al., 2011).

4.2.4.1 Particle Swarm Optimization

Particle swarm optimization (PSO) is a population based stochastic optimization technique introduced originally by Kennedy and Eberhart in 1995. It is inspired by social behaviour and movement dynamics of birds flocking or fish schooling. PSO has been applied successfully to a wide variety of search and optimization problems.

Rao (2009) explains that while birds are searching for food in an area, they have no prior knowledge of the food source. They start at random locations in the field and might go together or scatter to locate food. During the search, they share information of the locations they have been to and when a good food source is discovered, they eventually flock to the place.

As far as Particle Swarm Optimization is concerned, each potential solution represents a bird and is called a particle. Particles fly through the problem space by following the current optimum particles at a velocity dynamically adjusted according to the historical behaviours of the particle and its companions.

The basic PSO algorithm is shown in Figure 4.13. All the particles have a fitness value, which are evaluated by the fitness function to be optimized. PSO is initialized with a group of random particles and then searches for optima by updating generations. The particles have memory and each particle keeps tracks of its coordinates in the problem space, which are associated with the best solution achieved so far by that particle. This personal best value is called as pbest. Another

best value that is tracked by the particle swarm optimizer is the best value obtained so far by any particle in the neighbours of the particle. This local value is called lbest. When a particle takes all the population as its topological neighbours, the best value is a global best and is called as gbest.

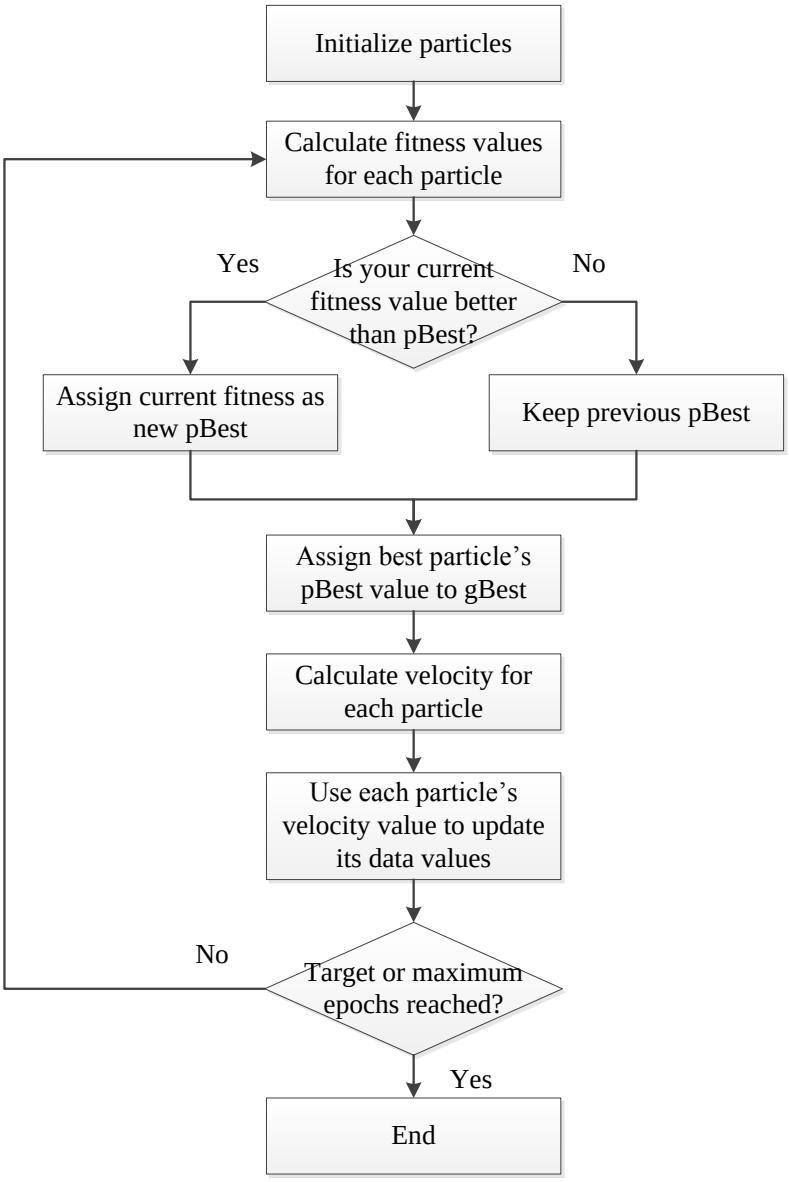

Figure 4.13 : Flowchart of the particle swarm optimization algorithm.

Particles attempts to change its location to a point where it had a better fitness value (pbest) at previous iterations, which models cognitive behaviour, and in a direction where other particles had a better fitness value (lbest), which models social behaviour. The velocity and position of each particle are updated after each successive iteration with following equations, respectively.

$$V_i^{k+1} = V_i^k + c_1 r_1{}^k \left(pbest_i^k - x_i^k\right) + c_2 r_2^k (gbest^k - x_i^k) \quad (4.24)$$

$$x_i^{k+1} = x_i^k + V_i^{k+1} \quad (4.25)$$

Where,

V_i^k : Velocity of particle i at iteration k,

V_i^{k+1} : Velocity of particle i at iteration k+1,

x_i^k : Position of particle i at iteration k,

x_i^{k+1} : Position of particle i at iteration k+1,

$pbest_i{}^k$: pbest of particle I,

$gbest$: gbest of the group,

c_1 : Cognitive acceleration coefficient,

c_2 : Social acceleration coefficient,

r_1, r_2 : Uniformly distributed random number between 0 and 1.

Although being a powerful technique, PSO shows some disadvantages, too: it sometimes is easy to be trapped in local optima, and the convergence rate decreased considerably in the later period of evolution. Several attempts have been made to overcome the limitations and to improve the performance of the PSO algorithm (Yang et al., 2007).

Shi and Eberhart (1998) proposed an inertia weight ω, which improves the performance of the original PSO algorithm by modifying equation 4.26 to:

$$V_i^{k+1} = \omega V_i^k + c_1 r_1{}^k \left(pbest_i^k - x_i^k\right) + c_2 r_2^k (gbest^k - x_i^k) \quad (4.26)$$

where $\omega \geq 0$ is defined as inertia weight factor.

As explained by Yang et al. (2007) “Empirical studies of PSO with inertia weight have shown that a relatively large x have more global search ability while a relatively small x results in a faster convergence”.

Moreover, Clerc and Kennedy (2002) introduced a new version of PSO with a constriction coefficient χ. The constriction coefficient reduces the velocity according to the following formula:

$$V_i^{k+1} = \chi\{V_i^k + c_1 r_1{}^k(pbest_i^k - x_i^k) + c_2 r_2^k(gbest^k - x_i^k)\} \quad (4.27)$$

Where,

$$\chi(\kappa, \varphi) \triangleq \begin{cases} \dfrac{2\kappa}{\left|2 - \varphi - \sqrt{\varphi^2 - 4\varphi}\right|}, & \varphi = c_1 + c_2 > 4 \\ \kappa, & otherwise \end{cases} \quad (4.28)$$

Since the newer version of PSO is found to be more effective than originally proposed algorithm, the updated versions of PSO is used as optimization algorithm in this research.

The parameters used in the definition of particle swarm optimization control the behaviour of a swarm and they have a strong influence on the overall performance of the algorithm. The most influential parameters are swarm size, inertia weight, constriction coefficient and acceleration coefficient. However, there is not an established approach for correct selection of the PSO parameters. Past studies in similar domains can serve as a good basis thus, it may certainly be beneficial to tune the parameters based on the individual problem at hand.

In the proposed methodology, the parameters of PSO algorithm are chosen in advance during pre-optimization phase based on the expertise of the authors, previous authoritative studies and design of experiments methods. Design of experiment methods considers the run of an algorithm as an experiment, gaining insightful conclusions into the behaviour of the algorithm and the interaction and significance of its parameters. Once the parameters are established, they are kept fixed during the calculation.

4.3 Summary

In this chapter, the proposed simulation based-optimization methodology, which is aimed to be developed for supporting the whole-building design process from energy efficiency perspective, is presented.

The whole-building design is a multi-disciplinary approach that aims to integrate all aspects of site development, building and system design, construction, and operations in order to create energy-efficient, resource conscious, environmentally responsible and comfortable built-environments. Today, common design approaches are not sufficient to meet the requirements of high energy performance buildings and there is a strong need for new approaches that attempt to bridge the gap between different steps of building design process. Therefore, in the current study, an integrative simulation-based optimization methodology was proposed. In the solution approach, improving building performance was taken integrally as one-problem and the interactions between building structure, HVAC systems and building-integrated renewable energy production were simultaneously and dynamically solved while looking for a balanced combination of several design options.

The method specifically aimed at supporting cost-effective building and system design for real-world design challenges via mathematical computation by minimizing global costs in long term while ensuring required thermal comfort is provided to user within minimized CO_2 emission rates. The methodology had the capability to right size then chooses HVAC and renewable system equipment that is balanced with building architectural design options. The study covered multi-dimensional building design aims through a single-objective optimization approach where multi objectives are represented in a ε-Constraint penalty approach.

The optimization scheme was realized through the collaboration of updated and enhanced generic optimization environment GenOpt, a dynamic building simulation tool EnergyPlus, and a user-created dedicated database.

The objective of the optimization is formularized as a single-objective optimization with constraints. The main criterion is taken as global cost where building CO_2 emissions and occupancy thermal comfort are imposed as constraints. Moreover, when evaluating renewable systems together with building and HVAC system design alternatives, payback period of the considered renewable technology is also taken into account in the form of penalty function.

The PSO technique, which is capable of dealing with complex optimization problems where discrete and continuous variables exits with discontinuities, was adopted as the optimization algorithm of the study.

The definitions of decision variables, the formulation of objective function and constraints, and finally the selection of appropriate solution computation techniques were explained in detail within the chapter.

One of the most important contributing factors of this methodology is that it can efficiently handle large number of variables with different nature. For instance, the best combinations of building architectural characteristics, envelope features, and HVAC system equipment and building related renewable systems are sought simultaneously while taking into account dynamic interaction between building loads and building systems. Moreover, variables are represented in discrete form and all the variable related information is stored in a user-created database that can interact with the optimization engine therefore, the economic and energy performances of actual market products can be easily tested and compared as design options. In addition, the single objective formulization of objective function supported with penalty functions provides quick convergence opportunities.

In order to test the efficacy and applicability of the proposed methodology and to assess its advantages and disadvantages, a case study has been carried out as the next step of the current work.

5. CASE STUDY RESULTS AND DISCUSSION

5.1 Introduction

This chapter illustrates how the proposed simulation-based optimization methodology can be applied to the building design projects to provide decision support for evaluating different design alternatives for cost-effective energy efficiency. The functioning and the effectiveness of the optimization framework are assessed through a case study implementation where different design scenarios are created, optimized and analysed.

Following sections firstly introduces a hypothetical base case building that serves as an initial reference for calculations, and then the test cases of interest are explained. Optimization scenarios are described in terms of design variables, objective function, optimization algorithm, financial data and parameter settings.

Finally, optimization analyses are carried out and the results are presented. The boundary of the methodology is discussed and recommendations for future improvements are suggested.

5.2 Case Study

5.2.1 Base case building description

The base case building serves as a baseline reference for comparison and evaluation in the optimization analysis therefore; the establishment of the base case building model is one of the main steps of the proposed methodology. The building model definition should include all the details about building architectural characteristics and building system characteristics in consideration.

In this study, the methodology is intended to be applied to a hypothetical generic office building. Three cities in Turkey including Istanbul, Ankara and Antalya are selected as building locations hence, the performance of the methodology under different climatic conditions can be observed.

The prototypical building represents common construction practices where buildings are designed without giving attention to building energy performance. Since the base case building is non-existing, the building model is developed based on the conventional building stock in Turkey.

The data about the envelope structures, schedules, and internal gains etc. are obtained from the National Building Energy Performance Calculation Methodology for Turkey. Moreover, it has been benefited from an expert opinion to highlight HVAC system types and equipment that are frequently used in Turkey.

The description of the base case building model covers the following subjects: weather conditions, general building description, building envelope, occupancy, interior lighting, plugged-in equipment, HVAC system and water heating system.

5.2.1.1 Climate

Three cities in Turkey, which are Istanbul (latitude N 40° 58' and longitude E 28° 49'), Ankara (latitude N 39° 56' and longitude E 32° 52') and Antalya (latitude N 36° 53' and longitude E 30° 43'), are selected as main locations of the base case building.

The Istanbul's climate is characterized as a warm, marine and subtropical. Summer weather in Istanbul is warm, where a maximum daily average dry-bulb temperature is 24.2 °C occurring in August. Winters are cold and wet, where a minimum daily average dry-bulb temperature is 4.9 °C occurring in February. Spring and autumn are mild, but often wet and unpredictable. Istanbul has persistently medium to high humidity. Hours of sunshine range between 2.6 hours per day in January and 11.6 hours per day in July.

Ankara's climate is characterized as continental with the climatic features of a semi-arid region. The summers are hot and winters are cold where relative humidity is higher in winter. The maximum daily average dry-bulb temperature is 21.5 °C occurring in July and the minimum daily average dry-bulb temperature is -2.4 °C occurring in January.

The Antalya's climate is characterized as a Mediterranean climate with hot and humid summers and mild and rainy winters. Around 300 days of the year are sunny, with over 3000 hours of sunlight per year. The maximum daily average dry-bulb

temperature is 29.2 °C occurring in July and the minimum daily average dry-bulb temperature is 10.1 °C occurring in January.

In the study, International Weather for Energy Calculations weather data, including temperature, humidity, wind, and, solar radiation is used as input to simulation model. The weather information is obtained in annual hourly format representing the typical long-term weather patterns. The Figure 5.1 illustrates average outdoor air temperatures for Istanbul, Ankara and Antalya. The maximum and minimum monthly temperatures are given in APPENDIX A.

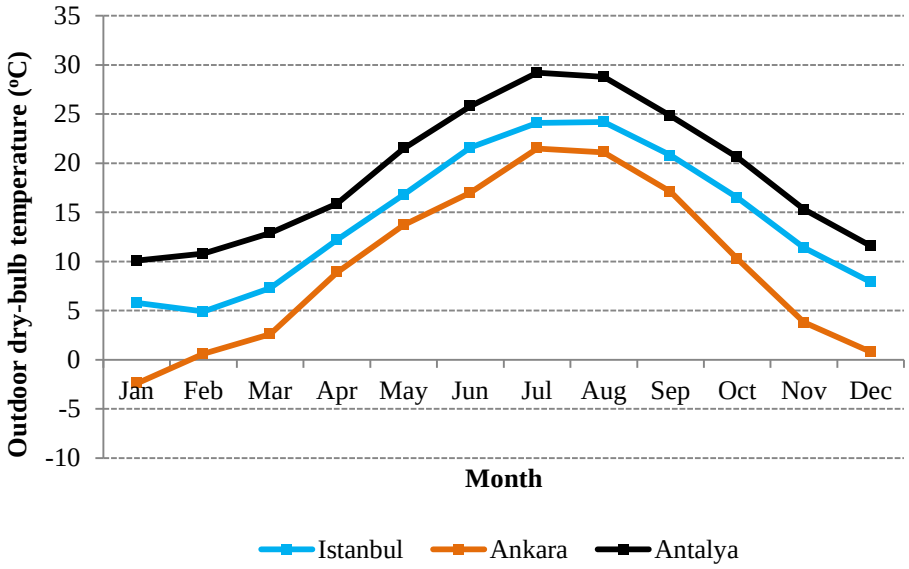

Figure 5.1 : Monthly average outdoor air temperatures.

Similarly, the Figure 5.2 summarizes average global horizontal solar radiation received in Istanbul, Ankara and Antalya on monthly basis. The graphics on monthly direct solar radiation is given in APPENDIX A.

For design day equipment sizing calculations, the extreme weather conditions are taken as following: The maximum dry-bulb temperatures for summer design day are 31.1 °C, 33 °C, and 38 °C for Istanbul, Ankara and Antalya, respectively. The minimum dry-bulb temperatures for winter design day are -2.6 °C, -15.7 °C, and 1.4 °C for Istanbul, Ankara and Antalya, respectively.

The details of summer and winter design day are given in APPENDIX A.

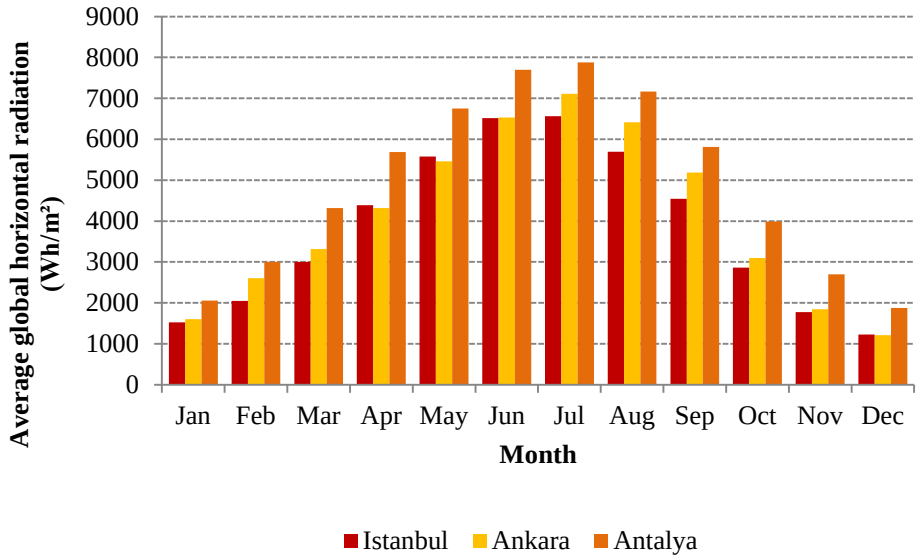

Figure 5.2 : Monthly average global solar radiation.

5.2.1.2 General building description

The building under study is a three-story office building with a total above-basement floor area of 8709 m^2. It has a square L shape with main dimensions of 57.6 m by 57.6 m. The building floor-to-floor height is 3 m and the floor-to-roof height is 9 m. The building is aligned with true north. A graphical representation of the base case building model can be seen in Figure 5.3.

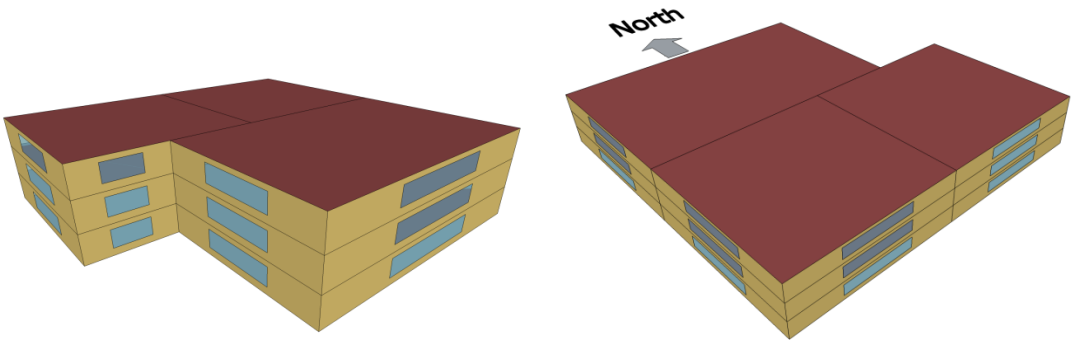

Figure 5.3 : The front and back 3D view of base case building model.

Each building floor is divided into 3 conditioned zones, which makes, in total, 9 thermal zones. All the zone space is assumed for office use. The building layout is illustrated in Figure 5.4. All the floors have the same footprint. The long axis is along the East-West direction and the front facade faces South direction. There are no adjacent buildings or trees surrounding the building.

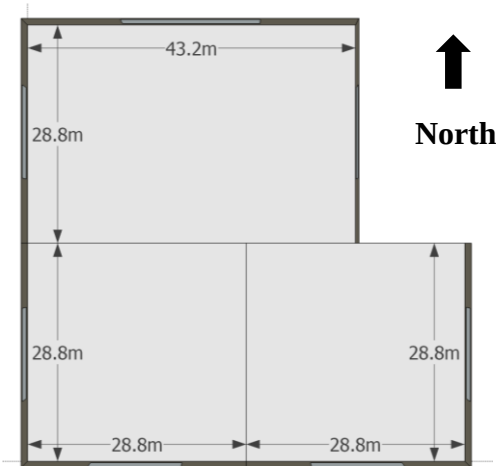

Figure 5.4 : The layout of base case building.

5.2.1.3 Building envelope

Opaque constructions of the base case building include brick walls as external walls, an inverted concrete flat roof, a slab-on-grade floor, ceilings and interior partition walls.

The brick wall element consists of the following sequence of layers from outside to inside: common exterior paint, exterior plaster, insulation, extra plaster, brick, interior plaster and interior paint. Buildings in each city are identical except for external wall exterior paint. To follow real life construction practices, a common dark colour exterior paint with a solar absorptivity of 0.7 is chosen for the base case buildings located in Istanbul and Ankara however, a light colour paint with a solar absorptivity of 0.4 is preferred for the base case building in Antalya.

The roof type of the base case building considered in this case study is a conventional inverted flat roof system composed of the following sequence of layers from outside to inside: surface loading gravel, paving slab, geotextile, insulation, water proofing layer, screed floor, concrete deck, and interior plaster. The solar absorptivity of the outside layer that is composed of gravel is taken as 0.9.

The thickness of insulation layers in external wall and roof elements are assumed zero to represent uninsulated initial design conditions however, the optimum insulation thickness will be investigated as an optimization design variable.

The slab-on-grade floor consists of the following sequence of layers from outside to inside: Concrete deck, rigid insulation, plaster, and linoleum finish.

The main construction elements are summarized in Table 5.1. These envelope constructions represent common building elements in Turkey and the materials are obtained from the product catalogues.

Table 5.1 : Base case building construction elements.

Building Elements	**Construction (from outside to inside)**
External Walls	Exterior paint + Exterior plaster (0.02m) + insulation (to investigate)+ Extra plaster (0.02m) + Brick (0.19m) + Interior plaster (0.02m)
Roof	Gravel (0.03m) + Paving slab (0.05m)+ Geotextile (0.001m) + insulation (to investigate)+ water proofing (0.006m) + Screed floor (0.15m) + Concrete deck (0.15m) + Interior plaster (0.02m)
Floor	Concrete deck (0.35m) + Rigid insulation (0.05m) + Plaster (0.05m) + Linoleum finish (0.01m)
Ceiling	Concrete deck (0.10m) + Air gap + Acoustic tile (0.01m)
Interior wall	Plaster (0.05m) + Brick (0.10m) + Plaster(0.05m)

The U-values for, external walls, the roof and floor are 2.06, 2.161, and 0.45 W/m^2K, respectively. Since no insulation is applied to external walls and roof, these building elements do not comply with the recommended numbers by national building standard TS 825 (2008). However, after the application of optimization, appropriate levels of insulation will be determined.

The thermal properties of the building floor comply with the national standard.

Transparent building construction includes windows with double pane glazing. Windows are distributed on each face of the building and all windows have a height of 1.5 m. The overall window-to-wall ratio of the base case building is set at 25%. Each glazing unit is made up of double windows with clear glass and 12 mm air space. U-value of the glazing unit is set to 2.9 W/m^2K, SHGC is set to 0.75, and Tvis is set to 0.85, which represents a manufactured glazing unit commonly used in Turkey. The thermal performance of glazing unit is below the recommended levels of 2.4 W/m^2K by TS 825 standard. However, a standard-complying unit will be explored during optimization process. The window frame is ignored for simplification.

Building air infiltration through building elements is assumed 0.5 ach for all the zones. Furthermore, an infiltration schedule is assumed to vary the peak infiltration

rate given above with HVAC fan on/off operation, assuming that the building is positively pressurized when the HVAC fan is on. Therefore, the schedule assumes full infiltration when the HVAC system is scheduled off and 25% of the peak infiltration when the HVAC system is scheduled on.

5.2.1.4 Occupancy

The value of the peak occupancy for the base case building is set in accordance with National Building Energy Performance Calculation Methodology for Turkey. The national methodology identifies four levels of occupancy density based on floor space per person as given in Table 5.2.

Table 5.2 : Density of people for office buildings.

People Density	Low	Medium	High	Very high
Floor area per person (m^2/person)	15.5	11.6	9.3	7.8

In this study, medium occupancy density (11.6 m^2/person) is assumed for base case building model therefore, the actual number of maximum occupancy is about 750. The total heat gain from each occupant is set at 130 W per person for moderately active office work activity in offices. This value is taken from ASHRAE 2009 Fundamentals Handbook, Table 1 of Chapter 18. The heat given off by people is directly added in building energy balance.

Moreover, the base case building operating hours are assumed to follow typical office occupancy patterns in Turkey with peak occupancy occurring from 8 AM to 6 PM weekdays and Saturday. In addition, a limited occupancy is assumed to include janitorial functions and after-hours workers beginning at 7 AM and extending until 7 PM. For Sunday, the building is assumed to be closed. Hourly profile of occupation in the building during 24 hours is given in APPENDIX B.

5.2.1.5 Interior lighting

In order to achieve IESNA (Illuminating Engineering Society of North America) recommended illumination levels (500 lux) in the office space, 11 W/m2 lighting power density is applied to all zones in the base case model. This value is consistent with the Turkish National Calculation Methodology. A lighting schedule given in Appendix B is assumed to modify the given peak value in order to incorporate the

effect of the manual controls. The base case building does not include any dimming control of artificial lights based on indoor daylighting levels.

Internal heat loads generated due to lighting is added directly in building energy balance.

No exterior lighting assumed for this case study.

5.2.1.6 Plugged-in equipment

Office buildings have miscellaneous equipment plugged in to receptacles as plug loads, including office equipment (computers, monitors, copiers, fax machines and printers, etc.), and possibly refrigerators, coffee makers, and beverage vending machines.

The value of the peak power of office equipment for the base case building is set again in accordance with National Building Energy Performance Calculation Methodology for Turkey. The methodology identifies four levels of interior load according to occupancy density as shown in Table 5.3. For the base case building, medium level equipment load, which is 10.8 W/m^2, is taken in coherence with previously selected occupancy density.

Table 5.3 : Density of people vs equipment load for office buildings.

People Density	**Low**	**Medium**	**High**	**Very high**
Equipment load (W/m^2)	5.4	10.8	16.1	21.5

The peak loads are modified according to plugged-in load schedule given in Appendix B. The schedule follows occupancy schedule pattern.

Internal heat loads generated due to plugged-in equipment is added directly in building energy balance.

5.2.1.7 HVAC system

The HVAC system of the base case building is developed based on the non-residential reference building description given in Turkish National Building Performance Calculation Methodology, Appendix IV (BEP-TR, 2010). Moreover, an expert opinion is taken in selecting initial HVAC system equipment.

Reference building description of Turkey assumes central water heating system with natural gas boiler for space heating purposes. Cooling is provided through a chiller-based system where Fan coil units are acting as secondary system elements. Ventilation is assumed to be brought into the building space through an air handling unit.

Based on the acquired information, the heating, cooling and ventilation need of the base case building is assumed to be served by a central hybrid air-water HVAC system as illustrated in Figure 5.5. The heat exchange between the centrally conditioned water and room air is taking place through a four pipe fan-coil system located in each thermal zone where hot water is provided by a boiler and chilled water is provided by a chiller. Moreover, for ventilation purposes, a dedicated outdoor air system that is also served by the central plant equipment is adapted.

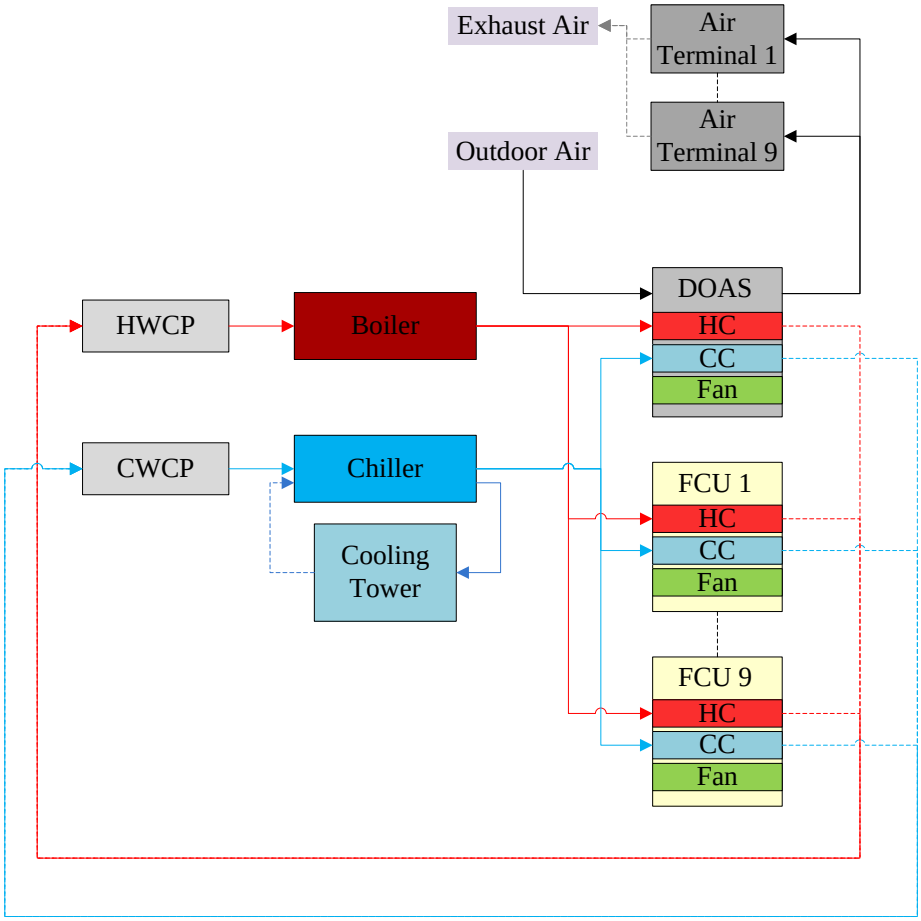

FCU : Fan Coil Unit
HC : Heating Coil
CC : Cooling Coil
HWCP : Hot Water Circulation Pump
CWCP : Chilled Water Circulation Pump
DOAS : Dedicated Outdoor Air System

Figure 5.5 : HVAC system schematic.

The author investigated available system equipment in the Turkish market and determined the related equipment efficiency coefficients based on actual products dominating the market.

The central heating plant equipment is a natural gas-fired hot water boiler, which provides hot water to the ventilation system main heating coil and fan-coil system heating coils. The nominal thermal efficiency of the plant is assumed 82%. Moreover, the efficiency is assumed to be varying during annual operation according to the boiler's biquadratic efficiency curve where the efficiency is a function of part load- ratio and boiler leaving water temperature.

The boiler nominal capacity is calculated first through sizing calculations based on the given design day weather information, then a market equipment that matches the calculated load is selected from the user-created equipment database.

There is a hot water circulating pump with a motor efficiency set at 0.875 and it operates against a 179352 Pa head. Motor is located outside of fluid and adds no heat to fluid. Hot water loop piping is assumed to be perfectly insulated, so there is no heat loss from the loop.

The central cooling plant equipment is a water-cooled electric chiller and it works together with an associated cooling tower. The chilled water is produced for the ventilation system main cooling coil and fan-coil system cooling coils. The initial rated Energy Efficiency Ratio (EER) of the chiller is assumed 4.45 kW/kW. The chiller nominal capacity is then calculated through sizing calculation based on given design day weather information. However, after establishing the required equipment capacity, actual market equipment that matches the calculated cooling load is selected from the user-created equipment database and the EER is updated accordingly. Moreover, EER is assumed to be varying during annual operation according to the chillers three efficiency curves that are Cooling Capacity Function of Temperature Curve, Cooling Capacity Function of Temperature Curve and Electric Input to Cooling Output Ratio Function of Part Load Ratio Curve. The curves are created based on manufacturers' equipment technical data sheets.

There is a variable speed chilled water pump with a motor efficiency of 90% operates against a 179352 Pa head. Motor is located outside of fluid and adds no heat to fluid. There is also a variable speed condenser water pump with a motor efficiency

of 87% operates against a 197740 Pa head. Motor is located outside of fluid and adds no heat to fluid. Chilled water and condenser water flows are assumed to be varying so that the temperature leaving the chiller matches a set point. Chilled water and condenser water loop piping are assumed to be perfectly insulated so there is no heat loss.

There are four-pipe fan coil units serving each zone. The units include cycling type fans so the fan is cycled to match unit output with the load. Heating and cooling capacities of the units are obtained through sizing calculations.

There is one central dedicated outdoor air system, which supplies 100% outdoor air to the building zones during operation hours when required. There are air terminal units in each room. The ventilation system's heating and cooling coils are also served by the central plant equipment. The main supply fan is a variable air volume fan and the total fan efficiency is 61%. The electric power input varies according to a performance curve as a function of flow fraction.

Outdoor air ventilation rate is chosen 0.0125 m3/second per person, which satisfies related ventilation standards such as ASHRAE 62.1-2010: Ventilation for Acceptable Indoor Air Quality and EN 15251: Indoor environmental input parameters for design and assessment of energy performance of buildings - addressing indoor air quality, thermal environment, lighting and acoustics.

HVAC system main operation is assumed to follow occupancy schedule. When the systems are on, the ventilation fan run continuously to supply the required ventilation air, while the fan coils cycle on and off to meet the building's cooling and heating loads. During off hours, each system will shut off, and only cycle on when the corresponding setback thermostat control calls for heating or cooling to maintain the setback temperature.

The HVAC systems maintain 21 °C heating setpoint and 24 °C cooling setpoint during occupied hours. During off hours, a thermostat setback control strategy is also applied, assuming a 15 °C for heating and 50 °C for cooling. Moreover, the HVAC system schedules allow earlier startup times to bring the space to the desired temperature at the beginning of normal occupancy. The heating and cooling is available all around the year whenever there is need.

The HVAC schedule pattern together with set point schedules are given in APPENDIX B.

5.2.1.8 Water heating system

A stand-alone storage water heater is adopted for the case study building to prepare required hot water for occupancy use. The system consists of a storage tank and a natural gas burner unit. Hot water requirement in the case study building is to supply lavatories during the day and for clean-up during the evening. The hot water consumption is assumed 7.5 litres per person per day and since there are 750 people, the daily hot water consumption is around 5625 litres. The peak flow rate is assumed 0.000469 m^3/s and a modifying hot water use schedule is used as given in APPENDIK B to obtain hourly flow rates.

The water is assumed to be heated to 50 °C. The volume of the tank and the heater capacity is sized based on peak draw, assumed start and finish temperatures and a user defined time for recovery. After establishing the hot water load, equipment that matches the calculated needs is selected from the equipment database.

The schematic of water heating system is given in Figure 5.6.

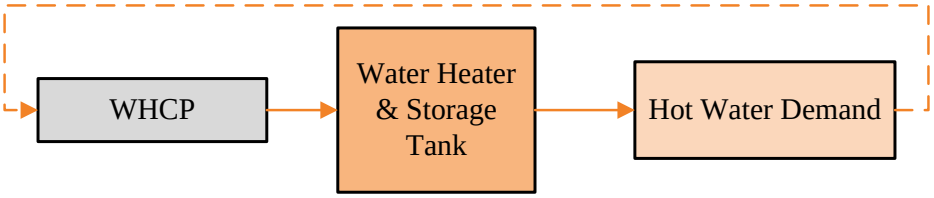

WHCP : Water Heater Circulation Pump

Figure 5.6 : Water heating system schematic.

5.2.2 Design variables

5.2.2.1 Variable description

The definition of design variables highly depend on the limitations imposed by the simulation tool that is coupled with the optimization algorithm. Therefore, in this study, decision variables are formed based on the structure of the EnergyPlus simulation tool.

As mentioned in previous chapters, there are three main factors that determine a building's demand for energy: exterior load, interior load and building heat loss or gain. Moreover, HVAC system type, equipment efficiency and control strategies affect the amount of energy consumption and indoor comfort level. Similarly, characteristics of renewable systems together with outdoor conditions determine the level of energy generation. Therefore, in this study, the considered variables are categorized into three main groups: building-related variables, HVAC-related variables and renewable system-related variables. It is assumed that building loads are served by the reference central HVAC system explained in the previous section and the renewable energy production will be supplied by photovoltaic and solar thermal systems.

The possible values of the design variables are prepared based on the actual materials and system equipment available in the Turkish construction market.

5.2.2.2 Building-related variables

Orientation

Orientation is defined by the azimuth angle between the true north and the building north axis. The orientation is measured in degrees and it is considered to be varying from 0 to 360 degrees by user defined steps.

In this case study implementation, the orientation is set as a discrete variable varying between 0 and 360 degrees with a step of 10 degrees. The initial value of the orientation is set to 0 degree.

The corresponding variable name is assigned *Ort*.

Insulation level for building main elements

Insulation level and consequent overall heat transfer coefficient of the building main structures are defined by the thickness of insulation layer exists within each structure. The lower value is taken zero, which represents no insulation condition. Insulation thickness is then varied in user defined steps, up to a user-defined maximum value.

In the case study, insulation thickness of external wall and roof elements are investigated as design variables.

For wall insulation, the thickness of only one type of wall insulation material which is extruded polystyrene is investigated. The insulation thickness within the external

wall construction is set to be varying between 0 and 0.15 meter with an incremental step of 0.005 meter. Insulation materials usually manufactured in 0.01 m thickness however, they can be also produced in 0.005m thickness on demand. Therefore, to increase the precision, 0.005m insulation thickness step is preferred. The initial value is taken zero to start with a no-insulation case. The corresponding variable name is assigned *iEW*.

Similarly, the thickness of only one type of roof insulation material which is extruded polystyrene is investigated. The insulation thickness within the roof construction is set to be varying between 0 and 0.15 meter with an incremental step of 0.005 meter. The initial value is taken zero to consider a no-insulation case. The corresponding variable name is assigned *iR*.

Solar reflectivity of roof system (roof type)

Reflective surfaces can deliver high solar reflectance and high thermal emittance therefore; they can maintain lower roof temperatures. Therefore, the performance of roof systems depending on their ability to reflect solar radiation is investigated within the course of this study. In EnergyPlus, thermal, solar and visible absorptance values of materials can be user-defined, and consequent solar reflectance and Solar Reflectance Index (SRI) values for a particular layer then can be calculated. Thus, in the optimization scheme, the solar absorptance value of the outer layer of a given roof system is taken as discrete decision variable. The absorptance value of the each product to be tested must be between 0.0 and 1.0; however designer can test and compare as many products as required.

In the case study, a reflective cool roof surface coating and a conventional dark-coloured gravel surface are investigated and compared through optimization as discrete options.

Roof layer 1 represents a dark coloured gravel layer for a conventional roof where the solar absorptivity is 0.9 (reflectivity is 0.1), emissivity is 0.9 and resulting SRI value is 6.

Roof layer 2 represents a cool roof coating material produced in Turkey and available for national market. The coating has a solar absorptivity of 0.18 (reflectivity of 0.82), emissivity of 0.9 and a resulting SRI value of 103.

The corresponding variable name is assigned *RT*.

Glazing type

In the methodology, glazing type is taken as a discrete variable where each possible integer number corresponds to a glazing unit ID number stored in the user-created database.

Glazing ID number relates the variable to the actual product information including U-value, SHGC and visible transmittance value all together. Therefore, by this approach, the designer can test and compare the actual performances of as many glazing products as required.

A database of actual glazing units available in the Turkish market has been prepared as given in Table 5.4. All the units are made of double-glazing with a filling gas and with variations of different coatings.

There are twenty-seven products in the database covering a wide range of glazing types. The U value of the products varies between 2.9 W/m2K and 1.1 W/m2K while the total solar energy transmittance (SHGC) value ranges between 0.75 and 0.21 and visible transmittance value ranges between 0.8 and 0.21. The units have either an air or argon filling of 12mm or 16mm cavity. The solar and optical properties of the units vary based on different coatings and technologies applied.

Table 5.4 : Glazing database.

Glazing Type (ID)	U Value	SHGC	Tvis	Glazing Type (ID)	U Value	SHGC	Tvis
1	2.9	0.75	0.80	15	1.6	0.39	0.64
2	2.8	0.46	0.64	16	1.6	0.29	0.45
3	2.8	0.34	0.35	17	1.6	0.21	0.21
4	2.8	0.28	0.21	18	1.3	0.56	0.79
5	2.7	0.75	0.80	19	1.3	0.44	0.71
6	2.7	0.46	0.64	20	1.3	0.39	0.64
7	2.7	0.34	0.35	21	1.3	0.29	0.45
8	2.7	0.28	0.21	22	1.3	0.21	0.21
9	2.6	0.75	0.80	23	1.1	0.56	0.79
10	2.6	0.46	0.64	24	1.1	0.44	0.71
11	2.6	0.34	0.35	25	1.1	0.39	0.64
12	2.6	0.28	0.21	26	1.1	0.29	0.45
13	1.6	0.56	0.79	27	1.1	0.21	0.21
14	1.6	0.44	0.71				

There are 27 values from 1 to 27 available as values of design variables.

The initial glazing type is taken Glazing 1 with a U-value of 2.9 W/m2K, SHGC of 0.75 and Tvis of 0.8.

The corresponding variable name is assigned *GT*.

Window-to-wall ratio

Window-to-wall ratio is defined by the varying window size. It is assumed that the external wall accommodates a single rectangular window placed at its centre and the window size is calculated based on the window width and height.

Window-to-wall ratio is taken as a discrete variable where each possible design variable is a pre-defined window coordinate value corresponding to a w-t-w ratio. Therefore as each window coordinate changes, so does the percentage of the glazed surface.

In the case study, six w-t-w ratio options that are 5%, 15%, 25%, 35%, 45%, and 55% considered as decision variables.

Building facades with different orientations may have different window-to-wall ratios however for each orientation the w-t-w is required to be same.

In the case study, window height is fixed at 1.5 m. As illustrated in Figure 5.7, only the x coordinates of the window corners are allowed to vary. The maximum value of the window coordinates cannot exceed the coordinate values of the base walls that contain the window.

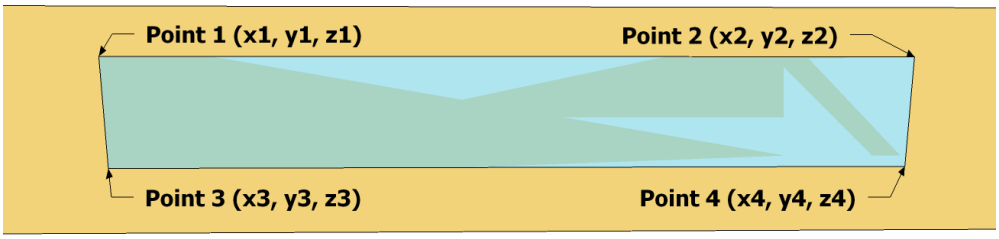

Figure 5.7 : Window coordinates.

The initial window-to-wall ratios of all windows are set to 25%.

The corresponding variable name is assigned *WTW*.

Artificial lighting control

A building's daylight potential and the answer to whether or not to integrate electric lights with a daylighting dimming control system is explored in discrete form where design variables are either 0 or 1. If the variable takes 0 there is only a manual

control system available, however if variable takes 1, a pre-defined daylighting based dimming control system is integrated into the building simulation model and building lights are allowed to be dimmed according to a user set daylighting control scheme.

The corresponding variable name is assigned *DL*.

In the case study, the predefined dimming control operates with a design value of 500 lux and two points inside each zone at a height of 0.8 m (desk level) are selected as reference points as shown in Figure 5.8.

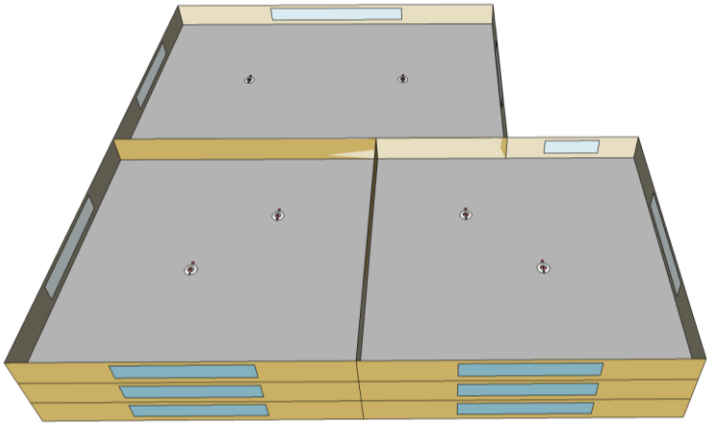

Figure 5.8 : Location of daylighting reference points.

At each time step the required power of the artificial lights is calculated according to the illuminance levels evaluated at the reference points and the parameters established by the control strategy.

5.2.2.3 HVAC system-related variables

In the current study, a selection of HVAC plant equipment is realized through optimization. Each chiller or boiler equipment has a unique ID number that relates it to the physical equipment information and related performance curves stored in the database. Therefore, optimization searches among discrete equipment ID numbers for the suitable equipment that can match the required capacity and load requirements while showing the best performance throughout the year. The developed optimization code makes sure at each iteration step the equipment capacity, reference efficiency ratio and off-reference equipment performance curves which define the dynamic equipment performance is read from the user-prepared equipment database and loaded to simulation model for the analysis.

The number of chiller or boiler equipment to investigate is set by the designer; however enough equipment that can cover a wide range of equipment capacities should be available in the database.

In addition, the capacity of depending equipment such as cooling towers and fan coil units are calculated based on building loads and selected equipment simultaneously within the process as a depending variable.

Chiller Type

The chiller equipment type is taken as a discrete variable where given values of design variable is integers indicating chiller equipment stored in a user-created chiller database. The corresponding variable name is assigned *CL*.

In the database, each chiller is defined with a nominal cooling capacity, full load energy efficiency ratio and off-reference performance curves including Capacity as a Function of Temperature curve (CAPFT), Energy Input Ratio as a Function of Temperature curve (EIRFT), and Energy Input Ratio as a Function of Part-load Ratio curve (EIRFPLR).

CAPFT is a biquadratic performance curve that parameterizes the variation of the cooling capacity as a function of the leaving chilled water temperature and the entering condenser fluid temperature. EIRFT is again a biquadratic performance curve that parameterizes the variation of the energy input to cooling output ratio as a function of the leaving chilled water temperature and the entering condenser fluid temperature. Lastly, EIRFPLR is quadratic performance curve that parameterizes the variation of the energy input ratio (EIR) as a function of the part-load ratio. The EIR is the inverse of the COP, and the part-load ratio is the actual cooling load divided by the chiller's available cooling capacity. The three curves define the impact of varying chilled water temperature, condenser temperature, and load on chiller performance and capacity.

For case study under investigation, a chiller database including 44 chiller equipment, which are commercially available in Turkish market, is prepared. A sample the library is given in Table 5.5 below. The library covers a range of products with cooling capacities from 270 kW to 1750 kW. Moreover, there are two product categories based on their efficiencies: moderate-efficiency chiller category (average EER: 4.72) as shown in Group A of Table 5.5 and high-efficiency chiller category

(average EER: 5.63) as shown in Group B of Table 5.5. The initial chiller type is also selected after the base case sizing calculations from this database.

Table 5.5 : A sample of chiller equipment database.

Group A: Moderate-efficiency chillers

Chiller Type	Capacity (kW)	EER	Efficiency curves		
			CAPFT	EIRFT	EIRFPLR
1	287	5.04	CAP1	EIR1	EPLR1
2	312	4.8	CAP2	EIR2	EPLR2
3	349	4.85	CAP3	EIR3	EPLR3
4	375	4.57	CAP4	EIR4	EPLR4
...	...	...	...	...	...
20	1420	4.7	CAP20	EIR20	EPLR20
21	1630	4.76	CAP21	EIR21	EPLR21
22	1750	4.73	CAP22	EIR22	EPLR22

Group B: High-efficiency chillers

Chiller Type	Capacity (kW)	EER	Efficiency curves		
			CAPFT	EIRFT	EIRFPLR
23	270	5.64	CAP23	EIR23	EPLR23
24	304	5.61	CAP24	EIR24	EPLR24
25	355	5.53	CAP25	EIR25	EPLR25
26	380	5.6	CAP26	EIR26	EPLR26
...	...	...	...	...	...
42	1442	5.5	CAP42	EIR42	EPLR42
43	1614	5.81	CAP43	EIR43	EPLR43
44	1742	5.72	CAP44	EIR44	EPLR44

Similarly, a sample of related chiller curves is also shared in Table 5.6. The curve coefficients are calculated by the author based on equipment test measurements published by manufacturers through application of appropriate curve fitting procedures.

Table 5.6 : A sample of chiller performance curve database.

Name	CAPFT1	EIRFT1	EIRFPLR1
Coefficient1 Constant	9.62E-01	7.96E-01	4.15E-02
Coefficient2 x	4.01E-02	-1.25E-03	6.54E-01
Coefficient3 x**2	8.71E-05	7.38E-04	3.04E-01
Coefficient4 y	-4.60E-03	-9.84E-03	N.A
Coefficient5 y**2	-6.97E-05	8.11E-04	N.A
Coefficient6 x*y	-2.26E-04	-1.23E-03	N.A
Minimum Value of x	5	5	0.25
Maximum Value of x	12	12	1.01
Minimum Value of y	25	25	N.A
Maximum Value of y	40	40	N.A

The complete chiller database with physical product information and chiller performance curves can be found in APPENDIX C.

Boiler type

The boiler equipment type is taken as a discrete variable where given values of design variable are integers indicating a boiler equipment stored in the user-created boiler database. The corresponding variable name is assigned *BL*.

Each boiler is defined with a nominal heating capacity, nominal thermal efficiency and a performance curve.

The thermal efficiency-curve is called Normalized Boiler Efficiency Curve (NBEC) and it is required for describing the normalized heating efficiency (as a fraction of nominal thermal efficiency) of the boiler's burner. NBEC parameterizes the boiler's efficiency as a function of the part-load ratio and boiler outlet water temperature.

For this case study, a boiler database including 54 boiler equipment, which are commercially available in Turkish market, is prepared by the author. A sample of the boiler library is given in Table 5.7 below. The library covers a range of products with heating capacities from 55 kW to 1210 kW. Moreover, there are two product categories based on their efficiencies: low-efficiency boiler category (efficiency: 84%) as shown in Group A of Table 5.7 and high-efficiency boiler category (efficiency: 95%) as shown in Group B of Table 5.7. The initial boiler type is also selected after sizing calculations from this database.

Table 5.7 : A sample of boiler equipment database.

Group A: Low-efficiency Boilers				**Group B:** High-efficiency Boilers			
Boiler Type	**Capacity (kW)**	**Thermal Efficiency**	**Efficiency Curve**	**Boiler Type**	**Capacity (kW)**	**Thermal Efficiency**	**Efficiency Curve**
1	55	0.84	BLE1	28	58	0.95	BLE28
2	76	0.84	BLE2	29	70	0.95	BLE29
3	93	0.84	BLE3	30	85	0.95	BLE30
…	...	...	…	...	...	...	...
25	1025	0.84	BLE25	52	1020	0.95	BLE52
26	1115	0.84	BLE26	53	1110	0.95	BLE53
27	1210	0.84	BLE27	54	1200	0.95	BLE54

Similarly, a sample of boiler efficiency curve database is also shared in Table 5.8. The curve coefficients are generated by the author based on equipment test

measurement data published by manufacturer through imposing a curve fitting procedure.

Table 5.8 : A sample of boiler curve database.

Name	BLE
Coefficient1 Constant	1.112
Coefficient2 x	7.86E-02
Coefficient3 x**2	-4.00E-01
Coefficient4 y	0
Coefficient5 y**2	-1.57E-04
Coefficient6 x*y	9.38E-03
Coefficient7 x**3	2.34E-01
Coefficient8 y**3	1.33E-06
Coefficient9 x**2*y	-4.45E-03
Coefficient10 x*y**2	-1.22E-05
Minimum Value of x	0.1
Maximum Value of x	1
Minimum Value of y	20
Maximum Value of y	80

The complete boiler library including physical product information and boiler performance curves can be found in APPENDIX C.

5.2.2.4 Renewable system-related variables

In the case study, sizing and equipment selection of Photovoltaic and solar water heating systems are carried out through proposed optimization scheme.

Photovoltaic module type

Photovoltaic technology is evolving quickly and as a result, new products are introduced to the market. Each module in the market has different dynamic performance characteristics. In the base case building, there is no PV system available. However, in order to investigate the ideal PV system that can complement the new design proposal, a generic PV system is added to the simulation-optimization model and analyses are carried out. The generic system consists of a PV array and a simple inverter. Energy storage is ignored for simplification. In the optimization methodology, different PV module types and their physical and efficiency data are stored in the database by a unique ID number. PV module type is then taken as a discrete design variable therefore allowing designer to compare the performance of different products. The number of different PV modules to compare is up to the designer. The corresponding variable name is assigned *PVtyp*.

In the case study, the performance of two PV types, which are Poly Crystalline Silicon Cells and Thin Film Cells, are evaluated and compared. Table 5.9 shows the characteristics of the PV modules included in the database.

Table 5.9 : Photovoltaic module library.

Photovoltaic Type	**PV 1**	**PV 2**
Cell type	Poly Crystalline Silicon	Thin film
Number of Cells in Series	60	90
Active Area (m2)	1.46	0.9216
Shunt Resistance (ohm)	1000000	400
Maximum Power under standard test conditions	250 Wp	60 Wp
Short Circuit Current (A)	8.64	1.19
Open Circuit Voltage (V)	37.6	92
Reference Temperature (^{o}C)	25	25
Reference Insolation	1000	1000
Module Current at Maximum Power (A)	8.12	0.9
Module Voltage at Maximum Power (V)	30.8	67
Temperature Coefficient of Short Circuit Current	0.0029376	0.000895
Temperature Coefficient of Open Circuit Voltage	-0.12784	-0.2806
Nominal Operating Cell Temperature Test Ambient Temperature	20	20
Nominal Operating Cell Temperature Test Cell Temperature	46	46
Nominal Operating Cell Temperature Test Insolation	800	800
Module Heat Loss Coefficient	30	30
Total Heat Capacity	50000	50000

The data is obtained from technical data sheets of actual market products. The PV 1 has a module efficiency of 14.91% and the PV 2 has a module efficiency of 6.3 % under standard test conditions.

Number of available photovoltaic modules

The optimization methodology can also calculate the optimum installed PV capacity and consequent power output for a particular building based on the total number of PV modules in an array. Therefore, the number of installed modules is taken as the design variable. The corresponding variable name is assigned *PVnum*.

The minimum number of modules is assumed 1. The maximum number of modules is obtained based on the availability of the area for modules, module size and the minimum distance between the modules. In the case study, the building roof is considered as module location as shown in Figure 5.9. The rows of modules are arranged at a distance to each other such that the shadow from each module in no

case reaches the next row. Taking into account all the influential parameters, the maximum available module number is calculated as 858 for the base case building where 26 of them are connected in parallel and 33 of them are connected in series.

The PV module orientation and inclination angle is set as a fixed parameter where modules are arranged facing south and tilted according to the latitude of each building location.

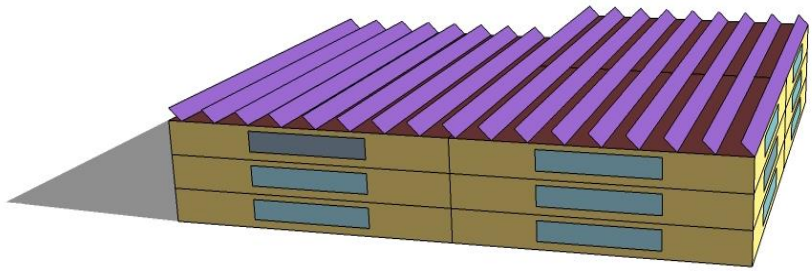

Figure 5.9 : The PV system integrated into base case building.

Solar thermal module type

Using thermal storage systems to gain hot water is becoming very popular and there are many solar collector products available in the market. Solar collectors (SC) can have diverse thermal and optical properties therefore in the methodology the collector module characteristics including the coefficients for the energy conversion efficiency and incident angle modifier are stored in the library by an ID number together with physical module data. Module type is then taken as a discrete variable that can take the value of product ID number.

In the base case building, there is no solar water heating system available. However, in order to investigate the ideal system configuration that can improve the performance of the base case building, a generic system is added to the simulation-optimization model. The system consists of a collector array, a water tank and a backup system.

Solar collector module type is taken as the discrete variable where possible variable values are integers indicating a collector module stored in a user-created collector database. The corresponding variable name is assigned *SCtyp*.

In the case study, there are three glazed flat-plate solar collectors which are a high-efficiency selective surface collector (SC1), a medium-efficiency selective surface collector (SC2) and a low-efficiency black painted collector (SC3) are evaluated and

compared. All three collectors have a gross area about 2.5 m^2. The collector thermal performances are compared in Table 5.10 below based on kilowatt-hours thermal collector output per panel per day published by Solar Rating & Certification Corporation (SRCC).

Table 5.10 : Solar collector thermal performance rating.

Climate ->		**High Radiation**	**Medium Radiation**	**Low Radiation**
Category (Ti-Ta)*	**Collector type**	**(6.3 kWh/m².day)**	**(4.7 kWh/m².day)**	**(3.1 kWh/m².day)**
C (20 °C)	SC 1	8.8	6	3.3
	SC 2	7.9	5.4	3
	SC 3	6.3	3.9	1.8
D (50 °C)	SC 1	5.8	3.3	1
	SC 2	5.1	2.9	0.9
	SC 3	2.5	0.8	0

** difference between collector inlet fluid temperature (Ti) and the ambient air temperature (Ta).*
*** C- Water Heating (Warm Climate) D- Space & Water Heating (Cool Climate.*

Moreover, the collector library that includes the thermal and optical characteristics of the solar collectors under consideration is given in Table 5.11. The data is obtained from actual market products.

Table 5.11 : Solar collector database.

Solar Collector Name	**SC 1**	**SC 2**	**SC 3**
Surface type	Selective Surface High Efficiency	Selective Surface Medium Efficiency	Black painted Low Efficiency
Gross Area (m2)	2.52	2.50	2.49
Test Fluid	water	water	water
Test Flow Rate	0.0000498	0.0000471316	0.0000499400
Test Correlation Type	Inlet	Inlet	Inlet
Coefficient 1 of Efficiency Equation	0.7162	0.708	0.659
Coefficient 2 of Efficiency Equation	-3.0562	-3.7334	-5.3999
Coefficient 3 of Efficiency Equation	-0.00674	-0.00591	-0.01871
Coefficient 2 of Incident Angle Modifier	-0.07070	-0.13886	-0.27781
Coefficient 3 of Incident Angle Modifier	-0.12320	-0.00901	-0.08253

Number of available solar thermal modules

The total number of collector modules determines thermal output of the system. In EnergyPlus simulation engine, a solar collector is defined with an individual associated surface that determines the collector location, tilt, azimuth, and gross area. Therefore, the physical presence of an associated surface represents a module's existence. The surfaces are defined in the 3D coordinate system (x, y, z) thus, the surfaces coordinates become design variables. In particular, when the x and y coordinate values of a module's upper left and right corners equals to actual coordinates, the collector exist. However, when the x and z coordinates equal to the values of lower left and right corners, the collector does not exist. Thus, based on the user-specified coordinate values, the total number of available modules can be calculated. The corresponding variable name is assigned *SCnum*.

The maximum number of modules is obtained based on the building water heating load, availability of the area for modules, module size and the minimum distance between the modules. In the case study, it was assumed that collectors would be installed next to the building site. Moreover, the rows of modules would be arranged at a distance to each other such that the shadow from each module in no case reaches the next row. Taking into account building occupancy density and hot water needs, the maximum available module number is assumed 140 for the base case building as shown in Figure 5.10.

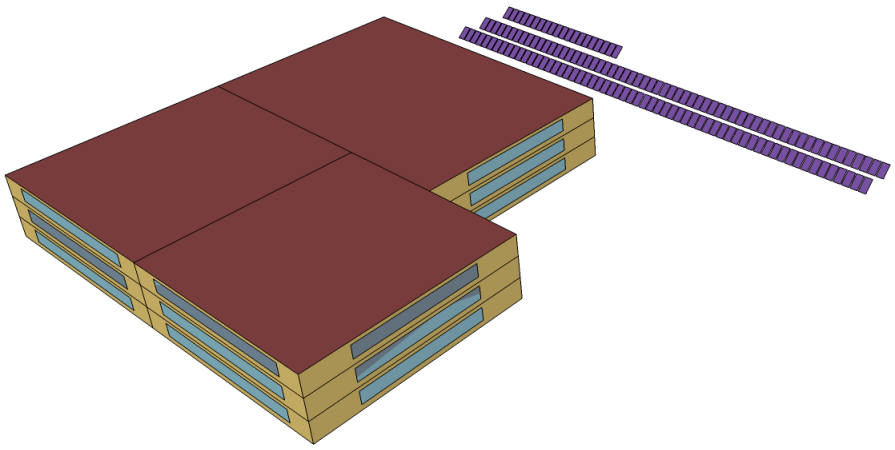

Figure 5.10 : The solar thermal system integrated into the base case building.

The collector orientation and inclination angle is set as a fixed parameter where modules are arranged facing south and tilted according to the latitude of building location.

5.2.3 Objective function

In the current investigation, the objective function is represented by the global cost per square meter building floor area difference between any design combination that is created through optimization and base case design, added with the sum of all the penalty functions due to constraint violations. Therefore, only the additional cost incurred to achieve a given level of energy savings can be determined and compared while considering design limitations. The objective formula is given in equation 5.1.

$$h(x) = \frac{dGC_i}{Building\ Floor\ Area} + PEN \tag{5.1}$$

Where

dGC_i : Global cost difference between any design combination and base case building,

PEN : Sum of all penalty function results.

The reason to divide the GC to the floor area is to reduce the magnitude of the value for better readability.

As explained previously in the methodology section, the purpose of this study is to assist designers in achieving cost-effective high performance building design, therefore the cost function was defined to minimize building energy, water, material, and system related service life costs while maintaining or improving user comfort and reducing building CO_2 emission rates. The elements of the main objective function of the case study are therefore as given in equation 5.2:

$$\begin{aligned} h(x) \quad &= d(\textstyle\sum_1^n NPV_{Energy} + \sum_1^n NPV_{Water} + \sum_1^n NPV_{Material} + \\ &\textstyle\sum_1^n NPV_{Equipment} + \sum_1^n NPV_{Renewable})/Area + \sum_1^{k4} \mu_x PEN_k \end{aligned} \tag{5.2}$$

Each cost component is discounted to the present considering the time value of money. The main function is then adapted specifically for the case studies and reformulated.

5.2.3.1 Global cost components

The energy component of the main formula includes net present value of end-use energy consumption due to operation of boiler, chiller, fans (including fan coils and

ventilation fans), circulation pumps, water heating, interior lighting and plugged-in equipment. Moreover, in cases with PV optimization, the net present value of the surplus electricity generated through PV system is subtracted from overall energy cost as a benefit. Equation 5.3 shows end use types and related energy sources. It is assumed that the building maintains its annual energy efficiency performance throughout the long-term calculation period.

$$\sum_{1}^{n} NPV_{Energy} = NPV_{Natural\ gas}^{Boiler} + NPV_{Electricity}^{Chiller} + NPV_{Electricity}^{Cooling\ tower} + NPV_{Electriciy}^{Fans} + NPV_{Electriciy}^{Pumps} + NPV_{Natural\ gas}^{Water\ heating} + NPV_{Electricity}^{Lighting} + NPV_{Electricity}^{Plugged\ equipment} - (NPV_{Electricity}^{PV\ Surplus}) \quad (5.3)$$

The water component of the main formula includes net present value of water use due to HVAC cooling tower operation and occupancy hot water use, as given in equation 5.4.

$$\sum_{1}^{n} NPV_{Water} = NPV_{Water}^{Cooling\ tower} + NPV_{Hot\ Water}^{Occupancy} \quad (5.4)$$

The material component of the main formula includes net present value of ownership costs of building materials tested through optimization including insulation for external walls and roof, roof cover layer, glazing unit and external wall element, as given in equation 5.5. As the window-to-wall-ratio of external wall varies, the cost of external brick wall also varies as a dependent variable; therefore, its influence is also taken into account. The net present value covers initial, installation, maintenance, replacement and disposal costs of each element.

$$\sum_{1}^{n} NPV_{Material} = NPV_{Material}^{External\ wall\ insulation} + NPV_{Material}^{Roof\ insulation} + NPV_{Material}^{Roof\ cover} + NPV_{Material}^{Window} + NPV_{Material}^{External\ wall} \quad (5.5)$$

The equipment component of the main formula given in equation 5.6 includes net present value of HVAC equipment selected during optimization including boiler and chiller. Moreover net present value of depending equipment including cooling tower

and fan coils are taken into account as well. The cost of ventilation fans and circulation pumps are ignored for simplification. The formula also includes NPV of water heating equipment and lighting control system. The value covers initial, installation, maintenance, replacement and disposal costs of each element.

$$\sum_{1}^{n} NPV_{Equipment} = NPV_{Equipment}^{Boiler} + NPV_{Equipment}^{Chiller} + NPV_{Equipment}^{Cooling\ tower} + NPV_{Equipment}^{Water\ heater} + NPV_{Equipment}^{Fan\ coil} + NPV_{Equipment}^{Lighting\ contol} \quad (5.6)$$

When the base case is integrated with the PV and solar water heating systems, renewable system component given in equation 5.7 is also added to the global cost.

$$\sum_{1}^{n} NPV_{Renewable} = NPV_{Renewable}^{PV} + NPV_{Renewable}^{SWH} \quad (5.7)$$

The renewable system component includes net present value of ownership of selected and sized renewable system equipment, namely photovoltaic and solar thermal collectors, and rest of the supporting equipment required for a successful implementation. The net present value covers initial, installation, maintenance, replacement and disposal costs of each equipment.

5.2.3.2 Penalty function components

There are four penalty functions, which are thermal comfort, CO_2 emission rate, equipment capacity and payback period of renewables, used to restrict the design space to a user-defined eligible region.

Equipment capacity

The methodology requires the HVAC equipment to be sized first through a sizing calculation then, the optimization attempts to select a suitable equipment from the equipment database that can satisfy the autosized capacities while performing well at on and off-reference conditions. Sizing factors are applied to determine an allowable capacity range.

In the case study, for boiler equipment, the capacity lower limit factor is set as 0.99, and the capacity upper limit is chosen as 1.25.

Thus, the capacity penalty equation for boiler takes the form in equation 5.8.

$$PEN_{CapacityBoiler} = \mu_{blmax}\left(max\left(0,\ (BLC_{actual} - BLC_{autosize} * 1.25\ )\right)\right)^{q} + \mu_{blmin}\left(max\left(0,\ (BLC_{autosize} * 0.99 - BLC_{actual})\right)\right)^{q} \quad (5.8)$$

Similarly, the capacity lower limit factor is set as 0.99, and the capacity upper limit is chosen as 1.15 for chiller equipment. Therefore, the capacity penalty equation for chiller is expressed as in equation 5.9.

$$PEN_{CapacityChiller} = \mu_{clmax}\left(max\left(0,\ (CLC_{actual} - CLC_{autosize} * 1.15\ )\right)\right)^{q} + \mu_{clmin}\left(max\left(0,\ (CLC_{autosize} * 0.99 - CLC_{actual})\right)\right)^{q} \quad (5.9)$$

Penalty parameters μ_{blmax}, μ_{blmin}, μ_{clmax}, μ_{clmin} and penalty power factor q are determined in the pre-optimization phase based on design of experiments.

The application of capacity constraints makes sure that optimization selects right-sized equipment.

Thermal Comfort

In thermal comfort penalty function, the target thermal comfort metric is chosen according to European standard EN 15251. The standard indicates four categories of state of comfort for mechanically heated and cooled buildings through PMV and PPD metrics, as shown in Table 5.12.

Table 5.12 : Recommended categories for design of mechanically heated and cooled buildings according to EN 15251.

Category	PPD %	PMV
I (high level of expectation),	< 6	-0.2 < PMV < + 0.2
II (normal level of expectation),	<10	-0.5 < PMV < + 0.5
III (moderate level of expectation),	<15	-0.7 < PMV < + 0.7
IV (acceptable only for a limited part of the year).	>15	PMV < - 0.7; or + 0.7 < PMV

"Category II: normal level of expectation" is taken to define the boundaries of the comfort zone, therefore the target PPD index is determined as 10 per cent. Equation 5.10 introduces the penalty formula used for the case study application.

$$PEN_{Comfort} = \mu_{cf}\left(max\left(0,\ (PPD_{actual} - 10)\right)\right)^{q} \tag{5.10}$$

The PDD index of actual building is computed for each hour of the occupancy work schedule through the year for each thermal zone. For simplification, hourly PPD indices are averaged for the whole year. Then, an area-weighted average PPD of all zones is calculated to represent the comfort conditions in the entire building as given in equation 5.11.

$$PPD_{Actual} = \frac{\sum_{n=1}^{9} PPD_n^{Avg} * ZoneArea_n}{\sum_{1}^{9} ZoneArea_n} \tag{5.11}$$

Penalty parameter μ_{cf} and power factor q are determined in the pre-optimization phase based on design of experiments.

CO_2 emission rate

In CO_2 emission penalty function, a penalty is applied to force the optimum solution into the target zone when the emitted overall building CO_2 emission rate exceeds a user-set target.

In the case study, 10 per cent reduction in building annual CO_2 emission is aimed to be achieved therefore the final formula becomes as in equation 5.12.

$$PEN_{Emission} = \mu_{em}\left(max\left(0,\ (CO2_{actual} - CO2_{base} * 0.9)\right)\right)^{\mathrm{q}} \tag{5.12}$$

The actual amount of CO_2 released from base case building due to energy consumption is obtained through application of appropriate carbon dioxide equivalent intensity indexes for each energy carrier. In this study, CO_2 emission factor is set at 0.234 kg.eqCO2/kWh for natural gas and 0.617 kg.eqCO2/kWh for electricity in compliance with published national data by Ministry of Environment and Urbanization of Turkey.

Therefore, the actual amount of CO_2 emission rate is formulated as in equation 5.13:

$$CO2_{Actual} = 0.617 * \sum Electricy + 0.234 * \sum Natural\ Gas \quad (5.13)$$

Penalty parameter μ_{em} and power factor q are determined in the pre-optimization phase based on design of experiments.

Payback period

The payback period of a renewable system investment is limited according to a user set time-period. In the case study, 25 years period is chosen as maximum payback limit both for photovoltaic and solar thermal system applications and the related formula is expressed as in equation 5.14. The reason to choose a long period as payback time is to have an opportunity to observe the payback behaviour of renewable systems under different climatic conditions within building life-cycle and to compare climate responsive performances without eliminating systems unless they are not beneficial within the building life.

$$PEN_{payback\ PV/SC} = \mu_{pbPV/SC} \left(max(0,\ (SPB_{actual} - 25))\right)^{q} \quad (5.14)$$

Penalty parameter μ_{pb} and power factor q are determined in the pre-optimization phase based on design of experiments.

5.2.4 Financial data

Cost analysis is only as valid as its data; therefore, it is crucial that data used for the calculations are accurate and representative of the present conditions. Calculating the global cost of a building is generally a complicated process involving factors such as product, installation and maintenance costs, predicted energy and water use and prices, discount rates, etc. The author of the study thus carried out an extensive market survey to collect cost data on design variables including building materials, HVAC system equipment and photovoltaic and solar thermal renewable systems. A price database has been established. Data regarding commonly used products in Turkish construction sector is collected directly from manufacturers and retail offices. When required, unit cost data which is published by Ministry of Environment and Urbanization of Turkey inside the Building Construction Unit Cost

Data Book was also used. Usually more than one price for a product group is obtained, therefore prices are averaged to represent generic market situation.

Moreover, the historical time-series data about Turkish financial markets including inflation, market interest rate and price escalation rates were investigated, too. The year 2012 is selected as the representative year for financial indicators.

The cost data libraries are introduced in the following sections.

5.2.4.1 Financial market data

Since the global cost calculation in the methodology is based on the net-present value approach, all the costs and revenues occur during building life span requires to be discounted to the present while considering the time value of money.

Inflation rate and the market interest rate (normal discount rate) for Turkey are obtained from Central Bank of Turkey, as summarized in Table 5.13. Annual average inflation rate is calculated as 8.936 % based on monthly Consumer Price Index in 2012 and market interest rate is calculated as 10.264 % based on Average Cost of Domestic Borrowing, Zero Coupon index. The case study uses constant dollars approach that is cost value after adjustment for inflation. As a result, real discount rate is calculated as 1.21 % based on the given information. After establishment of real discount rate, NPV of each cost or revenue can be calculated.

Table 5.13 : Nominal discount rate and inflation rate for Turkey.

Month (2012)	Market interest rate (Annual Compound, %)	Inflation rate (Year to Year % Changes)
January	11.07	6.16
February	11.38	6.37
March	11.1	7.8
April	10.84	9.19
May	10.71	8.88
June	10.87	9.07
July	10.71	8.87
August	10.39	8.28
September	9.61	11.14
October	9.15	10.43
November	8.83	10.43
November	8.51	10.61
Average	10.264	8.936

5.2.4.2 Cost estimates for energy and water

Annual energy and water cost due to building operation is calculated as a product of building operating source consumption which is estimated through simulation and a corresponding utility tariff.

Utility rate for electricity is obtained from Turkish Electricity Distribution Company (TEDAS). The year 2012 average retail price of 0.32 TL/kWh (including Value added tax (VAT) and all other taxes) is used as building's unit cost of electricity consumption. Moreover, the utility electricity prices since 1995 that are published by TEDAS were investigated and escalation rate for electricity is computed as 11% including inflation. When the price is adjusted for inflation, the real electricity price escalation rate is calculated as 1.89 %.

To obtain the feed-in tariff applicable to renewable electricity production, it has been benefitted from national renewable energy regulation. Therefore, the unit price is set at 0.305 TL/kWh for electricity fed back into the electricity grid as recommended by the national bodies.

Utility rate for natural gas is obtained from IGDAS (Istanbul Gas Distribution Industry and Trade Incorporated Company). The year 2012 average retail price of 0.09 TL/kWh (including VAT and all other taxes) is used as building's unit cost of natural gas consumption. Moreover, the utility gas prices since 2008 that are published by IGDAS were investigated and nominal price escalation rate for natural gas is computed as 14.4 % including inflation. When the price is adjusted for inflation, the real natural gas price escalation rate is calculated as 5 %.

Utility rate for water is obtained from ISKI (Istanbul Water and Sewerage Administration). The year 2012 average retail price of 8.217 TL/m3 (including VAT and all other taxes) is used as building's unit cost of water consumption. Moreover, the utility water prices since 2006 that are published by ISKI were investigated and escalation rate for water is computed as 11.7 % including inflation. When the price is adjusted for inflation, the real water price escalation rate is calculated as 2.58 %.

5.2.4.3 Cost estimates for design variables

In the building service life, costs are incurred in construction, operation, and disposal of a facility. Therefore, to perform global cost analyses for a building design project

initial, operating, maintenance and disposal costs for each design variable are needed.

The initial cost for a building material including insulation, glazing type, roof cover, and wall construction is calculated as a product of unit price of the material and the amount that is actually required. Similarly cost for maintenance, replacement and disposal are also directly related with the amount of material used.

On the other hand, each system equipment has a unique list price collected from the market. Maintenance, replacement and disposal costs are associated with the equipment itself.

In the calculation, the study period is estimated 25 years. Therefore, in cases where the life expectancy of the equipment or material is shorter than building life, replacement costs are taken into account.

Similarly, if the product life ends after building life, a scrap value is calculated based on percentage of remaining equipment life and corresponding initial cost. The present value of this value is subtracted from the final net present value.

Cost data for each design element is given below. All the prices include VAT of 18 percent.

Orientation

Variation in building orientation only influences building energy demand, energy and HVAC water consumption levels and consequent costs. There is no other cost associated with orientation variable.

External wall / roof insulation

The average market price of a Extruded polystyrene insulation panel with a density of 150 kg/m3 and a heat transfer coefficient of 0.031 W/m.K is used in the cost analysis. The panels can be applied to walls, floor and flat roof construction. The price of the insulation is calculated based on per m3 and it linearly increases as thickness grows. The unit price of the panel is obtained as 360 TL/m3. The installation cost is assumed as 9.56 TL/m2 including labour and installation material.

Insulation is assumed to have no maintenance and repair requirements. The life expectancy of insulation panel is assumed as lifespan of the building therefore neither replacement cost nor scrap value occurs.

External wall element

The area of external walls change with the variation in building window-to-wall ratio since it is one of the design variables of the study. Therefore, to take into account the cost of building external wall element, the price of a generic wall composition is created based on National Construction Data Book for Turkey. The insulation price is excluded from the sum as it is calculated and used separately in the analysis. The unit price for a brick wall construction is calculated as 95m2/TL based on the breakdown given in Table 5.14.

Table 5.14 : External wall construction cost.

Description of Steps	Unit	Unit Cost
To paint the wall with emulsion paint	M2	4.88 TL
To plaster the wall with cement mortar	M2	19.36 TL
To build the brick wall	M2	34.00 TL
To plaster the wall with mortar	M2	10.06 TL
To paint the wall with emulsion paint	M2	12.19 TL
Total Cost		80.49 TL/m2
Total Cost inc VAT 18%		95 TL/m2

The external wall element is assumed to have no maintenance and repair requirements. The life expectancy of external wall is assumed as lifespan of the building therefore neither replacement cost nor scrap value occurs.

Roof cover

The prices of a conventional roof finish with gravel and cool roof paint are explored.

The unit cost of gravel is obtained as 59TL/m3 including material and labour cost. Since the roof area is fixed at 2903 m2, the total initial cost for covering the flat roof in consideration with 0.08 m gravel becomes 13702 TL. The life expectancy of gravel layer is assumed as long as life span of the building and no maintenance is required during this period. Similarly, no scrap value is assumed.

To cover the same roof with cool roof paint requires application of a base and a coating layer. The price of base layer is 8.26 TL/kg and 315 kg is required for the case study building. The price of the paint layer is 6.49 TL/kg and 1188 kg is required for two layer application. Therefore, the total initial material cost is calculated as 10312 TL. The labour cost for material application is obtained as 2.36 TL/m2; therefore the total labour cost becomes 6851 TL.

The upper paint coating is required to be renewed in single layer in every five years because the solar reflectivity of the coating is decreased by time. The maintenance cost 6758 TL in total including material and labour cost and the value is required to be discounted to present value using appropriate discount factors.

There is no scrap value associated with cool roof paint as well.

Glazing units

Cost of glazing systems vary based on the production technology and the type of the glass. The market survey taken aimed to cover commonly available and frequently used products in Turkey. Table 5.15 summarizes cost per square meter for all the glazing products available in the library.

Table 5.15 : Glazing cost data.

Glazing Type	U Value	SHGC	Tvis	Cost TL/m2	Glazing Type	U Value	SHGC	Tvis	Cost TL/m2
1	2.9	0.75	0.80	38.9	15	1.6	0.39	0.64	61.4
2	2.8	0.46	0.64	46.6	16	1.6	0.29	0.45	88.5
3	2.8	0.34	0.35	82.6	17	1.6	0.21	0.21	75.5
4	2.8	0.28	0.21	64.9	18	1.3	0.56	0.79	48.4
5	2.7	0.75	0.80	42.5	19	1.3	0.44	0.71	54.3
6	2.7	0.46	0.64	53.1	20	1.3	0.39	0.64	64.9
7	2.7	0.34	0.35	86.1	21	1.3	0.29	0.45	92
8	2.7	0.28	0.21	68.4	22	1.3	0.21	0.21	79.1
9	2.6	0.75	0.80	46	23	1.1	0.56	0.79	51.9
10	2.6	0.46	0.64	56.6	24	1.1	0.44	0.71	57.8
11	2.6	0.34	0.35	89.7	25	1.1	0.39	0.64	68.4
12	2.6	0.28	0.21	72	26	1.1	0.29	0.45	95.6
13	1.6	0.56	0.79	44.8	27	1.1	0.21	0.21	82.6
14	1.6	0.44	0.71	50.7					

The cheapest glazing unit costs 38.9 TL per square meter and the most expensive glazing unit costs 95.6 TL per square meter.

The installation cost for glazing system is assumed 80 TL/m2 including labour and installation material. The annual glazing maintenance cost is assumed 15 TL/m2. The life expectancy of glazing system is assumed as long as building life span therefore no replacement cost occurs. The glazing scrap value is ignored.

The total cost of glazing installation is obtained as a product of unit price and current window-to-wall ratio.

Boiler

A representative price list for low and high efficient boiler groups, which are available in Turkish HVAC market and used-frequently in design solutions, is prepared. Figure 5.11 illustrates the entire capacity-price range used in the study for low thermal efficiency and high-thermal efficiency boiler groups.

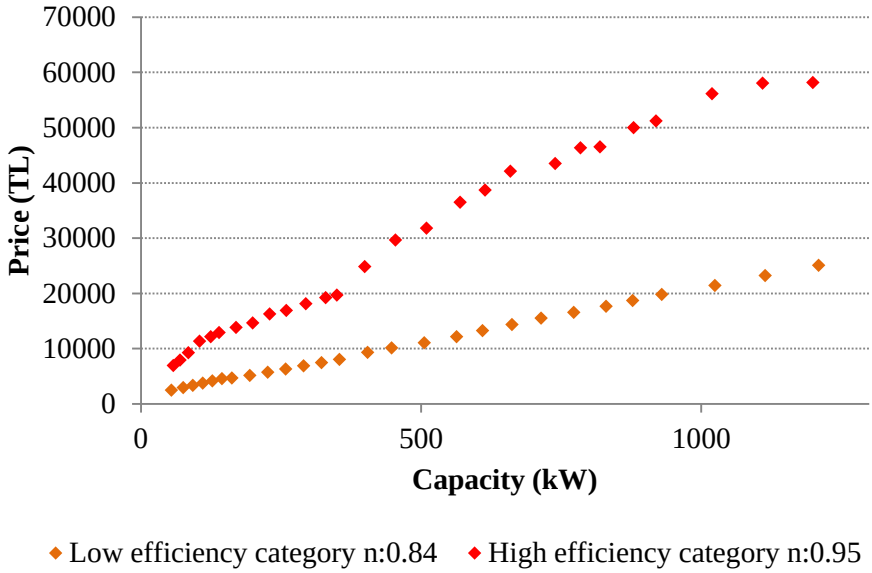

Figure 5.11 : Boiler initial price curve.

The Table 5.16 below demonstrates a sample of boiler cost library including equipment initial price. The full list is given in APPENDIX D.

Table 5.16 : A sample of boiler cost library.

Low efficiency category - Eff: 0.84			**High-efficiency category - Eff: 0.95**		
Boiler Number	**Capacity (kW)**	**Price (TL)**	**Boiler Number**	**Capacity (kW)**	**Price (TL)**
1	55	2453	28	58	6948
2	76	2942	29	70	7884
3	93	3339	30	85	9268
4	111	3736	31	105	11345
…	…	…	…	…	…
25	1025	21420	52	1020	56112
26	1115	23180	53	1110	58012
27	1210	25037	54	1200	58147

The costs for equipment installation and annual maintenance are calculated according to the data published in Building Construction Unit Cost Data Book. A curve fitting procedure is applied to the published data as shown in Figure 5.12, and

then the obtained capacity-installation price function is used to calculate the actual installation cost for each boiler in the library.

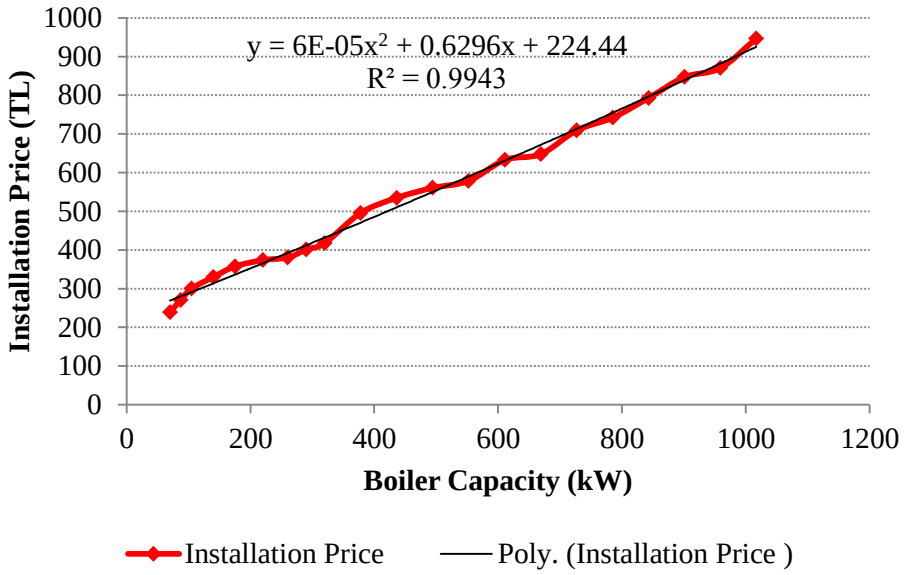

Figure 5.12 : Boiler installation price curve.

The annual maintenance cost is assumed as half of the installation cost that is in coherence with published data.

Boiler life expectancy is assumed 25 years as recommended in Chartered Institution of Building Services Engineers (CIBSE) Guide M – Maintenance Engineering & Management Appendix 13.A1.

For the 25-year calculation period, no replacement cost occurs. The replacement cost is equal to the sum of initial and installation costs discounted to present.

For both cases, the equipment's life ends with building span therefore no scrap value occurs.

Chiller

A representative price list for moderate and high efficiency chiller groups, which are available in Turkish HVAC market and used-frequently in design solutions, is prepared. Figure 5.13 demonstrates the entire capacity-price range used in the study for both equipment categories. The full load ERR value of moderate efficiency category varies between 4.45 and 5.05 with the average EER of 4.71. The full load ERR value of high efficiency category varies between 5.49 and 5.81 with the average EER of 5.63.

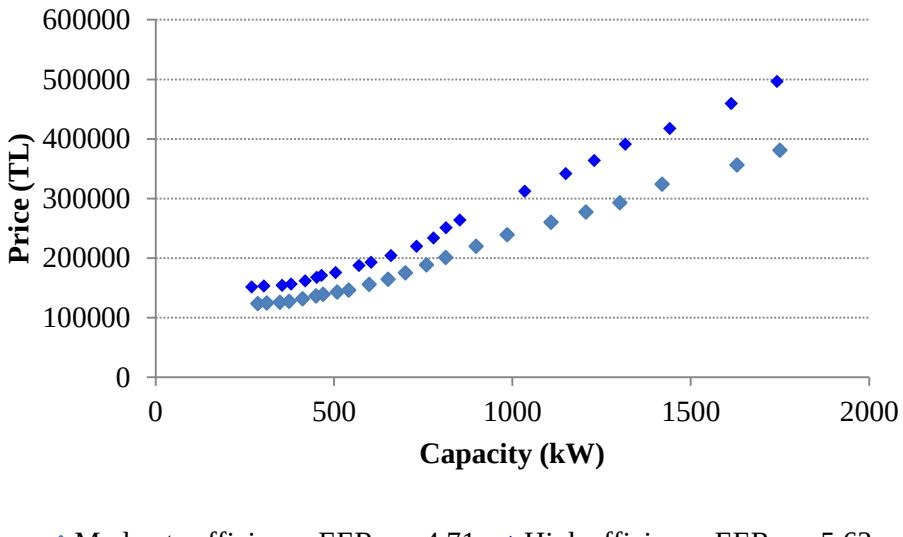

Figure 5.13 : Chiller initial price curve.

The Table 5.17 below demonstrates a sample of chiller cost library including equipment initial price. The full list is given in APPENDIX D.

Table 5.17 : A sample of chiller cost library.

Moderate efficiency category				High efficiency category			
Chiller Number	**Capacity (kW)**	**EER**	**Price (TL)**	**Chiller Number**	**Capacity (kW)**	**EER**	**Price (TL)**
1	287	5.04	123229	23	270	5.64	151420
2	312	4.8	124326	24	304	5.61	152767
3	349	4.85	125308	25	355	5.53	153975
4	375	4.57	126977	26	380	5.6	156026
…				…			
20	1420	4.7	323780	42	1442	5.5	417272
21	1630	4.76	355795	43	1614	5.81	459320
22	1750	4.73	380899	44	1742	5.72	496423

The costs for equipment installation and annual maintenance are calculated according to the data published in Building Construction Unit Cost Data.

A curve fitting procedure is applied to the collected data as shown in Figure 5.14, and then the obtained chiller capacity-installation price function is used to calculate the actual installation cost for each chiller in the library.

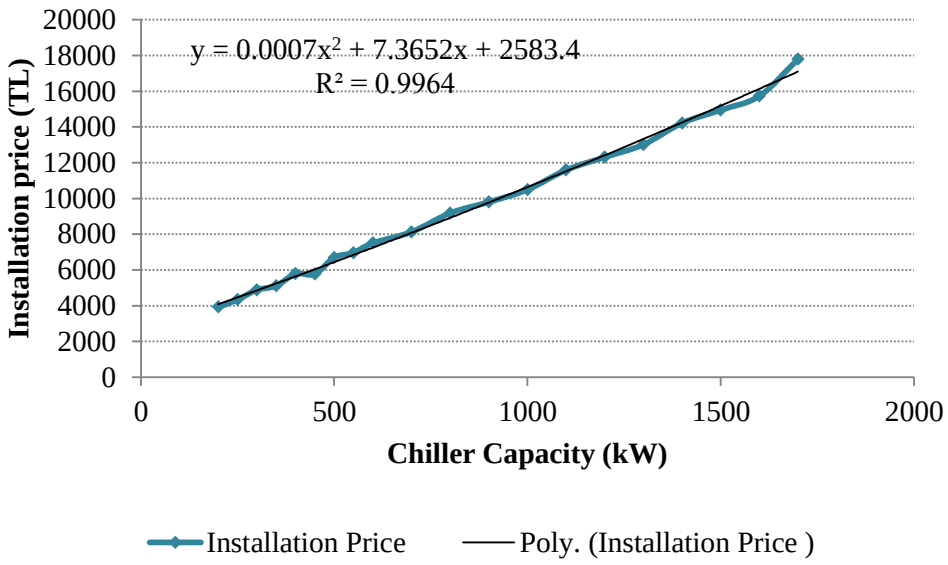

Figure 5.14 : Chiller installation price curve.

The annual maintenance cost is assumed about 22 % of the installation cost that is in coherence with published maintenance data.

Chiller life expectancy is assumed 20 years as recommended in CIBSE Guide M. Therefore, the equipment is required to be renewed once in the 25-year calculation period. The renewal cost is equal to the sum of initial and installation cost discounted to present.

At the end of the 25-year analysis period the chiller would still have 15 years of life remaining or 15/20 = 75 percent of its useful life due to the replacement at 20th year. Therefore 75 % of initial value can be assumed as scrap value and discounted to present.

Cooling tower

Cooling tower is a dependent equipment and it is capacity is related to the cooling load and selected chiller capacity.

An equipment price list representing average market products is prepared.

A tower capacity-price curve is established through curve fitting procedures as given in Figure 5.15 and therefore for each autosized cooling tower equipment, a corresponding product price can be calculated.

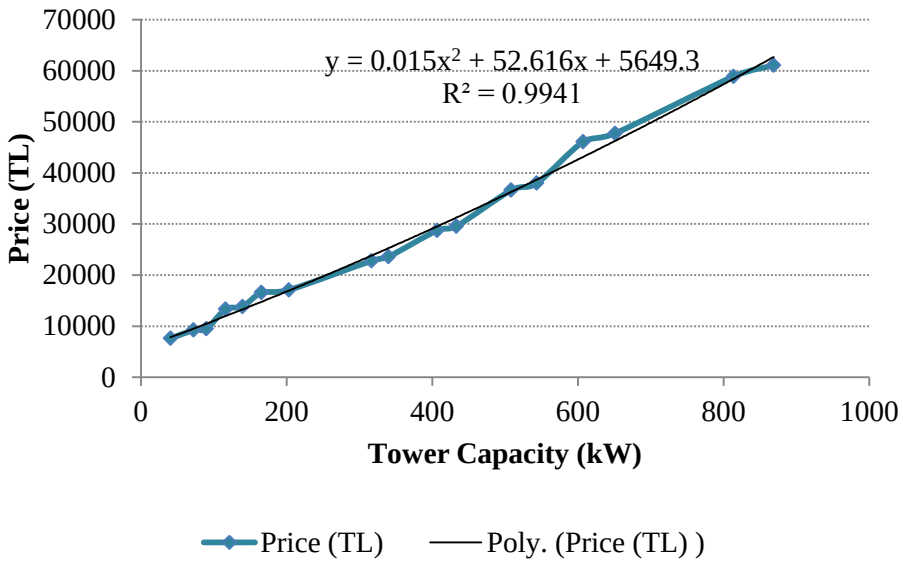

Figure 5.15 : Cooling tower initial price curve.

Moreover, the costs for equipment installation and annual maintenance are calculated according to the data published in Building Construction Unit Cost Data book. A curve fitting procedure is applied to the collected data as illustrated in Figure 5.16, and then the obtained cooling tower capacity-installation price function is used to calculate the actual installation cost for each autosized tower equipment.

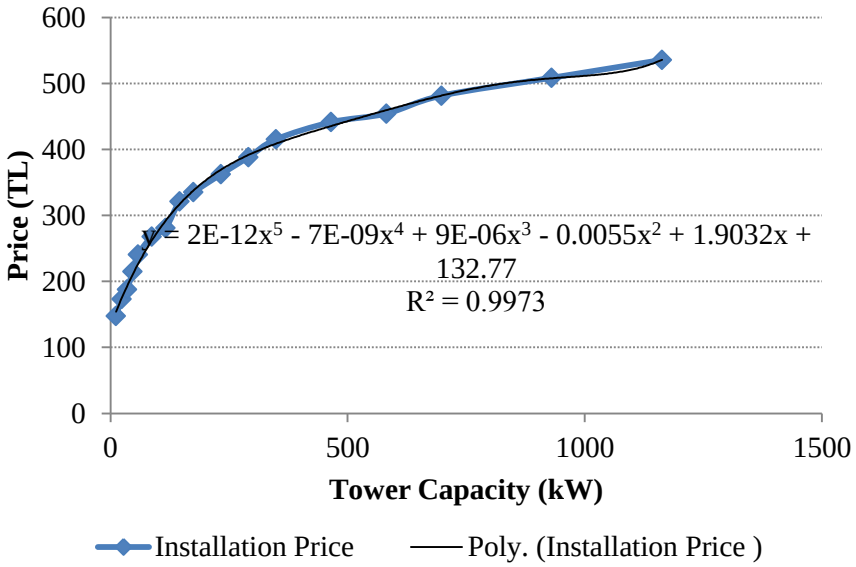

Figure 5.16 : Cooling tower installation price curve.

Similarly, when the published data for cooling tower annual maintenance costs is investigated, it was seen that the maintenance cost is usually equal almost 12% of installation cost.

Cooling tower life expectancy is assumed 25 years as recommended in CIBSE Guide M. There is no replacement or scrap value occur during 25-year analysis as the equipment life ends with study period.

Fan coil

Fan coil is another dependent equipment and the number of required fan coils are calculated at each run based building load requirements.

A generic, moderate-capacity fan coil unit with details given in Table 5.18 is selected as the representative equipment. Based on the calculated building loads and the total heating and cooling capacities of the considered equipment, the required number of fan coil units is calculated for each thermal zone. The price of the equipment is taken from the market as average. Then the initial system price is obtained as the product of equipment price and total number of equipment to install.

Table 5.18 : Fan coil unit details.

	Total cooling capacity (kW)			**Total heating capacity (kW)**			**Price (TL)**
Equipment	**Low**	**Medium**	**High**	**Low**	**Medium**	**High**	
Fan Coil Unit	6.34	7.33	8.19	8.24	9.3	10.15	1732

The equipment installation cost is obtained from Building Construction Unit Cost Data Book as 29.5 TL per equipment. Similarly, the same source suggests 29.5 TL annual maintenance cost per equipment as well.

Fan coil unit life expectancy is assumed 15 years as recommended in CIBSE Guide M. In 25-year analysis period, the fan coil units are required to be replaced once at the end of 15^{th} year. Replacement cost is equal to the sum of initial cost and installation cost.

In 25-year analysis period, fan coil units would still have 5 years of life remaining at the end of 25^{th} year. Therefore 5/15= 33 percent of its useful life corresponding to 33 % of initial equipment cost is assumed as scrap value and discounted to present.

Water heater

In the case study, the water heater includes a natural gas burner and a storage tank. A representative price list for this type of common water heater equipment, which is

available in Turkish HVAC market and used-frequently in design solutions, is prepared. A sample of the list is given in Table 5.19.

Table 5.19 : Water heater price list.

Water heating system	Cap (kW)	Heater Price (TL)	Water Tank Price (TL)	Total system price (TL)
1	69.8	1300	3900	5200
2	93	1745	4700	6445
3	116	1880	5400	7280
...	...	...	...	...

The costs for water heater installation and annual maintenance are calculated according to the data published in Building Construction Unit Cost Data Book. A curve fitting procedure is applied to the published data as shown in Figure 5.17, and then the obtained heater capacity-installation price function is used to calculate the actual installation cost for each water heater in the library.

The Building Construction Unit Cost Data Book suggests that same curve and function can be used to calculate annual maintenance cost.

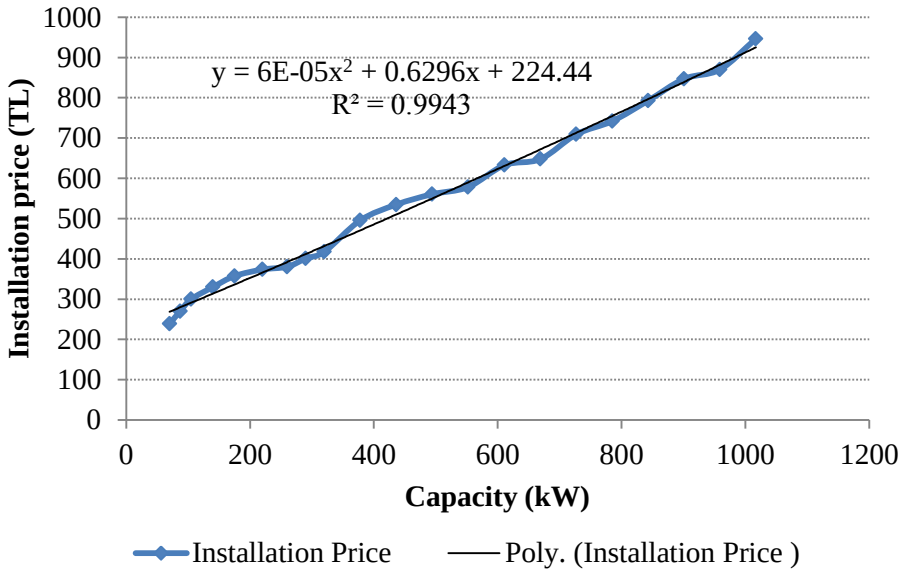

Figure 5.17 : Water heater installation price curve.

Water heater life expectancy including water tank and burner is assumed 25 years as recommended in CIBSE Guide M.

For the 25-year calculation period no replacement cost occurs.

Moreover, the equipment's life ends with building life span therefore no scrap value occurs, too.

Dimming lighting control system

In the methodology two lighting control systems, namely manual control and a dimming control based on daylighting is investigated and compared. Based on the information including two sensors per zone, 11 W/m2 lighting load and 8709 m2 floor area, two cost scenarios are prepared as given in Table 5.20 according to actual market prices.

Table 5.20 : Lighting control cost breakdown.

Cost breakdown (TL)	Manual control	Dimming control
Controller and sensor	2795	4554
Ballast	183678	275517
Total system price	186473	280071
Sensor Installation	1035	1294
Ballast installation	48774	65053
Total Installation price	49809	66346

The maintenance cost is ignored as it was equal in two cases.

The life expectancy of lighting sensors and ballast are assumed 15 years and 20 years respectively, as recommended in CIBSE Guide M.

In 25-year analysis period both sensors and ballasts are required to be renewed once, end of their equipment life. Replacement costs are equal to the sum of equipment and installation costs.

In 25-year analysis period, sensors would still have 10 years of life remaining at the end of 25^{th} year. Therefore 5/15= 33 percent of its useful life corresponding to 33 % of initial equipment cost is assumed as scrap value and discounted to present. For the ballast however, 5 years of its useful life remains end of study period, which is equal to 5/20= 25 percent of initial equipment cost as scrap value.

Photovoltaic system

The average market cost for installing a PV system either with poly-crystalline silicon modules or with thin-film modules are investigated. The cost of a PV system is measured in price-per-peak-watt (TL/Wp). Watt peak is the amount of power that a PV module is able to supply when it receives 1000 watts per square meter of solar irradiance at standard test condition. Price per peak watt is the usual figure-of-merit that is used to measure the cost of solar electric installations inclusive the cost for module, inverter, construction, wiring and labour. The average market prices are

estimated at 5.699 TL/Wp for Poly-crystalline Silicon and 4.342 TL/Wp for thin-film systems. The cost breakdown is given in Table 5.21.

Table 5.21 : Photovoltaic system cost breakdown.

Price breakdown	Polycrystalline (TL/Wp)	Thin-Film (TL/Wp)
PV Module	2.985	1.628
Inverter	0.814	0.814
Construction	0.814	0.814
Cable- material	0.543	0.543
Labour	0.543	0.543
Total	5.699	4.342

The annual maintenance cost is assumed 20 TL per module, which is in line with market prices.

The module life span is assumed 25 years and inverter lifespan is assumed 12.5 years based on the information provided by manufacturers.

In 25-year analysis period only the inverter is required to be renewed once. Replacement costs are equal to equipment cost plus installation cost including 1.09 TL/Wp for modules and 0.27 TL/Wp for inverters.

There is no scrap value assumed for the analysis period since equipment life ends with the study period.

Solar water heating system

In the case study, for water heating purpose three solar thermal systems with varying solar collector types are investigated and compared.

A market survey is taken to obtain average prices for a selective surface high efficiency collector, selective surface moderate efficiency collector and a black paint low efficiency collector. Moreover, construction and installation prices are acquired, too.

The Table 5.22 introduces the solar thermal system cost data.

Table 5.22 : Solar thermal system cost breakdown.

	SC1 (high efficiency)	**SC2** (moderate efficiency)	**SC3** (low efficiency)
Module cost (TL)	1200	790	515
Construction cost per module (TL)	60	60	60
Installation cost per module (TL)	40	40	40

An average market price list for water tank is also prepared as given in Table 5.23.

Table 5.23 : Water tank price list.

Water storage number	**Volume(litre)**	**Price (TL)**
1	1260	3900
2	1690	4700
3	2110	5400

The annual maintenance cost is assumed 40 TL per collector.

The life expectancy of both the collector and water tank is assumed 25 years.

Solar thermal systems also require a backup system in case there isn't sufficient sunlight. Initial cost, installation cost and maintenance cost for backup system is assumed same as the burner of the water heater system explained previously.

For the 25-year calculation period no replacement cost occurs.

Moreover, the equipment's life ends with building life span therefore no scrap value occurs, too.

5.3 Results and Discussion

In this section, firstly, pre-optimization steps are taken and prerequisite calculations are carried out. Upon determination of necessary parameters, the formulated optimization problems of the study are run and the results are shared and discussed. Moreover, the results of the validation analysis are given and conclusions are drawn.

5.3.1 Design variable refinement

As explained in the methodology, the optimization problem becomes more complex as the number of design variables grows. Therefore, to reduce the size of the

optimization problem, a simple sensitivity analysis is carried out on the base case buildings.

The aim of the analysis is to capture the influential parameters directly on building primary heating, cooling and lighting energy consumption. A parametric analysis using an EnergyPlus model of case study buildings is applied only to the candidate architectural design variables including, building orientation, wall and roof insulation thicknesses, roof reflectivity, glazing type, and window-to-wall ratio.

The value of each parameter is varied from its minimum value to the maximum with user-defined steps while the rests of the parameters are kept constant at their initial values. Then the percentage of difference between minimum and maximum energy consumption values relative to the maximum value is calculated.

The sensitivity of roof insulation thickness is investigated under two conditions depending on the roof SRI value: a high SRI value of 103 and a low SRI value of 6.

The window-to-wall ratio of each façade (South, North, East and West) is investigated separately as they are independently optimized.

Two sets of calculations are carried out for Istanbul, Ankara and Antalya cases. In the first set, there is no dimming control of artificial lighting according to daylighting. In the second set however, the impact of lighting control strategies on design variables are also taken into account. The percentage of sensitivity of each variable on boiler primary natural gas consumption, chiller primary electricity consumption, lighting primary electricity consumption and building overall source energy consumption are given separately.

The Table 5.24 summarizes the calculated sensitivity indexes for Istanbul, Ankara and Antalya cases where no daylighting strategy and dimming control is applied.

In all three cases, the most influential parameter on overall building source energy consumption is obtained as roof insulation thickness in both SRI conditions. Roof SRI value itself is the second most influential parameter among all.

The least influential parameter is found as building orientation. The parameter sensitivity on boiler and chiller source energy consumption can differ for each parameter.

Window-to-wall ratios influence mostly energy consumption for cooling, especially in Southern and Western façades. However due to lack of dimming control; their overall influence is relatively small.

Similarly, glazing type has a moderate importance since the building cannot benefit from a dimming control.

Table 5.24 : Sensitivity index given in percentage for Istanbul, Ankara and Antalya cases where no dimming control available.

Cases	Energy End Use	Ort	Wall Ins	Roof Ins		Roof SRI	Win Type	W-W-R			
				SRI1	SRI2			S	W	N	E
Istanbul	N.G. Boiler	0.14	9.22	26.97	37.32	14.72	4.74	2.68	1.21	0.70	1.23
	Elc. Chiller	0.56	4.66	3.24	12.79	18.03	11.53	9.00	8.49	3.27	6.88
	Elc. Lighting	0.00	0.00	0.00	0.00	0.00	0.00	0.00	0.00	0.00	0.00
	Total P.Uses	0.14	0.46	4.97	5.04	0.43	1.95	1.54	1.57	0.48	1.1
Ankara	N.G. Boiler	0.20	10.38	28.49	39.63	16.62	5.14	2.80	1.34	0.66	1.42
	Elc. Chiller	1.16	9.02	5.01	22.00	29.85	17.20	12.20	11.57	4.70	11.41
	Elc. Lighting	0.00	0.00	0.00	0.00	0.00	0.00	0.00	0.00	0.00	0.00
	Total P.Uses	0.17	1.45	7.85	9.95	1.95	1.68	0.94	1.14	0.36	0.95
Antalya	N.G. Boiler	0.52	9.75	18.88	44.08	31.42	6.42	5.66	2.51	0.88	2.52
	Elc. Chiller	0.90	3.69	10.34	8.59	20.66	10.47	8.64	9.27	2.78	7.58
	Elc. Lighting	0.00	0.00	0.00	0.00	0.00	0.00	0.00	0.00	0.00	0.00
	Total P.Uses	0.29	0.6	4.08	2.26	3.34	2.88	2.44	2.76	0.76	2.12

When the dimming control is activated, the sensitivity indexes are updated due to the reduction in lighting consumption and consequent reduction in overall energy consumption, as given in Table 5.25.

The roof insulation thickness is still the most influential parameter in all three cases. Similarly, the orientation is again the least influential parameter in all energy consumption categories.

The glazing type and the window-to-wall ratio in all orientations become more significant in presence of dimming control. The influence of glazing type becomes almost five times higher in comparison to no dimming control condition.

Table 5.25 : Sensitivity index given in percentage for Istanbul, Ankara and Antalya cases where there is dimming control available.

Cases	Energy End Use	Ort	Wall Ins	Roof Ins		Roof SRI	Win Type	W-W-R			
				SRI1	SRI2			S	W	N	E
Istanbul	N.G. Boiler	0.18	9.46	27.64	38.36	15.43	3.19	1.71	0.46	0.20	0.47
	Elc. Chiller	0.77	3.37	5.99	9.96	17.77	6.65	6.05	5.69	1.58	4.53
	Elc. Lighting	0.67	0.00	0.00	0.00	0.00	25.60	17.30	16.32	10.35	14.91
	Total P. Uses	0.17	0.85	6.18	6.69	0.1	6.83	2.95	2.63	2.04	2.61
Ankara	N.G. Boiler	0.21	10.72	28.67	40.05	17.17	3.59	1.85	0.52	0.17	0.70
	Elc. Chiller	1.44	7.85	9.78	17.96	30.04	11.09	9.01	8.96	2.78	8.67
	Elc. Lighting	0.88	0.00	0.00	0.00	0.00	26.58	17.43	17.20	10.48	15.21
	Total P.Uses	0.25	2.03	9.4	12.23	2.88	7.17	3.11	2.7	1.9	2.48
Antalya	N.G. Boiler	0.70	10.29	20.99	47.01	33.42	4.11	4.80	1.58	0.42	1.69
	Elc. Chiller	0.95	2.65	12.72	6.25	20.77	6.24	6.18	6.46	1.28	5.68
	Elc. Lighting	1.29	0.00	0.00	0.00	0.00	30.66	18.68	19.58	10.90	17.25
	Total P.Uses	0.37	0.39	5.3	3.5	3.04	7.97	2.53	2.5	1.95	2.22

When all the results are analysed it was seen that the influence of variation in building orientation demonstrated an insignificant importance as a decision variable in all cases and in all energy consumption categories.

The rest of the parameters however showed from high to moderate correlation at least in one energy consumption category. Therefore, only the building orientation was eliminated from candidate design variables.

The final list of variables including building design parameters, HVAC and renewable system parameters used in this case study are listed in Table 5.26, which introduces the name, the symbol, and the range or value of each variable.

In the column Range or Value, the boundary values are used for a discrete variable that is spaced linearly based on user specified number of intervals, and a series of admissible values are used for a discrete variable that denotes the indices in the library file corresponding to that discrete variable.

Table 5.26 : Final list of design variables.

Variable Name	Symbol	Range or Value
Building architectural characteristics		
External wall insulation thickness	iEW	[0 ; 0.15] (meter)
Roof insulation thickness	iR	[0 ; 0.15] (meter)
Roof SRI	RT	RT1, RT2
Glazing type	GT	GT1 – GT27
Window-to-wall ratio	WTW	5, 15, 25, 35, 45, 55 %
Building HVAC system characteristics		
Boiler type	BL	BL1 – BL54
Chiller type	CL	CL1 – CL 44
Building renewable system characteristics		
PV type	PVtyp	PV1, PV2
Number of PV Modules	PVnum	[1 ; 858]
Solar collector type	SCtyp	SC1, SC2
Number of solar collectors	SCnum	[1 ; 140]

5.3.2 Base case energy performance

When all the necessary information is collected, the simulation models of the base case scenarios are developed in EnergyPlus which is the simulation engine adopted in the methodology.

Firstly, base case sizing calculations are carried out to calculate initial building thermal loads and to determine required capacities of plant equipment including chiller, boiler and water heater. After the capacities are established, the sizing factors are applied and upper and lower limits of allowed capacity range for each equipment is obtained. Then, suitable equipment that has the lowest capacity within the capacity range are selected from the equipment database as initial base case equipment.

The results of the boiler sizing calculations are given in Table 5.27. The required boiler thermal capacities for the buildings in Istanbul, Ankara and Antalya are determined as 591 kW, 857 kW, and 499 kW, respectively. It can be seen from the results that the impact of climate conditions is directly reflected on the capacities where the highest boiler capacity is required in Ankara and lowest in Antalya. The sizing factors of 0.99 and 1.25 are applied to determine the allowable lower and upper equipment capacity limits. Then, a low-efficiency boiler falls within the capacity range of each scenario is selected as base case equipment from the boiler

database given in APPENDIX C, Table C.1 where traditional low efficiency equipment are available.

Boiler 18 that has a nominal capacity of 610 kW is selected for Istanbul, Boiler 23 that has a nominal capacity of 878 kW is selected for Ankara and Boiler 16 that has a nominal capacity of 506 kW is selected for Antalya. Thermal efficiency of all the boilers is 84%.

Table 5.27 : Calculated boiler capacity and selected boiler equipment.

Cases	Equipment sizing [kW]			Equipment Selection [kW]	
	Required Capacity	Min allowed capacity (0.99 *ReqCap)	Max allowed capacity (1.25*ReqCap)	Equipment Library Number	Equipment Capacity
Istanbul	591	585	738	BL 18	610
Ankara	857	848	1071	BL 23	878
Antalya	499	494	624	BL 16	506

The results of the chiller sizing calculations are summarized in Table 5.28. The required chiller nominal capacities for the buildings in Istanbul, Ankara and Antalya are determined as 712 kW, 583 kW, and 756 kW, respectively.

Table 5.28 : Calculated chiller capacity and selected chiller equipment.

Cases	Equipment sizing [kW]			Equipment Selection [kW]	
	Required Capacity	Min allowed capacity (0.99 *ReqCap)	Max allowed capacity (1.15*ReqCap)	Equipment Library Number	Equipment Capacity
Istanbul	712	705	819	CL 13	760
Ankara	583	577	670	CL 10	599
Antalya	756	749	870	CL 13	760

The impact of climate conditions is also reflected on the chiller capacities where the highest capacity chiller is required in Antalya and lowest in Ankara, as expected.

The sizing factors of 0.99 and 1.15 are applied to determine the allowable lower and upper equipment capacity limits. Then, a moderate efficiency chiller falls within the capacity range of each scenario is selected as base case equipment from the chiller database given in APPENDIX C, Table C.5, where traditional equipment are available.

Chiller 13 with a capacity of 760 kW and an EER of 4.72 is chosen for Istanbul, Chiller 10 with a capacity of 599 kW and an EER of 4.68 is chosen for Ankara and finally, Chiller 13 again with a capacity of 760 kW and an EER of 4.72 is chosen for Antalya. The reason for the same chiller selected for Istanbul and Antalya is that there is no other smaller capacity equipment within the allowed capacity range in the equipment database suitable for the Istanbul case study.

The sizing calculation is performed lastly for obtaining the power capacity and tank volume of water heaters.

The capacity of the water heater depends on water use, flow rate and hot water set point. Since the hot water requirements are assumed same in all three cases, the required equipment capacities are also resulted in same values as given in Table 5.29 below.

Table 5.29 : Water heater sizing and selected equipment.

Cases	**Required Capacity [kW]**	**Water Heater Selection**		
		Equipment Library Number	Equipment Capacity [kW]	Storage Volume [m3]
Istanbul	83	WH 2	93	1.69
Ankara	83	WH 2	93	1.69
Antalya	83	WH 2	93	1.69

Once the boiler, chiller and water heater equipment are chosen, they are added to the simulation models together with their efficiency curves. Thus, the models became complete. Annual simulations are run now to evaluate the overall energy performances of the base case scenarios.

Table 5.30 summarizes the base case annual site energy consumption per floor area for Istanbul, Ankara and Antalya based on fuel type and end use type. According to the numbers, heating is the dominant load in the base case buildings located in Istanbul and Ankara. However, in Antalya the cooling load becomes dominant.

Table 5.30 : Base case site energy consumption breakdown per floor area.

End use type [kWh/m2]	Istanbul	Ankara	Antalya
Natural Gas Boiler	46.2	76.5	15.2
Electricity Chiller	16.8	8.4	26.2
Electricity Cooling Tower	0.6	0.2	1.0
Electricity HVAC Fans	9.8	9.9	10.1
Electricity HVAC Pumps	4.9	4.1	5.7
Natural Gas Water Heating	7.6	9.1	6.3
Electricity Interior Lighting	34.7	34.7	34.7
Electricity Interior Equipment	32.9	32.9	32.9

Moreover, energy consumption per conditioned floor area in source energy (primary) form is given in Table 5.31. National site-to-source energy conversion factors for Turkey of 2.36 is applied for electricity and of 1.0 applied for natural gas, as recommended by Ministry of Environment and Urbanization of Turkey. The primary energy use intensity (PEUI) of the baseline buildings is found to be 288.9, 298.2, and 282.3 kWh/m2/year for Istanbul, Ankara and Antalya respectively.

Table 5.31 : Base case primary energy consumption breakdown per floor area.

End use type [kWh/m2]	Istanbul	Ankara	Antalya
Natural Gas Boiler	46.2	76.5	15.2
Electricity Chiller	39.6	19.8	61.8
Electricity Cooling Tower	1.4	0.5	2.3
Electricity HVAC Fans	23.2	23.3	23.8
Electricity HVAC Pumps	11.5	9.7	13.5
Natural Gas Water Heating	7.6	9.1	6.3
Electricity Interior Lighting	81.8	81.8	81.8
Electricity Interior Equipment	77.5	77.5	77.5
Total End Uses	288.9	298.2	282.3

The results also show that the most space heating energy consumption occurs in Ankara that is five times higher than Antalya and 1.6 times higher than Istanbul. The most space cooling energy consumption occurs in Antalya that is 3.1 times higher than Ankara and 1.5 times higher than Istanbul. The cooling tower energy consumption profile follows the energy profile of the chiller however, the amounts are very small.

Fan energy consumption due to fan coils and ventilation system are similar in all three cases since they are mostly related to the operating hours. Energy consumption for lighting is equal in all three cases since same lighting power density is used in all

cases and there is no dimming control of artificial lights according to daylighting. Similarly, equal amount of energy is consumed by plugged-in equipment since the equipment power density is assumed same in all cases. Even though the hot water consumption, and capacity and volume of the water heaters are same in all three cases, the water heater energy consumption differs greatly due to the different outdoor conditions the buildings are exposed to. Energy need for water heating is highest in Ankara where mains water temperature, which depends on outdoor air temperature, is relatively colder than other cases. Electricity consumption of circulation pumps constitutes a small space in the overall energy use.

There is not a building performance database currently covering buildings located in Turkey, therefore the base case final energy consumption values are compared to the values published in Data Hub for the Energy Performance of Buildings by Building Performance Institute Europe (BPIE, 2014). According to their Europe's Buildings Under the Microscope Report, which is a country-by-country review of the energy performance of European buildings, the average specific energy consumption in the non-residential sector is estimated 280kWh/m2 covering all end-uses. The values ranges from 200 kWh/m2 to 360 kWh/m2 for the buildings constructed between the years 1980-2000.

The PEUI of base cases in Istanbul, Ankara and Antalya are higher than their average European counterparts. In general, the results show that PEUI of the base case models are within a reasonable range.

The water consumption due to occupancy hot water use and HVAC cooling tower use is also given in Table 5.32 below. Highest amount of cooling tower water consumption occurs in Antalya followed by Istanbul and Ankara. Occupancy hot water use is equal in all cases since occupancy hot water requirements are assumed same in all three cases

Table 5.32 : Water end use.

Water Consumption	**Istanbul [m3/m2]**	**Ankara [m3/m2]**	**Antalya [m3/m2]**
Cooling Tower Water Use	0.191	0.140	0.337
Hot Water Use	0.202	0.202	0.202
Total Use	0.393	0.342	0.539

Annual CO_2 emission rates for each base case building are calculated by application of national CO_2 conversion factors of 0.234 for natural gas and 0.617 for electricity as given in Table 5.33.

Table 5.33 : Base case annual CO_2 emission rates.

End-use CO2 emission rate (kgCO2 /m2)	Istanbul	Ankara	Antalya
Electricity based CO2 rate	61.5	55.6	68.2
Natural gas based CO2 rate	12.6	20.0	5.0
Total CO2 emission rate	74.1	75.6	73.2

According to BPIE survey, and Eurostat database, the average specific CO2 emission in Europe is 54 $kgCO_2/m^2$ where the national values of $kgCO_2$ per floor space vary in the range from 5-120 $kgCO_2/m^2$. Therefore, the CO_2 emission from base case buildings is within the range of European building stock.

5.3.3 Parameter settings for the optimization algorithm

For the case study optimization, the algorithm used the von Neumann topology, 40 particles, 300 generations, a seed number of 1, a cognitive acceleration constant of 2.8, a social acceleration constant of 1.3 and velocity clamping with a maximum velocity gain of 0.5. Since the updated version of PSO algorithm with constriction coefficient has been adopted in the study, 0.6 is assumed as constriction gain coefficient.

The parameters are adjusted based on the literature review by Carlisle and Dozier, 2001; Zhang et al., 2004 and the previous experience of the author based on experiments on a small case study building.

5.3.4 Penalty parameter adjustment

Before initializing the optimization, a test optimization case with a small PSO population size was created to establish the magnitude range that each penalty function and the global cost term of the main objective function is likely to have. Then penalty parameters are assumed and tuned with an aim to give each penalty an equal importance without being dominated among them or by the cost objective.

The purpose of the current optimization study is to eliminate any design option that cannot satisfy all of the constraints simultaneously. Therefore, each time a constraint

is violated, a significant penalty value is aimed to be added to the objective function to create a jump from the unfeasible neighbourhood.

ΔCO2 (The difference between the CO2 emission rate of any design option and a target rate), ΔPPD (The difference between the PPD index of any design option and a target index), ΔCLmin (the difference between minimum allowed chiller capacity and recommended chiller equipment capacity), ΔCLmax (the difference between recommended chiller equipment capacity and maximum allowed chiller capacity), ΔBLmin (the difference between minimum allowed boiler capacity and recommended boiler equipment capacity), ΔBLmax (the difference between recommended boiler equipment capacity and maximum allowed boiler capacity) value ranges are obtained for Istanbul, Ankara and Antalya cases.

Then, the power of the penalty term is set as 2 to obtain quadratic penalty function values of each penalty constraint. Therefore the amount of penalty becomes proportional to the square of the amount of violation and it increase at a faster rate. Therefore, the penalty function returns zero when it is under the given limits but the penalty term becomes increasingly larger as solutions moves away from the feasible region. Once the magnitude ranges of quadratic penalty function values are obtained, suitable penalty parameters (μ) that can balance the contribution range of each penalty are selected by trial.

The results of the test cases and the selected penalty parameters are given in APPENDIX D.

5.3.5 Optimization results

In this section, the ability of the proposed methodology to solve the whole building design optimization problem is investigated. Three case studies located in Istanbul, Ankara and Antalya demonstrate how the developed method can be used to generate least-cost and energy-efficient design recommendations among several options specific to a building, its use pattern, and its climate and location.

In the first step of the case study analysis, the base case buildings are optimized without considering any renewable system integration possibility. Only the optimal combinations of building and HVAC system variables are sought simultaneously in a 25-year service life analysis period. Then the photovoltaic and solar water heating system schemes, which are described in previous sections, are integrated into the

building models and the optimizations are re-run to find the best combination of building, HVAC and renewable system options together this time.

The main objective function is the difference between the Global Cost (GC) per square meter building floor area of any design option that is created through optimization and base case design added with the sum of the all penalty functions due to constraint violations. Therefore, the additional cost incurred to achieve a given level of energy savings can be determined and compared practically while considering design limitations. Since the objective function is calculated relative to the base case, the dGC intends to go below zero as improvements are being made during search process when the GC of new design alternatives becomes smaller than GC of the base case. However, if the new design combinations worsen the total building performance, dGC then can take positive values. In addition, if a candidate solution violates any of the penalty criteria, a large penalty value is added to the main objective function therefore the total cost value of objective function is sharply increased to eliminate constraint-violating design recommendations.

5.3.5.1 Istanbul case study

The graphic given in Figure 5.18 illustrates the results of the optimization search in Istanbul case as a dense cloud of black circles where each circle represents a different combination of the optimization variables and the resulting objective function value.

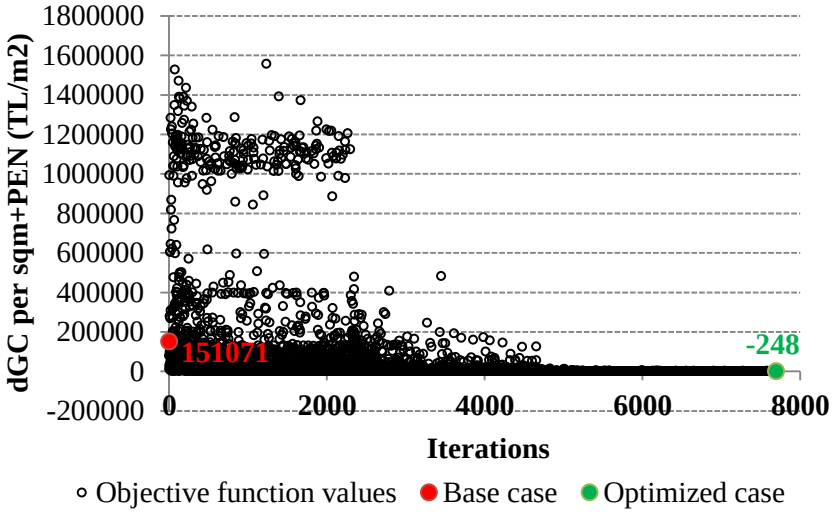

Figure 5.18 : Distribution of optimization results obtained with Istanbul case.

PSO search involves iteratively trying arbitrarily selected parameters while always remembering the best solution found in the process. As the figure indicates, the solution space constitutes a wide range of possibilities due to the large number of variables involved.

The main objective function for the initial case is calculated as 151071 where, after optimization, it was reduced to -248.

Since the objective function is calculated based on building global cost (GC) performance and how well the building satisfies user-set penalty limitations, a breakdown of objective function is also illustrated in Figure 5.19, where dark blue circles represents dGC per floor area and orange circles represents the corresponding total penalty function value.

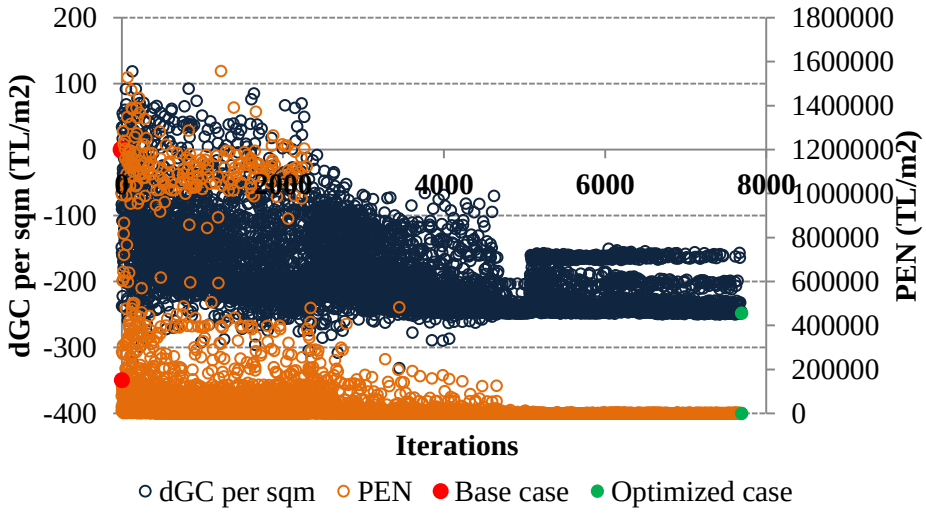

Figure 5.19 : Breakdown of optimization results obtained with Istanbul case.

As figure shows, a large portion of the solution space constitute invalid solutions due to violations of the problem constraints, even some of the solutions show a better GC performance than the optimized case.

The dGC per sqm value of base case is calculated as zero since it is the reference point of the optimization. However, its corresponding penalty function is calculated as 151071. The positive value indicates that the initial case violates some penalty criteria.

When the penalty values of the two cases are further investigated, it was seen that base case violates comfort and CO_2 emission criteria as given in Figure 5.20.

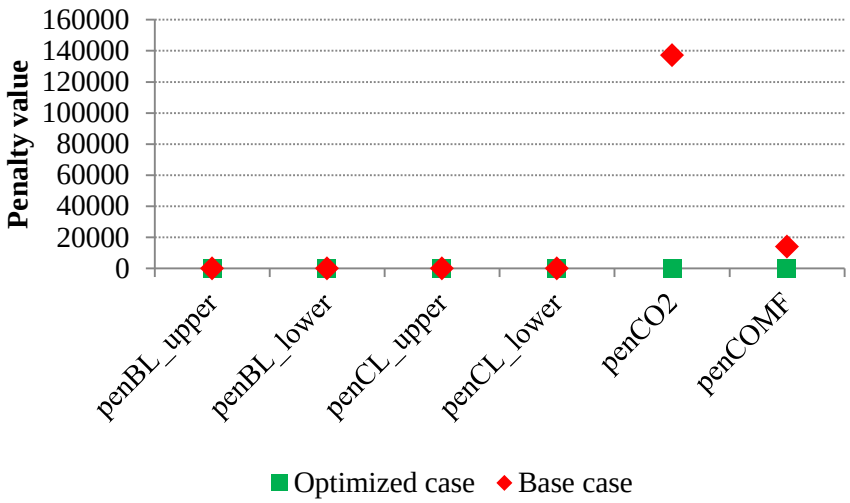

Figure 5.20 : Penalty values obtained with Istanbul case.

The dGC per sqm value of the optimized case is calculated as -248 TL/m2 and the corresponding penalty value is obtained as zero. Therefore, the optimization was successful at reducing building GC without violating any of the optimization constraints.

When the absolute GC per sqm values of base case and optimized cases are compared as given in Figure 5.21, it was found that in optimized case, 248 TL/m2 GC saving has been achieved relative to base case and the application of optimization has achieved reducing the overall GC by 18.7 % in Istanbul case study.

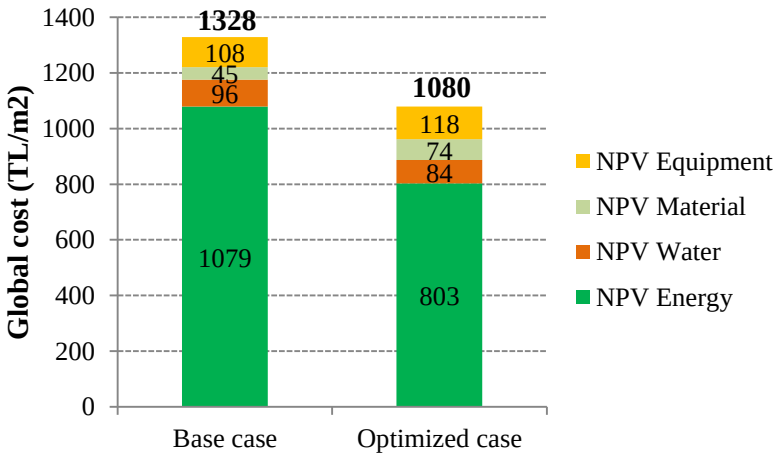

Figure 5.21 : Comparison of global cost breakdown obtained with Istanbul case.

Total GC is a summation of net-present value of energy cost, water cost, building material cost and system equipment cost in the 25 year calculation period and Figure 5.21 shows how absolute values of each GC element contributed to the total value.

The application of the proposed optimization methodology has reduced the NPV of energy cost by 25.6 %, and the NPV of water cost by 12.6 %. However, to improve building energy and HVAC water use efficiency, the NPV of building material cost has increased by 65.2 % and the NPV of building equipment cost has increased by 9.2 % due to investments in new design alternatives.

Table 5.34 provides the base case and final set of recommended design solutions obtained with the proposed optimization methodology for Istanbul case study.

Table 5.34 : Base case and optimized case design options with Istanbul case.

	iEW (m)	**iR (m)**	**RT**	**GT**	**WTW South (%)**	**WTW West (%)**	**WTW North (%)**	**WTW East (%)**	**BLtyp**	**CLtyp**	**DL**
B.C	0	0	1	1	25	25	25	25	18	13	0
O.C	0.025	0.045	2	13	45	35	55	35	43	32	1

According to the given numbers, the optimization recommended increasing the external wall insulation thickness from zero to 0.025 meters and the roof insulation thickness from zero to 0.045 meters.

Moreover, optimization also recommended cool roof paint (RT2) instead of conventional gravel roof (RT1) as final layer of the roof element.

The initial air filled double glazed glazing unit GT1 (U: 2.9 W/m2K, SHGC: 0.75, Tvis: 0.8, Cost: 38.9 TL/m2) was replaced with double glazed argon filled glazing unit GT13 (U: 1.6 W/m2K, SHGC: 0.56, Tvis: 0.79, Cost: 44.8 TL/m2).

Furthermore, the moderate window-to-wall ratios were increased from 25 % to 45 % in Southern facade and to 35 % in Western and Eastern facades and to 55 % in northern facade. The increase in w-t-w ratios naturally let the net area of external wall decrease accordingly.

The change in NPV due to the changes that occur in independent and dependent variables of building material category are summarized in Table 5.35.

The improvements in building façade were also combined and supported with the improvements in building systems.

Table 5.35 : NPV breakdown of building material cost with Istanbul case.

Building Materials	Base case (TL/m2)	Optimized case (TL/m2)
External wall insulation	0.0	2.5
Roof insulation	0.0	8.6
Roof coating type	1.6	4.6
Glazing type	26.2	45.2
Wall composition	17.0	13.0
Total Material Cost	44.8	73.9

To begin with, the optimization selected dimming control of artificial lights according to daylight levels as a cost effective and energy-efficient design option over manual lighting control.

The integration of dimming control of lights with the rest of the new design recommendations for building facade caused a decrease in building heating and cooling loads. The load reduction was simultaneously reflected both on chiller and boiler equipment sizes. The base case boiler equipment BL 18 (Capacity: 610 kW, Eff: 0.84, Cost: 13240 TL) was replaced with BL 43 (Capacity: 510 kW, Eff: 0.95, Cost: 31795 TL) which is in the high-efficiency equipment category. However, similar size lower-efficiency boiler BL10 (Capacity: 506 kW, Eff: 0.84, Cost: 11053 TL) wasn't found to be favourable even though its lower initial cost.

Similarly, the base case chiller CL 13 (Capacity: 760 kW, EER: 4.72, Cost: 188210 TL) was replaced with CL 32 (Capacity: 605, EER: 5.65, Cost: 192610) which is in the high-efficiency equipment category. Similar size lower-efficiency alternative CL 10 (Capacity: 599 kW, EER: 4.68, Cost: 155377 TL) wasn't found to be worth investing under circumstances.

The penalty values due to boiler and chiller equipment allowable capacities are calculated as zero as given in Figure 5.20 before, which indicates that optimization, was successful at selecting right size equipment while considering the dynamic load changes.

The reductions in building heating and cooling loads were also reflected on dependent equipment. The number of required fan coil units was decreased from 64 to 47. Similarly, the required cooling tower capacity was decreased from 731kW to 565 kW as well.

The change in NPV due to the changes that occur in independent and dependent building system variables are summarized in Table 5.36.

Table 5.36 : NPV breakdown of building system cost with Istanbul case.

Building Systems	Base case (TL/m2)	Optimized case (TL/m2)
Lighting Control	36.7	53.4
Boiler	2.4	4.4
Chiller	33.1	32.7
Cooling Tower	8.4	6.7
Fan Coil Units	25.3	18.5
Water Heater	2.5	2.5
Total Equipment Cost	108.2	118.2

The capital cost of the recommended boiler is more than twice the capital cost of recommended boiler. Moreover, the NPV of the recommended boiler is almost double the NPV of initial boiler. However, the improved thermal efficiency combined with reduced equipment capacity made the investment worth the cost.

When the initial and recommended chiller equipment are compared it was found that even the capital cost of initial chiller (CL13) is lower than the capital cost of the selected chiller (CL43), the selected chiller shows a better NPV performance due to its lower installation and maintenance costs because of its lower capacity. In addition, the recommended chiller also offers improved energy performance and improved energy cost, which makes CL43 a suitable design option.

The NPV of cooling tower decreased due to the reduction in cooling capacity and consequent equipment capacity. Similarly, NPV of fan coil units reduced in parallel to the reduction in the number of required units.

The impact of optimization on 25-year operating energy costs are given in Table 5.37.

Table 5.37 : NPV breakdown of energy cost with Istanbul case.

Energy Cost Type	Base case (TL/m2)	Optimized case (TL/m2)
Electricity Cost	872.6	654.7
Natural Gas Cost	206.5	148.5
Total Energy Cost	1079.1	803.2

The largest energy cost is due to electricity use, which is about more than 4 times natural gas cost in both cases. The recommended design strategies however

succeeded decreasing energy cost about 25 % for electricity and about 28 % for natural gas.

The direct influence of optimization on annual building primary energy consumption is summarized in Figure 5.22. The application of the recommended design options achieved lowering total annual primary energy use from 288.9 kWh/m2 to 215.1 kWh/m2 that is equal to 25.6 % reduction in total. The reduction occurred in every end use type except the natural gas use for water heating since there was not any design option influencing water heating system performance.

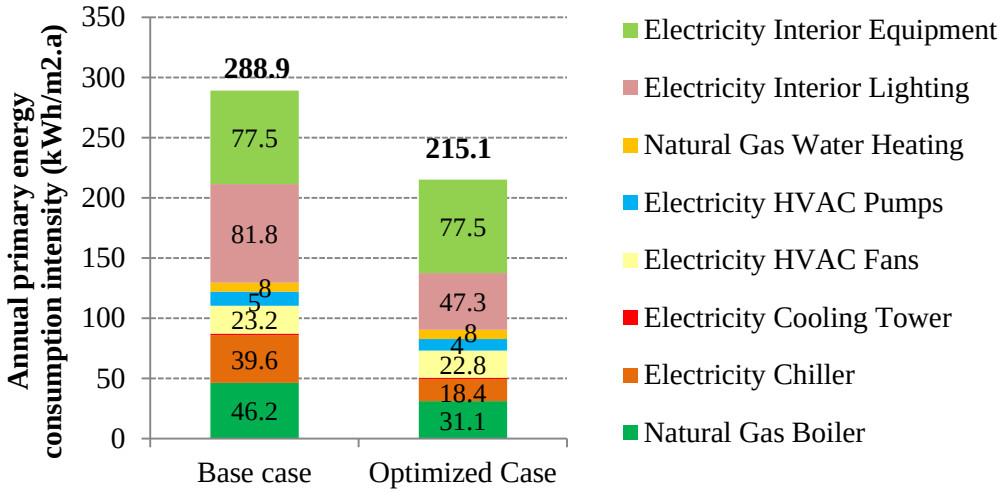

Figure 5.22 : Comparison of annual primary energy consumption breakdown obtained with Istanbul case.

The decrease in energy use also resulted in a decrease in the value of annual CO_2-eq emission rate as shown in Figure 5.23.

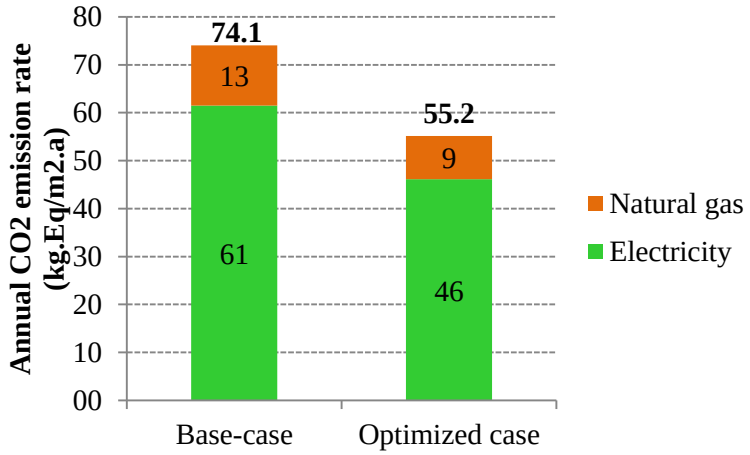

Figure 5.23 : Comparison of annual CO_2 emission rate breakdown obtained with Istanbul case.

The overall annual building emission rate was decreased from 74 kg.Eq-CO2/m2 to 55 kg.Eq-CO2/m2. The percentage of reduction is equal to 25.5 that is much higher than the minimum target reduction of 10 %. Therefore, the recommended design strategies are perfectly capable of satisfying CO_2 emission constraint for the Istanbul case.

The impact of optimization on NPV water cost is given in Table 5.38. The water cost because of cooling tower water use decreased by 26 % due to the reduction in building cooling needs. However, the available design strategies have no influence on building hot water use, which is only linked with building occupancy density. Therefore, the related water cost remained same in two cases.

Table 5.38 : Comparison of NPV breakdown of water cost and water end use with Istanbul case.

Water End Use Type	NPV water cost (TL/m2)		Annual water consumption [m3/m2]	
	Base case	Optimized case	Base case	Optimized case
Cooling tower	46.9	34.7	0.191	0.141
Hot water	49.6	49.6	0.202	0.202
Total	96.4	84.3	0.393	0.343

In addition, the new design strategies also improved building comfort as the average building discomfort index of initial case has decreased from 10.45 PPD to 7.56 PPD.

The optimization finds a single solution which is the energy and water performance level leading to the lowest cost during the estimated economic lifecycle as a result of combination of various energy efficiency measures available for the Istanbul case study. However, cost versus energy cloud of optimization search is very useful to determine a cost-effective range.

Figure 5.24 shows global cost vs net primary energy performance of investigated design options that are capable of satisfying CO_2 and comfort restrictions. The design combinations that cannot satisfy penalty criteria are filtered. The base case and optimized case scenarios are highlighted. The optimized case represents an economic optimum as it is the minimum global cost option among the considered energy efficiency measures for this particular building. The figure shows that optimization creates a sharp fall both in global cost and primary energy consumption levels in comparison to base case.

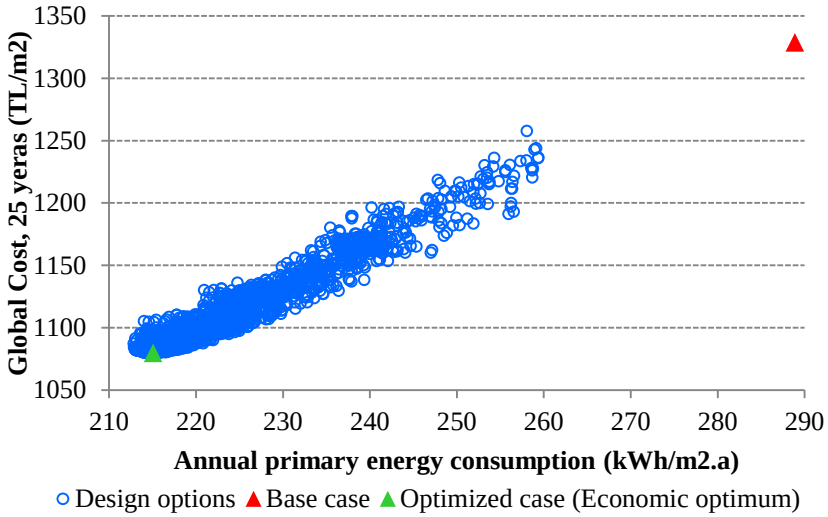

Figure 5.24 : Global cost vs primary energy cloud obtained with Istanbul case.

Figure 5.25 focuses on the lower part of the cost-energy cloud where a frontier curve is represented in black dashes.

Design options from optimized case (the economic optimum) within a 5% increase in global cost range towards minimum primary energy case following the frontier curve constitute a solution that can be considered as a cost-effective alternative range. Therefore, various types of solutions with reasonable low global cost, closed to the lower frontier of cost-energy cloud are investigated.

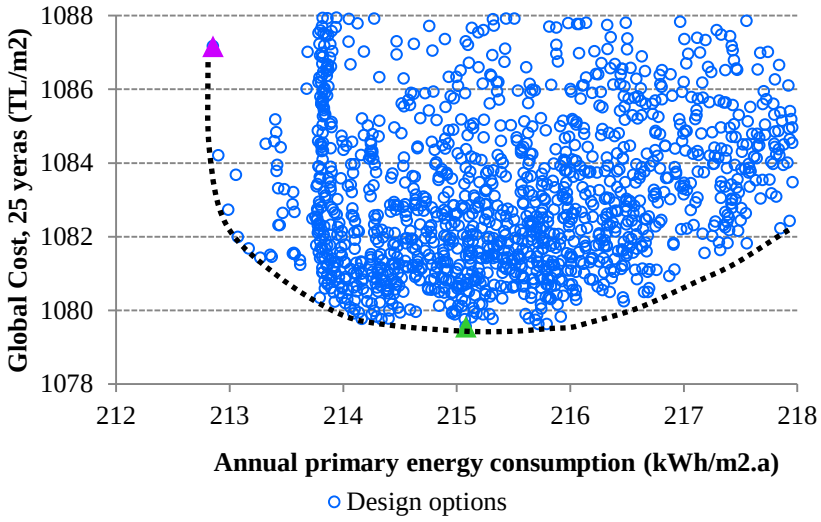

Figure 5.25 : Cost-effective alternative solutions obtained with Istanbul case.

The area of the curve to the right of the economic optimum represents solutions that underperform in both cost and energy.

Results show that, to save 2.22 kWh/m2.a primary energy, 7.61 TL/m2 extra global cost is required for 25 years calculation period. Lower primary energy alternatives required more investment in insulation and glazing type, larger windows resulting all together a smaller size boiler. Lower primary energy alternatives that have slightly higher global cost values than the economic optimum is presented in Table 5.39.

Table 5.39 : Cost-effective alternative solutions with Istanbul case.

	Net Primary Energy (kWh/m2.a)	Global Cost (TL/m2)	iEW (m)	iR (m)	RT	GT	WTW South (%)	WTW West (%)	WTW North (%)	WTW East (%)	BLtyp	CLtyp	DL
1(Min.En)	212.86	1087.16	0.09	0.08	2	24	55	55	55	45	42	32	1
2	212.90	1084.20	0.04	0.08	2	14	55	45	55	55	42	32	1
3	212.99	1082.72	0.025	0.045	2	19	55	55	55	55	43	32	1
4	213.08	1081.99	0.03	0.055	2	19	55	55	55	45	43	32	1
5	213.17	1081.67	0.03	0.05	2	19	55	55	55	45	43	32	1
6	213.27	1081.42	0.04	0.045	2	19	55	55	55	45	43	32	1
7	213.36	1081.49	0.025	0.045	2	19	55	55	55	45	43	32	1
8	214.09	1079.91	0.02	0.055	2	19	55	45	55	35	43	32	1
9	214.17	1079.76	0.025	0.05	2	19	55	45	55	35	43	32	1
10 (O.C)	215.08	1079.55	0.025	0.045	2	13	45	35	55	35	43	32	1

In the second step of the investigation, the optimization problem was extended to optimize building, HVAC system and renewable systems simultaneously.

First, the roof-mounted PV scheme described in previous section is added to building model and then, optimum PV capacity and PV type was searched simultaneously together with other design options. Table 5.40 introduces the initial and recommended design alternatives.

Table 5.40 : Base case and optimized case design options after PV integration with Istanbul case.

	iEW (m)	iR (m)	RT	GT	WTW South (%)	WTW West (%)	WTW North (%)	WTW East (%)	BLtyp	CLtyp	DL	Pv Type	PV Number
B.C	0	0	1	1	25	25	25	25	18	13	0	-	-
O.C	0.025	0.045	2	13	45	35	55	35	43	32	1	1	858

As numbers indicate, all the design recommendations including external wall insulation thickness, roof insulation thickness, roof coating type, window-to-wall ratios, dimming control system based on daylighting, chiller equipment and boiler equipment are remained same as the optimum case without PV integration.

The Figure 5.26 below shows the objective function values calculated with each PV type during the search process. The values obtained with PV2 are always much higher than the values obtained with PV1. Therefore, the optimization selected PV1 (polycrystalline silicone cell) over PV2 (thin film cell) as ideal PV system for Istanbul case study.

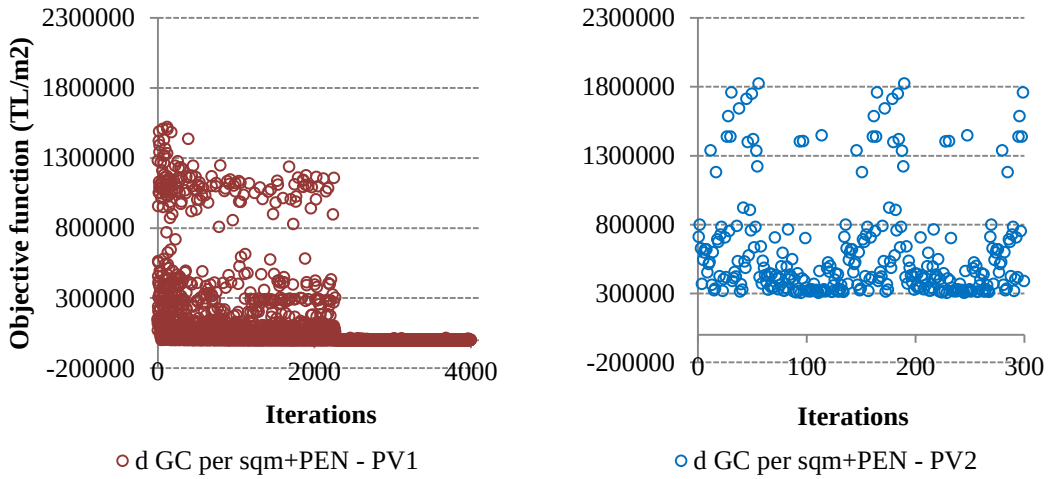

Figure 5.26 : Distribution of optimization results with each PV type obtained with Istanbul case.

When the elements of the objective function are investigated it was seen that the design case with PV 2 is constantly penalized due to payback constraint because it is not able to satisfy 25-year payback criteria.

However, the recommended system with PV1 has an average payback period of 21 years that is less than the target period and no penalty due to time constraint was imposed. Therefore, the energy savings within building life span was able to pay back the ownership cost of the system PV1.

Moreover, the annual cost benefits obtained with PV2 is less than PV1. The optimum number of PV modules is calculated as 858 that is the maximum number of modules that can be installed on rooftop based on physical constraints.

The absolute GC per sqm of the optimized case with PV is calculated as 1053 TL/m2 that is 508 TL/m2 less than initial case and 232 TL/m2 less then optimized case without a PV system. A comparison of absolute GC values is illustrated in Figure 5.27.

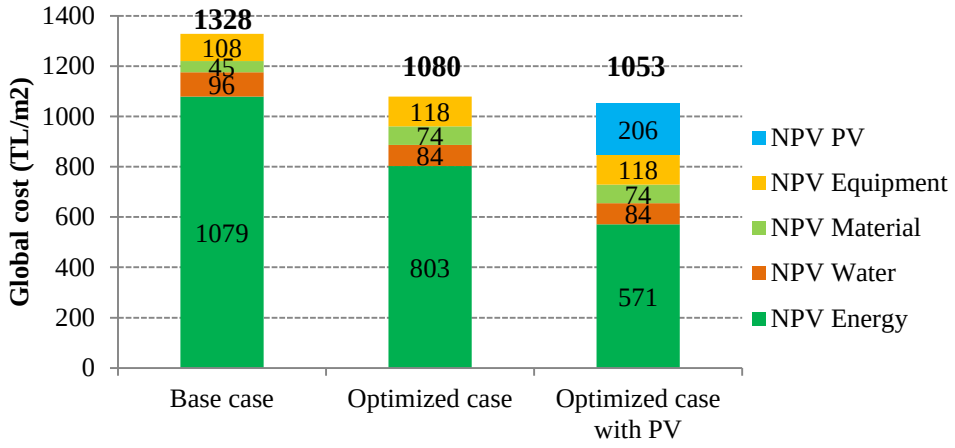

Figure 5.27 : Global cost breakdown after PV integration with Istanbul case.

The application of PV system has reduced the NPV energy costs by 47.1 % in comparison to base case and by 28.9 % in comparison to optimized case without PV. The NPV of equipment and material cost remained same in two optimized cases since rest of the design variables remained same. The recommended PV system has a 214.5 kW installed peak-power and it is capable of annually producing 235,273 kWh electricity. 233,562 kWh of that amount directly satisfies the building electricity load that is equal to 35.7 % of the total building electricity need. Consequently, the building CO_2 emission rate was decreased to 38.8 kg/m2.a that is equal to a 47.6% decrease in comparison to initial case and a 29.7 % decrease in comparison to optimized case without PV system as given in Figure 5.28.

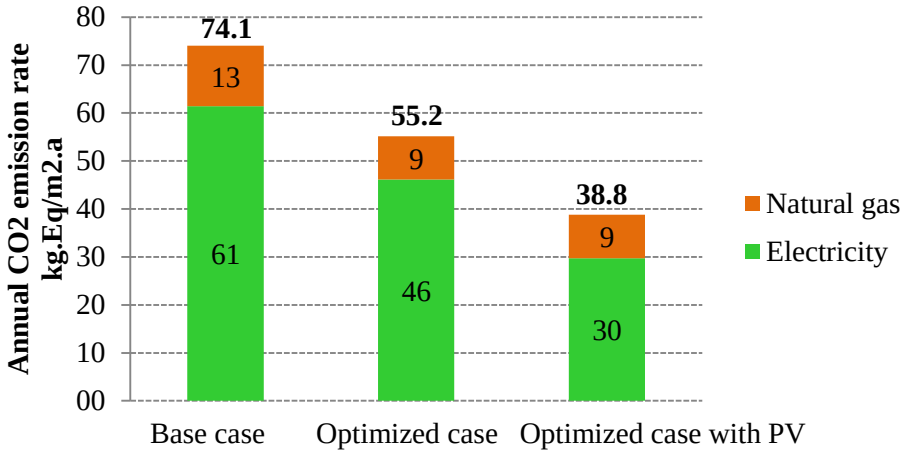

Figure 5.28 : Comparison of annual CO_2 emission rate after PV integration obtained with Istanbul case.

The total NPV ownership cost of the selected PV system is calculated as 206 TL/m2 for 25 years period. The initial investment requires 140 TL/m2 for PV modules, inverter and installation fees. The rest of the money is required for system

maintenance and replacement of aging equipment. The cost of annual electricity saving is equal to 8.6 TL/m2. The annual surplus electricity generated back to the grid is 1711 kWh and is equal to a 0.047 TL/m2 income. When combined with annual electricity saving the annual cost benefit obtained from the PV system is equal to 8.65 TL/m2.

Design variables related to PV system have no influence on building comfort therefore the discomfort index of the optimized case with PV system is obtained same as the discomfort index of optimized case without PV system, which was able to satisfy the comfort criteria.

Lastly, the solar water heating (SWH) system described in previous section is added to the building model and the optimization is re-run for an aim to find the optimal solar collector type, and collector number. Since the so-called system is only for sanitary water heating and there is no HVAC interaction, the results are presented only for SWH system. The main objective function consists of NPV per sqm of ownership of SWH system, NPV per sqm of natural gas use due to water heating by backup system and penalty value in case the investment payback period is not satisfied.

The Figure 5.29 below illustrates the optimization search space. As shown in the figure, the payback period of the solar thermal systems start exceeding the target period of 25 years with all three solar collector types after installation of 60 collectors and large penalties occurs.

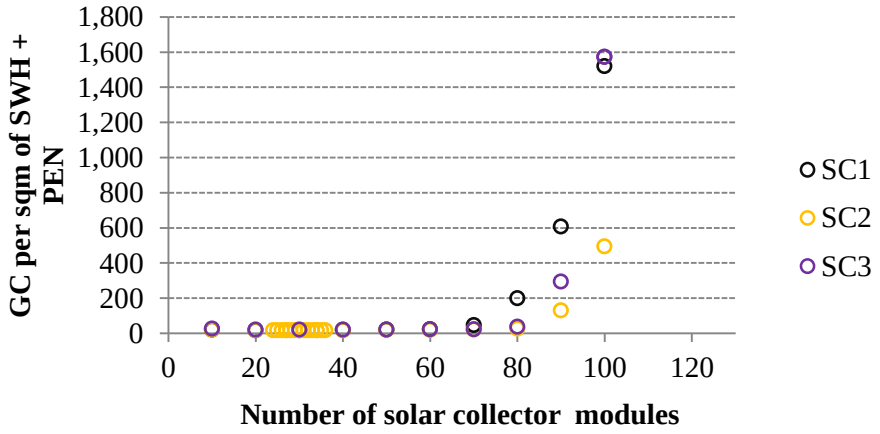

Figure 5.29 : Optimization results with each solar collector type with Istanbul case.

Therefore, the maximum value of feasible design region is obtained as 60 collectors. The feasible design region is then investigated in detail and a comparison of the GC

performances of solar systems with all collector types is provided in Figure 5.30. According to the given numbers, the optimum collector type for this case study building is obtained as SC 2 (selective surface, moderate efficiency collector) and the optimum number of collector modules is obtained as 31.

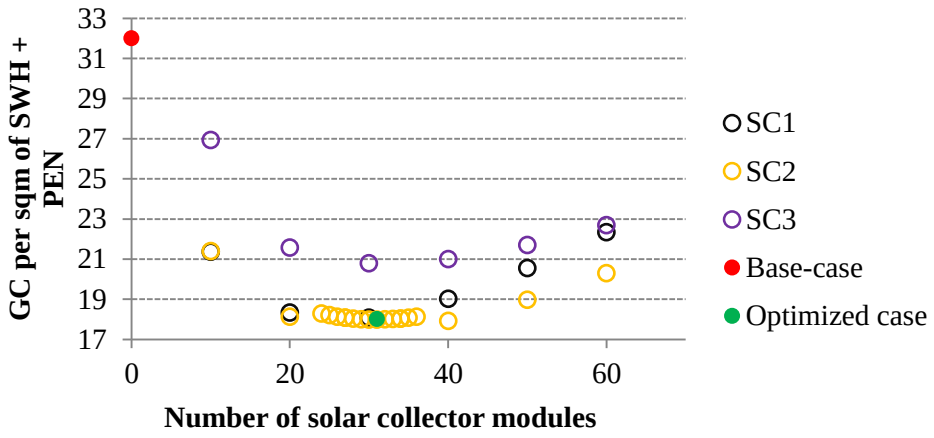

Figure 5.30 : Optimization results with each solar collector type within feasible region obtained with Istanbul case.

Table 5.41 summarizes the cost performances of initial and recommended systems. As results shows the NPV ownership cost of the recommended solar water heating system is 2.6 times higher than the conventional natural gas water heating system. However, the contribution of the solar thermal system was capable of decreasing the natural gas annual energy use from 8 kWh/m2 to 3 kWh/m2 with a corresponding NPV energy saving of 60 % for water heating purposes. Therefore, the energy savings were able to pay back the investments cost in 6.2 years, which is less than the target value.

Table 5.41 : Global cost breakdown of conventional and solar thermal water heating system obtained with Istanbul case.

Cost type	Conventional water heater system	Solar thermal system
NPV energy	29	11.4
NPV system ownership	2.5	6.6
Total GC	31.5	18

In addition to cost saving benefits, the reduction in annual natural gas water heating requirement resulted in 1.1 kg-eq/m2 reduction in annual CO2 emissions.

The recommended SWH system is combined with rest of the recommended design options and the GC performance of different design cases are compared in Figure 5.31.

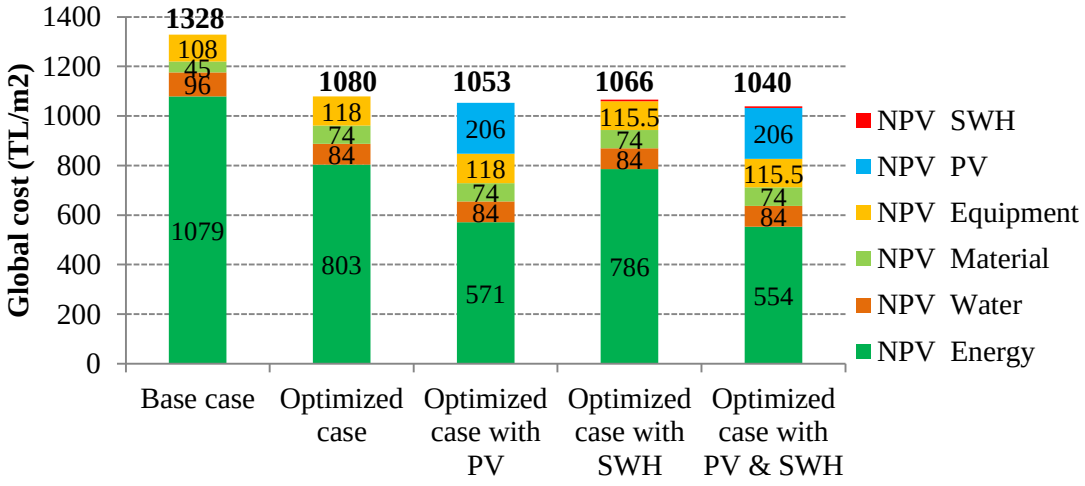

Figure 5.31 : Comparison of all design scenarios obtained with Istanbul case.

If all design suggestions given by the proposed optimization method are adopted, the building overall energy consumption from non-renewables can be decreased by 44%, annual CO2 emission rate can be decreased by 49 % and the building global costs can be decreased by 21.7 % while improving the overall building comfort for the Istanbul case study.

5.3.5.2 Ankara case study

The graphic in Figure 5.32 illustrates the results of the optimization search in Ankara case as a dense cloud of black circles.

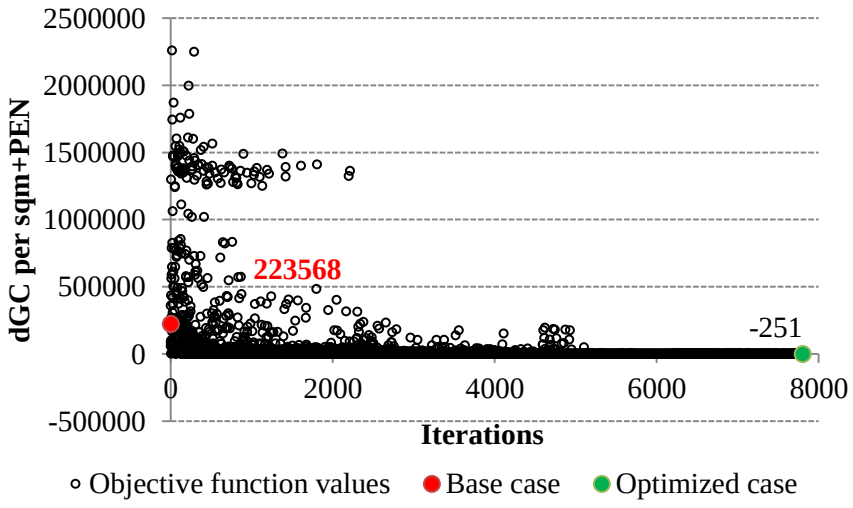

Figure 5.32 : Distribution of optimization results obtained with Ankara case.

In the figure each black circle represents a different combination of the optimization variables and the resulting objective function value that includes dGC per floor area and total penalty value.

As the figure indicates, many different combinations of design variables are created and investigated during optimization search therefore, the solution space covers a wide region. The main objective function for the base case is calculated as 223,568 where, after optimization, it was reduced to -251.

Since the objective function is based on building global cost performance and how well the building satisfies the user-set penalty limitations, a breakdown of objective function is also illustrated in Figure 5.33, where dark circles represents dGC per sqm and orange circles represents the corresponding total penalty function value.

As Figure shows, a large portion of the solution space constitute invalid solutions due to violations of the problem constraints even some of the solutions show a better GC performance than the optimized case.

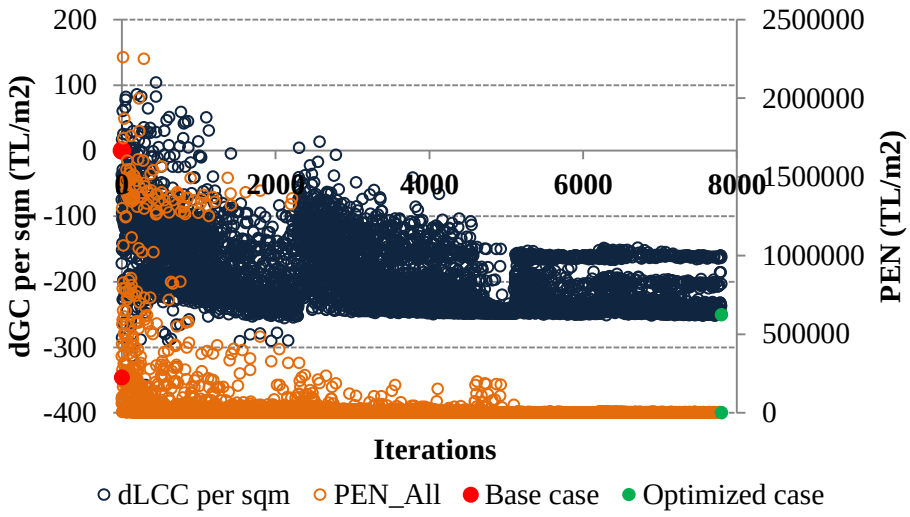

Figure 5.33 : Breakdown of optimization results obtained with Ankara case.

The dGC per sqm of initial case is calculated as zero since it is the reference point of the optimization. However, its corresponding penalty function is calculated as 223,568. The positive value indicates that the initial case violates some penalty criteria. When the penalty values of initial case are further investigated it was seen that base case violates comfort and CO_2 emission criteria as given in Figure 5.34.

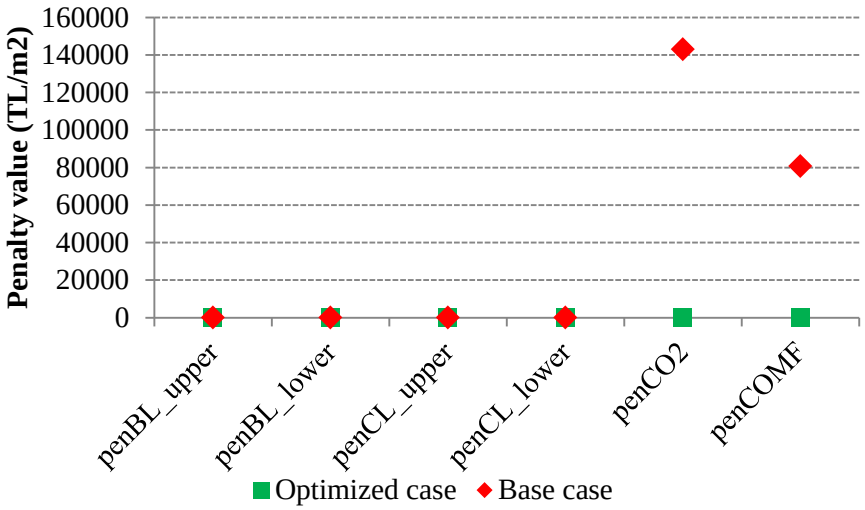

Figure 5.34 : Penalty values obtained with Ankara case.

The dGC per sqm of the optimized case is calculated as -251 TL/m2 and the corresponding penalty value is obtained as zero. Therefore, the optimization was successful at reducing building global cost without violating any of the optimization constraints.

When the absolute GC per sqm values of base case and optimized cases are compared as given in Figure 5.35 it was found that in optimized case 251 TL/m2 global cost saving has been achieved relative to base case and the application of optimization has achieved reducing the overall GC by 18.6 % in Ankara case study.

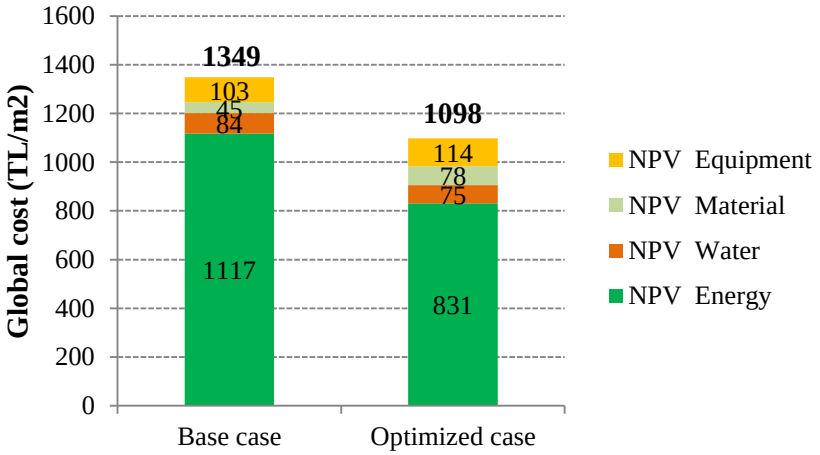

Figure 5.35 : Comparison of global cost breakdown obtained with Ankara case.

Total global cost is a summation of net-present value of energy cost, water cost, building material cost and system equipment cost and Figure 5.35 shows how absolute values of each GC element contributed to the total value.

The application of the proposed optimization methodology has reduced the NPV of energy cost by 25.6 %, and the NPV of water cost by 10.6 %. However, to improve building energy and water efficiency, the NPV of building material cost has increased by 74.4 % and the NPV of building equipment cost has increased by 11 % due to investments in new design options.

Table 5.42 provides the base case and final set of recommended design options.

Table 5.42 : Base case and optimized case design options with Ankara case.

	iEW (m)	**iR (m)**	**RT**	**GT**	**WTW South (%)**	**WTW West (%)**	**WTW North (%)**	**WTW East (%)**	**BLtyp**	**CLtyp**	**DL**
B.C.	0	0	1	1	25	25	25	25	23	10	0
O.C.	0.05	0.085	2	13	45	45	45	25	45	30	1

According to the given numbers, the optimization recommended increasing the external wall insulation thickness from zero to 0.05 meters and the roof insulation thickness from zero to 0.085 meters.

Moreover, optimization also recommended cool roof paint (RT2) instead of conventional gravel roof (RT1) as final layer of the roof element.

The initial air filled double glazed glazing unit GT1 (U: 2.9 W/m2K, SHGC: 0.75, Tvis: 0.8, Cost: 38.9 TL/m2) was replaced with double glazed argon filled glazing unit GT13 (U: 1.6 W/m2K, SHGC: 0.56, Tvis: 0.79, Cost: 44.8 TL/m2).

Moreover, the moderate window-to-wall ratios were increased from 25 % to 45 % in Southern, Western and Northern facades. However, the window-to-wall ratio of Eastern facades remained the same. The increase in w-t-w ratios naturally let the net area of external wall decrease accordingly.

The change in NPV due to the changes that occur in independent and dependent variables of building material category are summarized in Table 5.43.

The improvements in building façade were also combined and supported with the improvements in building systems.

To begin with, the optimization selected dimming control of artificial lights according to daylight levels as a cost effective and energy-efficient design option over manual lighting control.

Table 5.43 : NPV breakdown of building material cost with Ankara case.

Building Materials	Base case (TL/m2)	Optimized case (TL/m2)
External wall insulation	0.0	3.9
Roof insulation	0.0	13.4
Roof coating type	1.6	4.6
Glazing type	26.2	42.5
Wall composition	17.0	13.6
Total Material Cost	44.8	78.1

Moreover, when the lighting control was integrated with the rest of the new building façade recommendations, a decrease in building heating and cooling loads were obtained.

The reduction in building loads was dynamically reflected both on chiller and boiler equipment sizes in the calculation. The base case boiler equipment BL 23 (Capacity: 878 kW, Eff: 0.84, Cost: 18689 TL) was replaced with BL 45 (Capacity: 615 kW, Eff: 0.95, Cost: 38689 TL) which is in the high-efficiency equipment category. However, similar size lower-efficiency boiler BL18 (Capacity: 610 kW, Eff: 0.84, Cost: 13240 TL) wasn't found to be favourable.

Similarly, the bas case chiller CL 10 (Capacity: 599 kW, EER: 4.68, Cost: 155377 TL) was replaced with CL 30 (Capacity: 505, EER: 5.63, Cost: 175251) which is in the high-efficiency equipment category. Similar size lower-efficiency alternative CL 8 (Capacity: 510 kW, EER: 4.72, Cost: 142623 TL) wasn't found to be worth investing under circumstances.

The penalty values due to boiler and chiller equipment allowable capacities are calculated as zero which shows that optimization algorithm was successful at finding right-sized equipment while.

The reductions in building heating and cooling loads were also reflected on dependent equipment. The number of required fan coil units was decreased from 66 to 44. Similarly, the required cooling tower capacity has decreased from 577 kW to 472 kW as well.

The change in NPV due to the changes that occur in independent and dependent building system variables are summarized in Table 5.44.

Table 5.44 : NPV breakdown of building system cost with Ankara case.

Building Systems	Base case (TL/m2)	Optimized case (TL/m2)
Boiler	3.3	5.3
Chiller	27.4	29.6
Cooling Tower	6.7	5.7
Fan Coil Units	26.0	17.4
Water Heater	2.5	2.5
Lighting Control	36.7	53.4
Total Equipment Cost	102.6	113.8

The recommended boiler has about twice the capital cost of initial boiler and 1.6 times the global cost of initial boiler however, improved thermal efficiency was found to be worth investing in to decrease energy costs.

When the initial and recommended chiller equipment are compared it was found that the capital cost of initial chiller (CL10) is lower than the capital cost of the selected chiller (CL30). Moreover, NPV of the initial chiller is also higher than the selected chiller. However, the energy efficiency due to the better EER of the recommended chiller makes the total investment worth the cost.

The NPV of cooling tower decreased due to the reduction in equipment capacity.

Similarly, NPV of Fan coil units reduced in parallel to the reduction in the number of required units.

The impact of optimization on global energy costs are given in Table 5.45. The largest energy cost is due to electricity use, which is about more than twice the natural gas cost in both cases. The recommended design strategies however succeeded decreasing energy cost about 22 % for electricity and about 34.4 % for natural gas.

Table 5.45 : NPV breakdown of energy cost with Ankara case.

Energy Cost Type	Base case (TL/m2)	Optimized case (TL/m2)
Electricity Cost	789.3	615.8
Natural Gas Cost	328.1	215.2
Total Energy Cost	1117.4	831.0

The influence of optimization on annual building energy performance is summarized in Figure 5.36. The application of the recommended design options achieved lowering total annual building primary energy use intensity from 298.2 kWh/m2 to 222 kWh/m2 which is equal to 25.6 % decrease. The reduction occurred in every end use type except the natural gas use for water heating since there was not any design option directly influencing water heating system performance.

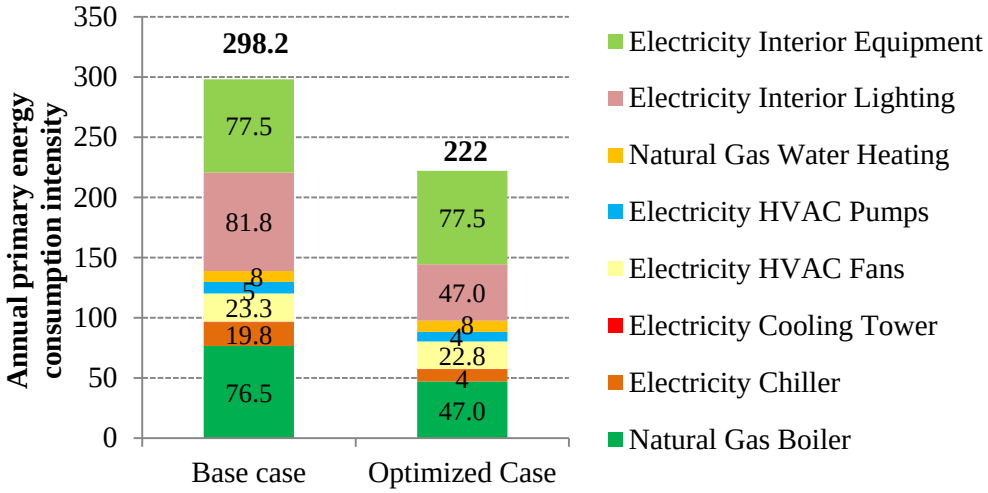

Figure 5.36 : Comparison of annual primary energy consumption breakdown obtained with Ankara case.

The reduction in energy use also resulted in a reduction in the value of annual CO2-eq emission rate as shown in Figure 5.37.

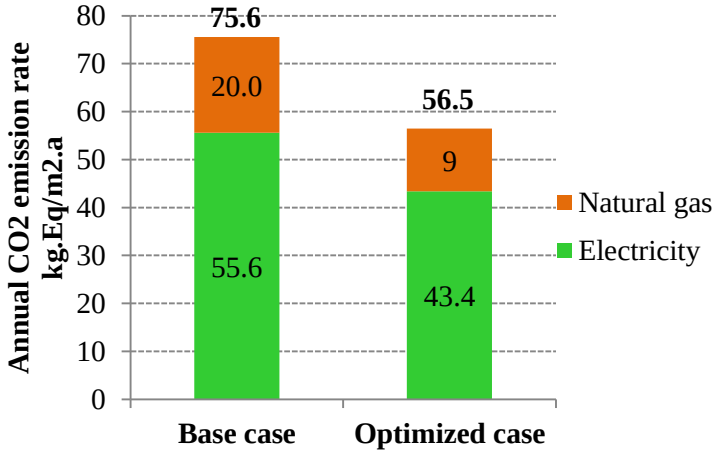

Figure 5.37 : Comparison of annual CO_2 emission rate breakdown obtained with Ankara case.

The overall annual building emission rate was decreased from 75.6 kg.Eq-CO2/m2 to 56.5 kg.Eq-CO2/m2. The percentage of reduction is equal to 25.3 that is much higher than the minimum target reduction of 10 %. Therefore, the recommended design

strategies are perfectly capable of satisfying CO_2 emission constraint for the Ankara case.

The impact of optimization on NPV of water cost is given in Table 5.46. The service life water cost due to cooling tower water use decreased by 25.8 % due to the reduction in building cooling needs and consequent cooling tower operating hours. However, the available design strategies have no influence on building hot water use, which is only linked with building occupancy density. Therefore, the related water cost remained same in two cases.

Table 5.46 : Comparison of NPV breakdown of water cost and water end use with Ankara case.

Water End Use Type	**NPV water cost (TL/m2)**		**Annual water consumption [m3/m2]**	
	Base case	Optimized case	Base case	Optimized case
Cooling tower	34.3	25.4	0.140	0.103
Hot water	49.6	49.6	0.202	0.202
Total	83.8	75.0	0.341	0.305

In addition, the new design strategies also improved building comfort as the average building discomfort index of base case has decreased from 12.69 PPD to 7.94 PPD.

The optimization finds a single solution which is the energy and water performance level leading to the lowest cost during the estimated economic lifecycle as a result of combination of various energy efficiency measures available for the Ankara case study. However, cost vs energy cloud of optimization search is very useful to determine a cost-effective alternative range.

Figure 5.38 shows global cost vs net primary energy performance of investigated design options that are capable of satisfying CO_2 and comfort restrictions. The design combinations that cannot satisfy penalty criteria are filtered. The base case and optimized case scenarios are highlighted. The optimized case represents an economic optimum as it is the minimum global cost option among the considered energy efficiency measures for this particular building. The figure shows that optimization creates a sharp fall both in global cost and primary energy consumption levels in comparison to base case.

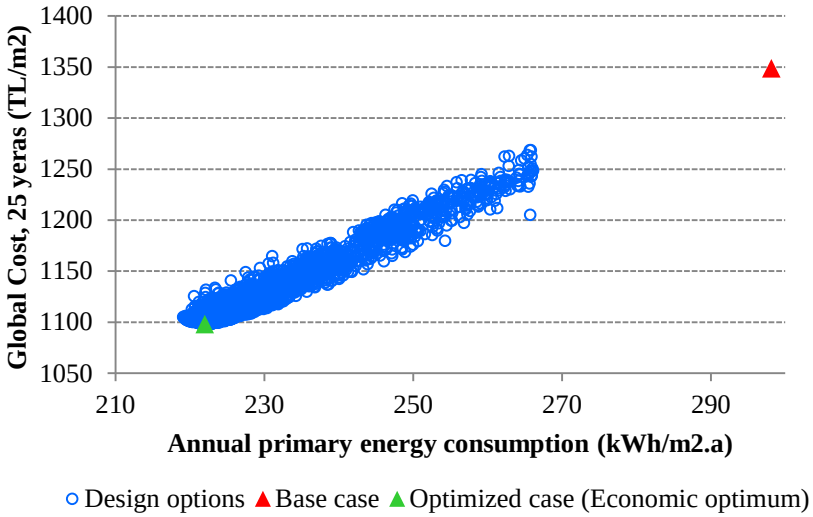

Figure 5.38 : Global cost vs primary energy cloud obtained with Ankara case.

Figure 5.39 focuses on the lower part of the cost-energy cloud where a frontier curve is represented in black dashes. Design options from optimized case (the economic optimum) within a 5% increase in global cost range towards minimum primary energy case following the frontier curve constitute a solution that can be considered as a cost-effective alternative range. Therefore, various types of solutions with reasonable low global cost, closed to the lower frontier of cost-energy cloud is investigated.

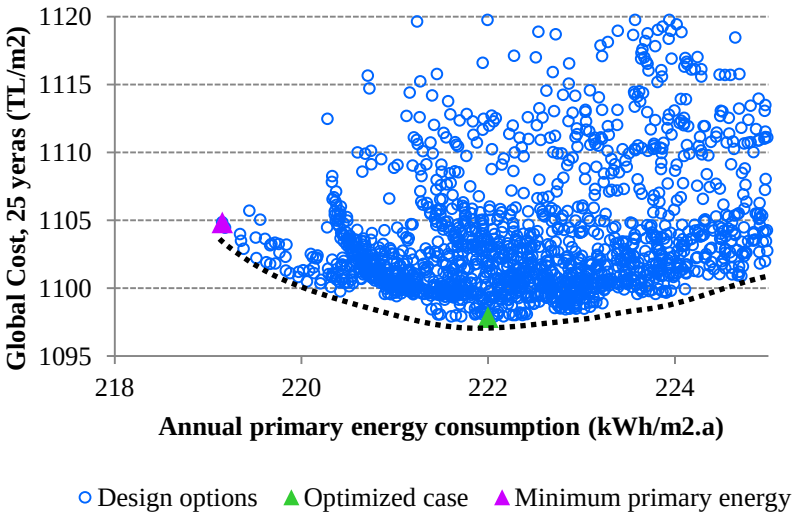

Figure 5.39 : Cost-effective alternative solutions obtained with Ankara case.

The area of the curve to the right of the economic optimum represents solutions that underperform in both cost and energy.Results show that, to save 2.85 kWh/m2.a primary energy, 6.97 TL/m2 extra global cost is required for 25 years calculation period. Lower primary energy alternatives required more investment in insulation

and glazing type, larger windows. Lower primary energy alternatives that have slightly higher global cost values than the economic optimum is presented in Table 5.47.

Table 5.47 : Cost-effective alternative solutions with Ankara case.

	Net Primary Energy (kWh/m2.a)	Global Cost (TL/m2)	iEW (m)	iR (m)	RT	GT	WTW South (%)	WTW West (%)	WTW North (%)	WTW East (%)	BLtyp	CLtyp	DL
1(Min.En)	219.15	1104.84	0.075	0.100	2	24	55	55	55	55	45	30	1
2	219.18	1104.44	0.065	0.100	2	24	55	55	55	55	45	30	1
3	219.38	1102.90	0.040	0.115	2	24	55	55	55	45	45	30	1
4	219.52	1102.19	0.055	0.100	2	24	55	55	55	45	45	30	1
5	220.06	1100.48	0.040	0.095	2	24	55	55	55	35	45	30	1
6	220.42	1099.75	0.040	0.085	2	19	55	55	55	35	45	30	1
7	221.46	1098.04	0.040	0.085	2	18	45	45	55	25	45	30	1
8	221.61	1097.91	0.040	0.080	2	18	45	45	55	25	45	30	1
9	221.72	1097.92	0.045	0.075	2	18	45	45	55	25	45	30	1
10(O.C)	222.00	1097.87	0.050	0.085	2	13	45	45	45	25	45	30	1

In the second step of the investigation, the optimization problem was extended to optimize building, HVAC system and renewable systems simultaneously.

First, the roof-mounted PV scheme described in previous section is added to building model and then, optimum PV capacity and PV type was searched simultaneously together with other design options. Table 5.48 introduces the initial and recommended design alternatives.

Table 5.48 : Base case and optimized case design options with PV integration with Ankara case.

	iEW (m)	iR (m)	RT	GT	WTW South (%)	WTW West (%)	WTW North (%)	WTW East (%)	BLtyp	CLtyp	DL	Pv Type	PV Number
B.C	0	0	1	1	25	25	25	25	23	10	0	-	-
O.C	0.05	0.08	2	13	45	45	45	25	45	30	1	1	858

As numbers indicate, all the design recommendations except external wall insulation thickness are remained same as the optimum case without PV integration. However, the optimum thickness of roof insulation is obtained as 0.08 m, which is half centimetre less than the case without PV system.

The Figure 5.40 illustrates the objective function values calculated with each PV type during the search process. The values obtained with PV2 are much higher than the

values obtained with PV1 most of the time. Therefore, the optimization selected PV module type 1 (polycrystalline silicone cell) over PV module type 2 (thin film cell) as ideal PV system for the Ankara case study.

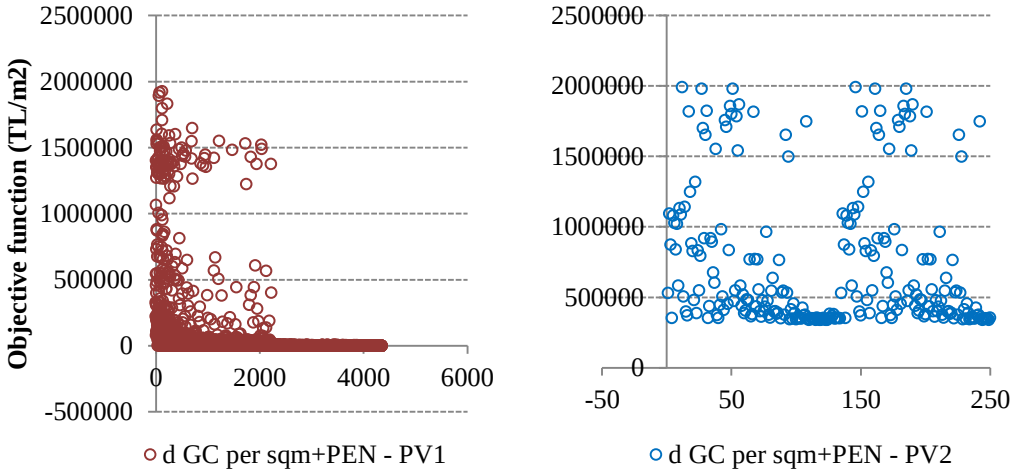

Figure 5.40 : Distribution of optimization results with each PV type obtained with Ankara case.

When the elements of the objective function are investigated it was seen that the design case with PV 2 is constantly penalized due to payback constraint because it is not able to satisfy 25-year payback criteria.

However, the recommended system with PV1 has an average payback period of 18.8 years that is less than the target period and no penalty due to time constraint was imposed. Therefore, the energy savings within building life span was able to pay back the ownership cost of the system PV1. Moreover, the annual cost benefits obtained with PV2 is less than PV1.

The optimum number of PV modules is calculated as 858 that is the maximum number of modules that can be installed on rooftop based on physical constraints.

The absolute overall GC per sqm of the optimized case with PV is calculated as 1050 TL/m2 that is 539 TL/m2 less than base case and 252 TL/m2 less then optimized case without a PV system. A comparison of absolute GC values is illustrated in Figure 5.41.

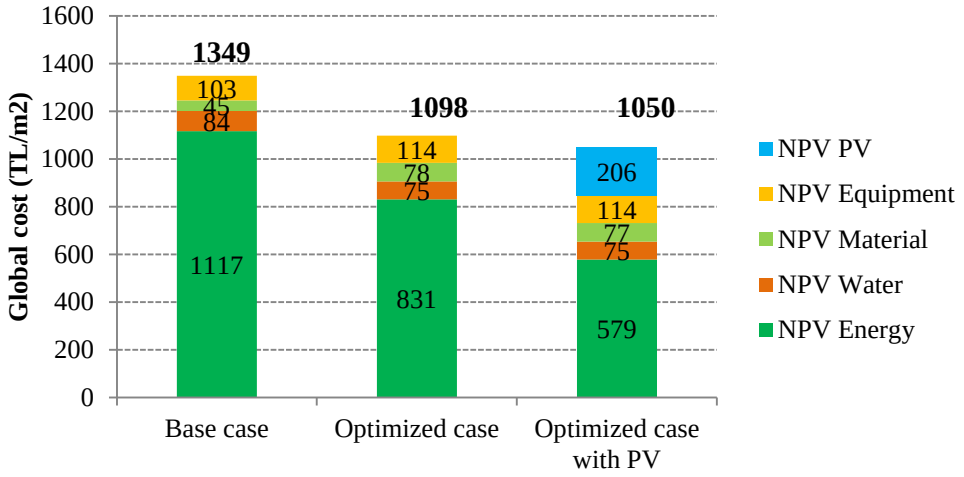

Figure 5.41 : Global cost breakdown after PV integration with Ankara case.

The application of PV system has reduced the NPV energy costs by 48.2 % in comparison to base case and by 30.4 % in comparison to optimized case without PV. The NPV of equipment cost remained same in two optimized cases since rest of the design variables remained same. However, NPV of material cost slightly decreased due to the 0.05m reduction in optimum roof insulation level. The recommended PV system has a 214.5 kW installed peak-power and it is capable of annually producing 256,846 kWh electricity. 251,950 kWh of that amount directly satisfies the building electricity load that is equal to 40 % of the total building electricity need. Consequently, the building CO_2 emission rate was decreased to 38.7 kg/m2.a that is equal to a 48.8 % decrease in comparison to base case and a 31.5 % decrease in comparison to optimized case without PV system as shown in Figure 5.42.

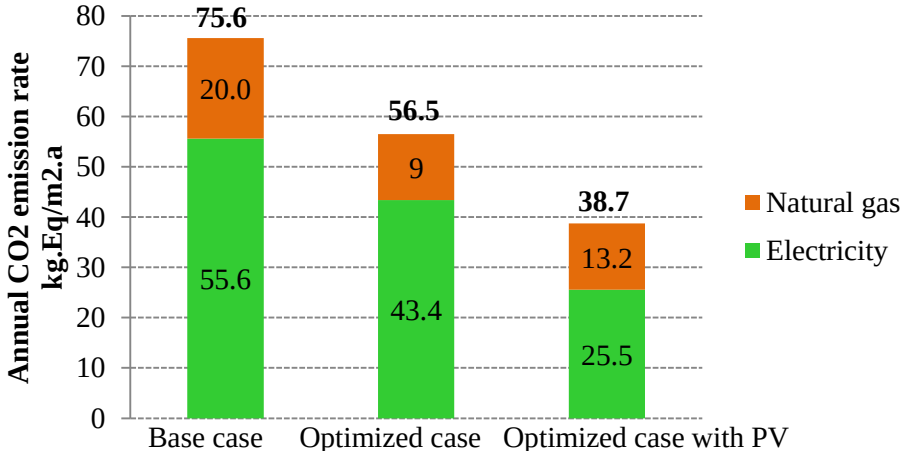

Figure 5.42 : Comparison of annual CO_2 emission rate after PV integration obtained with Ankara case.

The total NPV ownership cost of the selected PV system is calculated as 206 TL/m2 for 25 years period. The initial investment requires 140 TL/m2 for PV modules, inverter and installation fees. The rest of the money is required for system maintenance and replacement of aging equipment. The cost equal of annual electricity saving is 9.4 TL/m2. The annual surplus electricity generated back to the grid is 4897 kWh and is equal to a 0.135 TL/m2 income. When combined with annual electricity saving the annual cost benefit obtained from the PV system is equal to 9.556 TL/m2.

The change in design variables resulted in a decrease in the average building discomfort index where initial level was reduced from 12.69 PPD to 8 PPD.

Lastly, the solar water heating system described in previous section is added to the building model and the optimization is re-run for an aim to find the optimal solar collector type, and collector number. Since the so-called system is only for sanitary water heating, the system is optimized without considering the building and HVAC system interaction. The main objective function consists of NPV per sqm of ownership of solar water heating system, NPV per sqm of natural gas use due to water heating by backup system and penalty value in case the investment payback period is not satisfied.

The Figure 5.43 below illustrates the optimization search space. As shown in the figure, the payback period of the solar thermal systems start exceeding the target period of 25 years with all three solar collector types after installation of 70 collectors and large penalties occurs. Therefore, the maximum value of feasible design region is obtained as 70 collectors.

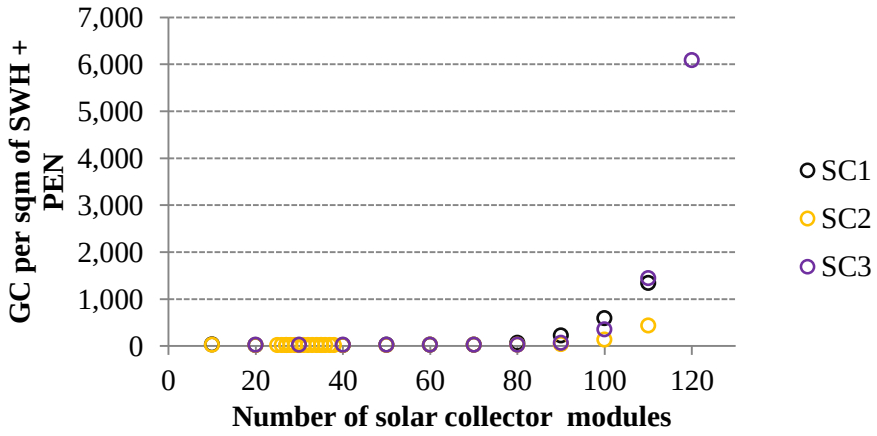

Figure 5.43 : Optimization results with each solar collector type with Ankara case.

The feasible design region is then investigated in detail and a comparison of the cost performances of solar systems with all collector types is provided in Figure 5.44. According to the given numbers, the optimum collector type for this case study building is obtained as SC 2 (selective surface, moderate efficiency collector) and the optimum number of collector modules is obtained as 34.

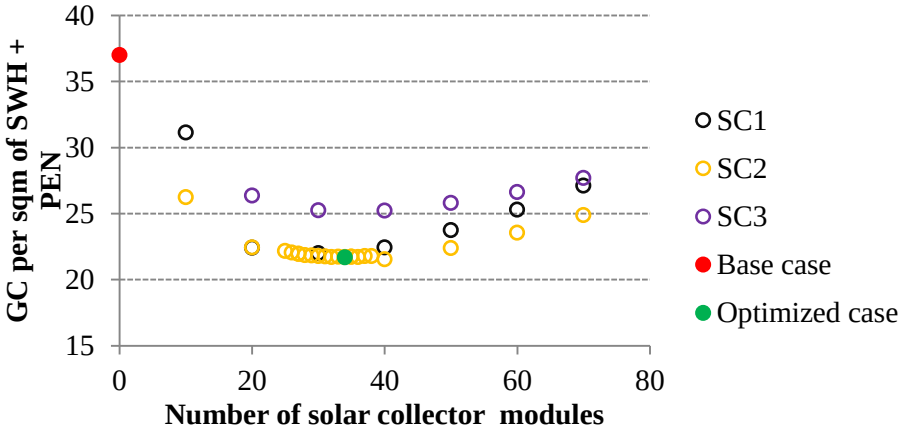

Figure 5.44 : Optimization results with each solar collector type within feasible region obtained with Ankara case.

Table 5.49 summarizes the GC performances of base case and recommended optimized case systems. As results shows the NPV of ownership of the recommended solar water heating system is 2.8 times higher than the conventional natural gas water heating system. However, the contribution of the solar thermal system was capable of decreasing the natural gas annual energy use from 9.1 kWh/m2 to 3.8 kWh/m2 with a corresponding NPV energy cost saving of 58 %. Therefore, the energy savings were able to pay back the investments cost in 6.3 years, which is less than the target value.

Table 5.49 : Global cost breakdown of conventional and solar thermal water heating system with Ankara case.

Cost type	Conventional water heater system	Solar thermal system
NPV energy	34.8	14.6
NPV system ownership	2.5	7.1
Total GC	37.3	21.7

In addition to cost saving benefits, the reduction in annual natural gas water heating requirement resulted in 1.2 kg-eq/m2 reduction in annual CO_2 emissions.

The recommended SWH system is combined with rest of the recommended design options and the GC performance of different design cases are compared in Figure 5.45. If all design suggestions given by the proposed optimization method are adopted, the building overall energy consumption from non-renewables can be decreased by 47.3%, annual CO2 emission rate can be decreased by 50.4 % and the building global costs can be decreased by 23.3 % while improving the overall building comfort for the Ankara case study.

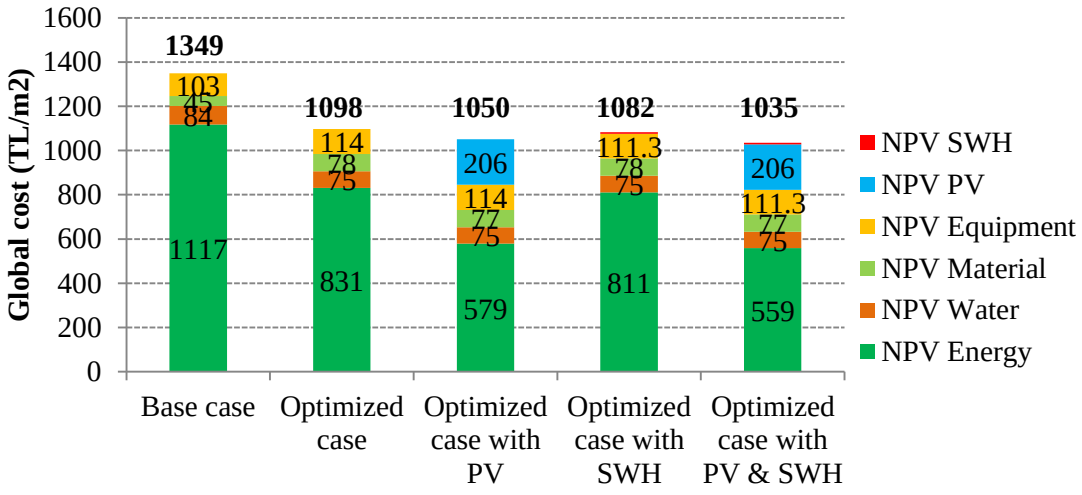

Figure 5.45 : Comparison of all design scenarios obtained with Ankara case.

5.3.5.3 Antalya case study

The graphic in Figure 5.46 illustrates the results of the optimization search in Antalya case as a dense cloud of black circles.

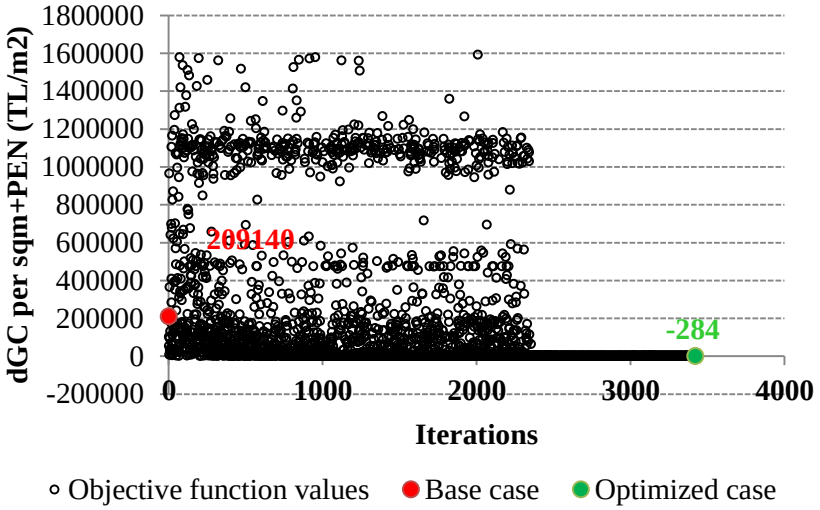

Figure 5.46 : Distribution of optimization results obtained with Antalya case.

In the figure each black circle represents a different combination of the optimization variables and the resulting objective function that includes dGC per floor area and total penalty value.

As the figure indicates, the solution space constitutes a wide range of possibilities due to the large number of variables involved. The main objective function for the base case is calculated as 209140 where, after optimization, it was reduced to -284.

Since the objective function is based on building global cost performance and how well the building satisfies the user-set penalty limitations, a breakdown of objective function is also illustrated in Figure 5.47, where dark circles represents dGC per sqm and orange circles represents the corresponding total penalty function value. As figure shows, a large portion of the solution space constitute invalid solutions due to violations of the problem constraints even they show an improved GC performance than the base case.

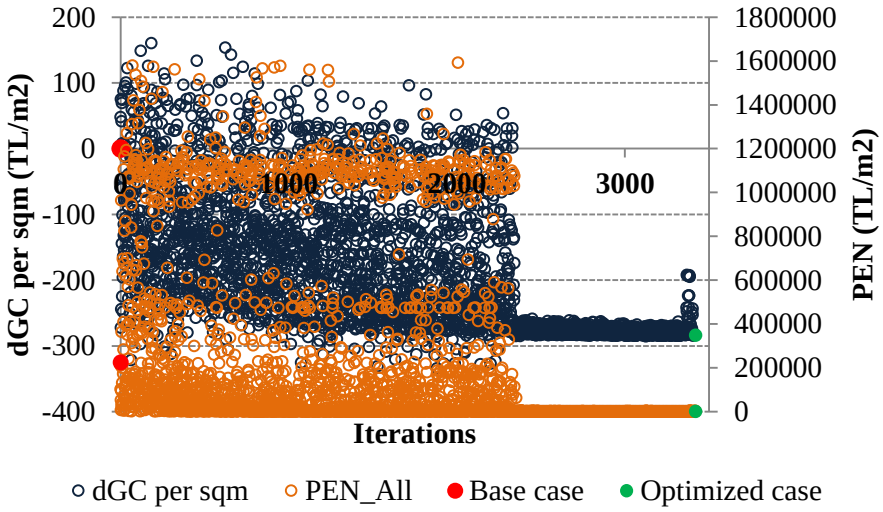

Figure 5.47 : Breakdown of optimization results obtained with Antalya case.

The dGC per sqm of base case is calculated as zero since it is the reference point of the optimization. However, its corresponding penalty function is calculated as 209140. The positive value indicates that the base case violates some penalty criteria.

When the penalty values of base case are further investigated it was seen that base case violates comfort and CO2 emission criteria as given in Figure 5.48.

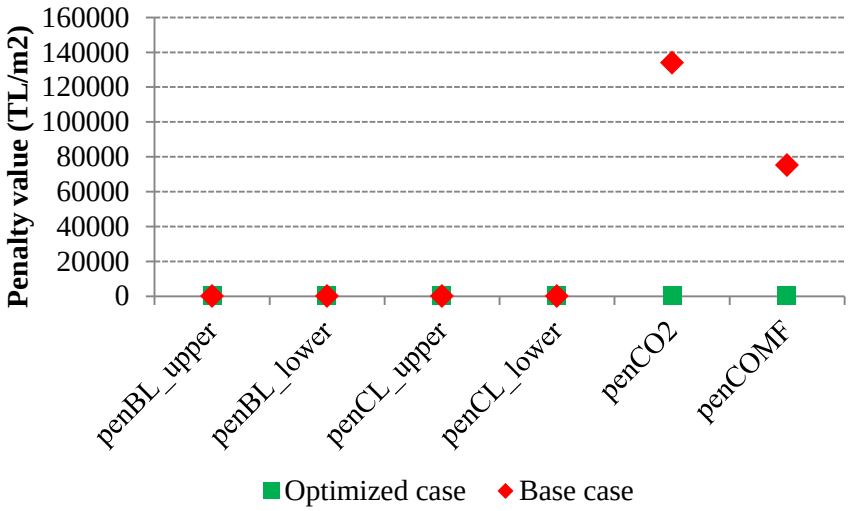

Figure 5.48 : Penalty values obtained with Antalya case.

The dGC per sqm of the optimized case is calculated as -284 TL/m2 and the corresponding penalty value is obtained as zero. Therefore, the optimization was successful at reducing building global cost without violating any of the optimization constraints.

When the absolute global cost per sqm values of base case and optimized cases are compared it was found that in optimized case 284 TL/m2 GC saving has been achieved relative to base case and the application of optimization has achieved reducing the overall global cost by 21.2 % in Antalya case study.

Total global cost is a summation of NPV of energy, water, building material and system equipment and Figure 5.49 below shows how absolute values of each GC element contributed to the total value.

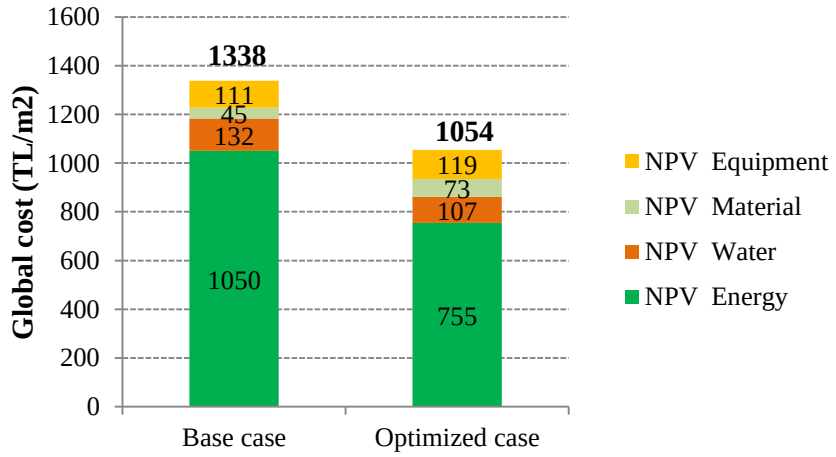

Figure 5.49 : Comparison of global cost breakdown obtained with Antalya case.

The application of the proposed optimization methodology has reduced the NPV of energy cost by 28.1 %, and the NPV of water cost by 19.2 %. However, to improve building energy and water efficiency, the NPV of building material cost has increased by 62.8 % and the NPV of building equipment cost has increased by 7.6 % due to investments in new design alternatives.

Table 5.50 provides the base case and final set of recommended design options for Antalya case study.

Table 5.50 : Base case and optimized case design options with Antalya case.

	iEW (m)	**iR (m)**	**RT**	**GT**	**WTW South (%)**	**WTW West (%)**	**WTW North (%)**	**WTW East (%)**	**BLtyp**	**CLtyp**	**DL**
B.C	0	0	1	1	25	25	25	25	16	13	0
O.C	0.02	0.03	2	19	45	45	45	35	42	32	1

According to the given numbers, the optimization recommended increasing the external wall insulation thickness from zero to 0.02 meters and the roof insulation thickness from zero to 0.03 meters.

Moreover, optimization also recommended cool roof paint (RT2) instead of conventional gravel roof (RT1) as final layer of roof construction.

The initial air filled double glazed glazing unit GT1 (U: 2.9 W/m2K, SHGC: 0.75, Tvis: 0.8, Cost: 38.9 TL/m2) was replaced with double glazed argon filled glazing unit GT19 (U: 1.3 W/m2K, SHGC: 0.44, Tvis: 0.71, Cost: 54.3 TL/m2).

Moreover, the moderate window-to-wall ratios were increased from 25 % to 45 % in Southern, Western and Northern façades. However, the window-to-wall ratio of Eastern facades was increased from 25 % to 35 %. The increase in w-t-w ratios naturally let the net area of external wall decrease accordingly.

The change in NPV due to the changes that occur in independent and dependent variables of building material category are summarized in Table 5.51.

Table 5.51 : NPV breakdown of building materials with Antalya case.

Building Materials	Base case (TL/m2)	Optimized case (TL/m2)
External wall insulation	0.0	2.3
Roof insulation	0.0	6.8
Roof coating type	1.6	4.6
Glazing type	26.2	46.1
Wall composition	17.0	13.0
Total material cost	44.8	72.9

The improvements in building façade were also combined and supported with the improvements in building systems.

To begin with, the optimization selected daylighting control system as a cost effective and energy-efficient design option over manual lighting control. When the lighting control was integrated with the rest of the building façade design recommendations, a decrease in building heating and cooling loads were obtained.

The reduction in building loads have been reflected both on chiller and boiler equipment sizes.

The base case boiler equipment BL 16 (Capacity: 506 kW, Eff: 0.84, Cost: 11053 TL) was replaced with BL 42 (Capacity: 455 kW, Eff: 0.95, Cost: 29623 TL) which is in the high-efficiency equipment category. However, similar size lower-efficiency alternative boiler, BL15 (Capacity: 448 kW, Eff: 0.84, Cost: 10113 TL), wasn't found to be favourable.

Similarly, the base case chiller CL 13 (Capacity: 760 kW, EER: 4.72, Cost: 188210 TL) was replaced with CL 32 (Capacity: 605, EER: 5.65, Cost: 192610) which is in the high-efficiency equipment category. Similar size lower-efficiency alternative CL 10 (Capacity: 599 kW, EER: 4.68, Cost: 155377 TL) wasn't found to be worth investing in under circumstances.

The reductions in building heating and cooling loads were also reflected on dependent equipment. The number of required fan coil units was decreased from 72 to 51. Similarly, the required cooling tower capacity has decreased from 731 kW to 565 kW as well.

The change in NPV due to the changes that occur in independent and dependent building system variables are summarized in Table 5.52.

Table 5.52 : NPV breakdown of building systems with Antalya case.

Building Systems	Base case (TL/m2)	Optimized case (TL/m2)
Boiler	2.0	4.1
Chiller	33.1	32.7
Cooling Tower	8.4	6.7
Fan Coil Units	28.4	20.1
Water Heater	2.5	2.5
Lighting Control	36.7	53.4
Total Equipment Cost	111.0	119.4

The capital cost of the recommended boiler is almost three times higher than the initial boiler. Similarly it also has higher net-present value for service life. However, the optimization found that improved thermal efficiency was worth investing in.

When the base case and recommended chiller equipment are compared it was found that the capital cost of base case chiller (CL13) is slightly lower than the capital cost of the recommended chiller (CL32) even though the selected chiller is among the higher efficient and more expensive equipment category. This is because the optimization succeeded lowering building cooling load and selected smaller size equipment. When the net-present values of chiller equipment ownership are compared it was seen that smaller size new chiller is more economic due to smaller installation and maintenance costs. Moreover, when combined with the benefits of improved equipment efficiency, the recommended chiller was found to be a better investment.

The NPV ownership of cooling tower decreased due to the reduction in cooling load and corresponding equipment capacity. Similarly, NPV ownership of Fan coil units reduced in parallel to the reduction in the number of required units.

The impact of optimization on NPV energy costs are given in Table 5.53. The largest energy cost is due to electricity use, which is about ten times the natural gas cost in both cases. The recommended design strategies however succeeded decreasing energy cost about 29.2 % for electricity and about 15.3 % for natural gas.

Table 5.53 : NPV breakdown of energy use with Antalya case.

Energy Cost Type	Base case (TL/m2)	Optimized case (TL/m2)
Electricity Cost	968.0	685.4
Natural Gas Cost	82.4	69.8
Total Energy Cost	1050.4	755.2

The influence of optimization on building annual primary energy performance is summarized in Figure 5.50. The application of the recommended design options achieved lowering total building annual primary energy use intensity from 282.3 kWh/m2 to 202.9 kWh/m2 with a 28.1 % decrease. The reduction occurred in every end use type except the natural gas use for water heating since there was not any design option directly influencing water heating system performance.

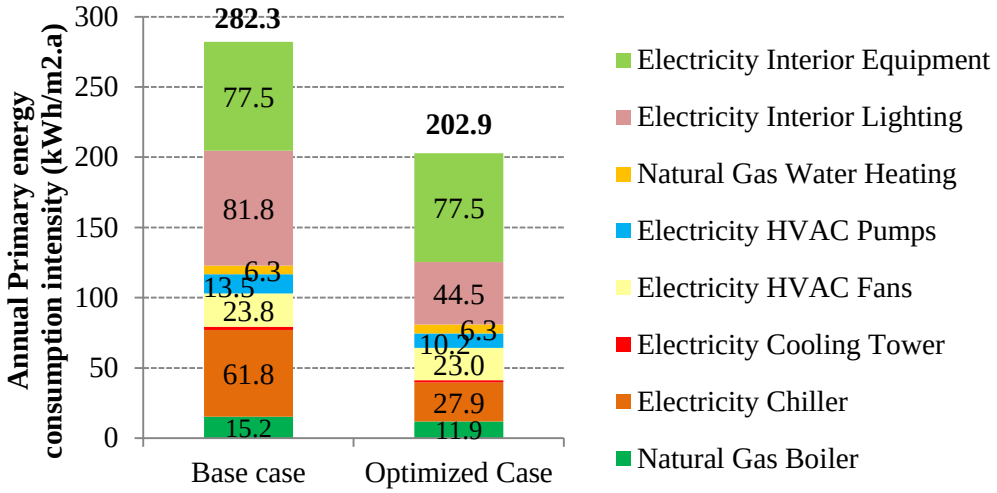

Figure 5.50 : Comparison of annual primary energy consumption breakdown obtained with Antalya case.

The reduction in primary energy use also resulted in a reduction in the value of annual CO2-eq emission rate as shown in Figure 5.51. The overall annual building emission rate was decreased from 73.2 kg.Eq-CO2/m2 to 52.5 kg.Eq-CO2/m2.

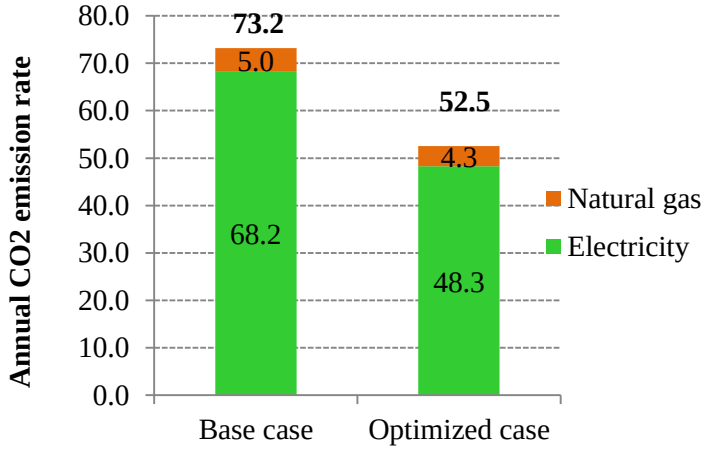

Figure 5.51 : Comparison of annual CO2 emission rate breakdown obtained with Antalya case.

The reduction is equal to 28.2 % that is much higher than the minimum target reduction of 10 %. Therefore, the recommended design strategies are perfectly capable of satisfying CO_2 emission constraint.

The impact of optimization on water costs are given in Table 5.54. The NPV water cost due to cooling tower water use decreased by 30.7 % because of the reduction in building cooling needs and consequent cooling tower operating hours. However, the available design strategies have no influence on building hot water use, which is only linked with building occupancy density. Therefore, the related water cost remained same in two cases.

Table 5.54 : NPV breakdown of water cost and water end use with Antalya case.

Water End Use Type	**NPV water cost (TL/m2)**		**Annual water consumption [m3/m2]**	
	Base case	Optimized case	Base case	Optimized case
Cooling tower	82.8	57.4	0.337	0.234
Hot water	49.6	49.6	0.202	0.202
Total	132.3	106.9	0.539	0.435

In addition, the new design strategies also improved building comfort as the average building discomfort index of initial case has decreased from 12.5 PPD to 7.62 PPD.

The proposed optimization methodology finds a single solution which is the energy and water performance level leading to the lowest cost during the estimated economic lifecycle as a result of combination of various energy efficiency measures available for the Antalya case study. However, cost vs energy cloud of optimization search is very useful to determine a cost-effective range. Figure 5.52 shows global cost vs net primary energy performance of investigated design options that are capable of satisfying CO_2 and comfort restrictions. The design combinations that cannot satisfy penalty criteria are filtered. The base case and optimized case scenarios are highlighted. The optimized case represents an economic optimum as it is the minimum global cost option among the considered energy efficiency measures for this particular building. The figure shows that optimization creates a sharp fall both in global cost and primary energy consumption levels.

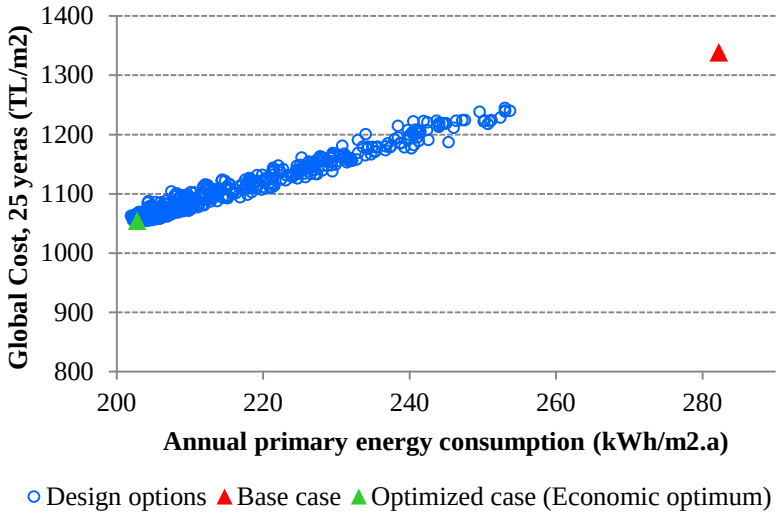

Figure 5.52 : Global cost vs primary energy cloud obtained with Antalya case.

Figure 5.53 focuses on the lower part of the cost-energy cloud where a frontier curve is represented in black dashes. Design options from optimized case (the economic optimum) within a 5% increase in global cost range towards minimum primary energy case following the frontier curve constitute a solution that can be considered as a cost-effective alternative range. Therefore, various types of solutions with reasonable low global cost, close to the lower frontier of cost-energy cloud is investigated.

The area of the curve to the right of the economic optimum represents solutions that underperform in both cost and energy.

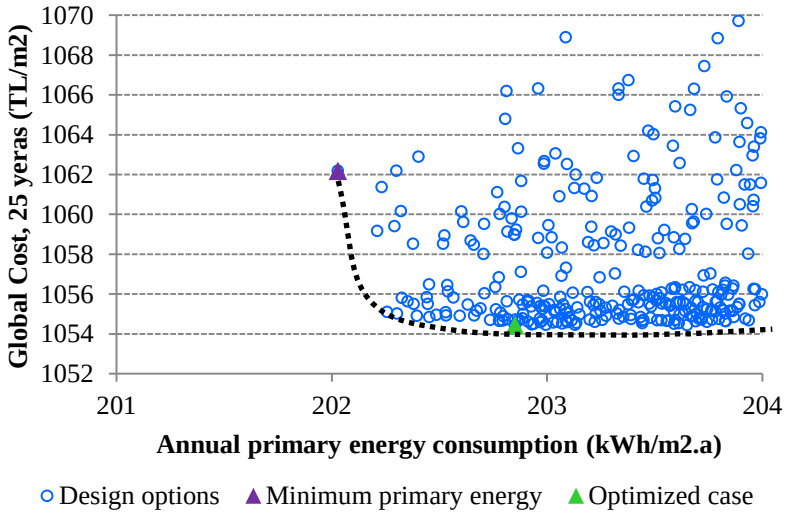

Figure 5.53 : Cost-effective alternative solutions obtained with Antalya case.

Results show that, to save 0.82 kWh/m2.a primary energy, 7.73 TL/m2 extra global cost is required for 25 years calculation period in comparison to economic optimum

point. Lower primary energy alternatives required more investment in insulation and glazing type, larger windows. Lower primary energy alternatives that have slightly higher global cost values than the economic optimum is presented in Table 5.55.

Table 5.55 : Cost-effective alternative solutions with Antalya case.

	Net Primary Energy (kWh/m2.a)	Global Cost (TL/m2)	iEW (m)	iR (m)	RT	GT	WTW South (%)	WTW West (%)	WTW North (%)	WTW East (%)	BLtyp	CLtyp	DL
1 (Min.En)	202.03	1062.18	0.03	0.035	2	24	55	55	45	35	42	33	1
2	202.21	1059.16	0.025	0.035	2	19	55	35	55	35	42	33	1
3	202.26	1055.09	0.02	0.035	2	19	45	45	55	35	42	32	1
4	202.31	1055.01	0.015	0.035	2	19	45	45	55	35	42	32	1
5	202.40	1054.91	0.02	0.03	2	19	45	45	55	35	42	32	1
6	202.45	1054.84	0.015	0.03	2	19	45	45	55	35	42	32	1
7	202.53	1054.91	0.025	0.025	2	19	45	45	55	35	42	32	1
8	202.74	1054.70	0.02	0.035	2	19	45	45	45	35	42	32	1
9	202.78	1054.66	0.03	0.03	2	19	45	45	45	35	42	32	1
10 (O.C)	202.85	1054.44	0.02	0.03	2	19	45	45	45	35	42	32	1

In the second step of the investigation, the optimization problem was extended to optimize building, HVAC system and renewable systems simultaneously.

First, the roof-mounted PV scheme described in previous section is added to building model and then, optimum PV capacity and PV type was searched simultaneously together with other design options. Table 5.56 introduces the base case and optimized case design alternatives.

Table 5.56 : Base case and optimized case design options with PV integration with Antalya case.

	iEW (m)	iR (m)	RT	GT	WTW South (%)	WTW West (%)	WTW North (%)	WTW East (%)	BLtyp	CLtyp	DL	PV Type	PV Number
B.C	0	0	1	1	25	25	25	25	16	14	0	-	-
O.C	0.015	0.03	2	19	45	35	45	35	42	32	1	1	858

As numbers indicate, all the design recommendations except external wall insulation thickness are remained same as the optimum case without PV integration. However, the optimum thickness of external wall insulation is obtained as 0.015 m that is half centimetre less than the optimized case without PV system. Moreover, w-t-w ratio of west wall is 10 % less than the optimum case without PV integration.

The Figure 5.54 below shows the objective function values calculated with each PV type during the search process. The lowest objective function value obtained with PV1 is -392 where lowest objective function value obtained with PV2 is -285 Therefore, the optimization selected PV module type 1 (polycrystalline silicone cell) over PV module type 2 (thin film cell) as ideal PV system for this case study.

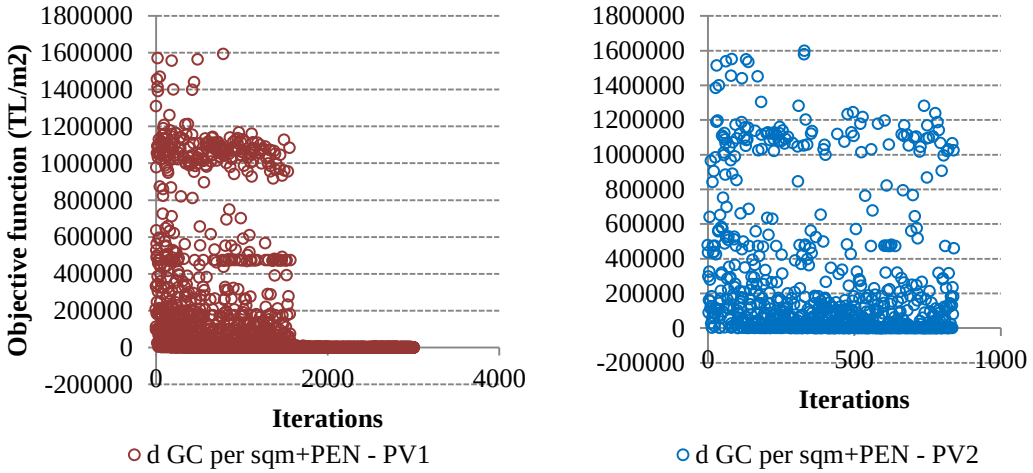

Figure 5.54 : Distribution of optimization results with each PV type obtained with Antalya case.

When the elements of the objective function are investigated it was seen that the design case with both PV types are not penalized due to PV system payback violation. PV1 has an average SPB time of 14.5 years where PV2 has 22.5 years. Therefore, the energy savings within building life span was able to pay back the ownership cost of the both PV systems in consideration. However, the annual cost benefits obtained with PV2 is less than PV1 therefore the optimization did not select it as the optimal option.

The optimum number of PV modules is calculated as 858 that is the maximum number of modules that can be installed on rooftop based on physical constraints.

The absolute GC per sqm of the optimized case with PV is calculated as 946 TL/m2 that is 606 Tl/m2 less than initial case and 311 TL/m2 less then optimized case without a PV system. A comparison of absolute GC values is illustrated in Figure 5.55.

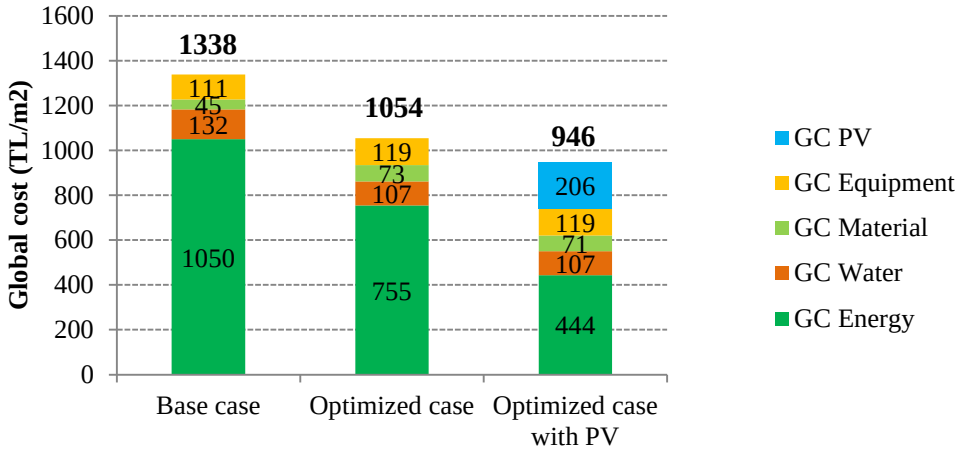

Figure 5.55 : Global cost breakdown after PV integration obtained with Antalya case.

The application of PV system has reduced the NPV energy costs by 57.7 % in comparison to initial case and by 41.2 % in comparison to optimized case without PV. The NPV ownership of equipment remained same in two optimized cases since rest of the design variables remained same. However, NPV ownership of material slightly decreased due to the 0.05m reduction in optimum external wall insulation level. The recommended PV system has a 214.5 kW installed peak-power and it is capable of annually producing 315,514 kWh electricity. 312,608 kWh of that amount directly satisfies the building electricity load that is equal to 46 % of the total building electricity need. Consequently, the building CO_2 emission rate was decreased to 30.6 kg/m2.a that is equal to a 58.7 % decrease in comparison to initial case and a 41.9 % decrease in comparison to optimized case without PV system as shown in Figure 5.56.

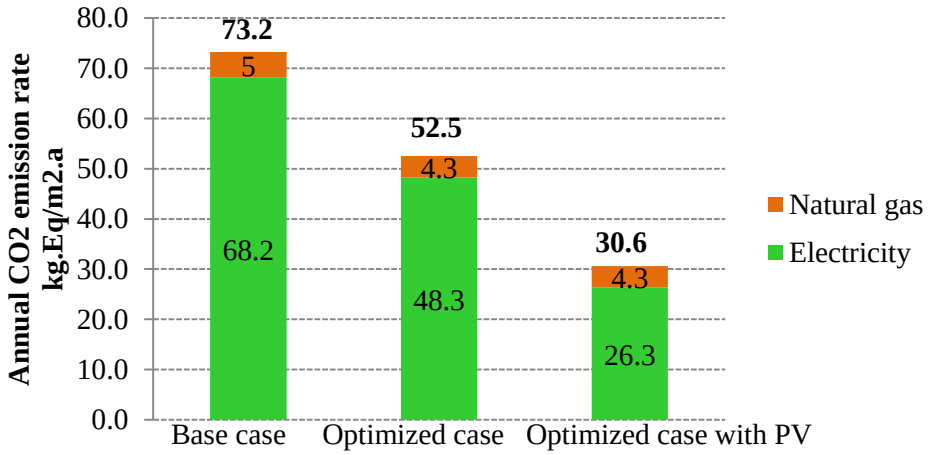

Figure 5.56 : Comparison of annual CO_2 emission rate after PV integration obtained with Antalya case.

The NPV ownership of the selected PV system is calculated as 206 TL/m2 for 25 years period. The initial investment requires 140 TL/m2 for PV modules, inverter and installation fees. The rest of the money is required for system maintenance and replacement of aging equipment. The cost equal of annual electricity saving is 11.6 TL/m2. The annual surplus electricity generated back to the grid is 2906 kWh and is equal to a 0.08 TL/m2 income. When combined with annual electricity saving the annual cost benefit obtained from the PV system is equal to 11.68 TL/m2.

The change in design variables resulted in a decrease in the average building discomfort index where initial level was reduced from 12.69 PPD to 7.54 PPD.

Lastly, the solar water heating system (SHW) described in previous section is added to the building model and the optimization is re-run for an aim to find the optimal solar collector type, and collector number. Since the so-called system is only for sanitary water heating, the system is optimized without considering the building and HVAC system interaction. The main objective function, GC consists of NPV per sqm of ownership of solar water heating system, NPV per sqm of natural gas use due to water heating by backup system and penalty value in case the investment payback period is not satisfied.

The Figure 5.57 illustrates the optimization search space. As shown in the figure, the payback period of the solar thermal systems start exceeding the target period of 25 years with all three solar collector types and large penalties occurs after installation of 70 collectors. Therefore, the maximum value of feasible design region is obtained as 60 collectors.

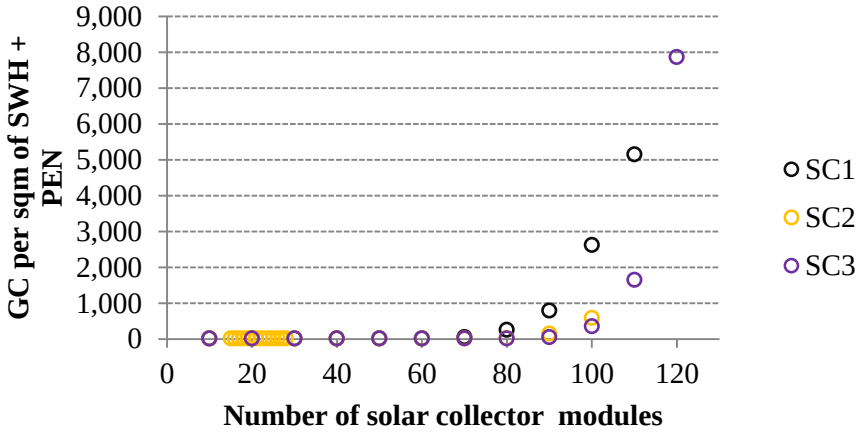

Figure 5.57 : Optimization results with each solar collector type obtained with Antalya case.

The feasible design region is then investigated in detail and a comparison of the GC performances of solar systems with all collector types is provided in Figure 5.58. According to the given numbers, the optimum collector type for this case study building is obtained as SC 2 (selective surface, moderate efficiency collector) and the optimum number of collector modules is obtained as 25.

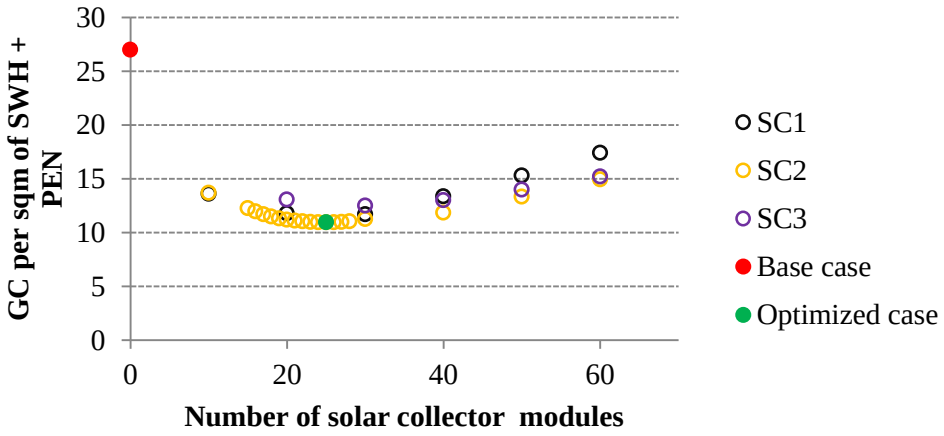

Figure 5.58 : Optimization results with each solar collector type within feasible region obtained with Antalya case.

Table 5.57 summarizes the GC performances of base case and optimized systems. As results shows the NPV of ownership of the recommended solar water heating system is about twice the conventional natural gas water heating system. However, the contribution of the solar thermal system was capable of decreasing the natural gas annual energy use from 6.3 kWh/m2 to 1.4 kWh/m2 with a corresponding global energy cost saving of 77 %. Therefore, the energy savings were able to pay back the investments cost in 4.1 years, which is less than the target value.

Table 5.57 : Global cost breakdown of conventional and solar thermal water heating system with Antalya case.

Cost type	Conventional water heater system	Solar thermal system
NPV energy	24.3	5.5
NPV system ownership	2.5	5.4
Total GC	26.8	10.9

In addition to cost saving benefits, the reduction in annual natural gas water heating requirement resulted in 1.1 kg-eq/m2 reduction in annual CO2 emissions.

The recommended SWH system is combined with rest of the recommended design options and the GC performance of different design cases are compared in Figure 5.59.

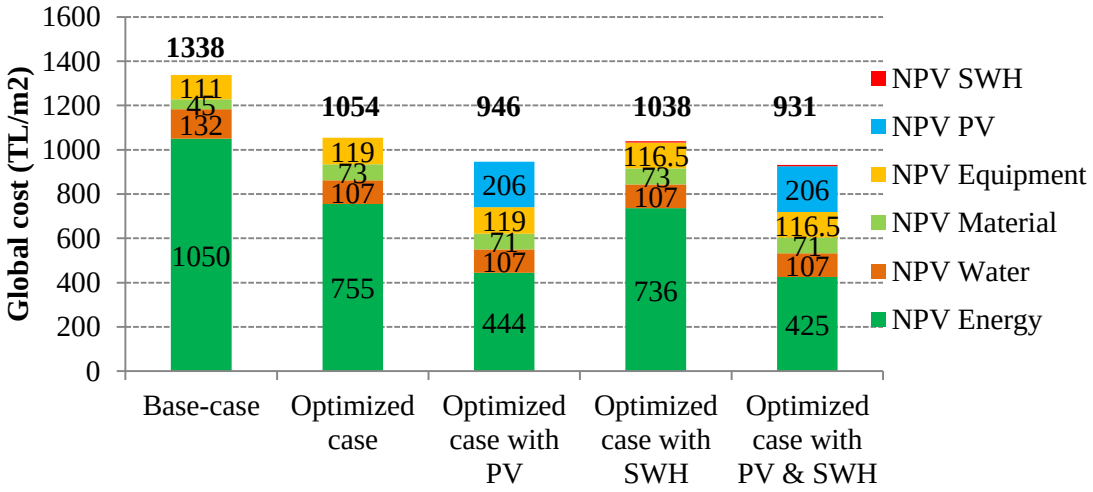

Figure 5.59 : Comparison of all design scenarios obtained with Antalya case.

If all design suggestions given by the proposed optimization method are adopted, the building overall energy consumption from non-renewables can be decreased by 57.5%, annual CO2 emission rate can be decreased by 60.3 % and the building global costs can be decreased by 30.4 % while improving the overall building comfort for the Antalya case study.

5.3.5.4 Comparison of case studies

The optimization methodology that is developed within the course of this study was applied to three case study buildings located in Istanbul, Ankara and Antalya. The cities represent three different climate regions available in Turkey. Therefore, the performance of the proposed method on recommending least-cost design options at various levels of energy savings in the different climates is investigated.

Istanbul has a mild climate where heating and cooling loads are equally dominant. Ankara however has a colder climate where heating load plays the dominant part. On the contrary, Antalya has a very warm climate therefore it is a cooling load dominant city.

First, building architectural elements and HVAC system equipment types are optimized without considering renewable system integration. The application of the

optimization methodology has resulted in different recommendations in different cities as summarized in Table 5.58.

Table 5.58 : Comparison of base case and recommended design solutions for Istanbul , Ankara and Antalya cases.

		iEW (m)	iR (m)	RT	GT	WTW South (%)	WTW West (%)	WTW North (%)	WTW East (%)	BLtyp	CLtyp	DL
Istanbul	B.C	0	0	1	1	25	25	25	25	18	13	0
	O.C	0.025	0.045	2	13	45	35	55	35	43	32	1
Ankara	B.C	0	0	1	1	25	25	25	25	23	10	0
	O.C	0.05	0.085	2	13	45	45	45	25	45	30	1
Antalya	B.C	0	0	1	1	25	25	25	25	16	13	0
	O.C	0.02	0.03	2	19	45	45	45	35	42	32	1

For instance, the external wall insulation was increased from uninsulated condition to 0.025 m, 0.005 m, 0.02 m in Istanbul, Ankara and Antalya, respectively that is in line with climate requirements.

Similarly, roof insulation was increased to 0.045 m, 0.085 m, 0.03 m in Istanbul, Ankara and Antalya, respectively.

Introduction of insulation not only improved building thermal resistance to heat losses but also introduced an improvement of the mean radiant temperature of the inner surfaces of the external opaque envelope; therefore it also contributed to the thermal comfort.

The cool roof paint (RT2) that was described in the previous sections was recommended for all three cases over roof gravel (RT1), as an economic option to deal with the building cooling load. Even in heating load dominated Ankara case, when combined with appropriate levels of roof insulation, the cool roof paint coating was found to be a cost-effective energy efficiency solution.

In Istanbul and Ankara cases same glazing element, GT13 (U: 1.6 W/m2K, SHGC: 0.56, Tvis: 0.79, Cost: 44.8 TL/m2) is found as the ideal glazing type and it replaced the initial glazing unit GT1 (U: 2.9 W/m2K, SHGC: 0.75, Tvis: 0.8, Cost: 38.9

TL/m2). GT13 has an improved U value of 1.6 W/m2K that provides required resistance to heat flow. SHGC of GT13 is 0.56, which is a moderate value however; it is lower than SHGC of the base case glazing. The moderate value prevents unwanted heat gain while still allowing the beneficial part of it in the building. Visible transmittance of GT13, 0.79, is one of the highest glazing units in the database. Therefore, it transmits most of the daylight that strikes the glazing. GT13 also has mid-range price in comparison to other windows in the library. Therefore, when the glazing unit combined with the increased w-t-w ratio and a dimming control of lights according to daylighting, it showed the best performance in two case studies.

GT19 (U: 1.3 W/m2K, SHGC: 0.44, Tvis: 0.71, Cost: 54.3 TL/m2) was obtained as the ideal glazing for the Antalya case study building and outperformed GT1. It has a U value of 1.3 W/m2K. The lower U value of GT19 yields lower peak cooling loads in summer therefore makes it a suitable glazing candidate for the Antalya climate. GT19 also has lower SHGC of 0.44 and it reduces heat gain from sun striking the glass in summer. However, visible transmittance of GT19 has high value of 0.71. Therefore, the building can still benefit from daylighting when combined with daylighting control system. Even though GT19 is more expensive than GT13, still its thermal and optical properties make it the ideal option for the Antalya case study.

In addition to lowering thermal losses, the installation of the new heat resisting windows is also a contributing factor to thermal comfort through improving mean radiant temperature.

The window-to-wall ratios for all façade orientations were mostly increased in addition to glazing improvements in all three cases. In the methodology, w-t-w ratio is generally optimized based on the interacting influence of the solar and optical properties of the glazing unit, orientation of the glazing unit, climate conditions, net present value of the glazing unit, daylighting potential and the floor area of the lit space, artificial lighting power, dimming control strategy and net present value of the wall unit that holding the glazing.

In all three cases, the w-t-w ratio of south exposed façade increased to 45 %. Combination of artificial lighting control according to daylighting with new recommended glazing units that have an improved U value, reduced SHGC and high

Tvis, allowed higher w-t-w ratios to be cost effectively realized. The glazing unit that was selected for Antalya case has a lower U-value and SHGC value than the windows selected for Istanbul and Ankara. Therefore, still 45% w-t-w ratio for south glazing in hot climate was feasible.

Considering w-t-w ratio of north facing façade, in Istanbul case 55% was found to be optimal where, in Ankara and Antalya 45 % was ideal. Large northern windows compared to base case provided better daylighting potential and when combined with improved thermal and optical performances of glazing units, heat gain and losses were balanced.

In eastern and western facades, the w-t-w ratios of Istanbul case were obtained both 35%. However, in Ankara and Antalya western facade w-t-w ratios were obtained both 45 % where eastern w-t-w ratios were 25% and 35 % respectively. The non-symmetrical L-shape of the building introduced shading effect on the eastern façade. Moreover when combined with glazing characteristics and cost value of glazing and wall, there has been variation in the optimal w-t-w ratios.

The base case boiler capacities for Istanbul, Ankara and Antalya cases were obtained as 610, 878 and 506 kW, respectively. The application of optimization methodology however reduced the heating loads and new boiler equipment was selected simultaneously from the database with the following capacities: 510 kW for Istanbul, 615 kW for Ankara and 455 kW for Antalya. The penalties calculated based on upper and lower allowable equipment capacity range are equal to zero, therefore the optimization was successful at reducing building heating loads and choosing the right size boiler equipment for each case study building while maintaining the thermal comfort. All the recommended new boilers are from the high-efficient equipment category. The reduced equipment capacities combined with higher efficiency operating characteristics (therefore reduced service life energy consumption values) were able to compensate for the initial investment costs.

The base case chiller capacities for Istanbul, Ankara and Antalya cases were obtained as 760, 599 and 760 kW, respectively. The application of optimization methodology however reduced the cooling loads and new boiler equipment was selected simultaneously from the database with the following capacities: 605 kW for Istanbul, 505 kW for Ankara and 605 kW for Antalya. The penalties calculated based on upper

and lower allowable equipment capacity range are equal to zero, therefore the optimization was successful at reducing building cooling loads and choosing the right size chiller equipment for each case study building while maintaining the thermal comfort. All the recommended new equipment are from the high-efficient equipment category. The reduced equipment capacities combined with higher efficiency operating characteristics (therefore reduced service life energy consumption values) were able to compensate for the initial investment costs.

The Table 5.59 summarizes the objective function values, which is the total global cost due to energy consumption for heating, cooling, ventilating and plugged load, water consumption for HVAC system use and hot water occupancy use, ownership of building materials and ownership of building HVAC and water heating systems for 25 year period.

Table 5.59 : Comparison of base case and optimized case global cost breakdown for Istanbul, Ankara and Antalya cases.

	Istanbul		**Ankara**		**Antalya**	
Global Cost element (TL/m2)	Base case	Optimized case	Base case	Optimized case	Base case	Optimized case
NPV Energy	1079	803	1117	831	1050	755
NPV Water	96	84	84	75	132	107
NPV Material	45	74	45	78	45	73
NPV Equipment	108	118	103	114	111	119
GC Sum	1328	1080	1349	1098	1338	1054

In all cases the energy costs constitutes the largest amount followed by water/equipment costs and finally material costs. Application of the optimization methodology resulted in a serious decrease in energy and water cost due to the investments is energy efficiency measures in materials and HVAC equipment category. In the end, total global costs were cut 18.7%, 18.6%, 21.2% for Istanbul, Ankara and Antalya cases, respectively.

Table 5.60 summarizes the influence of optimization on building primary energy performance. The numbers show that the recommended design options achieved lowering building energy consumption significantly in all cases. In Istanbul case where cooling and heating is equally dominant, design options were able to decrease both natural gas use for boiler and electric use for chiller in a balance. In Ankara case where heating load is dominant, most reduction was occurred in natural gas boiler

use while still chiller electricity use was taken into account. Similarly, in Antalya case recommended design options achieved decreasing chiller electricity use considerably without increasing boiler natural gas use.

Table 5.60 : Comparison of base case and optimized case primary energy consumption breakdown for Istanbul, Ankara and Antalya cases.

Primary Energy Consumption [kWh/m2]	**Istanbul**		**Ankara**		**Antalya**	
	Base case	Optimized Case	Base case	Optimized Case	Base case	Optimized Case
N.g Boiler	46.2	31.1	76.5	47.0	15.2	11.9
Elc. Chiller	39.6	18.4	19.8	10.0	61.8	27.9
Elc. Cooling Tower	1.4	1.0	0.5	0.3	2.3	1.5
Elc. HVAC Fans	23.2	22.8	23.3	22.8	23.8	23.0
Elc. HVAC Pumps	11.5	9.4	9.7	8.2	13.5	10.2
N.g Water Heating	7.6	7.6	9.1	9.1	6.3	6.3
Elc. Interior Lighting	81.8	47.3	81.8	47.0	81.8	44.5
Elc. Equipment	77.5	77.5	77.5	77.5	77.5	77.5
Total End Uses	288.9	215.1	298.2	222.0	282.3	202.9

The design optimization in this study also focused on finding the optimal renewable energy system sizes and photovoltaic and solar collector module types along with architectural and HVAC options.

When the base case buildings are integrated with the PV system and optimization calculations are repeated, it was seen that photovoltaic module type 1, PV1 (Poly Crystalline Silicon), was recommended as ideal option for all three cases. In Istanbul and Ankara cases, PV2 (thin film) wasn't able to satisfy 25-year pay-back criteria therefore it was eliminated from the feasible solution list through penalty function. In Antalya case, even though PV2 option satisfied the payback criteria, still the obtained cost benefits were less than PV1 thus it wasn't selected as optimal.

The ideal number of modules was obtained as 858 for all cases that is the maximum allowable module number and the consequent investment and running cost is calculated as 206 TL/m2. The installed peak-power of the recommended PV system is 214.5 kW. However, the annual electricity production obtained with each case study differs due to different climate conditions each city has. The most electricity was annually produced in Antalya case (315,514 kWh: 46 % of the total building electricity need), followed by Ankara case (256,846 kWh) and Istanbul case (235,273 kWh; 35.7 % of the total building electricity need).

Optimization of building, HVAC system and PV system together has let minor changes in building-side variables in Ankara and Antalya cases in comparison to building and HVAC optimization. In Ankara, optimal roof insulation thickness was lowered 0.005m. In Antalya, external wall insulation thickness was obtained 0.015m with PV installation which is 0.005m lower than without PV optimization case. Moreover, w-t-w of west facade was lowered 10%.

Furthermore, when the initial buildings are integrated with the solar hot water system and optimization calculations are run once more, it was seen that collector module type 2 (SC2: selective-surface, moderate efficiency) was recommended as ideal collector for all three cases. However, optimal number of solar collector modules is found as 31, 34, and 25 for Istanbul, Ankara and Antalya case studies, respectively for same hot water requirements.

Figure 5.60 illustrates a summary of the optimization results where design options of building architectural elements, HVAC systems and renewable systems are sought together. The figure shows that the simultaneous optimization of building, systems and renewables decreased global cost per sqm values by 21.7%, 23.3%, and 30.4% for Istanbul, Ankara and Antalya cases. Moreover, the figure also demonstrates that the cost-effective solutions lead to consistent energy savings where global cost for energy sharply decreased.

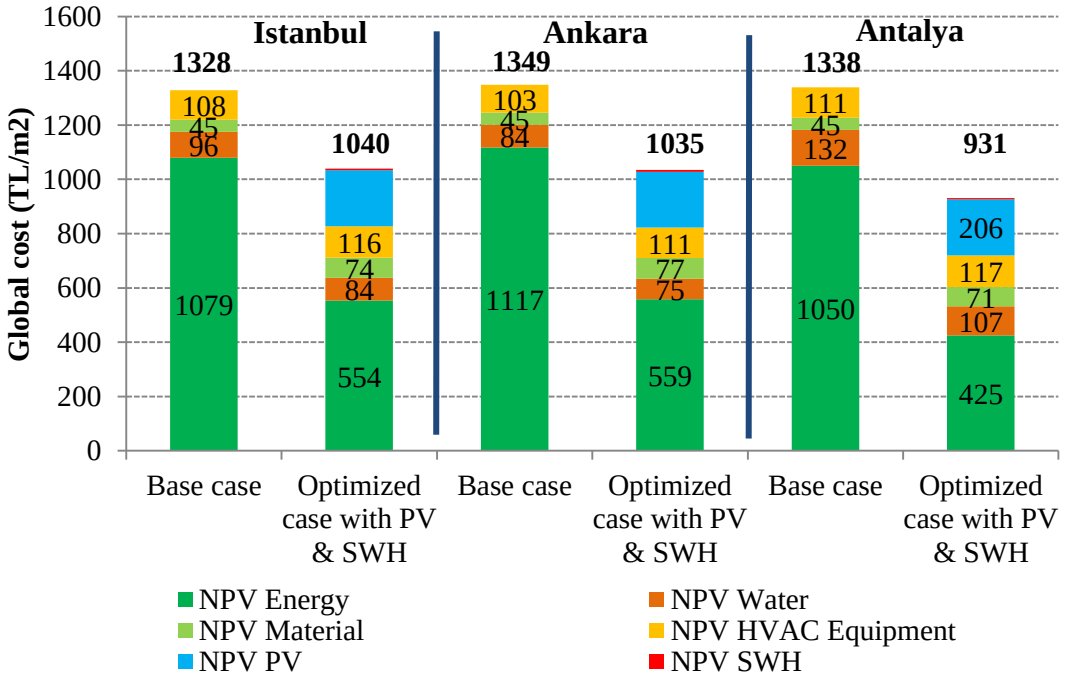

Figure 5.60 : Comparison of all design scenarios.

Table 5.61 summarizes the annual CO_2 emission breakdown obtained with base case and optimized cases. Results show that the application of the proposed methodology successfully generated building, HVAC and renewable system design configurations that can emits less CO_2 than the target level. Combination of PV and SWH systems together with more efficient HVAC and building envelope options resulted in a decrease of 49.2 %, 50.4% and 61.4% in annual kgEq CO_2 emissions for Istanbul, Ankara and Antalya cases, respectively.

Moreover, the building average discomfort indexes were improved from 10.46 to 7.56 in Istanbul case, from 12.69 to7.94 in Ankara case and from 12.5 to 7.62 in Antalya case. Therefore, optimization methodology achieved giving design recommendations that can also provide thermal comfort to the building occupants.

Table 5.61 : Comparison of annual CO_2 emission rate for base case and optimized cases for Istanbul, Ankara and Antalya.

Case	Base case	Optimized case with PV & SWH
Istanbul	74.1	37.7
Ankara	75.6	37.5
Antalya	73.2	29.5

To conclude, the comparison of the three case studies shows that the proposed optimization methodology is capable of recommending cost-effective design options that are consistent with the climate and feasible to realize under actual market conditions. Any combination of design options that does not meet target thermal comfort requirements and CO_2 emission rate is automatically eliminated from the possible optimal solutions by implemented penalty approach. Therefore, the application of the recommended design strategies achieved lowering building overall global cost, annual energy consumption and CO2 emission a great deal while improving building comfort for the all three case studies.

5.3.6 Validation of the results

The validation of the results obtained with the proposed methodology consists of two tasks: the validation of the simulation tool that acts as the calculation engine of the optimization scheme and the validation of the optimization output.

In the methodology, EnergyPlus simulation engine is used to calculate objective function value and it is a validated tool according to industry standard methods

including ANSI/ASHRAE Standard 140-2011 criteria. Therefore, the simulation results are assumed to provide required calculation accuracy.

A search space constitutes the combinations of all the possible values of design variables within their allowable ranges. In the current study, combination of design variables creates 3.19E11 design possibilities and calculating the objective value of all search points requires about 665820778 days on a high capacity computer. Since the number of cases to evaluate becomes far too large for this case study and for the most real-world problems, it becomes impossible to carry out a full enumeration search within a reasonable amount of time. Therefore, a simplified parametric approach is adopted for validation of the optimization study.

In the proposed validation approach, each variable of the optimized design case is parametrically investigated within its given range while the rest of the variables were kept fixed at their optimized values. Therefore, variables were tested individually to see if there is a better option than its recommended value that can further improve the optimized case around the optimal neighborhood.

5.3.6.1 Validation of Istanbul case study

External wall insulation thickness (iEW)

The application of the proposed optimization methodology to Istanbul case study recommended 0.025m of insulation for the external walls as the optimal thickness in combination with the rest of the design recommendations. The results of the parametric investigation in Table 5.62 demonstrate that the introduction of external wall insulation reduced the total global cost only until 0.025m, but then the GC started increasing with the increase in insulation thickness.

Table 5.62 : Parametric analysis of external wall insulation thickness based on total global cost breakdown (TL/m2) for Istanbul.

iEW	PEN All	Total GC	NPV Energy	NPV Water	NPV Material	NPV Equipment
0.010	0	1080.62	804.33	84.13	73.21	118.95
0.015	0	1080.43	803.85	84.17	73.45	118.95
0.020	0	1079.96	803.45	84.26	73.70	118.55
0.025	**0**	**1079.55**	**803.17**	**84.28**	**73.95**	**118.16**
0.030	0	1079.75	803.12	84.28	74.19	118.16
0.035	0	1080.01	803.07	84.34	74.44	118.16
0.040	0	1080.13	802.89	84.39	74.69	118.16

Moreover, the GC breakdown explains that increase in external wall insulation decreased NPV in energy and equipment cost categories however, NPV for water and material cost conversely increased. In addition, no penalty occurred within the tested insulation range.

According to the Table 5.63 below, the increase in external wall insulation levels decreased boiler energy cost because of the reduction in associated energy consumption and heating loads. On the other hand, it also slightly increased chiller and cooling tower electricity costs and the related energy use. There were also minor changes in fan and pump energy costs due to the changes in building heating and cooling needs. The rest of the energy categories remained same.

Table 5.63 : Parametric analysis of external wall insulation thickness based on NPV energy cost breakdown (TL/m2) for Istanbul.

iEW	NPV N.G. Boiler	NPV Elc. Chiller	NPV Elc. CTower	NPV Elc. HVACFan	NPV Elc. Pump	NPV N.G DWH	NPV Elc. Lights	NPV Elc. Equipment
0.010	121.65	67.75	3.626	84.60	34.14	29.30	175.47	287.80
0.015	120.63	67.93	3.625	84.59	34.51	29.30	175.47	287.80
0.020	119.81	68.09	3.626	84.59	34.77	29.30	175.47	287.80
0.025	**119.17**	**68.23**	**3.626**	**84.59**	**34.98**	**29.30**	**175.47**	**287.80**
0.030	118.73	68.41	3.630	84.58	35.19	29.30	175.47	287.80
0.035	118.43	68.52	3.630	84.58	35.34	29.30	175.47	287.80
0.040	118.03	68.61	3.630	84.58	35.47	29.30	175.47	287.80

Table 5.64 summarizes the NPV cost breakdown for water. The water costs due to cooling tower use slightly increased as the insulation thickness increased. However, water costs due to hot water use remained unchanged since associated water use is kept fixed in the calculation.

Table 5.64 : Parametric analysis of external wall insulation thickness based on NPV water cost breakdown (TL/m2) for Istanbul.

iEW	NPV CTower	NPV Hot water
0.010	34.57	49.56
0.015	34.62	49.56
0.020	34.70	49.56
0.025	**34.72**	**49.56**
0.030	34.73	49.56
0.035	34.79	49.56
0.040	34.84	49.56

Table 5.65 next shows that the decrease in NPV equipment cost is due to the decrease in Fan coil equipment ownership cost only as the required number of FCUs was reduced from 49 to 47 due to the reduction in heating loads that is the dominant load and determines the required number of FCUs. NPV ownership cost of boiler, chiller, cooling tower, water heating and lighting control remained same, as they were kept fixed in the parametric analysis.

Table 5.65 : Parametric analysis of external wall insulation thickness based on NPV equipment cost breakdown (TL/m2) for Istanbul.

iEW	NPV Boiler	NPV Chiller	NPV CTower	NPV FCU	NPV WH	NPV LC
0.010	4.41	32.71	6.66	19.33	2.47	53.37
0.015	4.41	32.71	6.66	19.33	2.47	53.37
0.020	4.41	32.71	6.66	18.94	2.47	53.37
0.025	**4.41**	**32.71**	**6.66**	**18.54**	**2.47**	**53.37**
0.030	4.41	32.71	6.66	18.54	2.47	53.37
0.035	4.41	32.71	6.66	18.54	2.47	53.37
0.040	4.41	32.71	6.66	18.54	2.47	53.37

Table 5.66 explains that the increase in NPV material cost is due to the increase in external wall insulation levels. Since the rest of the variables were kept fixed in the parametric analysis, the associated cost values remained unchanged.

Table 5.66 : Parametric analysis of external wall insulation thickness based on NPV material cost breakdown (TL/m2) for Istanbul.

iEW	NPV EW Insul.	NPV Roof Insul.	NPV Roof layer	NPV Glazing	NPV EWOther
0.010	1.80	8.59	4.64	45.17	13.01
0.015	2.05	8.59	4.64	45.17	13.01
0.020	2.29	8.59	4.64	45.17	13.01
0.025	**2.54**	**8.59**	**4.64**	**45.17**	**13.01**
0.030	2.79	8.59	4.64	45.17	13.01
0.035	3.03	8.59	4.64	45.17	13.01
0.040	3.28	8.59	4.64	45.17	13.01

To conclude, the results showed that 0.025 m of external wall insulation was able to balance heating and cooling loads, associated energy costs together with the water cost due to cooling purposes and FCU ownership costs. Therefore, the proposed optimization methodology was successful at recommending a cost-effective external wall insulation solution within the given boundaries for the Istanbul case study.

Roof insulation thickness (iR)

The application of the proposed optimization methodology to Istanbul case study recommended 0.045m of insulation for the roof element as the optimal choice, in combination with rest of the design recommendations. The results of the parametric investigation in Table 5.67 demonstrate that the introduction of roof insulation reduced the total global cost only until 0.045m but then the cost started increasing with the increase in insulation thickness. The GC breakdown explains that increase in roof insulation levels decreased NPV in energy category only however NPV for water, material and equipment increased inversely. In addition, no penalty occurred within the tested insulation range.

Table 5.67 : Parametric analysis of roof insulation thickness based on total Global Cost breakdown (TL/m2) for Istanbul.

iR	PEN All	Total GC	NPV Energy	NPV Water	NPV Material	NPV Equipment
0.030	0	1081.04	806.94	83.79	72.15	118.16
0.035	0	1080.20	805.31	83.98	72.75	118.16
0.040	0	1079.76	804.09	84.16	73.35	118.16
0.045	**0**	**1079.55**	**803.17**	**84.28**	**73.95**	**118.16**
0.050	0	1080.15	802.62	84.43	74.55	118.55
0.055	0	1080.44	802.21	84.53	75.15	118.55
0.060	0	1080.68	801.79	84.59	75.75	118.55

According to the Table 5.68, the increase in roof insulation decreased the boiler energy cost because of the reduction in associated heating load and energy consumption.

Table 5.68 : Parametric analysis of roof insulation thickness based on NPV energy cost breakdown (TL/m2) for Istanbul.

iR	NPV N.G. Boiler	NPV Elc. Chiller	NPV Elc. CTower	NPV Elc. HVACFan	NPV Elc. Pump	NPV N.G DWH	NPV Elc. Lights	NPV Elc. Equipment
0.030	124.67	66.79	3.573	84.59	34.75	29.30	175.47	287.80
0.035	122.41	67.35	3.594	84.58	34.81	29.30	175.47	287.80
0.040	120.58	67.85	3.613	84.58	34.90	29.30	175.47	287.80
0.045	**119.17**	**68.23**	**3.626**	**84.59**	**34.98**	**29.30**	**175.47**	**287.80**
0.050	118.09	68.64	3.641	84.59	35.10	29.30	175.47	287.80
0.055	117.21	69.00	3.654	84.59	35.19	29.30	175.47	287.80
0.060	116.42	69.29	3.664	84.60	35.26	29.30	175.47	287.80

On the other hand, it also slightly increased chiller and cooling tower electricity costs and related energy use due to the increase in cooling loads in summer period. There was also a minor increase in fan and pump electricity costs due to the changes in building heating and cooling needs. The rest of the energy categories remained same, as they do not interact with the insulation.

Table 5.69 summarizes the NPV cost breakdown for water. The water costs due to cooling tower use slightly increased with the increase in insulation level and resulting cooling needs. However, NPV hot water cost remained unchanged since associated water use is kept fixed in the calculation.

Table 5.69 : Parametric analysis of roof insulation thickness based on NPV water cost breakdown (TL/m2) for Istanbul.

iR	NPV CTower	NPV Hot water
0.030	34.231	49.558
0.035	34.422	49.558
0.040	34.603	49.558
0.045	**34.723**	**49.558**
0.050	34.873	49.558
0.055	34.968	49.558
0.060	35.030	49.558

Table 5.70 below shows that there is only a minor increase in NPV ownership cost of FCUs after the application of 0.045m insulation, as the required number of FCU is increased from 47 to 48. The rest of the categories remain unchanged, as they were kept fixed in the parametric analysis.

Table 5.70 : Parametric analysis of roof insulation thickness based on NPV equipment cost breakdown (TL/m2) for Istanbul.

iR	NPV Boiler	NPV Chiller	NPV CTower	NPV FCU	NPV WH	NPV LC
0.030	4.41	32.71	6.66	18.54	2.47	53.37
0.035	4.41	32.71	6.66	18.54	2.47	53.37
0.040	4.41	32.71	6.66	18.54	2.47	53.37
0.045	**4.41**	**32.71**	**6.66**	**18.54**	**2.47**	**53.37**
0.050	4.41	32.71	6.66	18.94	2.47	53.37
0.055	4.41	32.71	6.66	18.94	2.47	53.37
0.060	4.41	32.71	6.66	18.94	2.47	53.37

The increase in NPV material cost is due to the increase in roof insulation levels. Since the rest of the variables were kept fixed in the parametric analysis, the associated cost values remained unchanged as shown in Table 5.71.

Table 5.71 : Parametric analysis roof insulation thickness based on NPV material cost breakdown (TL/m2) for Istanbul.

iR	NPV EW Insul.	NPV Roof Insul.	NPV Roof layer	NPV Glazing	NPV EWOther
0.030	2.54	6.79	4.64	45.17	13.01
0.035	2.54	7.39	4.64	45.17	13.01
0.040	2.54	7.99	4.64	45.17	13.01
0.045	**2.54**	**8.59**	**4.64**	**45.17**	**13.01**
0.050	2.54	9.19	4.64	45.17	13.01
0.055	2.54	9.79	4.64	45.17	13.01
0.060	2.54	10.39	4.64	45.17	13.01

To conclude, the results showed that 0.045 m of roof insulation was able to balance heating and cooling loads, associated energy costs together with the water cost due to cooling purposes and FCU ownership costs. Therefore, the proposed optimization methodology was successful at recommending a cost-effective roof insulation solution within the given boundaries for the Istanbul case study.

Roof type (RT)

The application of the proposed optimization methodology to Istanbul case study recommended the cool roof coating (RT2) over conventional gravel layer (RT1) as the optimal choice, in combination with the rest of the design recommendations.

The results of the parametric investigation given in Table 5.72 demonstrate that switching from conventional gravel roof to cool roof coating decreased total global cost. In addition, a penalty also occurred with RT1 because the recommended chiller used in the analysis was not able to meet the building cooling load.

Table 5.72 : Parametric analysis of roof type based on total Global Cost breakdown (TL/m2) for Istanbul.

RT	PEN All	Total GC	NPV Energy	NPV Water	NPV Material	NPV Equipment
1	188.05	1088.60	811.12	87.27	70.88	119.34
2	**0**	**1079.55**	**803.17**	**84.28**	**73.95**	**118.16**

The GC breakdown table also explains that application of cool roof coating decreased NPV in energy, water and equipment categories however, NPV for material increased.

According to the Table 5.73, the cool roof coating increased the boiler natural gas cost because of the increase in associated heating load and energy consumption. On the other hand, it also significantly decreased the chiller and cooling tower electricity costs and related energy use together with electricity cost for fans and pumps. The electricity cost due to artificial lighting and plugged-in equipment remained same in both cases since they were kept fixed in the analysis.

Table 5.73 : Parametric analysis of roof type based on NPV energy cost breakdown (TL/m2) for Istanbul.

RT	NPV N.G. Boiler	NPV Elc. Chiller	NPV Elc. CTower	NPV Elc. HVACFan	NPV Elc. Pump	NPV N.G DWH	NPV Elc. Lights	NPV Elc. Equipment
1	115.78	77.44	4.016	85.00	36.32	29.30	175.47	287.80
2	119.17	68.23	3.626	84.59	34.98	29.30	175.47	287.80

Table 5.74 summarizes the NPV breakdown for water cost. The water costs due to cooling tower use decreased with cool roof coating in line with the decrease in chiller operation. However, hot water cost remains unchanged since associated water use was kept fixed in the calculation.

Table 5.74 : Parametric analysis of roof type based on NPV water cost breakdown (TL/m2) for Istanbul.

RT	NPV CTower	NPV Hot water
1	37.707	49.558
2	**34.723**	**49.558**

Table 5.75 shows that the decrease in NPV equipment cost is due to the decrease in NPV ownership of fan coil equipment cost as the required number of FCU is reduced from 50 to 47 due to the reduction in cooling loads. NPV ownership cost of boiler, chiller, cooling tower, water heating and lighting control remained same, as they were kept fixed in the parametric analysis.

Table 5.75 : Parametric analysis of roof type based on NPV equipment cost breakdown (TL/m2) for Istanbul.

RT	NPV Boiler	NPV Chiller	NPV CTower	NPV FCU	NPV WH	NPV LC
1	4.41	32.71	6.66	19.73	2.47	53.37
2	**4.41**	**32.71**	**6.66**	**18.54**	**2.47**	**53.37**

The increase in NPV ownership material cost is due to the switch from the gravel roof to cool roof coating only. Since the rest of the variables were kept fixed in the parametric analysis, the associated cost values remained unchanged as given in Table 5.76.

Table 5.76 : Parametric analysis of roof type based on NPV material cost breakdown (TL/m2) for Istanbul.

RT	NPV EW Insul.	NPV Roof Insul.	NPV Roof layer	NPV Glazing	NPV EWOther
1	2.54	8.59	1.57	45.17	13.01
2	**2.54**	**8.59**	**4.64**	**45.17**	**13.01**

To conclude, the results showed that cool roof coating (RT2) was able to balance heating and cooling related costs together with water and equipment costs for a reasonable price. Therefore, it was successfully recommended by the proposed optimization methodology as the cost-effective solution for the Istanbul case study within the given boundaries.

Glazing Type (GT)

The application of the proposed optimization methodology recommended GT13 out of 27 glazing alternatives as the optimal glazing choice for Istanbul case study, in combination with the rest of the design recommendations. Table 5.77 summarizes the total global cost breakdown. GT13 has the lowest total GC value. Moreover, it also shows the best performance in NPV energy category as well. According to the results GT1, GT5 and GT9 were penalized. When we further investigated the penalty breakdown, it was found out that all three glazing units have high U values, SHGC values and Tvis values and they were penalized because the capacity of the optimized chiller is not enough to meet the occurring building cooling load.

Table 5.77 : Parametric analysis of glazing type based on total Global Cost breakdown (TL/m2) for Istanbul.

GT	PEN All	Total GC	NPV Energy	NPV Water	NPV Material	NPV Equipment
1	1390.49	1095.23	814.42	86.93	73.35	120.52
2	0.00	1093.56	819.70	82.76	74.13	116.97
3	0.00	1140.26	863.92	82.38	77.77	116.18
4	0.00	1164.68	890.00	82.51	75.98	116.18
5	1374.53	1095.68	814.35	87.09	73.71	120.52
6	0.00	1094.22	819.66	82.81	74.79	116.97
7	0.00	1140.73	863.95	82.47	78.13	116.18
8	0.00	1165.10	889.99	82.59	76.33	116.18
9	1367.06	1096.31	814.56	87.16	74.07	120.52
10	0.00	1094.44	819.48	82.85	75.14	116.97
11	0.00	1140.87	863.75	82.44	78.49	116.18
12	0.00	1165.24	889.77	82.58	76.70	116.18
13	**0.00**	**1079.55**	**803.17**	**84.28**	**73.95**	**118.16**
14	0.00	1081.76	807.82	82.82	74.54	116.58
15	0.00	1090.03	815.75	82.47	75.63	116.18
16	0.00	1119.75	843.09	82.10	78.37	116.18
17	0.00	1163.95	887.98	82.73	77.05	116.18
18	0.00	1080.41	803.43	84.51	74.31	118.16
19	0.00	1080.33	805.87	82.97	74.91	116.58
20	0.00	1091.40	816.44	82.79	75.98	116.18
21	0.00	1124.70	846.96	82.83	78.72	116.18
22	0.00	1165.85	889.31	82.94	77.42	116.18
23	0.00	1081.17	803.60	84.75	74.67	118.16
24	0.00	1080.82	805.87	83.11	75.26	116.58
25	0.00	1091.93	816.44	82.97	76.33	116.18
26	0.00	1125.35	847.07	83.01	79.09	116.18
27	0.00	1166.51	889.39	83.16	77.77	116.18

GT13, GT14, GT19, GT23 and GT24 were selected for detailed inspection and comparisons.

According to the Table 5.78 below, GT13 demonstrated a moderate performance in terms of boiler natural gas cost, which is in correlation with energy consumption. Building with GT23 required less boiler energy costs than GT13 however; it cost more for electricity due to chiller, cooling tower, fans and pump operation. Similarly, natural gas costs obtained with GT24 was less than with GT13; however, it cost more for electricity for lighting.

Even GT13 does not show the best performance in heating and cooling related costs categories, it showed a good cost performance in terms of lighting.

Table 5.78 : Parametric analysis of glazing type based on NPV energy cost breakdown (TL/m2) for Istanbul.

GT	NPV N.G. Boiler	NPV Elc. Chiller	NPV Elc. CTower	NPV Elc. HVACFan	NPV Elc. Pump	NPV N.G DWH	NPV Elc. Lights	NPV Elc. Equipment
13	**119.17**	**68.23**	**3.626**	**84.59**	**34.98**	**29.30**	**175.47**	**287.80**
14	120.56	63.83	3.440	84.39	33.75	29.30	184.74	287.80
19	119.41	64.17	3.445	84.39	34.13	29.30	183.22	287.80
23	117.22	69.63	3.663	84.63	35.89	29.30	175.47	287.80
24	118.55	64.62	3.455	84.41	34.50	29.30	183.22	287.80

Table 5.79 summarizes the NPV cost breakdown for water. The building with GT13 showed a moderate performance in cooling tower water cost category. The hot water cost remained unchanged with all windows since associated water use is kept fixed in the calculation.

Table 5.79 : Parametric analysis of glazing type based on NPV water cost breakdown (TL/m2) for Istanbul.

GT	NPV CTower	NPV Hot water
13	**34.723**	**49.558**
14	33.264	49.558
19	33.412	49.558
23	35.191	49.558
24	33.553	49.558

Table 5.80 shows that the only NPV equipment ownership cost variation occurred in FCU category since the rest of the equipment is kept fixed in the parametric analysis. When we further investigated the number of required fan coils in detail, it was seen that 47 units were required with GT13 and GT23 and 43 units were required with GT14, GT19 and GT24.

Table 5.80 : Parametric analysis of glazing type based on NPV equipment cost breakdown (TL/m2) for Istanbul.

GT	NPV Boiler	NPV Chiller	NPV CTower	NPV FCU	NPV WH	NPV LC
13	**4.41**	**32.71**	**6.66**	**18.54**	**2.47**	**53.37**
14	4.41	32.71	6.66	16.97	2.47	53.37
19	4.41	32.71	6.66	16.97	2.47	53.37
23	4.41	32.71	6.66	18.54	2.47	53.37
24	4.41	32.71	6.66	16.97	2.47	53.37

The increase in NPV material cost category is due to the variation in glazing type variable as Table 5.81 suggests. Since the rest of the variables were kept fixed in the parametric analysis, the associated cost values remained unchanged. The NPV ownership cost of GT13 is among the lowest.

Table 5.81 : Parametric analysis of glazing type based on NPV material cost breakdown (TL/m2) for Istanbul.

GT	NPV EW Insul.	NPV Roof Insul.	NPV Roof layer	NPV Glazing	NPV EWOther
13	**2.54**	**8.59**	**4.64**	**45.17**	**13.01**
14	2.54	8.59	4.64	45.77	13.01
19	2.54	8.59	4.64	46.13	13.01
23	2.54	8.59	4.64	45.89	13.01
24	2.54	8.59	4.64	46.48	13.01

To conclude, the results showed that GT13 was able to balance building heating and cooling loads, lighting energy needs, associated energy costs and HVAC water costs for a reasonable price. Therefore, the optimization methodology was successful at recommending a cost-effective glazing solution for the Istanbul case study within the given boundaries.

Window-to-wall ratio of southern façade (WTW S)

The application of the proposed optimization methodology to Istanbul case study recommended 45 % of window-to-wall ratio for the south facing facade as the optimal solution, in combination with rest of the design recommendations.

The results of the parametric investigation in Table 5.82 demonstrated that increasing w-t-w ratio reduced the total global cost until 45% but then the cost started increasing.

Table 5.82 : Parametric analysis of southern façade window-to-wall ratio based on total Global Cost breakdown (TL/m2) for Istanbul.

WTW S	PEN All	Total GC	NPV Energy	NPV Water	NPV Material	NPV Equipment
5	0	1096.55	830.13	83.42	66.02	116.97
15	0	1087.76	819.27	83.51	68.00	116.97
25	0	1082.42	811.38	83.69	69.98	117.37
35	0	1080.39	806.37	83.90	71.97	118.16
45	**0**	**1079.55**	**803.17**	**84.28**	**73.95**	**118.16**
55	0.16	1080.45	801.36	84.61	75.93	118.55

Moreover, a penalty occurred at 55% because the cooling capacity of the recommended chiller became insufficient with the introduction of 55 % w-t-w ratio.

The GC breakdown shows that larger windows decreased only NPV energy costs where NPV costs for water, material and equipment increased.

When we further investigated the cost breakdown for the energy category given in Table 5.83, it was seen that increasing w-t-w ratio in the southern orientation decreased natural gas cost for boiler since larger windows provided more heat gain in the southern orientation and reduced heating loads in winter period. Similarly, increasing w-t-w ratio also decreased electricity cost for artificial lighting due to the enhanced daylighting potential of the building when combined with the dimming control. On the other hand, larger south facing windows increased electricity cost for chiller, cooling tower, HVAC fans, and circulation pumps due to the higher heat gains and resulting cooling load in the summer period. The cost for water heating and plugged-in equipment remained unchanged since they were kept fixed in the analysis.

Table 5.83 : Parametric analysis of southern façade window-to-wall ratio based on NPV energy cost breakdown (TL/m2) for Istanbul.

WTWS	N.G. Boiler	NPV Elc. Chiller	NPV Elc. CTower	NPV Elc. HVACFan	NPV Elc. Pump	NPV N.G DWH	NPV Elc. Lights	NPV Elc. Equipment
5	120.01	65.67	3.523	84.47	33.94	29.30	205.41	287.80
15	119.90	65.98	3.537	84.49	34.06	29.30	194.22	287.80
25	119.73	66.49	3.558	84.51	34.29	29.30	185.69	287.80
35	119.54	67.24	3.587	84.55	34.62	29.30	179.74	287.80
45	**119.17**	**68.23**	**3.626**	**84.59**	**34.98**	**29.30**	**175.47**	**287.80**
55	118.92	69.37	3.670	84.64	35.39	29.30	172.27	287.80

Table 5.84 summarizes the NPV cost breakdown for water.

Table 5.84 : Parametric analysis of southern façade window-to-wall ratio based on NPV water cost breakdown (TL/m2) for Istanbul.

WTW_S	NPV CTower	NPV Hot water
5	33.866	49.558
15	33.950	49.558
25	34.128	49.558
35	34.337	49.558
45	**34.723**	**49.558**
55	35.053	49.558

The water costs due to cooling tower use increased as w-t-w ratio increased, which is in line with the increase in cooling load and consequent chiller operation. However, hot water cost remained unchanged since associated water use was kept fixed in the analysis.

Table 5.85 shows that only the NPV ownership cost of FCUs increased with the variation in w-t-w ratio, which is in parallel with the increase in cooling load and the requirement for more FCUs. The number of the required FCUs was 44 at 5% w-t-w where it became 48 at 55%. However, the rest of the equipment cost categories remained unchanged, as they were kept fixed in the parametric analysis.

Table 5.85 : Parametric analysis of southern façade window-to-wall ratio based on NPV equipment cost breakdown (TL/m2) for Istanbul.

WTW_S	NPV Boiler	NPV Chiller	NPV CTower	NPV FCU	NPV WH	NPV LC
5	4.41	32.71	6.66	17.36	2.47	53.37
15	4.41	32.71	6.66	17.36	2.47	53.37
25	4.41	32.71	6.66	17.76	2.47	53.37
35	4.41	32.71	6.66	18.54	2.47	53.37
45	**4.41**	**32.71**	**6.66**	**18.54**	**2.47**	**53.37**
55	4.41	32.71	6.66	18.94	2.47	53.37

The increase in NPV material cost is due to the changes in wall area and glazed area as given in Table 5.86. When w-t-w ratio increased, the area of wall component that holding the glazing decreased, therefore the cost for wall insulation and the rest of the non-insulation wall materials decreased accordingly. Conversely, the cost of glazing material increased with the w-t-w ratio, as it was expected.

The roof insulation and roof coating has no interaction with the w-t-w ratio therefore the associated cost values remained unchanged.

Table 5.86 : Parametric analysis of southern façade window-to-wall ratio based on NPV material cost breakdown (TL/m2) for Istanbul.

WTW_S	NPV EW Insul.	NPV Roof Insul.	NPV Roof layer	NPV Glazing	NPV EWOther
5	2.98	8.59	4.64	34.54	15.27
15	2.87	8.59	4.64	37.20	14.70
25	2.76	8.59	4.64	39.85	14.14
35	2.65	8.59	4.64	42.51	13.57
45	**2.54**	**8.59**	**4.64**	**45.17**	**13.01**
55	2.43	8.59	4.64	47.83	12.44

To conclude, the results showed that 45% of w-t-w ratio at the southern façade was able to balance heating and cooling loads, artificial lighting and daylighting potential together with the ownership cost for FCU, wall insulation, non-insulation wall materials and glazing cost itself. Therefore, the optimization methodology was successful at recommending a cost-effective w-t-w ratio solution for the Istanbul case study within the given boundaries.

Window-to-wall ratio of western façade (WTW W)

The application of the proposed optimization methodology to Istanbul case study recommended 35 % of window-to-wall ratio for the west-facing facade as the optimal solution, in combination with the rest of the design recommendations. The results of the parametric investigation in Table 5.87 demonstrated that increasing w-t-w reduced the total global cost until 35% but then the cost started increasing. The GC breakdown explains that larger windows decreased only NPV energy costs where NPV costs for water, material and equipment increased. In addition, penalty values started occurring with the introduction of 45% of w-t-w ratio because the cooling capacity of the recommended chiller started to become insufficient to meet the resulting cooling load.

Table 5.87 : Parametric analysis of western facade window-to-wall ratio based on total Global Cost breakdown (TL/m2) for Istanbul.

WTW W	PEN All	Total GC	NPV Energy	NPV Water	NPV Material	NPV Equipment
5	0	1089.97	821.38	83.61	68.00	116.97
15	0	1083.72	812.64	83.73	69.98	117.37
25	0	1080.41	806.74	83.94	71.97	117.76
35	**0**	**1079.55**	**803.17**	**84.28**	**73.95**	**118.16**
45	4.18	1080.69	801.16	84.66	75.93	118.95
55	105.33	1081.82	799.94	85.02	77.91	118.95

When we further investigated the NPV cost breakdown for the energy category given in Table 5.88, it was seen that increasing w-t-w ratio in the western orientation slightly changed natural gas cost for boiler as a result of increased heat gain due to larger windows combined with the less heat gain from artificial lighting with dimming control.

On the other hand, larger west facing windows increased electricity cost for chiller, cooling tower, HVAC fans, and circulation pumps due to higher heat gains and

resulting cooling load in the summer period. The cost for water heating and plugged-in equipment remained unchanged since they were kept fixed in the analysis.

Similarly, increasing w-t-w ratio also decreased electricity cost for artificial lighting due to the enhanced daylighting potential of the building when combined with the dimming control.

Table 5.88 : Parametric analysis of western facade window-to-wall ratio based on NPV energy cost breakdown (TL/m2) for Istanbul.

WTWW	NPV N.G. Boiler	NPV Elc. Chiller	NPV Elc. CTower	NPV Elc. HVACFan	NPV Elc. Pump	NPV N.G DWH	NPV Elc. Lights	NPV Elc. Equipment
5	119.03	66.08	3.526	84.48	34.76	29.30	196.41	287.80
15	119.17	66.50	3.546	84.50	34.78	29.30	187.04	287.80
25	119.21	67.27	3.582	84.53	34.87	29.30	180.18	287.80
35	**119.17**	**68.23**	**3.626**	**84.59**	**34.98**	**29.30**	**175.47**	**287.80**
45	119.23	69.38	3.677	84.64	35.18	29.30	171.96	287.80
55	119.20	70.62	3.731	84.70	35.39	29.30	169.20	287.80

Table 5.89 summarizes the NPV cost breakdown for water. The water costs due to cooling tower use increased as w-t-w ratio increased, which is in line with the increase in cooling load and consequent chiller operation. However, hot water cost remained unchanged since associated water use was kept fixed in the analysis.

Table 5.89 : Parametric analysis of western facade window-to-wall ratio based on NPV water cost breakdown (TL/m2) for Istanbul.

WTW_W	NPV CTower	NPV Hot water
5	34.054	49.558
15	34.170	49.558
25	34.378	49.558
35	**34.723**	**49.558**
45	35.101	49.558
55	35.465	49.558

Table 5.90 below shows that only the NPV ownership cost of FCUs increased with the variation in w-t-w ratio, in parallel with the increase in cooling load and the requirement for more FCUs. The number of required FCUs was 44 at 5% w-t-w where it became 49 at 55%. However, the rest of the systems were kept fixed during the analysis so there were no cost variations.

Table 5.90 : Parametric analysis of western facade window-to-wall ratio based on NPV equipment cost breakdown (TL/m2) for Istanbul.

WTW_W	NPV Boiler	NPV Chiller	NPV CTower	NPV FCU	NPV WH	NPV LC
5	4.41	32.71	6.66	17.36	2.47	53.37
15	4.41	32.71	6.66	17.76	2.47	53.37
25	4.41	32.71	6.66	18.15	2.47	53.37
35	**4.41**	**32.71**	**6.66**	**18.54**	**2.47**	**53.37**
45	4.41	32.71	6.66	19.33	2.47	53.37
55	4.41	32.71	6.66	19.33	2.47	53.37

The increase in NPV material cost is due to the changes in wall area and glazing area as given in Table 5.91. When w-t-w ratio increased, the area of wall component that holding the glazing decreased accordingly, therefore the cost for wall insulation and the rest of the non-insulation wall materials decreased. Moreover, the ownership cost of glazing material increased with the w-t-w ratio as it was expected.

The roof insulation and roof coating has no interaction with the w-t-w ratio therefore the associated cost values remained unchanged.

Table 5.91 : Parametric analysis of western facade window-to-wall ratio based on NPV material cost breakdown (TL/m2) for Istanbul.

WTW_W	NPV EW Insul.	NPV Roof Insul.	NPV Roof layer	NPV Glazing	NPV EWOther
5	2.87	8.59	4.64	37.20	14.70
15	2.76	8.59	4.64	39.85	14.14
25	2.65	8.59	4.64	42.51	13.57
35	**2.54**	**8.59**	**4.64**	**45.17**	**13.01**
45	2.43	8.59	4.64	47.83	12.44
55	2.32	8.59	4.64	50.48	11.87

To conclude, the results showed that 35% of w-t-w ratio at the western façade was able to balance heating and cooling loads, artificial lighting and daylighting potential together with the ownership cost for FCU, wall insulation, non-insulation wall materials and glazing cost itself. Therefore, the optimization methodology was successful at recommending a cost-effective w-t-w ratio solution for the Istanbul case study within the given boundaries.

Window-to-wall ratio of northern façade (WTW N)

The application of the proposed optimization methodology to Istanbul case study recommended 55 % of window-to-wall ratio for the north facing facades as the optimal solution in combination with the rest of the design recommendations. The

results of the parametric investigation in Table 5.92 demonstrated that increasing w-t-w ratio reduced the total global cost with no penalties occurring. The GC breakdown explains that larger windows decreased only NPV energy costs where NPV costs for water, and material increased. The NPV equipment cost however remained same.

Table 5.92 : Parametric analysis of northern facade window-to-wall ratio based on total Global Cost breakdown (TL/m2) for Istanbul.

WTWN	PENAll	Total GC	NPV Energy	NPV Water	NPV Material	NPV Equipment
5	0	1085.12	819.03	83.89	64.04	118.16
15	0	1083.35	815.26	83.91	66.02	118.16
25	0	1081.63	811.48	83.99	68.00	118.16
35	0	1080.44	808.24	84.05	69.98	118.16
45	0	1079.74	805.44	84.17	71.97	118.16
55	**0**	**1079.55**	**803.17**	**84.28**	**73.95**	**118.16**

When we further investigated the NPV cost breakdown for the energy category given in Table 5.93, it was seen that increasing w-t-w ratio in the northern orientation increased natural gas cost for boiler a little because of thermal heat losses due to larger windows combined with the less heat gain from artificial lighting with dimming control. Since the U value of the glazing was improved, having large windows could be tolerated.

Table 5.93 : Parametric analysis of northern facade window-to-wall ratio based on NPV energy cost breakdown (TL/m2) for Istanbul.

WTWN	NPV N.G. Boiler	NPV Elc. Chiller	NPV Elc. CTower	NPV Elc. HVACFan	NPV Elc. Pump	NPV N.G DWH	NPV Elc. Lights	NPV Elc. Equipment
5	118.68	66.99	3.565	84.52	34.87	29.30	193.31	287.80
15	118.92	67.15	3.573	84.53	34.88	29.30	189.12	287.80
25	118.89	67.39	3.586	84.54	34.91	29.30	185.05	287.80
35	119.13	67.61	3.596	84.55	34.93	29.30	181.32	287.80
45	119.18	67.90	3.611	84.57	34.95	29.30	178.12	287.80
55	**119.17**	**68.23**	**3.626**	**84.59**	**34.98**	**29.30**	**175.47**	**287.80**

Moreover, larger north facing windows also increased electricity cost slightly for chiller, cooling tower, HVAC fans, and circulation pumps. The cost for water heating and plugged-in equipment remained unchanged since they were kept fixed in the analysis.

However, increasing w-t-w ratio decreased electricity cost for artificial lighting a great deal due to the enhanced daylighting potential of the building when combined with the dimming control.

Table 5.94 summarizes the NPV cost breakdown for water. The water costs due to cooling tower use increased very slightly as w-t-w ratio increased, which is in line with the increase in chiller electricity costs. However, hot water cost remained unchanged since associated water use was kept fixed in the analysis.

Table 5.94 : Parametric analysis of northern facade window-to-wall ratio based on NPV water cost breakdown (TL/m2) for Istanbul.

WTW_N	NPV CTower	NPV Hot water
5	34.332	49.558
15	34.347	49.558
25	34.428	49.558
35	34.495	49.558
45	34.613	49.558
55	**34.723**	**49.558**

Table 5.95 shows that no changes were observed in the NPV equipment ownership cost category. The changes in the building thermal loads were minor therefore there was no need to update the number of FCUs. Moreover, since the rest of the systems were kept fixed during the analysis, there were no cost variations as well.

Table 5.95 : Parametric analysis of northern facade window-to-wall ratio based on NPV equipment cost breakdown (TL/m2) for Istanbul.

WTW_N	NPV Boiler	NPV Chiller	NPV CTower	NPV FCU	NPV WH	NPV LC
5	4.41	32.71	6.66	18.54	2.47	53.37
15	4.41	32.71	6.66	18.54	2.47	53.37
25	4.41	32.71	6.66	18.54	2.47	53.37
35	4.41	32.71	6.66	18.54	2.47	53.37
45	4.41	32.71	6.66	18.54	2.47	53.37
55	**4.41**	**32.71**	**6.66**	**18.54**	**2.47**	**53.37**

The increase in NPV material cost is due to the changes in wall area and glazing area as given in Table 5.96. When w-t-w ratio increased, the area of wall component that holding the glazing decreased, therefore the cost for wall insulation and the rest of the non-insulation wall materials decreased accordingly. Moreover, the cost of glazing material increased with the w-t-w ratio as it was expected.

The roof insulation and roof coating has no interaction with the w-t-w ratio therefore the associated cost values remained unchanged.

Table 5.96 : Parametric analysis of northern facade window-to-wall ratio based on NPV material cost breakdown (TL/m2) for Istanbul.

WTW_N	NPV EW Insul.	NPV Roof Insul.	NPV Roof layer	NPV Glazing	NPV EWOther
5	3.09	8.59	4.64	31.88	15.83
15	2.98	8.59	4.64	34.54	15.27
25	2.87	8.59	4.64	37.20	14.70
35	2.76	8.59	4.64	39.85	14.14
45	2.65	8.59	4.64	42.51	13.57
55	**2.54**	**8.59**	**4.64**	**45.17**	**13.01**

To conclude, the results showed that 55% of w-t-w ratio at the northern façade was able to balance heating and cooling loads, artificial lighting and daylighting potential together with the ownership cost for FCU, wall insulation, non-insulation wall materials and glazing cost itself. Therefore, the optimization methodology was successful at recommending a cost-effective w-t-w ratio solution for the Istanbul case study within the given boundaries.

Window-to-wall ratio of eastern façade (WTW E)

The application of the proposed optimization methodology to Istanbul case study recommended 35 % of window-to-wall ratio for the east-facing facade as the optimal solution, in combination with the rest of the design recommendations. The results of the parametric investigation in Table 5.97 demonstrated that increasing w-t-w reduced the total global cost until 35% but then the cost started increasing. Moreover, no penalty values occurred within the tested w-t-w ratio range. The GC breakdown showed that larger windows decreased only e NPV energy costs where NPV costs for water, material and equipment increased.

Table 5.97 : Parametric analysis of eastern facade window-to-wall ratio based on total Global Cost breakdown (TL/m2) for Istanbul.

WTW E	PEN All	Total GC	NPV Energy	NPV Water	NPV Material	NPV Equipment
5	0	1086.62	817.68	83.56	68.00	117.37
15	0	1081.76	810.28	83.72	69.98	117.76
25	0	1079.62	805.54	83.96	71.97	118.16
35	**0**	**1079.55**	**803.17**	**84.28**	**73.95**	**118.16**
45	0	1081.15	801.71	84.56	75.93	118.95
55	0	1082.18	800.43	84.89	77.91	118.95

When we further investigated the cost breakdown for the NPV energy category given in Table 5.98, it was seen that increasing w-t-w ratio in the eastern orientation increased slightly the natural gas cost for boiler as a result of the enlarged heat loss due to larger windows and less heat gain from artificial lighting with dimming control.

On the other hand, larger east facing windows increased electricity cost for chiller, cooling tower, HVAC fans, and circulation pumps due to higher heat gains and resulting cooling load in the summer period. The cost for water heating and plugged-in equipment remained unchanged since they were kept fixed in the analysis.

Furthermore, increasing w-t-w ratio decreased a great deal electricity cost for artificial lighting due to the enhanced daylighting potential of the building when combined with the dimming control.

Table 5.98 : Parametric analysis of eastern facade window-to-wall ratio based on NPV energy cost breakdown (TL/m2) for Istanbul.

WTWE	NPV N.G. Boiler	NPV Elc. Chiller	NPV Elc. CTower	NPV Elc. HVACFan	NPV Elc. Pump	NPV N.G DWH	NPV Elc. Lights	NPV Elc. Equipment
5	119.09	66.07	3.525	84.48	34.71	29.30	192.71	287.80
15	119.14	66.53	3.548	84.50	34.75	29.30	184.71	287.80
25	119.15	67.28	3.583	84.54	34.85	29.30	179.04	287.80
35	**119.17**	**68.23**	**3.626**	**84.59**	**34.98**	**29.30**	**175.47**	**287.80**
45	119.26	69.26	3.672	84.64	35.16	29.30	172.63	287.80
55	119.33	70.20	3.714	84.70	35.28	29.30	170.10	287.80

Table 5.99 summarizes the NPV cost breakdown for water. The water costs due to cooling tower use increased slightly as the w-t-w ratio increased, which is in line with the increase in cooling load and consequent chiller operation.

Table 5.99 : Parametric analysis of eastern facade window-to-wall ratio based on NPV water cost breakdown (TL/m2) for Istanbul.

WTW_E	NPV CTower	NPV Hot water
5	34.005	49.558
15	34.166	49.558
25	34.398	49.558
35	**34.723**	**49.558**
45	35.004	49.558
55	35.335	49.558

However, hot water cost remained unchanged since associated water use was kept fixed in the analysis.

Table 5.100 shows that only the NPV ownership cost of FCUs increased with the variation in w-t-w ratio, in parallel with the increase in thermal loads and the resulting requirement for more FCUs. The number of required FCUs was 45 at 5% w-t-w where it became 49 at 55%. However, the rest of the systems were kept fixed during the analysis so there were no cost variations. The capacity of the recommended central plant equipment stayed within allowed ranges in the parametric analysis as no penalty occurred.

Table 5.100 : Parametric analysis of eastern facade window-to-wall ratio based on NPV equipment cost breakdown (TL/m2) for Istanbul.

WTW_E	NPV Boiler	NPV Chiller	NPV CTower	NPV FCU	NPV WH	NPV LC
5	4.41	32.71	6.66	17.76	2.47	53.37
15	4.41	32.71	6.66	18.15	2.47	53.37
25	4.41	32.71	6.66	18.54	2.47	53.37
35	**4.41**	**32.71**	**6.66**	**18.54**	**2.47**	**53.37**
45	4.41	32.71	6.66	19.33	2.47	53.37
55	4.41	32.71	6.66	19.33	2.47	53.37

The increase in NPV material cost is due to the changes in wall area and glazed area as given in Table 5.101. When w-t-w ratio increased, the area of wall component that holding the glazing decreased, therefore the cost for wall insulation and the rest of the non-insulation wall materials decreased accordingly. Moreover, the ownership cost of glazing material increased with the w-t-w ratio as it was expected.

The roof insulation and roof coating has no interaction with the w-t-w ratio therefore the associated cost values remained unchanged.

Table 5.101 : Parametric analysis of eastern facade window-to-wall ratio based on NPV material cost breakdown (TL/m2) for Istanbul.

WTW_E	NPV EW Insul.	NPV Roof Insul.	NPV Roof layer	NPV Glazing	NPV EWOther
5	2.87	8.59	4.64	37.20	14.70
15	2.76	8.59	4.64	39.85	14.14
25	2.65	8.59	4.64	42.51	13.57
35	**2.54**	**8.59**	**4.64**	**45.17**	**13.01**
45	2.43	8.59	4.64	47.83	12.44
55	2.32	8.59	4.64	50.48	11.87

To conclude, the results showed that 35% of w-t-w ratio at the eastern façade was able to balance heating and cooling loads, artificial lighting and daylighting potential together with the ownership cost for FCU, wall insulation, non-insulation wall materials and glazing cost itself. Therefore, the optimization methodology was successful at recommending a cost-effective w-t-w ratio solution for the Istanbul case study within the given boundaries.

Boiler type (BLtype)

The application of the proposed optimization methodology to Istanbul case study recommended Boiler 43 from the equipment database as the optimal choice in combination with rest of the design recommendations. The parametric analysis carried out with a sample of low efficiency (BL 15-17) and high efficiency (BL 42-44) boiler equipment from the database. The results of the parametric investigation in Table 5.102 demonstrate that the switching from low efficiency equipment to high efficiency equipment decreased total global costs. In addition, BL15 and BL42 were penalized because their heating capacities were not able to satisfy resulting heating loads.

The GC breakdown explains that improvement on the boiler thermal efficiency let to a considerable reduction in NPV energy category while causing a little rise on the NPV equipment costs depending on the capacity of the tested equipment. However, NPV for water and material remained unchanged, as they were not influenced with the boiler replacement.

Table 5.102 : Parametric analysis of boiler type based on total Global Cost breakdown (TL/m2) for Istanbul.

BLtyp	PEN All	Total GC	NPV Energy	NPV Water	NPV Material	NPV Equipment
15	365.90	1090.39	816.56	84.28	73.95	115.61
16	0	1092.03	818.03	84.28	73.95	115.77
17	0	1093.59	819.41	84.28	73.95	115.95
42	147.10	1078.15	802.05	84.28	73.95	117.86
43	**0**	**1079.55**	**803.17**	**84.28**	**73.95**	**118.16**
44	0	1081.42	804.44	84.28	73.95	118.75

According to the Table 5.103 improving boiler efficiency only improved boiler NPV energy cost as expected. Moreover, the increase in equipment capacity also increased the natural gas boiler costs. The rest of the energy categories assumed to be remained same as minor changes occurred in electricity cost for fans and circulation pumps.

Table 5.103 : Parametric analysis of boiler type based on NPV energy cost breakdown (TL/m2) for Istanbul.

BLtyp	NPV N.G. Boiler	NPV Elc. Chiller	NPV Elc. CTower	NPV Elc. HVACFan	NPV Elc. Pump	NPV N.G DWH	NPV Elc. Lights	NPV Elc. Equipment
15	132.56	68.23	3.626	84.59	34.98	29.30	175.47	287.80
16	134.03	68.23	3.626	84.59	34.98	29.30	175.47	287.80
17	135.42	68.23	3.626	84.59	34.98	29.30	175.47	287.80
42	118.06	68.23	3.626	84.59	34.98	29.30	175.47	287.80
43	**119.17**	**68.23**	**3.626**	**84.59**	**34.98**	**29.30**	**175.47**	**287.80**
44	120.45	68.23	3.626	84.59	34.98	29.30	175.47	287.80

Table 5.104 summarizes the NPV cost breakdown for water. Both the water costs due to cooling tower use and hot water cost remained unchanged since associated water use did not interact with the boiler replacement.

Table 5.104 : Parametric analysis of boiler type based on NPV water cost breakdown (TL/m2) for Istanbul.

BLtyp	NPV CTower	NPV Hot water
15	34.722	49.558
16	34.722	49.558
17	34.722	49.558
42	34.722	49.558
43	**34.722**	**49.558**
44	34.722	49.558

As demonstrated in Table 5.105, the only change in NPV equipment cost occurred in boiler category as expected.

Table 5.105 : Parametric analysis of boiler type based on NPV equipment cost breakdown (TL/m2) for Istanbul.

BLtyp	NPV Boiler	NPV Chiller	NPV CTower	NPV FCU	NPV WH	NPV LC
15	1.86	32.71	6.66	18.54	2.47	53.37
16	2.02	32.71	6.66	18.54	2.47	53.37
17	2.20	32.71	6.66	18.54	2.47	53.37
42	4.11	32.71	6.66	18.54	2.47	53.37
43	**4.41**	**32.71**	**6.66**	**18.54**	**2.47**	**53.37**
44	5.00	32.71	6.66	18.54	2.47	53.37

The efficiency and capacity changes increased the NPV ownership equipment costs. The more efficient equipment cost almost double of the low efficiency group. BL15 and BL42 were not able to satisfy heating loads as penalties occurred. Even BL17

and BL44 remained in the allowed equipment capacity range; they were not preferred since there was smaller size equipment that can still meet the load.

As given in Table 5.106, there were no cost changes in the NPV material category since there were no interactions between building material and boiler replacement in the parametric analysis.

Table 5.106 : Parametric analysis boiler type based on NPV material cost breakdown (TL/m2) for Istanbul.

BLtyp	NPV EW Insul.	NPV Roof Insul.	NPV Roof layer	NPV Glazing	NPV EWOther
15	2.54	8.59	4.64	45.17	13.01
16	2.54	8.59	4.64	45.17	13.01
17	2.54	8.59	4.64	45.17	13.01
42	2.54	8.59	4.64	45.17	13.01
43	**2.54**	**8.59**	**4.64**	**45.17**	**13.01**
44	2.54	8.59	4.64	45.17	13.01

To conclude, the results showed that BL43 showed an improved energy performance while being capable of meeting building heating loads for an affordable equipment price in Istanbul case study. Therefore, the proposed optimization methodology successfully recommended a cost-effective boiler solution within the given boundaries.

Chiller type (CLtype)

The application of the proposed optimization methodology to Istanbul case study recommended Chiller 32 from the equipment database as the optimal choice when combined with rest of the design recommendations. The parametric analysis carried out with a sample of moderate efficiency (CL 9-11) and high efficiency (CL 31-33) chiller equipment. The results of the parametric investigation in Table 5.107 demonstrate that the switching from moderate efficiency equipment to high efficiency equipment decreased total global costs. However, only CL11, CL32 and CL33 were able to comply with constraints and not penalized.

The GC breakdown explains that improvement on the chiller efficiency let to a considerable reduction in NPV energy category while causing a little rise on NPV equipment costs depending on the capacity of the tested equipment. However, NPV cost for water and material were not influenced with the chiller replacement.

Table 5.107 : Parametric analysis of chiller type based on total Global Cost breakdown (TL/m2) for Istanbul.

CLtyp	PEN All	Total GC	NPV Energy	NPV Water	NPV Material	NPV Equipment
9	3311.18	1101.85	832.17	85.00	73.95	110.73
10	0.29	1104.55	831.93	85.73	73.95	112.94
11	0	1109.08	833.56	86.51	73.95	115.06
31	814.70	1078.78	804.15	83.81	73.95	116.87
32	**0**	**1079.55**	**803.17**	**84.28**	**73.95**	**118.16**
33	0	1083.05	803.46	85.02	73.95	120.62

According to the Table 5.108 improving chiller efficiency improved chiller NPV energy cost together with cooling tower electricity costs as expected.

Moreover, the chiller electricity cost increased in parallel with the increase in the equipment capacity. In addition, minor changes occurred in electricity cost for fans and circulation pumps. The rest of the energy cost categories remained uninfluenced, as they did not interact with the chiller.

Table 5.108 : Parametric analysis of chiller type based on NPV energy cost breakdown (TL/m2) for Istanbul.

CLtyp	NPV N.G. Boiler	NPV Elc. Chiller	NPV Elc. CTower	NPV Elc. HVACFan	NPV Elc. Pump	NPV N.G DWH	NPV Elc. Lights	NPV Elc. Equipment
9	119.17	98.723	3.812	84.591	33.302	29.30	175.47	287.80
10	119.17	96.314	3.812	84.586	35.477	29.30	175.47	287.80
11	119.17	95.863	3.808	84.586	37.563	29.30	175.47	287.80
31	119.17	70.453	3.637	84.586	33.729	29.30	175.47	287.80
32	**119.17**	**68.232**	**3.626**	**84.586**	**34.984**	**29.30**	**175.47**	**287.80**
33	119.17	66.433	3.608	84.586	37.089	29.30	175.47	287.80

Table 5.109 summarizes the NPV cost breakdown for water.

Table 5.109 : Parametric analysis of chiller type based on NPV water cost breakdown (TL/m2) for Istanbul.

CLtyp	NPV CTower	NPV Hot water
9	35.439	49.558
10	36.169	49.558
11	36.953	49.558
31	34.255	49.558
32	**34.723**	**49.558**
33	35.466	49.558

Water costs due to cooling tower use was slightly improved with higher efficiency chiller equipment depending on equipment capacity where and hot water cost remained same.

As demonstrated in Table 5.110, the only major change in equipment cost occurred in chiller category as expected. The efficiency and capacity improvements increased equipment costs. CL9, CL10 and CL32 were not able to satisfy cooling loads as penalties occurred. However, even CL11 and CL33 remained in the allowed equipment capacity range; they were not preferred since there was smaller size equipment that can still meet the resulting cooling load.

Table 5.110 : Parametric analysis of chiller type based on NPV equipment cost breakdown (TL/m2) for Istanbul.

CLtyp	NPV Boiler	NPV Chiller	NPV CTower	NPV FCU	NPV WH	NPV LC
9	4.41	25.74	6.20	18.54	2.47	53.37
10	4.41	27.41	6.75	18.54	2.47	53.37
11	4.41	29.00	7.27	18.54	2.47	53.37
31	4.41	31.74	6.35	18.54	2.47	53.37
32	**4.41**	**32.71**	**6.66**	**18.54**	**2.47**	**53.37**
33	4.41	34.63	7.20	18.54	2.47	53.37

As shown in Table 5.111, there were no cost changes in the NPV material category since there were no interactions between building material and chiller equipment in the parametric analysis.

Table 5.111 : Parametric analysis chiller type based on NPV material cost breakdown (TL/m2) for Istanbul.

CLtyp	NPV EW Insul.	NPV Roof Insul.	NPV Roof layer	NPV Glazing	NPV EWOther
9	2.54	8.59	4.64	45.17	13.01
10	2.54	8.59	4.64	45.17	13.01
11	2.54	8.59	4.64	45.17	13.01
31	2.54	8.59	4.64	45.17	13.01
32	**2.54**	**8.59**	**4.64**	**45.17**	**13.01**
33	2.54	8.59	4.64	45.17	13.01

To conclude, the results showed that CL32 showed an improved energy performance while being capable of meeting building cooling loads for an affordable equipment price in Istanbul case study. Therefore, the proposed optimization methodology successfully recommended a cost-effective chiller solution within the given boundaries.

Lighting control (LC)

The application of the proposed optimization methodology to Istanbul case study recommended dimming control of artificial lights (option 1) according to indoor daylighting levels as the optimal choice over manual lighting control (option 0), when combined with rest of the design recommendations. The results of the parametric investigation in Table 5.112 demonstrate that dimming control of lights resulted in a major GC reduction. Moreover, the cost breakdown explains that dimming control reduces not only NPV energy costs but also NPV water cost as well. NPV for material were not influenced however, NPV for equipment was increased.

In addition, the case with manual light control was penalized because the recommended chiller could not satisfy resulting cooling load in this combination.

Table 5.112 : Parametric analysis of lighting control strategies based on total Global Cost breakdown (TL/m2) for Istanbul.

LC	PEN All	Total GC	NPV Energy	NPV Water	NPV Material	NPV Equipment
0	1643.44	1212.28	946.22	88.67	73.95	103.44
1	**0**	**1079.55**	**803.17**	**84.28**	**73.95**	**118.16**

According to the Table 5.113, dimming control of lights over daylighting increased boiler natural gas cost to some extent due to the reduction in heat gain from lighting system. However, it decreased electricity cost for chiller, cooling tower, fans, and pumps a great deal in addition to the decrease in lighting electricity cost. The rest of the energy cost categories remained uninfluenced, as they did not interact with the lighting system.

Table 5.113 : Parametric analysis of lighting control strategies based on NPV energy cost breakdown (TL/m2) for Istanbul.

LC	NPV N.G. Boiler	NPV Elc. Chiller	NPV Elc. CTower	NPV Elc. HVACFan	NPV Elc. Pump	NPV N.G WH	NPV Elc. Lights	NPV Elc. Equipment
0	116.33	81.66	4.127	85.22	38.13	29.30	303.65	287.80
1	**119.17**	**68.23**	**3.626**	**84.59**	**34.98**	**29.30**	**175.47**	**287.80**

Table 5.114 summarizes the NPV cost breakdown for water. Water costs due to cooling tower use were significantly improved with dimming control where hot water cost remained same.

Table 5.114 : Parametric analysis of lighting control strategies based on NPV water cost breakdown (TL/m2) for Istanbul.

LC	NPV CTower	NPV Hot water
0	39.112	49.558
1	**34.723**	**49.558**

As demonstrated in Table 5.115, the major change in NPV equipment ownership cost occurred in lighting control category as installing dimming control costs more than manual control system. In addition, the cost for FCUs decreased with dimming control due to the decrease in heat gain from lighting system, the decrease in resulting cooling load and the required number of FCUs from 52 to 47.

Table 5.115 : Parametric analysis of lighting control strategies based on NPV equipment cost breakdown (TL/m2) for Istanbul.

LC	NPV Boiler	NPV Chiller	NPV CTower	NPV FCU	NPV WH	NPV LC
0	4.41	32.71	6.66	20.52	2.47	36.68
1	**4.41**	**32.71**	**6.66**	**18.54**	**2.47**	**53.37**

As shown in Table 5.116, there were no cost changes in the NPV material category since there were no interactions between building material and the lighting system.

Table 5.116 : Parametric analysis of lighting control strategies based on NPV material cost breakdown (TL/m2) for Istanbul.

LC	NPV EW Insul.	NPV Roof Insul.	NPV Roof layer	NPV Glazing	NPV EWOther
0	2.54	8.59	4.64	45.17	13.01
1	**2.54**	**8.59**	**4.64**	**45.17**	**13.01**

To conclude, the results showed that dimming control of artificial lights according to daylighting levels decreased the electricity cost for lighting together with electricity cost for cooling system for an affordable price. The slight increase in NPV energy cost for heating was compensated with other benefits. Therefore, the proposed optimization methodology successfully recommended a cost-effective lighting control solution within the given boundaries.

5.3.6.2 Validation of Ankara case study

External wall insulation thickness (iEW)

The application of the proposed optimization methodology to Ankara case study recommended 0.05m of insulation for the external walls as the optimal choice, in combination with the rest of the design recommendations.

The results of the parametric investigation in Table 5.117 demonstrate that the introduction of external wall insulation had a trend for reducing the total global cost only until 0.05m, but then the cost started increasing continuously. Moreover, the GC breakdown explains that increase in external wall insulation decreased NPV in energy cost category only. However, NPV cost for water and material conversely increased. The NPV cost for equipment did not vary within the tested range of insulation variable.

In addition, the penalties occurred at 0.035m and 0.04m insulation thicknesses are due to under capacity boiler equipment.

Table 5.117 : Parametric analysis of external wall insulation thickness based on total global cost breakdown (TL/m2) for Ankara.

iEW	PEN All	Total GC	NPV Energy	NPV Water	NPV Material	NPV Equipment
0.035	13.06	1097.84	831.83	74.88	77.28	113.84
0.040	2.00	1097.71	831.42	74.90	77.54	113.84
0.045	0	1097.89	831.26	74.98	77.79	113.84
0.050	**0**	**1097.87**	**831.00**	**74.98**	**78.05**	**113.84**
0.055	0	1097.96	830.76	75.04	78.31	113.84
0.060	0	1098.12	830.64	75.07	78.57	113.84
0.065	0	1098.17	830.43	75.07	78.82	113.84

According to the Table 5.118 below, the increase in external wall insulation levels decreased boiler natural gas cost because of the reduction in associated energy consumption and heating loads.

On the other hand, it also slightly increased chiller and cooling tower electricity costs and the related energy use. There were also minor changes in fan and pump energy costs due to the changes in building heating and cooling needs. The rest of the energy categories remained same.

Table 5.118 : Parametric analysis of external wall insulation thickness based on NPV energy cost breakdown (TL/m2) for Ankara.

iEW	NPV N.G. Boiler	NPV Elc. Chiller	NPV Elc. CTower	NPV Elc. HVACFan	NPV Elc. Pump	NPV N.G WH	NPV Elc. Lights	NPV Elc. Equipment
0.035	181.96	36.80	1.206	84.697	30.13	34.78	174.46	287.80
0.040	181.29	36.95	1.207	84.697	30.25	34.78	174.46	287.80
0.045	180.89	37.08	1.209	84.699	30.35	34.78	174.46	287.80
0.050	**180.41**	**37.19**	**1.210**	84.698	**30.45**	**34.78**	**174.46**	**287.80**
0.055	180.00	37.29	1.211	84.698	30.53	34.78	174.46	287.80
0.060	179.72	37.38	1.212	84.699	30.59	34.78	174.46	287.80
0.065	179.36	37.46	1.213	84.700	30.65	34.78	174.46	287.80

Table 5.119 summarizes the NPV breakdown for water cost. The water costs due to cooling tower use slightly increased as the insulation thickness increased.

Table 5.119 : Parametric analysis of external wall insulation thickness based on NPV water cost breakdown (TL/m2) for Ankara.

iEW	NPV CTower	NPV Hot water
0.035	25.321	49.558
0.040	25.346	49.558
0.045	25.427	49.558
0.050	**25.426**	**49.558**
0.055	25.484	49.558
0.060	25.514	49.558
0.065	25.516	49.558

Table 5.120 below shows that the variation in external wall insulation levels did not cause any cost changes at NPV equipment category within the tested insulation range.

Table 5.120 : Parametric analysis of external wall insulation thickness based on NPV equipment cost breakdown (TL/m2) for Ankara.

iEW	NPV Boiler	NPV Chiller	NPV CTower	NPV FCU	NPV WH	NPV LC
0.035	5.30	29.64	5.71	17.36	2.47	53.37
0.040	5.30	29.64	5.71	17.36	2.47	53.37
0.045	5.30	29.64	5.71	17.36	2.47	53.37
0.050	**5.30**	**29.64**	**5.71**	**17.36**	**2.47**	**53.37**
0.055	5.30	29.64	5.71	17.36	2.47	53.37
0.060	5.30	29.64	5.71	17.36	2.47	53.37
0.065	5.30	29.64	5.71	17.36	2.47	53.37

The ownership cost of boiler, chiller, cooling tower, water heating and lighting control were kept fixed in the parametric analysis however, FCUs were allowed to adjust to the building heating and cooling load needs. Results indicate that load changes did not require any FCU update.

As shown in Table 5.121, the increase in NPV material cost is due to the increase in external wall insulation levels. Since the rest of the variables were kept fixed in the parametric analysis, the associated cost values remained unchanged.

Table 5.121 : Parametric analysis of external wall insulation thickness based on NPV material cost breakdown (TL/m2) for Ankara.

iEW	NPV EW Insul.	NPV Roof Insul.	NPV Roof layer	NPV Glazing	NPV EWOther
0.035	3.17	13.39	4.64	42.51	13.57
0.040	3.42	13.39	4.64	42.51	13.57
0.045	3.68	13.39	4.64	42.51	13.57
0.050	**3.94**	**13.39**	**4.64**	**42.51**	**13.57**
0.055	4.19	13.39	4.64	42.51	13.57
0.060	4.45	13.39	4.64	42.51	13.57
0.065	4.71	13.39	4.64	42.51	13.57

To conclude, the results showed that 0.05 m of external wall insulation was able to balance heating and cooling loads, associated NPV energy costs together with the water cost due to cooling purposes. Therefore, the proposed optimization methodology was successful at recommending a cost-effective external wall insulation solution within the given boundaries for the Ankara case study.

Roof insulation thickness (iR)

The application of the proposed optimization methodology to Ankara case study recommended 0.085m of insulation for the roof element as the optimal choice, when combined with rest of the design recommendations. The results of the parametric investigation given in Table 5.122 demonstrate that the introduction of roof insulation reduced the total global cost only until 0.085m but then the cost started increasing. The GC breakdown explains that increase in roof insulation levels decreased NPV in energy category only however NPV for water, material and equipment increased inversely within the tested insulation range.

In addition, penalties occurred until 0.85 m of insulation due to the under capacity boiler equipment. Without enough insulation, the boiler used in the analysis was not

able to satisfy building heating load. Therefore, less insulation required a higher capacity boiler, which was not preferred in the optimization.

Table 5.122 : Parametric analysis of roof insulation thickness based on total Global Cost breakdown (TL/m2) for Ankara.

iR	PEN All	Total GC	NPV Energy	NPV Water	NPV Material	NPV Equipment
0.065	63.09	1098.28	834.24	74.54	75.65	113.84
0.070	26.28	1097.99	833.20	74.70	76.25	113.84
0.075	6.14	1097.90	832.43	74.78	76.85	113.84
0.080	0.01	1097.92	831.69	74.93	77.45	113.84
0.085	**0**	**1097.87**	**831.00**	**74.98**	**78.05**	**113.84**
0.090	0	1098.06	830.46	75.10	78.65	113.84
0.095	0	1098.26	830.00	75.16	79.25	113.84

According to the Table 5.123, the increase in roof insulation decreased the boiler natural gas cost because of the reduction in associated heating load and energy consumption.

On the other hand, insulation also slightly increased chiller and cooling tower electricity costs and related energy use due to the increase in cooling loads in summer period. There was also a minor increase in fan and pump electricity costs due to the changes in building heating and cooling needs. The rest of the energy categories remained same, as they do not interact with the insulation.

Table 5.123 : Parametric analysis of roof insulation thickness based on NPV energy cost breakdown (TL/m2) for Ankara.

iR	NPV N.G. Boiler	NPV Elc. Chiller	NPV Elc. CTower	NPV Elc. HVACFan	NPV Elc. Pump	NPV N.G WH	NPV Elc. Lights	NPV Elc. Equipment
0.065	184.94	36.15	1.177	84.69	30.23	34.78	174.46	287.80
0.070	183.52	36.47	1.188	84.69	30.29	34.78	174.46	287.80
0.075	182.43	36.72	1.195	84.69	30.35	34.78	174.46	287.80
0.080	181.40	36.96	1.203	84.70	30.40	34.78	174.46	287.80
0.085	**180.41**	**37.19**	**1.210**	**84.70**	**30.45**	**34.78**	**174.46**	**287.80**
0.090	179.61	37.40	1.216	84.70	30.50	34.78	174.46	287.80
0.095	178.88	37.61	1.222	84.70	30.55	34.78	174.46	287.80

Table 5.124 summarizes the NPV breakdown for water cost. The water costs due to cooling tower use slightly increased with the increase in insulation level and resulting cooling needs. However, hot water cost remains unchanged since associated water use is kept fixed in the calculation.

Table 5.124 : Parametric analysis of roof insulation thickness based on NPV water cost breakdown (TL/m2) for Ankara.

iR	NPV CTower	NPV Hot water
0.065	24.986	49.558
0.070	25.137	49.558
0.075	25.218	49.558
0.080	25.376	49.558
0.085	**25.426**	**49.558**
0.090	25.539	49.558
0.095	25.601	49.558

Table 5.125 shows that the variation in roof insulation levels did not cause any cost changes at NPV equipment ownership category within the tested insulation range. Cost of boiler, chiller, cooling tower, water heating and lighting control were kept fixed in the parametric analysis however, FCUs were allowed to adjust to the building heating and cooling load needs. Results indicate that load changes did not require any FCU update.

Table 5.125 : Parametric analysis of roof insulation thickness based on NPV equipment cost breakdown (TL/m2) for Ankara.

iR	NPV Boiler	NPV Chiller	NPV CTower	NPV FCU	NPV WH	NPV LC
0.065	5.30	29.64	5.71	17.36	2.47	53.37
0.070	5.30	29.64	5.71	17.36	2.47	53.37
0.075	5.30	29.64	5.71	17.36	2.47	53.37
0.080	5.30	29.64	5.71	17.36	2.47	53.37
0.085	**5.30**	**29.64**	**5.71**	**17.36**	**2.47**	**53.37**
0.090	5.30	29.64	5.71	17.36	2.47	53.37
0.095	5.30	29.64	5.71	17.36	2.47	53.37

As shown in Table 5.126, the increase in NPV material cost is due to the increase in roof insulation levels.

Table 5.126 : Parametric analysis roof insulation thickness based on NPV material cost breakdown (TL/m2) for Ankara.

iR	NPV EW Insul.	NPV Roof Insul.	NPV Roof layer	NPV Glazing	NPV EWOther
0.065	3.94	10.99	4.64	42.51	13.57
0.070	3.94	11.59	4.64	42.51	13.57
0.075	3.94	12.19	4.64	42.51	13.57
0.080	3.94	12.79	4.64	42.51	13.57
0.085	**3.94**	**13.39**	**4.64**	**42.51**	**13.57**
0.090	3.94	13.99	4.64	42.51	13.57
0.095	3.94	14.59	4.64	42.51	13.57

Since the rest of the variables were kept fixed in the parametric analysis, the associated cost values remained unchanged.

To conclude, the results showed that 0.085 m of roof insulation was able to balance heating and cooling loads, associated energy costs together with the water cost due to cooling purposes. Therefore, the proposed optimization methodology was successful at recommending a cost-effective roof insulation solution within the given boundaries for the Ankara case study.

Roof type (RT)

The application of the proposed optimization methodology to Ankara case study recommended the cool roof coating (RT2) over conventional gravel layer (RT1) as the optimal choice in combination with the rest of the design recommendations.

The results of the parametric investigation given in Table 5.127 demonstrate that switching from conventional gravel roof to cool roof coating decreased total global cost. In addition, a penalty also occurred with RT1 because the recommended chiller used in the analysis was not able to meet the building cooling loads.

The GC breakdown table also explains that application of cool roof coating decreased NPV in energy, water and equipment categories however, NPV for material increased.

Table 5.127 : Parametric analysis of roof type based on total Global Cost breakdown (TL/m2) for Ankara.

RT	PEN All	Total GC	NPV Energy	NPV Water	NPV Material	NPV Equipment
1	14.32	1101.74	834.18	77.55	74.98	115.03
2	**0**	**1097.87**	**831.00**	**74.98**	**78.05**	**113.84**

According to the Table 5.128, the cool roof coating increased the boiler natural gas cost because of the increase in associated heating load and energy consumption.

Table 5.128 : Parametric analysis of roof type based on NPV energy cost breakdown (TL/m2) for Ankara.

RT	NPV N.G. Boiler	NPV Elc. Chiller	NPV Elc. CTower	NPV Elc. HVACFan	NPV Elc. Pump	NPV N.G WH	NPV Elc. Lights	NPV Elc. Equipment
1	175.74	43.21	1.442	85.03	31.72	34.78	174.46	287.80
2	**180.41**	**37.19**	**1.210**	**84.70**	**30.45**	**34.78**	**174.46**	**287.80**

On the other hand, it also significantly decreased the chiller and cooling tower electricity costs and related energy use together with electricity cost for fans and pumps. The electricity cost due to artificial lighting and plugged-in equipment remained same in both cases since they were kept fixed in the analysis.

Table 5.129 summarizes the NPV cost breakdown for water. The water costs due to cooling tower use decreased with cool roof coating in line with the decrease in chiller operation. However, hot water cost remains unchanged since associated water use was kept fixed in the calculation.

Table 5.129 : Parametric analysis of roof type based on NPV water cost breakdown (TL/m2) for Ankara.

RT	NPV CTower	NPV Hot water
1	27.996	49.558
2	**25.426**	**49.558**

Table 5.130 shows that the decrease in NPV equipment ownership cost is due to the decrease in fan coil equipment cost as the required number of FCU is reduced from 47 to 44 due to the reduction in cooling loads. Cost of boiler, chiller, cooling tower, water heating and lighting control remained same, as they were kept fixed in the parametric analysis.

Table 5.130 : Parametric analysis of roof type based on NPV equipment cost breakdown (TL/m2) for Ankara.

RT	NPV Boiler	NPV Chiller	NPV CTower	NPV FCU	NPV WH	NPV LC
1	5.30	29.64	5.71	18.54	2.47	53.37
2	**5.30**	**29.64**	**5.71**	**17.36**	**2.47**	**53.37**

As shown in Table 5.131, the increase in NPV material cost is due to the switch from the gravel roof to cool roof coating only. Since the rest of the variables were kept fixed in the parametric analysis, the associated cost values remained unchanged.

Table 5.131 : Parametric analysis of roof type based on NPV material cost breakdown (TL/m2) for Ankara.

RT	NPV EW Insul.	NPV Roof Insul.	NPV Roof layer	NPV Glazing	NPV EWOther
1	3.94	13.39	1.57	42.51	13.57
2	**3.94**	**13.39**	**4.64**	**42.51**	**13.57**

To conclude, the results showed that cool roof coating (RT2) was able to balance heating and cooling related costs together with water and equipment costs for a reasonable price. Therefore, it was successfully recommended by the proposed optimization methodology as the cost-effective solution for the Ankara case study within the given boundaries.

Glazing Type (GT)

The application of the proposed optimization methodology recommended GT13 out of 27 glazing alternatives as the optimal glazing choice for Ankara case study, in combination with the rest of the design recommendations. Table 5.132 summarizes the total global cost breakdown. GT13 has the lowest total GC value. Moreover, it also shows the best performance in energy category after GT23 and GT18.

Table 5.132 : Parametric analysis of glazing type based on total Global Cost breakdown (TL/m2) for Ankara.

GT	PEN All	Total GC	NPV Energy	NPV Water	NPV Material	NPV Equipment
1	2188.29	1113.03	841.38	77.55	77.49	116.61
2	390.54	1115.78	850.60	73.12	78.22	113.84
3	390.54	1162.45	895.06	72.69	81.65	113.05
4	390.54	1187.57	921.41	72.74	79.97	113.45
5	2039.98	1113.25	841.09	77.72	77.83	116.61
6	328.20	1116.17	850.33	73.15	78.84	113.84
7	328.20	1162.50	894.73	72.73	81.98	113.05
8	328.20	1187.66	921.08	72.83	80.30	113.45
9	1949.95	1113.65	841.06	77.82	78.17	116.61
10	270.34	1116.22	850.00	73.21	79.18	113.84
11	270.34	1162.60	894.40	72.82	82.33	113.05
12	270.34	1187.68	920.73	72.87	80.64	113.45
13	**0**	**1097.87**	**831.00**	**74.98**	**78.05**	**113.84**
14	0	1102.38	836.86	73.46	78.61	113.45
15	0	1110.76	844.99	73.08	79.63	113.05
16	0	1140.68	872.74	72.67	82.21	113.05
17	0	1184.44	917.19	73.23	80.98	113.05
18	0	1098.27	830.65	75.38	78.39	113.84
19	0	1100.35	834.34	73.61	78.96	113.45
20	0	1111.61	845.10	73.49	79.97	113.05
21	0	1144.65	875.54	73.51	82.55	113.05
22	0	1185.98	918.07	73.54	81.32	113.05
23	0	1098.70	830.46	75.67	78.73	113.84
24	0	1100.45	833.86	73.85	79.29	113.45
25	0	1111.61	844.51	73.75	80.30	113.05
26	0	1144.68	875.05	73.68	82.89	113.05
27	0	1186.08	917.56	73.81	81.65	113.05

In addition to the cost performance, the results also show that the windows between GT1 –GT12 were penalized. When we further investigated the penalty conditions, it was found out that all the penalized glazing units have high U-values varying between 2.9 and 2.6 W/m2K and the penalties occurred due to under boiler capacity where optimized boiler used in the analysis was not enough to meet the occurring building heating load. Moreover, GT1, GT5 and GT18 that have a SHGC of 0.75 were also penalized second time because the capacity of the optimized chiller used in the analysis was not enough to meet the occurring building cooling load.

GT13, GT18, GT19, GT23 and GT24 were selected for detailed inspection and comparisons.

According to the Table 5.133, GT13 demonstrated a moderate performance in terms of boiler natural gas cost, which is in correlation with energy consumption. GT18, GT23 and GT24 cost less since they have a lower U value than GT13.

In terms of chiller electricity cost, the performance of GT13 comes after GT19 and GT24 where they had lower SHGC values. Moreover, GT19 and GT24 also cost less for electricity due to cooling tower, fans and pumps.

Only GT 24 costs less both for heating and cooling purposes than GT13 however, it had a much higher electricity cost for lighting due to its lower Tvis value.

Table 5.133 : Parametric analysis of glazing type based on NPV energy cost breakdown (TL/m2) for Ankara.

GT	NPV N.G. Boiler	NPV Elc. Chiller	NPV Elc. CTower	NPV Elc. HVACFan	NPV Elc. Pump	NPV N.G WH	NPV Elc. Lights	NPV Elc. Equipment
13	**180.41**	**37.19**	**1.210**	**84.70**	**30.45**	**34.78**	**174.46**	**287.80**
18	178.50	38.14	1.231	84.73	31.01	34.78	174.46	287.80
19	180.66	33.99	1.074	84.50	29.24	34.78	182.29	287.80
23	177.15	38.87	1.247	84.75	31.40	34.78	174.46	287.80
24	179.10	34.62	1.088	84.52	29.67	34.78	182.29	287.80

Table 5.134 summarizes the NPV breakdown for water cost. The building with GT13 showed a moderate performance in cooling tower water cost category. GT19 and GT24 had the least cost requirement among all. The hot water cost remains unchanged with all windows since associated water use is kept fixed in the calculation.

Table 5.134 : Parametric analysis of glazing type based on NPV water cost breakdown (TL/m2) for Ankara.

GT	NPV CTower	NPV Hot water
13	**25.426**	**49.558**
18	25.821	49.558
19	24.050	49.558
23	26.113	49.558
24	24.293	49.558

Table 5.135 shows that the only equipment ownership cost variation occurred in FCU category since the rest of the equipment was kept fixed in the parametric analysis. When we further investigated the details, the number of required fan coils units were obtained as 44 for GT13, GT18 and GT23 and as 43 for GT19 and GT24.

Table 5.135 : Parametric analysis of glazing type based on NPV equipment cost breakdown (TL/m2) for Ankara.

GT	NPV Boiler	NPV Chiller	NPV CTower	NPV FCU	NPV WH	NPV LC
13	**5.30**	**29.64**	**5.71**	**17.36**	**2.47**	**53.37**
18	5.30	29.64	5.71	17.36	2.47	53.37
19	5.30	29.64	5.71	16.97	2.47	53.37
23	5.30	29.64	5.71	17.36	2.47	53.37
24	5.30	29.64	5.71	16.97	2.47	53.37

The increase in NPV material cost category is due to the variation in glazing type variable as Table 5.136 suggests. Since the rest of the variables were kept fixed in the parametric analysis, the associated cost values remained unchanged. The ownership cost of GT13 is the lowest among the selected windows.

Table 5.136 : Parametric analysis of glazing type based on NPV material cost breakdown (TL/m2) for Ankara.

GT	NPV EW Insul.	NPV Roof Insul.	NPV Roof layer	NPV Glazing	NPV EWOther
13	**3.94**	**13.39**	**4.64**	**42.51**	**13.57**
18	3.94	13.39	4.64	42.85	13.57
19	3.94	13.39	4.64	43.42	13.57
23	3.94	13.39	4.64	43.19	13.57
24	3.94	13.39	4.64	43.75	13.57

To conclude, the results showed that GT13 was able to balance building heating and cooling loads, lighting energy needs, associated energy costs and HVAC water costs for a reasonable glazing price. Therefore, the optimization methodology was

successful at recommending a cost-effective glazing solution for the Ankara case study within the given boundaries.

Window-to-wall ratio of southern façade (WTW S)

The application of the proposed optimization methodology to Ankara case study recommended 45 % of window-to-wall ratio for the south facing facade as the optimal solution, when combined with rest of the design recommendations. The results of the parametric investigation in Table 5.137 demonstrated that increasing w-t-w reduced the total global cost until 45% but then the cost started increasing. Moreover, a penalty occurred at 55% because the cooling capacity of the recommended chiller became insufficient with the introduction of 55 % w-t-w ratio. The GC breakdown shows that larger windows decreased only NPV energy costs where NPV costs for water, material and equipment increased.

Table 5.137 : Parametric analysis of southern façade window-to-wall ratio based on total Global Cost breakdown (TL/m2) for Ankara.

WTWS	PEN All	Total GC	NPV Energy	NPV Water	NPV Material	NPV Equipment
5	0	1116.74	858.78	74.17	70.34	113.45
15	0	1108.00	847.63	74.25	72.27	113.84
25	0	1101.89	839.45	74.40	74.20	113.84
35	0	1098.76	834.19	74.60	76.12	113.84
45	**0**	**1097.87**	**831.00**	**74.98**	**78.05**	**113.84**
55	16.17	1099.44	829.04	75.39	79.98	115.03

When we further investigated the cost breakdown for the NPV energy category given in Table 5.138, it was seen that increasing w-t-w ratio in the southern orientation decreased natural gas cost for boiler since larger windows provided more heat gain in the southern orientation and reduced heating loads in winter period.

Table 5.138 : Parametric analysis of southern façade window-to-wall ratio based on NPV energy cost breakdown (TL/m2) for Ankara.

WTWS	NPV N.G. Boiler	NPV Elc. Chiller	NPV Elc. CTower	NPV Elc. HVACFan	NPV Elc. Pump	NPV N.G WH	NPV Elc. Lights	NPV Elc. Equipment
5	181.09	35.24	1.135	84.58	29.31	34.78	204.85	287.80
15	181.03	35.45	1.145	84.60	29.39	34.78	193.45	287.80
25	180.92	35.83	1.160	84.62	29.64	34.78	184.71	287.80
35	180.69	36.42	1.182	84.66	29.98	34.78	178.69	287.80
45	**180.41**	**37.19**	**1.210**	**84.70**	**30.45**	**34.78**	**174.46**	**287.80**
55	180.16	38.07	1.241	84.75	30.88	34.78	171.34	287.80

Similarly, increasing w-t-w ratio also decreased significantly electricity cost for artificial lighting due to the enhanced daylighting potential of the building when combined with the dimming control.

On the other hand, larger south facing windows increased electricity cost for chiller, cooling tower, HVAC fans, and circulation pumps due to the higher heat gains and resulting cooling load in the summer period. The cost for water heating and plugged-in equipment remained unchanged since they were kept fixed in the analysis.

Table 5.139 summarizes the NPV cost breakdown for water. The water costs due to cooling tower use increased as w-t-w ratio increased, which is in line with the increase in cooling load and consequent chiller operation. However, hot water cost remained unchanged since associated water use was kept fixed in the analysis.

Table 5.139 : Parametric analysis of southern façade window-to-wall ratio based on NPV water cost breakdown (TL/m2) for Ankara.

WTW_S	NPV CTower	NPV Hot water
5	24.609	49.558
15	24.696	49.558
25	24.837	49.558
35	25.043	49.558
45	**25.426**	**49.558**
55	25.834	49.558

Table 5.140 below shows that only the NPV ownership cost of FCUs increased with the variation in w-t-w ratio, which is in parallel with the increase in cooling load and the requirement for more FCUs.

Table 5.140 : Parametric analysis of southern façade window-to-wall ratio based on NPV equipment cost breakdown (TL/m2) for Ankara.

WTW_S	NPV Boiler	NPV Chiller	NPV CTower	NPV FCU	NPV WH	NPV LC
5	5.30	29.64	5.71	16.97	2.47	53.37
15	5.30	29.64	5.71	17.36	2.47	53.37
25	5.30	29.64	5.71	17.36	2.47	53.37
35	5.30	29.64	5.71	17.36	2.47	53.37
45	**5.30**	**29.64**	**5.71**	**17.36**	**2.47**	**53.37**
55	5.30	29.64	5.71	18.54	2.47	53.37

The number of the required FCUs was 43 at 5% w-t-w and 44 at 15 to 45 % and it became 47 at 55%. However, the rest of the equipment cost categories remained unchanged, as they were kept fixed in the parametric analysis.

The increase in NPV material cost is due to the changes in wall area and glazed area as given in Table 5.141. When w-t-w ratio increased, the area of wall component that holding the glazing decreased, therefore the cost for wall insulation and the rest of the non-insulation wall materials decreased accordingly. Conversely, the cost of glazing material increased with the w-t-w ratio, as it was expected.

The roof insulation and roof coating has no interaction with the w-t-w ratio therefore the associated cost values remained unchanged.

Table 5.141 : Parametric analysis of southern façade window-to-wall ratio based on NPV material cost breakdown (TL/m2) for Ankara.

WTW_S	NPV EW Insul.	NPV Roof Insul.	NPV Roof layer	NPV Glazing	NPV EWOther
5	4.59	13.39	4.64	31.88	15.83
15	4.43	13.39	4.64	34.54	15.27
25	4.27	13.39	4.64	37.20	14.70
35	4.10	13.39	4.64	39.85	14.14
45	**3.94**	**13.39**	**4.64**	**42.51**	**13.57**
55	3.77	13.39	4.64	45.17	13.01

To conclude, the results showed that 45% of w-t-w ratio at the southern façade was able to balance heating and cooling loads, artificial lighting and daylighting potential together with the ownership cost for FCU, wall insulation, non-insulation wall materials and glazing cost itself. Therefore, the optimization methodology was successful at recommending a cost-effective w-t-w ratio solution for the Ankara case study within the given boundaries.

Window-to-wall ratio of western façade (WTW W)

The application of the proposed optimization methodology to Ankara case study recommended 45 % of window-to-wall ratio for the west-facing facade as the optimal solution, in combination with the rest of the design recommendations. The results of the parametric investigation in Table 5.142 demonstrated that increasing w-t-w reduced the total global cost until 45% but then the cost started increasing. The GC breakdown explains that larger windows decreased only NPV energy costs where NPV costs for water, material and equipment increased.

In addition, a penalty values occurred with the introduction of 55% of w-t-w ratio because the cooling capacity of the recommended chiller started to became insufficient to meet the resulting cooling load.

Table 5.142 : Parametric analysis of western facade window-to-wall ratio based on total Global Cost breakdown (TL/m2) for Ankara.

WTWW	PENAll	Total GC	NPV Energy	NPV Water	NPV Material	NPV Equipment
5	0	1112.68	855.12	74.17	70.34	113.05
15	0	1104.81	845.27	74.22	72.27	113.05
25	0	1100.26	838.21	74.41	74.20	113.45
35	0	1098.51	833.87	74.67	76.12	113.84
45	**0**	**1097.87**	**831.00**	**74.98**	**78.05**	**113.84**
55	25.33	1099.12	829.19	75.32	79.98	114.63

When we further investigated the cost breakdown for the NPV energy category given in Table 5.143, it was seen that increasing w-t-w ratio in the western orientation slightly increased natural gas cost for boiler as a result of increased heat gain due to larger windows combined with the less heat gain from artificial lighting with dimming control.

On the other hand, larger west facing windows increased electricity cost for chiller, cooling tower, HVAC fans, and circulation pumps due to higher heat gains and resulting cooling load in the summer period. The cost for water heating and plugged-in equipment remained unchanged since they were kept fixed in the analysis.

Similarly, increasing w-t-w ratio also decreased electricity cost for artificial lighting due to the enhanced daylighting potential of the building when combined with the dimming control.

Table 5.143 : Parametric analysis of western facade window-to-wall ratio based on NPV energy cost breakdown (TL/m2) for Ankara.

WTWW	NPV N.G. Boiler	NPV Elc. Chiller	NPV Elc. CTower	NPV Elc. HVACFan	NPV Elc. Pump	NPV N.G WH	NPV Elc. Lights	NPV Elc. Equipment
5	179.49	35.12	1.108	84.56	29.95	34.78	202.32	287.80
15	179.62	35.32	1.119	84.58	29.93	34.78	192.12	287.80
25	179.86	35.75	1.142	84.60	30.04	34.78	184.24	287.80
35	180.23	36.41	1.174	84.64	30.22	34.78	178.61	287.80
45	**180.41**	**37.19**	**1.210**	**84.70**	**30.45**	**34.78**	**174.46**	**287.80**
55	180.62	38.05	1.247	84.77	30.64	34.78	171.28	287.80

Table 5.144 summarizes the NPV cost breakdown water. The water costs due to cooling tower use increased as w-t-w ratio increased, which is in line with the increase in cooling load and consequent chiller operation. However, hot water cost remained unchanged since associated water use was kept fixed in the analysis.

Table 5.144 : Parametric analysis of western facade window-to-wall ratio based on NPV water cost breakdown (TL/m2) for Ankara.

WTW_W	NPV CTower	NPV Hot water
5	24.608	49.558
15	24.660	49.558
25	24.849	49.558
35	25.113	49.558
45	**25.426**	**49.558**
55	25.767	49.558

Table 5.145 below shows that only the NPV ownership cost of FCUs increased with the variation in w-t-w ratio, in parallel with the increase in cooling load and the requirement for more FCUs. The number of required FCUs was 42 at 5% and 15 %w-t-w ratio, where it became 43 at 25%, 44 at 35% and 45%, and finally 46 at 55%. However, the rest of the systems were kept fixed during the analysis so there were no cost variations.

Table 5.145 : Parametric analysis of western facade window-to-wall ratio based on NPV equipment cost breakdown (TL/m2) for Ankara.

WTW_W	NPV Boiler	NPV Chiller	NPV CTower	NPV FCU	NPV WH	NPV LC
5	5.30	29.64	5.71	16.57	2.47	53.37
15	5.30	29.64	5.71	16.57	2.47	53.37
25	5.30	29.64	5.71	16.97	2.47	53.37
35	5.30	29.64	5.71	17.36	2.47	53.37
45	**5.30**	**29.64**	**5.71**	**17.36**	**2.47**	**53.37**
55	5.30	29.64	5.71	18.15	2.47	53.37

The increase in NPV material cost is due to the changes in wall area and glazed area as given in Table 5.146. When w-t-w ratio increased, the area of wall component that holding the glazing decreased accordingly, therefore the ownership cost for wall insulation and the rest of the non-insulation wall materials decreased. Moreover, the ownership cost of glazing material increased with the w-t-w ratio as it was expected.

The roof insulation and roof coating has no interaction with the w-t-w ratio therefore the associated cost values remained unchanged.

Table 5.146 : Parametric analysis of western facade window-to-wall ratio based on NPV material cost breakdown (TL/m2) for Ankara.

WTW_W	NPV EW Insul.	NPV Roof Insul.	NPV Roof layer	NPV Glazing	NPV EWOther
5	4.59	13.39	4.64	31.88	15.83
15	4.43	13.39	4.64	34.54	15.27
25	4.27	13.39	4.64	37.20	14.70
35	4.10	13.39	4.64	39.85	14.14
45	**3.94**	**13.39**	**4.64**	**42.51**	**13.57**
55	3.77	13.39	4.64	45.17	13.01

To conclude, the results showed that 45% of w-t-w ratio at the western façade was able to balance heating and cooling loads, artificial lighting and daylighting potential together with the ownership cost for FCU, wall insulation, non-insulation wall materials and glazing cost itself. Therefore, the optimization methodology was successful at recommending a cost-effective w-t-w ratio solution for the Ankara case study within the given boundaries.

Window-to-wall ratio of northern façade (WTW N)

The application of the proposed optimization methodology to Ankara case study recommended 45 % of window-to-wall ratio for the north-facing facade as the optimal solution, in combination with the rest of the design recommendations. The results of the parametric investigation in Table 5.147 demonstrated that increasing w-t-w ratio reduced the total global cost until 55% and no penalties occurred. The GC breakdown explains that larger windows decreased only NPV energy costs where NPV costs for water, and material increased. The NPV equipment ownership cost however remained same.

Table 5.147 : Parametric analysis of northern facade window-to-wall ratio based on total Global Cost breakdown (TL/m2) for Ankara.

WTW N	PEN All	Total GC	NPV Energy	NPV Water	NPV Material	NPV Equipment
5	0	1103.18	844.22	74.77	70.34	113.84
15	0	1101.33	840.38	74.83	72.27	113.84
25	0	1099.73	836.85	74.83	74.20	113.84
35	0	1098.52	833.64	74.91	76.12	113.84
45	**0**	**1097.87**	**831.00**	**74.98**	**78.05**	**113.84**
55	0	1097.90	828.98	75.10	79.98	113.84

When we further investigated the cost breakdown for the NPV energy category given in Table 5.148, it was seen that increasing w-t-w ratio in the northern orientation

increased natural gas cost for boiler to some extent because of thermal heat losses due to larger windows combined with the less heat gain from artificial lighting with dimming control. However, since the glazing had an improved U-value, having large windows could be tolerated.

Moreover, larger north facing windows also increased electricity cost slightly for chiller, cooling tower, HVAC fans, and circulation pumps. The cost for water heating and plugged-in equipment remained unchanged since they were kept fixed in the analysis.

However, increasing w-t-w ratio decreased electricity cost for artificial lighting a great deal due to the enhanced daylighting potential of the building when combined with the dimming control.

Table 5.148 : Parametric analysis of northern facade window-to-wall ratio based on NPV energy cost breakdown (TL/m2) for Ankara.

WTWN	NPV N.G. Boiler	NPV Elc. Chiller	NPV Elc. CTower	NPV Elc. HVACFan	NPV Elc. Pump	NPV N.G WH	NPV Elc. Lights	NPV Elc. Equipment
5	179.10	36.76	1.180	84.66	30.34	34.78	189.60	287.80
15	179.34	36.82	1.185	84.67	30.35	34.78	185.44	287.80
25	179.69	36.92	1.194	84.67	30.40	34.78	181.40	287.80
35	180.07	37.03	1.201	84.68	30.42	34.78	177.66	287.80
45	**180.41**	**37.19**	**1.210**	**84.70**	**30.45**	**34.78**	**174.46**	**287.80**
55	180.80	37.38	1.221	84.72	30.48	34.78	171.80	287.80

Table 5.149 summarizes the NPV cost breakdown for water. The water costs due to cooling tower use increased very slightly as w-t-w ratio increased, which is in line with the increase in chiller electricity costs. However, hot water cost remained unchanged since associated water use was kept fixed in the analysis.

Table 5.149 : Parametric analysis of northern facade window-to-wall ratio based on NPV water cost breakdown (TL/m2) for Ankara.

WTW_N	NPV CTower	NPV Hot water
5	25.217	49.558
15	25.275	49.558
25	25.276	49.558
35	25.354	49.558
45	**25.426**	**49.558**
55	25.542	49.558

Table 5.150 below shows that no changes were observed in the NPV equipment cost category. The changes in the building thermal loads were minor therefore there was no need to update the number of FCUs. Moreover, since the rest of the systems were kept fixed during the analysis, there were no cost variations as well.

Table 5.150 : Parametric analysis of northern facade window-to-wall ratio based on NPV equipment cost breakdown (TL/m2) for Ankara.

WTW_N	NPV Boiler	NPV Chiller	NPV CTower	NPV FCU	NPV WH	NPV LC
5	5.30	29.64	5.71	17.36	2.47	53.37
15	5.30	29.64	5.71	17.36	2.47	53.37
25	5.30	29.64	5.71	17.36	2.47	53.37
35	5.30	29.64	5.71	17.36	2.47	53.37
45	**5.30**	**29.64**	**5.71**	**17.36**	**2.47**	**53.37**
55	5.30	29.64	5.71	17.36	2.47	53.37

The increase in NPV material cost is due to the changes in wall area and glazed area as given in Table 5.151. When w-t-w ratio increased, the area of wall component that holding the glazing decreased, therefore the cost for wall insulation and the rest of the non-insulation wall materials decreased accordingly. Moreover, the ownership cost of glazing material increased with the w-t-w ratio as it was expected.

The roof insulation and roof coating has no interaction with the w-t-w ratio therefore the associated cost values remained unchanged.

Table 5.151 : Parametric analysis of northern facade window-to-wall ratio based on NPV material cost breakdown (TL/m2) for Ankara.

WTW_N	NPV EW Insul.	NPV Roof Insul.	NPV Roof layer	NPV Glazing	NPV EWOther
5	4.59	13.39	4.64	31.88	15.83
15	4.43	13.39	4.64	34.54	15.27
25	4.27	13.39	4.64	37.20	14.70
35	4.10	13.39	4.64	39.85	14.14
45	**3.94**	**13.39**	**4.64**	**42.51**	**13.57**
55	3.77	13.39	4.64	45.17	13.01

To conclude, the results showed that 45% of w-t-w ratio at the northern façade was able to balance heating and cooling loads, artificial lighting and daylighting potential together with the ownership cost for wall insulation, non-insulation wall materials and glazing cost itself. Therefore, the optimization methodology was successful at recommending a cost-effective w-t-w ratio solution for the Ankara case study within the given boundaries.

Window-to-wall ratio of eastern façade (WTW E)

The application of the proposed optimization methodology to Ankara case study recommended 25 % of window-to-wall ratio for the east-facing facade as the optimal solution, in combination with the rest of the design recommendations. The results of the parametric investigation in Table 5.152 demonstrated that increasing w-t-w reduced the total global cost only until 25% but then the cost started increasing. The GC breakdown showed that larger windows decreased only NPV energy costs where NPV costs for water, material and equipment increased.

In addition, penalty values occurred starting with the 35 % of w-t-w ratio. A further investigation revealed that penalty values were due to under-capacity chiller equipment. Moreover, 45% and 55% of w-t-w ratios were extra penalized because they were also not able to satisfy heating loads when combined with the selected boiler.

Table 5.152 : Parametric analysis of eastern facade window-to-wall ratio based on total Global Cost breakdown (TL/m2) for Ankara.

WTW E	PEN All	Total GC	NPV Energy	NPV Water	NPV Material	NPV Equipment
5	0	1105.67	843.21	74.42	74.20	113.84
15	0	1100.23	835.59	74.67	76.12	113.84
25	**0**	**1097.87**	**831.00**	**74.98**	**78.05**	**113.84**
35	6.83	1099.08	829.02	75.45	79.98	114.63
45	8.22	1100.25	827.85	75.86	81.91	114.63
55	47.50	1102.63	827.07	76.30	83.83	115.42

When we analysed the NPV cost breakdown for the energy category given in Table 5.153, it was seen that increasing w-t-w ratio in the eastern orientation increased slightly the natural gas cost for boiler as a result of the enlarged heat loss due to larger windows and less heat gain from artificial lighting with dimming control.

On the other hand, larger east facing windows also slightly increased electricity cost for chiller, cooling tower, HVAC fans, and circulation pumps due to higher heat gains and resulting cooling load in the summer period. The cost for water heating and plugged-in equipment remained unchanged since they were kept fixed in the analysis.

Increasing w-t-w ratio had the most influence on artificial lighting costs since the larger windows enhanced daylighting potential of the building when combined with the dimming control.

Table 5.153 : Parametric analysis of eastern facade window-to-wall ratio based on NPV energy cost breakdown (TL/m2) for Ankara.

WTWE	NPV N.G. Boiler	NPV Elc. Chiller	NPV Elc. CTower	NPV Elc. HVACFan	NPV Elc. Pump	NPV N.G WH	NPV Elc. Lights	NPV Elc. Equipment
5	179.86	35.98	1.152	84.62	30.18	34.78	188.84	287.80
15	180.16	36.44	1.174	84.66	30.25	34.78	180.32	287.80
25	**180.41**	**37.19**	**1.210**	**84.70**	**30.45**	**34.78**	**174.46**	**287.80**
35	180.66	38.13	1.252	84.76	30.66	34.78	170.98	287.80
45	180.82	39.12	1.295	84.83	30.88	34.78	168.32	287.80
55	181.02	40.12	1.338	84.91	31.11	34.78	166.00	287.80

Table 5.154 summarizes the NPV cost breakdown for water. The water costs due to cooling tower use increased slightly as the w-t-w ratio increased, which is in line with the increase in cooling load and consequent chiller operation. However, hot water cost remained unchanged since associated water use was kept fixed in the analysis.

Table 5.154 : Parametric analysis of eastern facade window-to-wall ratio based on NPV water cost breakdown (TL/m2) for Ankara.

WTW_E	NPV CTower	NPV Hot water
5	24.861	49.558
15	25.112	49.558
25	**25.426**	**49.558**
35	25.891	49.558
45	26.305	49.558
55	26.743	49.558

Table 5.155 below shows that only the NPV ownership cost of FCUs increased with the variation in w-t-w ratio, in parallel with the increase in thermal loads and the resulting requirement for more FCUs. The number of required FCUs was 44 at 5% to 25% of w-t-w where it became 46 at 35% to 45%, and 48 at 55% w-t-W ratio. However, the rest of the systems were kept fixed during the analysis so there were no cost variations. The capacity of the recommended central plant equipment stayed within allowed ranges in the parametric analysis as no penalty occurred.

Table 5.155 : Parametric analysis of eastern facade window-to-wall ratio based on NPV equipment cost breakdown (TL/m2) for Ankara.

WTW_E	NPV Boiler	NPV Chiller	NPV CTower	NPV FCU	NPV WH	NPV LC
5	5.30	29.64	5.71	17.36	2.47	53.37
15	5.30	29.64	5.71	17.36	2.47	53.37
25	**5.30**	**29.64**	**5.71**	**17.36**	**2.47**	**53.37**
35	5.30	29.64	5.71	18.15	2.47	53.37
45	5.30	29.64	5.71	18.15	2.47	53.37
55	5.30	29.64	5.71	18.94	2.47	53.37

The increase in NPV material cost is due to the changes in wall area and glazed area as given in Table 5.156. When w-t-w ratio increased, the area of wall component that holding the glazing decreased, therefore the cost for wall insulation and the rest of the non-insulation wall materials decreased accordingly. Moreover, the ownership cost of glazing material increased with the w-t-w ratio as it was expected.

The roof insulation and roof coating has no interaction with the w-t-w ratio therefore the associated cost values remained unchanged.

Table 5.156 : Parametric analysis of eastern facade window-to-wall ratio based on NPV material cost breakdown (TL/m2) for Ankara.

WTW_E	NPV EW Insul.	NPV Roof Insul.	NPV Roof layer	NPV Glazing	NPV EWOther
5	4.27	13.39	4.64	37.20	14.70
15	4.10	13.39	4.64	39.85	14.14
25	**3.94**	**13.39**	**4.64**	**42.51**	**13.57**
35	3.77	13.39	4.64	45.17	13.01
45	3.61	13.39	4.64	47.83	12.44
55	3.44	13.39	4.64	50.48	11.87

To conclude, the results showed that 25% of w-t-w ratio at the eastern façade was able to balance heating and cooling loads, artificial lighting and daylighting potential together with the ownership cost for FCU, wall insulation, non-insulation wall materials and glazing cost itself. Therefore, the optimization methodology was successful at recommending a cost-effective w-t-w ratio solution for the Ankara case study within the given boundaries.

Boiler type (BLtype)

The application of the proposed optimization methodology to Ankara case study recommended Boiler 45 from the equipment database as the optimal choice in combination with rest of the design recommendations. The parametric analysis

carried out with a sample of low-efficiency (BL 17-19) and high-efficiency (BL 44-46) boiler equipment from the database. The results of the parametric investigation in Table 5.157 demonstrate that the switching from low efficiency equipment to high efficiency equipment decreased noticeably total global costs.

In addition, BL17, BL18 and BL44 were penalized because their heating capacities were not able to satisfy resulting heating load of the recommended design combination.

The GC breakdown explains that improvement on the boiler thermal efficiency let to a considerable reduction in NPV energy category while causing a little rise on the equipment costs. However, NPV for water and material remained unchanged, as they were not influenced with the boiler replacement. The amount of the cost reduction depends on the thermal capacity of the tested equipment.

Table 5.157 : Parametric analysis of boiler type based on total Global Cost breakdown (TL/m2) for Ankara.

BLtyp	PEN All	Total GC	NPV Energy	NPV Water	NPV Material	NPV Equipment
17	2395.11	1115.83	852.06	74.98	78.05	110.75
18	8.64	1117.41	853.47	74.97	78.05	110.92
19	0	1119.16	855.04	74.98	78.05	111.09
44	1843.83	1096.37	829.80	74.97	78.05	113.55
45	**0**	**1097.87**	**831.00**	**74.98**	**78.05**	**113.84**
46	0	1099.33	831.99	75.00	78.05	114.28

According to the Table 5.158 improving boiler efficiency only improved boiler NPV energy cost as expected. Moreover, the increase in equipment capacity also increased the natural gas boiler costs. The rest of the energy categories assumed to be remained same as minor changes occurred in electricity cost for fans and circulation pumps.

Table 5.158 : Parametric analysis of boiler type based on NPV energy cost breakdown (TL/m2) for Ankara.

BLtyp	NPV N.G. Boiler	NPV Elc. Chiller	NPV Elc. CTower	NPV Elc. HVACFan	NPV Elc. Pump	NPV N.G WH	NPV Elc. Lights	NPV Elc. Equipment
17	201.47	37.192	1.210	84.698	30.451	34.78	174.46	287.80
18	202.89	37.192	1.210	84.697	30.451	34.78	174.46	287.80
19	204.45	37.192	1.210	84.697	30.451	34.78	174.46	287.80
44	179.21	37.192	1.210	84.700	30.451	34.78	174.46	287.80
45	**180.41**	**37.192**	**1.210**	**84.698**	**30.451**	**34.78**	**174.46**	**287.80**
46	181.41	37.192	1.210	84.697	30.451	34.78	174.46	287.80

Table 5.159 summarizes the NPV cost breakdown for water. Both the water costs due to cooling tower use and hot water cost remained unchanged since associated water use didn't interact with the boiler replacement.

Table 5.159 : Parametric analysis of boiler type based on NPV water cost breakdown (TL/m2) for Ankara.

BLtyp	NPV CTower	NPV Hot water
17	25.422	49.558
18	25.422	49.558
19	25.422	49.558
44	25.422	49.558
45	**25.422**	**49.558**
46	25.422	49.558

As demonstrated in Table 5.160, the only change in NPV equipment cost occurred in boiler category as expected. The efficiency and capacity changes increase equipment costs. The more efficient equipment cost almost double of the low efficiency group. BL17, BL18 and BL44 were not able to satisfy heating loads as penalties occurred. Even BL19 and BL46 remained in the allowed equipment capacity range; they were not preferred since there was smaller size equipment that can still meet the load.

Table 5.160 : Parametric analysis of boiler type based on NPV equipment cost breakdown (TL/m2) for Ankara.

BLtyp	NPV Boiler	NPV Chiller	NPV CTower	NPV FCU	NPV WH	NPV LC
17	2.20	29.64	5.71	17.36	2.47	53.37
18	2.37	29.64	5.71	17.36	2.47	53.37
19	2.54	29.64	5.71	17.36	2.47	53.37
44	5.00	29.64	5.71	17.36	2.47	53.37
45	**5.30**	**29.64**	**5.71**	**17.36**	**2.47**	**53.37**
46	5.73	29.64	5.71	17.36	2.47	53.37

As shown in Table 5.161, there were no NPV cost changes in the material category since there were no interactions between building material and boiler replacement in the parametric analysis.

Table 5.161 : Parametric analysis boiler type based on NPV material cost breakdown (TL/m2) for Ankara.

BLtyp	NPV EW Insul.	NPV Roof Insul.	NPV Roof layer	NPV Glazing	NPV EWOther
17	3.94	13.39	4.64	42.51	13.57
18	3.94	13.39	4.64	42.51	13.57
19	3.94	13.39	4.64	42.51	13.57
44	3.94	13.39	4.64	42.51	13.57
45	**3.94**	**13.39**	**4.64**	**42.51**	**13.57**
46	3.94	13.39	4.64	42.51	13.57

To conclude, the results showed that BL45 showed an improved energy performance while being capable of meeting building heating loads for an affordable equipment ownership price in Ankara case study. Therefore, the proposed optimization methodology successfully recommended a cost-effective boiler solution within the given boundaries.

Chiller type (CLtype)

The application of the proposed optimization methodology to Ankara case study recommended Chiller 30 from the equipment database as the optimal choice in combination with rest of the design recommendations. The parametric analysis carried out with a sample of moderate efficiency (CL 7-9) and high efficiency (CL 29-31) chiller equipment. The results of the parametric investigation in Table 5.162 demonstrate that the switching from moderate efficiency equipment to high efficiency equipment decreased total global costs. However, only CL8, CL9, CL30 and CL31 were able to comply with constraints and not penalized. CL7 and CL29 were penalized because they were not able to satisfy cooling load of the recommended design combination.

Table 5.162 : Parametric analysis of chiller type based on total Global Cost breakdown (TL/m2) for Ankara.

CLtyp	PEN All	Total GC	NPV Energy	NPV Water	NPV Material	NPV Equipment
7	1091.75	1110.53	848.77	75.47	78.05	108.24
8	0	1115.83	851.99	76.38	78.05	109.42
9	0	1119.46	853.80	77.16	78.05	110.44
29	1372.09	1098.41	833.41	74.38	78.05	112.56
30	**0**	**1097.87**	**831.00**	**74.98**	**78.05**	**113.84**
31	0	1104.65	833.80	76.22	78.05	116.58

The GC breakdown explains that improvement on the chiller efficiency let to a considerable reduction in NPV energy category while causing a little rise on NPV equipment costs depending on the capacity of the tested equipment. However, NPV for water and material cost were not influenced with the chiller replacement.

According to the Table 5.163 improving chiller efficiency improved chiller NPV energy cost together with cooling tower electricity costs as expected. Moreover, the chiller electricity cost increased in parallel with the increase in the equipment capacity. In addition, minor changes occurred in electricity cost for fans and circulation pumps. The rest of the energy cost categories remained uninfluenced, as they did not interact with the chiller.

Table 5.163 : Parametric analysis of chiller type based on NPV energy cost breakdown (TL/m2) for Ankara.

CLtyp	NPV N.G. Boiler	NPV Elc. Chiller	NPV Elc. CTower	NPV Elc. HVACFan	NPV Elc. Pump	NPV N.G WH	NPV Elc. Lights	NPV Elc. Equipment
7	180.41	55.579	1.344	84.698	29.709	34.78	174.46	287.80
8	180.41	57.383	1.309	84.698	31.153	34.78	174.46	287.80
9	180.41	57.947	1.267	84.698	32.447	34.78	174.46	287.80
29	180.41	40.950	1.256	84.698	29.062	34.78	174.46	287.80
30	**180.41**	**37.192**	**1.210**	**84.698**	**30.451**	**34.78**	**174.46**	**287.80**
31	180.41	37.693	1.132	84.698	32.836	34.78	174.46	287.80

Table 5.164 summarizes the NPV cost breakdown for water. Water costs due to cooling tower use was slightly improved with higher efficiency chiller equipment depending on equipment capacity where and hot water cost remained same.

Table 5.164 : Parametric analysis of chiller type based on NPV water cost breakdown (TL/m2) for Ankara.

CLtyp	NPV CTower	NPV Hot water
7	25.907	49.558
8	26.819	49.558
9	27.604	49.558
29	24.823	49.558
30	**25.426**	**49.558**
31	26.658	49.558

As demonstrated in Table 5.165, the only major change in NPV equipment ownership cost occurred in chiller category as expected. The efficiency and capacity improvements increased equipment costs. CL7 and CL29 were not able to satisfy

cooling load as penalties occurred. However, even CL8 and CL9 remained in the allowed equipment capacity range; they were not preferred because of their lower efficiency values that led to serious energy costs. Similarly, even CL31 remained in the allowed equipment capacity range; it was not preferred since there was smaller size equipment that can still meet the resulting cooling load for an improved efficiency.

Table 5.165 : Parametric analysis of chiller type based on NPV equipment cost breakdown (TL/m2) for Ankara.

CLtyp	NPV Boiler	NPV Chiller	NPV CTower	NPV FCU	NPV WH	NPV LC
7	5.30	24.26	5.48	17.36	2.47	53.37
8	5.30	25.06	5.86	17.36	2.47	53.37
9	5.30	25.74	6.20	17.36	2.47	53.37
29	5.30	28.72	5.34	17.36	2.47	53.37
30	**5.30**	**29.64**	**5.71**	**17.36**	**2.47**	**53.37**
31	5.30	31.74	6.35	17.36	2.47	53.37

As shown in Table 5.166, there were no cost changes in the NPV material category since there were no interactions between building material and chiller equipment in the parametric analysis.

Table 5.166 : Parametric analysis chiller type based on NPV material cost breakdown (TL/m2) for Ankara case.

CLtyp	NPV EW Insul.	NPV Roof Insul.	NPV Roof layer	NPV Glazing	NPV EWOther
7	3.94	13.39	4.64	42.51	13.57
8	3.94	13.39	4.64	42.51	13.57
9	3.94	13.39	4.64	42.51	13.57
29	3.94	13.39	4.64	42.51	13.57
30	**3.94**	**13.39**	**4.64**	**42.51**	**13.57**
31	3.94	13.39	4.64	42.51	13.57

To conclude, the results showed that CL30 showed an improved energy performance while being capable of meeting building cooling loads for an affordable equipment price in Ankara case study. Therefore, the proposed optimization methodology successfully recommended a cost-effective chiller solution within the given boundaries.

Lighting control (LC)

The application of the proposed optimization methodology to Ankara case study recommended dimming control of artificial lights (option 1) according to indoor

daylighting levels as the optimal choice over manual lighting control (option 0), in combination with rest of the design recommendations.

The results of the parametric investigation in Table 5.167 demonstrate that dimming control of lights resulted in a major GC reduction. Moreover, the cost breakdown explains that dimming control reduces not only NPV energy costs but also NPV water cost as well. NPV for material ownership were not influenced however, NPV for equipment ownership was increased.

In addition, the case with manual light control was penalized because the recommended chiller could not satisfy resulting cooling load in this combination.

Table 5.167 : Parametric analysis of lighting control strategies based on total Global Cost breakdown (TL/m2) for Ankara.

LC	PEN All	Total GC	NPV Energy	NPV Water	NPV Material	NPV Equipment
0	1635.09	1229.44	971.52	79.56	78.05	100.31
1	**0**	**1097.87**	**831.00**	**74.98**	**78.05**	**113.84**

According to the Table 5.168, dimming control of lights over daylighting increased boiler natural gas cost in part due to the reduction in heat gain from lighting system. However, it decreased electricity cost for chiller, cooling tower, fans, and pumps a great deal in addition to the major decrease in lighting electricity cost.

The rest of the energy cost categories remained uninfluenced, as they did not interact with the lighting system.

Table 5.168 : Parametric analysis of lighting control strategies based on NPV energy cost breakdown (TL/m2) for Ankara.

LC	NPV N.G. Boiler	NPV Elc. Chiller	NPV Elc. CTower	NPV Elc. HVACFan	NPV Elc. Pump	NPV N.G WH	NPV Elc. Lights	NPV Elc. Equipment
0	176.18	48.35	1.595	85.37	33.80	34.78	303.65	287.80
1	**180.41**	**37.19**	**1.210**	**84.70**	**30.45**	**34.78**	**174.46**	**287.80**

Table 5.169 summarizes the NPV cost breakdown for water. Water costs due to cooling tower use were moderately improved with dimming control where hot water cost remained same.

Table 5.169 : Parametric analysis of lighting control strategies based on NPV water cost breakdown (TL/m2) for Ankara.

LC	NPV CTower	NPV Hot water
0	29.998	49.558
1	**25.426**	**49.558**

As demonstrated in Table 5.170, the major change in NPV equipment ownership cost occurred in lighting control category as installing dimming control costs more than manual control system.

In addition, the ownership cost for FCUs decreased with dimming control due to the decrease in heat gain from lighting system and the decrease in cooling load and required number of FCUs from 52 to 44.

Table 5.170 : Parametric analysis of lighting control strategies based on NPV equipment cost breakdown (TL/m2) for Ankara.

LC	NPV Boiler	NPV Chiller	NPV CTower	NPV FCU	NPV WH	NPV LC
0	5.30	29.64	5.71	20.52	2.47	36.68
1	**5.30**	**29.64**	**5.71**	**17.36**	**2.47**	**53.37**

As shown in Table 5.171, there were no cost changes in the NPV material ownership category since there were no interactions between building material and the lighting system.

Table 5.171 : Parametric analysis of lighting control strategies based on NPV material cost breakdown (TL/m2) for Ankara.

LC	NPV EW Insul.	NPV Roof Insul.	NPV Roof layer	NPV Glazing	NPV EWOther
0	3.94	13.39	4.64	42.51	13.57
1	**3.94**	**13.39**	**4.64**	**42.51**	**13.57**

To conclude, the results showed that dimming control of artificial lights according to daylighting levels decreased the electricity cost for lighting together with electricity cost for cooling system for an affordable price. The slight increase in NPV energy cost for heating was compensated with other benefits. Therefore, the proposed optimization methodology was successful at recommending a cost-effective lighting control solution within the given boundaries.

5.3.6.3 Validation of Antalya case study

External wall insulation thickness (iEW)

The application of the proposed optimization methodology to Antalya case study recommended 0.02m of insulation for the external walls as the optimal choice, in combination with the rest of the design recommendations.

The results of the parametric investigation in Table 5.172 demonstrate that the introduction of external wall insulation had a trend for reducing the total global cost only until 0.02m, but then the cost started increasing. Moreover, the GC breakdown explains that increase in external wall insulation decreased NPV in energy category also only until 0.02m. Similarly, NPV water costs also decreased until introduction of 0.015m insulation. However, NPV for material continuously increased as the insulation thickness increased. The NPV for equipment cost did not vary within the tested range of insulation variable.

In addition, the minor penalties occurred at 0.005m and 0.01m insulation thicknesses and they were due to under capacity chiller equipment.

Table 5.172 : Parametric analysis of external wall insulation thickness based on total global cost breakdown (TL/m2) for Antalya.

iEW	PEN All	Total GC	NPV Energy	NPV Water	NPV Material	NPV Equipment
0.005	15.44	1054.86	756.36	106.94	72.12	119.44
0.010	0.28	1054.61	755.88	106.92	72.37	119.44
0.015	0	1054.47	755.53	106.89	72.62	119.44
0.020	**0**	**1054.44**	**755.22**	**106.93**	**72.86**	**119.44**
0.025	0	1054.71	755.23	106.94	73.11	119.44
0.030	0	1054.66	754.94	106.93	73.35	119.44
0.035	0	1054.89	754.92	106.94	73.60	119.44

According to the Table 5.173, the increase in external wall insulation levels decreased boiler natural gas cost because of the reduction in associated energy consumption and heating loads. On the other hand, it also slightly decreased chiller electricity costs until 0.02m then it had a reverse influence where the cost started to increase. There were also minor changes in fan and pump energy costs due to the changes in building heating and cooling needs. The rest of the energy categories remained same as they were kept fixed in the analysis.

Table 5.173 : Parametric analysis of external wall insulation thickness based on NPV energy cost breakdown (TL/m2) for Antalya.

iEW	NPV N.G. Boiler	NPV Elc. Chiller	NPV Elc. CTower	NPV Elc. HVACFan	NPV Elc. Pump	NPV N.G WH	NPV Elc. Lights	NPV Elc. Equipment
0.005	47.11	103.65	5.740	85.32	37.39	24.27	165.08	287.80
0.010	46.46	103.55	5.733	85.31	37.69	24.27	165.08	287.80
0.015	45.97	103.50	5.729	85.29	37.89	24.27	165.08	287.80
0.020	**45.54**	**103.49**	**5.726**	**85.29**	**38.03**	**24.27**	**165.08**	**287.80**
0.025	45.46	103.49	5.725	85.28	38.13	24.27	165.08	287.80
0.030	45.09	103.50	5.724	85.28	38.20	24.27	165.08	287.80
0.035	44.99	103.50	5.722	85.28	38.28	24.27	165.08	287.80

Table 5.174 summarizes the NPV water cost breakdown. The water costs due to cooling tower use slightly varied depending on the variation on cooling load and associated chiller operation as the insulation thickness increased. However, hot water cost remained unchanged since associated water use is kept fixed in the calculation.

Table 5.174 : Parametric analysis of external wall insulation thickness based on NPV water cost breakdown (TL/m2) for Antalya.

iEW	NPV CTower	NPV Hot water
0.005	57.380	49.558
0.010	57.363	49.558
0.015	57.336	49.558
0.020	**57.368**	**49.558**
0.025	57.379	49.558
0.030	57.368	49.558
0.035	57.381	49.558

Table 5.175 shows that the variation in external wall insulation levels did not cause any cost changes at NPV equipment category within the tested insulation range.

Table 5.175 : Parametric analysis of external wall insulation thickness based on NPV equipment cost breakdown (TL/m2) for Antalya.

iEW	NPV Boiler	NPV Chiller	NPV CTower	NPV FCU	NPV WH	NPV LC
0.005	4.106	32.705	6.664	20.123	2.466	53.371
0.010	4.106	32.705	6.664	20.123	2.466	53.371
0.015	4.106	32.705	6.664	20.123	2.466	53.371
0.020	**4.106**	**32.705**	**6.664**	**20.123**	**2.466**	**53.371**
0.025	4.106	32.705	6.664	20.123	2.466	53.371
0.030	4.106	32.705	6.664	20.123	2.466	53.371
0.035	4.106	32.705	6.664	20.123	2.466	53.371

Ownership cost of boiler, chiller, cooling tower, water heating and lighting control were kept fixed in the parametric analysis however, FCUs were allowed to adjust to the building heating and cooling load needs. Results indicate that load changes did not require any FCU update within the tested range.

Table 5.176 shows that the increase in NPV material cost is due to the increase in external wall insulation levels. Since the rest of the variables were kept fixed in the parametric analysis, the associated cost values remained unchanged.

Table 5.176 : Parametric analysis of external wall insulation thickness based on NPV material cost breakdown (TL/m2) for Antalya.

iEW	NPV EW Insul.	NPV Roof Insul.	NPV Roof layer	NPV Glazing	NPV EWOther
0.005	1.56	6.79	4.64	46.13	13.01
0.010	1.80	6.79	4.64	46.13	13.01
0.015	2.05	6.79	4.64	46.13	13.01
0.020	**2.29**	**6.79**	**4.64**	**46.13**	**13.01**
0.025	2.54	6.79	4.64	46.13	13.01
0.030	2.79	6.79	4.64	46.13	13.01
0.035	3.03	6.79	4.64	46.13	13.01

To conclude, the results showed that 0.02 m of external wall insulation was able to balance heating and cooling loads, associated NPV energy costs together with the NPV water cost due to cooling purposes. Therefore, the proposed optimization methodology was successful at recommending a cost-effective external wall insulation solution within the given boundaries for the Antalya case study.

Roof insulation thickness (iR)

The application of the proposed optimization methodology to Antalya case study recommended 0.03m of insulation for the roof element as the optimal choice, when combined with rest of the design recommendations. The results of the parametric investigation given in Table 5.177 demonstrate that the introduction of roof insulation reduced the total global cost only until 0.03m but then the cost started increasing. The GC breakdown explains that increase in roof insulation levels decreased NPV in energy category only however NPV for water and material increased inversely within the tested insulation range. The NPV cost for equipment however, did not change.

In addition, no penalties occurred within the tested variable range.

Table 5.177 : Parametric analysis of roof insulation thickness based on total Global Cost breakdown (TL/m2) for Antalya.

iR	PEN All	Total GC	NPV Energy	NPV Water	NPV Material	NPV Equipment
0.015	0	1057.01	760.16	106.35	71.06	119.44
0.020	0	1055.38	757.69	106.59	71.66	119.44
0.025	0	1054.65	756.15	106.80	72.26	119.44
0.030	**0**	**1054.44**	**755.22**	**106.93**	**72.86**	**119.44**
0.035	0	1054.70	754.77	107.04	73.46	119.44
0.040	0	1055.27	754.58	107.19	74.06	119.44
0.045	0	1055.94	754.53	107.31	74.66	119.44

According to the Table 5.178, the increase in roof insulation decreased the boiler natural gas cost because of the reduction in associated heating load and energy consumption.

On the other hand, insulation also slightly increased chiller and cooling tower electricity costs and related energy use due to the increase in cooling loads in summer period. There was also a minor increase in fan and pump electricity costs due to the changes in building heating and cooling needs. The rest of the energy categories remained same, as they do not interact with the insulation.

Table 5.178 : Parametric analysis of roof insulation thickness based on NPV energy cost breakdown (TL/m2) for Antalya.

iR	NPV N.G. Boiler	NPV Elc. Chiller	NPV Elc. CTower	NPV Elc. HVACFan	NPV Elc. Pump	NPV N.G WH	NPV Elc. Lights	NPV Elc. Equipment
0.015	52.12	101.70	5.648	85.30	38.25	24.27	165.08	287.80
0.020	49.05	102.39	5.679	85.29	38.13	24.27	165.08	287.80
0.025	46.97	102.98	5.704	85.29	38.07	24.27	165.08	287.80
0.030	**45.54**	**103.49**	**5.726**	**85.29**	**38.03**	**24.27**	**165.08**	**287.80**
0.035	44.60	103.95	5.746	85.29	38.04	24.27	165.08	287.80
0.040	43.95	104.37	5.763	85.30	38.05	24.27	165.08	287.80
0.045	43.49	104.74	5.778	85.31	38.07	24.27	165.08	287.80

Table 5.179 summarizes the NPV cost breakdown for water. The water costs due to cooling tower use slightly increased with the increase in insulation level and resulting cooling needs. However, hot water cost remained unchanged since associated water use is kept fixed in the calculation.

Table 5.179 : Parametric analysis of roof insulation thickness based on NPV water cost breakdown (TL/m2) for Antalya.

iR	NPV CTower	NPV Hot water
0.015	56.792	49.558
0.020	57.033	49.558
0.025	57.240	49.558
0.030	**57.368**	**49.558**
0.035	57.478	49.558
0.040	57.637	49.558
0.045	57.748	49.558

Table 5.180 below shows that the variation in roof insulation levels did not cause any cost changes at NPV equipment category within the tested range. The ownership cost of boiler, chiller, cooling tower, water heating and lighting control were kept fixed in the parametric analysis however, FCUs were allowed to adjust to the building heating and cooling load needs where load changes did not require any FCU update.

Table 5.180 : Parametric analysis of roof insulation thickness based on NPV equipment cost breakdown (TL/m2) for Antalya.

iR	NPV Boiler	NPV Chiller	NPV CTower	NPV FCU	NPV WH	NPV LC
0.015	4.106	32.705	6.664	20.123	2.466	53.371
0.020	4.106	32.705	6.664	20.123	2.466	53.371
0.025	4.106	32.705	6.664	20.123	2.466	53.371
0.030	**4.106**	**32.705**	**6.664**	**20.123**	**2.466**	**53.371**
0.035	4.106	32.705	6.664	20.123	2.466	53.371
0.040	4.106	32.705	6.664	20.123	2.466	53.371
0.045	4.106	32.705	6.664	20.123	2.466	53.371

As shown in Table 5.181, the increase in NPV material cost is due to the increase in roof insulation levels.

Table 5.181 : Parametric analysis roof insulation thickness based on NPV material cost breakdown (TL/m2) for Antalya.

iR	NPV EW Insul.	NPV Roof Insul.	NPV Roof layer	NPV Glazing	NPV EWOther
0.015	2.29	4.99	4.64	46.13	13.01
0.020	2.29	5.59	4.64	46.13	13.01
0.025	2.29	6.19	4.64	46.13	13.01
0.030	**2.29**	**6.79**	**4.64**	**46.13**	**13.01**
0.035	2.29	7.39	4.64	46.13	13.01
0.040	2.29	7.99	4.64	46.13	13.01
0.045	2.29	8.59	4.64	46.13	13.01

Since the rest of the variables were kept fixed in the parametric analysis, the associated cost values remained unchanged.

To conclude, the results showed that 0.03 m of roof insulation was able to balance heating and cooling loads, associated energy costs together with the water cost due to cooling purposes. Therefore, the proposed optimization methodology was successful at recommending a cost-effective roof insulation solution within the given boundaries for the Antalya case study.

Roof type (RT)

The application of the proposed optimization methodology to Antalya case study recommended the cool roof coating (RT2) over conventional gravel layer (RT1) as the optimal choice, in combination with the rest of the design recommendations.

The results of the parametric investigation given in Table 5.182 demonstrate that switching from conventional gravel roof to cool roof coating decreased total global cost. In addition, a strong penalty also occurred with RT1 because the recommended chiller used in the analysis was not able to meet the resulting building cooling load in this design combination. The GC breakdown table also explains that application of cool roof coating decreased NPV in energy, water and equipment categories however, NPV for material increased.

Table 5.182 : Parametric analysis of roof type based on total Global Cost breakdown (TL/m2) for Antalya.

RT	PEN All	Total GC	NPV Energy	NPV Water	NPV Material	NPV Equipment
1	717.76	1079.54	775.58	113.15	69.79	121.01
2	**0**	**1054.44**	**755.22**	**106.93**	**72.86**	**119.44**

According to the Table 5.183, the cool roof coating increased the boiler natural gas cost because of the increase in associated heating load and energy consumption.

Table 5.183 : Parametric analysis of roof type based on NPV energy cost breakdown (TL/m2) for Antalya.

RT	NPV N.G. Boiler	NPV Elc. Chiller	NPV Elc. CTower	NPV Elc. HVACFan	NPV Elc. Pump	NPV N.G WH	NPV Elc. Lights	NPV Elc. Equipment
1	42.34	123.31	6.527	86.43	39.84	24.27	165.08	287.80
2	**45.54**	**103.49**	**5.726**	**85.29**	**38.03**	**24.27**	**165.08**	**287.80**

On the other hand, it also significantly decreased the chiller and cooling tower electricity costs and related energy use together with electricity cost for fans and pumps. The electricity cost due to artificial lighting and plugged-in equipment remained same in both cases since they were kept fixed in the analysis.

Table 5.184 summarizes the NPV cost breakdown for water. The water costs due to cooling tower use decreased with cool roof coating in line with the decrease in chiller operation. However, hot water cost remained unchanged since associated water use was kept fixed in the calculation.

Table 5.184 : Parametric analysis of roof type based on NPV water cost breakdown (TL/m2) for Antalya.

RT	NPV CTower	NPV Hot water
1	63.595	49.558
2	**57.368**	**49.558**

Table 5.185 below shows that the decrease in NPV equipment cost is due to the decrease in fan coil ownership cost as the required number of FCU is reduced from 55 to 51 due to the reduction in cooling loads. Ownership cost of boiler, chiller, cooling tower, water heating and lighting control remained same.

Table 5.185 : Parametric analysis of roof type based on NPV equipment cost breakdown (TL/m2) for Antalya.

RT	NPV Boiler	NPV Chiller	NPV CTower	NPV FCU	NPV WH	NPV LC
1	4.11	32.71	6.66	21.70	2.47	53.37
2	**4.11**	**32.71**	**6.66**	**20.12**	**2.47**	**53.37**

The increase in NPV material cost is due to the switch from the gravel roof to cool roof coating only where ownership of cool roof later is almost four times higher than gravel roof. Since the rest of the variables were kept fixed in the parametric analysis, the associated cost values remained unchanged as given in Table 5.186.

Table 5.186 : Parametric analysis of roof type based on NPV material cost breakdown (TL/m2) for Antalya.

RT	NPV EW Insul.	NPV Roof Insul.	NPV Roof layer	NPV Glazing	NPV EWOther
1	2.29	6.79	1.57	46.13	13.01
2	**2.29**	**6.79**	**4.64**	**46.13**	**13.01**

To conclude, the results showed that cool roof coating (RT2) was able to balance heating and cooling related costs together with water and equipment costs for a reasonable price. Therefore, it was successfully recommended by the proposed optimization methodology as the cost-effective solution for the Antalya case study within the given boundaries.

Glazing Type (GT)

The application of the proposed optimization methodology recommended GT19 out of 27 glazing alternatives as the optimal glazing choice for Antalya case study, in combination with the rest of the design recommendations. Table 5.187 summarizes the total global cost breakdown. GT19 has the lowest total GC value. Moreover, it also shows the best performance in NPV energy cost category as well.

Table 5.187 : Parametric analysis of glazing type based on total Global Cost breakdown (TL/m2) for Antalya.

GT	PEN All	Total GC	NPV Energy	NPV Water	NPV Material	NPV Equipment
1	2799.02	1080.34	773.12	113.72	71.30	122.20
2	67.52	1066.72	767.52	107.29	72.08	119.83
3	1.10	1114.34	812.79	106.38	75.73	119.44
4	23.28	1144.30	844.51	106.42	73.93	119.44
5	2699.70	1080.83	773.45	113.91	71.67	121.80
6	63.21	1066.87	767.38	107.32	72.74	119.44
7	0.69	1114.55	812.66	106.38	76.08	119.44
8	20.99	1144.60	844.47	106.41	74.29	119.44
9	2665.84	1081.27	773.51	113.94	72.02	121.80
10	59.03	1067.28	767.40	107.36	73.09	119.44
11	0.37	1114.94	812.64	106.42	76.44	119.44
12	18.81	1144.94	844.41	106.44	74.65	119.44
13	171.88	1057.99	757.07	109.19	71.90	119.83
14	1.34	1056.09	757.21	106.95	72.50	119.44
15	0.00	1062.10	762.76	106.32	73.58	119.44
16	0.00	1090.43	789.10	105.57	76.32	119.44
17	0.00	1143.12	842.65	106.02	75.01	119.44
18	150.01	1058.99	757.45	109.44	72.26	119.83
19	**0.00**	**1054.44**	**755.22**	**106.93**	**72.86**	**119.44**
20	0.00	1063.79	763.82	106.60	73.93	119.44
21	0.00	1096.40	794.00	106.29	76.68	119.44
22	0.00	1145.64	844.55	106.28	75.37	119.44
23	136.06	1059.72	757.71	109.56	72.62	119.83
24	0.00	1055.00	755.36	106.99	73.22	119.44
25	0.00	1064.28	763.88	106.68	74.29	119.44
26	0.00	1097.04	794.14	106.42	77.04	119.44
27	0.00	1146.08	844.59	106.33	75.73	119.44

In addition to the cost performance, the results also show that the windows between GT1 –GT14, GT18 and GT23 were penalized due to under capacity chiller equipment where recommended chiller failed to meet resulting cooling load.

When we further investigated the penalty conditions, it was found out that windows with highest U-value and highest SHGC value were penalized the most where SGGC played a dominant part in determination of the penalty value.

GT15, GT19, GT20, GT24 and GT25 were selected for detailed inspection and comparisons.

According to the Table 5.188, GT19 demonstrated a moderate performance in terms of boiler natural gas cost, which is in correlation with energy consumption. GT24 and GT25 lead to less natural gas boiler cost since they have a lower U-value than GT13.

In terms of chiller electricity cost, the performance of GT13 comes after GT15, GT20 and GT25 where they had lower SHGC values.

Only GT 25 costs less both for heating and cooling purposes than GT13 however, it had a much higher electricity cost for lighting due to its lower Tvis value. GT19 performs well in term of lighting electricity cost.

Table 5.188 : Parametric analysis of glazing type based on NPV energy cost breakdown (TL/m2) for Antalya.

GT	NPV N.G. Boiler	NPV Elc. Chiller	NPV Elc. CTower	NPV Elc. HVACFan	NPV Elc. Pump	NPV N.G WH	NPV Elc. Lights	NPV Elc. Equipment
15	46.35	101.62	5.654	85.20	37.45	24.27	174.42	287.80
19	**45.54**	**103.49**	**5.726**	**85.29**	**38.03**	**24.27**	**165.08**	**287.80**
20	45.74	102.37	5.682	85.23	37.80	24.27	174.94	287.80
24	45.16	103.80	5.737	85.30	38.21	24.27	165.08	287.80
25	45.31	102.65	5.691	85.24	37.99	24.27	174.94	287.80

Table 5.189 summarizes the NPV cost breakdown for water.

The building with GT13 showed a moderate performance in cooling tower water cost category. GT15 had the least cost requirement among all. The hot water cost remained unchanged with all windows since associated water use is kept fixed in the calculation.

Table 5.189 : Parametric analysis of glazing type based on NPV water cost breakdown (TL/m2) for Antalya.

GT	NPV CTower	NPV Hot water
15	56.760	49.558
19	**57.368**	**49.558**
20	57.038	49.558
24	57.435	49.558
25	57.117	49.558

Table 5.190 shows that NPV ownership cost for equipment did not vary in any category. Only FCUs were allowed to vary to match changing building thermal loads however, no load changes led to FCU update within the tested range. The rest of the equipment was kept fixed in the parametric analysis.

Table 5.190 : Parametric analysis of glazing type based on NPV equipment cost breakdown (TL/m2) for Antalya.

GT	NPV Boiler	NPV Chiller	NPV CTower	NPV FCU	NPV WH	NPV LC
15	4.11	32.71	6.66	20.12	2.47	53.37
19	**4.11**	**32.71**	**6.66**	**20.12**	**2.47**	**53.37**
20	4.11	32.71	6.66	20.12	2.47	53.37
24	4.11	32.71	6.66	20.12	2.47	53.37
25	4.11	32.71	6.66	20.12	2.47	53.37

The increase in NPV material ownership cost category is due to the variation in glazing type variable as Table 5.191 suggests. Since the rest of the variables were kept fixed in the parametric analysis, the associated cost values remained unchanged. The ownership cost of GT13 is the lowest among the selected windows.

Table 5.191 : Parametric analysis of glazing type based on NPV material cost breakdown (TL/m2) for Antalya.

GT	NPV EW Insul.	NPV Roof Insul.	NPV Roof layer	NPV Glazing	NPV EWOther
15	2.29	6.79	4.64	46.85	13.01
19	**2.29**	**6.79**	**4.64**	**46.13**	**13.01**
20	2.29	6.79	4.64	47.20	13.01
24	2.29	6.79	4.64	46.48	13.01
25	2.29	6.79	4.64	47.56	13.01

To conclude, the results showed that GT13 was able to balance building heating and cooling loads, lighting energy needs, associated energy costs and HVAC water costs for a reasonable glazing price. Therefore, the optimization methodology was

successful at recommending a cost-effective glazing solution for the Antalya case study within the given boundaries.

Window-to-wall ratio of southern façade (WTW S)

The application of the proposed optimization methodology to Antalya case study recommended 45 % of window-to-wall ratio for the south facing facade as the optimal solution, when combined with rest of the design recommendations. The results of the parametric investigation in Table 5.192 demonstrated that increasing w-t-w reduced the total global cost until 45% but then the cost started increasing. Moreover, a penalty occurred at 55% because the cooling capacity of the recommended chiller became insufficient with the introduction of 55 % w-t-w ratio.

The GC breakdown shows that larger windows decreased only NPV energy costs where NPV costs for water and material increased. NPV cost for equipment did not change.

Table 5.192 : Parametric analysis of southern façade window-to-wall ratio based on total Global Cost breakdown (TL/m2) for Antalya.

WTW S	PEN All	Total GC	NPV Energy	NPV Water	NPV Material	NPV Equipment
5	0	1072.12	781.83	106.19	64.67	119.44
15	0	1063.50	771.12	106.23	66.72	119.44
25	0	1057.53	762.91	106.42	68.76	119.44
35	0	1054.97	758.08	106.64	70.81	119.44
45	**0**	**1054.44**	**755.22**	**106.93**	**72.86**	**119.44**
55	1.10	1055.53	753.92	107.26	74.91	119.44

When we further investigated the NPV cost breakdown for the energy category given in Table 5.193, it was seen that increasing w-t-w ratio in the southern orientation slightly decreased natural gas cost for boiler since larger windows provided more heat gain in the southern orientation and reduced heating loads in winter period. However since the heating load was not dominant, its overall influence was minor. Similarly, increasing w-t-w ratio also decreased significantly electricity cost for artificial lighting due to the enhanced daylighting potential of the building when combined with the dimming control. On the other hand, larger south facing windows increased electricity cost for chiller, cooling tower, HVAC fans, and circulation pumps due to the higher heat gains and resulting cooling load in the summer period. The cost for water heating and plugged-in equipment remained unchanged since they were kept fixed in the analysis.

Table 5.193 : Parametric analysis of southern façade window-to-wall ratio based on NPV energy cost breakdown (TL/m2) for Antalya.

WTWS	NPV N.G. Boiler	NPV Elc. Chiller	NPV Elc. CTower	NPV Elc. HVACFan	NPV Elc. Pump	NPV N.G WH	NPV Elc. Lights	NPV Elc. Equipment
5	46.47	101.39	5.645	85.19	36.86	24.27	194.20	287.80
15	46.47	101.63	5.655	85.20	37.01	24.27	183.09	287.80
25	46.12	102.03	5.670	85.22	37.26	24.27	174.55	287.80
35	45.87	102.66	5.695	85.25	37.66	24.27	168.88	287.80
45	**45.54**	**103.49**	**5.726**	**85.29**	**38.03**	**24.27**	**165.08**	**287.80**
55	45.34	104.57	5.768	85.33	38.48	24.27	162.36	287.80

Table 5.194 summarizes the NPV cost breakdown for water. The water costs due to cooling tower use increased as w-t-w ratio increased, which is in line with the increase in cooling load and consequent chiller operation. However, hot water cost remained unchanged since associated water use was kept fixed in the analysis.

Table 5.194 : Parametric analysis of southern façade window-to-wall ratio based on NPV water cost breakdown (TL/m2) for Antalya.

WTW_S	NPV CTower	NPV Hot water
5	56.632	49.558
15	56.673	49.558
25	56.860	49.558
35	57.083	49.558
45	**57.368**	**49.558**
55	57.704	49.558

Table 5.195 below shows that there were no changes in the NPV equipment ownership cost categories. The number of required FCUs was allowed to match the building loads however; the load changes did not require any FCU update. The rest of the equipment cost categories remained unchanged as well as they were kept fixed in the parametric analysis.

Table 5.195 : Parametric analysis of southern façade window-to-wall ratio based on NPV equipment cost breakdown (TL/m2) for Antalya.

WTW_S	NPV Boiler	NPV Chiller	NPV CTower	NPV FCU	NPV WH	NPV LC
5	4.11	32.71	6.66	20.12	2.47	53.37
15	4.11	32.71	6.66	20.12	2.47	53.37
25	4.11	32.71	6.66	20.12	2.47	53.37
35	4.11	32.71	6.66	20.12	2.47	53.37
45	**4.11**	**32.71**	**6.66**	**20.12**	**2.47**	**53.37**
55	4.11	32.71	6.66	20.12	2.47	53.37

The increase in NPV material ownership cost is due to the changes in wall area and glazed area as given in Table 5.196. When w-t-w ratio increased, the area of wall component that holding the glazing decreased, therefore the cost for wall insulation and the rest of the non-insulation wall materials decreased accordingly. Conversely, the cost of glazing material increased with the w-t-w ratio, as it was expected.

The roof insulation and roof coating has no interaction with the w-t-w ratio therefore the associated cost values remained unchanged.

Table 5.196 : Parametric analysis of southern façade window-to-wall ratio based on NPV material cost breakdown (TL/m2) for Antalya.

WTW_S	NPV EW Insul.	NPV Roof Insul.	NPV Roof layer	NPV Glazing	NPV EWOther
5	2.69	6.79	4.64	35.28	15.27
15	2.59	6.79	4.64	37.99	14.70
25	2.49	6.79	4.64	40.70	14.14
35	2.39	6.79	4.64	43.42	13.57
45	**2.29**	**6.79**	**4.64**	**46.13**	**13.01**
55	2.19	6.79	4.64	48.84	12.44

To conclude, the results showed that 45% of w-t-w ratio at the southern façade was able to balance heating and cooling loads, artificial lighting and daylighting potential together with the ownership cost for wall insulation, non-insulation wall materials and glazing cost itself. Therefore, the optimization methodology was successful at recommending a cost-effective w-t-w ratio solution for the Antalya case study within the given boundaries.

Window-to-wall ratio of western façade (WTW W)

The application of the proposed optimization methodology to Antalya case study recommended 45 % of window-to-wall ratio for the west-facing facade as the optimal solution, in combination with the rest of the design recommendations. The results of the parametric investigation in Table 5.197 demonstrated that increasing w-t-w reduced the total global cost until 45% but then the cost started increasing. The GC breakdown explains that larger windows decreased only NPV energy costs where NPV costs for water, material and equipment increased.

In addition, a penalty values occurred with the introduction of 55% of w-t-w ratio because the cooling capacity of the recommended chiller started to became insufficient to meet the resulting cooling load.

Table 5.197 : Parametric analysis of western facade window-to-wall ratio based on total Global Cost breakdown (TL/m2) for Antalya.

WTWW	PEN All	Total GC	NPV Energy	NPV Water	NPV Material	NPV Equipment
5	0	1071.20	781.25	105.84	64.67	119.44
15	0	1062.89	770.75	105.99	66.72	119.44
25	0	1057.07	762.67	106.20	68.76	119.44
35	0	1054.64	757.85	106.54	70.81	119.44
45	**0**	**1054.44**	**755.22**	**106.93**	**72.86**	**119.44**
55	18.80	1055.91	754.19	107.38	74.91	119.44

When we further investigated the cost breakdown for the energy category given in Table 5.198, it was seen that increasing w-t-w ratio in the western orientation slightly increased than decreased natural gas cost for boiler as a result of increased heat gain due to larger windows combined with the less heat gain from artificial lighting with dimming control.

On the other hand, larger west facing windows increased electricity cost for chiller, cooling tower, HVAC fans, and circulation pumps due to higher heat gains and resulting cooling load in the summer period.

Furthermore, increasing w-t-w ratio also significantly decreased electricity cost for artificial lighting due to the enhanced daylighting potential of the building when combined with the dimming control.

The energy cost for water heating and plugged-in equipment remained unchanged since they were kept fixed in the analysis.

Table 5.198 : Parametric analysis of western facade window-to-wall ratio based on NPV energy cost breakdown (TL/m2) for Antalya.

WTWW	NPV N.G. Boiler	NPV Elc. Chiller	NPV Elc. CTower	NPV Elc. HVACFan	NPV Elc. Pump	NPV N.G WH	NPV Elc. Lights	NPV Elc. Equipment
5	45.74	99.97	5.583	85.11	37.62	24.27	195.16	287.80
15	45.79	100.43	5.601	85.13	37.67	24.27	184.05	287.80
25	45.76	101.15	5.631	85.17	37.76	24.27	175.13	287.80
35	45.73	102.21	5.674	85.22	37.89	24.27	169.05	287.80
45	**45.54**	**103.49**	**5.726**	**85.29**	**38.03**	**24.27**	**165.08**	**287.80**
55	45.49	105.01	5.789	85.35	38.27	24.27	162.20	287.80

Table 5.199 summarizes the NPV cost breakdown for water. The water costs due to cooling tower use increased as w-t-w ratio increased, which is in line with the

increase in cooling load and consequent chiller operation. However, hot water cost remained unchanged since associated water use was kept fixed in the analysis.

Table 5.199 : Parametric analysis of western facade window-to-wall ratio based on NPV water cost breakdown (TL/m2) for Antalya.

WTW_W	NPV CTower	NPV Hot water
5	56.284	49.558
15	56.431	49.558
25	56.639	49.558
35	56.985	49.558
45	**57.368**	**49.558**
55	57.823	49.558

The number of required FCUs was allowed to match the building loads however; the load changes did not require any FCU update as shown in Table 5.200. The rest of the systems were kept fixed during the analysis therefore, there were no cost variations in equipment ownership cost category.

Table 5.200 : Parametric analysis of western facade window-to-wall ratio based on NPV equipment cost breakdown (TL/m2) for Antalya.

WTW_W	NPV Boiler	NPV Chiller	NPV CTower	NPV FCU	NPV WH	NPV LC
5	4.11	32.71	6.66	20.12	2.47	53.37
15	4.11	32.71	6.66	20.12	2.47	53.37
25	4.11	32.71	6.66	20.12	2.47	53.37
35	4.11	32.71	6.66	20.12	2.47	53.37
45	**4.11**	**32.71**	**6.66**	**20.12**	**2.47**	**53.37**
55	4.11	32.71	6.66	20.12	2.47	53.37

The increase in NPV material cost is due to the changes in wall area and glazed area as given in Table 5.201.

Table 5.201 : Parametric analysis of western facade window-to-wall ratio based on NPV material cost breakdown (TL/m2) for Antalya.

WTW_W	NPV EW Insul.	NPV Roof Insul.	NPV Roof layer	NPV Glazing	NPV EWOther
5	2.69	6.79	4.64	35.28	15.27
15	2.59	6.79	4.64	37.99	14.70
25	2.49	6.79	4.64	40.70	14.14
35	2.39	6.79	4.64	43.42	13.57
45	**2.29**	**6.79**	**4.64**	**46.13**	**13.01**
55	2.19	6.79	4.64	48.84	12.44

When w-t-w ratio increased, the area of wall component that holding the glazing decreased accordingly, therefore the cost for wall insulation and the rest of the non-insulation wall materials decreased. Moreover, the cost of glazing material increased with the w-t-w ratio as it was expected.

The roof insulation and roof coating has no interaction with the w-t-w ratio therefore the associated cost values remained unchanged.

To conclude, the results showed that 45% of w-t-w ratio at the western façade was able to balance heating and cooling loads, artificial lighting and daylighting potential together with ownership cost for wall insulation, non-insulation wall materials and glazing itself. Therefore, the optimization methodology was successful at recommending a cost-effective w-t-w ratio solution for the Antalya case study within the given boundaries.

Window-to-wall ratio of northern façade (WTW N)

The application of the proposed optimization methodology to Antalya case study recommended 45 % of window-to-wall ratio for the north-facing facade as the optimal solution, in combination with the rest of the design recommendations. The results of the parametric investigation in Table 5.202 demonstrated that increasing w-t-w ratio reduced the total global cost until 55% and no penalties occurred. The GC breakdown explains that larger windows decreased only NPV energy costs where NPV costs for water, and material increased. The NPV equipment cost however remained same.

Table 5.202 : Parametric analysis of northern facade window-to-wall ratio based on total Global Cost breakdown (TL/m2) for Antalya.

WTW N	PEN All	Total GC	NPV Energy	NPV Water	NPV Material	NPV Equipment
5	0	1057.56	766.76	106.69	64.67	119.44
15	0	1056.39	763.50	106.74	66.72	119.44
25	0	1055.29	760.31	106.78	68.76	119.44
35	0	1054.54	757.42	106.87	70.81	119.44
45	**0**	**1054.44**	**755.22**	**106.93**	**72.86**	**119.44**
55	0	1054.91	753.54	107.03	74.91	119.44

When we further investigated the cost breakdown for the energy category given in Table 5.203, it was seen that increasing w-t-w ratio in the northern orientation slightly increased and decreased natural gas cost for boiler depending on the balance

between the thermal heat losses due to larger windows combined with the less heat gain from artificial lighting with dimming control. However, since the glazing had an improved U-value, having large windows could be tolerated.

Moreover, larger north facing windows also increased electricity cost slightly for chiller, cooling tower, HVAC fans, and circulation pumps. The cost for water heating and plugged-in equipment remained unchanged since they were kept fixed in the analysis.

However, increasing w-t-w ratio decreased electricity cost for artificial lighting a great deal due to the enhanced daylighting potential of the building when combined with the dimming control.

Table 5.203 : Parametric analysis of northern facade window-to-wall ratio based on NPV energy cost breakdown (TL/m2) for Antalya.

WTWN	NPV N.G. Boiler	NPV Elc. Chiller	NPV Elc. CTower	NPV Elc. HVACFan	NPV Elc. Pump	NPV N.G WH	NPV Elc. Lights	NPV Elc. Equipment
5	45.60	102.61	5.691	85.24	37.95	24.27	177.60	287.80
15	45.65	102.77	5.697	85.25	37.96	24.27	174.11	287.80
25	45.60	102.96	5.705	85.26	37.98	24.27	170.74	287.80
35	45.51	103.18	5.714	85.27	38.00	24.27	167.67	287.80
45	**45.54**	**103.49**	**5.726**	**85.29**	**38.03**	**24.27**	**165.08**	**287.80**
55	45.64	103.79	5.739	85.30	38.05	24.27	162.95	287.80

Table 5.204 summarizes the NPV cost breakdown for water. The water costs due to cooling tower use increased very slightly as w-t-w ratio increased, which is in line with the small increase in chiller electricity costs. However, hot water cost remained unchanged since associated water use was kept fixed in the analysis.

Table 5.204 : Parametric analysis of northern facade window-to-wall ratio based on NPV water cost breakdown (TL/m2) for Antalya.

WTW_N	NPV CTower	NPV Hot water
5	57.131	49.558
15	57.178	49.558
25	57.218	49.558
35	57.309	49.558
45	**57.368**	**49.558**
55	57.473	49.558

Table 5.205 shows that no changes were observed in the NPV equipment ownership cost category. The changes in the building thermal loads were minor therefore there

was no need to update the number of FCUs. Moreover, since the rest of the systems were kept fixed during the analysis, there were no cost variations as well.

Table 5.205 : Parametric analysis of northern facade window-to-wall ratio based on NPV equipment cost breakdown (TL/m2) for Antalya.

WTW_N	NPV Boiler	NPV Chiller	NPV CTower	NPV FCU	NPV WH	NPV LC
5	4.11	32.71	6.66	20.12	2.47	53.37
15	4.11	32.71	6.66	20.12	2.47	53.37
25	4.11	32.71	6.66	20.12	2.47	53.37
35	4.11	32.71	6.66	20.12	2.47	53.37
45	**4.11**	**32.71**	**6.66**	**20.12**	**2.47**	**53.37**
55	4.11	32.71	6.66	20.12	2.47	53.37

The increase in NPV material cost is only due to the changes in wall area and glazed area as given in Table 5.206. When w-t-w ratio increased, the area of wall component that holding the glazing decreased, therefore the cost for wall insulation and the rest of the non-insulation wall materials decreased accordingly. Moreover, the cost of glazing material increased with the w-t-w ratio as it was expected.

The roof insulation and roof coating has no interaction with the w-t-w ratio therefore the associated cost values remained unchanged.

Table 5.206 : Parametric analysis of northern facade window-to-wall ratio based on NPV material cost breakdown (TL/m2) for Antalya.

WTW_N	NPV EW Insul.	NPV Roof Insul.	NPV Roof layer	NPV Glazing	NPV EWOther
5	2.69	6.79	4.64	35.28	15.27
15	2.59	6.79	4.64	37.99	14.70
25	2.49	6.79	4.64	40.70	14.14
35	2.39	6.79	4.64	43.42	13.57
45	**2.29**	**6.79**	**4.64**	**46.13**	**13.01**
55	2.19	6.79	4.64	48.84	12.44

To conclude, the results showed that 45% of w-t-w ratio at the northern façade was able to balance heating and cooling loads, artificial lighting and daylighting potential together with the ownership costs for wall insulation, non-insulation wall materials and glazing cost itself. Therefore, the optimization methodology was successful at recommending a cost-effective w-t-w ratio solution for the Antalya case study within the given boundaries.

Window-to-wall ratio of eastern façade (WTW E)

The application of the proposed optimization methodology to Antalya case study recommended 35 % of window-to-wall ratio for the east-facing facade as the optimal solution, in combination with the rest of the design recommendations.

The results of the parametric investigation in Table 5.207 demonstrated that increasing w-t-w reduced the total global cost only until 35% but then the cost started increasing. The GC breakdown showed that larger windows decreased only NPV energy costs where NPV costs for water and material increased. NPV equipment ownership cost however remained same.

In addition, a very small penalty value occurred with the introduction of 55 % w-t-w ratio. A further investigation revealed that penalty value was due to under-capacity chiller equipment where selected chiller started to became insufficient to meet cooling needs.

Table 5.207 : Parametric analysis of eastern facade window-to-wall ratio based on total Global Cost breakdown (TL/m2) for Antalya.

WTW E	PEN All	Total GC	NPV Energy	NPV Water	NPV Material	NPV Equipment
5	0	1065.01	772.78	106.07	66.72	119.44
15	0	1058.33	763.86	106.27	68.76	119.44
25	0	1054.66	757.88	106.54	70.81	119.44
35	0	1054.44	755.22	106.93	72.86	119.44
45	**0**	**1055.83**	**754.17**	**107.31**	**74.91**	**119.44**
55	0.06	1057.60	753.46	107.74	76.96	119.44

When we analysed the cost breakdown for the NPV energy category given in Table 5.208, it was seen that increasing w-t-w ratio in the eastern orientation decreased slightly the natural gas cost for boiler due to the combined impact of heat gain due to larger windows in winter and less heat gain from artificial lighting with dimming control.

On the other hand, larger east facing windows also slightly increased electricity cost for chiller, cooling tower, HVAC fans, and circulation pumps due to higher heat gains and resulting cooling load in the summer period. The cost for water heating and plugged-in equipment remained unchanged since they were kept fixed in the analysis.

Increasing w-t-w ratio had the most influence on artificial lighting costs since the larger windows enhanced daylighting potential of the building when combined with the dimming control.

Table 5.208 : Parametric analysis of eastern facade window-to-wall ratio based on NPV energy cost breakdown (TL/m2) for Antalya.

WTWE	NPV N.G. Boiler	NPV Elc. Chiller	NPV Elc. CTower	NPV Elc. HVACFan	NPV Elc. Pump	NPV N.G WH	NPV Elc. Lights	NPV Elc. Equipment
5	45.88	100.72	5.610	85.15	37.71	24.27	185.65	287.80
15	45.81	101.30	5.635	85.17	37.74	24.27	176.13	287.80
25	45.73	102.23	5.674	85.22	37.86	24.27	169.10	287.80
35	45.54	103.49	5.726	85.29	38.03	24.27	165.08	287.80
45	**45.55**	**104.87**	**5.783**	**85.37**	**38.22**	**24.27**	**162.31**	**287.80**
55	45.41	106.31	5.842	85.45	38.40	24.27	159.99	287.80

Table 5.209 summarizes the NPV cost breakdown for water.

Table 5.209 : Parametric analysis of eastern facade window-to-wall ratio based on NPV water cost breakdown (TL/m2) for Antalya.

WTW_E	NPV CTower	NPV Hot water
5	56.515	49.558
15	56.712	49.558
25	56.978	49.558
35	57.368	49.558
45	**57.756**	**49.558**
55	58.186	49.558

The water costs due to cooling tower use increased slightly as the w-t-w ratio increased, which is in line with the increase in cooling load and consequent chiller operation. However, hot water cost remained unchanged since associated water use was kept fixed in the analysis.

Table 5.210 shows that no changes were observed in the NPV equipment cost category. The changes in the building thermal loads were minor therefore there was no need to update the number of FCUs. Moreover, since the rest of the systems were kept fixed during the analysis, there were no cost variations as well.

Table 5.210 : Parametric analysis of eastern facade window-to-wall ratio based on NPV equipment cost breakdown (TL/m2) for Antalya.

WTW_E	NPV Boiler	NPV Chiller	NPV CTower	NPV FCU	NPV WH	NPV LC
5	4.11	32.71	6.66	20.12	2.47	53.37
15	4.11	32.71	6.66	20.12	2.47	53.37
25	4.11	32.71	6.66	20.12	2.47	53.37
35	4.11	32.71	6.66	20.12	2.47	53.37
45	**4.11**	**32.71**	**6.66**	**20.12**	**2.47**	**53.37**
55	4.11	32.71	6.66	20.12	2.47	53.37

The increase in NPV material cost is due to the changes in wall area and glazed area as given in Table 5.211. When w-t-w ratio increased, the area of wall component that holding the glazing decreased, therefore the ownership cost for wall insulation and the rest of the non-insulation wall materials decreased accordingly. Moreover, the ownership cost of glazing material increased with the w-t-w ratio as it was expected.

The roof insulation and roof coating has no interaction with the w-t-w ratio therefore the associated cost values remained unchanged.

Table 5.211 : Parametric analysis of eastern facade window-to-wall ratio based on NPV material cost breakdown (TL/m2) for Antalya.

WTW_E	NPV EW Insul.	NPV Roof Insul.	NPV Roof layer	NPV Glazing	NPV EWOther
5	2.59	6.79	4.64	37.99	14.70
15	2.49	6.79	4.64	40.70	14.14
25	2.39	6.79	4.64	43.42	13.57
35	2.29	6.79	4.64	46.13	13.01
45	**2.19**	**6.79**	**4.64**	**48.84**	**12.44**
55	2.09	6.79	4.64	51.56	11.87

To conclude, the results showed that 35% of w-t-w ratio at the eastern façade was able to balance heating and cooling loads, artificial lighting and daylighting potential together with the ownership cost for FCUs, wall insulation, non-insulation wall materials and glazing cost itself. Therefore, the optimization methodology was successful at recommending a cost-effective w-t-w ratio solution for the Antalya case study within the given boundaries.

Boiler type (BLtype)

The application of the proposed optimization methodology to Antalya case study recommended Boiler 42 from the equipment database as the optimal choice in combination with the rest of the design recommendations. The parametric analysis

carried out with a sample of low-efficiency (BL 14-16) and high-efficiency (BL 41-43) boiler equipment from the database. The results of the parametric investigation in Table 5.212 demonstrate that the switching from low efficiency equipment to high efficiency equipment decreased total global costs noticeably.

In addition, BL14, and BL41 were penalized because their heating capacities were not able to satisfy resulting heating load of the recommended design combination.

The GC breakdown explains that improvement on the boiler thermal efficiency let to a significant reduction in NPV energy category while causing a little rise on the NPV equipment costs. However, NPV cost for water and material remained unchanged, as they were not influenced with the boiler replacement. The amount of the cost reduction depends on the thermal capacity of the tested equipment.

Table 5.212 : Parametric analysis of boiler type based on total Global Cost breakdown (TL/m2) for Antalya.

BLtyp	PEN All	Total GC	NPV Energy	NPV Water	NPV Material	NPV Equipment
14	128.79	1057.50	760.68	106.90	72.86	117.06
15	0	1058.09	761.14	106.90	72.86	117.19
16	0	1058.81	761.69	106.90	72.86	117.35
41	267.28	1053.38	754.75	106.90	72.86	118.84
42	**0**	**1054.44**	**755.22**	**106.90**	**72.86**	**119.44**
43	0	1055.25	755.71	106.90	72.86	119.74

According to the Table 5.213 improving boiler efficiency only improved boiler NPV energy cost as expected. Moreover, the resulting boiler energy cost also depends also capacity of the tested boiler equipment. The rest of the energy cost categories remained same.

Table 5.213 : Parametric analysis of boiler type based on NPV energy cost breakdown (TL/m2) for Antalya.

BLtyp	NPV N.G. Boiler	NPV Elc. Chiller	NPV Elc. CTower	NPV Elc. HVACFan	NPV Elc. Pump	NPV N.G WH	NPV Elc. Lights	NPV Elc. Equipment
14	51.00	103.49	5.73	85.29	38.03	24.27	165.08	287.80
15	51.46	103.49	5.73	85.29	38.03	24.27	165.08	287.80
16	52.02	103.49	5.73	85.29	38.03	24.27	165.08	287.80
41	45.07	103.49	5.73	85.29	38.03	24.27	165.08	287.80
42	**45.54**	**103.49**	**5.73**	**85.29**	**38.03**	**24.27**	**165.08**	**287.80**
43	46.04	103.49	5.73	85.29	38.03	24.27	165.08	287.80

Table 5.214 summarizes the NPV cost breakdown for water. Both the water costs due to cooling tower use and hot water use remained unchanged since associated water use did not interact with the boiler replacement.

Table 5.214 : Parametric analysis of boiler type based on NPV water cost breakdown (TL/m2) for Antalya.

BLtyp	NPV CTower	NPV Hot water
14	57.341	49.558
15	57.341	49.558
16	57.341	49.558
41	57.341	49.558
42	**57.341**	**49.558**
43	57.341	49.558

As demonstrated in Table 5.215, the only change in NPV equipment cost occurred in boiler category as expected. The efficiency and capacity improvement increased the equipment costs. The more efficient equipment cost almost double of the low efficiency group. BL14 and BL41 were not able to satisfy heating loads as penalties occurred. Even BL15, BL16, and BL43 remained in the allowed equipment capacity range; they were not preferred since there was smaller size high-efficient equipment that can still meet the load.

Table 5.215 : Parametric analysis of boiler type based on NPV equipment cost breakdown (TL/m2) for Antalya.

BLtyp	NPV Boiler	NPV Chiller	NPV CTower	NPV FCU	NPV WH	NPV LC
14	1.73	32.71	6.66	20.12	2.47	53.37
15	1.86	32.71	6.66	20.12	2.47	53.37
16	2.02	32.71	6.66	20.12	2.47	53.37
41	3.51	32.71	6.66	20.12	2.47	53.37
42	**4.11**	**32.71**	**6.66**	**20.12**	**2.47**	**53.37**
43	4.41	32.71	6.66	20.12	2.47	53.37

As shown in Table 5.216, there were no cost changes in the NPV material category since there were no interactions between building material and boiler replacement in the parametric analysis.

Table 5.216 : Parametric analysis boiler type based on NPV material cost breakdown (TL/m2) for Antalya.

BLtyp	NPV EW Insul.	NPV Roof Insul.	NPV Roof layer	NPV Glazing	NPV EWOther
14	2.29	6.79	4.64	46.13	13.01
15	2.29	6.79	4.64	46.13	13.01
16	2.29	6.79	4.64	46.13	13.01
41	2.29	6.79	4.64	46.13	13.01
42	**2.29**	**6.79**	**4.64**	**46.13**	**13.01**
43	2.29	6.79	4.64	46.13	13.01

To conclude, the results showed that BL45 showed an improved energy performance while being capable of meeting building heating loads for an affordable equipment price in Antalya case study. Therefore, the proposed optimization methodology successfully recommended a cost-effective boiler solution within the given boundaries.

Chiller type (CLtype)

The application of the proposed optimization methodology to Antalya case study recommended Chiller 32 from the equipment database as the optimal choice in combination with the rest of the design recommendations. The parametric analysis carried out with a sample of moderate efficiency (CL 9-11) and high efficiency (CL 31-33) chiller equipment. The results of the parametric investigation in Table 5.217 demonstrate that the switching from moderate efficiency equipment to high efficiency equipment decreased total global costs.

The GC breakdown explains that improvement on the chiller efficiency let to a considerable reduction in NPV energy category while causing a little rise on NPV equipment costs depending on the capacity of the tested equipment. However, NPV cost for water and material were not influenced with the chiller replacement.

Table 5.217 : Parametric analysis of chiller type based on total Global Cost breakdown (TL/m2) for Antalya.

CLtyp	PEN All	Total GC	NPV Energy	NPV Water	NPV Material	NPV Equipment
9	3590.35	1085.24	793.20	107.16	72.86	112.01
10	8.52	1089.83	793.64	109.12	72.86	114.22
11	0	1094.87	794.85	110.82	72.86	116.34
31	956.02	1053.56	756.62	105.93	72.86	118.15
32	**0**	**1054.44**	**755.22**	**106.93**	**72.86**	**119.44**
33	0	1058.00	754.68	108.56	72.86	121.90

In addition, only CL11, CL32 and CL33 were able to comply with the constraints and not penalized. However, CL9, CL10 and CL31 were penalized because they were not able to satisfy cooling load of the tested design combination.

According to the Table 5.218 improving chiller efficiency improved chiller NPV energy cost together with cooling tower electricity costs as expected. Moreover, the chiller electricity cost increased in parallel with the increase in the equipment capacity. In addition, minor changes occurred in electricity cost for fans and circulation pumps. The rest of the energy cost categories remained uninfluenced, as they did not interact with the chiller

Table 5.218 : Parametric analysis of chiller type based on NPV energy cost breakdown (TL/m2) for Antalya.

CLtyp	NPV N.G. Boiler	NPV Elc. Chiller	NPV Elc. CTower	NPV Elc. HVACFan	NPV Elc. Pump	NPV N.G WH	NPV Elc. Lights	NPV Elc. Equipment
9	45.54	143.030	5.879	85.417	36.189	24.27	165.08	287.80
10	45.54	141.087	5.980	85.302	38.580	24.27	165.08	287.80
11	45.54	139.946	6.045	85.272	40.902	24.27	165.08	287.80
31	45.54	106.277	5.688	85.332	36.635	24.27	165.08	287.80
32	**45.54**	**103.488**	**5.726**	**85.288**	**38.031**	**24.27**	**165.08**	**287.80**
33	45.54	100.583	5.775	85.267	40.372	24.27	165.08	287.80

Table 5.219 summarizes the NPV cost breakdown for water. Water cost due to cooling tower use was slightly improved by switching to a higher efficiency chiller depending on equipment capacity. However, hot water cost remained same as it was kept fixed in the analysis.

Table 5.219 : Parametric analysis of chiller type based on NPV water cost breakdown (TL/m2) for Antalya case

CLtyp	NPV CTower	NPV Hot water
9	57.604	49.558
10	59.557	49.558
11	61.265	49.558
31	56.372	49.558
32	**57.368**	**49.558**
33	59.002	49.558

As demonstrated in Table 5.220, the only major change in NPV equipment cost occurred in chiller category as expected. The efficiency and capacity improvements increased equipment ownership cost accordingly.

Table 5.220 : Parametric analysis of chiller type based on NPV equipment cost breakdown (TL/m2) for Antalya.

CLtyp	NPV Boiler	NPV Chiller	NPV CTower	NPV FCU	NPV WH	NPV LC
9	4.11	25.74	6.20	20.12	2.47	53.37
10	4.11	27.41	6.75	20.12	2.47	53.37
11	4.11	29.00	7.27	20.12	2.47	53.37
31	4.11	31.74	6.35	20.12	2.47	53.37
32	**4.11**	**32.71**	**6.66**	**20.12**	**2.47**	**53.37**
33	4.11	34.63	7.20	20.12	2.47	53.37

As shown in Table 5.221, there were no cost changes in the material category since there were no interactions between building material and chiller equipment in the parametric analysis.

Table 5.221 : Parametric analysis chiller type based on NPV material cost breakdown (TL/m2) for Antalya.

CLtyp	NPV EW Insul.	NPV Roof Insul.	NPV Roof layer	NPV Glazing	NPV EWOther
9	2.29	6.79	4.64	46.13	13.01
10	2.29	6.79	4.64	46.13	13.01
11	2.29	6.79	4.64	46.13	13.01
31	2.29	6.79	4.64	46.13	13.01
32	**2.29**	**6.79**	**4.64**	**46.13**	**13.01**
33	2.29	6.79	4.64	46.13	13.01

To conclude, the results showed that CL32 showed an improved energy performance while being capable of meeting building cooling loads for an affordable equipment price in Antalya case study. Therefore, the proposed optimization methodology recommended successfully a cost-effective chiller solution within the given boundaries.

Lighting control (LC)

The application of the proposed optimization methodology to Antalya case study recommended dimming control of artificial lights (option 1) according to indoor daylighting levels as the optimal choice over manual lighting control (option 0), when combined with rest of the design recommendations. The results of the parametric investigation in Table 5.222 demonstrate that dimming control of lights resulted in a major GC reduction. Moreover, the cost breakdown explains that dimming control reduces not only NPV energy costs but also water cost as well. NPV for material were not influenced however, NPV for equipment was increased.

In addition, the case with manual light control was strongly penalized because the chiller equipment could not satisfy resulting cooling load in this combination.

Table 5.222 : Parametric analysis of lighting control strategies based on total Global Cost breakdown (TL/m2) for Antalya.

LC	PEN All	Total GC	NPV Energy	NPV Water	NPV Material	NPV Equipment
0	1136.52	1198.19	910.11	111.68	72.86	103.53
1	**0**	**1054.44**	**755.22**	**106.93**	**72.86**	**119.44**

According to the Table 5.223, dimming control of lights over daylighting increased boiler natural gas cost in part due to the reduction in heat gain from lighting system. However, it decreased electricity cost for chiller, cooling tower, fans, and pumps a great deal in addition to the major decrease in lighting electricity cost. The rest of the energy cost categories remained uninfluenced, as they did not interact with the lighting system.

Table 5.223 : Parametric analysis of lighting control strategies based on NPV energy cost breakdown (TL/m2) for Antalya.

LC	NPV N.G. Boiler	NPV Elc. Chiller	NPV Elc. CTower	NPV Elc. HVACFan	NPV Elc. Pump	NPV N.G WH	NPV Elc. Lights	NPV Elc. Equipment
0	43.71	117.94	6.279	86.06	40.40	24.27	303.65	287.80
1	**45.54**	**103.49**	**5.726**	**85.29**	**38.03**	**24.27**	**165.08**	**287.80**

Table 5.224 summarizes the NPV cost breakdown for water. Water costs due to cooling tower use were moderately improved with dimming control where hot water cost remained same as it was kept fixed in the analysis.

Table 5.224 : Parametric analysis of lighting control strategies based on NPV water cost breakdown (TL/m2) for Antalya.

LC	NPV CTower	NPV Hot water
0	62.120	49.558
1	**57.368**	**49.558**

As demonstrated in Table 5.225, the major change in equipment cost occurred in lighting control system category as installing dimming control costs more than manual control system. In addition, the ownership cost for FCUs decreased with dimming control due to the decrease in heat gain from lighting system and the decrease in cooling load and required number of FCUs from 53 to 51.

Table 5.225 : Parametric analysis of lighting control strategies based on NPV equipment cost breakdown (TL/m2) for Antalya.

LC	NPV Boiler	NPV Chiller	NPV CTower	NPV FCU	NPV WH	NPV LC
0	4.11	32.71	6.66	20.91	2.47	36.68
1	**4.11**	**32.71**	**6.66**	**20.12**	**2.47**	**53.37**

As shown in Table 5.226, there were no cost changes in the NPV material category since there were no interactions between building material and the lighting system.

Table 5.226 : Parametric analysis of lighting control strategies based on NPV material cost breakdown (TL/m2) for Antalya.

LC	NPV EW Insul.	NPV Roof Insul.	NPV Roof layer	NPV Glazing	NPV EWOther
0	2.29	6.79	4.64	46.13	13.01
1	**2.29**	**6.79**	**4.64**	**46.13**	**13.01**

To conclude, the results showed that dimming control of artificial lights according to daylighting levels decreased the electricity cost for lighting together with electricity cost for cooling system for an affordable price. The slight increase in energy cost for heating was compensated with other benefits. Therefore, the proposed optimization methodology was successful at recommending a cost-effective lighting control solution within the given boundaries.

5.4 Summary

In this chapter, the feasibility of applying the proposed simulation-based optimization methodology to high-performance building design process was demonstrated by three case studies located in Istanbul, Ankara and Antalya. The selected cities represent different climatic regions in Turkey including mild-humid, mild-dry and hot-humid conditions.

At first, a hypothetical generic office building was developed according to common construction practices in Turkey, where energy efficiency was not at the heart of the design priorities. Secondly, candidate design variables were selected and their value ranges were established. A parametric analysis was carried out then among candidate variables to find out the sensitivity index of each parameter. Based on the results, the parameters that are found to be insensitive within the scope of the problem were eliminated.

The solution-space of the case studies covered a wide range of discrete design variables including wall and roof insulation thickness, roof coating type, glazing type, window-to-wall ratio of each façade, chiller and boiler equipment size and type (considering full load and part load performances), number and type of photovoltaic module for PV system integration and number and type of solar collector module for solar water heating system integration.

In order to create a real-world application case, technical and cost information regarding the actual building materials and system equipment was collected from the Turkish construction market and a comprehensive product database was prepared. The database included data about thermal and optical properties of envelope materials, capacity, full load and part load efficiency of building system equipment and, product life, cost data of the each product including capital cost, installation fees, maintenance costs and scrap values. Collecting cost data was found to be problematic as no national level baseline cost levels are established and costs are highly volatile.

Lastly, the optimization calculations were carried out, results are analysed and discussed. Each optimization run took about 20 hours on a moderate capacity computer with 16 GB RAM and 3.4 GHz processor.

The results showed that proposed methodology succeeded in recommending climate-appropriate and feasible new design options that are cost-efficient and energy-efficient within building service life while improving occupant's comfort and building CO_2 emission performance.

The validation of the methodology was assessed through a parametric analysis where optimized case is taken as initial scenario. The results showed that no further improvements are available for the considered case studies and the design options recommended by the proposed methodology were found as the optimum values within the scope of each case study. Therefore, for the case study applications of the current study it was accepted that the optimization method is capable of reliably identifying the optimum combination of design options.

To conclude, the work presented in this chapter showed that the proposed methodology could be successfully applied to building design problem for cost-effective energy-efficient building design solutions.

6. CONCLUSION AND FUTURE WORK

Buildings are one of the major energy consuming sectors in the world where they account for one-third of all final energy use and half of global electricity consumption. They are also an important source of carbon dioxide emissions because of their high energy consumption intensities. Therefore achieving energy efficiency in building sector plays a key role in reaching global energy and environmental targets as explained in IPCC publications (IPCC, 2007a; IPCC, 2007b).

Unlocking the energy efficiency potential in the building sector is becoming a priority for many countries. The European Commission states in the Energy Efficiency Plan that the greatest energy saving potential lies in buildings (EC, 2011) and therefore the European Directive on Energy Performance of Buildings requires all new buildings to be nearly zero-energy buildings by the end of 2020, and all new buildings occupied and owned by public authorities are nearly zero-energy buildings by 31 December 2018.

Fortunately, the professionals in the sector are beginning to realize that conventionally designed, constructed and operated buildings where design decisions are made by different team members independent of each other are not sufficient to address building energy efficiency targets set by authorities and the consequent global environmental challenges. Therefore, new design concepts and technologies are being emerged today and high energy performance buildings that can exceed current requirements of basic building standards are evolving from theory to reality.

Advances in building science and technology have introduced many approaches and options that can help improving building performance; however, designing for energy efficiency is still not straightforward. There are many expectations from buildings, for example to use as minimum energy and resources possible, to improve the health, comfort and productivity of their occupants and to limit the harmful environmental effects during building lifespan. Moreover, buildings are also expected to offer all these competing merits at reasonable costs. For instance, the recast version of the European Directive on Energy Performance of Buildings

underlines the necessities of a future building activity aimed at the most proper level of energy efficiency with a view to achieving cost-optimal levels (EPBD, 2010).

Many building design goals are in conflict and require a trade-off, and when combined with numerous design alternatives it could be rather difficult to select what design strategies to adopt and which technologies to implement through the application of simple design approaches.

Whole Building Design concept, which refers to a design and construction technique that incorporates an integrated design approach and an integrated team process, is introduced in the last decade to support creation of high energy performance buildings (WBDG, 2014). Whole Building Design views the building as a system, rather than a collection of components and it requires a multi-disciplinary strategy that effectively integrates all aspects of site development, building design, construction, and operations and maintenance.

In order to apply effectively Whole Building Design concept in real-life building projects, quantitative methods that can provide insight information about the building performance is strongly required. The interactions between building and building systems need be analysed and performance indicators for design options are required to be calculated and compared before decision-making.

Building performance simulation is now a widely accepted technique that is capable of predicting building performance through numerical representation of a building and system model, prior to construction. BPS allows designer studying the influence of every design decision on the building energy response therefore it helps capturing an instance but it does not give an answer to what is the best solution for a particle design problem under given boundaries. Designer is required to set up several simulation studies, change the values of design variables manually and test performances of all the design combinations based on a trial-and-error approach. This labour-intensive and human-driven approach can lead to improved results but in many cases, it is extremely unlikely to achieve the best solution, especially for the cases with complex buildings. Therefore, there is a strong need to automate the search procedure.

Simulation-based building performance optimization has been introduced as a promising solution to deal with the difficulties of applying simulation based techniques into building design challenges. Coupling simulation tools with optimization engines allow computing the optimal values of several design alternatives automatically therefore it has a significant potential in informing building experts during decision-making.

There is a significant contribution to building design optimization in the literature therefore firstly a thorough discussion of achievements was given in the scope of this study.

The literature review showed that there is certain amount of work has been done on a variety of building design issues. Some of the research efforts mainly focused on developing efficient search techniques and algorithms suitable for the building design optimization problem, while majority of the studies concentrated on problem formulation.

Most of the problem formulation approaches focused mainly on optimal design of building architectural design characteristics (construction/envelope parameters). Moreover, HVAC system design and efficient operation of individual devices through optimization has been investigated, too. There are also some studies proposed to address renewable system and component design with application of optimization. However, holistic approaches that aim to combine building architectural features, HVAC system features and renewable generation features simultaneously while taking into account various dimensions of building performance were in limited number.

Therefore the aim of the this thesis has been to investigate a holistic simulation-based optimization methodology that can quantitatively assess combinations of actual technology choices from building architectural design, HVAC systems and renewable energy generation systems simultaneously for cost-effective energy efficiency together with building environmental performance and the occupants thermal comfort.

The main aim of the proposed optimization scheme was to computationally design buildings that can achieve energy efficiency for the lowest possible global costs while limiting building related CO_2 emission without sacrificing user thermal

comfort during building operation for real-world design challenges. Moreover, water consumption as a result of building HVAC system use was also addressed.

The developed optimization framework consisted of three main modules: the optimizer, the simulator, and a user-created energy efficiency measures database. The responsibility of the optimizer is to control the entire process by implementing the optimization algorithm, to trigger simulation for performance calculation, to assign new values to variables, to calculate objective function, to impose constraints, and to check stopping criteria. The optimizer module is based on GenOpt optimization environment. However, a sub-module was added to optimization scheme to enable GenOpt to communicate with the user-created database module. Therefore, every time the value of a variable is updated, the technical and financial information of a matching product or system equipment is read from the database and written into simulation model and fed to the objective formula.

The simulator evaluates energy-related performance metrics and functional constraints through dynamic simulation techniques provided by EnergyPlus.

The database defines and organizes design variables and stores user-collected cost related, technical and non-technical data about the building energy efficiency measures to be tested during the optimization.

An updated version of Particle Swarm Optimization with constriction coefficient is used as the optimization algorithm.

In the problem formulation, the building performance is taken integrally as one-problem and the interactions between building structure, lighting system, pre-designed HVAC systems, sanitary water heating system and building-integrated renewable energy systems are captured simultaneously. The full coupling of thermal load, secondary system, plant and energy sources where there is a feedback from the supply-side to the demand-side provided a better understanding of how a building responds to the changing indoor and outdoor environmental factors therefore was able to capture the dynamic changes when a proposed HVAC system equipment is capable or not capable of meeting thermal loads.

The optimization process was motivated by the aim to improve performance of a base case design scenario created by the user. The optimizer module initiated creating alternative design scenarios by combining the variable options according to

optimization search principles. At each optimization iteration, a design day calculation for summer and winter periods was run to predict the building heating and cooling loads. Once the load was established, the optimization algorithm sought to determine the most suitable boiler and chiller equipment among a user-created equipment library while preventing capacity mismatch through penalty approach. Equipment selection focused on both the equipment capacity to be able to meet the estimated maximum peak load and on-reference/off-reference equipment behaviour to provide the best dynamic performance throughout the year. In addition, dependent equipment such as cooling tower, room terminal units are also sized and selected with an aim to complement the HVAC design suitably. Moreover, when integrated with the rest of the building system, right-size of renewable systems together with ideal equipment components were also searched through optimization. The procedure was iterated until a predefined stopping criterion is satisfied.

The objective function of the study was formulated as a single objective function, which is capable of including multi-dimension design aims. The primary objective was taken as minimization of building global costs due to changes in design variables therefore it included minimization of costs occur due to operational energy and water consumption together with ownership costs of building materials and building systems. Moreover, a set of penalty functions including equipment capacity, user comfort, CO_2 emissions and renewable payback period were added to the main objective function in the form of constraints to restrict the solution region to user-set design target. Consequently, multi-objective design aims were translated into a single-objective where the penalty functions acted as secondary objectives.

After an exhaustive description of the method, the performance of the proposed optimization methodology was evaluated through a case study implementation where different design scenarios were created, optimized and analysed. A hypothetical base case office building was defined. Three cities located in Turkey namely Istanbul, Ankara and Antalya were selected as building locations. Therefore, the performance of the methodology in different climatic conditions was investigated. An equipment database consists of actual building materials and system equipment commonly used in Turkish construction sector was prepared. In addition, technical and financial data necessary for objective function calculation were collected from the market.

The results of the case studies showed that application of the proposed methodology achieved giving climate-appropriate design recommendations, which resulted in major cost reductions and energy savings. Moreover new design alternatives also showed significantly better environmental performances as the CO_2 rates sharply decreased. Similarly, occupant thermal comfort was improved with the new design suggestions.

In Istanbul case study, if all design suggestions given by the proposed optimization methodology including PV and SWH system configurations was adopted, the building overall energy consumption from non-renewables would decrease by 44%, annual CO2 emission rate would decrease by 49 % and the building global costs can be would decrease by 21.7 %.

Similarly, in Ankara case study, if all design suggestions given by the proposed optimization method was adopted, the building overall energy consumption from non-renewables would decrease by 47.3%, annual CO2 emission rate would decrease by 50.4 % and the building global costs would decrease by 23.3 % while improving the overall building comfort.

If all design suggestions given by the proposed optimization method are adopted, the building overall energy consumption from non-renewables can be decreased by 57.5%, annual CO2 emission rate can be decreased by 60.3 % and the building global costs can be decreased by 30.4 % while improving the overall building comfort.

Finally, in Antalya case study, if all design suggestions given by the proposed optimization method was adopted, the building overall energy consumption from non-renewables could decrease by 57.5%, annual CO2 emission rate could decrease by 60.3 % and the building global costs could decrease by 30.4 % while improving the overall building comfort.

The results of the case study were also validated through a set of parametric experiments. The outputs of the tests showed that optimization achieved obtaining reasonable optimum results within a good accuracy.

One of the most important contributing factors of this thesis is introducing an integrative method where building architectural elements, HVAC system equipment

and renewable systems are simultaneously investigated and optimized while interactions between building and systems are being dynamically captured.

Moreover, this research is distinctive from previous studies because it makes possible investigating actual market products as energy efficiency design options through its database application and a sub-program that connect optimization engine with the data library. Therefore, application of the methodology can provide support on real-world building design projects and can prevent a mismatch between the optimization recommendations and the available market solutions. However, great care has to be taken to collect accurate and consistent technical and cost data of the energy efficiency measures.

Furthermore, another contributing merit of this research is that it achieves formulating competing building design aims in a single objective function, which can still capture multi-dimensions of building design challenge. Global costs are minimized while energy savings are achieved, CO2-equivelient emission is reduced, right-sized equipment are selected, thermal comfort is provided to users and target payback periods of investments are assured.

In addition to capability to address several objectives, a large number of design variables could also be evaluated through the efficient structure of the framework due to database application.

This research also suggests a time-saving search method due to its PSO algorithm settings. A huge solution space with more than 3.19E11 design possibilities are explored efficiently by only an average of 5000 evaluations.

However, even though this research showed promise to design buildings as a cost-effective and energy-efficient engineered system, it can still be improved in different ways:

The adopted Particle Swarm Optimization Algorithm seems to be efficient for such optimization aims however, other evolutionary algorithms such as Genetic Algorithm and Hybrid Particle Swarm Algorithm can be included as an alternative to the optimization framework and the efficiencies of different algorithms can be compared.

The performance of single objective formulation of design aims can be expressed as multi-objective formulation and the optimization performances can be eventually analysed and compared.

The current method has the capability of optimizing components of only one type of HVAC system in one optimization run. Therefore, it would be interesting as a future work to expand the capacity to assess and compare different HVAC systems together.

Although the current methodology is able address a large number of common design variables and tested for many from different categories still new variables for instance building form, shading design, site design could be integrated into the optimization structure for a more realistic building architectural design investigation.

Optimization objective expresses building environmental performance based on building annual CO_2 emission rate, however, the impact of other greenhouse gases could be added to the objective formula for more detailed analysis.

Current methodology considers energy efficiency and energy performance only during building operational phase, therefore embodied energy is not considered. In the future, a cradle-to-cradle life cycle assessment approach could be adopted for a better representative of actual design considerations and to contribute more to the sustainability.

To conclude, the proposed methodology links building energy performance requirements to financial and environmental targets and it provides a promising structure for addressing real life building design challenges through fast and efficient optimization techniques.

REFERENCES

Adamski, M. (2007). Optimization of the form of a building on an oval base, *Building and Environment, 42*, 1632–1643.

Aitken, D. (1998). *Whole Buildings: An Integrating R&D and Policy Frameworkfor the 21st Century*, UCS Publications, Cambridge, MA.

Al-Anzi, A., Seo, D., Krarti M. (2009). Impact of building shape on thermal performance of office buildings in Kuwait, *Energy Conversion and Management, 50*(3), 822–828.

Al-Homoud M. S. (2005). A systematic approach for the thermal design optimization of building envelopes. *Journal of Building Physics, 29*(2), 95–119.

Al-Homoud, M. S. (2005). Performance characteristics and practical applications of common building thermal insulation materials, *Building and Environment, 40*, 353–366.

Al-Sanea, S.A. & Zedan, M.F. (2011). Improving thermal performance of building walls by optimizing insulation layer distribution and thickness for same thermal mass, *Applied Energy, 88*, 3113–3124.

Al-Tamimi, N. A., Fadzil, S. F. S., Harun W. M. (2011). The Effects of Orientation, Ventilation, and Varied WWR on the Thermal Performance of Residential Rooms in the Tropics, *Journal of Sustainable Development, 4*(2), 142-149.

Ali M., Vukovic V., M. Sahir H., Fontanella G. (2013). Energy analysis of chilled water system configurations using simulation-based optimization, *Energy and Buildings, 59*, 111–122**.**

Akbari, H., Kurn, D.M., Bretz, S.E., Hanford, J.W. (1997). Peak power and cooling energy savings of shade tree. *Energy and Buildings, 25*, 139–148.

Ander G. D. (2003). *Daylighting Performance and Design*, John Wiley & Sons. ISBN 0471262994.

Ardente F., Beccali G., Cellura M., Lo Brano V. (2005). Life cycle assessment of a solar thermal collector, *Renewable Energy, 30*, 1031–1054.

Arora, J. S. (2012). *Introduction to Optimum Design, Third Edition*, Oxford, UK: Academic Press.

Asadi E., Silva M. G., Antunes C. H., Dias L. (2012). A multi-objective optimization model for building retrofit strategies using TRNSYS simulations, GenOpt and MATLAB, *Building and Environment, 56*, 370-378.

Asadi E., Silva M. G., Antunes C. H., Dias L., Glicksmanf L. (2014). Multi-objective optimization for building retrofit: A model using genetic algorithm and artificial neural network and an application, *Energy and Buildings*, *81*, 444–456.

Al-Sanea, S.A., Zedan, M.F., Al-Hussain, S.N. (2012). Effect of thermal mass on performance of insulated building walls and the concept of energy savings potential, *Applied Energy*, *89*, 430–442.

Alzoubi, H. H. & Al-Zoubi, A. H. (2010). Assessment of building façade performance in terms of daylighting and the associated energy consumption in architectural spaces: Vertical and horizontal shading devices for southern exposure facades, *Energy Conversion and Management*, *51*, 1592–1599.

ANSI/ASHRAE Standard 140-2004. (2004). *Standard Method of Test for the Evaluation of Building Energy Analysis Computer Programs*. Atlanta, GA: American Society of Heating, Refrigerating, and Air Conditioning Engineers.

April J., Glover F., Kelly J. P., Laguna M. (2003). Simulation-based optimization: practical introduction to simulation optimization, *Proceedings of the 2003 Winter Simulation Conference*, (pp. 71-78), New Orleans, Louisiana.

Ashari, M., Nayar, C. V. (1999). An optimum dispatch strategy using set points for a Photovoltaic (PV)–Diesel–Battery hybrid power system, *Solar Energy,66*(1), 1–9.

ASHRAE Standard 55, (2004). *Thermal environmental conditions for human occupancy*, American Society of Heating, Refrigerating and Air-Conditioning Engineers, Atlanta.

ASHRAE (2009). *2009 ASHRAE Handbook – Fundamentals*, American Society of Heating, Refrigerating and Air-Conditioning Engineers, Inc., ISBN978-1-933742-54-0.

Ashraf, I, Chandra, A, Sodha, M. (2004). Techno-economic and environmental analysis for grid interactive solar photovoltaic power system of Lakshadweep islands. *International Journal of Energy Research, 28*(12), 1033-1042.

Attia S., Hamdy M., O'Brien W., Carlucci S. (2013). Assessing gaps and needs for integrating building performance optimization tools in net zero energy buildings design, *Energy and Buildings*, *60*, 110–124.

Baglivo C., P Congedo. M., Fazio A. (2014). Multi-criteria optimization analysis of external walls according to ITACA protocol for zero energy buildings in the mediterranean climate, *Building and Environment*, *82*, 467–480.

Balaras, C.A. (1996). The role of thermal mass on the cooling load of buildings—an overview of computational methods, *Energy and Buildings, 24*(1), l–10.

Bambrook, S. M., Sproul, A.B., Jacob, D. (2011). Design optimization for a low energy home in Sydney, *Energy and Buildings*, *43*(7), 1702-1711.

Bandyopadhyay, S. & Saha, S. (2013). *Unsupervised Classification: Similarity Measures, Classical and Metaheuristic Approaches and Applications*, Springer, ISBN 978-3-642-32450-5.

Berdahl, P., Akbari, H., Jacobs, J., Klink, F. (2008). Surface roughness effects on the solar reflectance of cool asphalt shingles. Solar Energy Materials and Solar Cells.;92(4):482-489.

Bernal-Agustin J. L. & Dufo-Lopez R. (2009). Simulation and optimization of stand-alone hybrid renewable energy systems, *Renewable and Sustainable Energy Reviews, 13*, 2111–2118.

BEopt, (2012). *Building Energy Optimization*, National Renewable Energy Laboratory, Date retrieved: 10.04.2012, from http://beopt.nrel.gov/

BEP-TR (2010). *Building Energy Performance National Calculation Methodology* (Binalarda Enerji Performansı Ulusal Hesaplama Yöntemi), Republic of Turkey, Ministry of Environment and Urbanization.

Bessoudo, M., Tzempelikos, A., Athienitis, A.K., Zmeureanu, R. (2010). Indoor thermal environmental conditions near glazed facades with shading devices Part I: Experiments and building thermal model, *Building and Environment, 45*, 2506-2516.

Bhuvaneswari, M.C. (Ed.) (2014). *Application of Evolutionary Algorithms for Multi-objective Optimization in VLSI and Embedded Systems*, Springer, ISBN 978-81-322-1957-6.

Bichiou, Y. & Krarti, M. (2011). Optimization of envelope and HVAC systems selection for residential buildings, *Energy and Buildings*, *43*, 3373–3382.

Bigot D., Miranville F., Boyer H., Bojic M., Guichard S., Jean A. (2013). Model optimization and validation with experimental data using the case study of a building equipped with photovoltaic panel on roof: Coupling of the building thermal simulation code ISOLAB with the generic optimization program GenOpt, *Energy and Buildings, 58*, 333–347.

Bojić M., Miletić M., Marjanović V., Nikolić D., Skerlić J. (2012). Optimization of thermal insulation to achieve energy savings, *Proceedings of Ecos 2012 - The 25th International Conference On Efficiency, Cost, Optimization, Simulation And Environmental Impact Of Energy Systems*, Perugia, Italy, June 26-29, 2012.

Bojic, M., Yik, F., Wan, K., Burnett, J. (2002). Influence of envelope and partition characteristics on the space cooling of high-rise residential buildings in Hong Kong, *Building and Environmen*t, *37*(4), 347-355.

Bojić, M., Nikolić, N., Nikolić, D., Skerlić, J., Miletić, I. (2011). A simulation appraisal of performance of different HVAC systems in an office building, *Energy and Buildings*, *43*, 1207–1215.

Boonbumroong U., Pratinthong N., Thepa S., Jivacate C., Pridasawas W. (2011). Particle swarm optimization for AC-coupling stand alone hybrid power systems, *Solar Energy, 85*, 560–569.

Boreham S. & Hadley P. (2009). *The SLL Lighting Handbook*, The Society of Light and Lighting, Chartered Institution of Building Services Engineers (CIBSE), ISBN 978-1-906846-02-2.

Bornatico R., Pfeiffer M., Witzig A., Guzzella L. (2012). Optimal sizing of a solar thermal building installation using particle swarm optimization. *Energy*, *41*(1), 31–7.

Borowy, B. & Salameh, Z. (1995). Methodology for optimally sizing the combination of a battery bank and PV Array in a Wind/PV Hybrid system, *IEEE Transactions on Energy Conversion*, *11*(2), 367–75.

Boyano, A., Hernandez P., Wolf O. (2013). Energy demands and potential savings in European office buildings: Case studies based on EnergyPlus simulations, *Energy and Buildings*, *65*, 19–28.

BP, (2012). *BP Statistical Review of World Energy June 2012*, Reports and publications, p.p 42, Date retrieved: 01.08.2012, from: bp.com/statisticalreview.

BPIE, (2014). Buildings Performance Institute Europe, Brussels, Belgium, Date retrieved: 01.08.2012, from www.bpie.eu.

Bronin, S.C. (2012). *Building-Related Renewable Energy and the Case of 360 State Street*, Vanderbilt Law Review, 1875.

Brownlee A. E., Wright J. A., Mourshed M. M. A. (2011). Multi-objective window optimisation problem, *Proceedings of the 13th annual conference companion on genetic and evolutionary computation, GECCO'11*,(pp.89–90). New York, NY, USA.

Bui L. T. & Alam S. (2008). *Multi-Objective Optimization in Computational Intelligence: Theory and Practice*, IGI Global.

Caldas L. G. & Norford L. K. (2002). A design optimization tool based on a genetic algorithm, *Automation in Construction*, *11*, 173–84.

Caldas, L.G. & Norford, L. K. (2003). Genetic algorithms for optimization of building envelopes and the design and control of HVAC systems, *Journal of Solar Energy Engineering*, *125*, 343–51.

Caldas L. (2006). GENE ARCH: an evolution-based generative design system for sustainable architecture, Lecture Notes in Computer Science 4200, 109.

Caramia M. & Dell'Olmo, P. (2008). *Multi-objective Management in Freight Logistics*, London, UK, Springer-Verlag, , ISBN 978-1-84996-796-9.

Carboni C. & Montanari R. (2008). Solar thermal systems: Advantages in domestic integration, *Renewable Energy*, *33*(6), 1364–1373.

Carson Y. & Maria A. (1997). Simulation Optimization: Methods and Applications, *Proceedings of the 1997 Winter Simulation Conference*, (pp. 118 - 126) Atlanta, GA, USA.

Castro-Lacouture, D., Sefair, J., Flórez, L., Medaglia, A. (2009). Optimization Model for the Selection of Materials Using the LEED Green Building Rating System, *Construction Research Congress 2009, (* pp. 608-617), Seattle, Washington, April 5-7.

Celik. (2006). Present status of photovoltaic energy in turkey and life cycle technoeconomic analysis of a grid-connected photovoltaic-house. *Renewable and Sustainable Energy Reviews, 10*(4), 370-387.

Chantrelle, F. P., Lahmidi, H., Keilholz, W., Mankibi, M., Michel, P. (2011). Development of a multicriteria tool for optimizing the renovation of buildings, *Applied Energy, 88*(2011), 1386–1394.

Charron, R. & Athienitis, A. K. (2006). Optimization of the performance of double-façades with integrated photovoltaic panels and motorized blinds, *Solar Energy, 80*(5), 482–491.

Chaudhry I. A. & Drake P.R. (2009). Minimizing total tardiness for the machine scheduling and worker assignment problems in identical parallel machines using genetic algorithms, *International Journal of Advanced Manufacturing Technologies, 42*, 581–594.

Cheng, V., Ng, E., Givoni, B. (2005). Effect of envelope color and thermal mass on indoor temperatures in hot humid climate, *Solar Energy, 78*(4), 528–534.

Chedid, R. & Saliba, Y. (1996). Optimization and control of autonomous renewable energy systems. *The International Journal of Energy Research, 20*(7), 609–24.

Chow, T.T., Zhang, G.Q., Lin, Z., Song, C.L. (2002). Global optimization of absorption chiller system by genetic algorithm and neural network. *Energy and Buildings, 34*(1), 103–9.

Clerc M. & Kennedy J. (2002). The particle swarm-explosion stability,and convergence in a multidimensional complex space. *IEEE Transactions on Evolutionary Computation, 6*(1), 58-73.

CO2Now, (2014). Date retrieved: 01.08.2014, from: http://co2now.org/.

Coffey B. A. (2008). *Development and testing framework for simulation-based supervisory control with application to optimal zone temperature ramping demand response using a modified genetic algorithm*, (Master Thesis). Concordia University, Quebec, Canada.

Coffey B., Haghighat F., Morofsky E., Kutrowski E. (2010). A software framework for model predictive control with GenOpt, *Energy and Buildings, 42*(7), 1084–1092.

Coley, D. A. & Schukat, S. (2002). Low-energy design: combining computer based optimization and human judgement. *Building and Environment, 37*(12), 1241-7.

Crawley D. B., Hand J. W., Kummert M, Griffith B.T. (2008). Contrasting the capabilities of building energy performance simulation programs. *Building and Environment, 43*(4),661–73.

Cucchiella F., D'Adamo I., Gastaldi M., Koh S.C. L. (2012). Renewable energy options for buildings: Performance evaluations of integrated photovoltaic systems, *Energy and Buildings, 55*, 208–217.

Cvetković D. & Bojić M. (2014). Optimization of thermal insulation of a house heated by using radiant panels, *Energy and Buildings, 85*, 329–336.

Dakota, (2012). Design Analysis Kit for Optimization and Terascale Applications Date retrieved: 05.04.2014, from: http://dakota.sandia.gov/.

Dalton G.J., Lockington D.A., Baldock T.E. (2009). Feasibility analysis of renewable energy supply options for a grid-connected large hotel, *Renewable Energy*, *34*, 955–964.

Danielski, I., Fröling, M., Joelsson, A. (2012). The impact of the shape factor on final energy demand in residential buildings in nordic climates, *World Renewable Energy Forum, WREF 2012, Including World Renewable Energy Congress XII and Colorado Renewable Energy Society (CRES) Annual Conference*, (pp. 4260-4264), Denver, Colorado, USA, May 13-17.

Datta, G. (2001). Effect of fixed horizontal louver shading devices on thermal perfomance of building by TRNSYS simulation, *Renewable Energy*, *23*, 497–507.

Davis, J.A. & Nutter D.W. (2010). Occupancy diversity factors for common university building types, *Energy and Buildings*, *42*, 1543 − 1551.

Deb K. & Agrawal S. (1999). A Niched-Penalty Approach for Constraint Handling in Genetic Algorithms, *Proceedings of the International Conference Artificial Neural Nets and Genetic Algorithms*, (pp. 235-243), Portorož, Slovenia.

Deb K. (2012). *Optimization for Engineering Design: Algorithms and Examples*, Prentice-Hall of India Pvt.Ltd, ISBN 8120346785.

Dellino G., Meloni C., Pierreval H. (2014). Simulation–optimization of complex systems: Methods and applications, *Simulation Modelling Practice and Theory*, *46*, Pages 1–3.

Depecker, P., Menezo, C., Virgone, J., Lepers S. (2001). Design of building shape and energetic consumption, *Building and Environment*, *30*(2), 201–222.

Diaconu, B. M. (2011). Thermal energy savings in buildings with PCM-enhanced envelope: Influence of occupancy pattern and ventilation, *Energy and Buildings*, *43*(1), 101-107.

Ding, H., Benyoucef L., Xie X. (2006). A simulation-based multi-objective genetic algorithm approach for networked enterprises optimization. *Engineering Applications of Artificial Intelligence*, *19*(6), 609-623.

Djuric, N., Novakovic, V., Holst, J., Mitrovic, Z. (2007). Optimization of energy consumption in buildings with hydronic heating systems considering thermal comfort by use of computer-based tools, *Energy and Buildings*, *39*, 471–7.

Doulos L., Tsangrassoulis A., Topalis F. (2008). Quantifying energy savings in daylight responsive systems: the role of dimming electronic ballasts, *Energy and Buildings*, *40*, 36–50.

Dufo-Lopez, R. & Bernal-Agustin, J. L. (2005). Design and control strategies of PV–diesel systems using genetic algorithms, *Solar Energy*, *79*(1), 33–46.

IEA, (2006). International Energy Agency. Light's Labour's Lost. IEA Publications, France.

IEA, (2011a). World Energy Outlook 2011, OECD/IEA, Paris, France

IEA, (2011b): Key World Energy Statistics 2011, Date retrieved: 15.06.2012, from http://www.iea.org/publications/freepublications/publication/key_world_energy_stats-1.pdf.

Eberhart, R. & Kennedy, J. (1995). A new optimizer using particle swarm theory. In: Micro Machine and Human Science, *Proceedings of the Sixth International Symposium on MHS '95*, Nagoya Municipal Industrial Research Institute, October 4-6.

Eisenhower B, O'Neill Z., Narayanan S., Fonoberov V. A., Mezic´ I. (2012). A methodology for meta-model based optimization in building energy models, *Energy and Buildings*, *47*, 292–301.

Ellis P. & Torcellini P. (2005). Simulating tall buildings in EnergyPlus, *Proceedings of IBPSA 2005 Conference*, Montreal, Canada.

EN 15251 (2007). Indoor environmental input parameters for design and assessment of energy performance of buildings addressing indoor air quality, thermal environment, lighting and acoustics, European Committee for Standardization.

EN 15459 (2007). Energy performance of buildings - Economic evaluation procedure for energy systems in buildings, European Committee for Standardization.

EN ISO 7730 (2006). Ergonomics of the thermal environment—analytical determination and interpretation of thermal comfort using calculation of the PMV and PPD indices and local thermal comfort criteria; 2006. International Organization for Standardization.

EPBD (2010). Directive 2010/31/EU, Energy Performance of Buildings (Recast), European Parliament and of the Council, 19.05.2010.

Erell E., Portnov B. A., Etzion Y. (2003). Mapping the potential for climate-conscious design of buildings, *Building and Environment, 38*, 271 – 281.

Erhorn H. & Kluttig H. (2011). *Terms and definitions for high performance buildings, Concerted Action, Energy Performance of Buildings*, Technical Report, Community's Intelligent Energy Europe programme, from www.epbd-ca.eu.

ESTECO, (2014). modeFrontier; from http://www.esteco.com/modefrontier.

EU, (2011). A Roadmap for moving to a competitive low carbon economy in 2050, European Commission, Date retrieved: 15.08.2013, from: http://ec.europa.eu/clima/policies/roadmap/documentation_en.htm.

European Directive 2010/31/EU, (2010). On the energy performance of buildings (recast), Directive of the European Parliament and of the Council of 19 May 2010, Bruxelles.

European Regulation 244/2012, (2012). Commission Delegated Regulation, Official Journal of the European Union, European Parliament, Bruxelles.

ESRU, (2006). Class notes: Climate, University of Strathclyde's Energy Systems Research Unit.

Evins R., Pointer P., Vaidyanathan R. (2010). Configuration of a genetic algorithm for multi-objective optimisation of solar gain to buildings, *Proceedings of the genetic and evolutionary computation GECCO '10,* (pp. 1327–28), New York, NY, USA.

Evins R., Pointer P., Vaidyanathan R., Burgess S. (2012). A case study exploring regulated energy use in domestic buildings using design-of-experiments and multi-objective optimisation, *Building and Environment*, *54*, 126–36.

Evins, R. (2013). A review of computational optimisation methods applied to sustainable building design, R*enewable and Sustainable Energy Reviews*, *22*(2013), 230–245.

Farhanieh, B. & Sattari S. (2006). Simulation of energy saving in Iranian buildings using integrative modelling for insulation, *Renewable Energy*, *31*, 417–425.

Ferrara M., Fabrizio E., Virgone J., Filippi M., (2014). A simulation-based optimization method for cost-optimal analysis of nearly Zero Energy Buildings, *Energy and Buildings*, *84*, 442–457.

Fesanghary M., Asadi S., Geem Z.W. (2012). Design of low-emission and energy-efficient residential buildings using a multi-objective optimization algorithm, *Building and Environment*, *49*, 245-250.

Filho, J.P., Henriquez, J.R., Dutra J.C.C. (2010). Effects of coefficients of solar reflectivity and infrared emissivity on the temperature and heat flux of horizontal flat roofs of artificially conditioned nonresidential buildings, *Energy and Buildings, 43*, 440–445.

Fishwick, P. A. (1995). Computer Simulation: The Art and Science of Digital World Construction, http://www.cis.ufl.edu/~fishwick/introsim/paper.html)

Fong, K., Hanby, V., Chow, T. (2006). HVAC system optimization for energy management by evolutionary programming, *Energy and Buildings*, *38*, 220–31.

Fong K. F., Hanby V. I., Chow T. (2009). System optimization for HVAC energy management using the robust evolutionary algorithm, *Applied Thermal Engineering, 29*, 2327–2334.

Fu, M. C., F. W. Glover, April J. (2005). Simulation optimization: a review, new developments, and applications, *Proceedings of the 37th conference on Winter simulation,* Orlando, Florida.

Fu M. C. (2002). Optimization for Simulation: Theory vs. Practice, *INFORMS Journal on Computing*, *14*(3).

Fuller S. K. & Petersen S. R. (1995). *Life-cycle Costing Manual for the Federal Energy Management Program*, NIST Handbook 135, US Department of Commerce.

Gagne J. & Anderson M. (2010). Multi-Objective Facade Optimization for Daylighting Design Using a Genetic Algorithm, *Fourth National Conference of IBPSA - USA*, (pp. 110-117).

Gansterer M., Almeder C., Hartl R. F. (2014). Simulation-based optimization methods for setting production planning parameters, *International Journal of Production Economics*, *151*, 206–213.

GEATbx, (2012). The Genetic and Evolutionary Algorithm Toolbox for Matlab, Date retrieved: 05.04.2012, from: http://www.geatbx. com/.

GenOpt, (2012). Generic Optimization Program, Lawrence Berkeley National Laboratory, US, Date retrieved: 05.04.2012, from: http://simulationresearch.lbl.gov/GO

Gregory, K., Moghtaderi, B., Sugo H., Page A. (2008). Effects of thermal mass on the thermal performance of various Australian residential constructions systems, *Energy and Buildings*, *40*(4), 459–465.

Griffith, B., Pless, S., Talbert, B., Deru, M., Torcellini P. (2003). *Energy design analysis and evaluation of a proposed air rescue and fire fighting administration building for teterboro airport*, National Renewable Energy Laboratory, Golden (CO).

Griffith B. & Crawley, D. (2006). A Methodology for Analyzing the Technical Potential for Energy Performance in the US Commercial Building Sector with Detailed Energy *Modeling, SimBuild 2006 Conference*, Cambridge, Massachusetts, August 2−4.

Griego, D., Krarti, M., Hernandez-Guerrero A. (2012). Optimization of energy efficiency and thermal comfort measures for residential buildings in Salamanca, Mexico, *Energy and Buildings*, in press.

Grondzik W. & Furst R. (2000). *HVAC Components and Systems*, Vital Signs Curriculum Materials Project, Center for Environmental Design, University of California, Berkeley.

Gunaratne A. & Wu Z. (2011). A Penalty Function Method for Constrained Molecular Dynamics Simulation, *International Journal of Numerical Analysis and Modeling*, *8*(3), 496–517.

Guillemin, A. & Molteni, S. (2002). An energy-effcient controller for shading devices self-adapting to the user wishes, *Building and Environment*, *37*, 1091 – 1097.

Gustafsson, M., Dermentzis, G., Myhren, J. A., Bales, C., Ochs, F., Holmberg, S. Feist, W. (2014). Energy performance comparison of three innovative HVAC systems for renovation through dynamic simulation, *Energy and Buildings*, *82*, 512–519.

Haines R. W. & Myers M. E. (2010). *HVAC Systems Design Handbook*, McGraw-Hill Education, ISBN: 9780071622974.

Hamby, D. M. (1994). A review of techniques for parameter sensitivity analysis of environmental models, *Environmental Monitoring and Assessment*, *32* (2), 135-154.

Hamdy, M., Hasan, A., Siren, K. (2011). Impact of adaptive thermal comfort criteria on building energy use and cooling equipment size using a multi-objective optimization scheme, *Energy and Buildings*, *43*(9), 2055–2067.

Harvey D. (2012). *A Handbook on Low-Energy Buildings and District-Energy Systems: Fundamentals, Techniques and Examples*, Routledge, ISBN 1136573038.

Hasan A., Vuolle M., Siren K. (2008). Minimisation of life cycle cost of a detached house using combined simulation and optimization, *Building and Environment*, Vol.43, 2022–2034.

Hamdy M., Hasan A., Siren K. (2009). Combination of optimisation algorithms for a multi-objective building design problem, *Proceedings of the Eleventh International IBPSA Conference*, Glasgow, Scotland, July 27-30.

Hamdy M., Hasan A., Sirén K. (2010). Optimum design of a house and its HVAC systems using simulation-based optimisation, *International Journal of Low-Carbon Technologies, 5* (3), 120–124.

Hamdy M., Hasan A.,Siren K. (2011). Applying a multi-objective optimization approach for design of low-emission cost-effective dwellings. *Building and Environment*, *46*, 109–23.

Hamdy M., Hasan A., Siren K. (2011). Impact of adaptive thermal comfort criteria on building energy use and cooling equipment size using a multi-objective optimization scheme, *Energy and Buildings*, 43(9), 2055–2067.

Haniff M. F., Selamat H., Yusof R., Buyamin S., Ismail F. S. (2013). Review of HVAC scheduling techniques for buildings towards energy-efficient and cost-effective operations, *Renewable and Sustainable Energy Reviews*, *27*, 94–103.

Hassan, M.A., Guirguis N.M., Shaalan M.R., El-Shazly K.M. (2007). Investigation of effects of window combinations on ventilation characteristics for thermal comfort in buildings, *Desalination, 209*, 251–260.

Hassan, R., Cohanim, B., Weck, O., Venter, G. (2005). A comparison of particle swarm optimization and the genetic algorithm, *Proceedings of the 1st AIAA multidisciplinary design optimization specialist conference*, (pp.18-21), Austin, Texas, 18 - 21 April.

Hassouneh, K., Alshboul, A., Al-Salaymeh, A. (2010). Influence of windows on the energy balance of apartment buildings in Amman, *Energy Conversion and Management, 51* (8), 1583-1591.

Hepbasli A. & Kalinci Y. (2009). A review of heat pump water heating systems, *Renewable and Sustainable Energy Reviews*, *13*(6-7), 1211–1229.

Hensen, J. L. M. & Lamberts, R. (2011). *Building Performance Simulation for Design and Operation*, Taylor & Francis, Oxford, UK.

Ho, M., Chiang, C., Chou P., Chang K., Lee C. (2008). Optimal sun-shading design for enhanced daylight illumination of subtropical classrooms, *Energy and Buildings*, *40*, 1844–1855.

Hoes P., Trcka M., Hensen J., Bonnema B. (2011). Optimizing building designs using a robustness indicator with respect to user behavior, *Proceedings of the 12th International IBPSA conference*, Sydney, 14-16 November.

Holst J. N. (2003). Using whole building simulation models and optimizing procedures to optimize building envelope design with respect to energy consumption and indoor environment, *Proceedings of the 8th international IBPSA conference*, (pp. 507–14), Eindhoven.

Huang, W. & Lam, H. N. (1997). Using genetic algorithms to optimize controller parameters for HVAC systems, *Energy and Buildings*, 26(3), 277–82.

Huang W., Zaheeruddin M., Cho S. H. (2006). Dynamic simulation of energy management control functions for HVAC systems in buildings, *Energy Conversation Management*, *47*(7–8), 926–43.

Ibanez, M., Lazaro A., Zalba B., Cabeza L. F. (2005). An approach to the simulation of PCMs in building applications using TRNSYS, *Applied Thermal Engineering*, *25*, 1796–1807.

Ibrahim O., Fardoun F., Younes R., Louahlia-Gualous H. (2014a). Review of water-heating systems: General selection approach based on energy and environmental aspects, *Building and Environment*, *72*, 259–286.

Ibrahim O., Fardoun F., Younes R., Louahlia-Gualous H. (2014b). Optimal management proposal for hybrid water heating system, *Energy and Buildings*, *75*, 342–357.

IDEP, (2012). *Republic of Turkey, Climate Change Action Plan, Technical Report*, Ministry of Environment and Urbanization, Özel Printing, Ankara.

IEA Online Statistics, (2010). Statistics and Balances. International Energy Agency (IEA) of the Organisation for Economic Cooperation and Development (OECD), Paris, France, Retrieved 06 June 2013, from www.iea.org/stats/index.asp.

Ihm, P. & Krarti M. (2012). Design optimization of energy efficient residential buildings in Tunisia, *Building and Environment*, *58*, 81-90.

IPCC, (2007a). *IPCC Fourth Assessment Report Climate Change 2007: Synthesis Report*, Intergovernmental Panel on Climate Change, Retrieved: 01.05.2012, from: http://www.ipcc.ch.

IPCC, (2007b). *IPCC Fourth Assessment Report, Climate Change 2007: Working Group III: Mitigation of Climate Change*, Intergovernmental Panel on Climate Change, Retrieved 01.05.2012, from: http://www.ipcc.ch.

Ishibuchi H., Murata T., Turksen I. B. (1997). Single-objective and two-objective genetic algorithms for selecting linguistic rules for pattern classification problems, *Fuzzy Sets and Systems, 89*(2), 135– 150.

Jaber, S. & Ajib, S. (2011). Optimum, technical and energy efficiency design of residential building in Mediterranean region, *Energy and Buildings*,*43*, 1829–1834.

Jacob D., Burhenne S., Florita A., Henze G. (2010). Optimizing building energy simulation models in the face of uncertainty, *The proceedings of Fourth National Conference of IBPSA-USA*, New York City, NY, August 11–13.

Jaimes L., Martinez S. Z., Coello C.A. (2009). *An Introduction to Multiobjective Optimization Techniques,* Nova Science Publishers, Inc., 1-26. Retrieved from http://delta.cs.cinvestav.mx/~ccoello/chapters/chapter-cunha-revised.pdf.gz

Jensen P.A. & Bard J. F. (2003). *Operations Research Models and Methods*, John Wiley and Sons, ISBN-13: 978-0471380047.

Jin J. & Jeong J. (2014). Optimization of a free-form building shape to minimize external thermal load using genetic algorithm, *Energy and Buildings, 85*, 473–482.

Joe J., Choi W., Kwak Y., Huh J. (2014). Optimal design of a multi-story double skin façade, *Energy and Buildings*, *76*, 143–150.

Johnson, R., Sullivan, R., Selkowitz, S., Nozaki, S., Conner, C., Arasteh, D. (2004). Glazing energy performance and design optimization with daylighting, *Energy and Buildings*, *6*(4), 305-317.

Jones, D. R., C. D. Perttunen, and B. E. Stuckman. (1993). Lipschitzian optimization without the Lipschitz constant, *Journal of Optimization Theory and Application, 79* (1), 157–181.

Joudi, A., Svedung, H., Rönnelid, M. (2011). Energy Efficient Surfaces on Building Sandwich Panels - A Dynamic Simulation Model, *Energy and Buildings*, *43*, 2462–2467.

Kaiser, R., Sauer, D.U., Armbruster, A., Bopp, G., Puls, H. G. (1997). New concepts for system design and operation control of photovoltaic systems, *Proceedings of the 14th European photovoltaic solar energy conference*, Barcelona, Spain, 30 June - 4 July.

Kalogiro, S. A. (2001). Use of TRNSYS for modelling and simulation of a hybrid PV-thermal solar system for Cyprus, *Renewable Energy, 23*, 247–260.

Kalogirou S.A. (2004). Environmental benefits of domestic solar energy systems, *Energy Conversion Management*, *45*, 3075–3092.

Kämpf J. H. & Robinson D. (2009). A hybrid CMA-ES and HDE optimisation algorithm with application to solar energy potential, *Applied Soft Computing, 9*(2), 738–745.

Kämpf J. H. & Robinson D. (2010). Optimisation of building form for solar energy utilization using constrained evolutionary algorithms, *Energy and Buildings*, *42* (6), 807–814.

Kämpf J. H., Wetter M., Robinson D. A. (2010). Comparison of global optimization algorithms with standard benchmark functions and real-world applications using EnergyPlus, *Journal of Building Performance Simulation*, *3*, 103–20.

Karlsson, J. & Roos, A. (2001). Annual energy window performance vs. glazing thermal emittance- the relevance of very low emittance values, *Thin Solid Films*, *392*(2), 345-348.

Krarti M., Erickson P.M., Hillman T.C. (2005). A simplified method to estimate energy savings of artificial lighting use from daylighting, *Building and Environment*, *40* (6), 747–754.

Kennedy, J. & Eberhart, R. (1995). Particle Swarm Optimization, *Proceedings of the IEEE International Conference on Neural Networks*, (pp. 1942 – 1948), 27 Nov-01 Dec.

Kim, J. & Moon, J. W. (2009). Impact of Insulation on Building Energy Consumption, *Eleventh International IBPSA Conference*, (pp.674-680).

Kim, G., Lim, H. S., Lim, T. S., Schaefer, L., Kim, J. T. (2012). Comparative advantage of an exterior shading device in thermal performance for residential buildings, *Energy and Buildings*, *46*, 105–111.

Kontoleon, K. J. & Bikas, D. K. (2002). Modeling the influence of glazed openings percentage and type of glazing on the thermal zone behavior, *Energy and Buildings*, *34*, 389–399.

Koutroulis, E., Kolokotsa, D., Potirakis, A., Kalaitzakis, K. (2006). Methodology for optimal sizing of stand-alone photovoltaic/wind-generator systems using genetic algorithms, *Solar Energy*, *80*(9), 1072–88.

Kusiak A., Li M., Tang F. (2010). Modeling and optimization of HVAC energy consumption, *Applied Energy*, *87*, 3092–3102.

Kusiak, A. & Xu, G. (2012). Modeling and optimization of HVAC systems using a dynamic neural network, *Energy*, *42*, 241-250.

Kusiak, A., Xu G., Tang F. (2011a). Optimization of an HVAC system with a strength multi-objective particle-swarm algorithm, *Energy*, *36*, 5935-5943.

Kusiak, A., Tang, F., Xu, G. (2011b). Multi-objective optimization of HVAC system with an evolutionary computation algorithm, *Energy*, *36*, 2440-2449.

Kwok, S. K., Yuen, K. K., Lee, W. M. (2011). An intelligent approach to assessing the effect of building occupancy on building cooling load prediction, *Building and Environment*, *46*(8), 1681–1690.

LANL, (2013). Sustainable Design Guide, Los Alamos National Laboratory, USA Retrieved: 01.05.2013 from: http://www1.eere.energy.gov/buildings/commercial_initiative/guides.html#sdg

Lam, J. C., Tsang, C. L., Yang L., Lia D. H. W. (2005). Weather data analysis and design implications for different climatic zones in China, *Building and Environment*, *40*, 277–296.

Lam, J. C., Tsang C. L., Yang, L. (2006). Impacts of lighting density on heating and cooling loads in different climates in China, *Energy Conversion and Management*, 1942 –1953.

Lechner, N. (1990). *Heating, Cooling, Lighting – Design Methods for Architects*. USA. John Wiley & Sons.

Li D. H.W., Lam T. N.T., Wong S.L., Tsang E. K.W. (2008). Lighting and cooling energy consumption in an open-plan office using solar film coating, *Energy*, *33* (8), 1288–1297.

Liberti L. (2008). *Introduction to Global Optimization*, LIX, ´Ecole Polytechnique, Palaiseau F-91128, France.

Linhart, F. & Scartezzini, J. L. (2011). Evening Office Lighting: Visual Comfort vs. Energy Efficiency vs. Performance, *Building and Environment* ,*46* (5), 981–989.

Ling, C. S., Ahmad, M. H., Ossen D. R. (2007). The Effect of Geometric Shape and Building Orientation on Minimising Solar Insolation on High-Rise Buildings in Hot Humid Climate, *Journal of Construction in Developing Countries*, *12*(1).

Liu, G., Rasul, M. G., Amanullah, M. T. O., Khan, M. M. K. (2012). Techno-economic simulation and optimization of residential grid-connected PV system for the Queensland climate, *Renewable Energy*, *45*, 146-155.

Lombard L. P., Ortiz J., Maestro I. R. (2011). The map of energy flow in HVAC systems, *Applied Energy*, *8* (12), 5020–5031.

Lollini, Barozzi, Fasano, Meroni, Zinzi. (2006). Optimisation of opaque components of the building envelope, energy, economic and environmental issues, *Building and Environment*, *41*, 1001–13.

Loonen R., Trcka M., Hensen J. (2011). Exploring the potential of climate adaptive building shells, *The proceedings of 12th Conference of International Building Performance Simulation Association*, (pp. 2148–2155), 14–16 November.

Lovell, J. (2009). *Building Envelopes: An Integrated Approach*, New York, NY: Princeton Architectural Press.

Lu L., Cai W., Soh Y. C., Xie L., Li S. (2004). HVAC system optimization - condenser water loop, *Energy Conversion and Management*, *45*(4), 613–630.

Lu L., Cai W., Soh Y. C., Xie L. (2005a). Global optimization for overall HVAC systems-Part I problem formulation and analysis, *Energy Conversion and Management*, *46*, 999–1014.

Lu L., Cai W., Soh Y. C., Xie L. (2005b). Global optimization for overall HVAC systems—Part II problem solution and simulations, *Energy Conversion and Management*, *46*, 1015–1028.

Lu, L., Cai, W., Xie, L., Li, S., Soh, Y. C. (2005). HVAC system optimization—in-building section, *Energy and Buildings*, *37*(1), 11–22.

Machairas, V., Tsangrassoulisb, A., Axarlic, K. (2014). Algorithms for optimization of building design: A review, *Renewable and Sustainable Energy Reviews*, *31*, 101–112.

Magnier L., Zhou L., Haghighat F. (2009). Multiobjective optimisation of building design using TRNSYS simulations, genetic algorithm, artificial Neural Network, *Building and Environment, 45* (3), 739–746.

Manioglu, G. & Yılmaz, Z. (2008). Energy efficient design strategies in the hot dry area of Turkey, *Building and Environment*, *43*, 1301–1309.

Manzan M. (2014). Genetic optimization of external fixed shading devices, *Energy and Buildings, 72*, 431–440.

Mardaljevic J., Heschong L., Lee E. (2009). Daylight metrics and energy savings, *Lighting Research and Technology*, *41*, 261–283.

Marino C., Nucara A., Pietrafesa M., Pudano A. (2013). An energy self-sufficient public building using integrated renewable sources and hydrogen storage, *Energy*, *57*, 95–105.

Marks, W. (1997). Multicriteria optimization of shape of energy saving buildings, *Building and Environment*, *32*(4), 331–9.

Matlab, (2012b). Global Optimization Toolbox, Date retrieved: 05.04.2012, from: http://www.mathworks.com/products/global-optimization/index.html.

Matlab, (2012a). Optimization Toolbox™, Date retrieved: 05.04.2012, from: http://www.mathworks.com/products/optimization/.

Merriam-webster, (2012). Merriam-webster Dictionary, Definition of optimization Date retrieved: 01.06.2012, from: http://www.merriam-webster.com/dictionary/optimization.

Moeseke, G., Bruyere, I., Herde, A. (2007). Impact of control rules on the efficiency of shading devices and free cooling for office buildings, *Building and Environment, 42*, 784–793.

Mohamad, I., Pascal, H.B., Wurtz, E., Achard P. (2014). Limiting windows offset thermal bridge losses using a new insulating coating, *Applied Energy, 123*, 220–231.

Morgan, T. R., Marshall, R. H., Brinkworth, B. J. (1997). ARES a refined simulation program for the sizing an optimizatio optimization of autonomous hybrid energy systems, *Solar Energy*, *59*(4–6), 205–15.

Mossolly M., Ghali K., Ghaddar N. (2009). Optimal control strategy for a multi-zone air conditioning system using a genetic algorithm, *Energy*, *34* (1), 58–66.

Murray S. N., Walsh B. P., Kelliher D., O'Sullivan D. T. J. (2014). Multi-variable optimization of thermal energy efficiency retrofitting of buildings using static modelling and genetic algorithms – A case study, *Building and Environment, 75*, 98–107.

Nabinger S. & Persily A. (2011). Impacts of airtightening retrofits on ventilation rates and energy consumption in a manufactured home, *Energy and Buildings*, *43*, 3059–3067.

Nasrollahi F. (2009). *Climate and Energy Responsive Housing in Continental Climates: The Suitability of Passive Houses for Iran's Dry and Cold Climate*, Univerlagtuberlin, ISBN 3798321442.

Nassif, N., Kajl, S., Sabourin, R. (2005). Optimization of HVAC Control System Strategy Using Two-Objective Genetic Algorithm, *HVAC&R Research, 11,* 459-486.

NIBS, (2014). Whole Building Design Guide, United States National Institute of Building Sciences (NIBS) Retrieved April 2014 from http://www.wbdg.org/design/sustainable.php.

Nilsson, A. M. & Roos, A. (2009). Evaluation of optical and thermal properties of coatings for energy efficient windows, *Thin Solid Films*, *517*, 3173–3177.

Nguyen A. T. & Reiter S. (2013) Passive designs and strategies for low-cost housing using simulation-based optimization and different thermal comfort criteria, *Journal of Building Performance Simulation*, *7*(1), 68-81.

Nguyen A., Reitera S., Rigob P. (2014). A review on simulation-based optimization methods applied to building performance analysis, *Applied Energy*, *113*, 1043–1058.

Nikoofard Sara, Ugursal V. I., Beausoleil-Morrison I. (2014) An investigation of the technoeconomic feasibility of solar domestic hot water heating for the Canadian housing stock, *Solar Energy*, *101*, 308–320.

Ochoa, C. E. & Capeluto, I. G. (2008). Strategic decision-making for intelligent buildings: Comparative impact of passive design strategies and active features in a hot climate, *Building and Environment*, *43* 1829–1839.

ODYSSEE/MURE, (2009). *Energy efficiency trends and policies in the household & tertiary sectors in the EU 27. Lessons from the ODYSSEE/MURE project,* ADEME-Agence de l'Environnement et la Maitrise de l'Energie.

Oh S., Yoo Y., Song J., Song S. J., Jang H., Kim K., Kwak H. (2014). A cost-effective method for integration of new and renewable energy systems in public buildings in Korea, *Energy and Buildings*, *74*, 120–131.

Ohnari M. (1998). *Simulation Engineering*, IOS Press, ISBN 9051993927.

Ouarghi, R. & Krarti, M. (2006). Building shape optimization using neural network and genetic algorithm approach, *ASHRAE Transactions*, 112, 484–91.

Padovan R. & Manzan M. (2014). Genetic optimization of a PCM enhanced storage tank for Solar Domestic Hot Water Systems, *Solar Energy*, *103*, 563–573.

Palmero-Marrero, A. I. & Oliveira, A. C. (2010). Effect of louver shading devices on building energy requirements, *Applied Energy*, *87*, 2040–2049.

Palonen M., Hasan A., Siren K., A. (2001). Genetic algorithm for optimisation of building envelope and HVAC system parameters, *Proceedings of the 11th IBPSA Conference*, Glasgow, Scotland.

Palonen M., Hamdy M., and Hasan A (2013). Mobo: A New Software For Multi-Objective Building Performance Optimization, *Proceedings of BS2013, 13th Conference of International Building Performance Simulation Association*, Chambery, France, August 26-28.

Panda S. & Padhy N. P. (2008). Comparison of particle swarm optimization and genetic algorithm for FACTS-based controller design, *Applied Soft Computing*, *8*(4), 1418–1427.

Papadrakakis M. & Lagaros N. D. (2002). Reliability-based structural optimization using neural networks and Monte Carlo simulation, *Computer Methods in Applied Mechanics and Engineering*, *191*(32), 3491-3507.

Parker, J.H. (1981). *Use of Landscaping for Energy Conservation*, Department of Physical Sciences, Florida International University, Miami, FL.

Petri I., Li H., Rezgui Y., Chunfen Y., Yuce B., Jayan B. (2014). A modular optimisation model for reducing energy consumption in large scale building facilities, *Renewable and Sustainable Energy Reviews*, *38*, 990–1002.

Peyvandi M., Zafarani M., Nasr E. (2011). Comparison of Particle Swarm Optimization and the Genetic Algorithm in the Improvement of Power System Stability by an SSSC-based Controller, *Journal of Electrical Engineering & Technology*, *6*(2), 182-191.

Public Law 110 - 140 – (2007). Energy Independence And Security Act Of 2007". U.S. Government Printing Office. Retrieved 17 April 2011.

Qi X., Zhao W., Liu L., Yang Y., Zhong G., Huang X. (2014). Optimization via simulation of a seeded directional solidification process for quasi-single crystalline silicon ingots by insulation partition design, *Journal of Crystal Growth*, *398*, 5-12.

Ramallo-González A. P. & Coley D. A. (2014). Using self-adaptive optimisation methods to perform sequential optimisation for low-energy building design, *Energy and Buildings*, *81*, 8–29.

Rao S. S. (2009). *Engineering Optimization: Theory and Practice*, John Wiley & Sons.

Raphael B. & Smith I. F. C. (2013). *Engineering Informatics: Fundamentals of Computer-Aided Engineering*, Second Edition, John Wiley & Sons, ISBN 1118536320.

Rapone G. & Saro O. (2012). Optimisation of curtain wall facades for office buildings by means of PSO algorithm, *Energy and Buildings*, *45*, 189–196.

Richardson, I., Thomson, M., Infield, D. (2008). A high-resolution domestic building occupancy model for energy demand simulations, Energy and Buildings, *40* (8), 1560-1566.

Robitu M, Musy M, Inard C, Groleau D. (2006). Modeling the influence of vegetation and water pond on urban microclimate, *Solar Energy, 80*(4), 435–47.

Sakamoto, Y., Nagaiwa, A., Kobayasi, S., Shinozaki T. (1999). An optimization method of district heating and cooling plant operation based on genetic algorithm, *ASHRAE Transactions, 105* (2), 1–11.

Salsbury T. & Diamond R. (2000). Performance validation and energy analysis of HVAC systems using simulation, *Energy and Buildings*, *32* (1), 5–17.

Seo D., Ihm P., Krarti M. (2011). Development of an optimal daylighting controller, *Building and Environment*, *46*, 5, 1011–1022.

Shahrestani M., Yao R., Cook G. K. (2013). Characterising the energy performance of centralised HVAC&R systems in the UK, *Energy and Buildings*, *62*, 239–247.

Shea K., Sedgwick A., Antonuntto G. (2006). Multicriteria optimization of paneled building envelopes using ant colony optimization, *Intelligent Computing in Engineering and Architecture*, 627–636.

Shen E., Hu J., Patel M. (2014). Energy and visual comfort analysis of lighting and daylight control strategies, *Building and Environment*, *78*, 155–170.

Shi X. (2011). Design optimization of insulation usage and space conditioning load using energy simulation and genetic algorithm, *Energy*, *36*, 1659–67.

Shi Y. & Eberhart R. C. (1998). A modified particle swam optimizer. *IEEE Word Congress on Computational Intelligence*, 69-73.

Srinivasan, R. S., J. Lakshmanan, D., Srivastav, E. S. (2011). Benchmarking Plug-Load Densities for K-12 Schools. *Proceedings of Building Simulation 2011, 12th Conference of International Building Performance Simulation Association*, (pp. 2746–2752), November 2011.

Stathopoulou, M, Synnefa A., Cartalis C., Santamouris S, Karlessi T., Akbari H. (2009). A surface heat island study of Athens using high-resolution satellite imagery and measurements of the optical and thermal properties of commonly used building and paving materials, *International Journal of Sustainable Energy*, *28*(1), 59-76.

Stephan L., Bastide A., Wurtz E. (2011). Optimizing opening dimensions for naturally ventilated buildings, *Applied Energy*, *88*(8), 2791–2801.

Spall J. C. (2012). Stochastic Optimization, Part II.7, Ha*ndbook of Computational Statistics*, Springer.

Su, X. & Zhang, X. (2010). Environmental performance optimization of window–wall ratio for different window type in hot summer and cold winter zone in China based on life cycle assessment, *Energy and Buildings*, *42*, 198–202.

Suga K., Kato S., Hiyama K. (2010). Structural analysis of Pareto-optimal solution sets for multi-objective optimisation: an application to outer window design problems using multiple objective genetic algorithms, *Building and Environment*, *45*, 1144–1152.

Surry P. D., Radcliffe N. J., Boyd I. D. (1995). A multi-objective approach to constrained optimisation of gas supply networks: The COMOGA method, Evolutionary Computing, *Lecture Notes in Computer Science* (Vol. 993, pp. 166-180), Springer.

Synnefa, A., Santamouris M., and K. Apostolakis, (2007). On the development, optical properties and thermal performance of cool colored coatings for the urban environment, *Solar Energy*, *81*, 488–497.

Talebizadeh P., Mehrabian M., Abdolzadeh M. (2011). Prediction of the optimum slope and surface azimuth angles using the genetic algorithm, *Energy and Building*s, *43*, 2998–3005.

Trcka, M. & Hensen, J. L. M. (2010). Overview of HVAC system simulation, *Automation in Construction*, *19*(2), 93-99.

Tresidder E., Zhang Y., Forrester A. I. J. (2012). Acceleration of building design optimisation through the use of Kriging surrogate models, *Proceedings of building simulation and optimization 2012*, (pp.1–8), Loughborough, Leicestershire, UK.

Trubiano F., Roudsari M. S., Ozkan A. (2013). Building Simulation and Evolutionary Optimization in The Conceptual Design Of A High-Performance Office Building, *Proceedings of BS2013: 13th Conference of International Building Performance Simulation Association*, Chambéry, France, August 26-28.

TS 825 (2008). Thermal insulation requirements for buildings, Turkish Standard, Turkish Standard Organization.

Tuhus-Dubrow D. & Krarti M. (2010). Genetic-algorithm based approach to optimize building envelope design for residential buildings, *Building and Environment*, *45*, 574–81.

Turiel I., Craig P., Levine M., McMahon J., McCollister G., Hesterberg B. Robinson M. (1987). Estimation of energy intensity by end-use for commercial buildings, *Energy*, *12*(6), 435-446.

Tzempelikos, A. & Athienitis, A. K. (2007). The impact of shading design and control on building cooling and lighting demand, *Solar Energy*, *81*, 369–382.

U.S National Institute of Building Sciences, (2008). Assessment to the US Congress and US Department of Energy on High Performance Buildings, U.S National Institute of Building Sciences, Technical Report.

UNEP (2011)**.** Towards a Green Economy: Pathways to Sustainable Development and Poverty Eradication, ISBN: 978-92-807-3143-9, Retrieved from www.unep.org/greeneconomy.

Vakiloroaya V., Samali B., Cuthbert S., Pishghadam K., Eager D. (2014). Thermo-economic optimization of condenser coil configuration for HVAC performance enhancement, *Energy and Buildings*, *84*, 1–12.

Vakiloroaya V., Samali B., Fakhar A., Pishghadam K. (2014). A review of different strategies for HVAC energy saving, *Energy Conversion and Management*, 77, 738–754.

Venter G. (2010). Encyclopedia of Aerospace Engineering, R*eview of Optimization Techniques*, pp. 5229–5238, John Wiley & Sons.

Wang W., Zmeureanu R., Rivard H. (2005). Applying multi-objective genetic algorithms in green building design optimization, *Building and Environment*, 40(11), 1512–1525.

Wang W., Zhang J., Jiang W., Liu B. (2011). Energy performance comparison of heating and air-conditioning systems for multi-family residential buildings, *HVAC&R Research*, *17* (3), 209–322.

WBDG, (2014). Net Zero Energy Buildings, Whole Building Design Guide**,** The National Institute of Building Science, Retrieved 15.04.2012, from http://www.wbdg.org/resources/netzeroenergybuildings.php.

Wyon, D.P. (1996). Individual microclimate control: required range, probable benefits and current feasibility. *Proceedings of Indoor Air '96,* Institute of Public Health, Tokyo, Japan.

Wang, W., Zmeureanu, R., Rivard, H. (2005). Applying multi-objective genetic algorithms in green building design optimization, *Building and Environment*, *40*, 1512–25.

Wang, W., Rivard H., Zmeureanu R. (2006). Floor shape optimization for green building design, *Advanced Engineering Informatics*, *20*, 363–78.

WBDG, (2014). Whole Building Design Guide**,** The National Institute of Building Science, Date retrieved: 15.03.2012, from http://www.wbdg.org/.

Weise T. (2009). Global Optimization Algorithms – Theory and Application, http://www.it-weise.de/

Wells D. B., Bhattacharya S., Carr R., Maffeo C., Ho A., Comer J., Aksimentiev A. (2012). Optimization of the molecular dynamics method for simulations of DNA and ion transport through biological nanopores, *Methods in Molecular Biology*, *870*, 165-86.

Westphalen D. & Koszalinski S. (2001a). Energy Consumption Characteristics of Commercial Building HVAC Systems, *Volume I: Chillers, Refrigerant Compressors, and Heating Systems*, Arthur D. Little, Inc. 20 Acorn Park, Cambridge, MA, Arthur D. Little Reference No. 36922-00.

Westphalen D. & Koszalinski S., (2001b). Energy Consumption Characteristics of Commercial Building HVAC Systems, *Volume II: Thermal Distribution, Auxiliary Equipment, and Ventilation*, Arthur D. Little, Inc. 20 Acorn Park, Cambridge, MA, Arthur D. Little Reference No. 33745-00.

Wetter, M. (2001). GenOpt—A generic optimization program. In: Lamberts R, Negarao COR, Hensen J, editors. *Proceedings of the Seventh International IBPSA Conference*, (pp. 601–8).

Wetter M. & Wright J. (2004). A comparison of deterministic and probabilistic optimization algorithms for nonsmooth simulation-based optimization, *Building and Environment*, *39*, 989 – 999.

Wetter, M. & Polak E. (2005). Building design optimization using a convergent pattern search algorithm with adaptive precision simulations, *Energy and Buildings*, *37*, 603–12.

Wetter, M. (2009). GenOpt, generic optimization program – user manual, version 3.0.0. *Technical report* LBNL-5419. Lawrence Berkeley National Laboratory.

Wright, J. A. (1986). *The optimised design of HVAC systems*, (Ph.D. Thesis), Loughborough University of Technology, UK,

Wright J. & Farmani R. (2001) The simultaneous optimisation of building fabric construction, HVAC system size, and the plant control strategy, *Proceedings of the 7th IBPSA Conference: Building Simulation*, (pp. 865–872), Rio de Janeiro, Brazil, 13-15 August.

Wright, J.A., Loosemore, H.A., Farmani, R. (2002). Optimization of building thermal design and control by multicriterion genetic algorithm. *Energy and Buildings*, *34*(9), 959–972.

Wright J. & Zhang Y. (2005). An "Ageing " Operator and Its Use in the Highly Constrained Topological Optimization of HVAC System Design, *The proceedings of Genetic and Evolutionary Computation Conference, GECCO 2005*, Washington DC, USA, June 25-29.

Wright J. & Mourshed M. (2009). Geometric optimisation of fenestration, *Proceeedings of IBPSA 11th International Building Performance Simulation Association Conference*, Glasgow, UK,

Wright J. A, Brownlee A, E., Mourshed M. M., Wang M. (2013). Multi-objective optimization of cellular fenestration by an evolutionary algorithm. *Journal of Building Performance Simulation*, *7*(1), 33-51.

Xiaoqi, X., Patricia, J. C., John, E. T. (2014). Energy saving alignment strategy: achieving energy efficiency in urban buildings by matching occupant temperature preferences with a building's indoor thermal environment, *Applied Energy*, *123*, 209–219.

Yagan D. & Tam C. K. (2006). Distributed Model free Stochastic Optimization in Wireless Sensor Networks, *Second IEEEInternational Conference Proceeedings DCOSS 2006*, (pp. 85-100), CA, USA.

Yang F., Zhang C., Sun T. (2008). Comparison of Particle Swarm Optimization and Genetic Algorithm for HMM training, *19th International Conference on Pattern Recognition*, (pp. 8-11).

Yang X., Yuan J., J. Yuan, Mao H. (2007). A modified particle swarm optimizer with dynamic adaptation, *Applied Mathematics and Computation*, *189*, 1205–1213

Yang X. (2010). *Engineering Optimization: An Introduction with Metaheuristic Applications*, Wiley, ISBN: 978-0-470-58246-6

Yao, R. & Steemers, K. (2005). A method of formulating energy load profile for domestic buildings in the UK, I*nternational Journal of Energy and Building*, *37* (6), 663-671.

Yi, Y. K. & Malkawi, A. (2009). Optimizing building form for energy performance based on hierarchical geometry relation, *Automation in Construction, 18*, 825–33.

Yohanis, Y.G. & Norton B. (2002). Useful solar heat gains in multi-zone nondomestic buildings as a function of orientation and thermal time constant, *Renewable Energy, 27*, 87–95.

Yun, G. Y., Kim, H., Kim, J. T. (2012). Effects of occupancy and lighting use patterns on lighting energy consumption, *Energy and Buildings, 46*, 152–158.

Zabinsky, Z. B. (2003). *Stochastic Adaptive Search For Global Optimization*, Kluwer Academic Publishers, University of Washington, Seattle, Washington, USA.

Zaheer-Uddin, M. & Zheng, G. R. (2000). Optimal control of time-scheduled heating, ventilating and air conditioning processes in buildings, *Energy Conversion and Management, 41*, 49–60.

Zhai, Z., Johnson M., Krarti M. (2011). Assessment of natural and hybrid ventilation models in whole-building energy simulations, *Energy and Buildings, 43*, 2251–2261.

Zhou, J.L., Zhang, G.Q., Lin, Y.L., Li Y.G. (2008). Energy analysis of buildings employing thermal mass in Cyprus, *Energy and Buildings, 40* (6), 979-986.

Zhou, D. & Park S. H. (2012). Simulation-Assisted Management and Control Over Building Energy Efficiency – A Case Study, *Energy Procedia, 14*, 592–600.

Ziębik, **A. & Hoinka, K.** (2013). *Energy Systems of Complex Buildings*, Springer, ISBN 978-1-4471-4381-9.

Zitzler, E. (1999). *Evolutionary Algorithms for Multiobjective Optimization: Methods and Applications*, (PhD Thesis), Swiss Federal Institute of Technology, Zurich.

Znouda, E., Ghrab-Morcos, N., Hadj-Alouane, (2007). A. Optimization of mediterranean building design using genetic algorithms, *Energy and Buildings,39*, 148–153.

Zogou, O. & Stapountzis, H. (2011a). Experimental validation of an improved concept of building integrated photovoltaic panels, *Renewable Energy*, 36(12), 3488–3498.

Zogou, O. & Stapountzis, H. (2011b). Energy analysis of an improved concept of integrated pv panels in an office building in central Greece, *Applied Energy, 88*(3), 853-66.

APPENDICES

APPENDIX A: Weather Data
APPENDIX B: Schedules
APPENDIX C: Chiller and boiler database
APPENDIX D: Penalty parameters

APPENDIX A: Weather Data

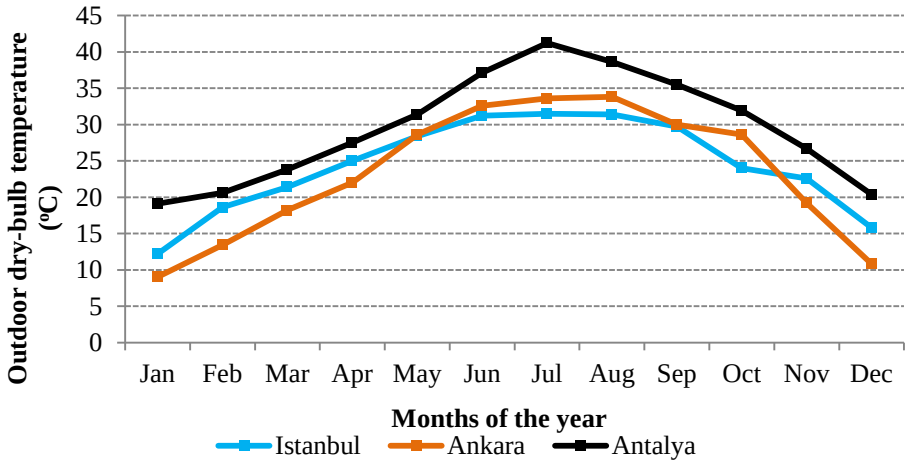

Figure A.1 : Monthly maximum outdoor air temperatures.

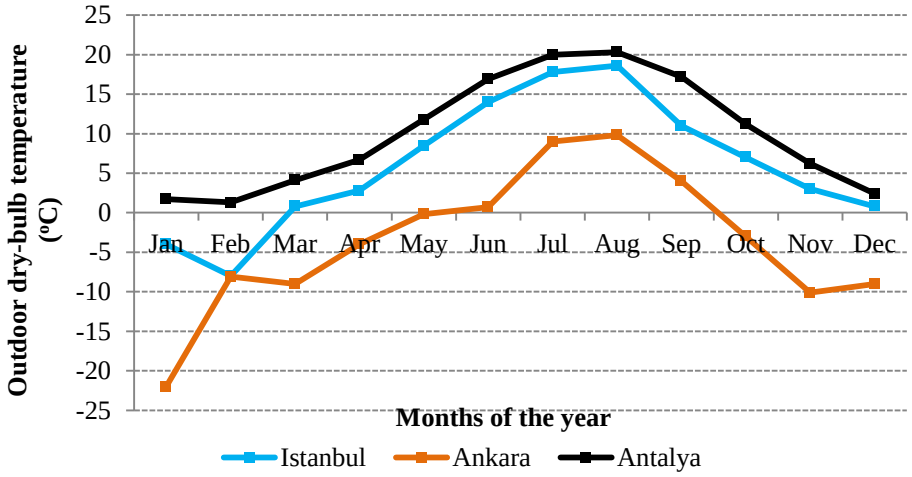

Figure A.2 : Monthly minimum outdoor air temperatures.

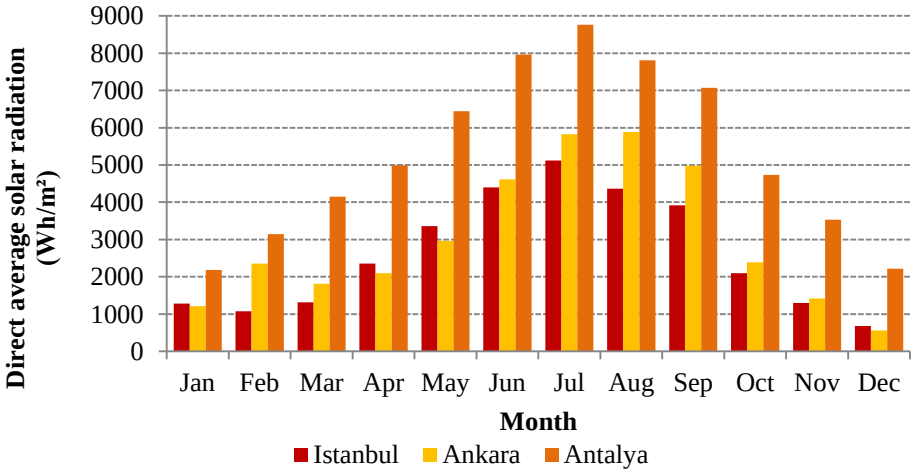

Figure A.3 : Monthly direct solar radiation.

Table A.1 : Winter design day for Istanbul, Ankara and Antalya.

Name	**Antalya**	**Ankara**	**Antalya**
Month	2	1	1
Day of Month	21	21	21
Maximum Dry-Bulb Temperature	-2.6	-15.7	1.4
Daily Dry-Bulb Temperature Range	0	0	0
Humidity Condition Type	Wetbulb	Wetbulb	Wetbulb
Wetbulb or DewPoint at Maximum Dry-Bulb	-2.6	-15.7	1.4
Barometric Pressure	100881	90432	100642
Wind Speed	6.2	0.5	4.5
Wind Direction	0	100	330
Solar Model Indicator	ASHRAE ClearSky	ASHRAE ClearSky	ASHRAE ClearSky

Table A.2 : Summer design day for Istanbul, Ankara and Antalya.

Name	**Antalya**	**Ankara**	**Antalya**
Month	8	8	7
Day of Month	21	21	21
Maximum Dry-Bulb Temperature	31.1	33	38
Daily Dry-Bulb Temperature Range	7.7	15.4	10.9
Humidity Condition Type	Wetbulb	Wetbulb	Wetbulb
Wetbulb or DewPoint at Maximum Dry-Bulb	21.4	17.6	21.9
Barometric Pressure	100881	90432	100642
Wind Speed	5.8	4	4.2
Wind Direction	30	230	0
Solar Model Indicator	ASHRAE Tau	ASHRAE Tau	ASHRAE Tau
ASHRAE Clear Sky Optical Depth for Beam Irradiance (taub)	0.47	0.52	0.504
ASHRAE Clear Sky Optical Depth for Diffuse Irradiance (taud)	1.973	1.726	1.87

APPENDIX B: Schedules

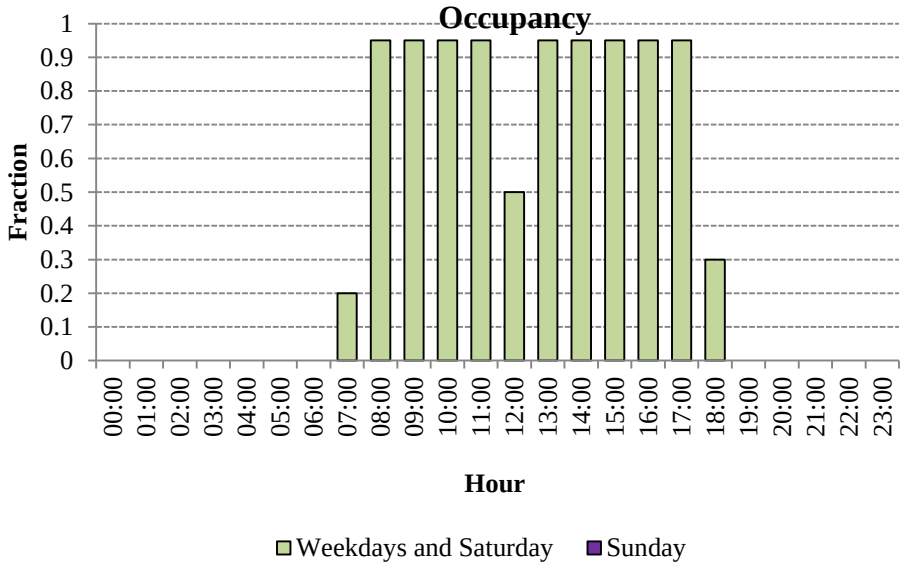

Figure B.1: Occupancy fraction schedule.

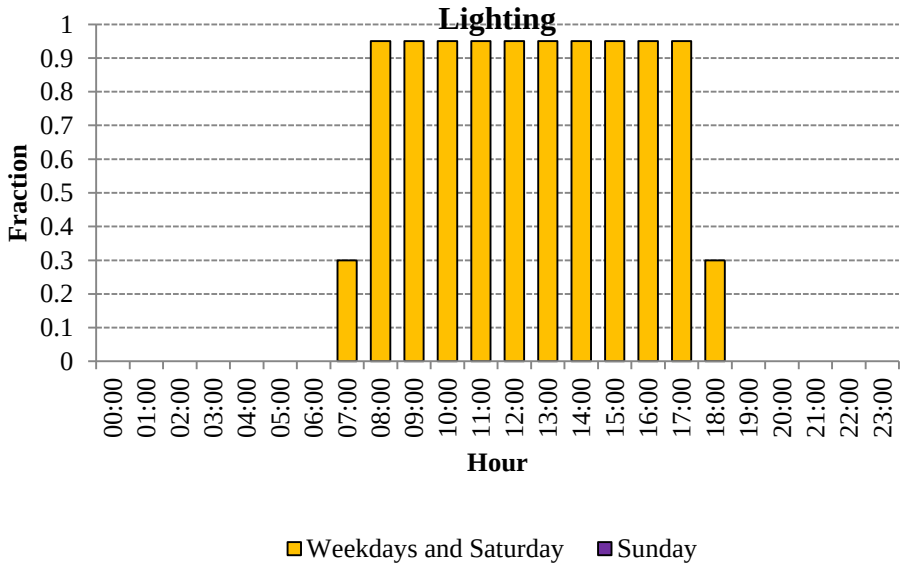

Figure B.2: Lighting fraction schedule.

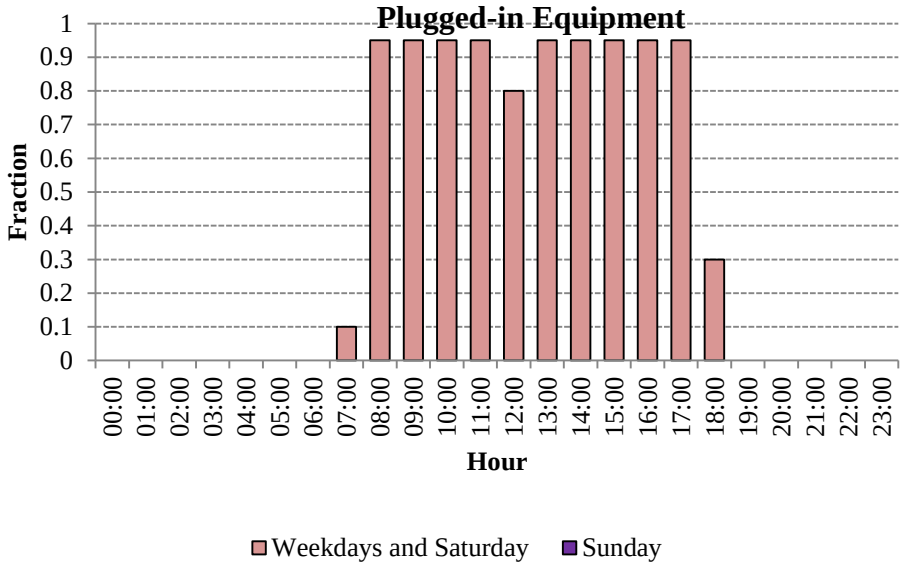

Figure B.3: Plugged-in equipment fraction schedule.

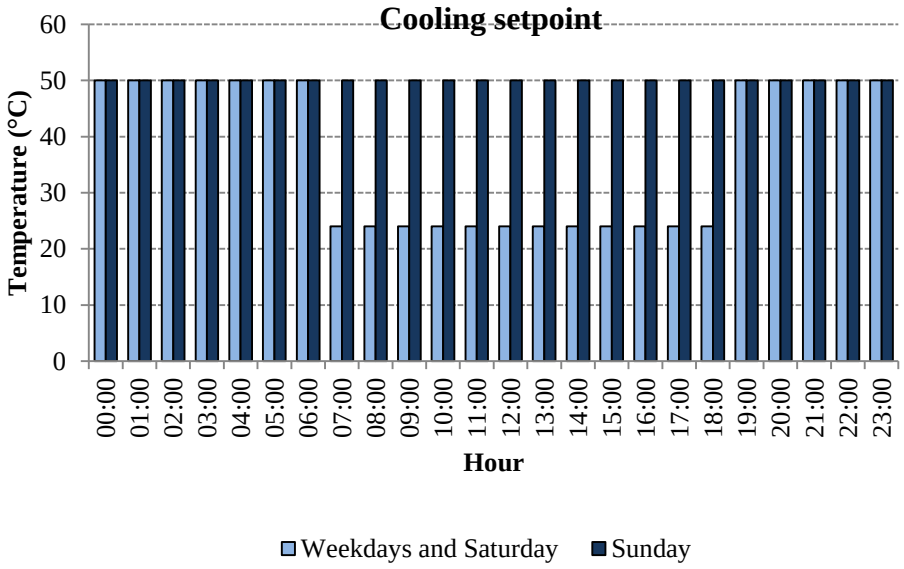

Figure B.4: Cooling setpoint schedule.

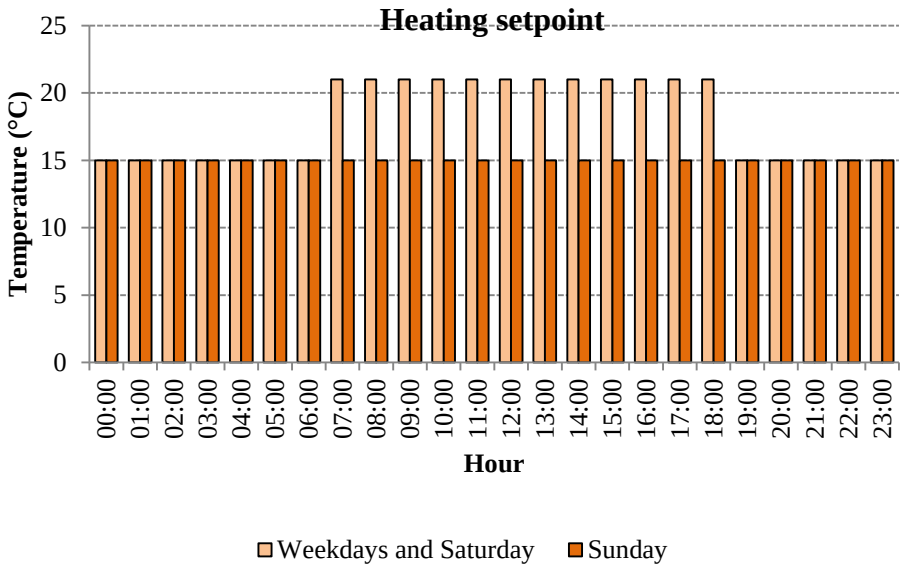

Figure B.5: Heating setpoint schedule.

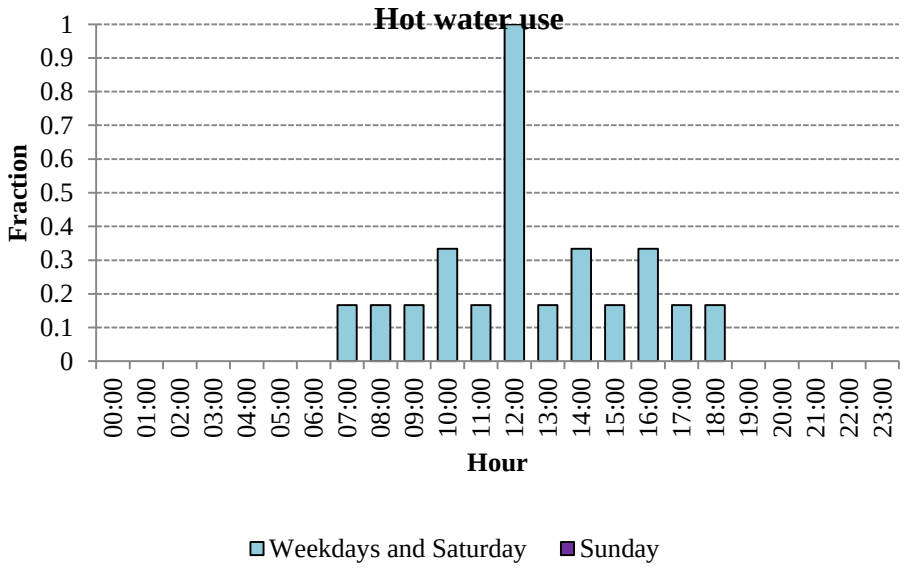

Figure B.6: Hot water use fraction schedule.

APPENDIX C: Chiller and boiler database

Table C.1: Boiler equipment database – low-efficiency equipment.

Group A: Low-efficiency Boilers				
Boiler ID	**Capacity (kW)**	**Nominal Thermal efficiency**	**Price (TL)**	**Efficiency curve**
1	55	0.84	2,453	BLE_1
2	76	0.84	2,942	BLE_2
3	93	0.84	3,339	BLE_3
4	111	0.84	3,736	BLE_4
5	128	0.84	4,135	BLE_5
6	145	0.84	4,531	BLE_6
7	163	0.84	4,637	BLE_7
8	195	0.84	5,114	BLE_8
9	227	0.84	5,710	BLE_9
10	259	0.84	6,281	BLE_10
11	291	0.84	6,869	BLE_11
12	323	0.84	7,448	BLE_12
13	355	0.84	8,029	BLE_13
14	405	0.84	9,297	BLE_14
15	448	0.84	10,113	BLE_15
16	506	0.84	11,053	BLE_16
17	564	0.84	12,146	BLE_17
18	610	0.84	13,240	BLE_18
19	663	0.84	14,332	BLE_19
20	715	0.84	15,511	BLE_20
21	773	0.84	16,553	BLE_21
22	831	0.84	17,647	BLE_22
23	878	0.84	18,689	BLE_23
24	930	0.84	19,782	BLE_24
25	1025	0.84	21,420	BLE_25
26	1115	0.84	23,180	BLE_26
27	1210	0.84	25,037	BLE_27

Table C.2: Boiler equipment database - high-efficiency equipment.

Group B: High-efficiency Boilers				
Boiler ID	**Capacity (kW)**	**Nominal Thermal efficiency**	**Price (TL)**	**Efficiency curve**
28	58	0.95	6,948	BLE_28
29	70	0.95	7,884	BLE_29
30	85	0.95	9,268	BLE_30
31	105	0.95	11,345	BLE_31
32	125	0.95	12,140	BLE_32
33	140	0.95	12,864	BLE_33
34	170	0.95	13,801	BLE_34
35	200	0.95	14,656	BLE_35
36	230	0.95	16,270	BLE_36
37	260	0.95	16,870	BLE_37
38	295	0.95	18,130	BLE_38
39	330	0.95	19,180	BLE_39
40	350	0.95	19,677	BLE_40
41	400	0.95	24,833	BLE_41
42	455	0.95	29,623	BLE_42
43	510	0.95	31,795	BLE_43
44	570	0.95	36,476	BLE_44
45	615	0.95	38,689	BLE_45
46	660	0.95	42,108	BLE_46
47	740	0.95	43,465	BLE_47
48	785	0.95	46,298	BLE_48
49	820	0.95	46,518	BLE_49
50	880	0.95	49,949	BLE_50
51	920	0.95	51,200	BLE_51
52	1020	0.95	56,112	BLE_52
53	1110	0.95	58,012	BLE_53
54	1200	0.95	58,147	BLE_54

Table C.3: Boiler thermal efficiency curves - low-efficiency equipment**.**

Group A – low efficiency boilers curve = C1 + C2*x + C3*x**2 + C4*y + C5*y**2 + C6*x*y + C7*x**3 + C8*y**3 + C9*x**2*y + C10*x*y**2	
Name	**BLE_1 – BLE_27**
Coefficient1 Constant	1.111720116
Coefficient2 x	0.078614078
Coefficient3 x**2	-0.400425756
Coefficient4 y	0
Coefficient5 y**2	-0.000156783
Coefficient6 x*y	0.009384599
Coefficient7 x**3	0.234257955
Coefficient8 y**3	1.33E-06
Coefficient9 x**2*y	-0.004446701
Coefficient10 x*y**2	-1.22E-05
Minimum Value of x	0.1
Maximum Value of x	1
Minimum Value of y	20
Maximum Value of y	80

Table C.4: Boiler thermal efficiency curves – high-efficiency equipment.

Group B – high efficiency boilers curve = C1 + C2*x + C3*x**2 + C4*y + C5*y**2 + C6*x*y	
Name	**BLE_28 – BLE_54**
Coefficient1 Constant	1.124970374
Coefficient2 x	0.014963852
Coefficient3 x**2	-0.02599835
Coefficient4 y	0
Coefficient5 y**2	-1.40E-06
Coefficient6 x*y	-0.00153624
Minimum Value of x	0.1
Maximum Value of x	1
Minimum Value of y	30
Maximum Value of y	85

Table C.5: Chiller equipment database – moderate-efficiency equipment**.**

Group A: Moderate-efficiency Chillers						
Chiller ID	**Capacity (kW)**	**EER**	**Price (TL)**	**Efficiency curves**		
				CAPFT	**EIRFT**	**EIRFPLR**
1	287	5.04	123,229	CAP_1	EIR_1	EPLR_1
2	312	4.8	124,326	CAP_2	EIR_2	EPLR_2
3	349	4.85	125,308	CAP_3	EIR_3	EPLR_3
4	375	4.57	126,977	CAP_4	EIR_4	EPLR_4
5	413	4.86	131,398	CAP_5	EIR_5	EPLR_5
6	450	4.69	136,273	CAP_6	EIR_6	EPLR_6
7	470	4.7	138,713	CAP_7	EIR_7	EPLR_7
8	510	4.72	142,623	CAP_8	EIR_8	EPLR_8
9	542	4.55	146,078	CAP_9	EIR_9	EPLR_9
10	599	4.68	155,377	CAP_10	EIR_10	EPLR_10
11	652	4.72	164,306	CAP_11	EIR_11	EPLR_11
12	701	4.74	174,659	CAP_12	EIR_12	EPLR_12
13	760	4.72	188,210	CAP_13	EIR_13	EPLR_13
14	814	4.73	200,847	CAP_14	EIR_14	EPLR_14
15	899	4.45	219,606	CAP_15	EIR_15	EPLR_15
16	986	4.76	238,666	CAP_16	EIR_16	EPLR_16
17	1109	4.76	259,971	CAP_17	EIR_17	EPLR_17
18	1207	4.55	276,983	CAP_18	EIR_18	EPLR_18
19	1302	4.65	292,566	CAP_19	EIR_19	EPLR_19
20	1420	4.7	323,780	CAP_20	EIR_20	EPLR_20
21	1630	4.76	355,795	CAP_21	EIR_21	EPLR_21
22	1750	4.73	380,899	CAP_22	EIR_22	EPLR_22

Table C.6: Chiller equipment database – high-efficiency equipment**.**

Group B: High-efficiency Chillers

Chiller ID	Capacity (kW)	EER	Price (TL)	Efficiency curves		
				CAPFT	EIRFT	EIRFPLR
23	270	5.64	151,420	CAP_23	EIR_23	EPLR_23
24	304	5.61	152,767	CAP_24	EIR_24	EPLR_24
25	355	5.53	153,975	CAP_25	EIR_25	EPLR_25
26	380	5.6	156,026	CAP_26	EIR_26	EPLR_26
27	420	5.63	161,458	CAP_27	EIR_27	EPLR_27
28	452	5.5	167,448	CAP_28	EIR_28	EPLR_28
29	466	5.65	170,446	CAP_29	EIR_29	EPLR_29
30	505	5.63	175,251	CAP_30	EIR_30	EPLR_30
31	571	5.54	187,228	CAP_31	EIR_31	EPLR_31
32	605	5.65	192,610	CAP_32	EIR_32	EPLR_32
33	660	5.7	203,827	CAP_33	EIR_33	EPLR_33
34	732	5.75	219,487	CAP_34	EIR_34	EPLR_34
35	780	5.53	233,732	CAP_35	EIR_35	EPLR_35
36	815	5.6	250,445	CAP_36	EIR_36	EPLR_36
37	853	5.56	263,747	CAP_37	EIR_37	EPLR_37
38	1035	5.68	311,982	CAP_38	EIR_38	EPLR_38
39	1150	5.71	341,345	CAP_39	EIR_39	EPLR_39
40	1230	5.7	363,633	CAP_40	EIR_40	EPLR_40
41	1317	5.73	390,737	CAP_41	EIR_41	EPLR_41
42	1442	5.5	417,272	CAP_42	EIR_42	EPLR_42
43	1614	5.81	459,320	CAP_43	EIR_43	EPLR_43
44	1742	5.72	496,423	CAP_44	EIR_44	EPLR_44

Table C.7: Chiller capacity as a function of temperature curve coefficients - moderate-efficiency equipment.

Group A: Moderate-efficiency Chillers

curve = C1 + C2*x + C3*x2 + C4*y + C5*y**2 + C6*x*y**

	Coef. 1	Coef. 2	Coef.3	Coef.4	Coef.5	Coef. 6	Min	Max	Min	Max
Name	**Constant**	**x**	**x**2**	**y**	**y**2**	**x*y**	**x**	**x**	**y**	**y**
CAP_1	9.62E-01	4.01E-02	8.71E-05	-4.60E-03	-6.97E-05	-2.26E-04	5	12	25	40
CAP_2	9.67E-01	4.15E-02	-4.01E-05	-5.35E-03	-5.61E-05	-2.11E-04	5	12	25	40
CAP_3	9.54E-01	4.17E-02	-3.58E-05	-4.70E-03	-6.45E-05	-2.16E-04	5	12	25	40
CAP_4	9.42E-01	4.40E-02	-4.81E-18	-4.54E-03	-5.33E-05	-3.13E-04	5	12	25	40
CAP_5	9.40E-01	4.16E-02	-1.85E-18	-4.34E-03	-6.05E-05	-2.25E-04	5	12	25	40
CAP_6	9.53E-01	4.03E-02	3.33E-18	-4.79E-03	-5.56E-05	-1.93E-04	5	12	25	40
CAP_7	9.53E-01	4.03E-02	3.33E-18	-4.79E-03	-5.56E-05	-1.93E-04	5	12	25	40
CAP_8	9.53E-01	4.09E-02	-2.45E-05	-5.02E-03	-5.39E-05	-1.86E-04	5	12	25	40
CAP_9	9.48E-01	4.18E-02	-2.31E-05	-4.96E-03	-5.07E-05	-2.11E-04	5	12	25	40
CAP_10	9.42E-01	4.24E-02	-2.09E-05	-4.76E-03	-5.43E-05	-2.20E-04	5	12	25	40
CAP_11	8.65E-01	3.55E-02	0.00E+00	-8.60E-04	-6.13E-05	-1.59E-04	5	12	25	40
CAP_12	9.47E-01	4.25E-02	-3.57E-05	-5.03E-03	-4.99E-05	-2.24E-04	5	12	25	40
CAP_13	9.47E-01	4.25E-02	-3.57E-05	-5.03E-03	-4.99E-05	-2.24E-04	5	12	25	40
CAP_14	9.54E-01	4.22E-02	-1.11E-18	-5.30E-03	-4.91E-05	-2.20E-04	5	12	25	40
CAP_15	9.39E-01	4.30E-02	-1.39E-05	-4.54E-03	-5.84E-05	-2.44E-04	5	12	25	40
CAP_16	8.83E-01	3.52E-02	-1.27E-05	-1.71E-03	-5.32E-05	-1.40E-04	5	12	25	40
CAP_17	9.39E-01	4.25E-02	-1.13E-05	-4.57E-03	-5.64E-05	-2.30E-04	5	12	25	40
CAP_18	9.47E-01	4.26E-02	-2.07E-05	-4.95E-03	-5.39E-05	-2.23E-04	5	12	25	40
CAP_19	8.77E-01	3.58E-02	-9.60E-06	-1.60E-03	-5.18E-05	-1.55E-04	5	12	25	40
CAP_20	9.47E-01	4.26E-02	-2.07E-05	-4.95E-03	-5.39E-05	-2.23E-04	5	12	25	40
CAP_21	8.77E-01	3.58E-02	-9.60E-06	-1.60E-03	-5.18E-05	-1.55E-04	5	12	25	40
CAP_22	8.77E-01	3.58E-02	-9.60E-06	-1.60E-03	-5.18E-05	-1.55E-04	5	12	25	40
CAP_23	7.68E-01	1.48E-02	-1.61E-04	1.05E-02	-3.03E-04	4.68E-04	5	18	25	45

Table C.8: Chiller capacity as a function of temperature curve coefficients - high-efficiency equipment.

Group B: High-efficiency Chillers

curve = C1 + C2*x + C3*x2 + C4*y + C5*y**2 + C6*x*y**

	Coef. 1	Coef. 2	Coef.3	Coef.4	Coef.5	Coef. 6	Min	Max	Min	Max
Name	**Constant**	**x**	**x**2**	**y**	**y**2**	**x*y**	**x**	**x**	**y**	**y**
CAP_24	7.32E-01	4.65E-04	-3.66E-04	1.56E-02	-4.17E-04	9.15E-04	5	18	25	45
CAP_25	7.80E-01	1.81E-02	-2.69E-04	8.87E-03	-2.82E-04	4.87E-04	5	18	25	45
CAP_26	7.80E-01	1.81E-02	-2.69E-04	8.87E-03	-2.82E-04	4.87E-04	5	18	25	45
CAP_27	9.27E-01	1.78E-02	-4.45E-04	2.64E-03	-2.68E-04	6.75E-04	5	18	25	45
CAP_28	9.27E-01	1.78E-02	-4.45E-04	2.64E-03	-2.68E-04	6.75E-04	5	18	25	45
CAP_29	7.29E-01	-2.06E-02	-1.99E-04	2.22E-02	-6.01E-04	1.43E-03	5	18	25	45
CAP_30	8.59E-01	3.32E-03	-3.47E-04	6.93E-03	-2.82E-04	8.55E-04	5	18	25	45
CAP_31	8.21E-01	5.95E-03	-3.92E-04	9.08E-03	-3.18E-04	8.34E-04	5	18	25	45
CAP_32	8.21E-01	5.95E-03	-3.92E-04	9.08E-03	-3.18E-04	8.34E-04	5	18	25	45
CAP_33	7.57E-01	1.33E-02	-2.76E-04	1.13E-02	-3.29E-04	6.02E-04	5	18	25	45
CAP_34	7.57E-01	1.33E-02	-2.76E-04	1.13E-02	-3.29E-04	6.02E-04	5	18	25	45
CAP_35	7.41E-01	1.58E-02	-1.71E-04	1.21E-02	-3.33E-04	4.81E-04	5	18	25	45
CAP_36	7.67E-01	1.39E-02	-2.23E-04	1.11E-02	-3.29E-04	5.50E-04	5	18	25	45
CAP_37	7.67E-01	1.39E-02	-2.23E-04	1.11E-02	-3.29E-04	5.50E-04	5	18	25	45
CAP_38	8.66E-01	3.43E-03	-3.50E-04	6.23E-03	-2.68E-04	8.48E-04	5	18	25	45
CAP_39	8.60E-01	1.60E-03	-2.79E-04	7.08E-03	-2.81E-04	8.44E-04	5	18	25	45
CAP_40	8.02E-01	1.38E-02	-2.12E-04	8.49E-03	-2.82E-04	5.45E-04	5	18	25	45
CAP_41	8.02E-01	1.38E-02	-2.12E-04	8.49E-03	-2.82E-04	5.45E-04	5	18	25	45
CAP_42	7.82E-01	2.37E-02	-9.99E-05	8.20E-03	-2.63E-04	2.68E-04	5	18	25	45
CAP_43	7.48E-01	1.34E-02	-2.19E-04	1.20E-02	-3.35E-04	5.49E-04	5	18	25	45
CAP_44	7.77E-01	1.37E-02	-2.43E-04	1.05E-02	-3.17E-04	5.53E-04	5	18	25	45

Table C.9: Chiller Energy Input Ratio as a Function of Temperature curve coefficients- moderate-efficiency equipment.

Group A: Moderate-efficiency Chillers

curve = C1 + C2*x + C3*x2 + C4*y + C5*y**2 + C6*x*y**

	Coef. 1	Coef. 2	Coef.3	Coef.4	Coef.5	Coef. 6	Min	Max	Min	Max
Name	**Constant**	**x**	**x**2**	**y**	**y**2**	**x*y**	**x**	**x**	**y**	**y**
EIR_1	7.96E-01	-1.25E-03	7.38E-04	-9.84E-03	8.11E-04	-1.23E-03	5	12	25	40
EIR_2	8.89E-01	-1.21E-02	1.40E-03	-1.29E-02	8.54E-04	-1.21E-03	5	12	25	40
EIR_3	8.68E-01	-1.27E-02	1.28E-03	-1.17E-02	8.32E-04	-1.12E-03	5	12	25	40
EIR_4	8.26E-01	-1.01E-02	1.10E-03	-1.04E-02	8.02E-04	-1.07E-03	5	12	25	40
EIR_5	8.49E-01	-7.00E-03	9.31E-04	-1.24E-02	8.41E-04	-1.10E-03	5	12	25	40
EIR_6	7.80E-01	-3.93E-03	8.92E-04	-9.62E-03	8.25E-04	-1.21E-03	5	12	25	40
EIR_7	7.80E-01	-3.93E-03	8.92E-04	-9.62E-03	8.25E-04	-1.21E-03	5	12	25	40
EIR_8	8.47E-01	-1.21E-02	1.24E-03	-9.95E-03	7.91E-04	-1.14E-03	5	12	25	40
EIR_9	8.66E-01	-1.14E-02	1.11E-03	-1.18E-02	8.37E-04	-1.15E-03	5	12	25	40
EIR_10	8.85E-01	-1.54E-02	1.34E-03	-1.09E-02	8.06E-04	-1.14E-03	5	12	25	40
EIR_11	8.73E-01	-1.04E-02	8.14E-04	-9.13E-03	6.81E-04	-8.60E-04	5	12	25	40
EIR_12	8.09E-01	-8.75E-03	1.11E-03	-1.01E-02	8.45E-04	-1.23E-03	5	12	25	40
EIR_13	8.09E-01	-8.75E-03	1.11E-03	-1.01E-02	8.45E-04	-1.23E-03	5	12	25	40
EIR_14	8.70E-01	-1.14E-02	1.16E-03	-1.17E-02	8.31E-04	-1.17E-03	5	12	25	40
EIR_15	8.61E-01	-8.16E-03	1.03E-03	-1.15E-02	8.27E-04	-1.21E-03	5	12	25	40
EIR_16	7.94E-01	-8.42E-03	7.42E-04	-5.39E-03	6.32E-04	-8.54E-04	5	12	25	40
EIR_17	8.45E-01	-9.51E-03	1.19E-03	-1.12E-02	8.51E-04	-1.27E-03	5	12	25	40
EIR_18	8.86E-01	-1.00E-02	1.08E-03	-1.25E-02	8.33E-04	-1.16E-03	5	12	25	40
EIR_19	8.53E-01	-1.10E-02	7.97E-04	-8.06E-03	6.65E-04	-8.17E-04	5	12	25	40
EIR_20	8.86E-01	-1.00E-02	1.08E-03	-1.25E-02	8.33E-04	-1.16E-03	5	12	25	40
EIR_21	8.53E-01	-1.10E-02	7.97E-04	-8.06E-03	6.65E-04	-8.17E-04	5	12	25	40
EIR_22	8.53E-01	-1.10E-02	7.97E-04	-8.06E-03	6.65E-04	-8.17E-04	5	12	25	40

Table C.10: Chiller Energy Input Ratio as a Function of Temperature curve coefficients - high-efficiency equipment.

Group B: High-efficiency Chillers

curve = C1 + C2*x + C3*x2 + C4*y + C5*y**2 + C6*x*y**

	Coef. 1	Coef. 2	Coef.3	Coef.4	Coef.5	Coef. 6	Min	Max	Min	Max
Name	**Constant**	**x**	**x**2**	**y**	**y**2**	**x*y**	**x**	**x**	**y**	**y**
EIR_23	6.14E-01	-2.31E-03	9.07E-04	-2.22E-03	7.81E-04	-1.33E-03	5	18	25	45
EIR_24	6.44E-01	1.18E-02	8.84E-04	-7.76E-03	9.02E-04	-1.65E-03	5	18	25	45
EIR_25	6.11E-01	-4.29E-03	1.01E-03	-2.84E-04	7.26E-04	-1.33E-03	5	18	25	45
EIR_26	6.11E-01	-4.29E-03	1.01E-03	-2.84E-04	7.26E-04	-1.33E-03	5	18	25	45
EIR_27	6.41E-01	4.59E-03	1.25E-03	-4.43E-03	8.62E-04	-1.82E-03	5	18	25	45
EIR_28	6.41E-01	4.59E-03	1.25E-03	-4.43E-03	8.62E-04	-1.82E-03	5	18	25	45
EIR_29	6.10E-01	1.53E-02	1.34E-03	-5.69E-03	9.31E-04	-2.13E-03	5	18	25	45
EIR_30	6.01E-01	1.02E-02	9.99E-04	-2.65E-03	8.02E-04	-1.72E-03	5	18	25	45
EIR_31	6.20E-01	8.10E-03	1.05E-03	-3.85E-03	8.27E-04	-1.70E-03	5	18	25	45
EIR_32	6.20E-01	8.10E-03	1.05E-03	-3.85E-03	8.27E-04	-1.70E-03	5	18	25	45
EIR_33	6.85E-01	2.17E-03	1.02E-03	-7.25E-03	8.72E-04	-1.53E-03	5	18	25	45
EIR_34	6.85E-01	2.17E-03	1.02E-03	-7.25E-03	8.72E-04	-1.53E-03	5	18	25	45
EIR_35	6.97E-01	2.73E-03	8.78E-04	-8.86E-03	8.97E-04	-1.45E-03	5	18	25	45
EIR_36	6.58E-01	4.03E-03	8.05E-04	-5.74E-03	8.17E-04	-1.39E-03	5	18	25	45
EIR_37	6.58E-01	4.03E-03	8.05E-04	-5.74E-03	8.17E-04	-1.39E-03	5	18	25	45
EIR_38	5.96E-01	9.43E-03	1.04E-03	-1.94E-03	7.92E-04	-1.73E-03	5	18	25	45
EIR_39	6.08E-01	1.09E-02	9.65E-04	-3.17E-03	8.06E-04	-1.68E-03	5	18	25	45
EIR_40	6.08E-01	1.09E-02	9.65E-04	-3.17E-03	8.06E-04	-1.68E-03	5	18	25	45
EIR_41	6.58E-01	2.87E-03	9.69E-04	-5.00E-03	8.19E-04	-1.49E-03	5	18	25	45
EIR_42	6.95E-01	-3.28E-04	8.63E-04	-7.43E-03	8.55E-04	-1.36E-03	5	18	25	45
EIR_43	6.95E-01	3.24E-03	9.45E-04	-8.57E-03	8.93E-04	-1.48E-03	5	18	25	45
EIR_44	6.70E-01	1.77E-03	9.42E-04	-5.79E-03	8.19E-04	-1.40E-03	5	18	25	45

Table C.11: Energy Input Ratio as a Function of Part-load Ratio curve- moderate-efficiency equipment.

Group A: Moderate-efficiency Chillers

curve = C1 + C2*x + C3*x2**

Name	Coeff.1 Constant	Coeff.2 x	Coeff.3 x**2	Min x	Max x
EPLR_1	4.15E-02	6.54E-01	3.04E-01	0.25	1.01
EPLR_2	3.30E-02	9.11E-01	5.57E-02	0.25	1.01
EPLR_3	3.30E-02	9.11E-01	5.57E-02	0.25	1.01
EPLR_4	3.30E-02	9.11E-01	5.57E-02	0.25	1.01
EPLR_5	3.30E-02	9.11E-01	5.57E-02	0.25	1.01
EPLR_6	1.98E-01	2.73E-01	5.28E-01	0.3	1.01
EPLR_7	1.98E-01	2.73E-01	5.28E-01	0.3	1.01
EPLR_8	1.82E-01	3.73E-01	4.45E-01	0.3	1.01
EPLR_9	3.06E-01	-1.55E-01	8.48E-01	0.3	1.01
EPLR_10	3.06E-01	-1.55E-01	8.48E-01	0.3	1.01
EPLR_11	3.06E-01	-1.55E-01	8.48E-01	0.3	1.01
EPLR_12	2.00E-01	6.75E-01	1.24E-01	0.28	1.01
EPLR_13	2.00E-01	6.75E-01	1.24E-01	0.28	1.01
EPLR_14	2.00E-01	6.75E-01	1.24E-01	0.28	1.01
EPLR_15	1.32E-01	1.01E+00	-1.41E-01	0.3	1.01
EPLR_16	1.01E-01	1.12E+00	-2.17E-01	0.3	1.01
EPLR_17	1.63E-01	7.90E-01	4.77E-02	0.25	1.01
EPLR_18	1.63E-01	7.90E-01	4.77E-02	0.25	1.01
EPLR_19	1.63E-01	7.90E-01	4.77E-02	0.25	1.01
EPLR_20	1.63E-01	7.90E-01	4.77E-02	0.25	1.01
EPLR_21	1.63E-01	7.90E-01	4.77E-02	0.25	1.01
EPLR_22	1.63E-01	7.90E-01	4.77E-02	0.25	1.01

Table C.12: Energy Input Ratio as a Function of Part-load Ratio curve - high-efficiency equipment.

Group B: High-efficiency Chillers

curve = C1 + C2*x + C3*x2**

Name	Coeff.1 Constant	Coeff.2 x	Coeff.3 x**2	Min x	Max x
EPLR_23	1.20E-01	1.40E-01	7.39E-01	0.19	1.02
EPLR_24	1.20E-01	1.40E-01	7.39E-01	0.19	1.02
EPLR_25	1.20E-01	1.40E-01	7.39E-01	0.19	1.02
EPLR_26	1.20E-01	1.40E-01	7.39E-01	0.19	1.02
EPLR_27	1.20E-01	1.40E-01	7.39E-01	0.19	1.02
EPLR_28	1.20E-01	1.40E-01	7.39E-01	0.19	1.02
EPLR_29	1.20E-01	1.40E-01	7.39E-01	0.19	1.02
EPLR_30	1.20E-01	1.40E-01	7.39E-01	0.19	1.02
EPLR_31	1.20E-01	1.40E-01	7.39E-01	0.19	1.02
EPLR_32	1.20E-01	1.40E-01	7.39E-01	0.19	1.02
EPLR_33	1.20E-01	1.40E-01	7.39E-01	0.19	1.02
EPLR_34	1.20E-01	1.40E-01	7.39E-01	0.19	1.02
EPLR_35	1.20E-01	1.40E-01	7.39E-01	0.19	1.02
EPLR_36	1.50E-01	-6.80E-02	9.17E-01	0.18	1.03
EPLR_37	1.50E-01	-6.80E-02	9.17E-01	0.18	1.03
EPLR_38	1.41E-01	-1.58E-01	1.01E+00	0.2	1.03
EPLR_39	1.61E-01	-2.06E-01	1.04E+00	0.19	1.01
EPLR_40	3.34E-01	-4.10E-01	1.08E+00	0.19	1.02
EPLR_41	3.34E-01	-4.10E-01	1.08E+00	0.19	1.02
EPLR_42	9.66E-02	7.48E-01	1.57E-01	0.18	1.03
EPLR_43	9.66E-02	7.48E-01	1.57E-01	0.18	1.03
EPLR_44	9.66E-02	7.48E-01	1.57E-01	0.18	1.03

APPENDIX D: Penalty Parameters

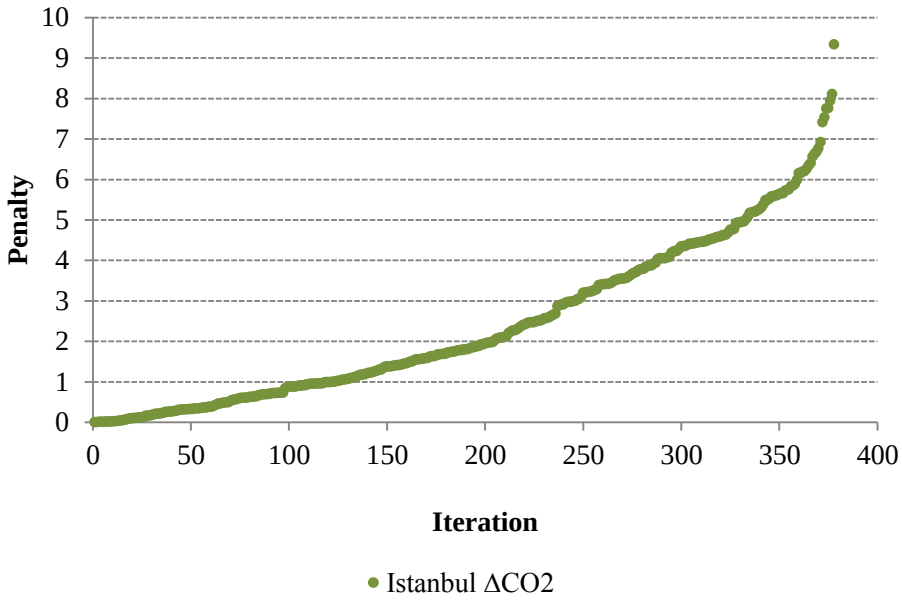

Figure D.1: The difference between the CO2 emission rate of any design option and the target rate for Istanbul case (ΔCO2).

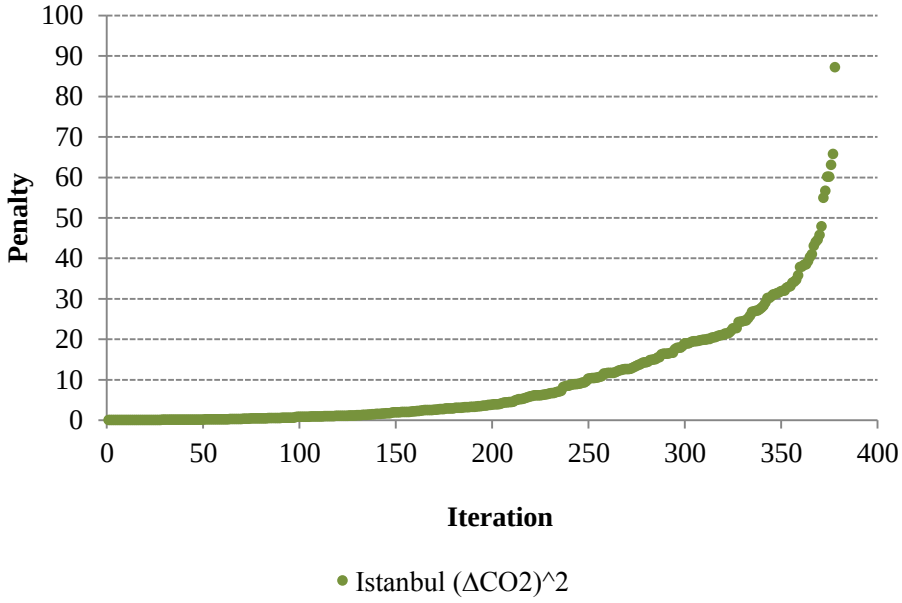

Figure D.2: The squared value of the ΔCO2 for Istanbul case.

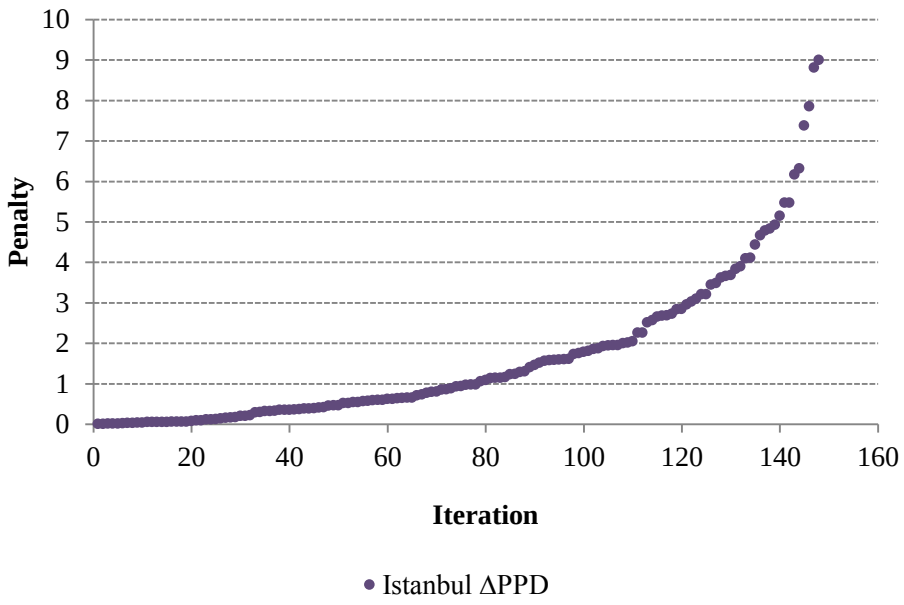

Figure D.3: The difference between the PPD index of any design option and the target index for Istanbul case (ΔPPD).

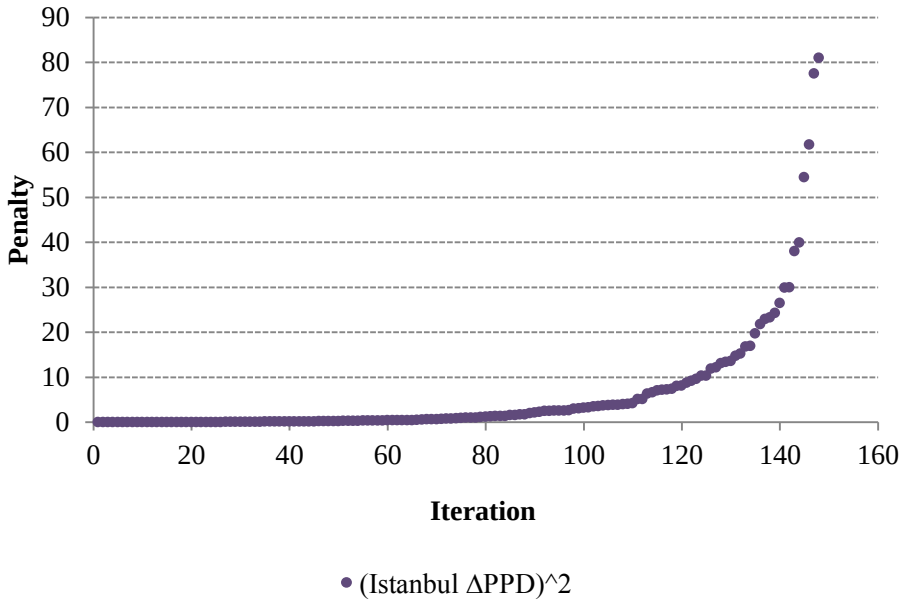

Figure D.4: The squared value of the ΔPPD for Istanbul case.

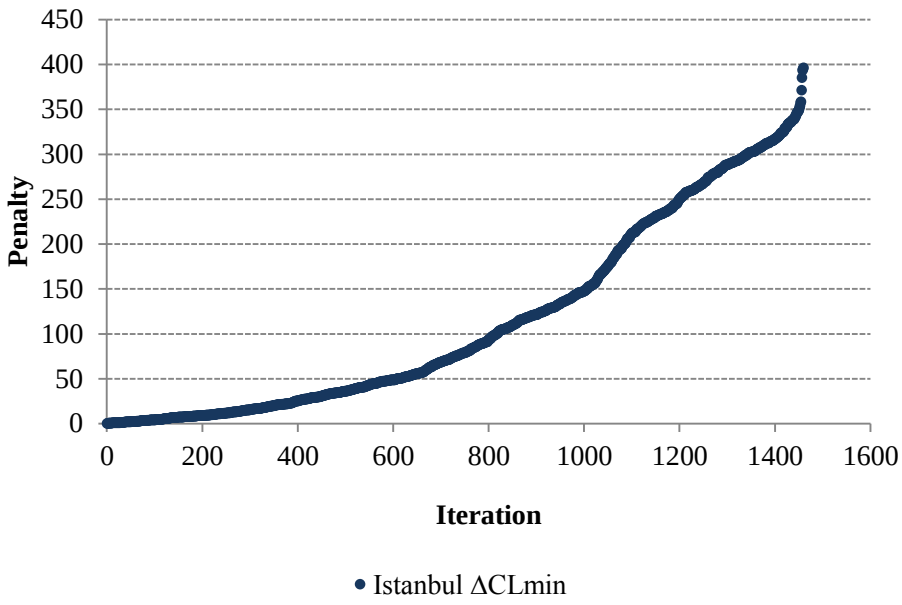

Figure D.5: The difference between the minimum allowed chiller capacity and the recommended chiller equipment capacity for Istanbul case (ΔCLmin).

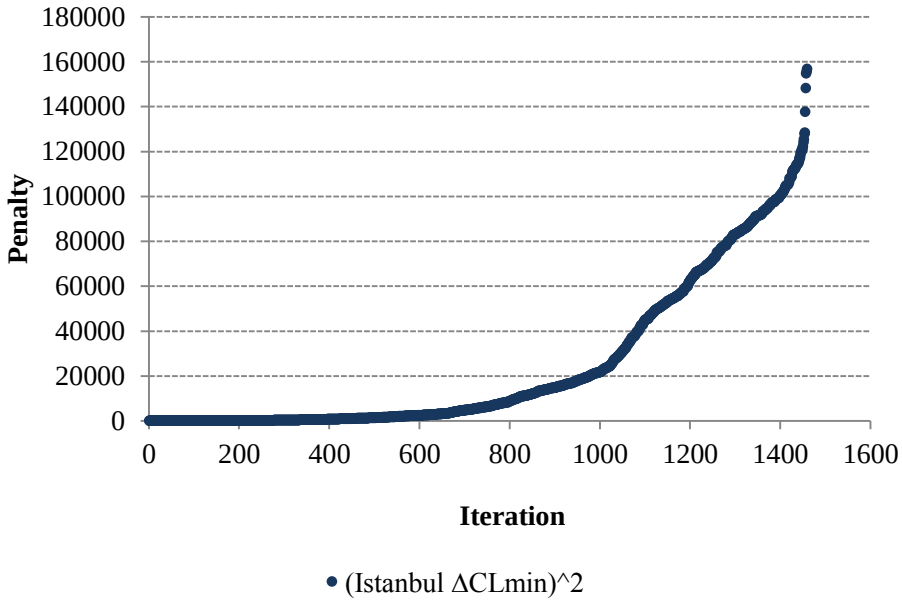

Figure D.6: The squared value of the ΔCLmin for Istanbul case.

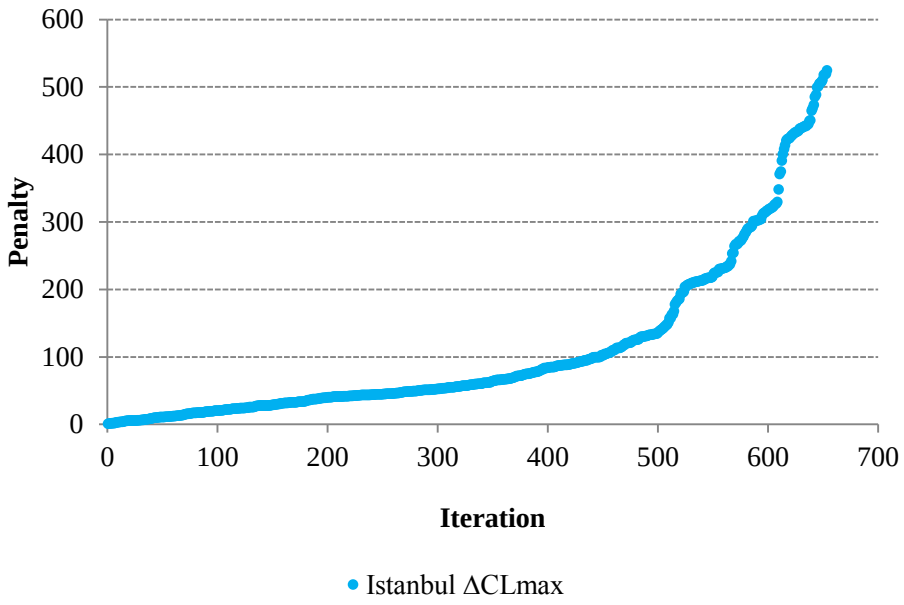

Figure D.7: The difference between the recommended chiller equipment capacity and the maximum allowed chiller capacity for Istanbul case (ΔCLmax).

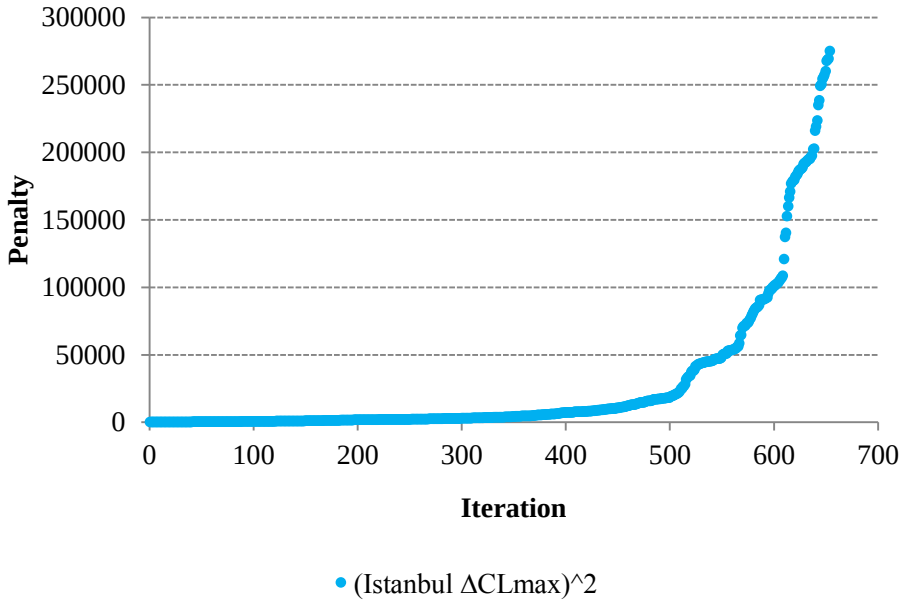

Figure D.8: The squared value of the ΔCLmax for Istanbul case.

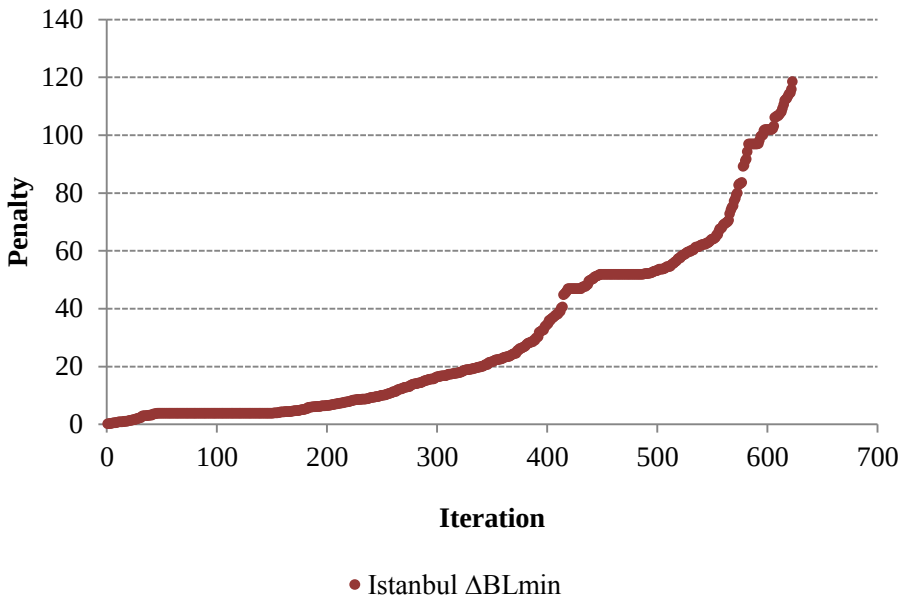

Figure D.9: The difference between the minimum allowed boiler capacity and the recommended boiler equipment capacity for Istanbul case (ΔBLmin).

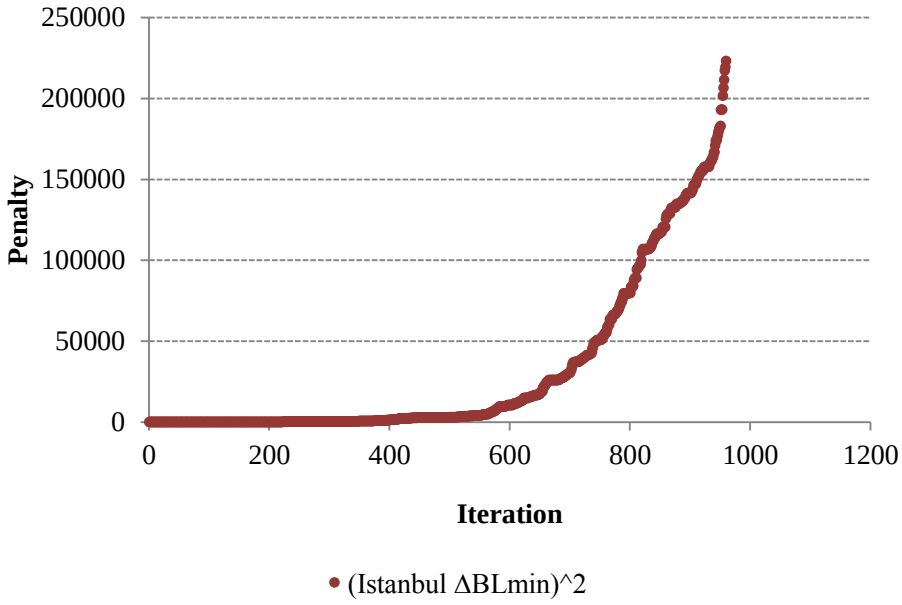

Figure D.10: The squared value of the ΔBLmin for Istanbul case.

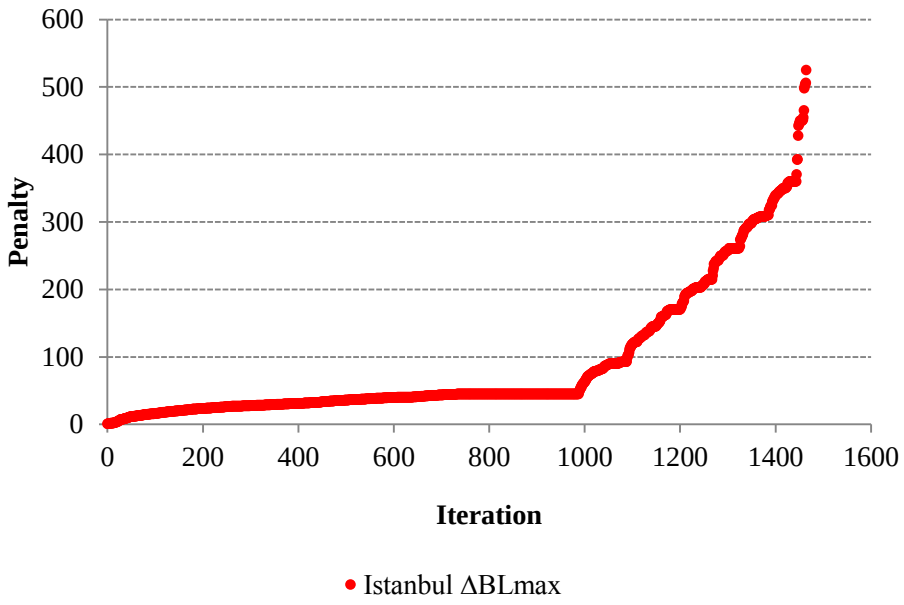

Figure D.11: The difference between the recommended boiler equipment capacity and the maximum allowed boiler capacity for Istanbul case (ΔBLmax).

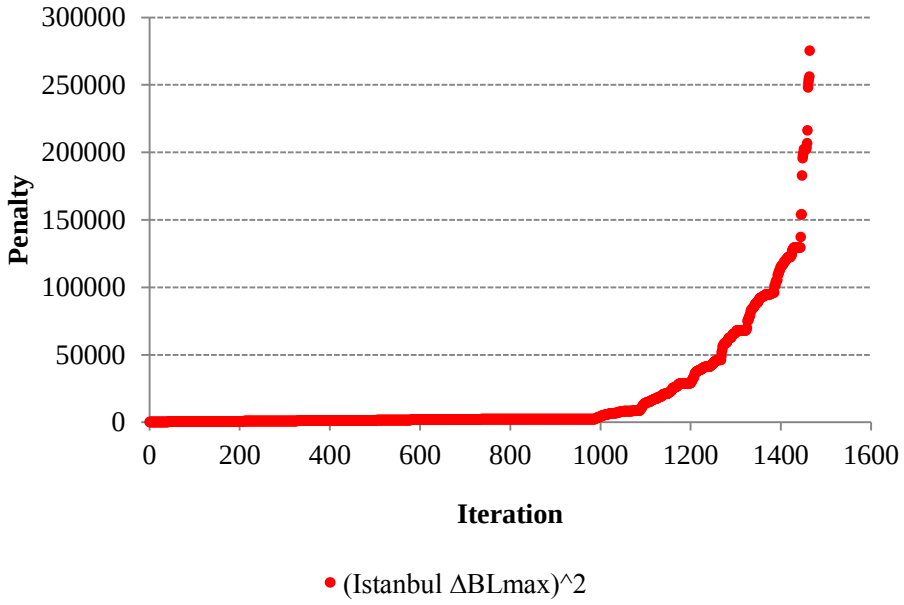

Figure D.12: The squared value of the ΔBLmax for Istanbul case.

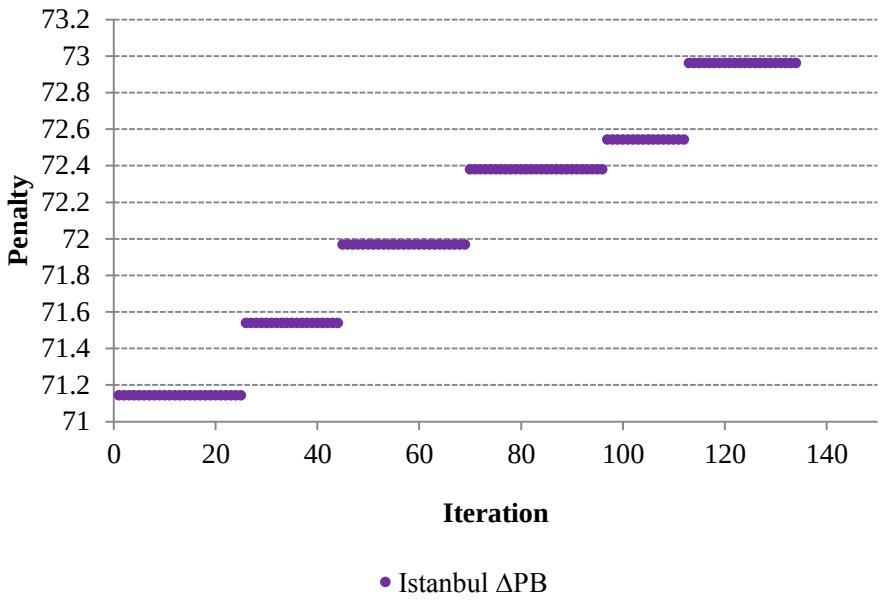

Figure D.13: The difference between the baypack period of any design option with PV and the target payback period for Istanbul case (ΔBLmax).

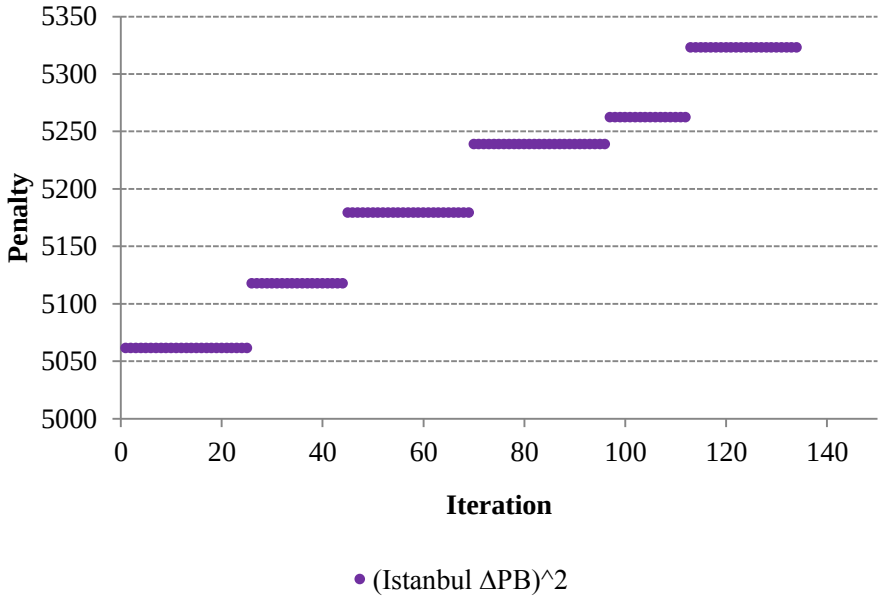

Figure D.14: The squared value of the ΔPB for Istanbul case.

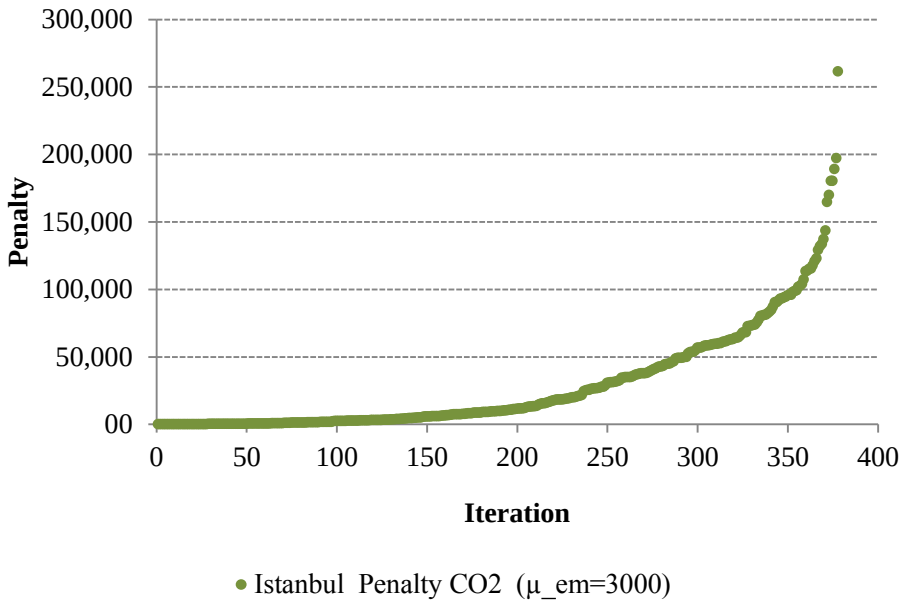

Figure D.15: Penalty function values of the CO2 emission for Istanbul case.

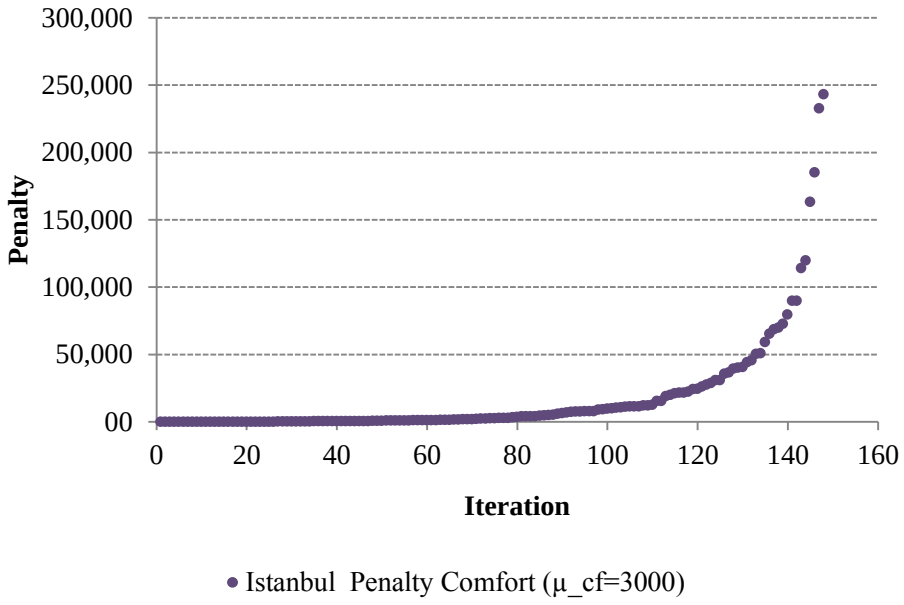

Figure D.16: Penalty function values of the PPD index for Istanbul case.

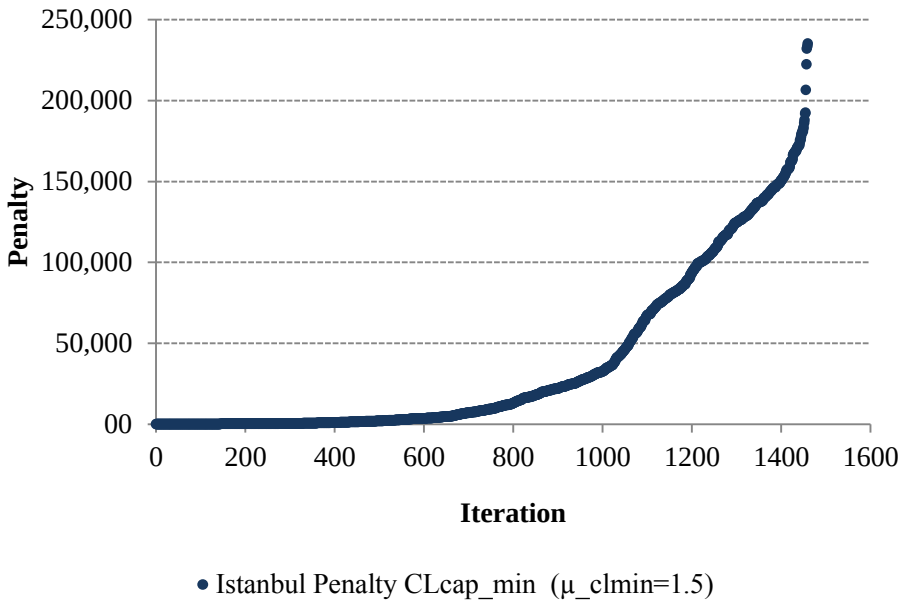

Figure D.17: Penalty function values of the chiller minimum capacity for Istanbul case.

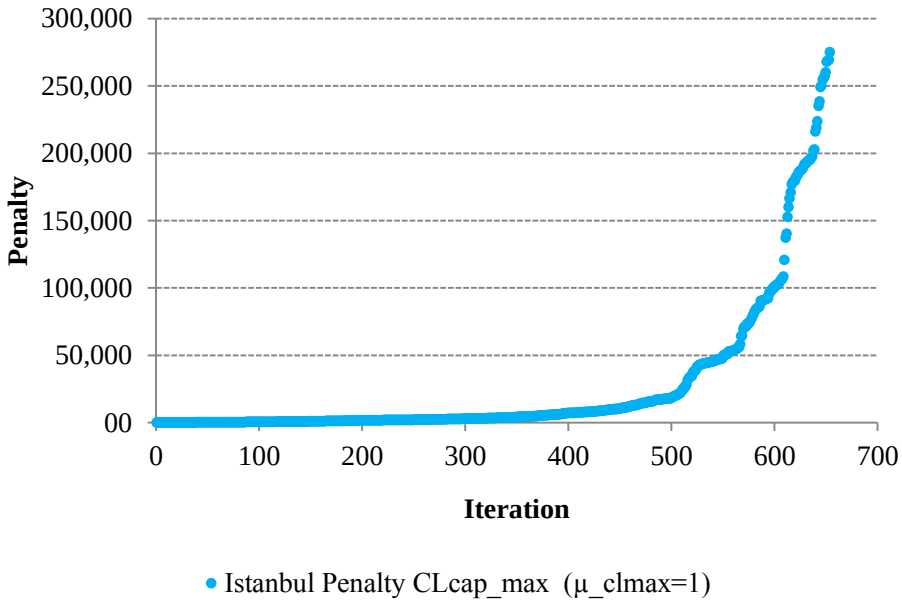

Figure D.18: Penalty function values of the chiller maximum capacity for Istanbul case.

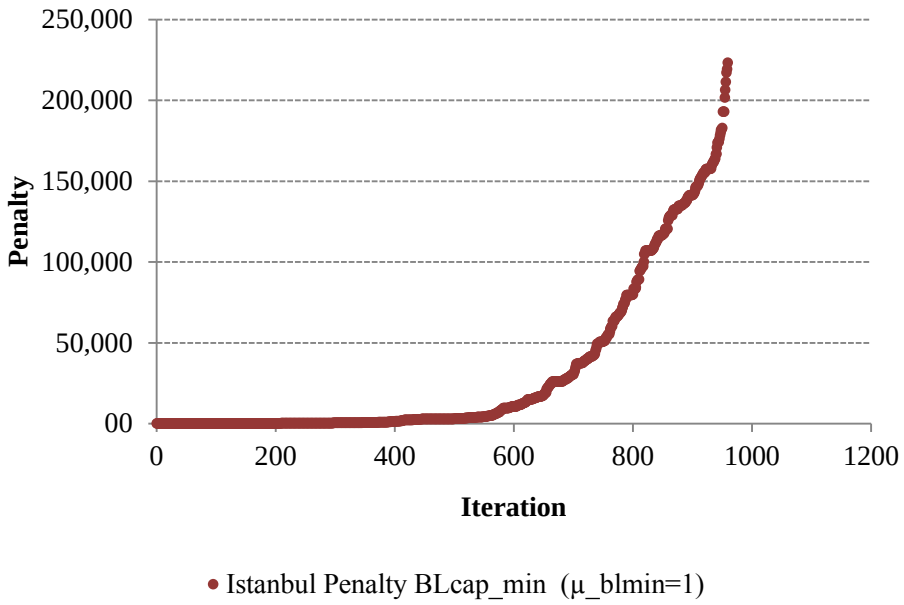

Figure D.19: Penalty function values of the boiler minimum capacity for Istanbul case.

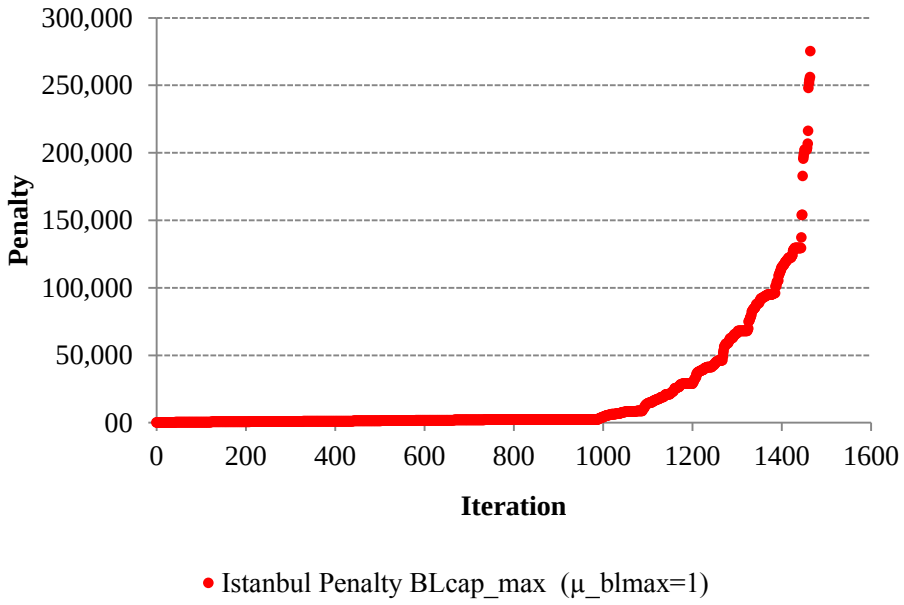

Figure D.20: Penalty function values of the boiler maximum capacity for Istanbul case.

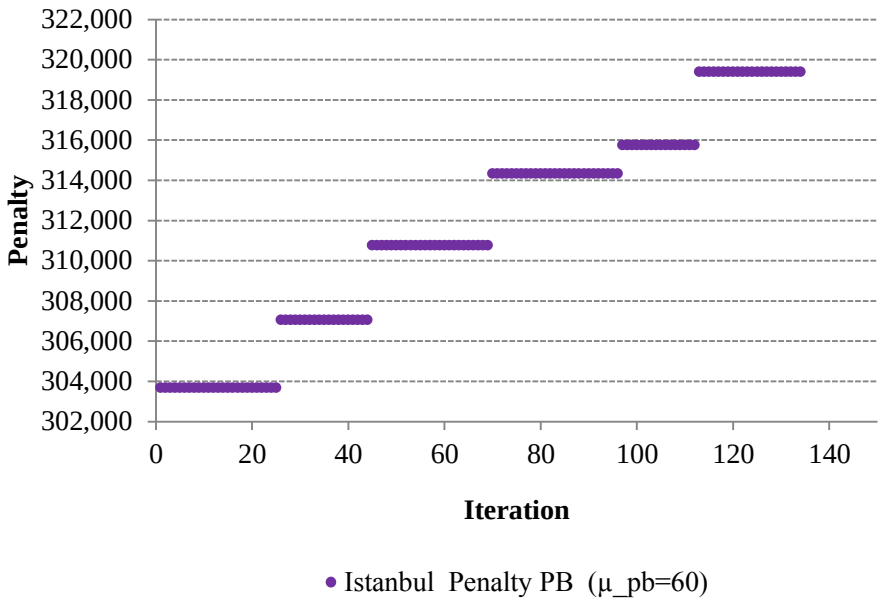

Figure D.21: Penalty function values of the payback period for Istanbul case.

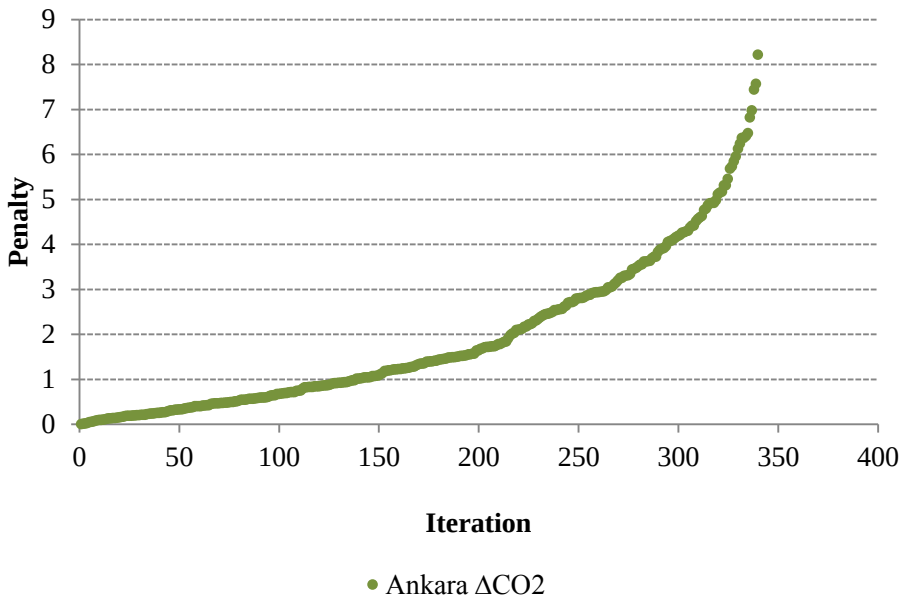

Figure D.22: The difference between the CO2 emission rate of any design option and the target rate for Ankara case (ΔCO2).

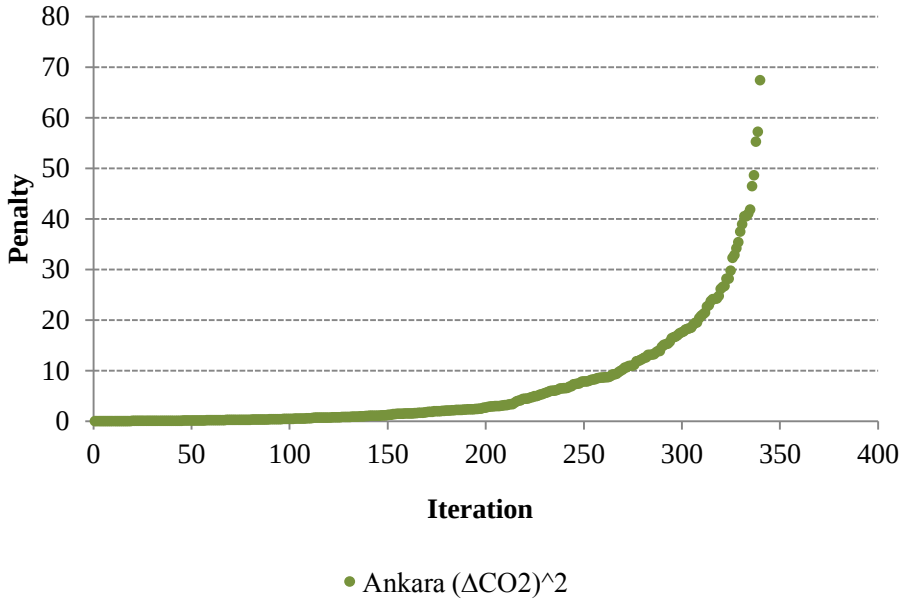

Figure D.23: The squared value of the ΔCO2 for Ankara case.

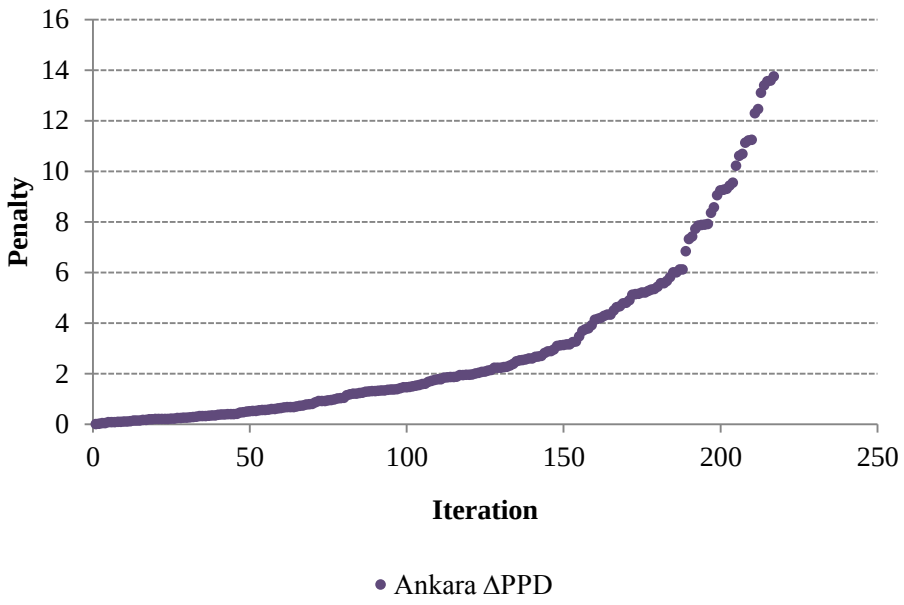

Figure D.24: The difference between the PPD index of any design option and the target index for Ankara case (ΔPPD).

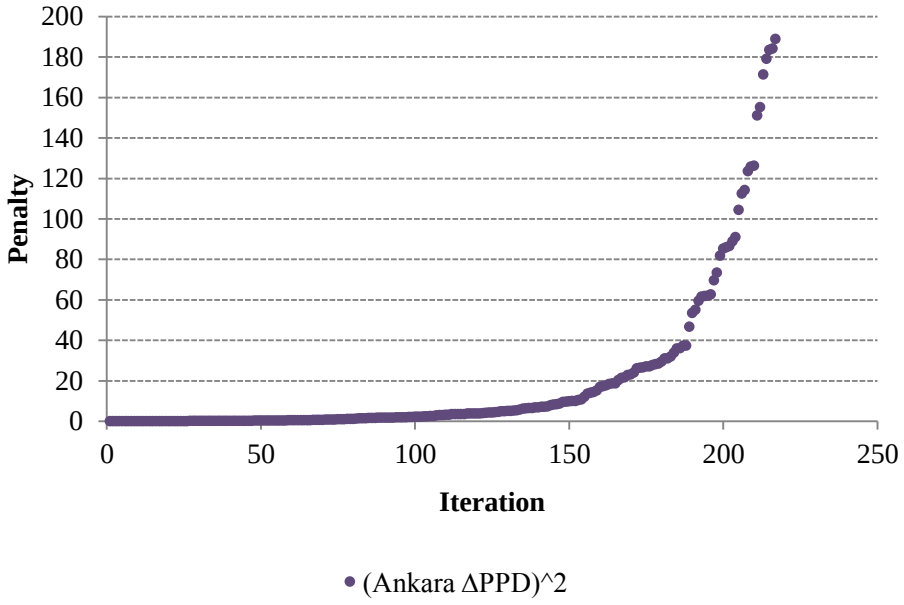

Figure D.25: The squared value of the ΔPPD for Ankara case.

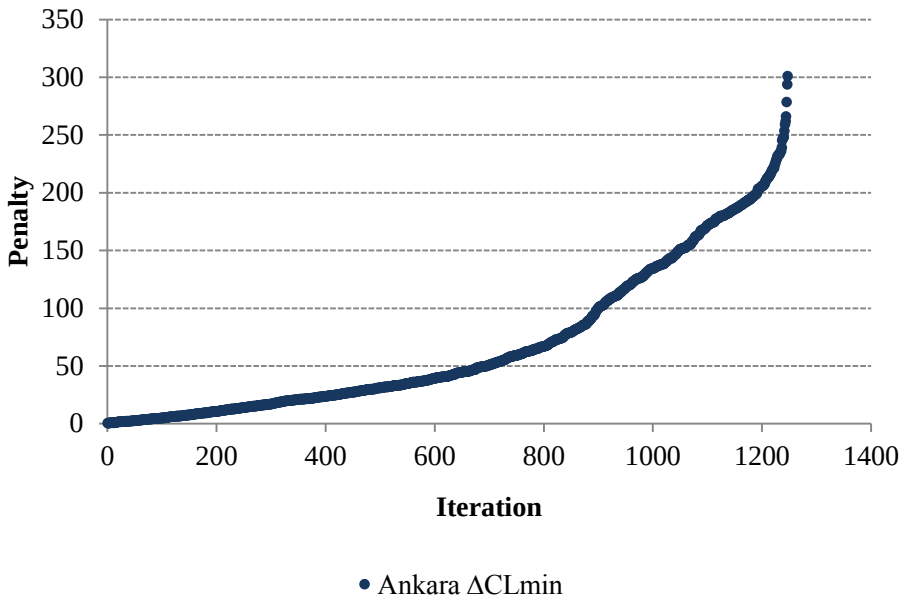

Figure D.26: The difference between the minimum allowed chiller capacity and the recommended chiller equipment capacity for Ankara case (ΔCLmin).

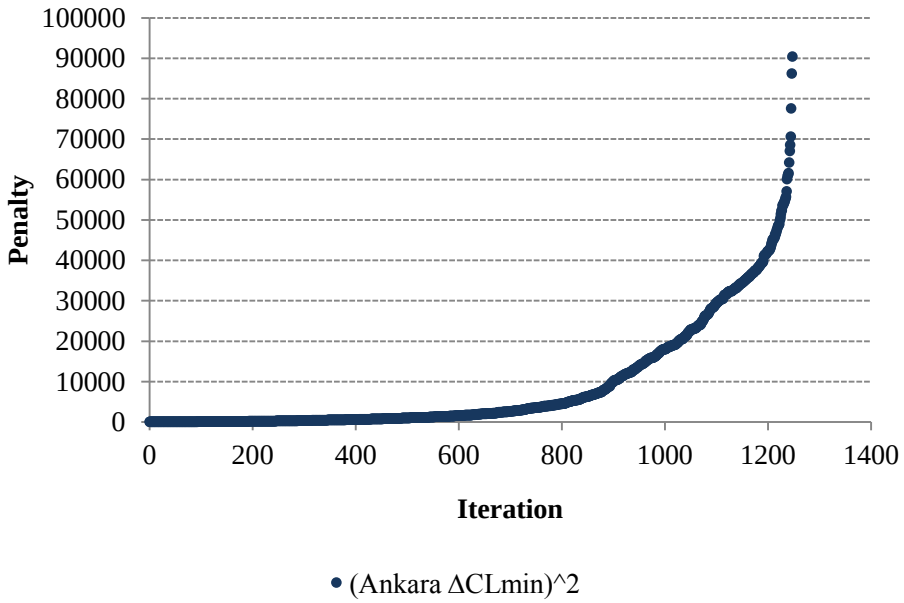

Figure D.27: The squared value of the ΔCLmin for Ankara case.

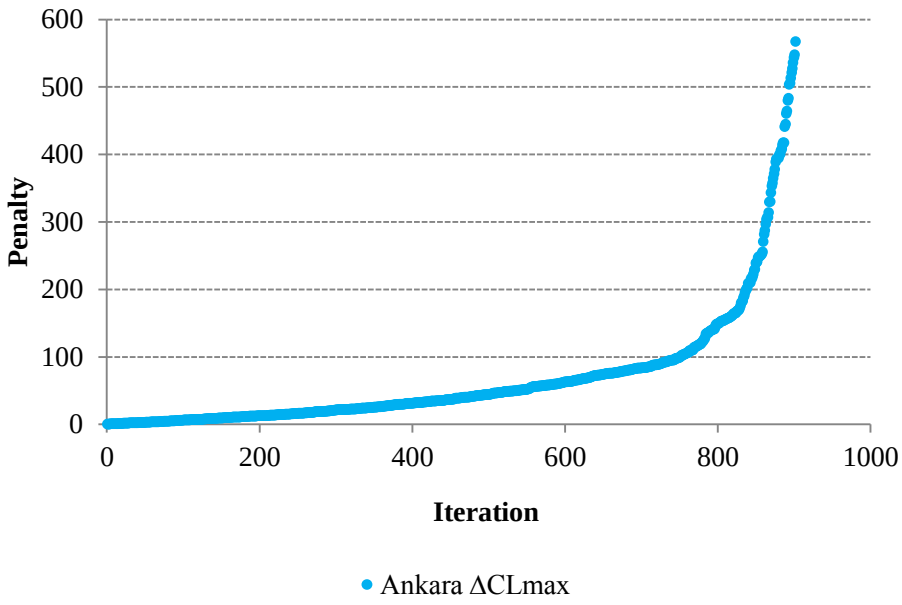

Figure D.28: The difference between the recommended chiller equipment capacity and the maximum allowed chiller capacity for Ankara case (ΔCLmax).

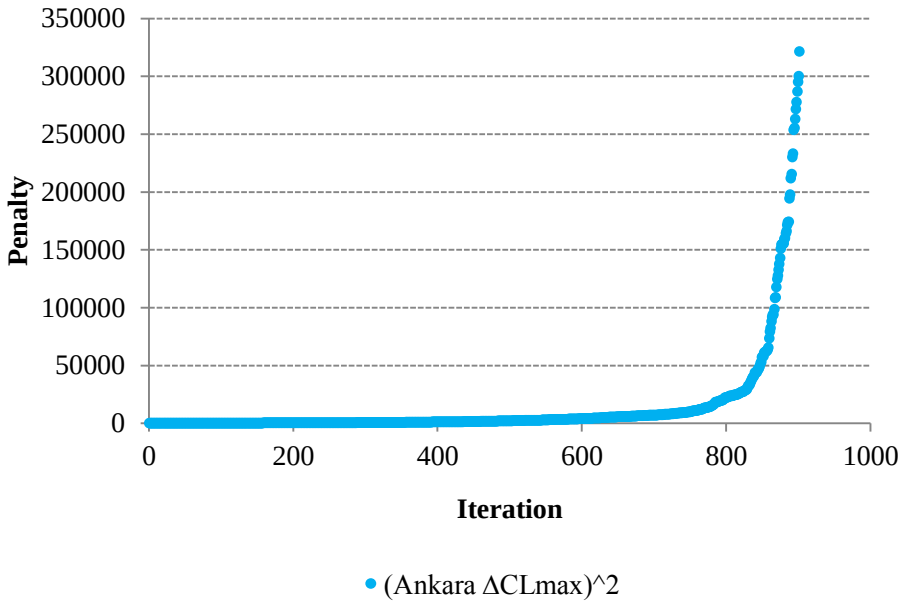

Figure D.29: The squared value of the ΔCLmax for Ankara case.

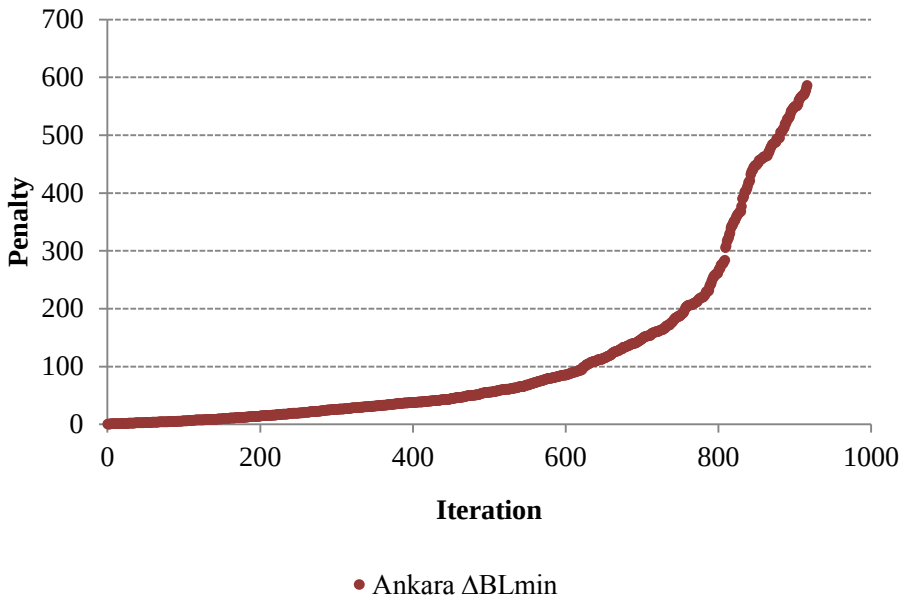

Figure D.30: The difference between the minimum allowed boiler capacity and the recommended boiler equipment capacity for Ankara case (ΔBLmin).

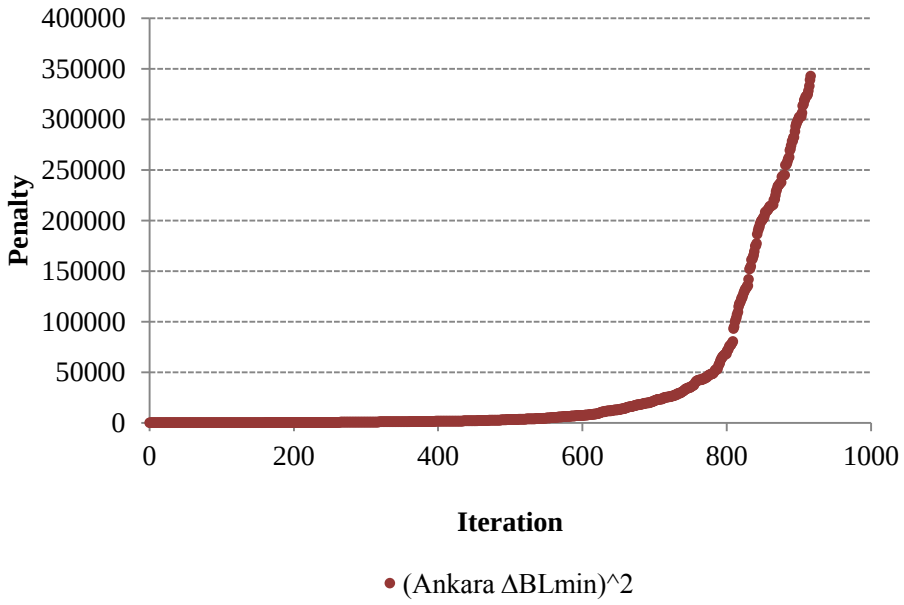

Figure D.31: The squared value of the ΔBLmin for Ankara case.

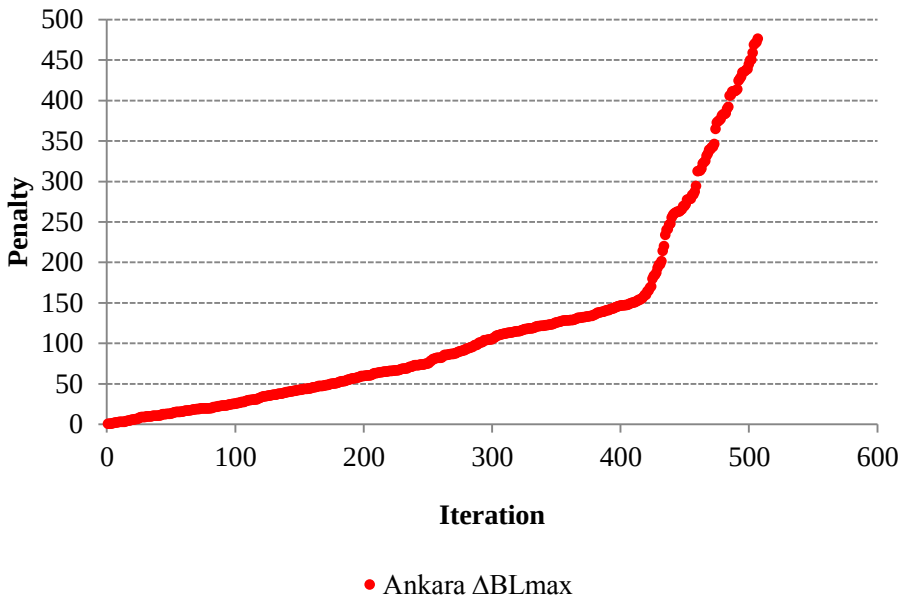

Figure D.32: The difference between the recommended boiler equipment capacity and the maximum allowed boiler capacity for Ankara case (ΔBLmax).

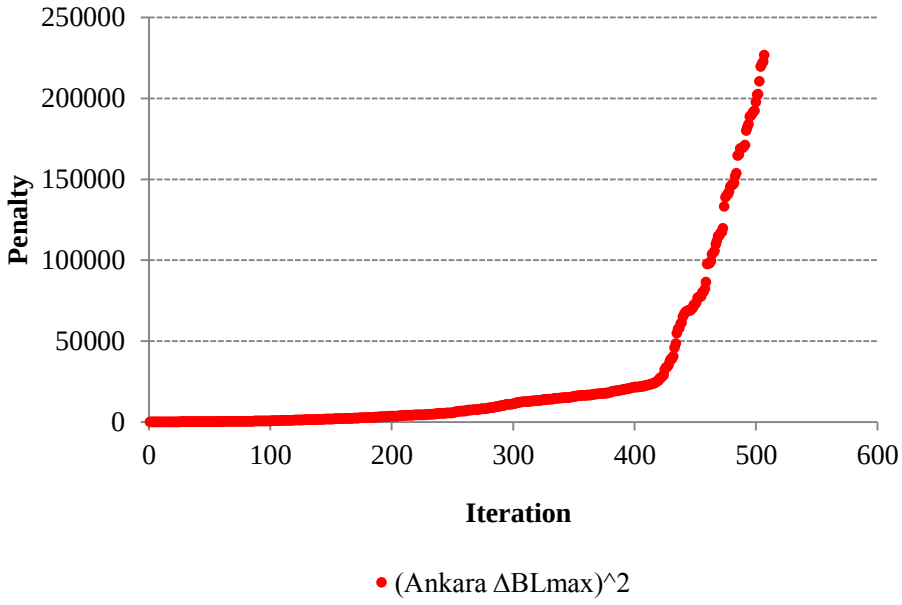

Figure D.33: The squared value of the ΔBLmax for Ankara case.

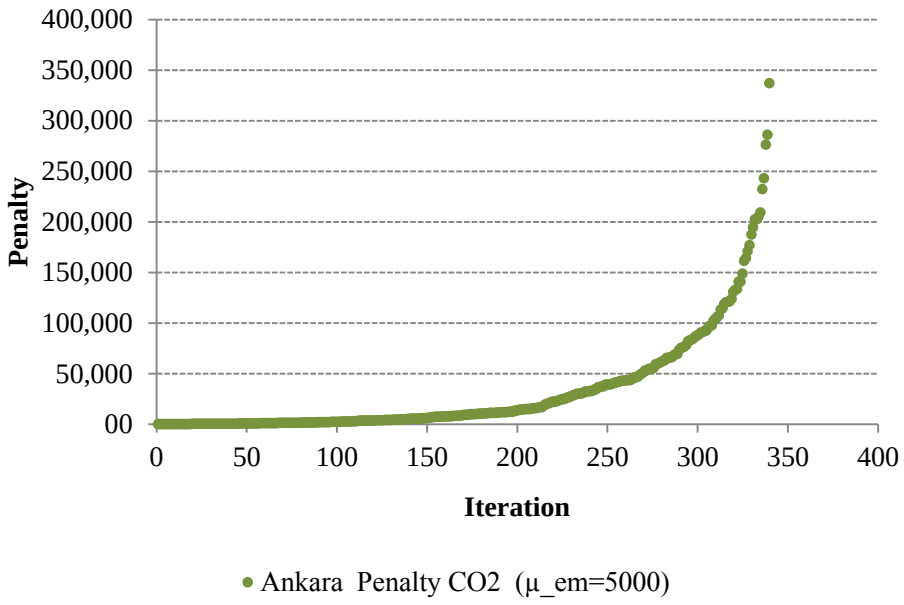

Figure D.34: Penalty function values of the CO2 emission for Ankara case.

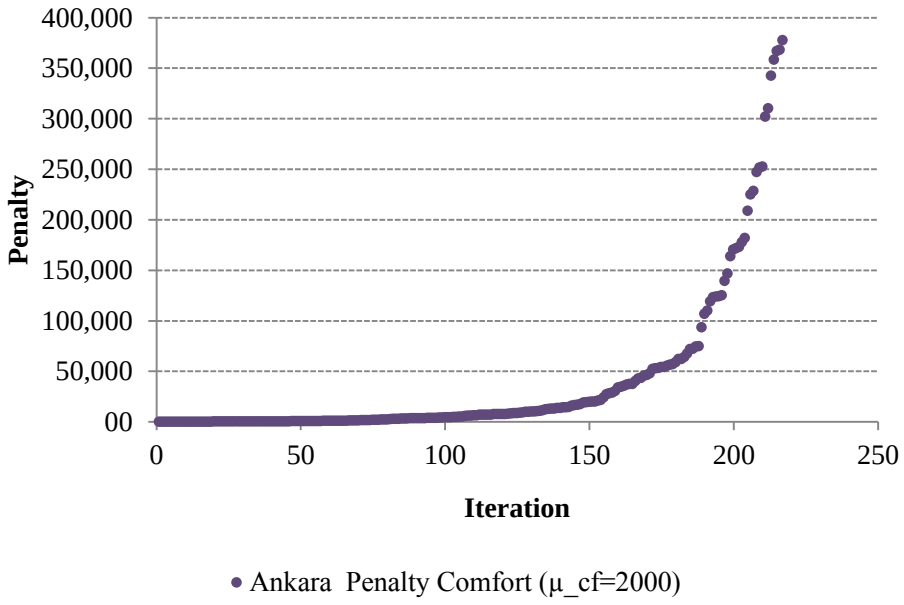

Figure D.35: Penalty function values of the PPD index for Ankara case.

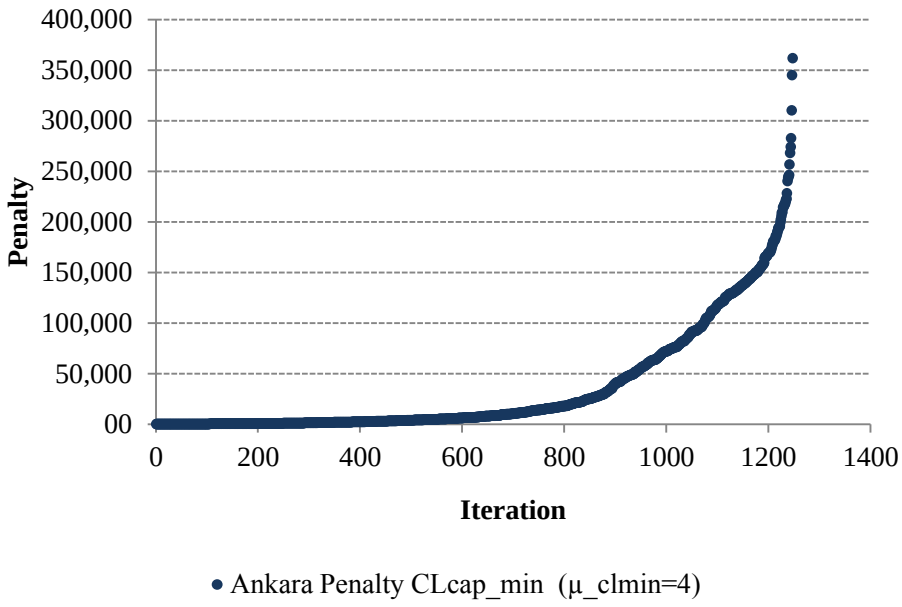

Figure D.36: Penalty function values of the chiller minimum capacity for Ankara case.

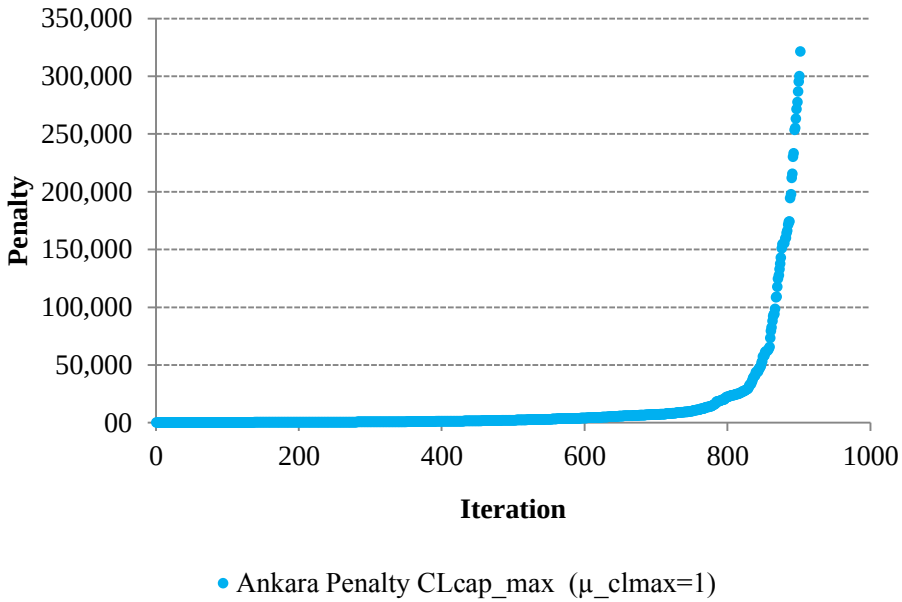

Figure D.37: Penalty function values of the chiller maximum capacity for Ankara case.

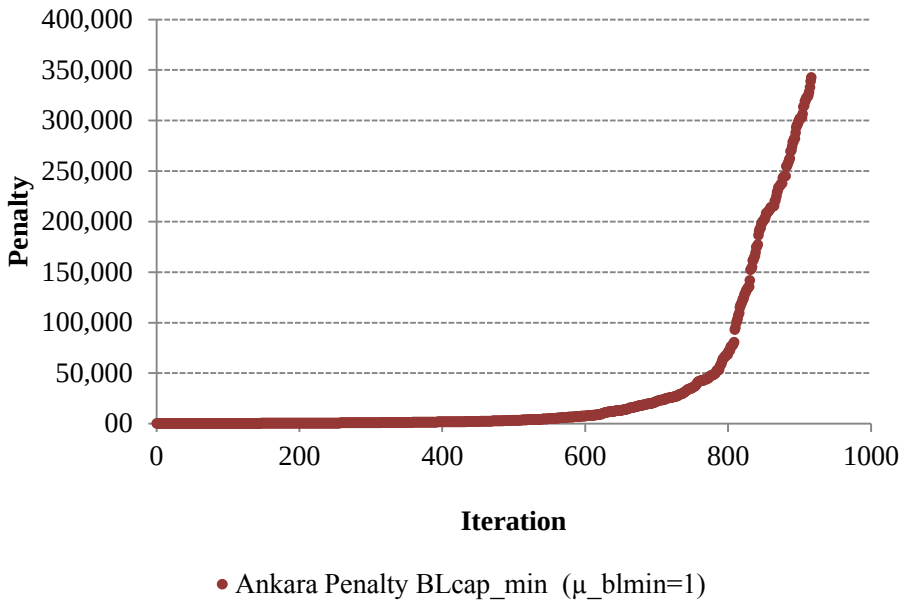

Figure D.38: Penalty function values of the boiler minimum capacity for Ankara case.

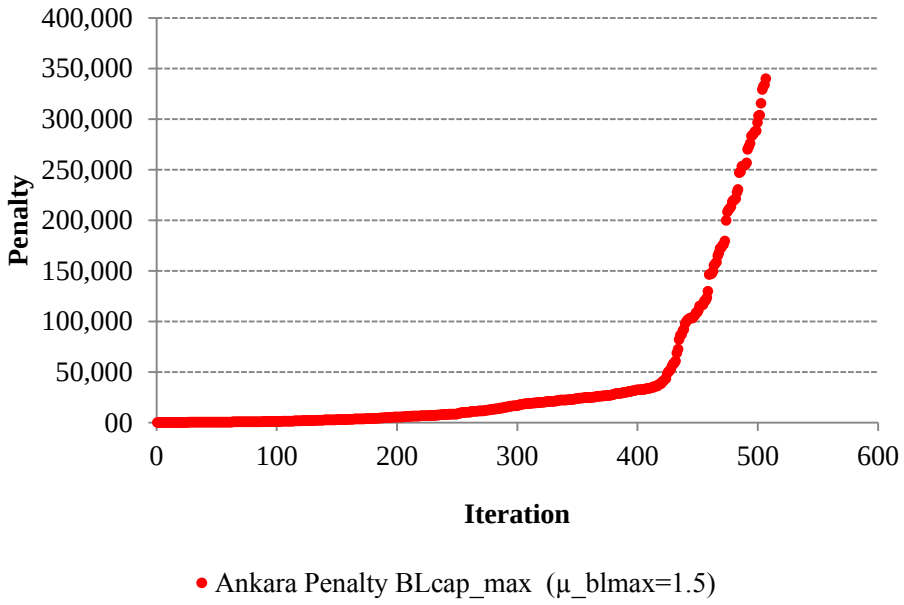

Figure D.39: Penalty function values of the boiler maximum capacity for Ankara case.

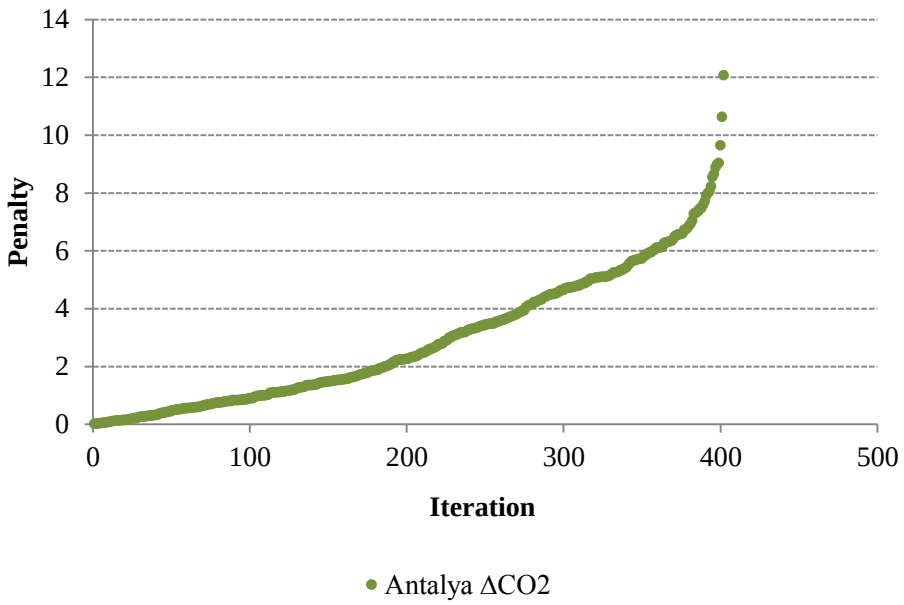

Figure D.40: The difference between the CO2 emission rate of any design option and the target rate for Antalya case (ΔCO2).

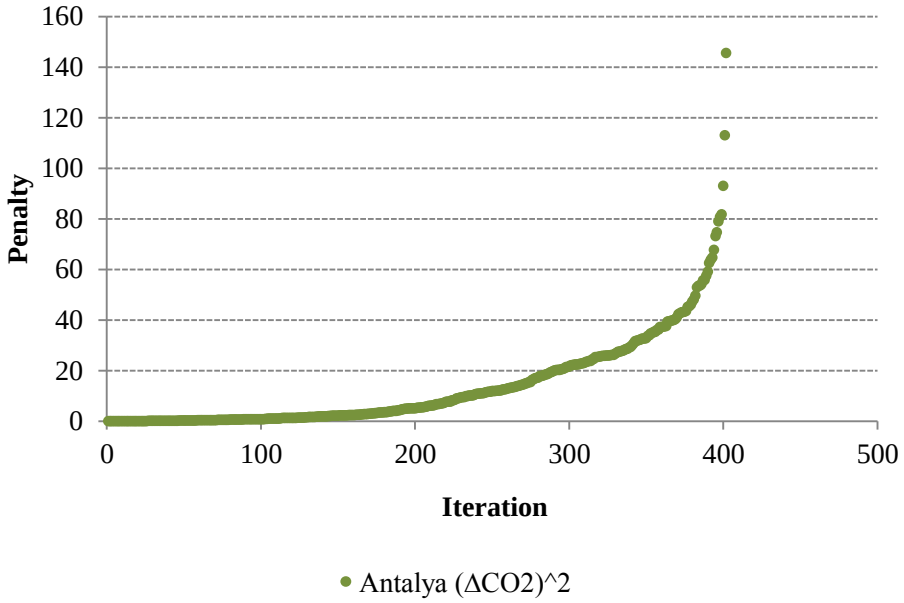

Figure D.41: The squared value of the ΔCO2 for Antalya case.

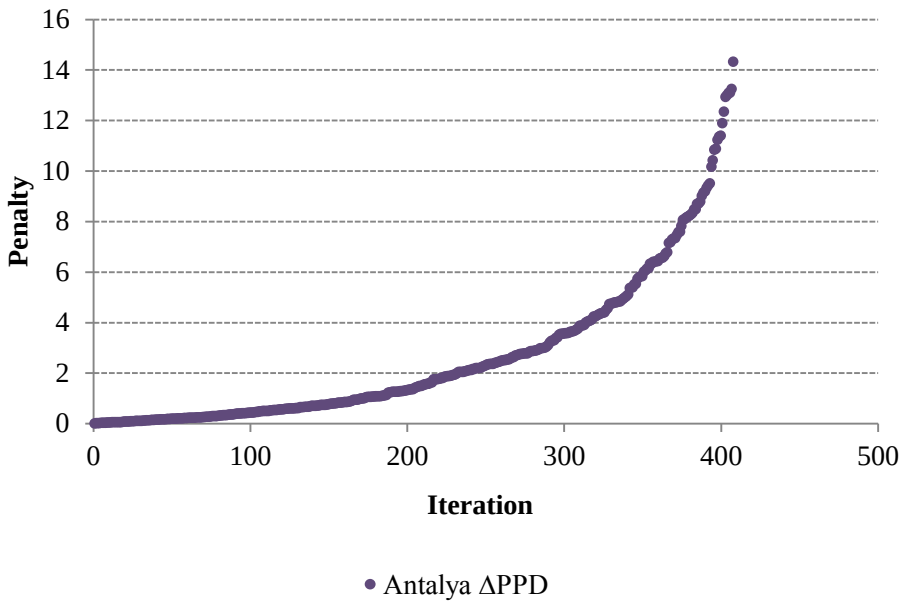

Figure D.42: The difference between the PPD index of any design option and the target index for Antalya case (ΔPPD).

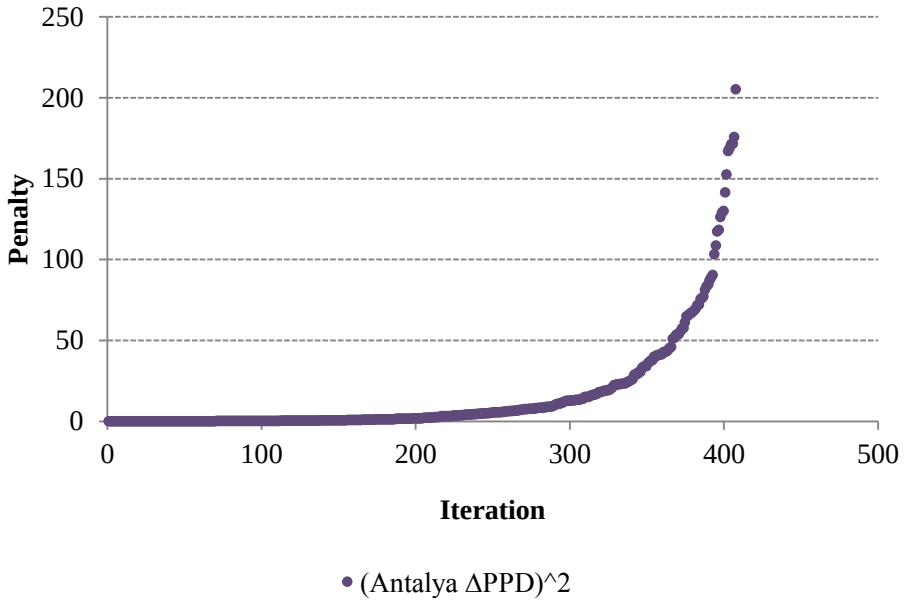

Figure D.43: The squared value of the ΔPPD for Antalya case.

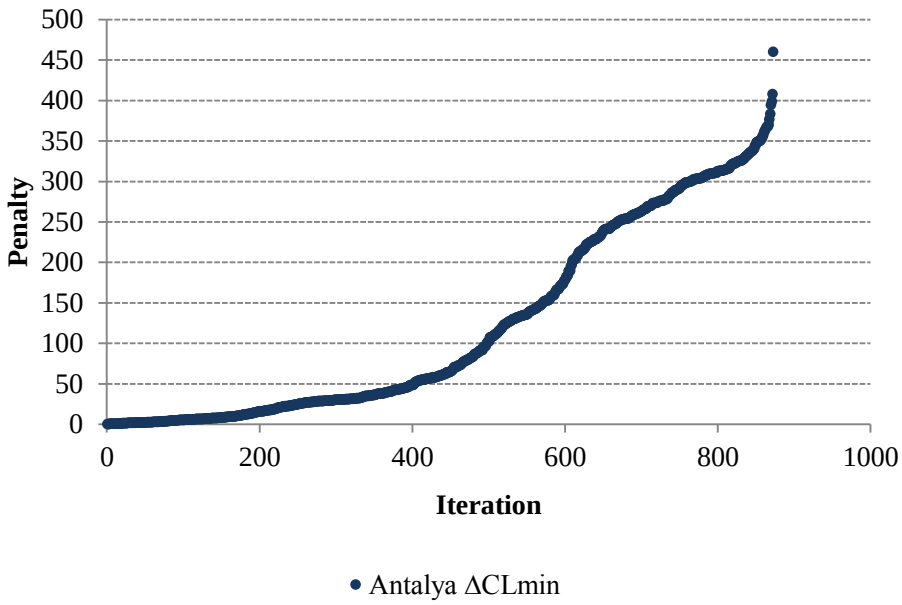

Figure D.44: The difference between the minimum allowed chiller capacity and the recommended chiller equipment capacity for Antalya case (ΔCLmin).

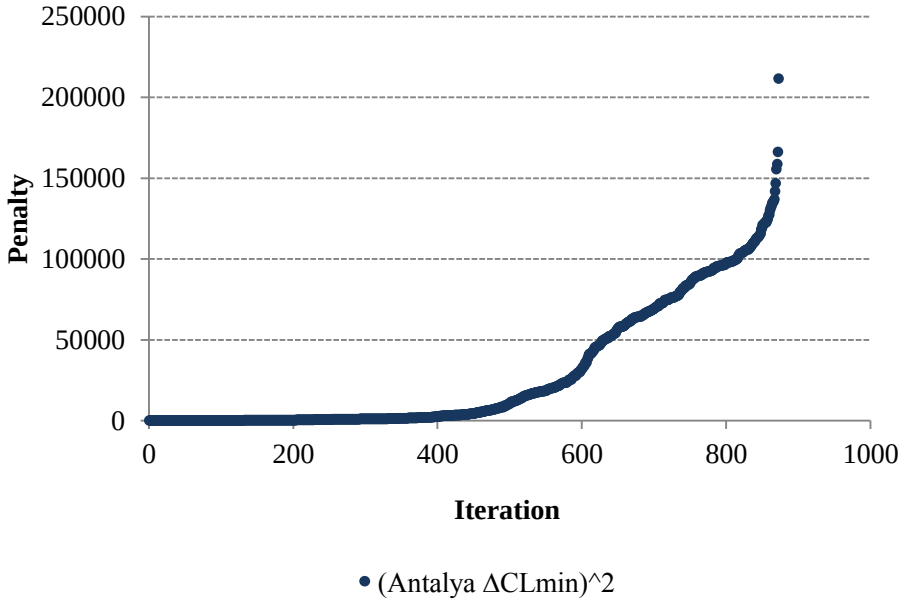

Figure D.45: The squared value of the ΔCLmin for Antalya case.

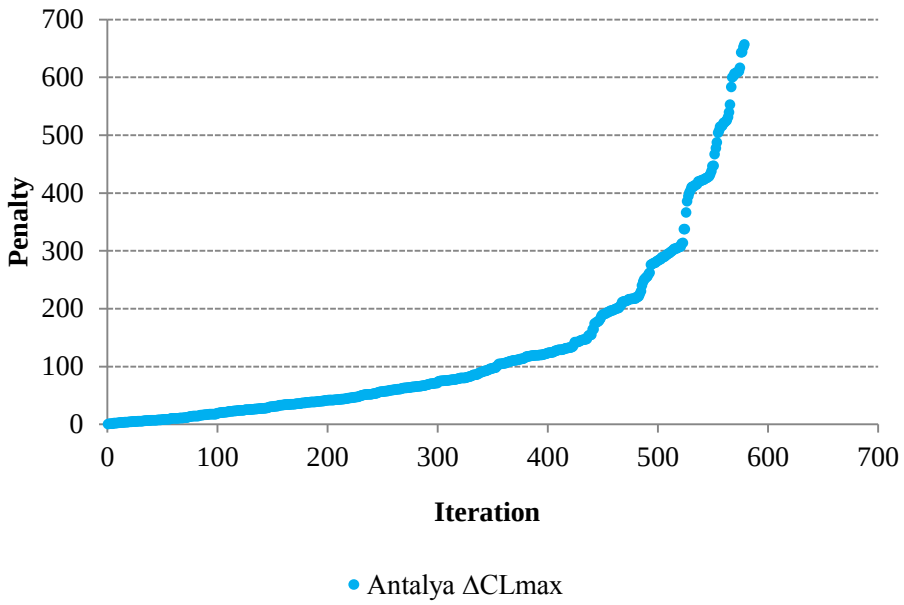

Figure D.46: The difference between the recommended chiller equipment capacity and the maximum allowed chiller capacity for Antalya case (ΔCLmax).

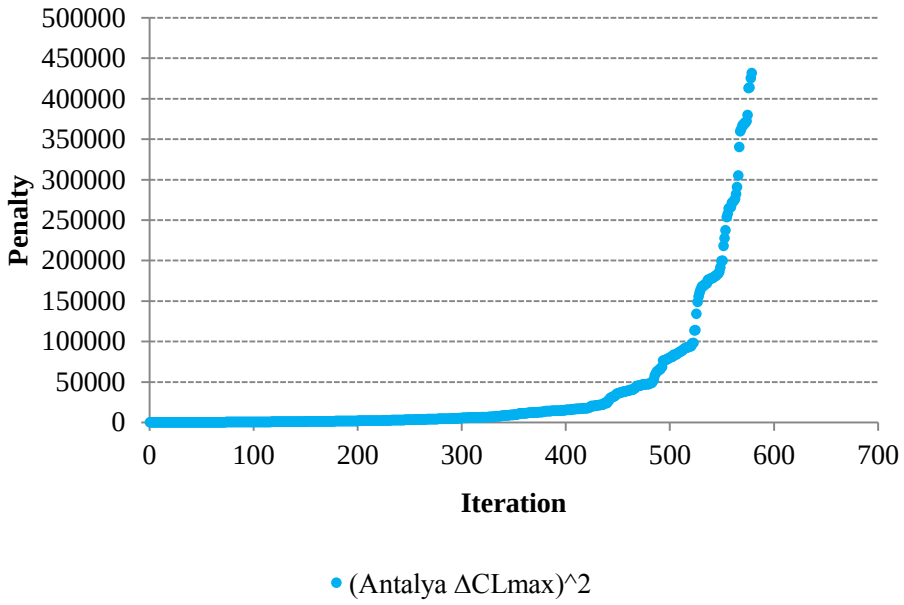

Figure D.47: The squared value of the ΔCLmax for Antalya case.

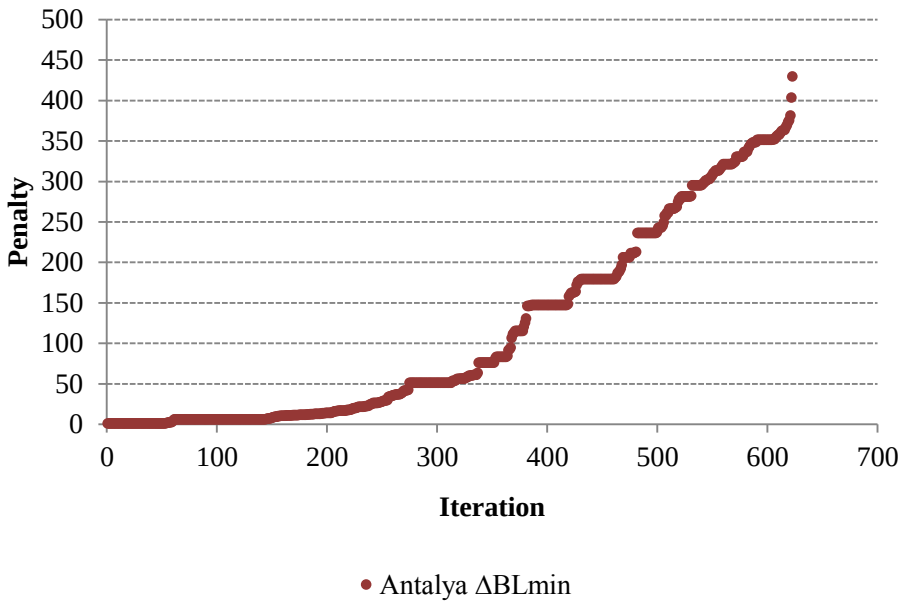

Figure D.48: The difference between the minimum allowed boiler capacity and the recommended boiler equipment capacity (ΔBLmin) for Antalya case.

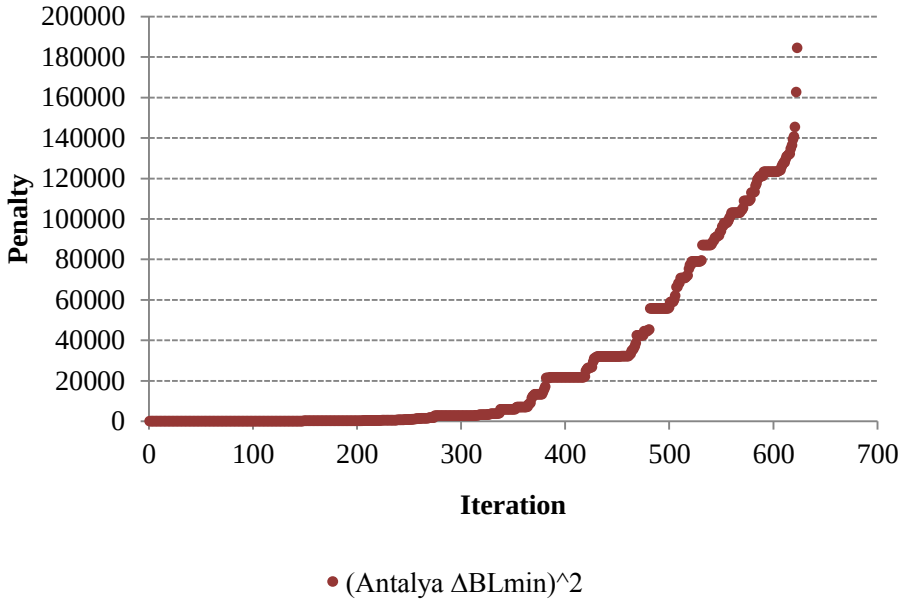

Figure D.49: The squared value of the ΔBLmin for Antalya case.

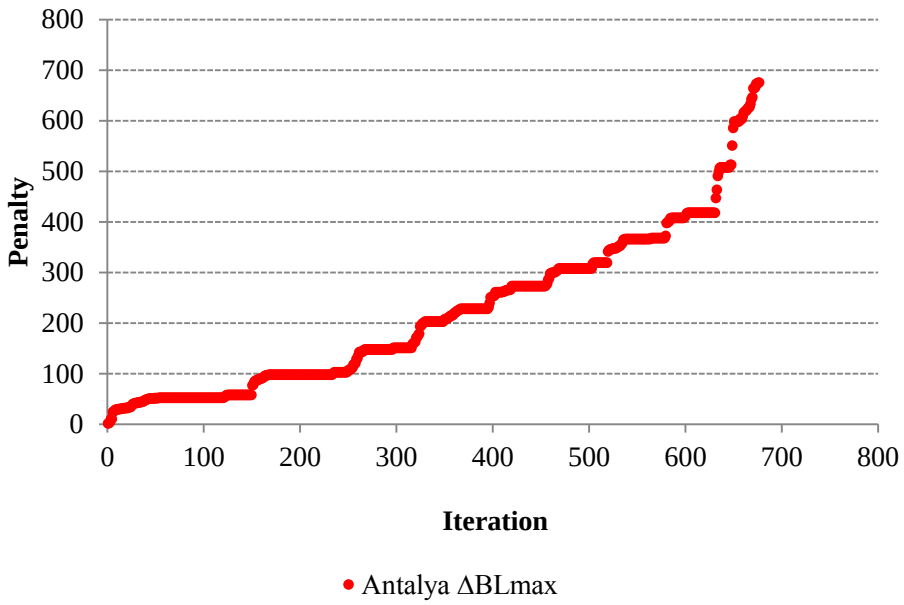

Figure D.50: The difference between the recommended boiler equipment capacity and the maximum allowed boiler capacity (ΔBLmax) for Antalya case.

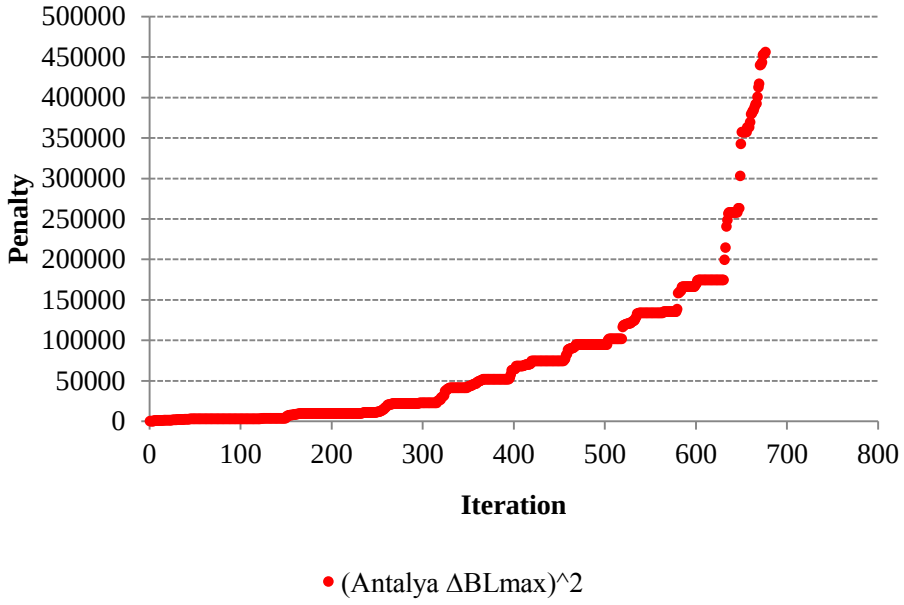

Figure D.51: The squared value of the ΔBLmax for Antalya case.

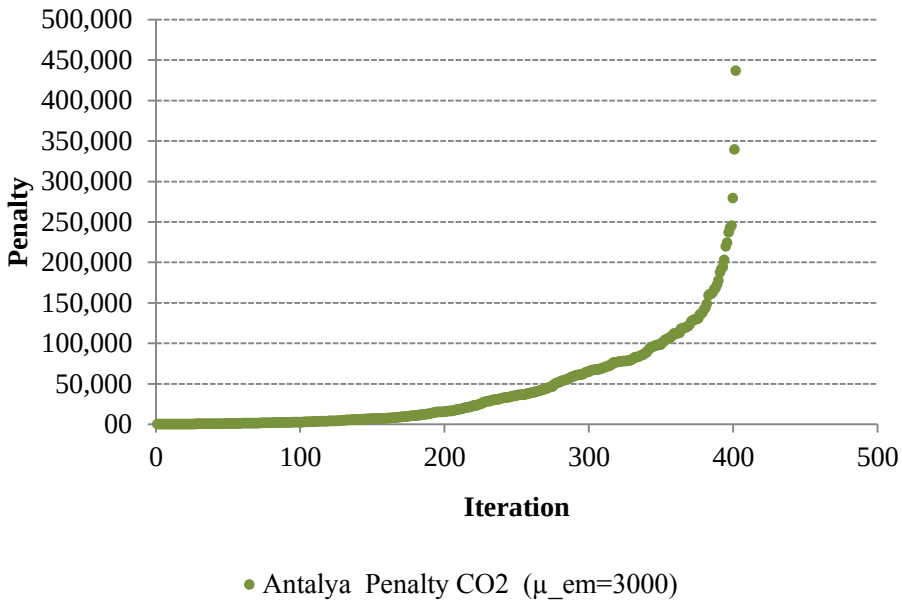

Figure D.52: Penalty function values of the CO2 emission for Antalya case.

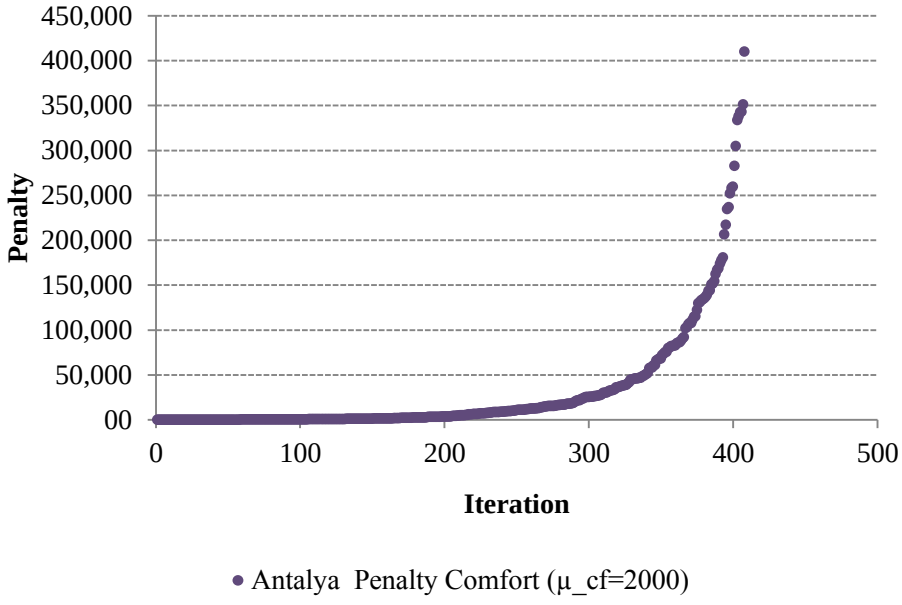

Figure D.53: Penalty function values of the PPD index for Antalya case.

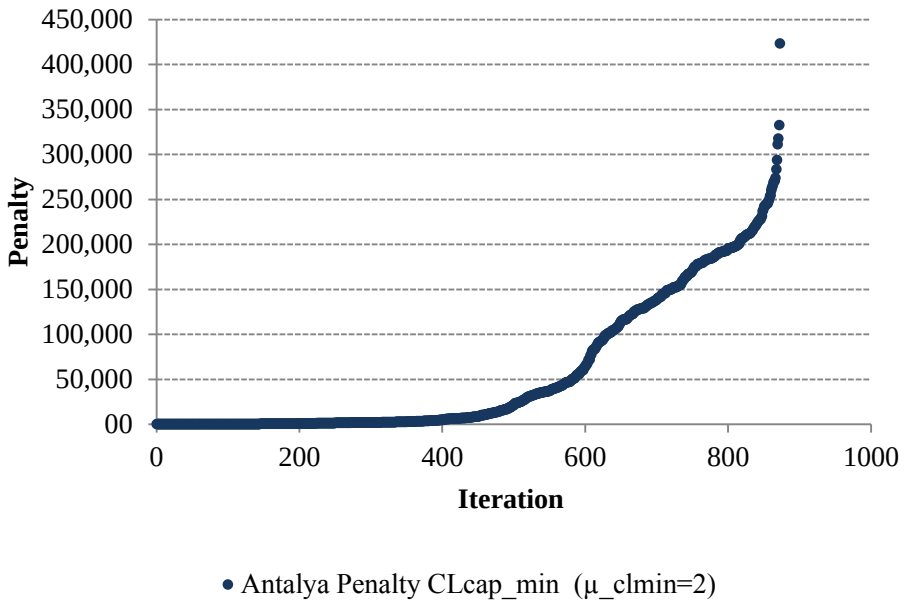

Figure D.54: Penalty function values of the chiller minimum capacity for Antalya case.

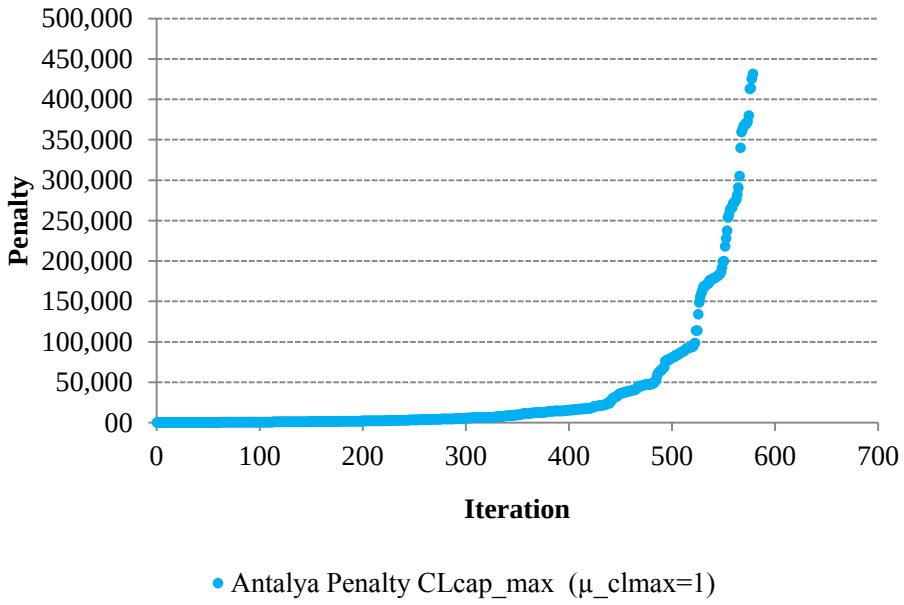

Figure D.55: Penalty function values of the chiller maximum capacity for Antalya case.

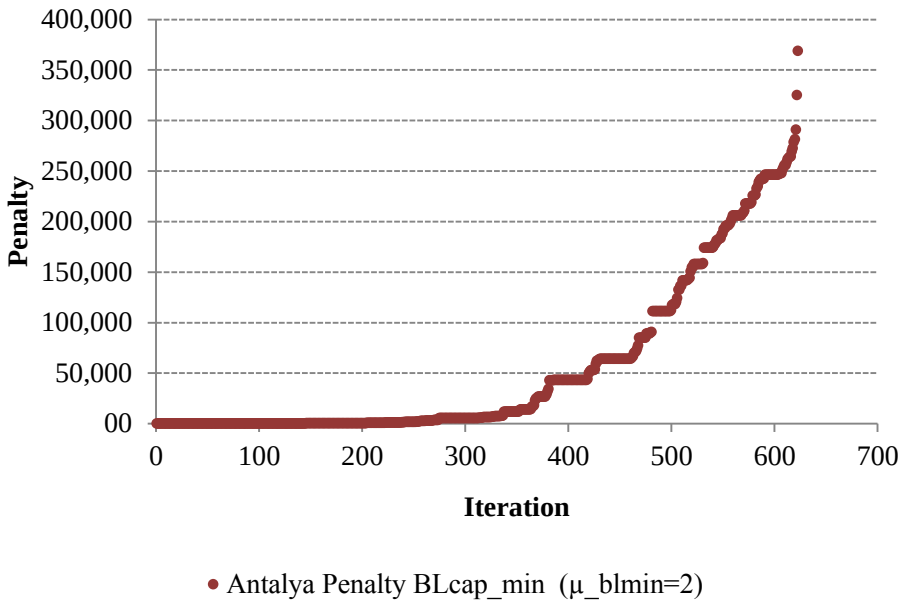

Figure D.56: Penalty function values of the boiler minimum capacity for Antalya case.

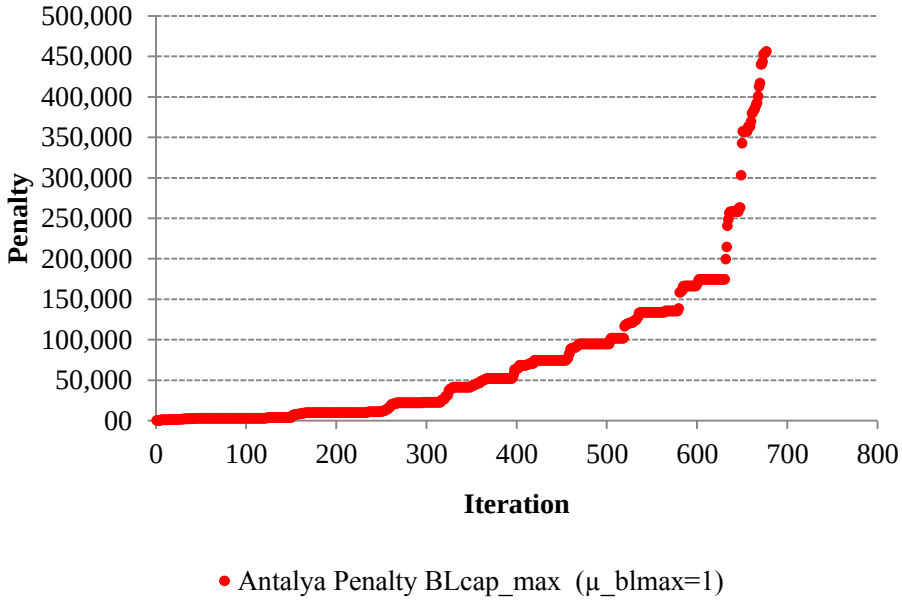

Figure D.57: Penalty function values of the boiler maximum capacity for Antalya case.

CURRICULUM VITAE

Name Surname **:** Meltem Bayraktar

E-Mail **:** bayraktarmeltem@yahoo.com

EDUCATION:

- **Bachelor of Science** **:** 2003, Istanbul Technical University, Faculty of Electrical and Electronic Engineering, Electrical Engineering Department
- **Master of Science** **:** 2006, Istanbul Technical University, Institute of Energy, Energy Science and Technologies Programme

PROFESSIONAL EXPERIENCE AND REWARDS:

- **March 2015 – Ongoing:** Chair of the Board of Directors**,** BINSIMDER- Turkish Branch of International Building Performance Simulation Association.
- **January 2011 – February 2012:** Building Energy Specialist, Ekomim Ecological Architectural Consulting.
- **May 2010 – March 2015**: Secretary-general, BINSIMDER- Turkish Branch of International Building Performance Simulation Association.
- **May 2008 – Ongoing:** Building energy modelling instructor, Independent.
- **June 2008 – December 2010:** Researcher, Politecnico di Torino, Department of Energy, EU Marie Curie Actions, CITYNET Research and Training Network, Italy.
- **November 2006 – January 2008:** Researcher, Istanbul Technical University, Project Management Centre, EU 6th FW I3CON Research Project, Turkey.
- **January 2005 – August 2005:** Researcher, Stuttgart University of Applied Sciences, EU Concerto Initiative, POLYCITY Project, Germany.

PUBLICATIONS, PRESENTATIONS AND PATENTS ON THE THESIS:

- **Bayraktar M.**, Fabrizio E., Perino M., 2012. The "extended building energy hub": a new method for the simultaneous optimization of energy demand and energy supply in buildings, *ASHRAE HVAC & R Research*, 18 (1-2), .67-87 (ISSN: 1078-9669).
- **Bayraktar M.**, Fabrizio E., Perino M., 2010. A Method for Simultaneous Optimization of Energy Demand and Energy Supply in Buildings, *Proceedings of the 7th International Conference on Indoor Air Quality, Ventilation and Energy Conversation in Buildings (IAQVEC 2010),* Syracuse, August 15-18, NY, USA.

OTHER PUBLICATIONS, PRESENTATIONS AND PATENTS :

- Yılmaz Z., Kalaycıoğlu E., Akgüç A., **Bayraktar M.**, 2012. Importance of Dynamic Energy Modelling in Energy Efficient and Green Building Design (Enerji Etkin ve Yeşil Bina Tasarımında Dinamik Enerji Modellemenin Önemi), *X. International HVAR+R Technology Symposium*, April 30 – May 2, Istanbul, Turkey.
- **Bayraktar M.**, Kalaycioğlu E., Yilmaz Z., 2011. A Real-Life Experience Of Using Dynamic Building Simulation For Building Environmental Performance Assessment In Turkey, *Proceedings of the 12th International Conference of the International Building Performance Simulation Association. (BS 2011)*, November 14-16, Sydney, Australia
- **Bayraktar M.**, Perino M., Yilmaz Z., 2010. Energy Performance And Comfort Level In High Rise And Highly Glazed Office Buildings, *Proceedings of the 10th International Conference for Enhanced Building Operations (ICEBO 2010)*, October 26 - 28, Kuwait City, Kuwait.
- **Bayraktar M.**, Celik B., Yilmaz Z., 2010. Energy Performance and Comfort Level Evaluation of an Office Building in Istanbul through Facade Design and Lighting Control, *Proceedings of the 10th International REHVA World Congress, Sustainable Energy Use in Buildings (CLIMA 2010)*, Antalya, Turkey.
- **Bayraktar M.**, 2009. An Approach for Optimization of Glazing Selection, Lighting and Shading Control Strategies for Commercial Buildings through a Case Study , *Proceedings of the 4th International Building Physics Conference*, ISBN 978-975-561- 350-5, pp 561-567, Istanbul,Turkey.
- **Bayraktar M.**, Yilmaz Z., 2007. Importance of Passive Intelligence in Building Energy Saving (Bina Enerji Tasarrufunda Pasif Akilliligin Önemi), *Proceedings of the 8th National Installation Engineering Congress*, İzmir, Turkey.
- **Bayraktar M.**, 2006. An approach to passive solar intelligent building design, M.Sc. Thesis, Istanbul Technical University, Institute of Energy.